Stony Brook University

OFFICIAL COPY

The official electronic file of this thesis or dissertation is maintained by the University Libraries on behalf of The Graduate School at Stony Brook University.

© All Rights Reserved by Author.

Mass spectrometry-based isotope-coded mass tag (ICMT) to study transmembrane peptide dynamics and protein-lipid interactions

A Dissertation Presented

by

Chiao-Yung Su

to

The Graduate School

in Partial Fulfillment of the

Requirements

for the Degree of

Doctor of Philosophy

in

Chemistry

Stony Brook University

May 2014

Stony Brook University

The Graduate School

Chiao-Yung Su

We, the dissertation committee for the above candidate for the
Doctor of Philosophy degree, hereby recommend
acceptance of this dissertation.

Nicole S. Sampson, Ph. D., Dissertation Advisor
Professor and Chair of Chemistry, Stony Brook University

Elizabeth M. Boon, Ph. D., Chairperson of Defense
Associate Professor of Chemistry, Stony Brook University

Daniel P. Raleigh. Ph. D., Third Member of Defense
Professor of Chemistry, Stony Brook University

Markus A. Seeliger, Ph. D., Outside Member of Defense
Assistant Professor of Pharmacological Sciences, Stony Brook University

This dissertation is accepted by the Graduate School

Charles Taber
Dean of the Graduate School

Abstract of the Dissertation

Mass spectrometry-based isotope-coded mass tag (ICMT) to study transmembrane peptide dynamics and protein-lipid interactions

by

Chiao-Yung Su

Doctor of Philosophy

in

Chemistry

Stony Brook University

2014

The plasma membrane contains a diverse array of proteins, including receptors, channels, and signaling complexes, that serve as decision-making centers. Investigation of membrane protein topology is important for understanding the function of these types of proteins. Here, we report a method to determine protein topology in the membrane that utilizes labeling of cysteine with isotope-coded mass tags (ICMT). The mass tags contain a thiol reactive moiety, linker, and a quaternary ammonium group to aid ionization in the mass spectrometer and were synthesized as both light and heavy (deuterated) forms. The probes are membrane impermeable.

To assess the utility of the probes for mapping peptide thiol topology, we employed a two-step labeling procedure. Vesicles containing α-helical transmembrane peptides were labeled with heavy (or light) probe, solubilized with detergent, and then labeled with an excess of the complementary probe. Peptides for which the cysteine was oriented in the center of the lipid bilayer were not labeled until the lipid vesicles were lysed with detergent, consistent with the membrane impermeability of the probes and reduced ionization of the thiol in the hydrophobic membrane. Peptides for which the cysteine was positioned in the headgroup zone of the lipid bilayer were labeled rapidly. Peptides for which the cysteine was positioned below the headgroup abutting the hydrocarbon region were labeled at a reduced rate compared to the fully

accessible cysteine. Moreover, the effect of lipid bilayer structure on the kinetics of peptide and lipid flipping in the bilayer was readily measured with our two-step labeling method. The small sample size required, the ease and rapidity of sample preparation, and the amenability of MALDI-TOF mass spectral analysis in the presence of lipids will enable future facile investigation of membrane proteins in a cellular context.

Interfacial proteins are water-soluble enzymes or regulatory macromolecules that bind transiently to the membrane surface during the course of the catalytic reaction or signaling event. The structures of the water-soluble state are often readily available to high resolution in a routine manner. However, characterizing the conformation of the active protein complex at the membrane interface is a major challenge in structural biology. Current methods rely primarily on the introduction of large, potentially structure altering, probes for EPR or fluorescence analysis, or detection of local structure by solid-state NMR spectroscopy. We are developing mass spectrometric methodology that will provide atomic resolution information about the nature of residues involved in protein-membrane binding.

Cholesterol oxidase from *Streptomyces sp.* SA-COO was employed as a model system because it is an interfacial enzyme that is easily expressed, and detailed kinetic analyses, and crystallographic structures are available. Multiple cysteines were introduced in a single protein, and the Michaelis-Menten kinetics of these mutants showed comparable activities to wild-type enzyme. These cysteine thiols were tagged with ICMT probes, and the reaction rates depended on the solvent accessibility of the cysteine being labeled. Moderate differences in labeling rate were detected at cysteines proposed to be in membrane contact. These studies serve as the foundation for future design of experiments to explore protein-membrane interactions in more detail.

Table of Contents

List of Figures

List of Tables

List of Schemes

List of Appendix Contents

List of Abbreviations

2 x YT	2 x Yeast extract tryptone
Ac	Acetyl
ACN	Acetonitrile
ALICE	Acid-labile isotope-coded extractants
Am	Amino
AMP	Ampicillin
APCI	Atmospheric pressure chemical ionization
BSA	Bovine serum albumin
CD	Circular dichroism
CHCA	α-Cyano-4-hydroxycinnamic acid
CI	Chemical ionization
CID	Collision-induced dissociation
CL	Cardiolipin
CMC	Critical micelle concentration
DEAE	Diethylaminoethanol
DHB	2,5-Dihydroxybenzoic acid
DHEA	Dehydroepiandrosterone
DLS	Dynamic light scattering
DMPC	1, 2-Dimymyristoyl-*sn*-glycero-3-phosphocholine
DNA	Deoxyribonuclein acid
DOPC	1, 2-Dioleoyl-*sn*-glycero-3-phosphocholine

DOPE	1, 2-Dioleoyl-*sn*-glycero-3-phosphoethanolamine
DOPG	1, 2-Dioleoyl-*sn*-glycero-3-phosphoglycerol
DPPC	1, 2-Dipalmitoyl-*sn*-glycero-3-phosphocholine
DOPS	1, 2-Dioleoyl-*sn*-glycero-3-phospho-L-serine
DTT	Dithiothreitol
E. coli	*Escherichia coli*
EI	Electron ionization
EPR	Electron paramagnetic resonance
eq	equivalents
ESI	Electrospray ionization
EtOAc	Ethyl acetate
EtOH	Ethanol
FAD	Flavin adenine dinucleotide
FPLC	Fast protein liquid chromatography
GMC	Glucose-methanol-choline
GPCR	G-protein couple receptor
HEPES	Hydroxyethyl piperazineethanesulfonic acid
HSQC	Heteronuclear single quantum coherence
Hz	Hertz
IAM	Iodoacetamide
ICAT	Isotope-coded affinity tag
ICMT	Isotope-coded mass tag

IF	Interfacial
IFA	Interfacial activation
IPTG	isopropyl β-D-thiogalactoside
IR	Infrared
isotope-ABPP	Isotopic tandem orthogonal proteolysis-activity-based protein profiling
ITC	Isothermal titration calorimetry
kb	kilobase
kDa	kilodalton
Km	Miclaelis-Menten constant
kV	kilovolts
LB	Luria-Bertani
LC	Liquid chromatography
LUV	Large unilamellar vesicles
NaPi	Sodium phosphate
NCI	Negative chemical ionization
NEM	*N*-Ethylmaleimide
NMR	Nuclear magnetic resonance
MALDI	Matrix-assisted laser desorption ionization
MCP	Microchannel plate
MD	Molecular dynamics
MS	Mass Spectrometry
MS/MS	Tandem mass

MWCO	Molucular weight cut off
m/z	mass-to-charge ratio
NCI	Negative chemical ionization
OD	Optical density
PCR	Polymerase chain reaction
PDA	Photodiode array
PDB	Protein data bank
PE	Phosphatidylethanolamine
PEG	Polyethylene glycol
PG	Phosphatidylglycerol
PI	Phosphatidylinositol 4,5-bisphosphate
PLA	Phospholipase A
PKC	Protein kinase C
POPC	1-Palmitoyl-2-oleoyl-*sn*-glycero-3-phosphocholine
PS	Phosphotidylserine
PTE	1, 2-Dipalmitoyl-*sn*-glycero-3-phosphothioethanol
RBF	Round-bottomed flask
rpm	Revolution per minute
SCAM	Substituted-cysteine accessibility methods
SDC	Sodium deoxycholate
SDS-PAGE	Sodium dodecyl sulfate polyacrylamide gel electrophoresis
SM	Sphingomyelin

SQ	Single quadrupole
SS	Solid-state
TCEP	Tris(2-carboxyethyl)phosphine
TFA	Trifluoroacetic acid
TLC	Thin layer chromatography
TOF	Time-of-flight
TROSY	Transverse relaxation optimized spectroscopy
UV/vis	Ultraviolet/visible

Chapter 1 Introduction

1.1 Specific aims

Despite the importance of membrane protein-lipid interactions in biological systems, it is still challenging in structural biology to understand the binding of interfacial protein to membranes or to monitor protein conformational changes at the membrane surface.

The goal of this thesis work is to develop an isotope-coded mass tag (ICMT)-based approach to investigate transmembrane peptide dynamics and peripheral membrane protein-lipid interactions by mass spectrometry. Experiments were designed to synthesize ICMTs, to differentially label dynamic transmembrane peptides and an interfacial enzyme, and to analyze the dynamics by mass spectrometry.

The specific aims are:

1. **Develop membrane impermeable isotope-coded mass tags (ICMTs).** We designed and synthesized ICMTs with various lengths of hydrocarbon linkers and PEG linker connecting the thiol reactive maleimide moiety and the positively charged quaternary ammonium group for isotope coding on the methyl groups. Membrane permeability of these mass tags was tested by fluorescence dye leakage assay and a NB-ECD-OMe peptide encapsulated vesicle labeling in native and lysed form with heavy and light probes respectively.

2. **Examine dynamic interactions of transmembrane peptides with lipid membranes.** We designed 3 α-helical transmembrane peptides with a (i) single cysteine located in a solvent-accessible region, (ii) partially buried in headgroups, or (iii) deeply embedded in the hydrophobic core when the peptide incorporates into membranes. By utilizing two-step or kinetic labeling of peptides with heavy and light ICMTs, we were able to probe the dynamics of peptide flipping in membranes in different lipid phases as well as regulation by anionic lipid headgroups. In addition, we also included thiol lipids in the synthetic vesicles in the presence and absence of solvent-accessible transmembrane peptide to study lipid flipping.

3. **Investigate the interfacial protein-lipid interactions of cholesterol oxidase by mapping protein-binding sites using ICMT strategy.** This strategy compares the differential cysteine reactivity of solvent-exposed thiols and membrane-embedded thiols in cholesterol oxidase. Multi-cysteines can be screened in a single mutant at time. Heavy probes were allowed to react with solvent-accessible cysteines and light probes were added in large excess to label the remainder of the cysteines upon denaturation. The heavy/light mass ratios for labeled peptide were assessed to determine if each cysteine is in membrane contact.

1.2 Biological importance of cell membranes

The cell membrane plays a pivotal role in living systems. The plasma membrane protects the cell from its surrounding and is involved in various cellular processes, such as cellular division, adhesion, ion conductivity and cell signaling (*1*). The plasma membrane is composed of lipid bilayers, which consist of a central hydrocarbon region and two flanking interfacial regions (Figure 1.1). The thickness of the hydrocarbon region is approximately 30 Å, and a single interface is roughly equal to 15 Å (*1*). The lipid bilayer is amphipathic, and consists of polar hydrophilic headgroups, which interact with the intracellular and extracellular faces, and long hydrophobic hydrocarbon chains, which are isolated from its surrounding (*1*). The composition of each lipid varies from different sources of the membrane. The most abundant lipids in cell membranes are phospholipids, sterols, and sphingolipids. The major lipid components to support membrane structures in mammalian cells are phosphatidylcholine (PC), phosphatidylserine (PS), phosphatidylethanolamine (PE), phosphatidylglycerol (PG), phosphatidylinositol 4,5-bisphosphate (PI), cardiolipin (CL), sphingomyelin (SM), and cholesterol; they differ in charge and size of the headgroup (Figure 1.2) (*1*).

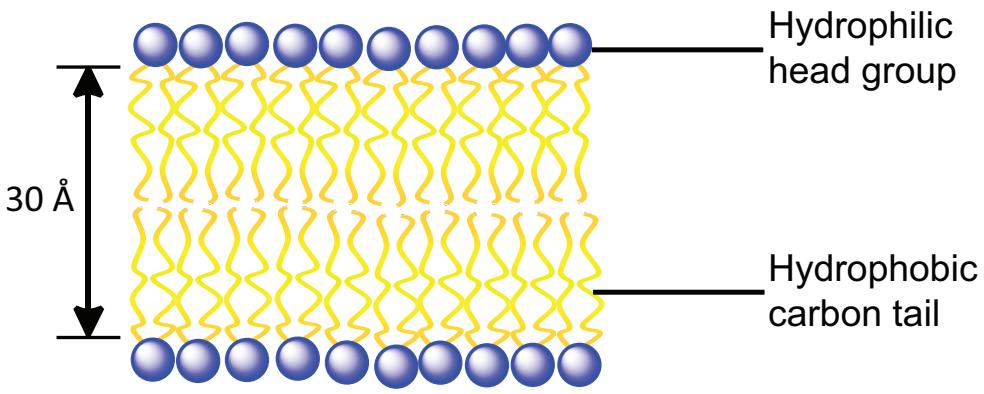

Figure 1.1 Schematic illustration of lipid bilayer architecture.

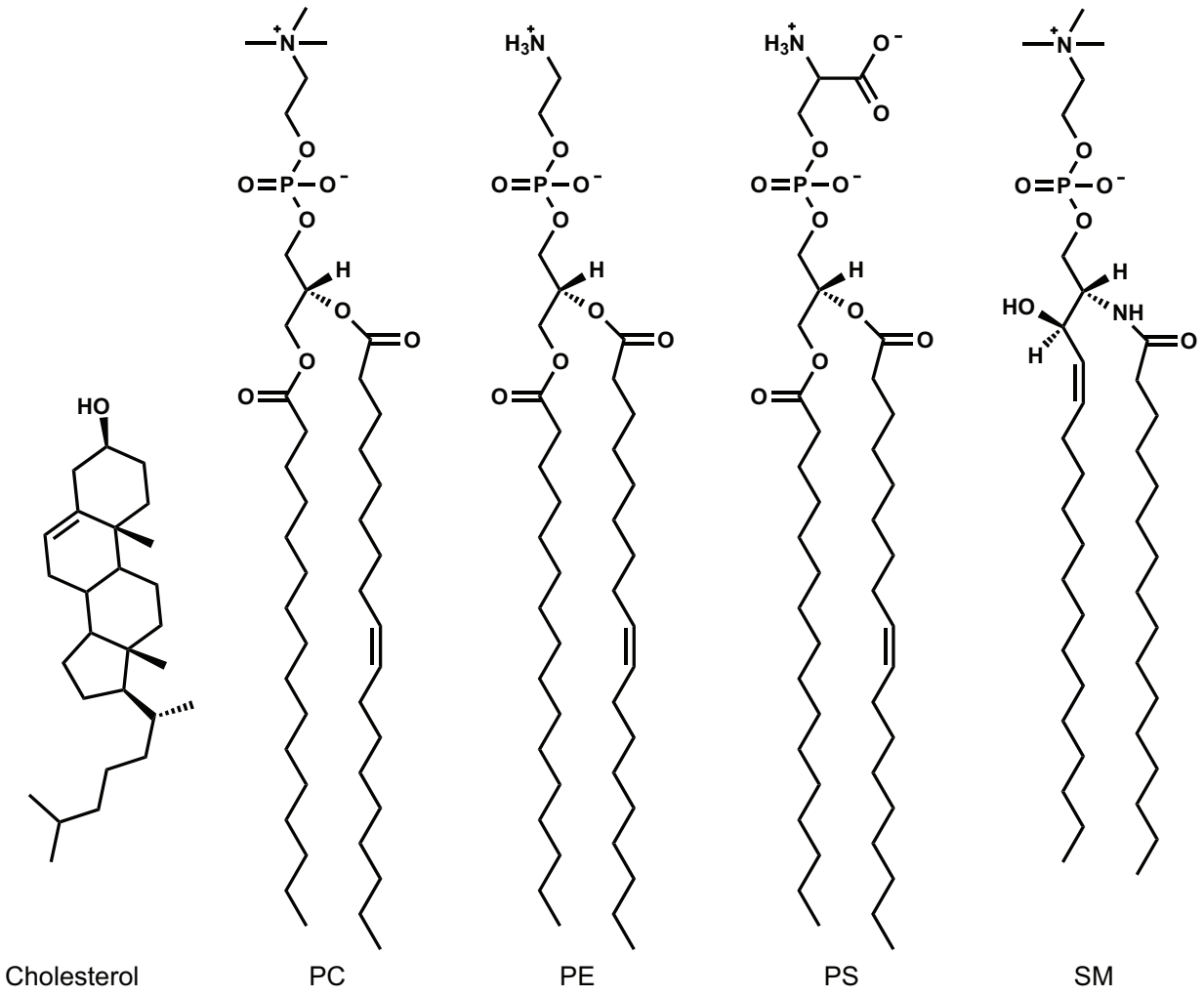

Figure 1.2 Structure representations of phospholipids abundant in mammalian cells and cholesterol.
Selected phospholipids are presented. The same fatty acid chains are shown for simplicity (*sn*-1: palmitoyl, *sn*-2: oleoyl for PC, PE, and PS). In lipid bilayers, cholesterol orients in the same position as phospholipids. The polar hydroxyl group is positioned toward the headgroups of the phospholipids, and the rigid hydrocarbon core and tail are associated with fatty acid chains.

Many plasma membranes are asymmetrically distributed between two monolayers (*2, 3*), for example, in *E. coli.*, PE and PS dominate in the inner monolayer, and PC and SM are mostly in the outer monolayer of the membrane (*1, 4, 5*). The fluidity of membranes is controlled by the chain length and degree of unsaturation of the fatty acid. Generally, shorter fatty acid hydrocarbon chains and saturated chains will lead to tight packing of the phospholipids. Cholesterol is normally found in mammalian cells and is known to affect membrane fluidity (*6,*

7). In contrast, unsaturated chains, especially *cis*-configuration lipids, interfere with phospholipid packing, making the membrane more flexible.

The flexibility of biological membranes is maintained by noncovalent interactions among lipids in the bilayer. Flexibility allows individual lipid molecules to diffuse freely within lipid bilayers. Cell membrane lipids are also involved in dynamic motions that assist alterations in membrane thickness, surface packing, lateral or rotational mobility. The structure and flexibility of membranes at different temperatures with various lipid compositions can be classified into three major phases: the gel state (s_o), the liquid-disordered state (l_d), and the liquid-ordered state (l_o). Cells tend to regulate the composition of the lipids to achieve their required membrane fluidity for specific cellular processes (*1*). The dynamics of membranes will dominate lipid properties, and will result in effects on membrane protein function.

1.3 Membrane proteins

Cell membranes are flexible and selectively permeable to polar substances via channels formed by protein complexes (*8*). The plasma membrane contains a diverse array of proteins, including receptors, channels, and signaling complexes that serve as an initial decision-making center for the cell (*8*). The structures, and thus the functions, of membrane-associated proteins are influenced by their environment in the membrane. Most of the cell functions proceed in or around the cell membranes, and they are controlled by membrane proteins.

It was estimated that the proportion of the putative membrane proteins in the human genome is around 30% (*9*). More than 60% of pharmaceutical drug targets are membrane-associated proteins (*10*), making them important for therapeutic purposes.

The membrane proteins can be divided into two major categories: integral (intrinsic) membrane proteins, and peripheral (extrinsic) membrane proteins (Figure 1.3). Integral proteins span the lipid bilayer with single or multiple α-helices, or a rolled-up β sheet (β barrel). Integral membrane proteins are amphiphilic, consisting of hydrophilic and hydrophobic regions. The hydrophilic part interacts with lipid headgroup as well as aqueous environment, and hydrophobic region interacts mostly with fatty acid hydrocarbon chains. Most integral proteins, e.g. sodium-potassium ATPase or hormone receptors, are structurally and functionally an essential intrinsic integral components of the membranes. Integral membrane proteins span into the hydrophobic core of the membranes with hydrophobic interactions with the fatty acid hydrocarbon chains. The transmembrane segment of an integral protein is very hydrophobic, and interacts with the hydrophobic lipids. Treatment with detergent is necessary to disrupt their hydrophobic interactions with plasma membranes. Conversely, peripheral proteins only transiently associate with the membrane. They either interact with integral proteins or penetrate into the region of the interface of the hydrocarbon core and polar headgroups. Membrane proteins play roles in signal transduction pathways, transport specific molecules across it, connect the cytoskeleton through the lipid bilayer, or catalyze membrane-associated reactions.

Membrane proteins can selectively bind defined lipids, and this specificity facilitates correct insertion, folding, and structural integrity and function of the proteins (*1*). To maintain the diffusion barrier and to keep the membrane electrochemically sealed, close interactions between membrane proteins and cell membranes are required.

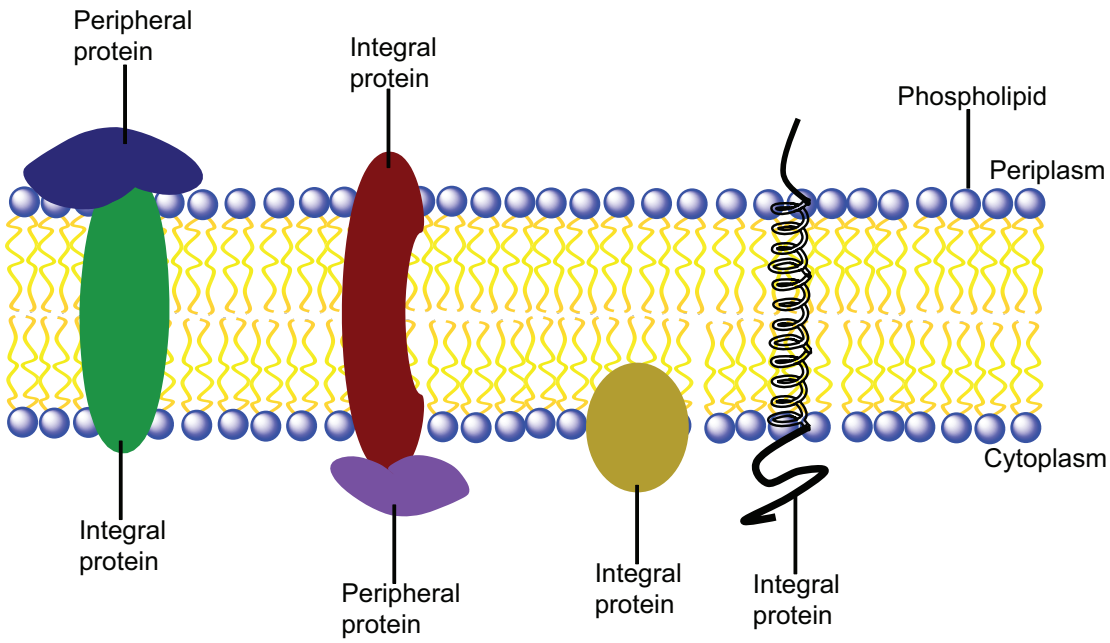

Figure 1.3 Schematic diagram of membrane proteins in cell membrane.
Integral proteins are embedded in the phospholipids containing cholesterol. Peripheral proteins are usually non-covalently attached to integral proteins.

1.4 Protein-lipid interactions

Membrane proteins control the transport of solutes and signals between the different functional areas of the cell (*11*). This is a critical process that ultimately affects the integrity of the cellular organelles. Integral membrane proteins form ion channels, e.g., sodium or potassium channel, transduce signals, e.g. G-protein couple receptor (GPCRs), or serve as transporters, e.g. ATPase. Despite the biological importance of these transmembrane proteins, the role of protein-lipid interactions involved in these processes is still not well understood (*12*). Lipids with different lateral packing, hydrophobic thickness, and headgroup charge can influence membrane proteins to alter their structure and activity. The transmembrane segments of integral proteins will in turn affect the organization and structure of lipids (*13-16*). Studying protein-lipid interactions is still a challenge in structural biology (*12*). The properties of transmembrane proteins are distinct from water-soluble proteins due to their hydrophobicity. The major difficulties for studying membrane proteins are expression of the proteins and reconstitution to their native environment (*17*).

Based on limited crystal structures of transmembrane proteins, the transmembrane segment consists of hydrophobic amino acids in the center interacting with the hydrocarbon chains of the bilayer and charged or aromatic amino acids on both sides interacting with the headgroup or the aqueous phase (*14*). In order to uncover how fundamental principles govern the molecular consequences of lipid-protein interactions, a simple model, i.e. a single α-helical transmembrane peptide, was developed to address these questions (*18-21*). Common examples of these peptides are KALP, WALP peptides (*22*) or polyLeu peptides (*23*), which are designed to span the lipid bilayer to form an α-helical structure, and participate in intermolecular interactions between amino acids and lipids.

KALP or WALP (Table 1.1) contains different numbers of leucine/alanine $(LA)_n$ repeating units (n = 5 ~ 12) in the central stretch and is flanked with two lysines or two tryptophans on both the N-termini and C-termini for KALP or WALP, respectively. pLeu (Table 1.1) consists of polyleucine on the central stretch and two lysine residues flanked on both side of the peptide as well as one tryptophan in the center with a total of 25 residues. These model transmembrane peptides are used to study peptide-lipid interactions, including hydrophobic mismatch with membranes, peptide tilt angle, or peptide oligomerization (*19*). For example, one

of the effects of the positive hydrophobic mismatch can be observed when hydrophobic thickness of the lipid bilayer is shorter than the transmembrane peptide hydrophobic length (*19*).

The pLeu transmembrane peptide used in London's lab has been extensively studied by fluorescence quenching methods. The studies include both the modification of peptides and changes in lipid compositions. They were able to determine the transmembrane and non-transmembrane states (*24*) of the peptide by using various hydrophobic lengths of the peptide (*25-27*), incorporating ionizable residues with the peptide at different pH (*28, 29*), and replacing different types of charged amino acid residues on the flanking position (*30, 31*).

Table 1.1 Sequences of selected transmembrane peptides designated to study hydrophobic matching effects.[a]

Analogue	N-terminal residues	Central stretch	C-terminal residues
KALP23	Ac-GKK	$(LA)_8L$	KKA-Am
KALP31	Ac-GKK	$(LA)_{12}L$	KKA-Am
WALP23	Ac-GWW	$(LA)_8L$	WWA-Am
WALP27	Ac-GWW	$(LA)_{10}L$	WWA-Am
pLeu19	Ac-KK	GL_9WL_9	KKA-Am

[a]Note that for WALPn and KALPn family, n corresponds to the total number of residues. This table is adapted from Killian, J.A. et al. (*19*).

Intrinsic proteins interact with the surrounding lipid via a range of interactions, including hydrophobic interactions, electrostatic interactions, hydrogen bonding, and dipolar interactions with the lipid-water interface. These interactions were revealed by available biophysical methods. EPR and ssNMR were used to assess polypeptide dynamics, topology, and interactions. CD and IR were utilized to monitor protein conformational dynamics and topologies on a picosecond time scale. ITC was used to quantitatively study the thermodynamics of polypeptide and membrane association. Fluorescence spectroscopy was used to assess the extent of membrane penetration (*13*).

The membrane-spanning regions of intrinsic proteins are divided into two categories: (i) a central hydrophobic region, which interacts with lipid hydrocarbons, and (ii) polar residues, which flank the surfaces of the bilayer and interact with the lipid-aqueous interfacial regions. Polar residues including proline, asparagine and serine are typically found on the N-terminus of

known membrane proteins (*21*). Hydrophobic residues including isoleucine, leucine, valine and alanine are commonly found in the transmembrane region of the integral membrane protein (*16, 19*). At the surface of the membrane, aromatic or charged amino acids including tryptophan, tyrosine, lysine, and arginine are typically found in known integral membrane proteins (*14*). Modification of transmembrane peptides in various lipid compositions may lead to the discovery of novel lipid-protein interactions. Experimental results gained from utilizing a simple model system can provide a more concrete picture of peptide-lipid interactions, and can provide further insight into the fundamental mechanism of protein-lipid interactions in more complex systems.

Unlike integral membrane proteins which are firmly associated with lipids, peripheral membrane proteins are water-soluble and only temporarily interact with membrane lipids. Research has shown that peripheral proteins regulate intrinsic membrane bound proteins by tethering them onto intracellular structures, and limiting their mobility (*1*). Peripheral proteins are also defined as "non-permanent membrane proteins". Non-permanent membrane protein can reversibly and irreversibly interact with the membrane. Membrane proteins that interact reversibly with lipids usually access their substrates from the membrane, for example, lipid transfer enzymes. Irreversible membrane bound proteins are usually not encoded by the cell's genome, and are instead from a parasite or any foreign organism. After insertion into the membranes, the foreign protein products can behave like integral proteins (*32*). Non-permanent membrane proteins can also be defined by the strength of the interactions. The interactions involved in weak association of proteins with membranes are hydrophobic interactions, electrostatic, or polar forces (*32*).

Location of peripheral membrane proteins can be arbitrarily categorized into three classes (*33*) (Figure 1.4): 1) S-type proteins which are usually localized on the membrane surface, and interact predominantly with polar headgroups, 2) I-type proteins which penetrate significantly into the interfacial region, mainly to the level of phosphate headgroups, and 3) H-type proteins which can penetrate into the hydrocarbon core region of the lipid bilayer.

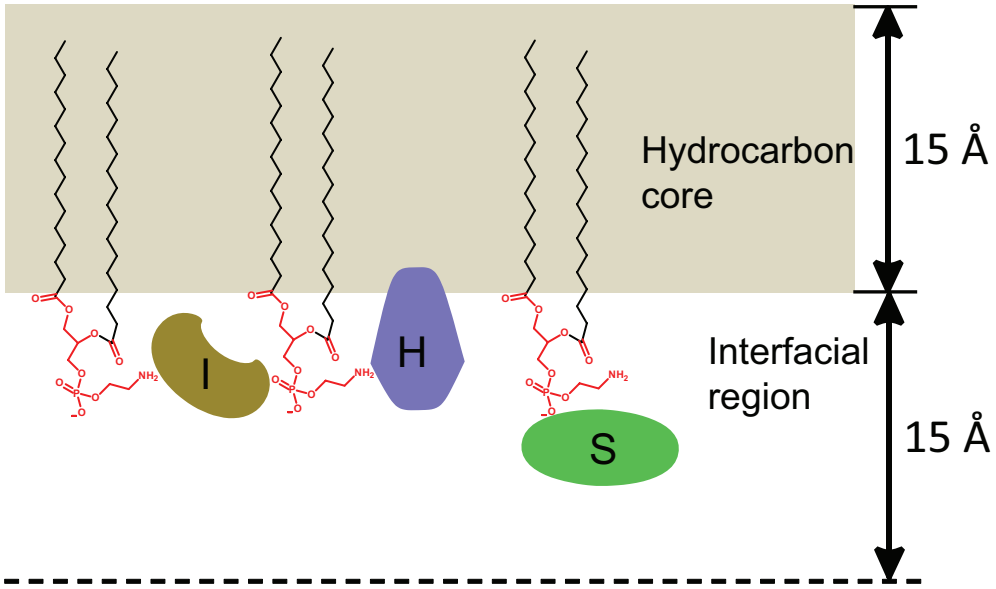

Figure 1.4 Structural representation of the phospholipid bilayer and the membrane location of three classes of peripheral membrane proteins.
The bilayer is comprised of a hydrophobic core and an interfacial region with approximately equal thickness. H-type and I-type proteins penetrate into the interfacial regions, whereas S-type protein localizes on the surface of the interfacial region. Phospholipid headgroups are colored in red. This figure was adapted from Cho and Stahelin, (*33*) and was made with Adobe Illustrator CS3.

Here, we focus on the interaction between peripheral membrane proteins and membrane lipids. Most membrane-bound enzymes access their substrate partitioned between the interface of lipids and the aqueous phase, and it is classified into two fundamental mechanisms: interfacial and non-interfacial (*34*). For interfacial enzymes, binding to the membrane is required in order for the substrate to interact with the protein's active site. In contrast, non-interfacial enzymes acquire their substrates from the aqueous environment, i.e. water-soluble substances.

Two types of enzymatic processes for interfacial enzymes should be considered: "interfacial" (IF) and "interfacial with interfacial activation" (IFA). In these two processes, binding to the membrane interface is required (*35*). In the IF process, the enzyme binds to the membrane lipids, facilitating the translocation of the substrate to the protein active site. In an IF + IFA process, the enzyme binds to the membrane, causing an allosteric activation of the enzyme before the substrate can enter the active site. It is important to understand the biophysical steps involved in interfacial recognition and association. Peripheral membrane proteins bind to the

lipid bilayer via hydrophobic interactions (*36*), electrostatic or ionic interactions (*33, 37*), and covalent bonding of the protein with membrane lipids (*38*) (Figure 1.5).

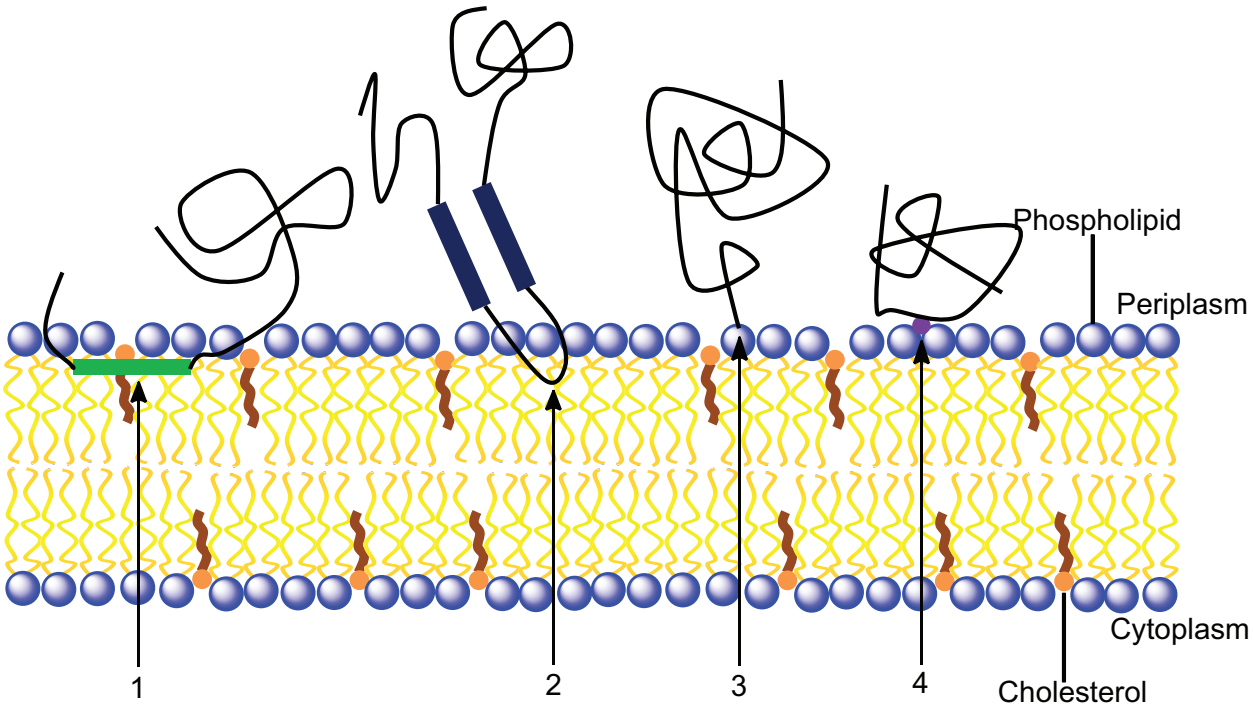

Figure 1.5 Schematic representation of the different types of peripheral protein-membrane interactions.
Interaction of an α-helix parallel to the membrane surface; 2) Interaction of a protein hydrophobic loop with lipids; 3) Covalent bond between protein and membrane lipids; 4) Electrostatic or ionic interaction of protein with membrane lipids, e.g. via Ca^{2+} ions. This figure was adapted from Nelson, D.L. and Cox, M.M, Lehninger Principles of Biochemistry (*1*), and was made with Adobe Illustrator CS3.

Studies of subcellular protein targeting have shown that localization to different cell compartments is induced by protein-lipid interactions, and in some cases, involves lipid ligand binding to the cell membrane (*8*). Efforts have been made to study the membrane-binding domains of these enzymes with different biophysical techniques, for example, NMR, EPR or X-ray crystallography (*8*). The C2 domains of protein kinase C (PKC) and cytosolic phospholipase A_2s (cPLA2) have been extensively studied. The C2 domain consists of about 120 residues and was discovered in the conserved sequence motif of Ca^{2+}-dependent PKCs (*8*). The binding site of the C2 domain was revealed by scanning mutagenesis and surface pressure measurements on PKCα (*39*) and $cPLA_2$ (*40*). It was shown that the concave face of C2 faces the lipid bilayer. Similar results were found by NMR and EPR experiments on cPLA2s (*41, 42*).

Another well studied interfacial enzyme is phospholipase A_2 (PLA2) in both its intracellular and secreted forms. PLA2 catalyzes the hydrolysis of the *sn*-2 fatty acid chain of dialkyl glycerophospholipid (Scheme 2.1). Soluble protein PLA2 binds to lipids on the membrane interface *i*-face, which results in activation of enzyme and substrate. The catalysis reaction then proceeds, and the product is released for the next catalytic cycle (*35*) (Figure 1.6). The binding surface "*i*-face" of PLA2 has been extensively studied. It is shown that binding of *i*-face to the lipid is crucial for protein function. The initial structure of PLA2 showed that the interfacial binding surface, *i*-face, is a flat surface near the active site. This flat region contains about 20 amino acid residues with a surface of about 1500 $Å^2$ (*43*). The *i*-face of PLA2 contains two or more cationic lysine or arginine residues, which can bind tightly to anionic phospholipids rather than zwitterionic phospholipids. This phenomenon indicates the interaction of interfacial binding is guided by electrostatic forces (*44*). However, aromatic residues, particularly tryptophan, have recently also been found to contribute to interfacial binding for some of the PLA2 family members. These proteins have one or more tryptophan(s) on their *i*-faces. Site-directed spin labeling (EPR) demonstrates that the binding surface of PLA2 sits on the membrane rather than penetrates into the lipid bilayers (*45*).

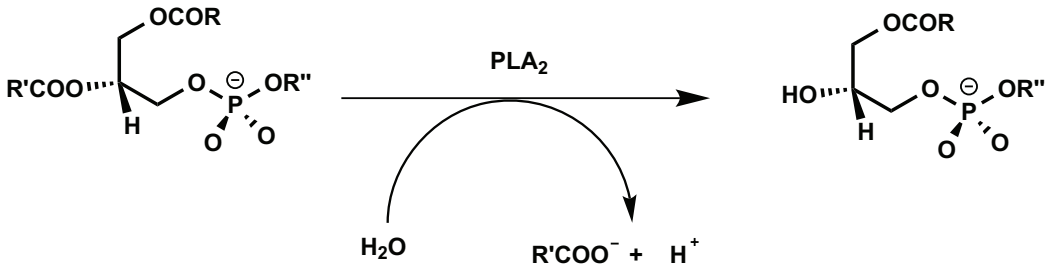

Scheme 1.1 The reaction catalyzed by phospholipase A_2.

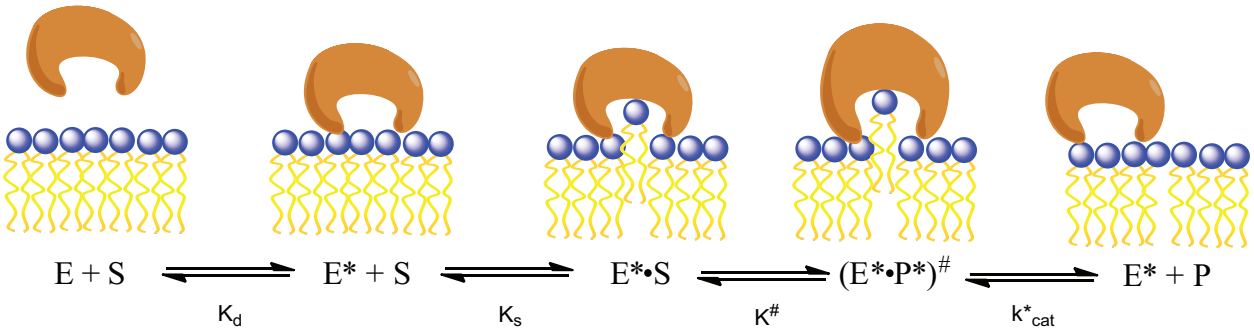

Figure 1.6 Interfacial catalysis of phospholipase A_2 (PLA2).
Key features of catalysis of PLA2. PLA2 catalyzes the formation of the enzyme-product complex once it is activated at the membrane interface. After releasing the product, the enzyme can diffuse to bind substrate and continue the turnover for next cycle. E: free enzyme in aqueous state; E*: Enzyme bound to the membrane surface; E*•S: enzyme-substrate complex of the interface bound form; $(E^*\bullet P^*)^{\#}$: additional anion activation step. This figure was adapted from Winget, Pan, and Bahnson, (*35*) and was made with Adobe Illustrator CS3.

Many important cellular processes are triggered and regulated in part by interactions between proteins and membranes, including signal transduction (*8*), inflammation (*46*), and membrane trafficking (*47-50*), so obtaining accurate structural information of membrane-docked proteins will be indispensible for elucidating the mechanism of these aforementioned biological functions. Conventional methods for studying membrane-proteins are available, e.g. EPR (*51-53*), NMR (*54-57*), fluorescence spectroscopy (*58-60*), H/D exchange (*61, 62*), and computational simulations (*63-66*). These methods are powerful tools for specific parts of the protein-lipid interactions, and they have advantages and limitations. More information about these methods will be discussed in the next section.

1.5 Current approaches for investigating protein-lipid interactions

Interfacial enzymes play important biological roles in signal transduction and lipid trafficking at the membrane interface. Due to the water-soluble nature of most interfacial enzymes, high-resolution crystal structures for these enzymes are readily available, but not in a lipid-bound state (*51*). The information gathered from crystallographic data does not provide dynamic details about changes in structural information due to protein-lipid interactions. Structural or dynamic descriptions of a membrane-bound state of the protein are essential for mechanistic studies. To understand the ensemble of protein at the membrane interface is still a considerable challenge for structural biology. Several approaches are currently available to investigate lipid-protein interactions, e.g. EPR, fluorescence spectroscopy, NMR, H/D exchange, and simulations.

1.5.1 Electron paramagnetic resonance (EPR)

The electron paramagnetic resonance (EPR) spectroscopy method (*67*) is one of the most powerful tools for determining membrane-docking protein structures. The EPR method reveals the insertion depth of a membrane-docking protein, and the angle of docked protein relative to the membrane surface. This approach utilizes a site-directed spin labeling and power saturation EPR method on the protein of interest. A nitroxide spin label probe is carefully introduced to selected sites on a single cysteine residue mutation on the enzyme surface via disulfide exchange or specific thiol-reactive iodoacetamido or maleimido groups (*68*). This method requires the removal of all native cysteine residues and the introduction of a single cysteine mutation for spin labeling.

To determine the depth of the spin labeled protein into the membrane, the rate of collision with extrinsic paramagnetic probes residing in the membrane or in the aqueous environment is monitored. These paramagnetic probes include molecular oxygen residing in the membrane, or nickel (II) ethylenediaminediacetic acid (NiEDDA) residing in the aqueous environments. These paramagnetic probes are utilized based on their apolar (O_2) and polar (NiEDDA) properties, respectively. With the wealth of information obtained from a library of spin labeling sites, typically 20 to 30 sites, the model of membrane-docking geometry and angular orientation relative to membrane surface can be created.

This method requires a small amount of protein (~ 1 nmol), and can be carried out at physiological temperature and various ionic buffer conditions. The EPR membrane depth experiment provides one of the most detailed molecular structures of protein membrane-docking geometry (*51*). However, there are still some limitations that should be taken into consideration. First, the local motion of the spin label should not be neglected. Second, preliminary structure information of a protein is required in order to carefully introduce cysteine mutation to the proper site on the protein surface. Third, since only a single cysteine can be introduced at a time, all native cysteine residues need to be removed, which may affect protein function and activity. Fourth, the uneven distribution of concentration gradients of the paramagnetic probe in the buffer and the membrane interface in depth measurement might complicate spectrum interpretation.

The binding structure of the C2 domain of some peripheral proteins, e.g. cytosolic phospholipase A_2 (cPLA2) (*69*), synaptotagmin I (SytIA) (*70*), and protein kinase Cα (PKCα) (*71*) are revealed from this EPR method, and the results from different proteins studied are consistent with similar functionalities. In addition, EPR can also be used to measure distance between pairs of two spin labels in one protein to provide a model of domain packing or to monitor structural changes (*53*).

1.5.2 Fluorescence spectroscopy

Fluorescence spectroscopy has proved to be useful in elucidating the organization, topology and orientation of membrane proteins. Fluorescence spectroscopy utilizes the sensitivity of a fluorophore, such as an intrinsic tryptophan or a fluorescent probe attached to the protein of interest, to the environmental polarity. Introduction of these fluorophores into a hydrophobic environment, such as the membrane, causes a shift of emission λ_{max} and the emission quantum yield. This approach can be employed in fluorescence quenching studies of membrane proteins to derive penetration depths of membrane-bound residues.

Fluorescence spectroscopy is a useful tool to map the membrane-binding region of a membrane protein. Multiple single-cysteine mutants are created and modified with a thiol-reactive fluorescein probe at the predicted membrane docking region. Fluorescein has the ability to serve as probe to monitor local environmental conditions by using fluorescence quenching. The mechanism of fluorescence quenching occurring in membranes is classified to be static due to slow lateral diffusion of membrane components. The docking of proteins to the membrane is

determined by the collisional encounter of fluorescein and the quencher iodide ion in the solution. Iodide is capable of efficiently quenching fluorescein emission, it is relatively impermeable to proteins and membranes, and is a good quencher to determine protein surface accessibility to lipid membranes. The fluorescence quencher method is used to determine the accessibility of fluorescein on the protein surface or the location of the probe embedded in model membranes. This method provides functional and spectroscopic information to map out the region of protein and membrane contacts. A well-developed fluorescence method to determine the depth of membrane insertion is parallax quenching (*25, 58, 59*), this measurement is based on the quenching of a tryptophan or an attached fluorophore, e.g. acrylodan (*60*), with the quencher, usually a spin label in the membrane. The protein insertion depth is obtained by fluorescence quenching of the spin label at different locations in phospholipids, such as the headgroup or hydrocarbon chain.

The location of the membrane-docking face of the C2 domain of cytosolic phospholipase A_2 was determined by Nalefski, E.A. et al. (*72*). Single cysteine mutations were introduced on the protein surface of the $cPLA_2$ C2 domain to generate 16 mutants, and structural integrity was tested for all mutants. Tryptophan fluorescence was used to determine protein-membrane docking after single cysteine substitution, and the results were comparable to wild-type protein. A fluorescein fluorophore was subsequently conjugated to the cysteine for the fluorescence quenching experiments with iodide. The fluorescence quenching results for all mutants was used to reveal the membrane docking region. This region for targeting membrane protein docking is initiated by binding of multiple calcium ions to a conserved residue segment with variable Ca^{2+}-binding loops. The fluorescence method was able to identify a localized region that is altered by Ca^{2+}-binding and membrane docking (*72*).

Like EPR, the fluorescence method also has similar limitations, multiple single site mutants need to be created, prior structural knowledge is preferred for mutation site selection, and the local motions of the relatively large probe should not be ignored.

1.5.3 Solid-state nuclear magnetic resonance (SS-NMR)

The use of NMR has had a tremendous impact on the study of proteins. NMR has been used to study functional conformational changes, lipid interactions, substrate-lipid interactions, substrate-protein interactions, protein oligomerization states, and the overall dynamics of

membrane transporters (*67*). This method relies on detection of NMR-active nuclei, such as ^{1}H, ^{13}C, ^{15}N, ^{19}F, or ^{31}P. NMR experiments with macromolecules such as proteins often require isotopically labeled ^{13}C, ^{15}N, or ^{2}H for aiding spectral assignments and enhancement of spectral resolution. Solution NMR is a useful tool in structural biology as well (*42, 55, 57*). However, long rotational correlation times cause line broadening, and thus limit the size of the complex of interest in this method to mostly less than 20 kDa (*57*).

Solid-state nuclear magnetic resonance (SS-NMR) (*54, 56, 57, 67, 73*) has increasingly been applied to study protein-membrane dynamics and the conformation of individual amino acid residues under conditions mimicking physiological environments. SS-NMR was used to investigate the interaction of the pleckstrin homology (PH) domain for the phospholipase C-δ1 with a model membrane (*74*). Tuzi, S. et al. selectively incorporated ^{13}C isotopes to alanine residues predicted to interact with membrane lipid for NMR acquisition. The results clearly showed that a conformational change was induced by localization of domain binding at the surface of PtdCho/PtdIns(4,5)P_2 vesicles.

Though beneficial, the study of proteins by NMR has some limitations. Due to the large size of proteins, reorientation of the complex is a slow process. High-resolution spectra are difficult to obtain for those proteins that are large, aggregated, or incorporated into supramolecular assemblies. NMR is relatively insensitive, so large protein quantity (ranging from micromoles to millimoles) is required. In addition, this method does not provide direct evidence regarding the depth of protein insertion into the membranes (*51*).

1.5.4 Hydrogen/deuterium (H/D) exchange

Deuterium exchange, is also a valuable tool to study protein dynamics (*75*). This approach is usually coupled with mass spectrometry to provide information regarding protein conformational changes during catalysis or membrane binding.

The exchange of amide hydrogens with deuterium in the presence of D_2O makes this method especially powerful to probe protein dynamic changes. The amide hydrogen on the polypeptide backbone can differentially exchange with deuterium. The rate of H/D exchange in the presence or absence of lipid membranes can be compared in order to predict if a protein-lipid interaction is occurring. Samples are then proteolyzed and analyzed by mass spectrometry in a

time course manner (*61, 62*). This method is able to determine the orientation of protein contacts on the membrane surface, and offers single amino acid resolution (*75*).

Burke, J.E. et al. utilized this method in studying group IA phospholipase A_2, which was highly disulfide bonded, with model membrane. The results showed that the two α-helical with 4 disulfide bond regions exhibited slow rates of exchange with deuterium. It was proposed that the rigidity of these two α-helices arose from the disulfide bond, and the *i*-face contacting area also showed decreasing rates of exchange (*61*).

1.5.5 Molecular dynamic (MD) simulation

With the emerging importance of computational biology, the use of molecular simulations (MD) to study protein-lipid interactions has grown in recent years (*63-66, 76*). This calculation approach is an alternative to experimental studies. Simulation methods can often provide much more atomic and dynamic details regarding protein-lipid interactions. The information gained from MD simulations primarily concerns the orientation and depth of protein insertion into lipid bilayers at the molecular level (*63, 77*). Coarse-grained molecular dynamics (CG-MD) simulations, initially developed for lipids, have been recently applied to integral or monotopic membrane proteins for determining protein structures (*77*). These predictions via calculations often require additional experimental biophysical constraints, such as EPR membrane penetration measurement or crystal structures, for more accurate results.

The finite difference Poisson-Boltzmann (FDPB) method is another simulation approach widely used to describe electrostatic properties of proteins, nucleic acids, and membranes (*37, 78, 79*). This method particularly focuses on the electrostatic forces between the charged residues on proteins and headgroups of the lipids. It reveals how electrostatic interactions drive the membrane association of basic proteins for more efficient catalysis. This method has been applied to study the FYVE membrane binding domain (*79*), and the membrane association of group IIA secreted phospholipase A_2 (*78*). Future simulations will extend to examine the importance of lipid mixtures, especially cholesterol which controls lipid bilayer fluidity, adaptability, and protein specificity on the interfacial surface of membranes (*65*).

1.6 Cholesterol oxidase as a model enzyme to study interfacial protein-lipid interactions

1.6.1 Introduction and applications of cholesterol oxidase

Cholesterol oxidase is a water-soluble enzyme that is isolated from a variety of microorganisms. Cholesterol oxidase is a flavoenzyme that catalyzes the oxidation and isomerization of cholesterol to cholest-4-en-3-one via the intermediate cholest-5-en-3-one. The cofactor flavin adenine dinucleotide (FAD) is required for the oxidation of the cholesterol. The reduced cofactor is subsequently oxidized by molecular oxygen, to produce hydrogen peroxide (Scheme 1.2) (*80-82*).

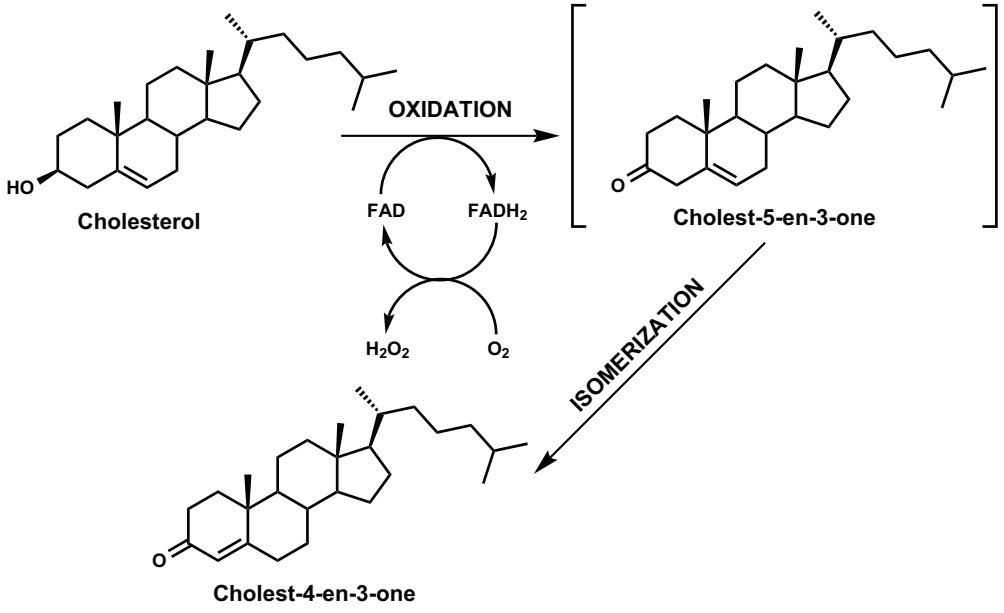

Scheme 1.2 The reaction catalyzed by cholesterol oxidase.
Cholesterol is first oxidized to cholest-5-en-3-one accompanying with FAD being reduced to $FADH_2$. $FADH_2$ is subsequently oxidized by molecular O_2 to FAD with formation of H_2O_2. Cholest-5-en-3-one is then undergoing isomerization to form cholest-4-en-3-one.

Cholesterol oxidase from bacteria was first found and isolated from *Nocardia erythropolis* in 1944 (*83-85*). Cholesterol oxidase is used in clinical laboratories to detect the total serum cholesterol level in the diagnosis of arteriosclerosis and other lipid disorders, which are among leading causes of death in the United States (*86-88*). The cholesterol oxidase assay is coupled to cholesterol esterase and peroxidase to determine total serum cholesterol level. The esterase is first incubated with serum in order to produce free cholesterol, since up to 70% of

cholesterol is esterified in blood serum. Cholesterol is then oxidized by cholesterol oxidase coupled with FAD cofactor, which is reduced during the oxidation step. The FAD is regenerated by the reduction of molecular oxygen to hydrogen peroxide (Scheme 1.1). A peroxidase reduces the hydrogen peroxide upon oxidation of an indicator molecule. A stable colored complex is formed that is quantitatively detected by absorption spectrometry. In this way, determination of total serum cholesterol is performed by cholesterol oxidase.

Cholesterol oxidase was also one of the earliest probes used to track cell cholesterol. The heterogeneity of cell membranes and the distribution of cholesterol in the plasma membrane has been determined (*89, 90*). The investigation of the dependence of cholesterol activity on the lipid phase by different lipid compositions also gives a better way of detecting microdomains in cellular membranes (*91*).

1.6.2 Structures and mechanism of Type I and Type II cholesterol oxidase

There are two types of cholesterol oxidase, Type I and Type II, (Figure 1.7) and they are classified according to their structure homologies. Although there are two types of enzymes, their catalytic reactions are the same, oxidation followed by isomerization. Type I cholesterol oxidase has a FAD cofactor non-covalently bound to the enzyme. Cholesterol oxidase is a monomeric 55 kDa protein with 509 amino acid residues. The three-dimensional crystal structure of Type I cholesterol oxidase has been solved from *Streptomyces sp.* SA-COO (*92*) and *Rhodococcus equi* (*93-95*). The crystal structure of Type II cholesterol oxidase from *Brevibacterium* BCO2 was also solved in 2001 (*96*).

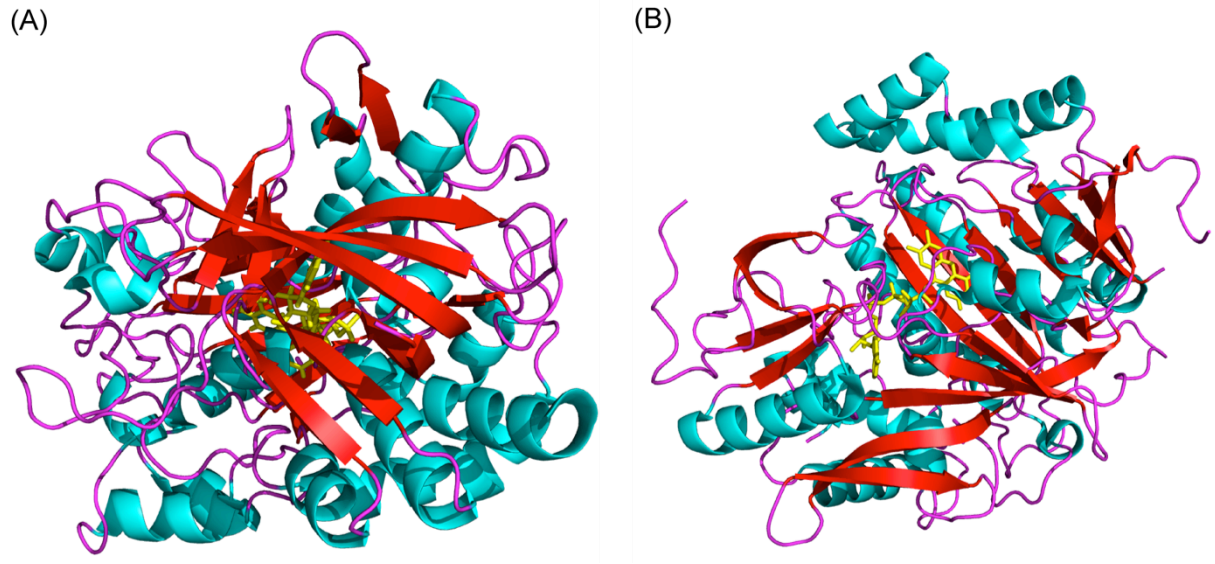

Figure 1.7 Crystal structure representations of cholesterol oxidase.
(A) Type I cholesterol oxidase (from *Streptomyces*, PDB entry 1MXT) (*92*). (B) Type II cholesterol oxidase (from *Brevibacterium* BCO2, PDB entry 1I19) (*96*). The substrate-binding cavity is deeply buried. The FAD cofactor is shown in ball-and-stick model and is colored in yellow for both structures. Cholesterol oxidases are colored based on secondary structures, α-helices in cyan, β-sheets in red, and coils in purple.

The enzymes are members of the GMC (glucose-methanol-choline) oxidoreductase family. A FAD cofactor that is non-covalently bound to type I cholesterol oxidase is required for oxidation. The conserved site for catalysis of cholesterol oxidase was revealed by crystallographic structures (*92-95*). Sequences and structural alignment of the active site revealed that there is complete conservation of His447 within the GMC oxidoreductase family (*94*). Using site-directed mutagenesis (*81, 97-100*) and X-ray crystallography (*92-95*), it has been shown that His447, Glu361, and Asn485 are the key residues for substrate positioning, oxidation, and isomerization in the active site. Glu361 acts as a general base for isomerization (*81, 97*), and His447 is proposed to orient the substrate with respect to the FAD cofactor. The Nε2 atom of His447 acts as a hydrogen bond donor rather than acceptor (*92*). Asn485 plays an important role in substrate oxidation by creating electrostatic potential around the FAD cofactor, hence enhancing the oxidation reaction through an N-H…π electrostatic interaction during the reaction (*100*). A bound water molecule, Wat541, has proven to occupy the position of the steroid substrate hydroxyl group in a sub-angstrom resolution (0.95 Å) crystal structure from *Streptomyces* enzyme (*92*).

Type II cholesterol from *Brevibacterium sterolicum* (BCO2) is structurally distinct from Type I cholesterol oxidase. In Type II cholesterol oxidase, the FAD cofactor is covalently bound to the enzyme via a histidine residue, His121. The X-ray crystal structure was also solved for the *Brevibacterium* BCO2 enzyme. Type II cholesterol oxidase has more hydrophilic residues than Type I enzyme. Four glutamate residues (Glu475, Glu551, Glu432, and Glu311), one arginine (Arg477), one lysine (Lys554), and one asparagine (Asn516) form a cavity in the active site around the pyrimidine region of Type II cholesterol oxidase (*101*). In the Type I enzyme, there are only three polar residues, Glu361, His447, and Asn485 in the active site. The midpoint reduction potential for the Type II enzyme is -101 mV (*102*), and that for Type I enzyme is -278 mV (*100*). The data show that Type II cholesterol oxidase is a better oxidizing agent than the Type I enzyme.

1.6.3 Interactions between cholesterol oxidase and lipid bilayer

The present study will focus on a Type I enzyme from *Streptomyces sp.* SA-COO, ChoA. Cholesterol oxidase is a water-soluble interfacial enzyme that is transiently associated with the membrane during the catalytic reaction.

Cholesterol oxidase is catalytically active at the membrane surface where the enzyme abstracts its hydrophobic substrate, cholesterol. Despite the wealth of information from kinetic studies (*60, 91, 97, 98*), mutagenesis (*81, 86, 99*), and X-ray crystal structures (*92, 95*) of cholesterol oxidase, the interfacial interaction between this enzyme and membrane lipids is still unclear. The catalytic turnover rate of cholesterol oxidase in the presence of membrane containing cholesterol is 5 orders of magnitude faster than the rate of cholesterol desorbing from the membrane (2×10^{-5} s^{-1} (*103*) vs. 24 s^{-1} (*104*)). This phenomenon means that cholesterol is embedded in lipid bilayers instead of dispersed in the aqueous phase. As a result cholesterol oxidase must interact to bind to the membrane in order to acquire cholesterol (*60, 104*).

The crystal structures of native cholesterol oxidase co-crystallized with substrate analogue, dehydroepiandrosterone (DHEA) (Figure 1.8 C), from *Rhodococcus equi* reveals that the active site of the protein is deeply buried and sequestered from the aqueous environment (*93, 94*) (Figure 1.8 A & B). It was proposed that the substrate-binding site was capped by two substrate-binding loops, loop 1 (residues 73-86) and loop 2 (residues 432-438) (*60, 95*). The poor electron density in the crystal structure of *Rhodococcus equi* enzyme means that these loops

are more flexible (*95*), and are able to be open and close during the course of substrate catalysis. The two loops on cholesterol oxidase are also proposed to form hydrophobic pathways between the active site of the protein and the lipid bilayer for access of cholesterol (*60, 104*).

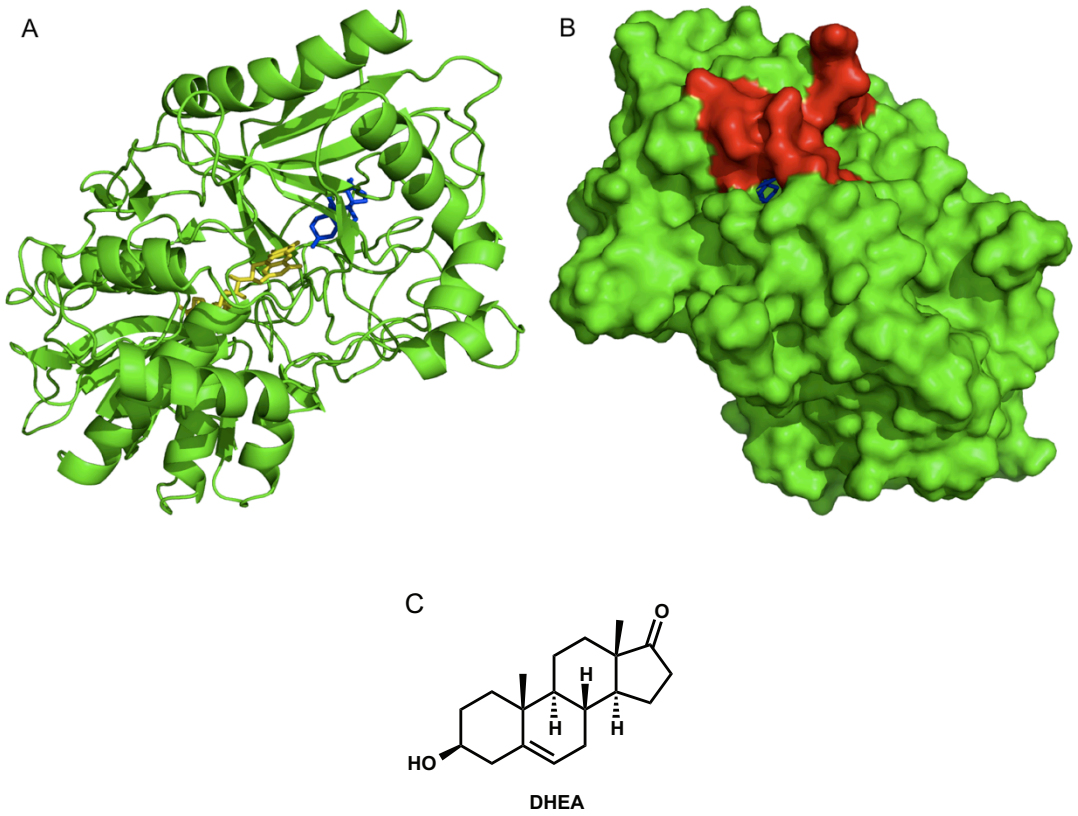

Figure 1.8 The overall structure of the complex of *Rhodococcus equi* cholesterol oxidase co-crystallized with dehydroepiandrosterone (DHEA).
(A) The structure shows DHEA is deeply buried in the binding cavity. The FAD cofactor is shown in stick model and is colored in yellow. DHEA is shown in ball-and-stick model and is blue-colored. (B) The surface structure of this enzyme shows DHEA, which is colored in blue, is completely separated from the bulk solvent. The two loops (residues 73-86 and residues 432-438) are shown in red. (C) The structure of dehydroepiandrosteron (DHEA). Cholesterol oxidase structure is from *Rhodococcus equi*. (PDB entry 1COY).

Truncated loop ($\Delta^{79\text{-}83}$) studies on *Streptomyces* cholesterol oxidase showed reduced substrate specificity compared to the wild-type enzyme (*104*). Interestingly, the DHEA specificity for the truncated mutant increased relative to wild-type enzyme, suggesting that the deletion of the looplet residues is required for packing the "tail" of cholesterol. Previous studies

employed labeling *Rhodococcus equi* enzyme with an acrylodan fluorophore on loop 73-86 (M81C-acrylodan) fluorescence spectroscopy analysis showed that the loop interacted with lipid headgroups but did not penetrate the bilayer (*60*). The acrylodan-labeled cholesterol oxidase in the fluorescence binding studies was also used to investigate the pH, ionic strength, and lipid headgroup effects on binding. These experiments suggested that the primary protein-lipid interaction was driven by hydrophobic forces, not ionic forces (*60*).

NMR analysis was also conducted on wild-type cholesterol oxidase metabolically labeled with an ^{15}N isotope (*105*). The heteronuclear single quantum coherence (HSQC) NMR spectra of wild-type cholesterol oxidase in the presence and absence of lipid vesicles (POPC/cholesterol) were obtained (Figure 1.9). The stacked HSQC spectra show shifts in peaks when cholesterol oxidase is in solution or interacts with membranes. The shift in peaks could represent two phenomena; (i) the shifted peaks could represent the binding site of the enzyme or (ii) a conformational change in protein structure has occurred as a result of lipid binding. This finding is evidence that cholesterol oxidase interacts with membrane.

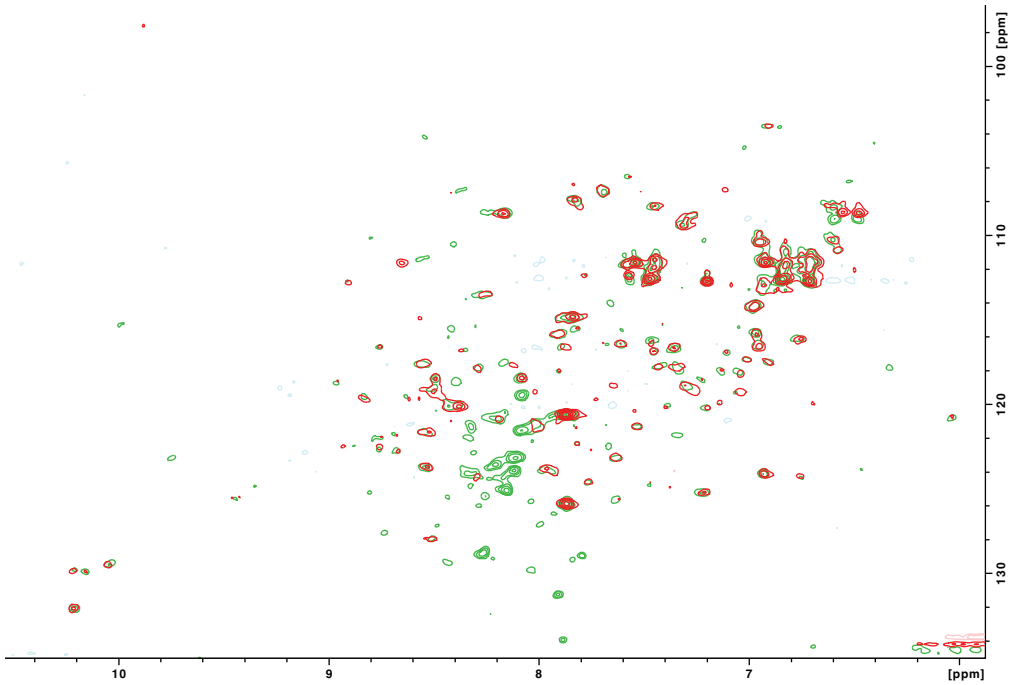

Figure 1.9 Stacked ^{1}H-^{15}N HSQC (700 MHz) NMR spectra of wild-type cholesterol oxidase in the presence and absence of vesicles (100 nm LUV, POPC/Cholesterol = 7/3).
Green lines are wild-type cholesterol oxidase (160 μM) resonances only, and red lines are resonances of wild-type cholesterol oxidase (120 μM) with lipid vesicles (500 μM). This figure was adapted from Ghang's thesis (*105*).

Although X-ray crystal structures of this enzyme with substrate analogues have been solved (*94*), crystal structures of cholesterol oxidase bound to cholesterol or interacting with the lipid bilayer are still not available. No direct evidence exists to show how the enzyme interacts with lipid bilayers, and other approaches should be developed to achieve this goal. From all the available experimental data, we postulate a working model of cholesterol oxidase interacting with the lipid bilayer (*106, 107*) (Figure 1.10). In this proposed model, cholesterol oxidase is likely to undergo a conformational change, and then closely approaches to the membrane surface to form a pathway to allow cholesterol to enter the active site. The enzyme oxidizes and isomerizes the substrate in the active site. After catalysis, the product is released to the bulk solution or the lipid bilayer, and the protein reverts to its original structure when leaving the lipid bilayer. During the catalytic process, the protein must alternate between an open and closed conformation in order to accept or release the substrate product. Since the crystal structure reveals that the FAD cofactor and DHEA are deeply buried in the protein active site cavity, the

extent to which the enzyme interacts with the membrane is still not well understood, and it is necessary to develop a novel method to address this question.

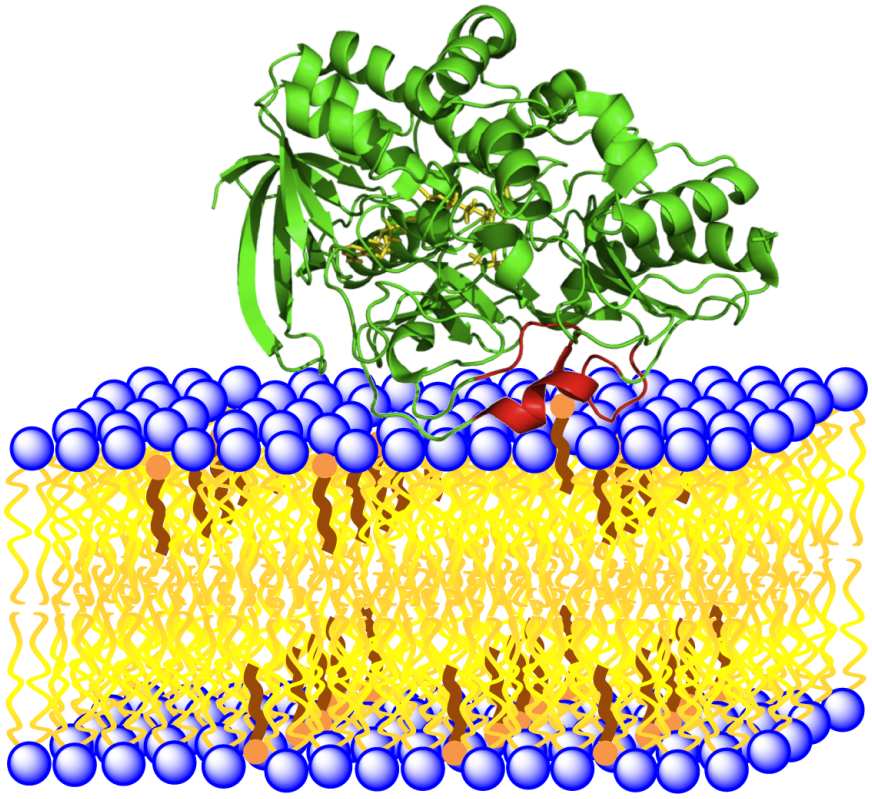

Figure 1.10 Proposed working model of how cholesterol oxidase interacts with the lipid bilayer. This model is to propose what is the orientation of the protein interacting with lipid membrane (*91*). Cholesterol oxidase (PDB entry 1MXT) is shown in green, FAD is shown in ball-and-stick model and is colored in yellow, and the two loops (73-86 and 432-438) are color in red. Cholesterol is shown with a head and a tail to represent the hydroxyl and hydrocarbon core respectively.

1.7 Protein bioconjugation, mass spectrometry, and stable isotope tagging in quantitative proteomics

1.7.1 Protein bioconjugation

NMR and X-ray crystallography are useful tools to obtain high resolution structural information in current research. Not all protein systems are amenable to analysis with these techniques because of size, aggregation, conformational flexibility or the amount of sample. Modification of specific functionalities on the macromolecules of interest combined with mass spectrometry is an attractive alternative (*108*).

Bioconjugation and modification techniques depend on two major related chemical properties: the reactive functionalities of the various derivatizing reagents and the functional groups on the target macromolecules to be modified. These techniques aim for analyzing specific targets including peptides, proteins, carbohydrates, lipids, nucleic acids, and oligonucleotides. Choosing the correct system of reactive groups leads to successful modifications. However, these modifications still rely on the availability of derivatizing reagents. An extensive understanding of the structure and reactivity of the target macromolecules leads to successful use of the all available modification techniques (*109*).

Bioconjugation reactions exploit the intrinsic or extrinsic chemical reactivity of macromolecules. For example, in proteins, intrinsic bioconjugation comes from the reactivity of natural amino acids, i.e. lysine, cysteine, glutamate, or tryptophan. Two-step reactions are required for extrinsic bioconjugation. The first step includes the introduction of reactive functionalities such as ketones, aldehydes, azides, alkenes, or alkynes into the target protein via genetic or chemical approaches. The second step involves the modification of the new functional groups to form oximes/hydrazones, Staudinger ligation products, or triazole-click products (*110*). Ideally, the bioconjugation reactions should proceed rapidly, selectively, and in high yields at physiological conditions. The most important concern is to preserve the target protein's biological activity regardless of the approach used.

Protein tagging is widely utilized in proteomics to analyze proteins in complex biological mixtures from a cell or an organism (*111, 112*). The advantage of labeling proteins in such complex systems is to reduce sample complexity and enrichment of the targeting proteins

(peptides). Most of the above protein modification methods can be combined with proteolytic digestion and mass spectrometry-based analysis (*111-114*).

Chemical labeling of natural amino acids is a commonly used modification strategy in proteomics (*111, 112*). Among the twenty natural amino acids, choices are limited to those with reactive side chains. Side chain reactivities of cysteine, lysine and tryptophan are used in thiol alkylation, amidination/guanidination, and modification of the indole system, respectively. Cysteine is probably the most well studied and efficient protein tagging target, as it is relatively rare (1.1%) across seven species (*115*) and it has specificity to a variety of sulfhydryl reagents (*111, 116*).

Here, we focus on cysteine modification. The labeling rates of the cysteine thiols are greatly influenced by their pK_a values, the inherent property of the protein, and by steric effect. Though crystal structure provides valuable information, proteins are dynamic. The crystal structure is only one of the conformations of the protein, and steric effect should also contribute to affect the rate of cysteine labeling (*117*). In aqueous solution, sulfhydryls have a pK_a around 8-9 (*118, 119*), and will be altered by its microenvironments (*118, 120-125*). Many proteins have domains which lower the cysteine thiol pK_a, and as a result the sulfhydryls are predominantly in their thiolate form at physiological pH. The effect of electrostatic interactions between cysteine sulfhydryl on the surface of the protein can change pK_a by ~2 units, and the effect is even larger when cysteine is an active site residue (> 2 units) (*126*). As a result, the reactivity of the cysteine thiols will be greatly affected by their microenvironment. Generally, the cysteine pK_a will be elevated via local electrostatic interactions when cysteine is exposed in a negatively charged environment (*121*). It is also possible that cysteine pK_a is raised to approximately 14 in a non-polar environment, such as the hydrocarbon region of the lipids (*125*).

A variety of sulfhydryl reagents, such as *N*-substituted maleimide-based, *N*-substituted iodoacetamide-based, acrylamide-based, vinyl-based, thiolsulfonate-based, and disulfide-linkage-based, are widely utilized in current proteomic applications (*111, 116, 127*). In aqueous media, the ionized sulfhydryls react with thiol specific reagents 9 orders of magnitude faster than in its un-ionized form at physiological conditions (*128*). The most commonly used cysteine modifiers are iodoacetamide-based and maleimide-based derivatives (Scheme 1.3). These reagents are easy to synthesize and couple to other functional groups, such as fluorophores.

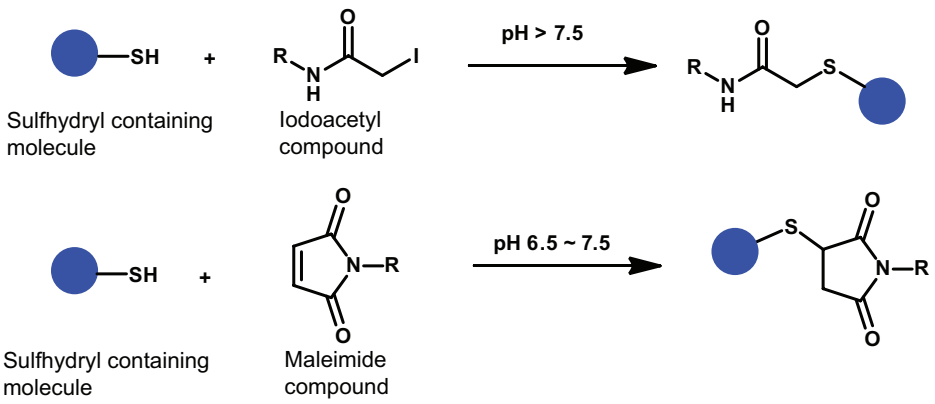

Scheme 1.3 Reaction scheme of sulfhydryl containing molecule with iodoacetyl or maleimide compounds.

In this thesis study, we chose maleimide-based thiol reagents for sulfhydryl bioconjugation, for example, *N*-Ethylmaleimide (NEM). NEM requires smaller molecular quantities of reagent, less reaction time, and is more effective at thiol alkylation at physiological pH compared to iodoacetamide (IAM), which requires a higher pH for alkylation of sulfhydryls. (pH 6.5 – 7.5 for NEM versus pH > 7.5 for IAM) (*129*). Synthesis of maleimide derivatives proceeds from simple starting material (*130*) (Scheme 1.4). In addition to enriching target proteins and reducing sample complexity, cysteine tagging can be used to study membrane protein topology using scanning cysteine accessibility mutagenesis (SCAM) (*120, 131, 132*). In native conditions, transmembrane proteins will undergo various conformational changes in the lipid bilayer or as a result of dynamic interactions with other proteins to achieve their functions. SCAM provides a systematic approach to map the residues on the solvent accessible surface or lipid embedded solvent inaccessible location by using membrane permeable or impermeable thiol-reactive reagents (*120*).

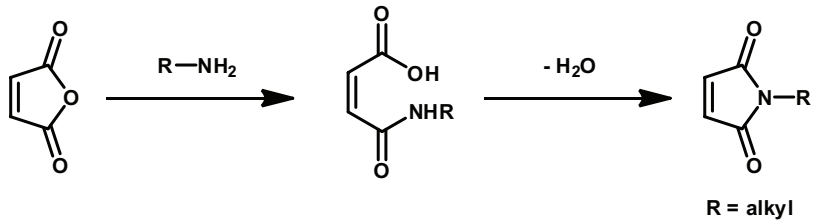

Scheme 1.4 Synthesis of *N*-alkylmaleimides from maleic anhydride with corresponding amine and followed by dehydration of maleamic acid to form *N*-alkylmaleimide.

1.7.2 Mass spectrometry

Mass spectrometry (MS) is an important and well-developed analytical technique with diverse applicability in research. Recent studies of mass spectrometry-based proteomics have been successful, and have identified mass spectroscopy as an indispensable tool for molecular and cellular biology (*113*). Sensitivity, resolution, dynamic range of measuring, and mass accuracy are key parameters for modern MS-based experiments in proteomics research (*133*).

Mass spectrometry is based on the mass-to-charge (m/z) ratios of the analytes, and traditional ionization methods, e.g. electron ionization (EI), chemical ionization (CI), negative chemical ionization (NCI), or atmospheric pressure chemical ionization (APCI), limit the applications of macromolecules in mass spectrometry (*133*). Large (or high molecular weight) molecules are not easily transferred into the gas phase to be ionized. More advanced ionization techniques have been discovered, which can tolerate macromolecules.

Electrospray ionization (ESI) (*134*) and matrix-assisted laser desorption ionization (MALDI) (*135*) are the most widely used soft ionization methods in the biological sciences. (Figure 1.11) The major differences between ESI and MALDI are described as follows: ESI can ionize the analytes out of a solution, and is used for a wide variety of compounds, including proteins, oligonucleotides, sugars, and polar lipids. MALDI ionizes the analytes out of a solid, a dry matrix complex, and can also be applied to a variety of samples, i.e. peptides or proteins. Because the source of the samples is liquid for ESI, it is often coupled to LC-MS (ESI) for protein identification, characterization and sequence analysis in tandem mass system. The mass spectra from both ESI and MALDI methods can be acquired in positive or negative mass-to-charge ratios. Due to different mechanisms of ionization in both methods, ESI is prone to generate multiple charges on analytes, and MALDI usually creates singly charged molecules.

In the following experiments, we exclusively use matrix-assisted laser desorption/ionization time-of-flight (MALDI-TOF) as this ionization method is less susceptible to lipid and detergent interference in comparison to electrospray methods. MALDI also has good mass accuracy, high resolution, excellent sensitivity, and very high throughput capability. In addition, data-interpretation analysis is relatively easy and straightforward. In preparation for MALDI analysis, the analyte is mixed well with the matrix in solution, and co-crystallized on an electrically conducting plate. A short laser pulse is first applied to the sample and the matrix crystal. Energy is absorbed by the matrix, and is subsequently transferred to the analyte. After

this process, the analyte is brought into the gas phase and ionized (Figure 1.11B). The exact mechanism of MALDI-ionization is still not fully understood.

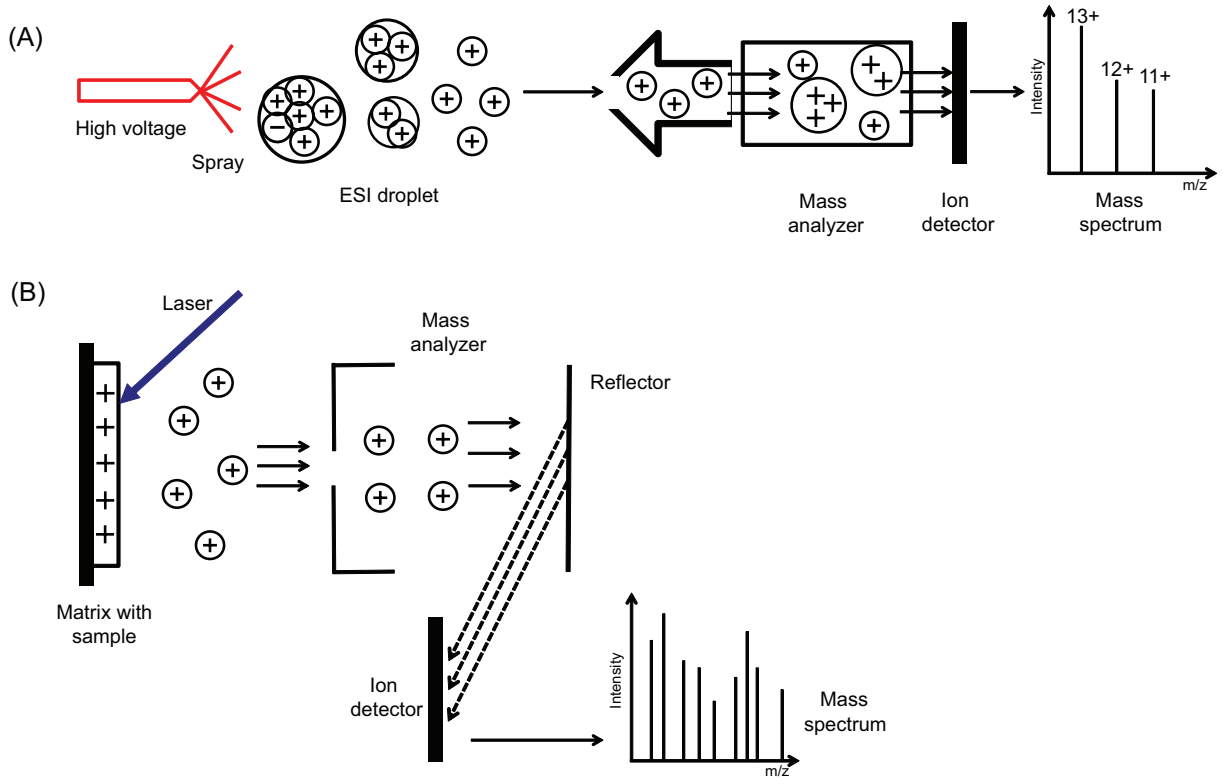

Figure 1.11 MS ionization sources.
(A) Electrospray ionization (ESI). (B) Matrix-assisted laser desorption/ionization (MALDI). This figure was adapted from Sokolowska et al. (*133*), and was made with Adobe Illustrator CS3.

1.7.3 Stable isotope tagging in quantitative proteomics

Besides qualitative protein identification in proteomics, quantitation of proteins is also necessary in order to detect changes in protein profiles which might be able to provide important diagnostics or functional insights (*136*). Currently, three major approaches are used for quantitative protein profiling, two-dimensional gel electrophoresis (2DE) analyzed by mass spectrometry, protein expression array analysis, and stable isotope labeling of protein or peptides analyzed by tandem mass spectrometry (*137*).

Stable isotope labeling is an important tool in modern quantitative proteomics. The general approaches for stable isotope tagging are metabolic labeling, mostly in growing cell cultures and enzymatically directed methods such as ^{18}O labeling, or chemical labeling with

external tags, i.e. ICAT reagent (*136*). Chemical labeling approaches are perhaps the most commonly used method in current quantitative proteomics (*138*). Chemical labeling can be classified into three categories: (i) small molecule chemical labeling, (ii) solid-phase-based labeling, (iii) nanopolymer-based labeling (Figure 1.12). Small molecule chemical labeling is straightforward, and is widely adopted in research. The reagents contain a reactive moiety for modification by amino acid side chain (i.e. lysine or cysteine), an isotope tag for coding and an affinity group for isolation, if necessary (Figure 1.12 A & B). Solid-support tagging combines label incorporation and purification in one step. In addition, the acid-cleavable functionality allows harsh washing conditions to remove non-specifically bound peptides or proteins (Figure 1.12C). Nanopolymer-based labeling of soluble polymers, i.e. dendrimers, combined with solid-support have some advantages: high structural and chemical homogeneity, a compact spherical shape, high branching, controlled surface functionalities, and the ability to permeate cells (*139*) (Figure 1.12D).

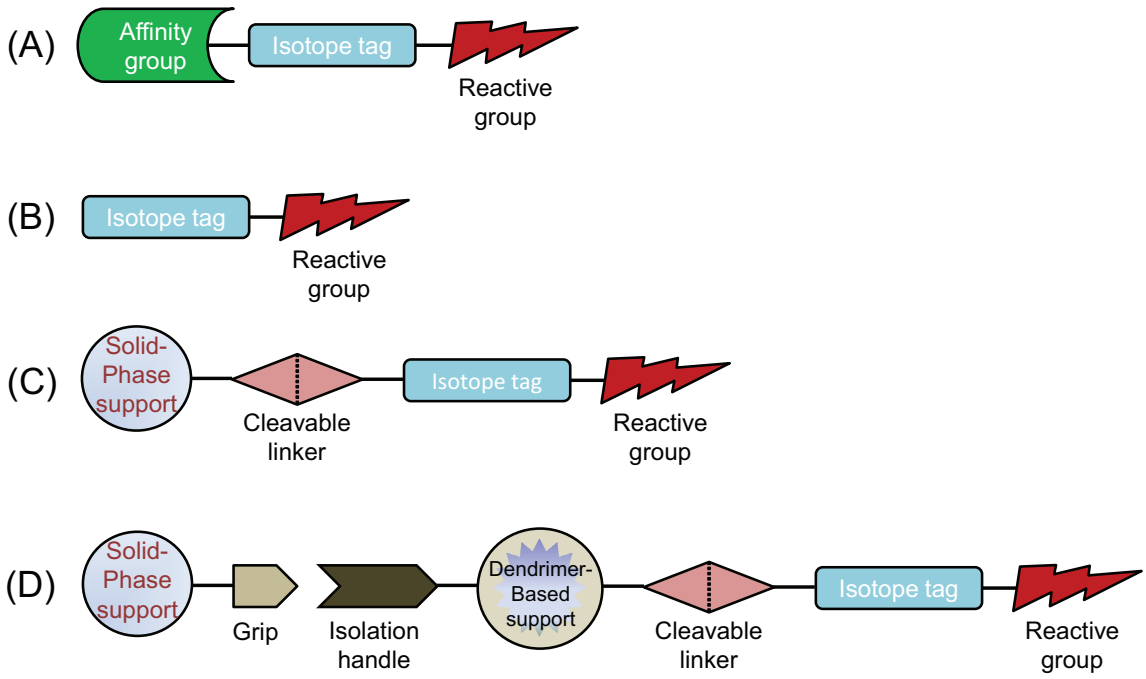

Figure 1.12 Common stable isotopic tagging reagents.
(A) A reagent containing a reactive group, an isotope tag, and an affinity tag for isolating tagging peptides. (B) A reagent that includes a reactive group and an isotope tag. (C) Solid-phase-based reagents functionalized with a cleavable linker, and isotope tag and a site-specific reactive group. (D) SoPIL reagents functionalized with a cleavable linker, a reactive group and an isotope tag. A "handle" group is also attached to the polymer agent that can efficiently bind to the solid beads functionalized with "grip" molecule. This figure was adapted from Iliuk, Galan, and Tao (*138*), and was made with Adobe Illustrator CS3.

Isotope-coded affinity tag (ICAT) was first introduced by Gygi, S.P. *et al.*, and was successfully employed in different cell states for quantitative analysis (*140*). The prototype of ICAT was comprised of a thiol-reactive group for cysteine modification, a linker for incorporating 8 deuterium atoms, and a biotin affinity tag for purification on streptavidin. The original application of this method was to quantitatively analyze complex protein mixtures (*140*). The following steps are required for quantitative analysis: 1) Sulfhydryl groups on cysteines are labeled with light version of ICAT in one cell state, and were labeled with heavy form of ICAT in the other cell state. 2) Samples were combined and proteolyzed. 3) Cysteine containing peptides with light or heavy forms of tag were separated by streptavidin affinity chromatography. 4) Purified peptides were analyzed by microcapillary liquid chromatography (μLC) and tandem mass spectrometry (MS/MS). 5) Peptides analyzed by mass spectrometry, mass to charge ratio (m/z) or sequence, were identified by automated database searching to determine proteins. However, first generation ICAT has some drawbacks. The biotin containing tag is relative large and bulky, and this could complicate data analysis under collision-induced dissociation (CID) conditions. The deuterium isotope in the heavy form could cause primary isotope effect in liquid chromatography (*141-143*), and might affect measurement accuracy. There are some second-generation ICAT tags available, and they introduced acid-labile groups on ICAT (*144*), attachment of tags on solid support (*145*), or uses of ^{13}C isotope in replacement with ^{2}H isotope to overcome current limitations on the first generation ICATs. With the use of the isotopic form of the tags, protein profiling could be quantitated by comparing a known quantity in one of the labeled peptides.

With successful applications of these isotope-coded affinity tags in complex systems, such as comparing expression levels of individual proteins, one can easily compare the differences quantitatively from complex samples modified with normal and isotope-coded tags in a mass spectrometer. The advantage of this method is the ability to compare the same analyte in different states. This concept can be extended to study interactions between peptides or proteins and membranes. The isotope-coded mass tag (ICMT) has similar components, a reactive moiety for a specific nucleophile, for example, cysteine thiols, and an isotope-coding region, but differs in the positively charged quaternary ammonium group for aiding ionization efficiency in mass

spectrometry. Details of the concepts and experimental designs will be discussed in the next chapter.

Chapter 2 Results and discussion

*Note: Some parts of this chapter are adapted from published work in *Bioconjugate Chemistry* (*146*)

2.1 Design and synthesis of ICMTs

Herein, we designed a series of *N*-alkyl(alkoxyl)maleimide ICMT reagents (Figure 2.1) to study transmembrane peptide dynamics and to map interfacial protein-membrane interactions. Because maleimides have relatively better reactivity than iodoacetyl derivatives at physiological pH, they were chosen as a thiol reactive component. The design is based on two considerations. First, the quaternary ammonium group ensures that proteolyzed peptides with mass tags will always bear at least a positive charge, which could improve ionization in the mass spectrometer. Second, the heavy isotope is introduced in the last step to make the experiment more cost efficient. The ICMT probes consist of three parts: a thiol reactive moiety, an alkyl or alkoxyl linker to mediate membrane permeability, and a quaternary ammonium group to aid ionization in the mass spectrometer. The syntheses of specific ICMT probes are shown in Scheme 2.1.

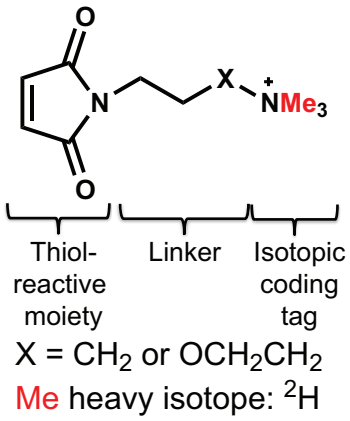

Figure 2.1 *N*-alkyl(alkoxyl)maleimide ICMT reagents.
The ICMT probes are comprised of three parts: a thiol reactive maleimide, an alkyl or alkoxyl linker, and a quaternary ammonium group bearing a positive charge and coding isotopes.

The synthesis of *tert*-butyl-aminoalkyl carbamates, **1** (Scheme 2.1), was performed according to procedures in the literature (*147-150*). The syntheses of compounds **2** and **3** were performed following a modification of the procedure to prepare *N*-ethylmaleimide reported by Niwayama et al. (*130*) as outlined in Scheme 2.1. The reaction was carried out by reacting maleic anhydride with the corresponding mono-BOC protected amine to form the maleamic acid intermediate, and subsequent ring closure by dehydration using acetic anhydride/sodium acetate. The ICMT reagents were prepared in excellent yields from the protected aminoalkyl maleimides **3a–3d** (Scheme 2.1). Quantitative deprotection of the terminal amines **3a–3d** (Scheme 2.1) to

free amine compound **4a**–**4d** and subsequent permethylation (*151*) with iodomethane provided the quaternary ammonium salts **5a-d$_0$**–**5d-d$_0$** in high purity (Scheme 2.1). Analogously, permethylation with corresponding iodomethane-d_3 provided the heavy isotope forms **5a-d$_9$**–**5d-d$_9$**.

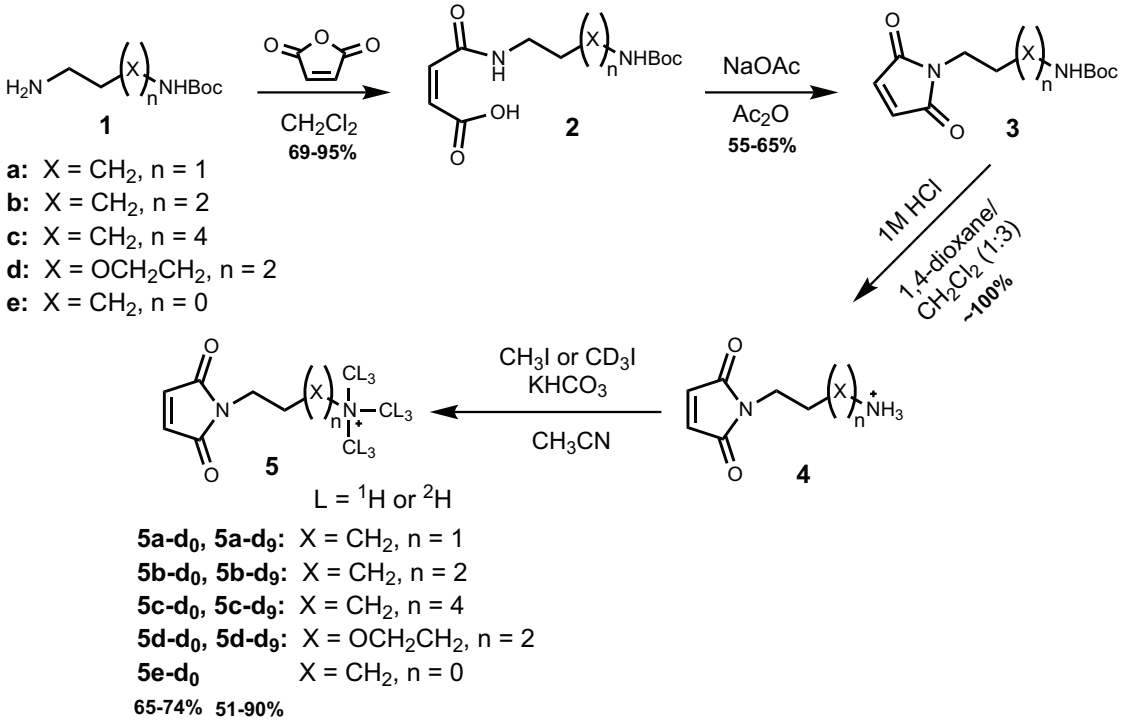

Scheme 2.1 Synthetic route for the preparation of ICMT probes.
Maleimide **4** was prepared in 3 steps from mono-BOC-protected diamine and maleic anhydride. Permethylation (*151*) of the maleimide amine **4** with iodomethane-d_0 (CH_3I) or iodomethane-d_3 (CD_3I) under mild basic conditions provides light version probes **5a-d$_0$**–**5d-d$_0$** or heavy version probes **5a-d$_9$**–**5d-d$_9$**, respectively, in 51–90 % yield.

Isotope-coded tag methods provide facile relative quantitation in mass spectrometry (*140*). The original ICAT tags include a thiol reactive iodoacetyl group, a biotin for purification, and a polyether linker. The polyether linker can be labeled with 8 deuterium atoms for isotope coding. Related labeling methods which utilize a combination of isotope tag, cysteine labeling, and mass spectrometry, include acid-labile isotope-coded extractants (ALICE) (*144*), and isotopic tandem orthogonal proteolysis-activity-based protein profiling (isoTOP-ABPP) (*152*). In ALICE, cysteine-containing peptides or proteins are captured on a maleimide resin. In isotope-ABPP, the differential reactivity of cysteine residues is elucidated. In each of these

methods, two different samples are labeled, one with light isotope and one with heavy isotope. Then, the samples are mixed and the ratio of heavy to light product is analyzed by mass spectrometry. Thus, cysteine-directed isotope-coded tags can fulfill a variety of needs in proteomic research.

Here, we have designed and synthesized a series of *N*-alkyl(alkoxy)maleimides, **5a-d_0**–**5d-d_9** to probe protein topologies in the presence of membranes. These probes comprise three components, a thiol-reactive maleimide, a positively charged quaternary ammonium group, and linkers of varying lengths between them. We focused on a cysteine labeling method because the amino acid functionality to be tagged, in this case a thiol, can reside in the membrane with little energetic penalty. Although lysine labeling has been used widely to map surface accessibility, due to lysine's cationic charge at physiologic pHs, it is not suitable for membrane studies. We utilized a covalent labeling strategy to avoid the problem of back exchange that is a limitation of hydrogen-deuterium exchange methods. The maleimide moiety reacts specifically with sulfhydryl groups, and in a physiological pH range, it reacts faster than other thiol-targeted reagents, e.g. iodoacetamide (*129*).

Alkyl and PEG-based linkers were selected as our linker between maleimide and quaternary ammonium group. We originally designed 2, 3, 4, and 6 carbon linkers and a PEG linker in our probes. A membrane impermeable tag for labeling in lipid bilayer system was desired, so we proposed shorter linkers may affect labeling of thiols which are in a charged environment. Probes containing a longer hydrophobic linker may bind non-specifically to proteins or may partition into the lipid membrane. We calculated clogP value and retention time from liquid chromatography to estimate the hydrophobicity of these probes (Figure 2.2). The clogP values show that the longer hydrocarbon linker (6C) is most hydrophobic, and the hydrophobicity of PEG linker is comparable to 2C- or 3C- linker probes. Tests of membrane permeability were empirical so various length linkers were evaluated.

Lastly, we developed the method such that a bottom-up analysis approach, in which the tagged protein is proteolytically reduced to smaller peptide fragments, could be employed. This approach enables monitoring the accessibility of several sites in a single protein simultaneously. Due to isotope effects on retention times (*141-143*), LC/MS methods require post-processing

alignment of spectra before evaluation of labeling ratios. Therefore, we chose to analyze tagged peptides with MALDI-TOF mass spectrometry in order to simplify the ratio analysis.

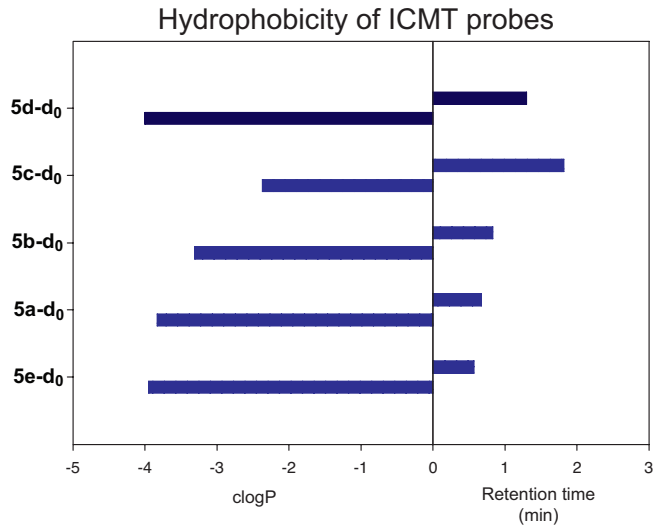

Figure 2.2 Hydrophobicity of ICMT probes.
Left: clogP values of ICMT probes calculated from Marvin Sketch, ChemAxon (*153, 154*). logP = $\log([I]_{Octanol}/[I]_{water})$, P: partition coefficient of organic compound, I, distribution in octanol and in water. Right: Retention time of ICMT probes in C18 column. (Waters ACQUITY Ultra Performance LC-MS, flow rate = 0.5 mL/min, linear gradient: 95% water to 95% acetonitrile in 20 min)

During the synthesis of the quaternary ammonium group in the last step, methanol was used as the solvent according to the published protocol (*151*). In that work, three methyl groups from iodomethane (CH_3I or CD_3I) were incorporated on the amine group of ϒ–aminobutyric acid. However, in the synthesis of **5c-d$_0$**, there were two major side products formed, the mono- or di-substituted Michael products produced from methanol attack on the alkenyl carbon (Figure 2.3A). We changed the reaction solvent to acetonitrile to synthesize ICMTs.

In the synthesis of **5e-d$_0$**, we again found more side products than desired compounds. For example, dimer or trimer was observed during the reaction (Figure 2.3B), and these side products probably came from nucleophilic attack of the amino group of one molecule on the maleimide double bond of another molecule. These reactions were monitored by mass spectrometry. Due to unexpected side products and difficulties in purification, we did not pursue the probe with a two-carbon alkyl linker. The hydrophobicity and retention time in reverse phase

C18 liquid chromatography of **5a-d$_0$**, with a three-carbon linker, are comparable to the **5e-d$_0$**, with a two-carbon linker (Figure 2.2) and thus we focused on **5a-d$_0$** as the hydrophilic probe.

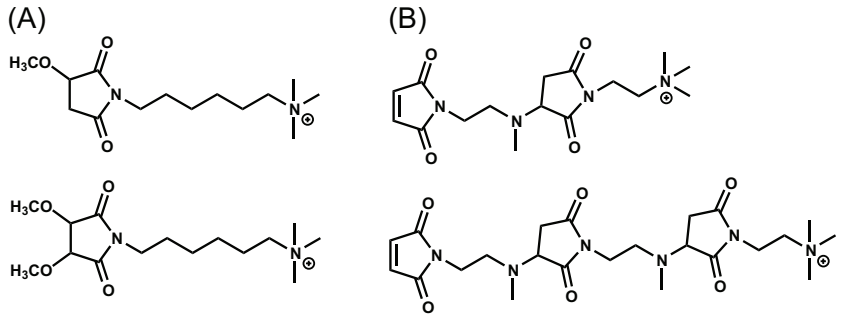

Figure 2.3 Reaction side products formed during synthesis of ICMTs.

We incorporated a quaternary ammonium mass tag for two reasons. First, the quaternary ammonium bears a positive charge regardless of the ionization conditions in the mass spectrometer. This tag eliminates the requirement for inclusion of basic amino acids in the peptide to be analyzed (*155-157*). Second, isotope incorporation is accomplished through per-methylation of a primary amine to form the quaternary ammonium in the last synthetic step. This reaction sequence provides an economical and efficient synthesis for heavy isotope incorporation. Isotopically labeled iodomethane with either ^{2}H or ^{13}C is commercially available. After per-methylation of amine, the ^{2}H and ^{13}C labels provide probes with +9 Da or +3 Da mass differences, respectively. Deuterium has two advantages: lower cost of starting material and complete separation of isotopic envelopes in the mass spectra, with 9 Da mass shifts. The hydrogen and deuterium probes were easily prepared in > 99 % purity and multi-gram quantities.

2.2 Design of transmembrane peptides for assessment of membrane access

We prepared three model transmembrane peptides each with a single cysteine to assess the reactivity of our probes with peptide thiols in lipid membranes. The peptide sequence Ac-$K_2GL_9WL_9K_2A$-NH_2 forms an α-helix and spans the lipid bilayer (*25*). This peptide and peptides with related sequences have been widely used to study membrane structure with fluorescence and EPR probes (*25*). The tryptophan fluorescence emission reports on the incorporation and orientation of peptide in the membrane, and a blue shift in tryptophan emission from 350 nm to 316 nm signifies that the transmembrane conformation has been adopted (Figure 2.4). We introduced a cysteine residue in the middle of the sequence to provide peptide **6** (Ac-$K_2GL_7WLCL_9K_2A$-NH_2), incorporated a cysteine at the N-terminus to provide peptide **7** (Ac-$CK_2GL_7WLAL_9K_2A$-NH_2), and placed a cysteine after the two lysines at the N-terminus to provide peptide **8** (Ac-$K_2CL_7WLAL_9K_2A$-NH_2) (Scheme 2.2). We expected the central cysteine in peptide **6**, which is buried in the membrane, would be inaccessible to our maleimide probes. Conversely, for that population of peptide **7** oriented with the terminal cysteine thiol protruding from the outer leaflet, we expected the thiol to be accessible to the probes. Peptide **8** was designed to place the cysteine in a position partially accessible to probe as the thiol is expected to reside at the boundary between the lipid headgroup region and hydrophobic core of the membrane (Figure 2.4). The relative position of cysteine on transmembrane peptides for peptide 6–8 is shown in Figure 2.5.

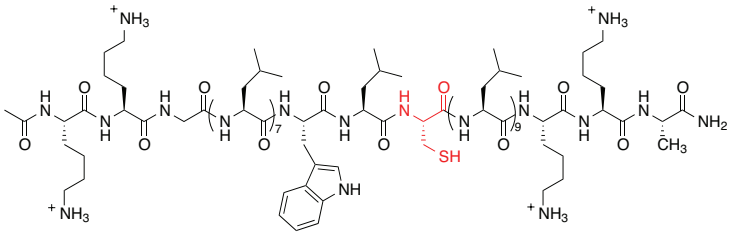

6

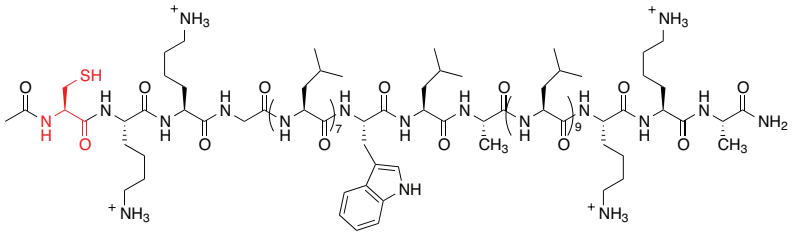

7

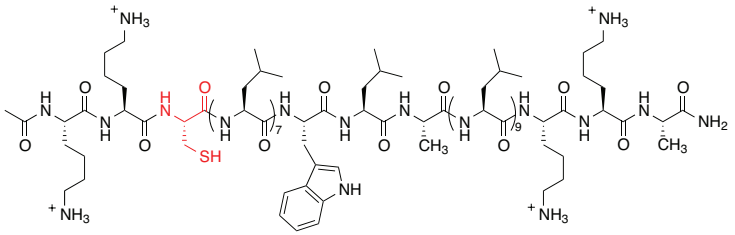

8

Scheme 2.2 Structures of model α-helical peptides.
Peptide **6** (cysteine inaccessible), peptide **7** (cysteine accessible), and peptide **8** (cysteine partially accessible).

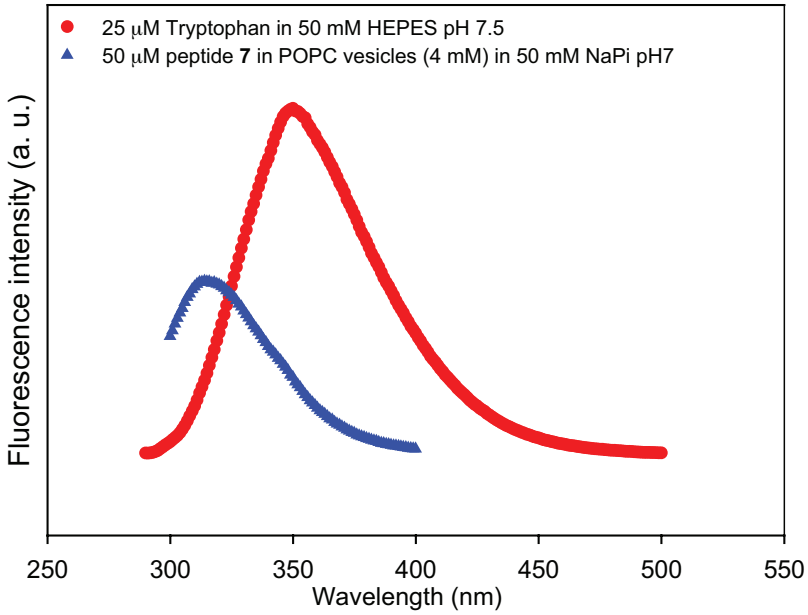

Figure 2.4 Tryptophan fluorescence spectra.
Red line: 25 μM tryptophan in 50 mM HEPES pH 7.5 buffer. Blue line: 50 μM peptide **7** in POPC vesicles (4 mM) in 50 mM NaPi pH 7 buffer, peptide **7**: Ac-$CK_2GL_7WLAL_9K_2A$-NH_2. Ex: 280 nm, $\lambda_{em,max}$ = 350 nm for Trp in buffer, $\lambda_{em,max}$ = 316 nm for peptide **7**/POPC vesicles.

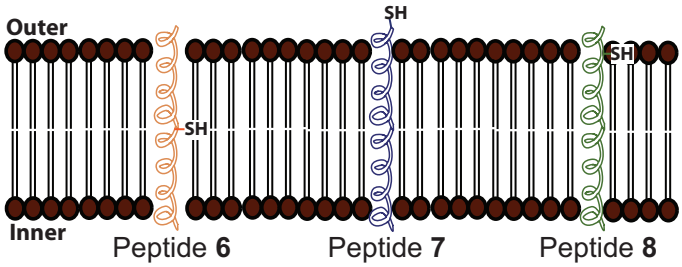

Figure 2.5 Representations of relative position of cysteine on transmembrane peptides.
Peptide **6** (cysteine inaccessible), peptide **7** (cysteine accessible), and peptide **8** (cysteine partially accessible) in lipid bilayers.

2.3 Assessment of ICMT labeling precision and accuracy

To test the accuracy and repeatability of mass spectral peak integration, we labeled peptide **6**, peptide **7**, or peptide **8** that had been suspended in 5% aqueous detergent solution with a 1:1 (molar) mixture of heavy and light probes. The experimental percentage of heavy and light labeling was determined in two different ways using Bruker flexAnalysis version 3.0 software. First, the average intensities of the heavy and light isotopomers were measured. Second, the areas under the entire heavy and light isotopic envelopes were measured. The percentage of heavy-labeled peptide was calculated from both sets of values. As shown in Figure 2.6, the ratio of labeling by heavy and light labels was close to 1:1. Only subtle variation was observed (generally 2-3%) in the percentage of heavy-labeled peptide using either method. The detection of light and heavy labels in the expected 1:1 ratio implies that there are no detectable isotope effects on either labeling rate or ionization efficiencies.

The results shown above demonstrate that reaction rates of both heavy and light version probes are the same, and the integration of the heavy and light peaks on mass spectra offer the utilities of our ICMT probes in quantitative measurements.

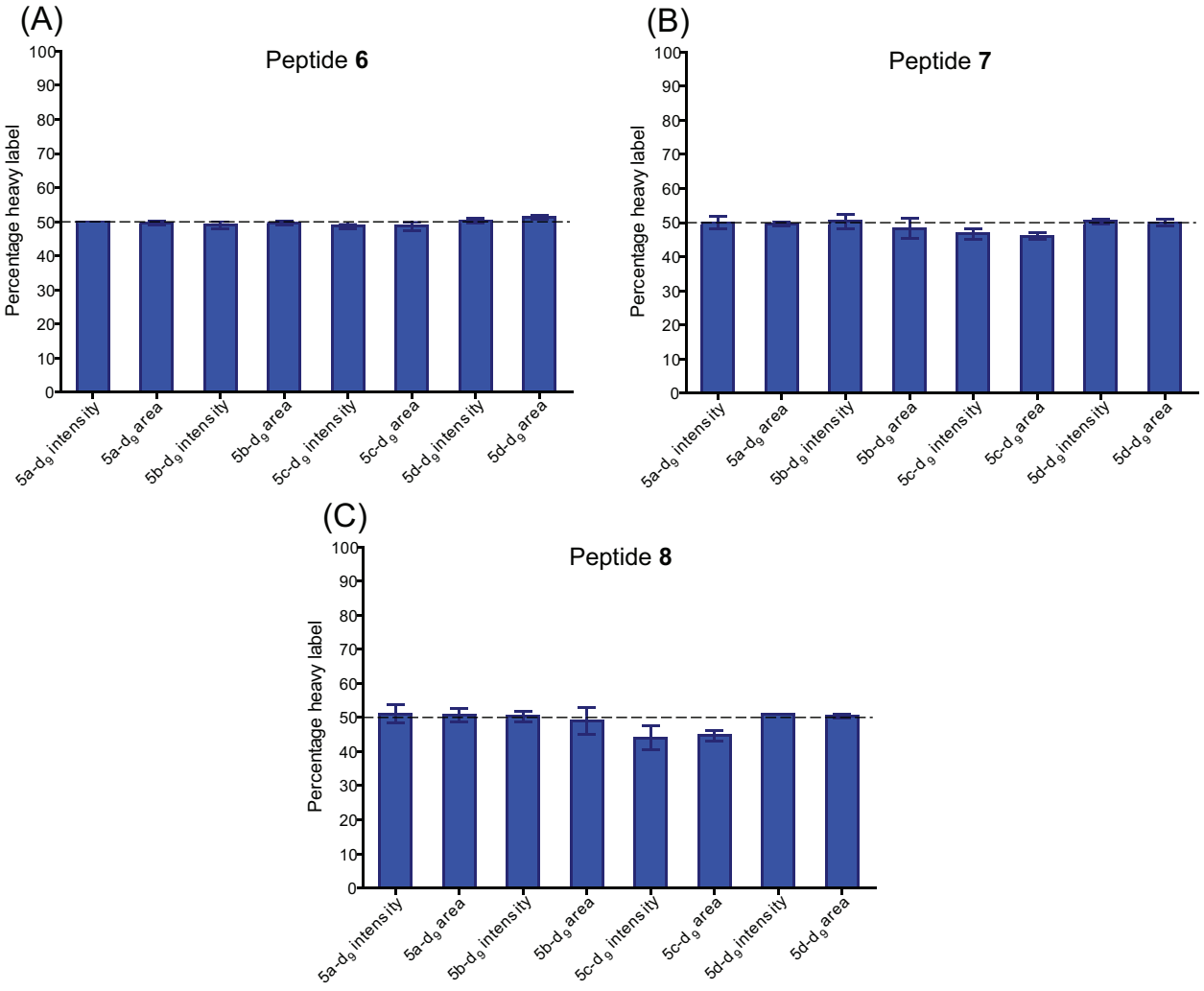

Figure 2.6 Accuracy and precision of labeling peptide 6, peptide 7, and peptide 8 with ICMT probes.

Peptide **6** (panel A), peptide **7** (panel B), or peptide **8** (panel C), all 50 μM, dissolved in 0.5 % (w/v) SDS, 50 mM sodium phosphate, pH 7 was labeled with a mixture of light (9 mM) and heavy (9 mM) ICMT probe. The percentage of peptide labeled with heavy probe was determined either the average intensity if the isotopmer in each envelop or the area under the entire isotopic envelop. Average values from three replicate experiments and the standards are shown. The dashed line represents the expected value of 50%. Errors are standard deviation based on triplicate measurement of three independent labeling experiments.

2.4 Membrane permeability of ICMT reagents

We performed a fluorescent dye leakage assay to test membrane permeability in the presence or absence of transmembrane peptides. We prepared POPC and peptide **7**/POPC vesicles with carboxyfluorescein encapsulated, and fluorescence intensity was monitored as a function of time. The fluorescence intensity for both POPC and peptide **7**/POPC vesicle solutions remained low and unchanged over 65 minutes. No significant dye leakage was observed until we added Triton X-100 to disrupt lipid vesicles (Figure 2.7B). This important control demonstrates that incorporation of transmembrane peptides does not increase the permeability of the membrane to anionic molecules.

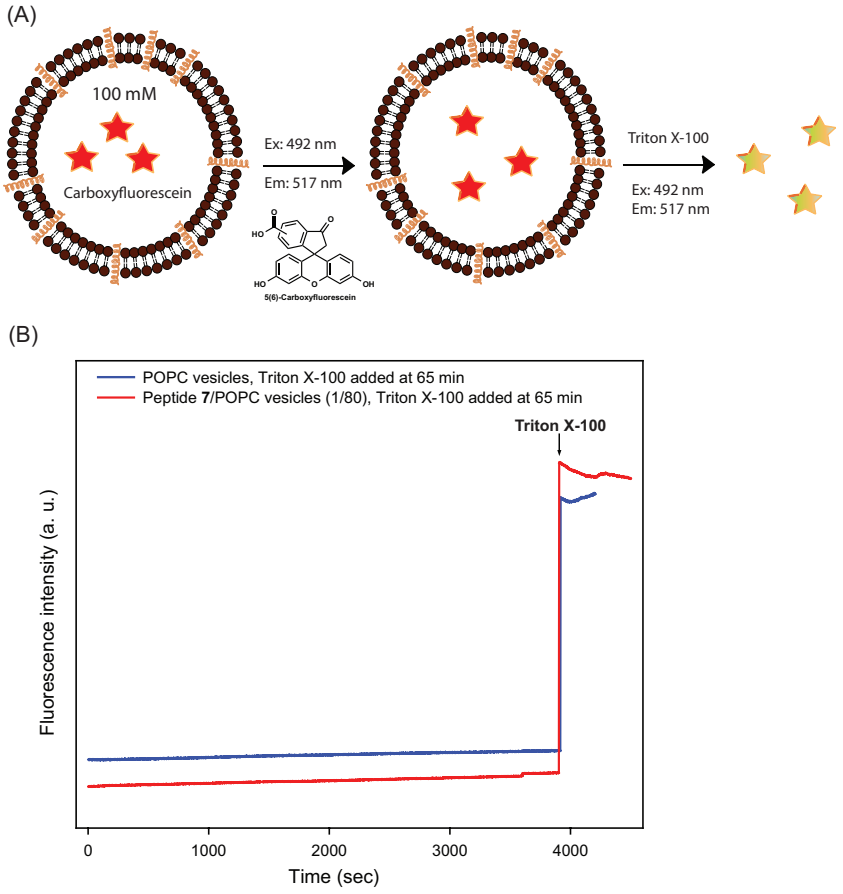

Figure 2.7 Vesicles permeability assay.
(A) Schematic illustration of membrane permeability assay. Carboxyfluorescein (100 mM) was encapsulated in peptide **7**/POPC (1/80) vesicles or POPC vesicles (285 μM total lipid). Fluorescence emission intensities (λ_{ex} = 492 nm, λ_{em} = 517 nm) were monitored for 70 min, and Triton X-100 was added to completely lyse vesicles at 65 min. (B) Time course of fluorescence emission intensity of carboxyfluorescein.

Because of the possibility that membrane permeation may be dependent on charge, we performed an additional experiment to test directly whether the cationic nature of the probe enables it to permeate the membrane. The modified tripeptide, NB-ECD-OMe, which contains a reactive thiol, was encapsulated in peptide **7**/POPC (1/80) vesicles. The tripeptide contains two acidic residues that are anions at neutral pH. As demonstrated for carboxyfluorescein, the anionic tripeptide is not expected to leak out of the vesicles.

We utilized a two-step labeling method as outlined in Figure 2.8. In the first step, the vesicles were labeled with the heavy isotope probe **5a-d$_9$**–**5d-d$_9$**. After a period of time (2–90 minutes), the probe was quenched with DTT, and then the vesicles were lysed with the detergent Triton X-100, and treated with light probe. If the ICMT probes were able to penetrate the lipid bilayer, the encapsulated NB-ECD-OMe peptide would be labeled with heavy probe during the first labeling step.

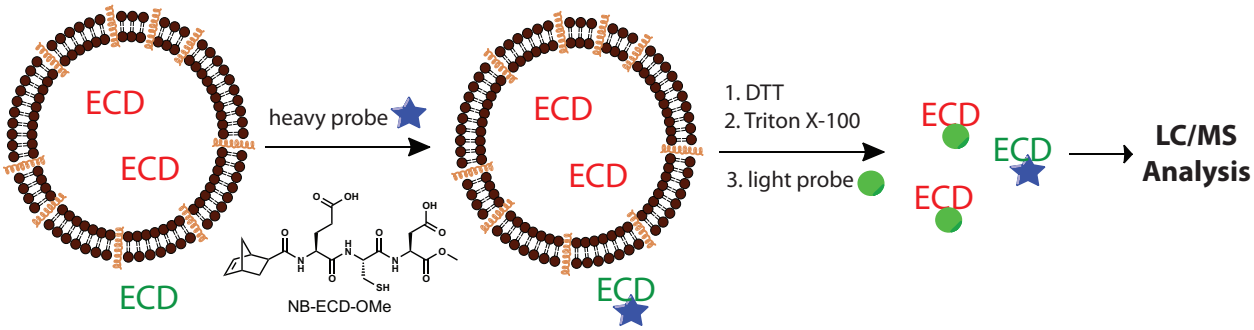

Figure 2.8 Schematic illustration of two-step labeling of NB-ECD-OMe.
NB-ECD-OMe (3 mM) was encapsulated in peptide **7**/POPC (4 mM) vesicles. In the heavy probe labeling, the remaining ECD in buffer was labeled, excess heavy probe was quenched with DTT, vesicles were lysed by Triton X-100, and light probe was added to label ECD released from vesicles. The heavy and light labeled ECD were analyzed by LC/MS.

Compared to phospholipid, the quantity of NB-ECD-OMe peptide in this experiment is quite small and difficult to detect by MALDI-TOF spectrometry. Therefore, we used LC/MS to separate labeled NB-ECD-OMe peptide from lipid and to analyze the percentage of heavy labeled peptide as a function of time. In each experiment, we observed a small amount of heavy labeled NB-ECD-OMe at the initial time point (2 minutes). Furthermore, we did not observe any increased labeling of the NB-ECD-OMe peptide with heavy probe over the course of 90 minutes (Figure 2.9). Almost all labeling was with the light probe, indicating that encapsulated NB-ECD-OMe was only accessible to label after the membranes were solubilized. The small amount

of heavy labeled NB-ECD-OMe is probably due to a trace of peptide that remains outside the vesicles after size exclusion chromatography. These data confirm the impermeability of the transmembrane-containing lipid bilayer to the ICMT probes (Figure 2.9).

We tested various lengths of carbon linker and a PEG linker to tune the membrane permeability and surface thiol reactivity of our probes. We sought a linker that both limited probe solubility in the membrane and that prevented interference of the quaternary ammonium mass tag with the thiol-labeling reaction. Permeability experiments with an encapsulated peptide confirmed that all the ICMT probes were membrane impermeable over at least a 90-minute period. This was true even in the presence of transmembrane peptides. Moreover, the rates of labeling were minimally affected by linker length. Therefore, all the ICMT probes are suitable to provide information on the position and dynamics of peptides in membranes. However, probe **5c** provided the least consistent labeling rates and efficiencies (Figures 2.6) of all the probes, perhaps due to its higher chain flexibility and greater hydrophobicity.

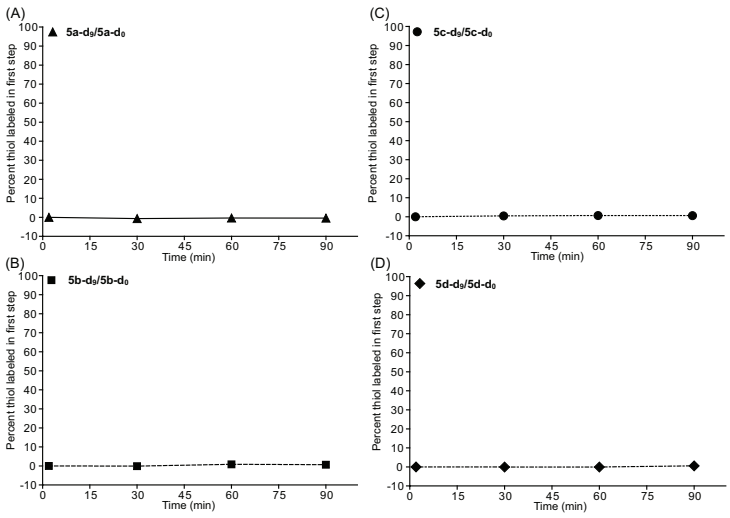

Figure 2.9 ICMT permeability tests with peptide 7/POPC (1/80) vesicles.
Tri-peptide NB-ECD-OMe (3 mM) was encapsulated in peptide **7**/POPC (1/80) vesicles. Intact vesicles were labeled with 6 mM **5a-d$_9$**, **5b-d$_9$**, **5c-d$_9$**, or **5d-d$_9$** heavy probe for 2, 30, 60 or 90 minutes, quenched with 7 mM DTT, 0.03% Triton X-100 to lyse vesicles, and were then labeled with 15 mM **5a-d$_0$**, **5b-d$_0$**, **5c-d$_0$**, or **5d-d$_0$** light probe for 1 hour. The reactions were analyzed by LC/MS and extracted ion chromatograms were integrated. Percentage heavy label indicates the percent of total labeling that occurred with intact vesicles. Average values from three replicate experiments and the standard deviations are shown. Tests with (A) **5a-d$_9$/5a-d$_0$** probe. (B) **5b-d$_9$/5b-d$_0$** probe. (C) **5c-d$_9$/5c-d$_0$** probe. (D) **5d-d$_9$/5c-d$_0$** probe. Errors are standard deviations based on triplicate measurements of three independent labeling experiments.

2.5 ICMT detection of peptide thiol membrane location

We prepared POPC vesicles with 1.25 mol percent of peptide **6** or peptide **7**. Each vesicle type was subjected independently to labeling with each of the ICMT heavy/light probe sets. We utilized a two-step labeling method similar to that used for the NB-ECD-OMe peptide, as outlined in Figure 2.10. In the first step, the vesicles were labeled with the heavy isotope probe. After 10 minutes, the probe was quenched with DTT, the vesicles were lysed with Triton X-100, and then treated with light probe. Because all four of the ICMT probes did not permeate the membrane, we expected that only thiols on the outer leaflet exposed to the aqueous environment would be labeled in the first step. Analogously, we expected that thiols buried in the membrane or with thiol exposed on the inner surface would be labeled after disruption of the lipid bilayers. We analyzed the heavy/light labeling percentage by integrating the full isotopic envelope as described above.

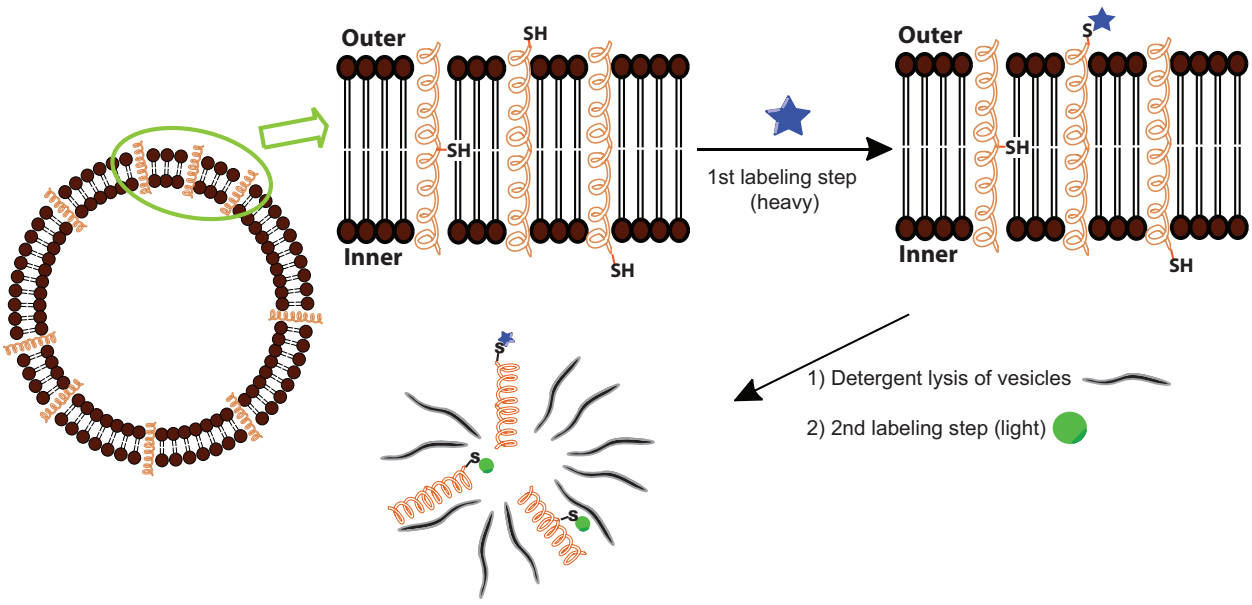

Figure 2.10 Labeling strategy for transmembrane α-helical peptides incorporated into POPC vesicles.
The cysteine is in a solvent inaccessible or accessible position for peptides **6** or **7**, respectively. In the case of peptide **7**, only the thiol on the outer leaflet is exposed to ICMT probe. The cysteine was first labeled with heavy probe in intact vesicles; the vesicles were lysed with detergent, and then labeled with light probe.

We found that neither heavy nor light ICMT probe labeled peptide **6** under these conditions. We postulated that the thiol in peptide **6** was too deeply buried in a hydrophobic environment to react with ICMT probe both in the vesicles and in the detergent micelles formed upon lysis of the membrane vesicles with Triton X-100 detergent. Therefore, we employed sodium cholate, which has a higher CMC and forms smaller micelles, that is unlikely to deeply bury the thiol group of Cys (*158*), to disrupt the vesicles, and also used elevated temperature to increase the labeling reaction rate. Under these conditions, the thiol of peptide **6** is labeled efficiently in the second step (Figure 2.11 A-D), consistent with our hypothesis.

In the case of peptide **7**, we found that the solvent accessible cysteine was readily labeled in the first step. However, with most of the ICMT probes, 100% of the cysteine in peptide **7** was labeled in the first step, rather than the 50% expected if the peptides were randomly oriented so that half of the thiol population is oriented toward the center of the vesicle and the other half faces the external solution (Figure 2.11 E-H). When we examined the kinetics of labeling peptide **7**, we found that within one minute over 90% of the thiol was labeled in the first step regardless of ICMT probe concentration. Previous work had identified a population of the a-helical peptide that orients parallel to the surface rather than in a transmembrane orientation, and found that equilibration between the two states is rapid (*31, 159*). Our data suggest that upon transitioning between the transmembrane and parallel orientations that the thiol orientation can invert from outer to inner leaflet and vice versa. If the timescale of this peptide flip is faster than the labeling time, then all of the solvent accessible thiol would be labeled in a single, fast step.

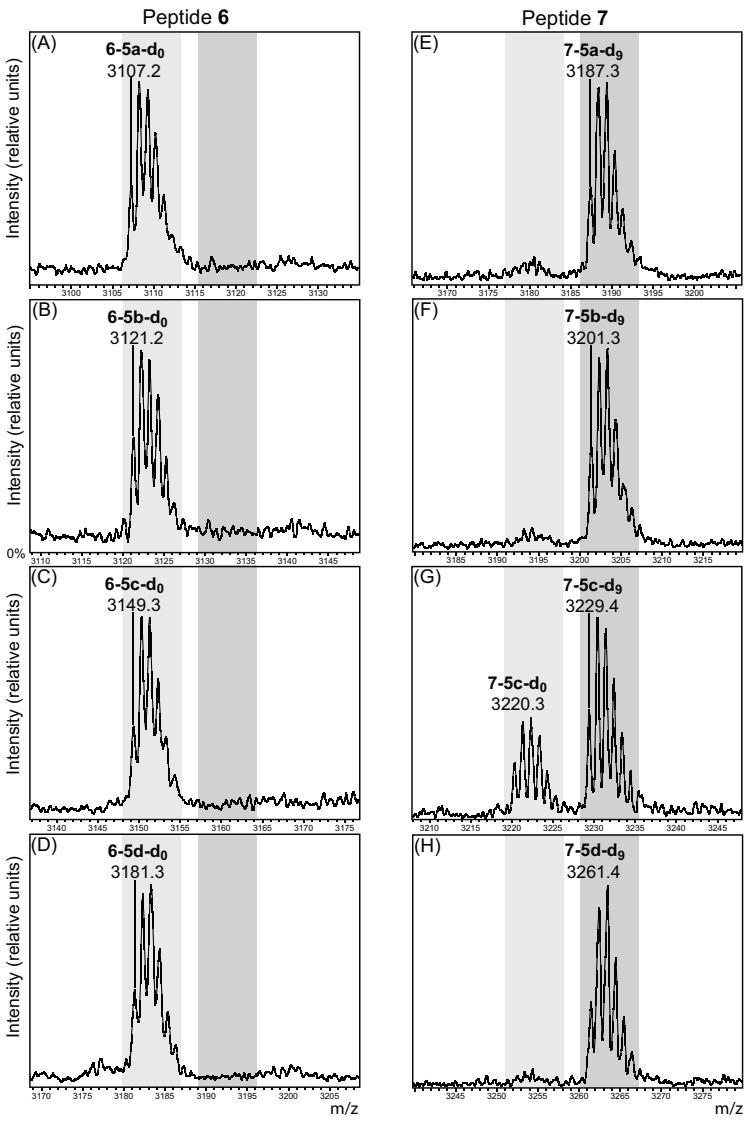

Figure 2.11 Mass spectra of peptide 6 and peptide 7 in POPC vesicles labeled in the two-step procedure.

Peptide/POPC vesicles were labeled with heavy probe for one hour in the first step, lysed with detergent, and then labeled with light probe for one hour as outlined in Figure 2.10. Peptide **6** labeled with heavy/light probes (A) **5a-d$_9$/5a-d$_0$**, (B) **5b-d$_9$/5b-d$_0$**, (C) **5c-d$_9$/5c-d$_0$**, or (D) **5d-d$_9$/5d-d$_0$** and peptide **7** labeled with heavy/light probes (E) **5a-d$_9$/5a-d$_0$**, (F) **5b-d$_9$/5b-d$_0$**, (G) **5c-d$_9$/5c-d$_0$**, or (H) **5d-d$_9$/5d-d$_0$**. Peptide **6**/POPC vesicles were lysed with 0.5% (w/v) sodium cholate at 25 °C and labeled with light probe at 75 °C. Peptide **7**/POPC vesicles were lysed with 0.03% (w/v) Triton X-100 and labeled with light probe at 25 °C. The peaks corresponding to light-labeled peptide are highlighted in light gray, and the peaks corresponding to heavy-labeled peptide are highlighted in dark gray. Intensities are relative to the highest peak in a single spectrum and each panel is not on the same scale.

We selected three peptides to model possible cysteine topologies in a protein. The sequences of all these peptides were identical except for the position of the cysteine residue. The peptide sequence was selected for its ability to form a transmembrane α-helix, and thus to position the cysteine in a mid-bilayer environment in the case of peptide **6**, in a lipid headgroup environment in the case of peptide **7**, or at the boundary of the lipid headgroup and the hydrocarbon region in the case of peptide **8**. Labeling was found to be very sensitive to the location of the Cys residue. Even the small difference in membrane depth for the Cys in peptide **7** and peptide **8** was sufficient to significantly slow labeling for the more deeply buried Cys in peptide **8**. The observation that peptide **6**, which had a Cys deeply buried in the bilayer, was not labeled by any of the ICMT labels shows that the ICMT approach will be able to readily identify Cys in membrane proteins that are deeply buried within lipid bilayers. The lack of labeling for a deeply buried Cys is due to two effects. First, the probes do not penetrate the bilayer. Second, a thiol in a hydrophobic environment will have an elevated pK_a and the level of ionization is expected to be lower than in solution. In aqueous solution, sulfhydryls have a pK_a around 8–9 (*118, 119*) and maleimides react with ionized sulfhydryls about 9 orders of magnitude faster than with un-ionized sulfhydryl groups (*128*).

We even found that upon disruption of vesicles with mild detergent conditions, the cysteine on peptide **6** still could not be labeled (Figure 2.11 A-D). Labeling was accomplished at 75 ^{o}C with the use of sodium cholate to lyse the vesicles. The results suggest that our probes cannot easily permeate detergent micelles in which the cysteine of peptide **6** is buried. The low aggregation number (4–8) of sodium cholate (*158*), which should enhance Cys accessibility to external solution in combination with elevated temperature, promoted labeling.

2.6 ICMT monitoring of peptide helix mobility kinetics in membranes

To assess whether peptide flipping in lipid membranes is occurring on the second time scale, we revised our labeling scheme and performed kinetics experiments (Figure 2.12). Peptide **7**/POPC vesicles (1/80) were labeled with **5a-d$_9$** or **5c-d$_9$** for 2 to 120 sec, then a ten-fold excess of **5a-d$_0$** or **5c-d$_0$** was added for five minutes before lysing vesicles for analysis. The amount of labeling observed in the first step increased with time and thiol labeling was complete within thirty seconds (Figure 2.13). The reaction rates were nearly identical for the two linkers tested (Figure 2.13B).

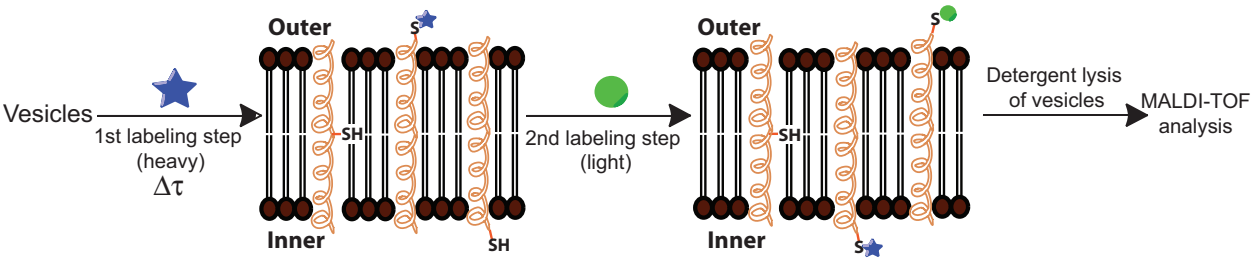

Figure 2.12 Schematic illustration of kinetic labeling strategy for transmembrane α-helical peptides incorporated into POPC vesicles.
The cysteine is in a solvent inaccessible or accessible position for peptides **6** or **7**, respectively. Peptide **6**/peptide **7**/POPC was first labeled with heavy probe, and 2, 5, 10, 30, 60, or 120 s after adding the first probe, a ten-fold excess of light probe was added.

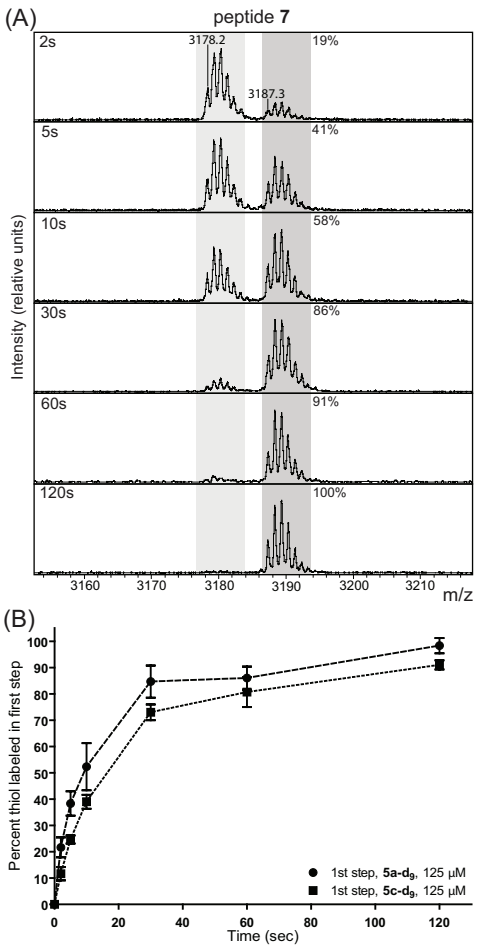

Figure 2.13 Kinetics of labeling peptide 7/POPC vesicles (1/80).
The vesicles were labeled with 125 µM **5a-d$_9$** or **5c-d$_9$**, after 2, 5, 10, 30, 60, or 120 s followed by 1.25 mM **5a-d$_0$** or **5c-d$_0$**, respectively. (A) Mass spectra of peptide **7** labeled with **5a-d$_9$**/**5a-d$_0$** at different time points. (B) Time courses for the two labeling experiments. Integrated areas under the isotopic envelope were used to calculate percent labeling. Errors are standard deviation based on triplicate measurements of three independent labeling experiments.

Next, we incorporated both peptide **6** and peptide **7** into the same POPC vesicle in order to assess the efficacy of labeling thiols in two different environments in a single membrane bilayer. The kinetic time courses for these mixtures of peptides labeled with **5a-d$_9$**/**5a-d$_0$** or **5c-d$_9$**/**5c-d$_0$** (Figure 2.14B) were identical to the time courses for the peptides incorporated into individual membranes (Figure 2.13B). Again, peptide **6** containing the inaccessible peptide was not labeled until the vesicles were lysed.

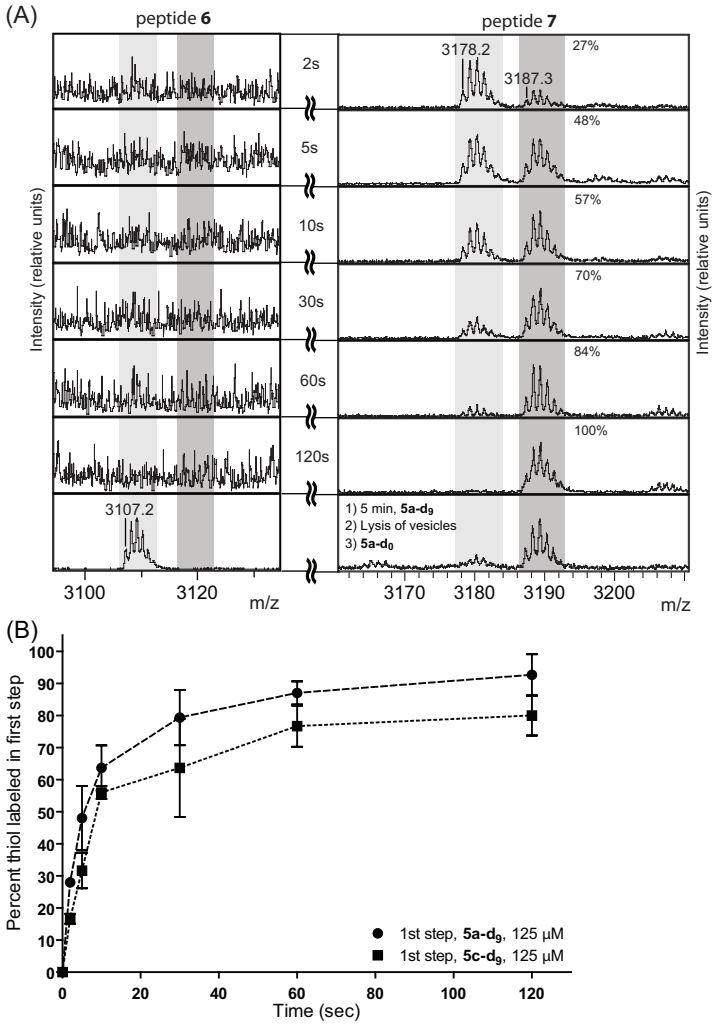

Figure 2.14 Kinetics of labeling peptide 6/peptide 7/POPC vesicles (1/1/127).
The vesicles were first labeled with 125 μM **5a-d$_9$** or **5c-d$_9$**, and 2, 5, 10, 30, 60, or 120 s after adding the first probe, 1.25 mM **5a-d$_0$** or **5c-d$_0$**, respectively, was added. (A) Mass spectra of peptide **6** (left) and peptide **7** (right) labeled with **5a-d$_9$**/**5a-d$_0$** at different time points. Bottom panel: after labeling 5 min with **5a-d$_9$**, the vesicles were lysed (sodium cholate, 75 °C) and a 300-fold excess of light probe, **5a-d$_0$**, was added. Intensities are relative to the highest peak in a single spectrum and each panel is not on the same scale. (B) Time courses for peptide **7** labeling for the two probes, **5a** and **5c**. Integrated areas under the isotopic envelope were used to calculate percent labeling. Errors are standard deviation based on triplicate measurements of three independent labeling experiments.

We also reversed the order of probe addition. We initially labeled with the light probe **5a-d$_0$**, and added an excess of heavy probe **5a-d$_9$** as a function of time (Figure 2.15A). Within experimental error, the rate of labeling in the first step was independent of which isotope or probe was used (compare Figure 2.15B to Figure 2.13B). From the combined results of these

experiments we conclude the flipping of peptide orientation is occurring within seconds. This is only an upper limit to the time required for flipping.

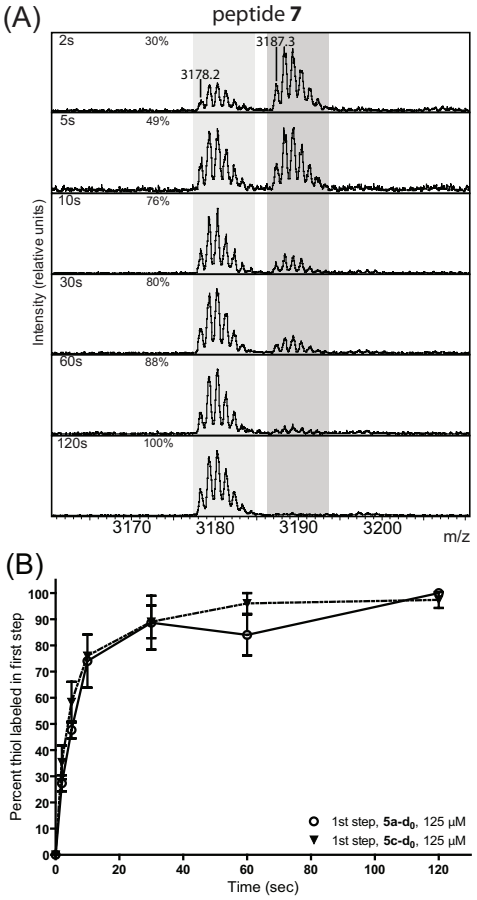

Figure 2.15 Kinetics of reversed-order of probe addition on labeling peptide 6/peptide 7/POPC vesicles (1/1/127).
The vesicles were first labeled with 125 µM **5a-d$_0$** or **5c-d$_0$**, and 2, 5, 10, 30, 60, or 120 s after adding the first probe, 1.25 mM **5a-d$_9$** or **5c-d$_9$**, respectively, was added. (A) Mass spectra of peptide **7** labeled with **5a-d$_0$/5a-d$_9$** at different time points. Intensities are relative to the highest peak in a single spectrum and each panel is not on the same scale. (B) Time courses for the two labeling experiments. Integrated areas under the isotopic envelope were used to calculate percent labeling in the first step for peptide **7**. Errors are standard deviation based on triplicate measurements of three independent labeling experiments.

A factor that could complicate interpretation of the labeling data in the case of the specific hydrophobic peptide used in this study is that, although they adopt a transmembrane topology, it was known from fluorescence experiments that a population of peptides that is too small to be detected orients parallel to the membrane surface and that sampling of this conformation is rapid, in the second time scale (*25*).

The orientation of the cysteine with respect to the aqueous probe containing environment in this conformation depends on whether the α-helical structure is strictly maintained and hydrogen propensity of the midhelix tryptophan, which would be expected to promote a topology in which the Trp faces the aqueous solution. Regardless, the peptides studied are so highly hydrophobic that they should be largely buried within the bilayer when oriented parallel to the membrane surface. Thus, the Cys could remain somewhat buried and the probability that it will be labeled could easily be 100- or 1000-fold lower than the probability that the cysteine in transmembrane-oriented peptide **7** would be labeled.

Combined with the fact that the nontransmembrane topography only exists for a small fraction of the time that the transmembrane topography is present, labeling of nontransmembrane oriented peptide is expected to make a minor contribution to the labeling in the presence of lipid vesicles. Alternatively, the peptide may simply flip about the center of mass, although this mechanism may be more energentically costly due to burying two sets of charged residues in the membrane simultaneously. Our present experiments cannot distinguish between these two mechanisms.

Nevertheless, the interchange between transmembrane and nontransmembrane topographies (Figure 2.16) did affect the labeling studies in another way. We found that over 90% of peptide **7** could be labeled in intact POPC vesicles within one minute. This strongly suggests that the orientation of the peptide parallel to the lipid bilayer allows flipping of the peptide cysteine orientation. That is, peptides with the cysteine facing the inside of the vesicle rapidly flip so as to reorient the cysteine to the outer bilayer, and vice versa. Through this flipping mechanism, the entire population of peptide **7** cysteine is accessible to probe labeling, regardless of the initial peptide orientation.

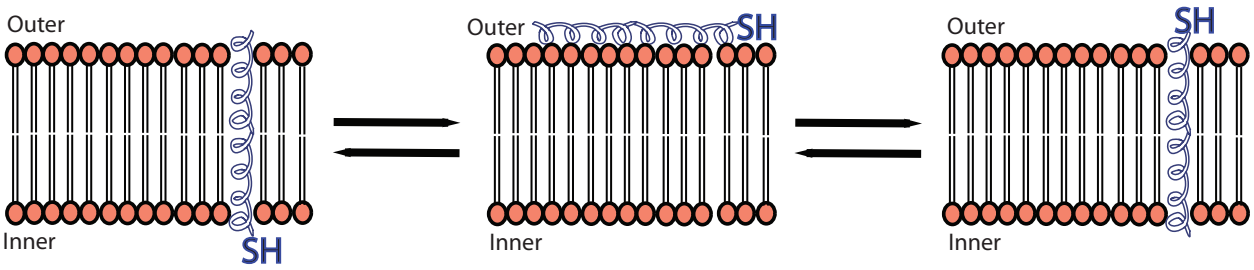

Figure 2.16 Schematic diagram of the proposed equilibrium of transmembrane peptide in lipid bilayers.
The equilibra representation show how the orientation of an inward cysteine in bilayer flips outward the bilayer with an intermediate parallel orientation with the membrane. This figure was adapted from Ren J. et al. (*25*), and was made with Adobe Illustrator CS3.

This process was readily monitored by adjusting our labeling protocol (Figure 2.12). We rapidly dilute the first reagent (heavy probe) by addition of an excess of the second probe (light probe). Then, the vesicles were lysed in order to label any inaccessible cysteine. Through this modified procedure, we observed the flipping of peptide **7**. Under the conditions of this experiment, the labeling kinetics are determined by both the probe labeling rate and the peptide flipping rate. This modified procedure is generally useful for the case in which peptides flip rapidly or proteins are peripherally associated with the membrane. It simplifies the labeling experiment because it eliminated the requirements to quench maleimide remaining from the first labeling step and to remove the quenching reagent before addition of the second probe.

2.7 Membrane can regulate accessibility to cysteine

To further investigate the effects of different lipid membrane compositions on peptide dynamics, we utilized the same kinetic labeling scheme outlined in Figure 2.12 with peptide **7**/POPC/cholesterol (1/60/20) and peptide **7**/POPC/cholest-4-en-3-one (1/60/20) lipid vesicles with probe **5a**. The introduction of cholesterol or cholest-4-en-3-one reduced both the initial rate of labeling, as well as the peptide flip rate (Figure 2.17A, Table 2.1). The labeling rate was reduced about 3-fold. Moreover, a population of peptide thiols remained inaccessible to probe when cholesterol was included in the lipid bilayer.

When the same comparison was performed with peptide **8**, 4-fold and 2-fold reductions in the rate of peptide labeling in the presence of cholesterol and cholest-4-en-3-one respectively were observed (Figure 2.17B, Table 2.1). Therefore, the relative changes in peptide labeling and flipping rates are independent of the position of thiol and are a consequence of lipid composition that influences bilayer structure.

The hydrophobic thicknesses of different types of lipid bilayers have been studied experimentally and computationally (*19, 160-163*). POPC has a 16-carbon saturated fatty acid and an 18-carbon fatty acid with one *cis* double bond on the glycerol backbone. The theoretically and experimentally determined hydrophobic thickness of POPC is 26 – 27 Å (*19, 160, 161*). Peptide **7** and peptide **8** are derived from pLeu19 transmembrane peptide, and the length of central stretch is about 30 Å. Hence, incorporation of peptide **7** and peptide **8** in POPC lipids should not cause any significant positive or negative mismatch. The 4-fold reduced labeling rate of peptide **8** compared to peptide **7** can be explained as the more accessible cysteine of peptide **7** to the probe. This result demonstrates that relative position of cysteine residues in model lipid vesicles can be identified by this method.

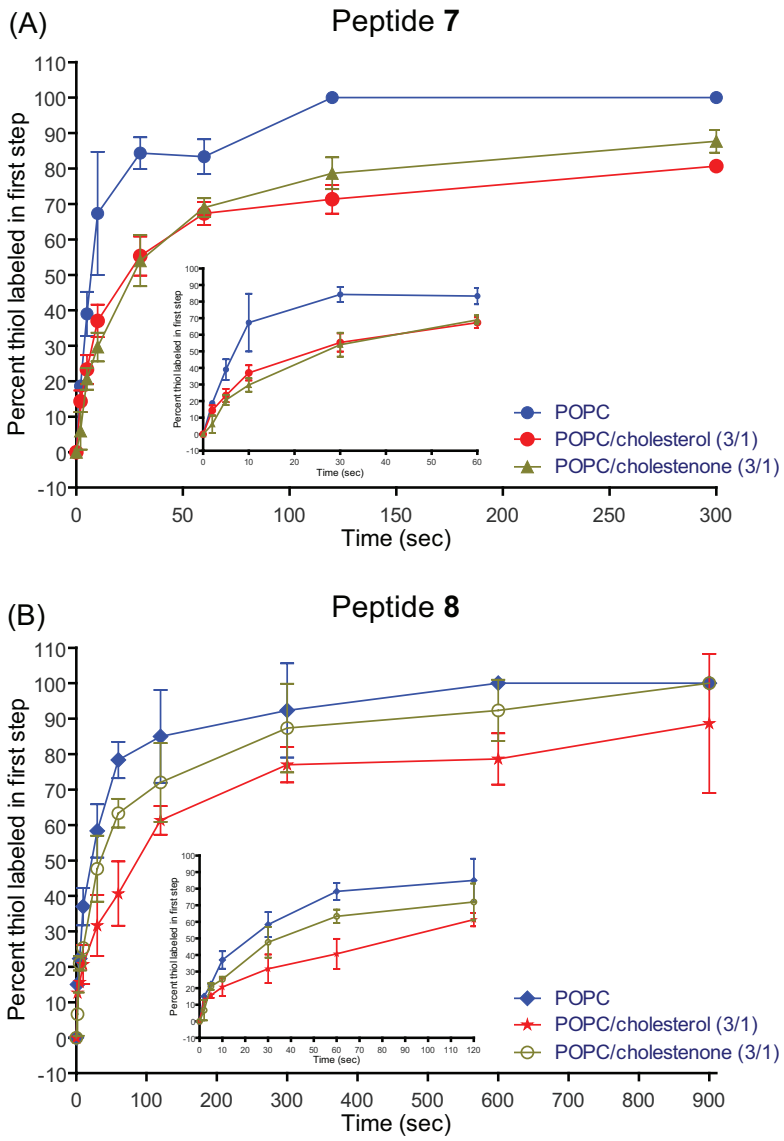

Figure 2.17 Kinetics of labeling peptide 7 and peptide 8 in various lipid compositions.
Peptide **7**/POPC (1/80), peptide **7**/POPC/cholesterol (1/60/20), peptide **7**/POPC/cholest-4-en-3-one (1/60/20), peptide **8**/POPC (1/80), peptide **8**/POPC/cholesterol (1/60/20), peptide **8**/POPC/cholest-4-en-3-one (1/60/20) vesicles were first labeled with 125 or 250 μM **5a-d$_9$** for peptide **7** and peptide **8** vesicles, respectively, and 2, 5, 10, 30, 60, or 120, 300, 600 and 900 s after adding the first probe, 1.25 or 2.50 mM **5a-d$_0$** for peptide **7** and peptide **8** vesicles, respectively, was added. (A) Time courses for peptide **7** labeling experiments. Inserted figure is a magnification of the first 60 s. (B) Time courses for peptide **8** labeling experiments. Inserted figure is a magnification of the first 120 s. Errors are standard deviation based on triplicate measurements of three independent labeling experiments.

Table 2.1 Relative rate of the transmembrane peptide labeling in different lipid compositions.[a]

Peptide/lipid	Time to label 50% (s)	[**5a-d$_9$**] (μM)	$1/t_{50}\times$[probe] ($M^{-1}s^{-1}$)
Peptide **7**/POPC (1/80)	7 ± 2	125	1081 ± 234
Peptide **7**/POPC/cholesterol (1/60/20)	25 ± 6	125	316 ± 72
Peptide **7**/POPC/cholest-4-en-3-one (1/60/20)	27 ± 5	125	292 ± 53
Peptide **8**/POPC (1/80)	24 ± 7	250	169 ± 47
Peptide **8**/POPC/cholesterol (1/60/20)	84 ± 19	250	48 ± 11
Peptide **8**/POPC/cholest-4-en-3-one (1/60/20)	35 ± 11	250	116 ± 38

[a]Time to label 50% thiol on peptide in different lipid compositions at different probe concentrations is reported. The reciprocal of the time to label 50% thiol multiplied by probe concentration used in the first step is calculated. This value should be proportional to the average rate constant over the 50% of the reaction. Errors are standard deviation based on triplicate measurements with three independent labeling experiments.

Cholesterol is an abundant sterols in mammalian membranes, and it has been shown that the presence of cholesterol increases membrane thickness (*164*). The thickness increases by 4.1 Å upon addition of 30 mol % cholesterol to POPC lipid (*161*). Likewise, the hydrophobic thickness increases upon addition of 25 mol % cholesterol in system, and the accessibility of cysteine to the probe is affected to some extent. The labeling rate of both peptide **7** and peptide **8** decreased in POPC/cholesterol vesicles.

An interesting phenomenon was observed when cholest-4-en-3-one was added to POPC. Cholest-4-en-3-one is the product of cholesterol oxidation and isomerization catalyzed by cholesterol oxidase. Cholest-4-en-3-one causes membranes to become leaky (*82*). The effects of cholest-4-en-3-one on membrane structure are mainly the lateral expansion of the lipid bilayer, and the increase in disorder of the membrane state (*82, 165*). The increased thickness of membrane also causes cysteine of the transmembrane peptide to be less accessible to the probe, and thus reduces the labeling rate of peptide **7** and peptide **8** in some extent. The labeling rate of peptide **7** in POPC/cholesterol is not distinguishable from that of peptide **7** in POPC/cholest-4-en-3-one vesicles. Nevertheless, labeling rate of peptide **8** in POPC/cholest-4-en-3-one is 3-fold

of magnitude faster than that in POPC/cholesterol. The differences are probably due to combined effects of membrane thickness change and disorder physical state of membrane. The presence of cholesterol is proved to alter membrane physical state from gel-like or liquid-disorder lipids to form a liquid-order state, and the extent of changes is regulated by the mole % of cholesterol in the membrane (*166*). Cholest-4-en-3-one in lipids is known to cause membrane disordered state, but the effects of its addition to lipids are not systematically and extensively studied. The labeling rate of peptide **7** and peptide **8** in POPC and sterol containing POPC vesicles might also be affected by the physical state of the membranes. These comparisons of peptide **7** in POPC and DPPC with various cholesterol and cholest-4-en-3-one compositions will be discussed in the next section.

2.8 ICMT monitoring of peptide flip rate in fluid and gel state membrane with various compositions of cholesterol and cholest-4-en-3-one

In addition to the comparison of peptide labeling and flipping rate using peptide **7** and peptide **8** in POPC and POPC/cholesterol (3/1), we also prepared vesicles of peptide **7** incorporated in different compositions of cholesterol and cholest-4-en-3-one in POPC and DPPC lipids. Peptide **7**/POPC/cholesterol (1/76/4), peptide **7**/POPC/cholesterol (1/68/12), peptide **7**/POPC/cholesterol (1/44/36), peptide **7**/POPC/cholest-4-en-3-one (1/76/4), peptide **7**/POPC/cholest-4-en-3-one (1/68/12), peptide **7**/POPC/cholest-4-en-3-one (1/44/36), peptide **7**/DPPC/cholesterol (1/64/16), peptide **7**/DPPC/cholesterol (1/48/32), peptide **7**/DPPC/cholest-4-en-3-one (1/64/16), and peptide **7**/DPPC/cholest-4-en-3-one (1/48/32) vesicles were prepared, and we used the same protocol to label peptide **7** in different lipid compositions. The relative rates of transmembrane peptide in different lipid compositions are listed and plotted in Table 2.2 and Figure 2.18. POPC is in the fluid state (l_d) at 30 °C, and its physical state behavior is altered by the addition of cholesterol to the lipid (*166*). The labeling rates of peptide **7** in pure POPC and POPC/cholesterol (95/5) vesicles did not differ significantly, while the labeling rate decreased in POPC/cholesterol (85/15), POPC/cholesterol (75/25), and POPC/cholesterol (55/45) vesicles. The rate was nearly 2-fold, 3-fold, and 8-fold slower in POPC/cholesterol (85/15), POPC/cholesterol (75/25) and POPC/cholesterol (55/45) vesicles than that in pure POPC vesicles (Figure 2.18A). When different mole fractions of cholest-4-en-3-one were added to POPC vesicles, a similar trend of decreasing labeling in vesicles with increasing mol % of cholest-4-en-3-one was observed. The labeling rates are very similar in POPC, POPC/cholest-4-en-3-one (95/5), and POPC/cholest-4-en-3-one (85/15) vesicles. However, the labeling rates are somewhat faster in the POPC vesicles containing higher mole percent (45%) of cholest-4-en-3-one (Figure 2.18A).

Table 2.2 Relative rate of the transmembrane peptide labeling in different lipid compositions.[a]

Peptide/lipid	Time to label 50% (s)	[**5a-d$_9$**] (μM)	$1/t_{50}\times$[probe] ($M^{-1}s^{-1}$)
Peptide **7**/POPC (1/80)	7 ± 2	125	1081 ± 234
Peptide **7**/POPC/cholesterol (1/76/4)	4 ± 0.1	250	1026 ± 26
Peptide **7**/POPC/cholesterol (1/68/12)	6 ± 2	250	690 ± 273
Peptide **7**/POPC/cholesterol (1/60/20)	25 ± 6	125	316 ± 72
Peptide **7**/POPC/cholesterol (1/44/36)	32 ± 4	250	125 ± 14
Peptide **7**/POPC/cholest-4-en-3-one (1/76/4)	4 ± 0.4	250	976 ± 95
Peptide **7**/POPC/cholest-4-en-3-one (1/68/12)	4 ± 0.5	250	976 ± 119
Peptide **7**/POPC/cholest-4-en-3-one (1/60/20)	27 ± 5	125	292 ± 53
Peptide **7**/POPC/cholest-4-en-3-one (1/44/36)	10 ± 0.7	250	412 ± 30
Peptide **7**/DPPC (1/80)	24 ± 3	455	90 ± 11
Peptide **7**/DPPC/cholesterol (1/64/16)	62 ± 7	250	64 ± 7
Peptide **7**/DPPC/cholesterol (1/48/32)	28 ± 2	250	144 ± 11
Peptide **7**/DPPC/cholest-4-en-3-one (1/64/16)	22 ± 5	250	180 ± 37
Peptide **7**/DPPC/cholest-4-en-3-one (1/48/32)	20 ± 2	250	197 ± 19

[a]Time to label 50% thiol on peptide in different lipid compositions at different probe concentrations is reported. The reciprocal of the time to label 50% thiol multiplied by probe concentration used in the first step is calculated. This value should be proportional to the average rate constant over the 50% of the reaction. Errors are standard deviations based on triplicate measurements with three independent labeling experiments.

The labeling rates in DPPC series vesicles are obviously slower than that in POPC series vesicles. We prepared peptide **7**/DPPC/cholesterol (1/64/16), peptide **7**/DPPC/cholesterol (1/48/32), peptide **7**/DPPC/cholest-4-en-3-one (1/64/16), and peptide **7**/DPPC/cholest-4-en-3-one (1/48/32) vesicles, and the same protocol was used to label peptide **7**. The relative rates are listed in Table 2.2. In the cholesterol containing DPPC vesicles, the rate is similar in pure DPPC

and DPPC/cholesterol (80/20) vesicles, and the rate in DPPC/cholesterol (60/40) vesicle is about 2-fold faster than the rate in DPPC vesicle. However, in cholest-4-en-3-one contained DPPC vesicles, there is almost no difference of labeling rate in DPPC with 20 or 40 mol % cholest-4-en-3-one vesicles, and it is roughly 2-fold faster than in pure DPPC vesicle (Figure 2.18B).

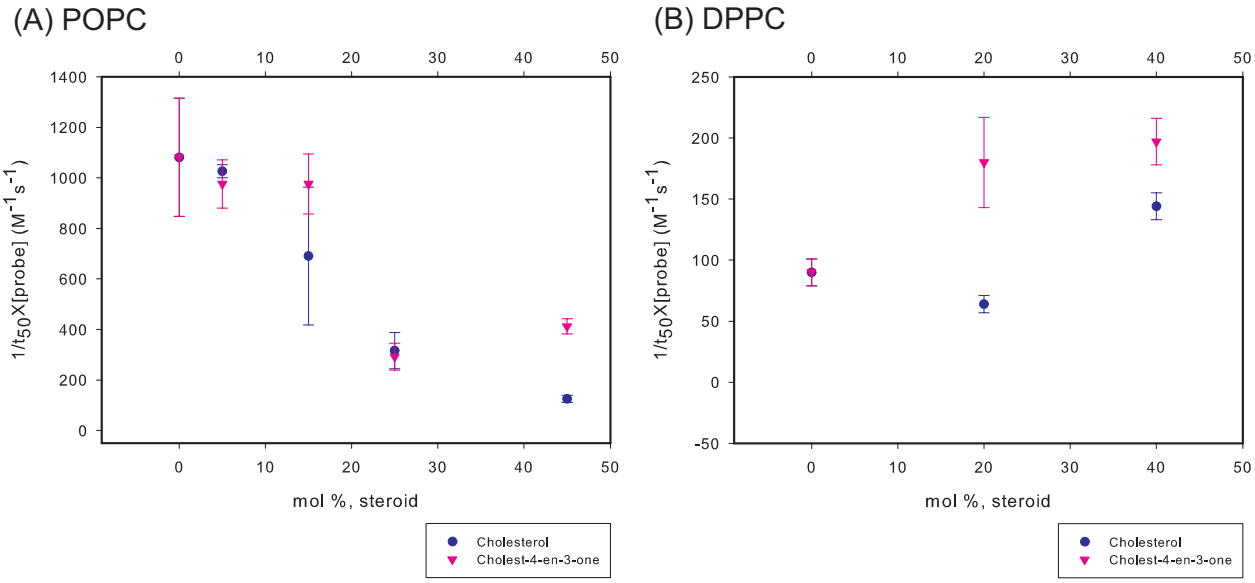

Figure 2.18 Relative rates of peptide 7 labeling at various mole fractions of cholesterol and cholest-4-en-3-one in POPC and DPPC vesicles.
(A) Relative labeling rate of peptide **7** in POPC vesicles. (B) Relative labeling rate of peptide **7** in DPPC vesicles. The plotted data are from Table. 2.2.

The peptide **7** labeling rates in DPPC vesicles are 10-fold slower than the rates in POPC vesicles. The lipid bilayer thicknesses of POPC and DPPC are 27 and 26.7 Å, respectively, (*19*) and the hydrophobic stretch of peptide **7** is about 30 Å in length. When transmembrane peptide **7** spans on POPC or DPPC bilayer, the cysteine thiol is accessible to the solvent and probes.

The explanation for the slower labeling rate in DPPC vesicles is probably due to the nature of the physical state of the lipids. The transition temperatures (T_m) of POPC and DPPC are -2 and 41 ^oC, respectively, and all labeling experiments were performed at 30 ^oC. Therefore, the vesicles of POPC and DPPC are in the liquid-disordered state (l_d) and in the gel state (s_o), respectively. Peptide flipping is slower in the gel state (s_o) than in the liquid-disordered state (l_d).

The physical state of lipids are altered upon addition of cholesterol, and increased cholesterol causes different shifts in phase behavior in the gel versus the fluid state (*166*).

Generally, addition of cholesterol to the fluid state lipid (fatty acid chains with un-saturated double bonds) will cause a phase transition from liquid disordered state (l_d) to liquid-ordered state (l_o). The packing of hydrocarbon fatty acid chains is not ordered, and the addition of cholesterol to organizes the packing. In contrast, the ordered packing in the gel state (s_o) is disordered by the addition of cholesterol. The disordered behavior represents a phase transition from the gel state (s_o) to the liquid-ordered state (l_o). The phase diagrams for cholesterol/POPC (*167*) and cholesterol/DPPC (*168*) mixtures are shown in Figure 2.19. The POPC and POPC/cholesterol (95/5) vesicles are liquid-disordered state (l_d), and the POPC/cholesterol (85/15) and POPC/cholesterol (75/25) vesicles are mixed liquid-disordered state (l_d) and liquid ordered state (l_o), and POPC/cholesterol (55/45) vesicles are liquid-ordered state (l_o) (Figure 2.19A). The labeling rates are faster in liquid disordered (l_d) lipid vesicles. The labeling rates decrease as the amount liquid-ordered state (l_o) increases. Addition of increasing amount of cholest-4-en-3-one to POPC vesicles also resulted in a decrease in labeling rate (Figure 2.18A). Therefore, peptide **7** in POPC/cholesten-4-en-3-one mixtures was always labeled at rates equal to or faster than peptide **7** in POPC/cholesterol mixtures (Figure 2.18A).

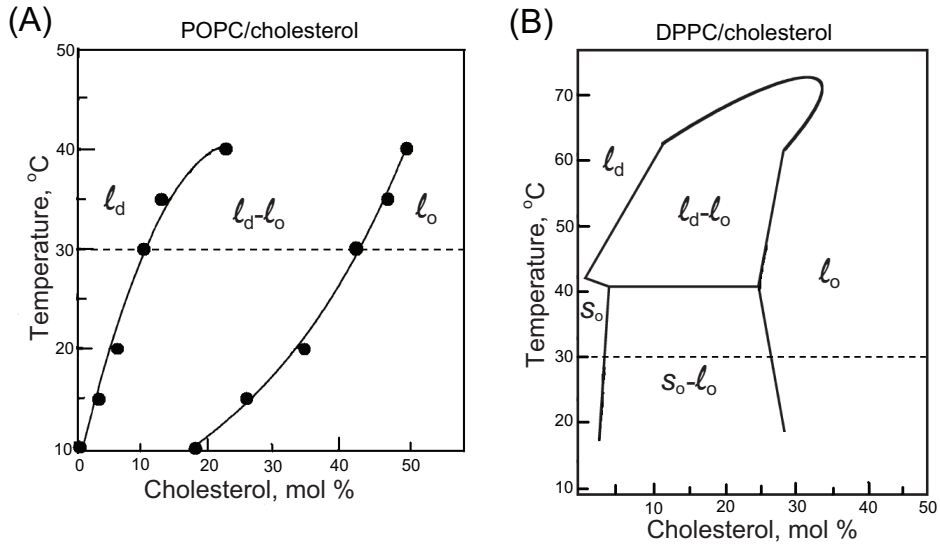

Figure 2.19 Temperature-composition phase diagram of the phospholipid-cholesterol system.
(A) POPC/cholesterol. (B) DPPC/cholesterol. The phase diagrams were based on the experimental data for POPC/cholesterol (*167*) and DPPC/cholesterol (*168*). The dash line represents the temperature (30 °C) at which labeling experiments were performed. s_o: gel state, ℓ_d: liquid-disordered state, ℓ_o: liquid-ordered state. These diagrams are adapted from Mateo, CR et al. (*167*) for POPC/cholesterol system and Sankaram, MB et al. (*168*) for DPPC/cholesterol system, and were made with Adobe Illustrator CS3.

Addition of cholesterol to DPPC vesicles causes a phase transition change from the gel state (s_o) for pure DPPC vesicle, to mixed states of gel state (s_o) and liquid-ordered state (l_o) for DPPC/cholesterol (80/20) vesicles, to liquid-ordered state (l_o) for DPPC/cholesterol (60/40) vesicle at 30 ^oC (Figure 2.19B). The labeling rates of peptide **7** increase with increasing liquidity of the membrane. The magnitude of the peptide **7** labeling rate is not as great in DPPC vesicles as in POPC/cholesterol vesicles. Peptide **7** in both DPPC/cholest-4-en-3-one (80/20) and DPPC/cholest-4-en-3-one (60/40) vesicles has almost the same rate increase compared to peptide **7** in DPPC vesicles (Figure 2.18B). Interestingly, if we compare the rates of labeling peptide **7**/POPC/cholesterol (1/44/36) to peptide **7**/DPPC/cholesterol (1/48/32) vesicles (Figure 2.18A & B), they are similar. Both types of vesicles are in the liquid-ordered state (l_o), suggesting that the peptide labeling is mainly determined by the physical state of the lipids despite the position of the cysteine in the headgroup region of the lipid bilayer. Our data suggest that lateral mobility of lipids is important for cysteine accessibility to the probe.

2.9 ICMT detection of peptide flip rate in anionic lipids

To further investigate the effects of lipid headgroup, especially anionic headgroup, on peptide labeling and flipping rate, we incorporated peptide **7** in DOPC, DOPC/cholesterol (3/1), DOPS, DOPG, and DOPC/DOPE (1/1) vesicles. The transition temperatures (T_m) of DOPC, DOPS, DOPG, and DOPE range from -11 °C – -18 °C. Therefore, at the peptide labeling temperature, 30 °C, all the lipids will exist in a liquid disordered state (l_d). We applied the same labeling protocol outlined in Figure 2.12, and the results of peptide **7** labeling in these various lipids are listed and plotted in Table 2.3 and Figure 2.20.

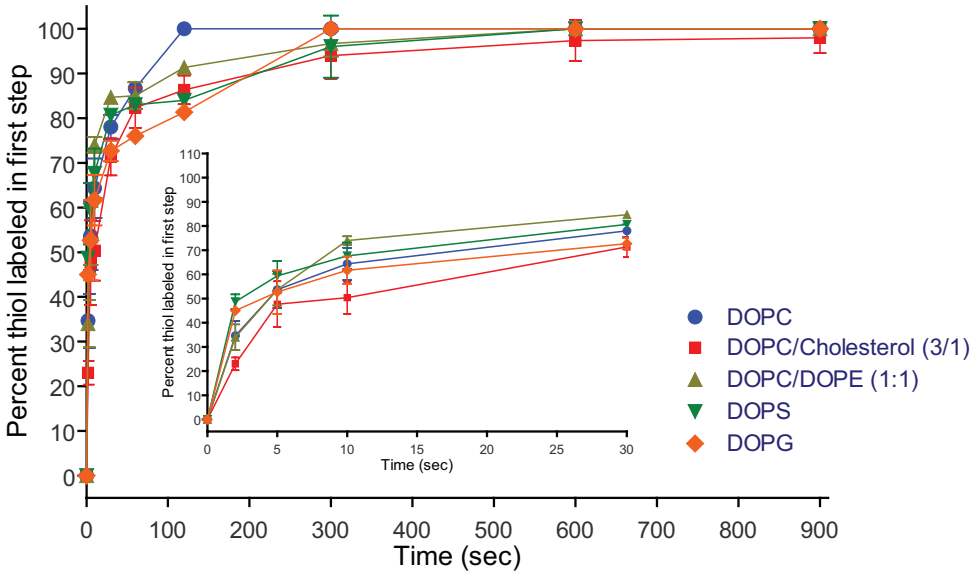

Figure 2.20 Kinetics of labeling peptide 7 in various type of zwitterionic and anionic lipid vesicles. Peptide **7**/DOPC (1/80), peptide **7**/DOPC/cholesterol (1/60/20), peptide **7**/DOPC/DOPE (1/40/40), peptide **7**/DOPS (1/80), peptide **7**/DOPG (1/80) vesicles were first labeled with 250 μM **5a-d$_9$** for peptide **7** vesicles. After 2, 5, 10, 30, 60, or 120, 300, 600 and 900 s, 2.50 mM of the second probe **5a-d$_0$** was added. Time courses for peptide **7** labeling experiments in different lipid compositions. Inserted figure is a magnification of the first 30 s. Errors are standard deviations based on triplicate measurements of three independent labeling experiments.

Given that both POPC and DOPC lipids are in a liquid-disordered state (l_d) at 30 °C, we expected the labeling rates to be similar when peptide **7** was incorporated. In order to make consistent comparison, we also prepared peptide **7** in DOPC and DOPC/cholesterol (3/1) vesicles. DOPC has two 18-carbon fatty acid chains (oleoyl) with one *cis* double bond, and POPC has an 18-carbon fatty acid chain (oleoyl) with one *cis* double bond and a saturated 16-carbon fatty acid chain (palmitoyl). Although they are in a fluid state at labeling temperature, 30

^{o}C, DOPC should be more fluid than POPC due to its lower T_m. The labeling rate of peptide **7** in DOPC vesicles was found to be slower than the rate of peptide **7** in POPC vesicles (Table 2.1 and Table 2.3). The labeling rates of peptide **7** in DOPC, DOPC/DOPE (1/1) and DOPG vesicles were similar. The labeling rate is nearly 2-fold faster in DOPS vesicles than the rate in DOPC vesicles (Table 2.3). The addition of 25 mol % cholesterol to DOPC vesicles was found to lower the labeling rate nearly 2-fold, and this result is consistent with the labeling rate of peptide **7** in POPC/cholesterol vesicles.

Table 2.3 Relative rate of the transmembrane peptide labeling in different lipid compositions.[a]

Peptide/lipid	Time to label 50% (s)	[**5a-d$_9$**] (μM)	$1/t_{50}\times$[probe] ($M^{-1}s^{-1}$)
Peptide **7**/DOPC (1/80)	5 ± 2	250	769 ± 237
Peptide **7**/DOPC/cholesterol (1/60/20)	8 ± 5	250	519 ± 350
Peptide **7**/DOPC/DOPE (1/40/40)	5 ± 0.9	250	851 ± 163
Peptide **7**/DOPS (1/80)	3 ± 0.8	250	1429 ± 408
Peptide **7**/DOPG (1/80)	5 ± 2	250	800 ± 320

[a]Time to label 50% thiol on peptide in different lipid compositions at different probe concentrations is reported. The reciprocal of the time to label 50% thiol multiplied by probe concentration used in the first step is calculated. This value should be proportional to the average rate constant over the 50% of the reaction. Errors are standard deviation based on triplicate of three independent labeling experiments.

Anionic lipids were shown to enhance binding of cationic polypeptides to the membrane. (*169, 170*) Peptide **7** is a poly-Leu transmembrane peptide with two lysine residues flanked on both termini. Electrostatic interactions between anionic lipids and cationic residues should have significant contribution to the stabilization of transmembrane (TM) topography (*159*). We expected that the labeling rate of peptide **7** in DOPS and DOPG vesicles should be slower than the labeling rate of peptide **7** in DOPC vesicle due to the negative charge present at pH 7. To our surprise, the labeling rate of peptide **7**/DOPG vesicles was comparable to peptide **7**/DOPC vesicles, while the rate of peptide **7**/DOPS vesicles was nearly 2-fold faster than rate of peptide **7**/DOPC vesicle. DOPE has a positive charge on its headgroup at pH 7, and the labeling rate of peptide **7** incorporated in equal mol % of DOPC/DOPE vesicles showed slightly faster labeling

rate compared to the rate of peptide **7**/DOPC vesicles. DOPE has a smaller headgroup than DOPC, and inclusion of DOPE in DOPC vesicles acts like cholesterol filling the available space surrounding the lipid chains. Therefore, the addition of DOPE to DOPC could increase the mechanical rigidity of fluid bilayers, and could theoretically decrease the labeling rate of peptide **7**. The labeling rate of peptide **7** in DOPC/cholesterol (3/1) vesicles was slower than the labeling rate of peptide **7** in DOPC vesicles, which could be due to decreased membrane fluidity, but the labeling rate of peptide **7** in DOPS vesicles is unexpectedly faster.

We proposed that the electrostatic interactions between an anionic lipid and a cationic residue could not only stabilize the TM configuration of the peptide (*159*) but could also slow down peptide flipping. The labeling results do not agree with this prediction. The transmembrane peptide flips faster in fluid lipids regardless of the charge of the headgroup or the composition of the lipids. The proposed TM topography is shown in Figure 2.21 (*159*). It was proposed that anionic lipids have a greater tendency of binding the membrane and forming a TM configuration. The stability TM configuration (relative to a non-TM configuration, membrane-bound) for lysine flanked transmembrane peptides represents an order: DOPS ≥ DOPG > DOPC ~ POPC > POPC/POPE (1/1) ~ POPC/cholesterol (6/4) (*159*). The rates of labeling of peptide **7** seem to follow this TM stability tendency. Nevertheless, the labeling rate of peptide **7**/DOPC/cholesterol (1/60/20) vesicles is about 2-fold slower than the rate of peptide **7**/DOPC/DOPE vesicles. Thus the peptide flipping is primarily determined by the physical state of the lipid membranes and probably also by the stabilization of TM topography. Other possible explanations are that the headgroup anions are solvated by the ions from bulk buffer solution or that the repulsion of the anions expands of the vesicles, and thus making vesicles more fluid.

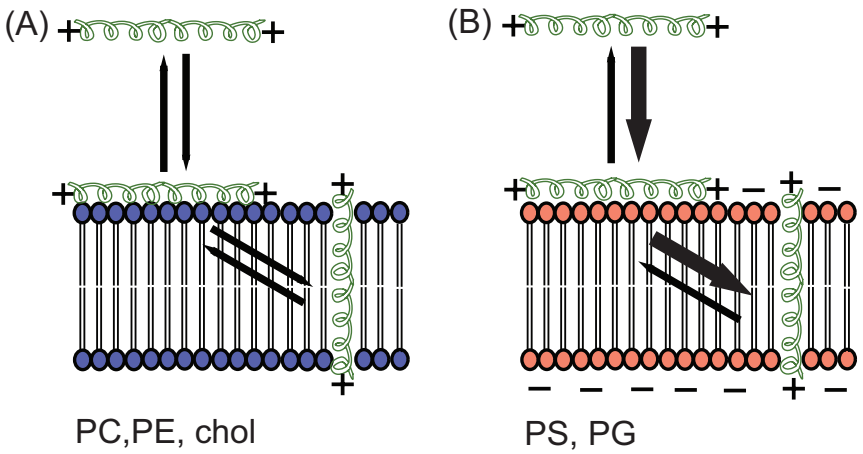

Figure 2.21 Schematic representation of the proposed differences in transmembrane peptide topography in cationic and anionic phospholipids.
This illustration shows the equilibra of the peptides between aqueous state, membrane surface-bound state, and transmembrane-spanning state. (A) Equilibra of TM in cationic phospholipids. (B) Equilibra of TM in zwitterionic phospholipids. This figure was adapted from Shahidullah, K et al. (*159*), and was made with Adobe Illustrator CS3.

2.10 ICMT monitoring of lipid flip rate in fluid and gel state membrane

We tested the ability of the ICMT probes to detect membrane dynamics using unilamellar vesicles that contain a synthetic lipid 1,2-dipalmitoyl-*sn*-glycero-3-phosphatidylthioethanol (PTE) (Figure 2.22). This lipid contains a terminal thiol in the headgroup in place of the amino group typically found in phosphatidylethanolamine (PE). Although phospholipids can move from the outer leaflet to the inner leaflet and *vice versa*, the transverse diffusion rate is usually in the order of hours to days (*171*). Thus, on the time scale of our labeling experiment, which is minutes, the thiolipid PTE should not exchange between leaflets. Assuming that in the vesicles PTE is randomly distributed between the inner monolayer (which has about 45% of the total lipids in 1000 Å vesicles) and outer monolayer (which has about 55% of the total lipids in 1000 Å vesicles), we expected that only 55% of the thiolipid would be labeled in intact vesicles, i.e., in the first labeling step, although introduction of transmembrane peptide or alteration of lipid composition can accelerate flopping rate in membranes (*172-174*).

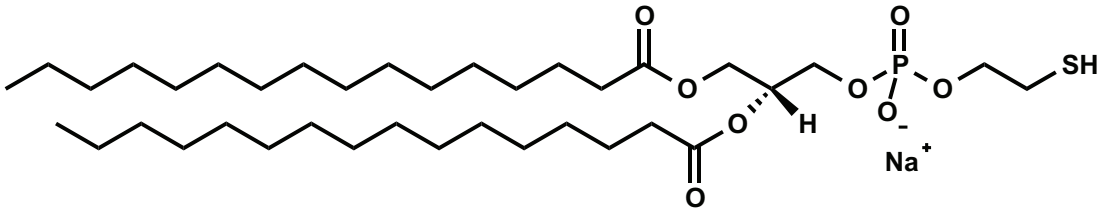

1,2-Dipalmitoyl-*sn*-Glycero-3-phosphothioethanol (PTE)

Figure 2.22 Structure of PTE.
Structure representation of PTE, 1,2-dipalmitoyl-*sn*-3-glycero-3-phosphothioethanol.

We prepared PTE/POPC (2/98), peptide **7**/PTE/POPC (1/1.6/78.4), PTE/DPPC (2/98), and peptide **7**/PTE/DPPC (1/1.6/78.4) vesicles, and performed a two-step labeling of thiolipid and peptide **7**. We compared the rate of thiolipid and peptide **7** labeling (Figure 2.23 & Table 2.4). We found that the rate of thiolipid labeling was about 100−150-fold slower than peptide **7** labeling, suggesting that the physical environment around the thiol of the PTE is quite different from the peptide. It is possible that the PTE pK_a is elevated due to its proximity to the phosphate group.

The initial rate of PTE labeling was reduced 2-3-fold upon changing the lipid composition from one that forms the liquid phase (POPC) to one that forms gel phase (DPPC) (Figure 2.23), consistent with tighter packing of headgroups in the gel phase. Introduction of 1.3

mol % peptide into the lipid bilayer increase the outer lipid labeling rate more than 7-fold. In the case of POPC membranes, the lipid flip rate also increased in the presence of peptide **7**. The change in flip rate can be attributed to decreased order in the bilayer structure upon addition of peptide. This effect was observed previously by de Kruijff and co-workers in 2001 and 2003. (*172, 173*) This change may also reflect an increase in the amount of reactive anionic thiolate in the presence of the peptide (which is cationic), or an increase in the thiol exposure to aqueous solution in the presence of the peptide.

Table 2.4 Relative rate of the transmembrane peptide labeling in different lipid compositions.[a]

Peptide/lipid	Time to label 50% (s)	[**5a-d$_9$**] (μM)	$1/t_{50}\times$[probe] ($M^{-1}s^{-1}$)
Peptide **7**/POPC (1/80)	3 ± 0.6	455	845 ± 195
Peptide **7**/POPC/PTE (1/78.4/1.6)	4 ± 0.6	455	563 ± 87
Peptide **7**/DPPC (1/80)	24 ± 3	455	90 ± 11
Peptide **7**/ DPPC/PTE (1/78.4/1.6)	31 ± 10	455	71 ± 23

[a]Time to label 50% thiol on peptide in different lipid compositions at different probe concentrations is reported. The reciprocal of the time to label 50% thiol multiplied by probe concentration used in the first step is calculated. This value should be proportional to the average rate constant over the 50% of the reaction. Errors are standard deviation based on triplicate measurements of three independent labeling experiments.

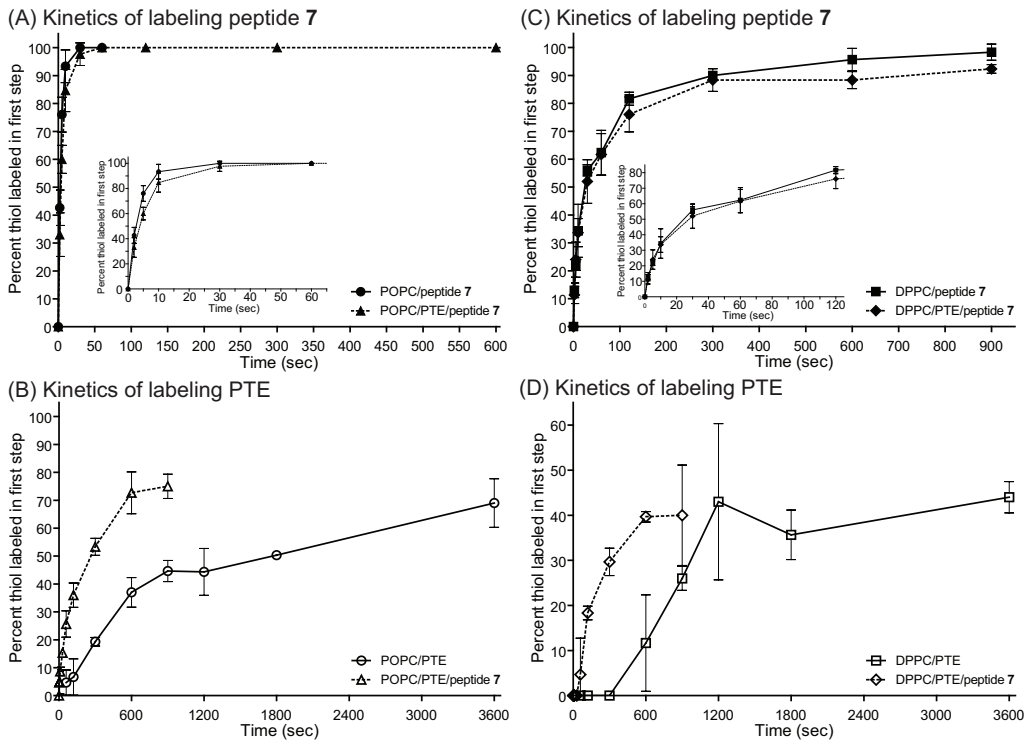

Figure 2.23 Kinetics of labeling peptide 7 in POPC (/PTE) and DPPC (/PTE) vesicles.
Peptide **7**/POPC (1/80), peptide **7**/PTE/POPC (1/1.6/78.4), PTE/POPC (2/98), peptide **7**/DPPC (1/80), and peptide **7**/PTE/DPPC (1/1.6/78.4), and PTE/DPPC (2/98) vesicles were labeled in the following procedures. The vesicles containing peptide **7** were first labeled with 455 mM **5a-d$_9$**, and 2, 5, 10, 30, 60, 120, 300, 600, or 900 s after adding the first probe, 4.55 mM **5a-d$_0$** was added. Samples in which PTE labeling was assayed in the absence of the peptide, labeling was carried out with 250 mM **5a-d$_9$** heavy probe for 1, 2, 5, 10, 15, 20, 30, and 60 min, quenched by 2 mM DTT, lysed with 0.03% Triton X-100, and labeled with 10 mM **5a-d$_0$** light probe for 1 h. (A) Time course for labeling peptide **7** in POPC or PTE/POPC vesicles. Inserted figure is a magnification of the first 60 s. (B) Time course for labeling thiolipid, PTE, in POPC or peptide **7**/POPC vesicles. (C) Time course for labeling peptide **7** in DPPC or PTE/DPPC vesicles. Inserted figure is a magnification of the first 120 s. (D) Time course for labeling of thiolipid, PTE, in DPPC or peptide **7**/DPPC vesicles. Errors are standard deviation based on triplicate measurements of three independent labeling experiments.

Interestingly, despite the fast initial rate of PTE labeling, the extent of labeling after 1 h was much lower than that of the peptide, confirming that the flipping of PTE between leaflets was slower than that of peptide **7** or peptide **8**. In POPC vesicles, there does seem to be an appreciable rate of PTE flip, as shown by the slow increase in reaction over 1 h and the observation that the level of labeling was greater than the 55% expected in the absence of lipid flipping, while in DPPC vesicles, which are in the gel state at 25 °C, PTE flip over hours appears to be negligible. The fact that the final level of PTE labeling was only 40% in DPPC may reflect a nonrandom distribution of PTE in the inner and outer leaflet.

In contrast, to the effect of peptide on lipid labeling, the introduction of 2 mol % thiolipid did not affect the rate of peptide **7** labeling in either POPC or DPPC vesicles (Figure 2.23 & Table 2.4). On the other hand, there was an effect of lipid physical state upon peptide labeling. We observed that incorporation of peptide **7** into gel phase DPPC reduced the initial rate of peptide labeling at least 10-fold. Moreover, the time to 100 % labeling is approximately 30-fold longer. Complete labeling is dependent on both label rate and peptide flip rate. Taken together it appears that the peptide flip rate is about three times slower in the gel phase than in the liquid phase. The decrease in labeling rate may again reflect a decrease in Cys exposure to aqueous solution.

Addition of 25 mole percent of cholesterol to liquid membranes reduced both the peptide labeling and flipping rates. A reduction was also observed upon incorporation of peptide **7** into gel phase membranes. The different membrane phases regulate the flipping rate of transmembrane peptide and our method detects these changes in peptide environment. We attribute the difference in the initial rate of labeling to the lipid structures. Since cholesterol and the gel phase both increase bilayer width they should dcrease Cys accessibility to solvent, which as noted above, showed slow labeling rates. Likewise, our labeling protocol detected changes in thiol lipid environment. These changes may also reflect a change in the burial of the thiol group.

2.11 Triply (^{2}H, ^{13}C, and ^{15}N) labeled wild-type cholesterol oxidase for solution NMR assignment

Uniformly ^{2}H, ^{13}C, and ^{15}N labeled wild-type cholesterol oxidase is required to study the cholesterol oxidase conformational changes in the presence of membrane by solution NMR. To optimize the expression conditions for triply labeled wild-type cholesterol oxidase, four commercially available rich media, BIOEXPRESS, ISOGRO, Silantes, and Spectra, were tested, and the cell growth curves and enzyme activity post IPTG induction were compared to M9 minimal medium.

The optical density of cells was monitored at 600 nm every hour during the growth period (Figure 2.24A). Enzymatic activity starting 12 h after IPTG induction was determined every 2 h for 12 h (Figure 2.24B), and the proteins were analyzed by SDS-PAGE (Figure 2.25).

The cells grew slowly in M9 minimal medium and ISOGRO rich medium, but grew quickly in BIOEXPRESS, Silantes, and Spectra rich media. Cells grown in BIOEXPRESS medium had the highest enzymatic activity, and interestingly, proteins expression in M9 medium yielded comparable enzymatic activity to that expressed in BIOEXPRESS medium. The protein gel (Figure 2.25) also showed that using BIOEXPRESS as medium produced a high concentration of enzyme. Considering the above results, we chose BIOEXPRESS rich medium for expression of triply labeled wild-type cholesterol oxidase.

Upon moving to a larger scale, 500-mL, we found that the growth rate in media was not as fast as that in the trial with unlabeled media. The culture took 12 h to reach an $OD_{600\ nm}$ of 1.35. Enzymatic activity was monitored starting 25 h after IPTG induction at 28 ^{o}C every 3 h for 9 h. After a total of 34 h of IPTG induction, the culture temperature was lowered to 18 ^{o}C for another 16 hours. The enzymatic activity did not decrease significantly before harvesting the cells, and the protein purification was carried out following existing methods.

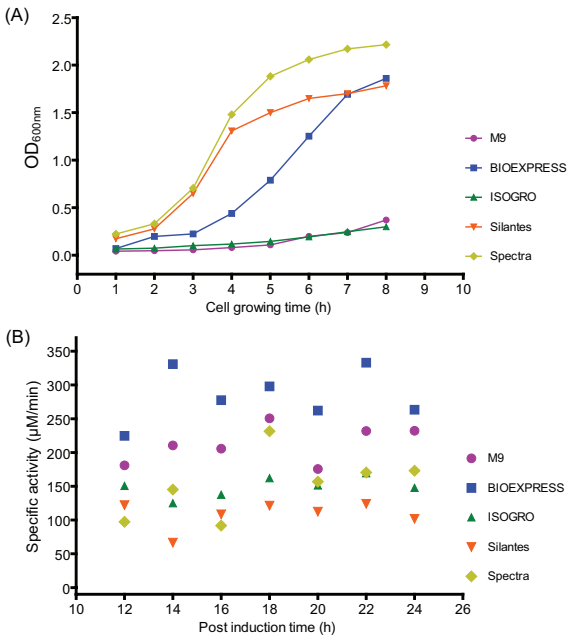

Figure 2.24 Time course of BL21(DE3)pLysS cell growth and cholesterol oxidase activity post IPTG induction.

(A) Time course of cell growth in BIOEXPRESS, ISGRO, Silantes, Spectra rich media, and M9 minimal medium. Cells were grown in 50 mL media, and 1 mL of cell cultures was aliquoted for optical density measurements at 600 nm. (B) Cholesterol oxidase activity from 12 to 24 h post IPTG induction. A 1 mL cell culture was harvested, and lysed by 5 freeze-and-thaw cycles. The supernatant was subsequently assayed in 50 mM sodium phosphate, pH 7, containing 0.025% (w/v) Triton X-100, 0.02% (w/v) BSA, and 0.45 mM cholesterol in 2% (v/v) isopropanol at 37 ^{o}C. These experiments are done once.

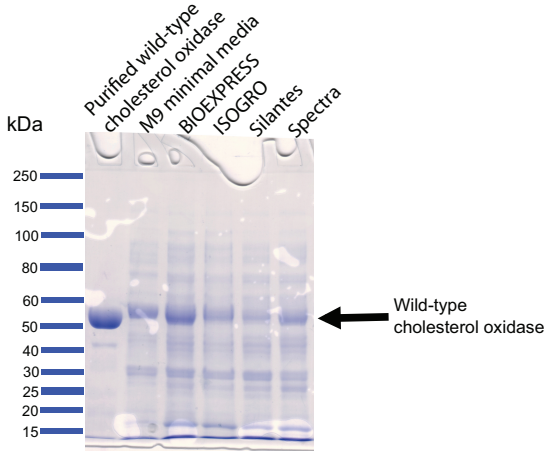

Figure 2.25 SDS-PAGE analysis of cholesterol oxidase expression trials in different growth media.

Protein expressed in M9 minimal medium, BIOEXPRESS, ISOGRO, Silantes, and Spectra rich media were compared. Cells (2 mL) were harvested 18 hours post IPTG induction, lysed, and proteins analyzed by SDS-PAGE.

The UV/vis absorption spectrum of purified triply-labeled wild-type ChoA (Figure 2.26) is similar to that of the unlabeled wild-type enzyme. Typically, there are three absorption peaks for this enzyme at 280, 391, and 468 nm in the UV/vis spectrum. The 280 nm peak is due to protein absorption and the other two peaks, are cofactor FAD absorption. The ratios of A_{280nm}/A_{391nm} and A_{280nm}/A_{468nm} are 10.5 and 11.5 respectively, and these values are identical to unlabeled wild-type cholesterol oxidase (*105*). The yield of triply labeled wild-type cholesterol oxidase was 34 mg from 500 mL BIOEXPRESS media. The purified triply labeled proteins were sent to our collaborator, Dr. Patrick Loria at Yale University, who used this enzyme for NMR experiments. A preliminary 2D TROSY-HSQC spectrum of triply labeled wild-type ChoA is given in Figure 2.27.

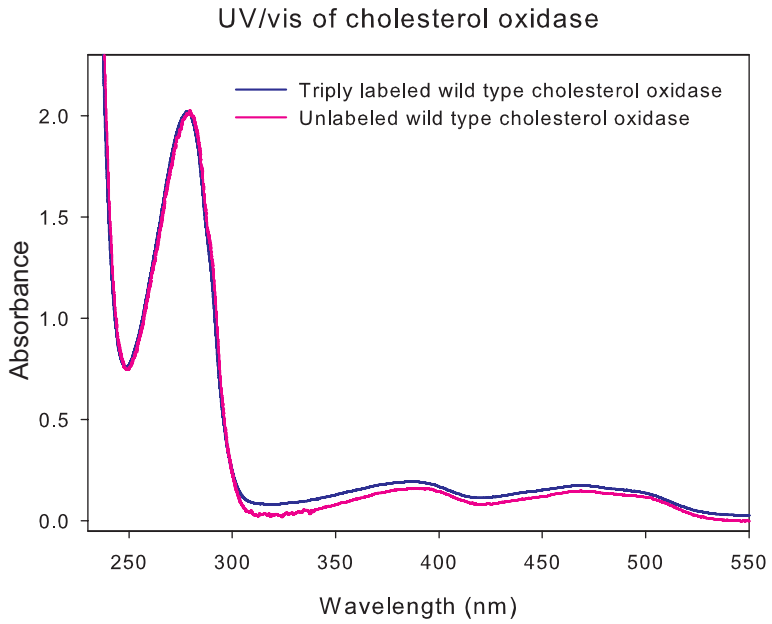

Figure 2.26 UV/vis spectra of triply ^{2}H, ^{13}C, and ^{15}N labeled and unlabeled wild-type cholesterol oxidase.
The 280 nm peak is the protein absorption maximum, and peaks at 391 and 468 nm are FAD absorption maxima. Spectra were normalized at 280 nm. Spectra is shown from 230 nm to 550 nm.

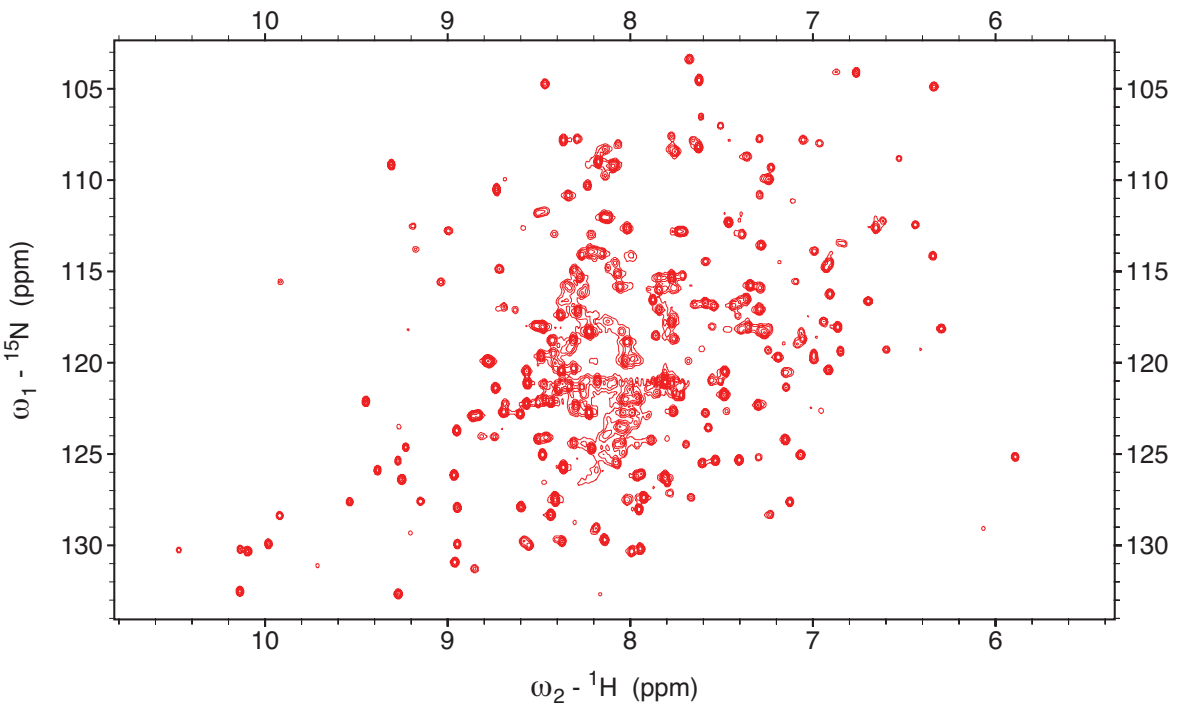

Figure 2.27 2D (^{1}H-^{15}N) TROSY-HSQC (600 MHz) spectrum of ^{2}H, ^{13}C, and ^{15}N labeled wild-type cholesterol oxidase.
This spectrum was adapted from collaborator, Dr. Nicolas Doucet and Prof. Patrick Loria, Department of Chemistry, Yale University.

In order to investigate what the the protein structure is altered upon interacting with membrane, NMR experiments in conjunction with mass-spectrometry-based ICMT were utilized. 2D and 3D NMR experiments were performed using triply labeled (^{2}H, ^{13}C, and ^{15}N) protein. The protocol for expressing isotopically labeled proteins is the same as that for un-labeled proteins. In previous M9 minimal medium expression protocol, cells had to be grown gradually in 50% D_2O, 70% D_2O, and finally 100% D_2O. The cell growth rate in M9 minimal medium was very slow. It took 14 h to reach mid-log phase in 70% D_2O, and the final yield of the triply labeled protein was only 2.6 mg per liter in M9 minimal media (*105*). Therefore, we tried to express the wild-type enzyme using rich media. Although it cost much more to use rich media, there was a great improvement using BIOEXPRESS rich medium in protein yield (33.5 mg/500 mL culture). Based on these considerations, expressing uniformly labeled protein in isotopically labeled rich media saved time, simplified purification, produced more proteins and was economical. The growth curves using rich media were similar to regular media, such as 2xYT medium. However, the critical determinant for selecting media was enzyme activity in the

culture. Wild-type cholesterol oxidase expressed in BIOEXPRESS media always had the highest specific activity. Although enzyme activity in M9 media had comparable high activity as well, the slow growth rate diminished its advantage. Thus, all considerations taken together, BIOEXPRESS was chosen for the production of triply labeled wild-type cholesterol oxidase.

2.12 Design and expression of cholesterol oxidase mutants

2.12.1 Construction of single cysteine mutants

Given that a large quantity of enzyme might be required for the ICMT approach, we tested protein expression efficiency with different plasmids carrying cholesterol oxidase. Plasmids pCO117 and pCO202 carrying wild-type cholesterol oxidase, pCO247 carrying the L80C mutant enzyme, and pCO273 carrying L80C/4CA (4CA: C56A, C282A, C445A and C452A) enzyme were transformed into BL21(DE3)pLysS cells and cultured in LB media. The plasmids used for wild-type cholesterol oxidase expression, pCO117 and pCO202, are derivatives of pKK223-3 and pUC19, respectively. Plasmid pCO247 carrying the L80C mutant in a pUC19 vector, and plasmid pCO273 carrying L80C/4CA mutant in a pET20b vector were used. A comparison of protein expression level was made with a small-scale cell cultures. pCO117 provides robust expression of wild-type cholesterol oxidase, and it gave higher expression yields than pCO202. The vector pKK223-3 has a strong *tac* promoter and strong *rrnB* ribosomal terminator, and derivatives give higher protein expression levels. However, this vector has a low copy number, and protein engineering in this plasmid is not as convenient. Plasmid pCO202 encoding wild-type cholesterol oxidase and pCO247 encoding L80C cholesterol oxidase are from pUC19 vector. This vector also has a *tac* promoter, but is missing the ribosomal terminator, and does not give as robust protein expression levels as the pKK223-3 vector.

We chose the pCO117 plasmid as a template for all subsequent PCR and cloning experiments. L80C, L274C, and W333C were useful mutants for fluorescence experiments in previous studies (*107*). All these mutants were sub-cloned into pCO117 using the *Xho*I to *Mlu*I restriction sites. The identity of the plasmid products was verified by *Hind*III restriction digest and by DNA sequencing.

2.12.2 Design and construction of multi-cysteine mutants

In order to introduce multiple cysteines into a single mutant protein, possible mutation sites on the solvent accessible surface of *Streptomyces sp.* SA-COO cholesterol oxidase (PDB entry 1MXT) were identified. Alanine, serine, and threonine residues were chosen as potential mutation sites because they are structurally similar and represent possible conservative mutations that will minimize disturbance of protein structural integrity. We aimed to introduce as many as

4 cysteine residues on the protein surface in a single protein, whilst also maintaining protein activity. From the selected 31 solvent exposed residues, we measured the distance from the Cα1 to Cα2 of the residues. In order to prevent formation of disulfide bonds, cysteine residues were introduced with a distance greater than 10 Å between each mutation. The *in silico* protease digestion pattern by trypsin and chymotrypsin was examined to assure that no more than two mutations were present on the same digested peptide. Another consideration for residue selection was dispersion across the protein surface, in order to get the highest interface scanning coverage. We chose 16 residues to introduce cysteine mutations. The multi-cysteine mutants are as follows (Figure 2.28): **mut1**, A32C/S129C/T371C/A423C, **mut2**, S153C/A205C/S312C/T435C, **mut3**, T168C/A276C/A301C/T394C, **mut4**, A184C/T239C/A407C/A465C, **mut5**, A32C/T168C/S312C/A465C and **mut6**, A184C/T239C/A301C/T394C. **Mut5** and **mut6** have a subset of the same cysteine mutations present in **mut1** – **mut4**. These mutants were prepared as controls for the possible perturbing effects of mutations on protein structure.

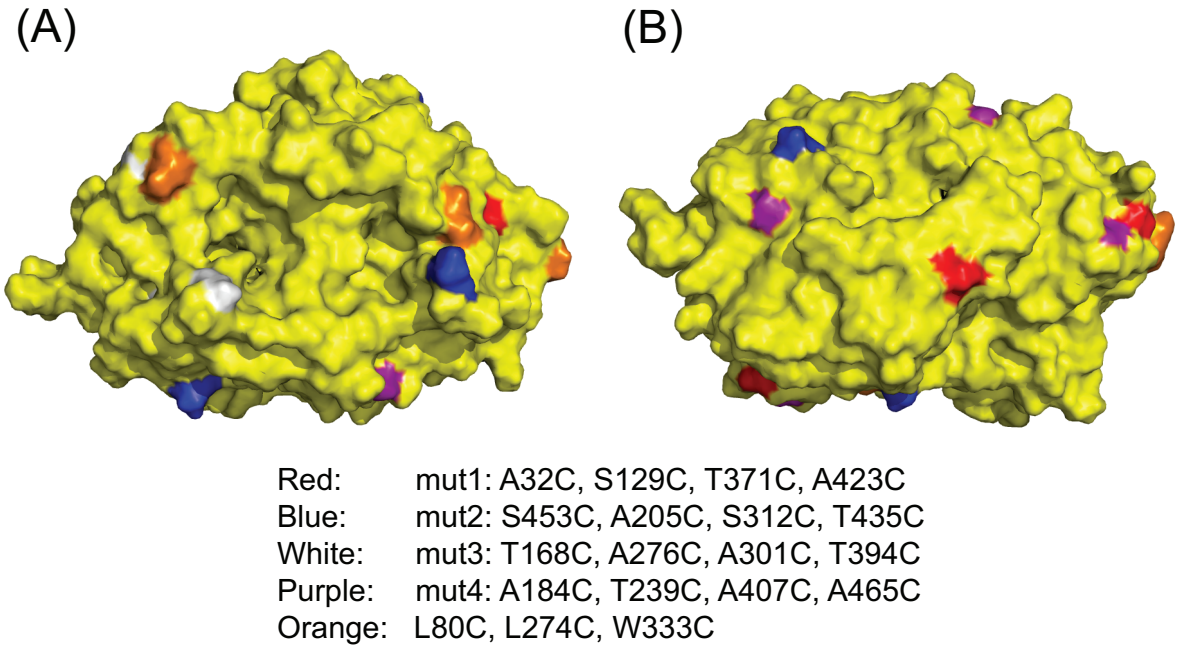

Figure 2.28 Representation of 19 cysteine mutations on cholesterol oxidase.
Crystal structure of *Streptomyces* cholesterol oxidase (PDB entry 1MXT) was used to generate this figure. Molecular surface of protein is shown, and protein is in yellow. Cysteine mutations on designated residues are in red, blue, white, purple, and orange as shown in the figure.

Plasmids encoding **mut1** – **mut6** were generated using QuickChange Lightning Multi Site-Directed Mutagenesis Kit (STRATAGENE) (*175-181*) with a high successful rate. Single strand DNA primer was need for each mutation site in PCR reaction. The enzyme blend extended the primer and ligated the nicks. Newly formed single strand DNA plasmid was transformed into the competent cells. Isolated plasmids of the correct size were selected for protein expression tests. Those plasmids that expressed cholesterol oxidase were sequenced to identify successful mutagenesis reactions. We could see 1, 2, 3, or 4 sites of mutations on the mutants. Details are discussed in discussion section.

In the first four mutagenesis reactions, we obtained **mut1** and 5 partial mutants: **mut2** (S153C/A205C/S312C), **mut2** (S153C/A205C/T435C), **mut3** (T168C/A276C), **mut4** (A184C/T239C/A407C), and **mut4** (T239C/A407C/A465C). Our ultimate goal was to introduce four cysteine residues in each mutant, so mutants which contained 3 mutations or less were further modified by PCR.

To obtain **mut2**, we sub-cloned the T435C mutation with restriction sites *Mlu*I and *Hind*III from plasmid 571-2 carrying S153C/A205C/T435C into plasmid 571-3 carrying S153C/A205C/S312C to generate plasmid 686-3 carrying **mut2** (S153C/A205C/S312C/T435C). The four cysteine mutant was successfully generated, but the protein aggregated after a few months. After re-examination of the DNA sequencing results, we found that there was an unexpected mutation, K438E, which might have cause protein aggregation and loss of protein activity. This mutation originateed from plasmid 571-2 during PCR reaction. We successfully mutated the nucleotide from Glu back to Lys by QuickChange Site-Directed Mutagenesis (*175-179*).

The other partial mutants with less than 4 mutations were performed using same procedures for **mut3** – **mut6** mutants.

Plasmids containing cysteine mutations T168C/A276C or A184C/T239C/A407C were used as templates. The A301C/T394C or A465C mutations were introduced to generate **mut3** and **mut4**, respectively. Using pCO117 as a template, PCR reactions were performed to generate **mut5** and **mut6** by the same multi site-directed mutagenesis protocol. We obtained **mut4**, **mut5**, a partial **mut3** (T168C/A276C) and a partial **mut6** (A184C/A301C/T394C).

For **mut3** mutant, the A301C and T394C mutations could not be introduced into the T168C/A276C template. Residues A301 and T394 could be mutated at the same time during construction of A184C/T239C/A301C/T394C mutant. The T_m of primers A301C and T394C is 77.2 ^oC and 78.8 ^oC, respectively, and both T_ms are higher than primers T168C and A276C, which are 73.8 ^oC and 73.6 ^oC respectively. The differences in T_m of these two sets of primers could be the reason that A301C and T394C mutations were hard to be introduced. In summary, 4 mutants, **mut1**: A32C/S129C/T371C/A423C, **mut2**: S153C/A205C/S312C/T435C, **mut4**: A184C/TT239C/A407C/A465C, and **mut5**: A32C/T168C/S312C/A465C, with 4 cysteine mutations; one mutant, **mut6**: A184C/A301C/T394C, with 3 cysteine mutations; and one mutant, **mut3**: T168C/A276C, with only 2 cysteine mutations. Of the 16 cysteine mutations, 11 are at single positions, the remaining 5 are duplicates, that serve as internal control. With 4 native cysteines, each cysteine mutant contains 5 to 8 cysteines in a single protein.

2.12.3 Over-expression of cholesterol oxidase

The over-expression and purification of wild-type cholesterol oxidase was carried out following the established protocol used in our laboratory (*91, 107*). We found that cysteine mutants formed intermolecular disulfide bonds during purification, as evident by the appearance of dimer on non-reducing protein gels. The dimer bands were not observed when proteins were incubated in a reducing reagent, such as TCEP.

Wild-type enzyme, single-cysteine, and multi-cysteine mutants, L80C, L274C, W333C, **mut1** (A32C/S129C/T371C/A423C), **mut2** (S153C/A205C/S312C/T435C), **mut3** (T168C/A276C), **mut4** (A184C/T239C/A407C/A465C), **mut5** (A32C/T168C/S312C/A465C), and **mut6** (A184C/A301C/T394C) were over-expressed using the same protocol with a yield 40, 47, 34, 11, 16, 21, 14, 14, 37, and 14 mg per 1L 2xYT medium, respectively. The purity of the wild-type enzyme and each mutant was shown in UV/vis spectra (Figure 2.29) and was confirmed by SDS-PAGE analysis (Figure 2.30).

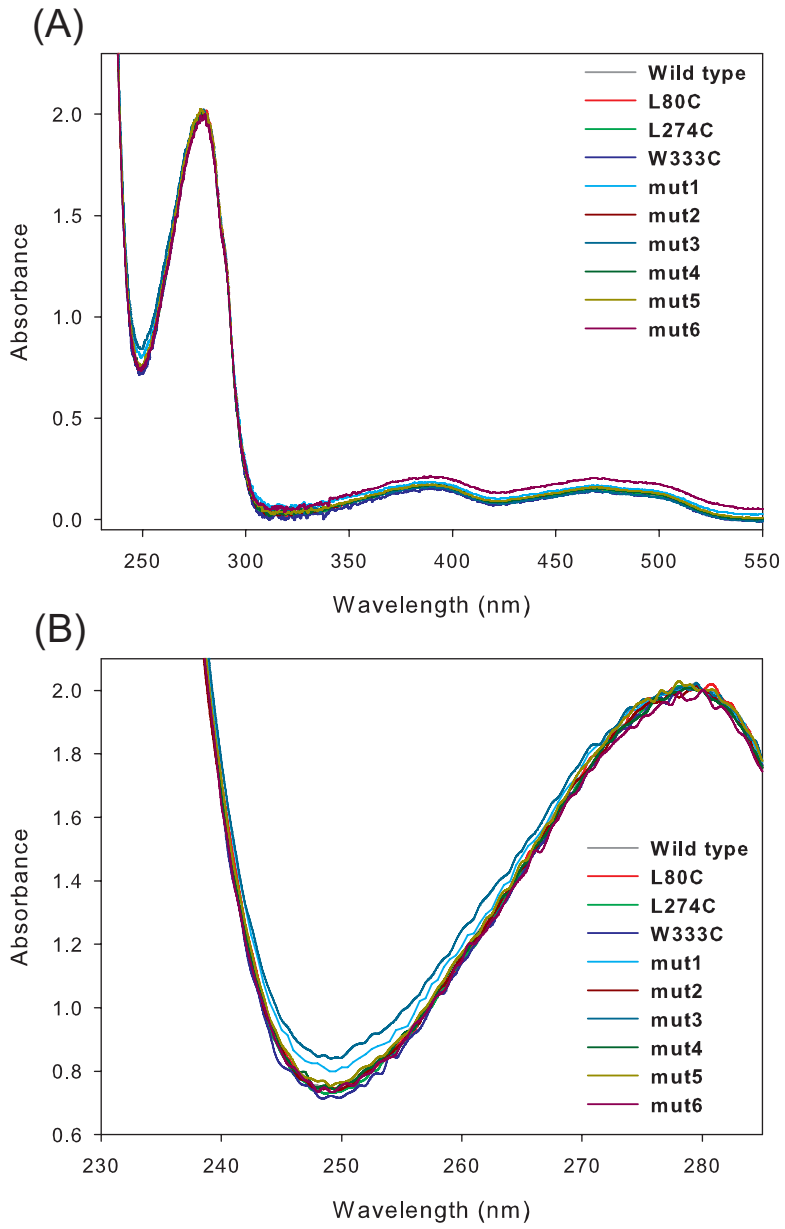

Figure 2.29 UV/vis spectra of wild-type and mutant cholesterol oxidase.
The 280 nm peak is protein absorption, and peaks at 391 and 468 nm are FAD absorption. Spectra were normalized at 280 nm. (A) Spectra are shown from 230 nm to 550 nm. (B) Spectra are shown from 230 nm to 285 nm.

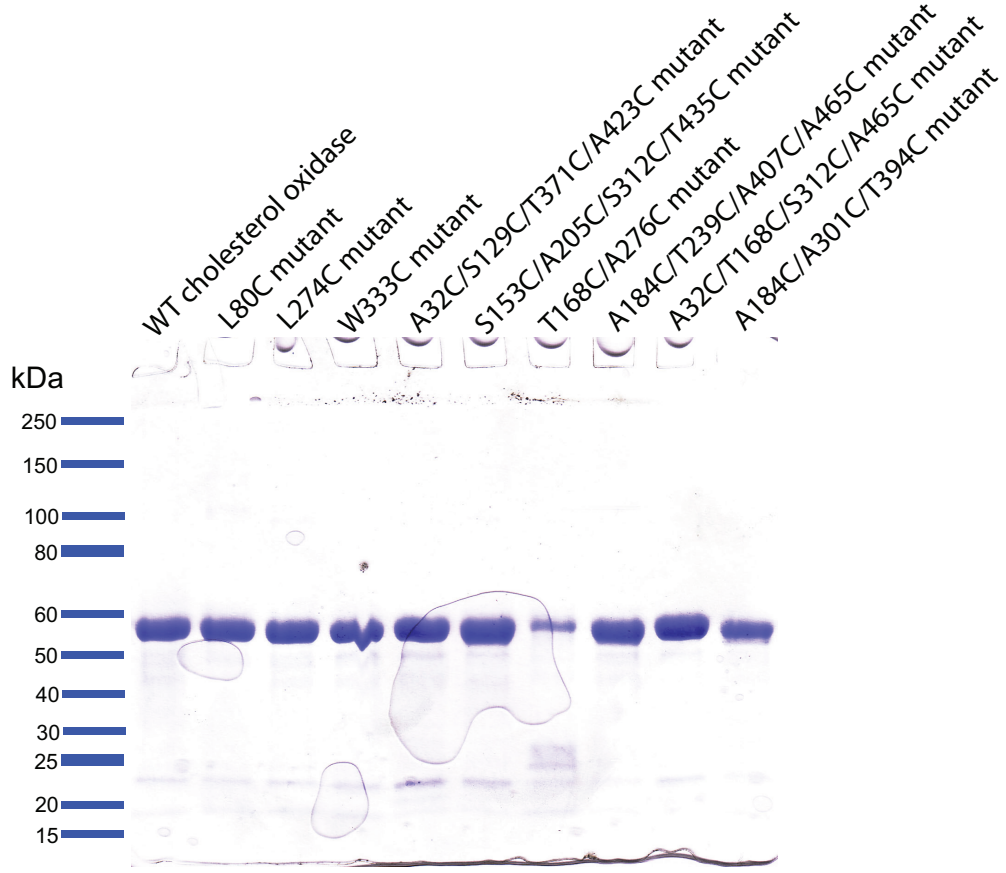

Figure 2.30 SDS-PAGE analysis of wild-type cholesterol oxidase, single-cysteine, and multi-cysteine mutants.
These proteins were analyzed in reducing conditions (TCEP), and the band at ~55 kDa is the monomer of cholesterol oxidase.

Steady-state enzyme kinetics and the intrinsic Trp fluorescence emission λ_{max} for wild type and all mutants were determined in order to confirm the folding and functional properties of the enzymes (Table 2.5). The fluorescence emission λ_{max} for the wild-type enzyme is 329 nm, and the emission λ_{max}s' for all mutants range from 328 nm to 332 nm, suggesting that all mutant proteins fold properly and maintain structural integrity. The mutants were found to have comparable catalytic activity to the wild-type cholesterol oxidase, which allowed us to use these mutant enzymes for ICMT-based labeling experiments to study protein binding orientations to the membranes. The yields of the multi-cysteine mutants ranged from 13 to 37 mg per liter culture, which was sufficient for various labeling experiments using different lipid compositions at various time points.

Table 2.5 Michaelis-Menten constant for wild-type and mutant cholesterol oxidase[a]

	k_{cat} (s^{-1})	K_m (μM)	k_{cat}/K_m ($M^{-1}s^{-1}$)	λ_{max} Trp (nm)[b]
Wild type	67 ± 6	13 ± 4	5.1×10^6	329
L80C	89 ± 7	11 ± 3	8.4×10^6	330
L274C	75 ± 8	17 ± 6	4.5×10^6	328
W333C	52 ± 6	16 ± 5	3.3×10^6	330
Mut1: A32C/S129C/T371C/A423C	23 ± 1	11 ± 2	2.0×10^6	332
Mut2: S153C/A205C/S312C/T435C	68 ± 8	10 ± 4	7.0×10^6	328
Mut3: T168C/A276C	46 ± 4	14 ± 3	3.4×10^6	328
Mut4: A184C/T239C/A407C/A465C	60 ± 6	13 ±4	4.6×10^6	330
Mut5: A32C/T168C/S312C/A465C	30 ± 2	12 ± 3	2.4×10^6	328
Mut6: A184C/A301C/T394C	57 ± 6	11 ± 4	5.0×10^6	329

[a]Assays conducted in 50 mM sodium phosphate, pH 7, containing 0.025% (w/v) Triton X-100, 0.02% (w/v) BSA, and 2% isopropanol at 37 °C. Errors are standard deviation based on triplicate measurements with three independent substrate preparations. [b]Excitation wavelength was 280 nm (slit width: 0.8 mm), emission was scanned from 300 nm 400 nm (slit width: 1.0 mm). Protein (1 μM) was in 50 mM sodium phosphate, pH 7.

2.13 Labeling and digestion of cholesterol oxidase

We labeled all proteins with a 1:1 (molar ratio) mixture of **5b-d_9/5b-d_0** (heavy/light) probes. The proteins were incubated at 70 ^{o}C in the presence of 1% sodium deoxycholate (SDC), a sterol detergent, for 1 h. Proteins were then digested with both trypsin and chymotrypsin for 16 ~ 18 h, SDC was removed by centrifugation after acidification with TFA. Digested peptides were mixed with matrix for MALDI-TOF analysis.

The protein digestion coverage for trypsin and chymotrypsin cleavages are shown in Table 2.6. The sequence coverage of all cholesterol oxidase proteins from these two proteases ranged from 49% - 63% and 34% - 63% for trypsin and chymotrypsin digest, respectively. In addition to the mutated cysteine mutations, there are four native cysteine residues in cholesterol oxidase C56, C282, C445, and C452. By trypsin digest we were able to identify a C445 and C452 labeled cysteine peptide, and in chymotrypsin digest we are able to identify C56, C445, and C452 labeled peptides.

Table 2.6 Percentage coverage of proteolyzed cholesterol oxidase by trypsin and chymotrypsin.[a]

	Trypsin	Chymotrypsin
	Coverage (%)	Coverage (%)
Wild type	59 ± 7	60 ± 14
L80C	60 ± 0.1	58 ± 5
L274C	61 ± 3	57 ± 2
W333C	53 ± 10	43 ± 8
Mut1: A32C/S129C/T371C/A423C	58 ± 5	49 ± 9
Mut2: S153C/A205C/S312C/T435C	58 ± 4	34 ± 14
Mut3: T168C/A276C	54 ± 3	56 ± 4
Mut4: A184C/T239C/A407C/A465C	61 ± 0.4	60 ± 7
Mut5: A32C/T168C/S312C/A465C	63 ± 10	61 ± 1
Mut6: A184C/A301C/T394C	49 ± 2	63 ± 10

[a]Conditions: 10 μM protein was labeled with 1 mM **5b-d_9/5b-d_0** probes in the presence of 1% SDC in 50 mM HEPES, pH 7 at 70 ^{o}C for 1 h. Trypsin or chymotrypsin was added and was incubated at 37 ^{o}C and 25 ^{o}C for trypsin digestion and chymotrypsin digestion for 16-18 h. Purified samples were analyzed by MALDI-TOF. Errors are standard deviation based on duplicate measurements of two independent labeling experiments.

The mass spectra of selected heavy/light, **5b-d_9/5b-d_0**, probe labeled peptide are shown in Figure 2.31. The three peaks in Figure 2.31A correspond to the C445 and C452 labeled peptides from trypsin digest. During the labeling process, the two cysteines could be labeled with both light probes, both heavy probes, or one heavy probe/one light probe, so there are three peaks corresponding to the labeled peptide. For the L80C labeled peptide (Figure 2.31 B & C), we can see a pair of peaks with a mass difference of 9 Da, which is the difference between the heavy and light probe. The peaks with an *m/z* 2016/2025 correspond to $peptide_{72\text{-}87}$ from the L80C mutant without any missing cleavage. The peaks with an *m/z* 2287/2296 are $peptide_{70\text{-}87}$ from the L80C mutant with one missing cleavage. In Figure 2.31D & E, the A184C labeled peptides are from two different mutants, **mut4**: A184C/T239C/A407C/A465C and **mut6**: A184C/A301C/T394C enzymes, and it shows that same peaks are found in the mass spectra from both proteins. The other two ICMT probe labeled cysteine peptides, S129C and S312C are from two mutants, and the masses of these two labeled peptides are *m/z* 1379/1388 and 3095/3104, respectively. The mass spectra in Figure 2.31 show that both the native and the mutated cysteine residues can be found in the range of 1000 to 3000 *m/z* with high mass resolution, and the isotopic envelope of heavy/light peaks can be integrated to calculate the ratios of heavy/light probe labeled peptides.

In chymotrypsin digest, we observed labeling of native C56 of the wild-type enzyme. Other cysteine mutation sites, such as A184C and S312C, could also be found in trypsin digest. The same T168C (**mut3** & **mut5**) mutation can be identified in two mutants, **mut3**: T168C/A276C and **mut5**: A32C/T168C/S312C/A465C. These labeled cysteine peptides are mostly in the range of 1000-2500 *m/z* from chymotrypsin digest. The labeling experiment of proteins with heavy/light probes provides information in identifying native and mutated cysteine residues. Generally, the results enable the identification of same cysteine from two peptides or same cysteine from two protein mutants. The SDC solubilized protein digestion with trypsin and chymotrypsin protocol successfully simplifies purification steps before mass analysis.

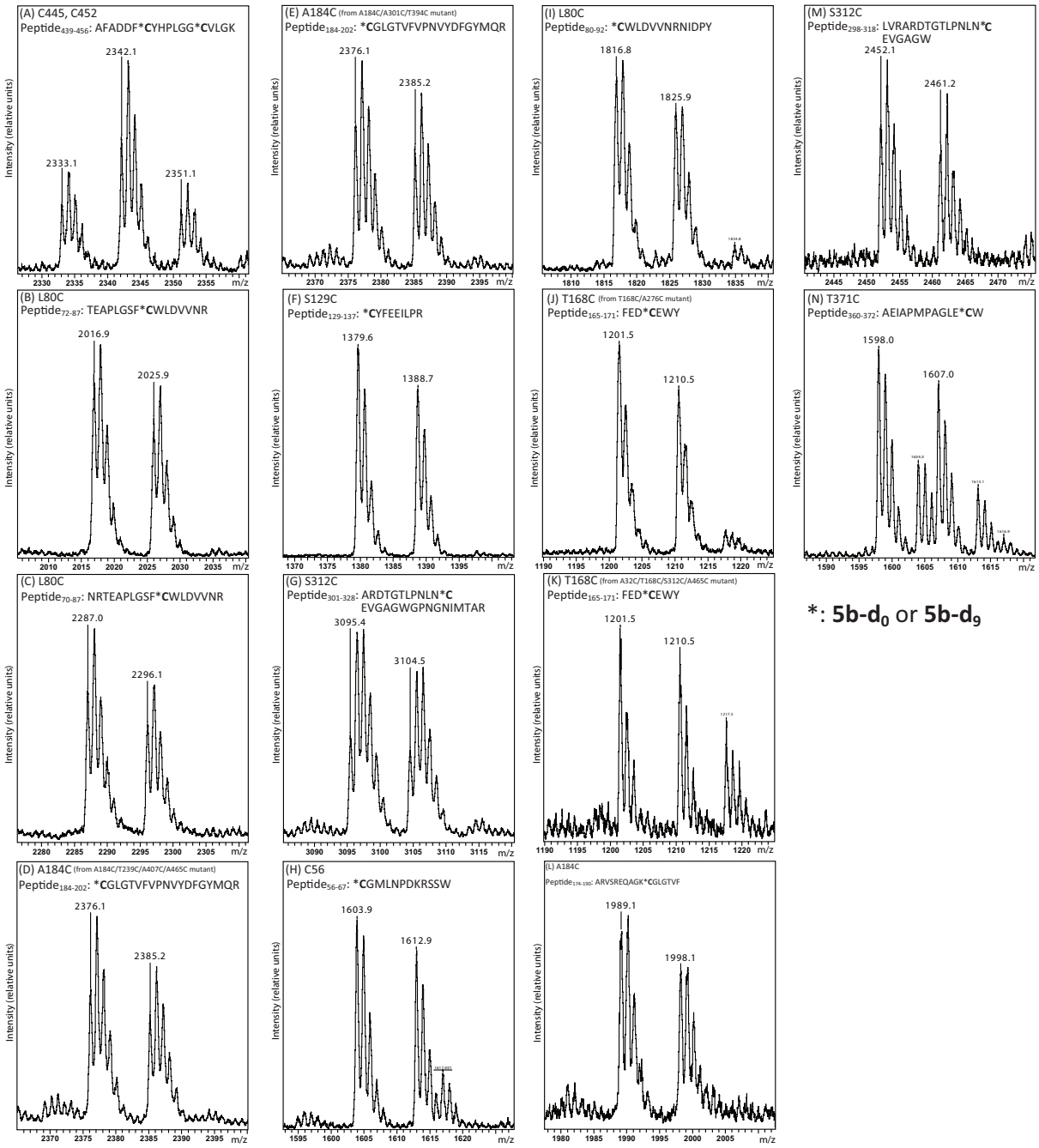

Figure 2.31 Mass spectra of heavy/light probes labeled cysteine peptides of wild-type and mutant cholesterol oxidase.

Proteins (10 μM) were labeled in 1 mM mixture of **5b-d_9/5b-d_0** probes with 1% SDC in 50 mM HEPES, pH 7 at 70 ^{o}C for 1h. Proteins were subsequently digested with trypsin or chymotrypsin, respectively, then purified, and analyzed by MALDI-TOF mass spectrometer.

The purpose of the labeling and sample preparation experiments shown here is to identify peptides containing mutated cysteine residues of interest as well as to optimize reaction and purification procedures for the following interfacial protein binding experiments. We carried out a digestion reaction in the presence of SDC at high temperature to help unfold the proteins as well as increase labeling rate between cysteine thiol and the maleimide probe. Sodium deoxycholate can be used as an alternative to SDS to denature protein (*182*). SDC is also able to solubilize hydrophobic transmembrane proteins in digestion solution, and it is known that trypsin works well in the presence of low concentration of SDC, typically less than 1% (w/v) (*183-186*). In our labeling experiment, we also found chymotrypsin worked well in the presence of 1% (w/v) SDC. We reduced the number of peptide purification steps by using SDC to denature and solubilize protein in the digestion step. Acidification by TFA after proteolysis precipitated SDC which could be removed by centrifugation prior to mass acquisition. Both trypsin and chymotrypsin were used to digest cholesterol oxidase. Trypsin hydrolyzes the C-terminal peptide bond of lysine (K) and arginine (R), and chymotrypsin hydrolyzes the C-terminal peptide bond of tyrosine (Y), phenylalanine (F), tryptophan (W), and leucine (L). The tryptic digested peptides will contain at least one positively charged amino acid residue whereas chymotryptic digested peptides do not always carry a charged residue on the peptide from their proteolytic specificity. The ICMT labeled cysteine-containing peptide always bear at least one positively charged peptide coming from the probe itself, which will aid ionization for mass spectroscopy (*155*). It was reported that enrichment of peptide by incorporation of a positive charged moiety to the cysteine substantially enhances the signals of peptide with less polar residues (*156*). We expected that ICMT labeling of cysteine would have more effects on chymotrypsin digested peptides. The combination of the two proteases can give complementary results from trypsin and chymotrypsin as well.

2.14 ICMT strategy for mapping cysteine accessibility on cholesterol oxidase with membrane

Results

Cholesterol oxidase is an interfacial enzyme that catalyzes the conversion of cholesterol to cholest-4-en-3-one. We know how the chemistry is processed from kinetic and structural analyses in our laboratory, and our kinetic and binding studies have also provided the substrate specificity toward the lipid bilayer (*91, 187, 188*). To understand how protein interacts with membranes, it is necessary to know how protein binds its substrate. Previous studies have shown that one of the loops is important for substrate binding during catalysis, (*104*) and acrylodan-labeled enzyme in fluorescence experiment has also revealed that the loop interacts with the lipid headgroup (*60*). The high resolution crystal structure of the soluble form of cholesterol oxidase is available, and it shows the catalytic site is deeply buried (*92*). Cholesterol is hydrophobic, and is embedded in the lipid membranes. In order to bind substrate, cholesterol oxidase must associate with the membrane (*91*), and make conformational changes. However, little is known how far the contact surface extends beyond the entrance to the substrate binding site, and how deep the protein inserts into the membrane. The changes of the contact surface and the insertion depth in different lipid structures are still unclear. Characterization of the active protein conformation at the membrane interface is still challenging in structural biology.

Cholesterol oxidase is a good example to study interfacial protein-lipid interactions. The enzyme from *Streptomyces* is heterologously expressed and stable, and structural information is available from crystal structure. Many conventional methods, e.g. EPR or ssNMR which are described in previous sections, have advantages and limitations to study membrane protein-lipid interactions. Here, we proposed a mass spectrometric methodology by applying an isotope-coded mass tag (ICMT) labeling strategy to study protein lipid interactions as outlined in Figure 2.32. This method utilizes the differential reactivity of the cysteine thiols in different states that are in contact with membranes or those are exposed to the solvent in combination with MALDI-TOF for mass analysis.

We designed ICMTs as previously discussed, and generated single-cysteine or multi-cysteine cholesterol oxidase mutants based on the crystal structure (PDB entry 1MXT). We originally proposed 4 basic steps (*107*): first, the native protein is labeled with heavy probe in the

presence of vesicles in a time course manner; second, reaction is quenched with DTT; third, protein is denatured (purification may be needed after this step); fourth, light probe is added in large excess to label the remainder cysteine thiols. Protein is then proteolyzed by trypsin or chymotrypsin, and peptides are purified by C18 Ziptip before mass analysis. In our modified procedure, we take the advantage of protocol used in the transmembrane peptide labeling experiment (Figure 2.12). Instead of quenching heavy probe after the first step, we add large excess (100-fold excess) of light probe to the aliquot at each time point, SDC is added, and reaction is incubated at 70 ^{o}C for 1hr. Trypsin or chymotrypsin is added to the solution to proteolyze the enzyme, and is subsequently analyzed by mass spectrometry.

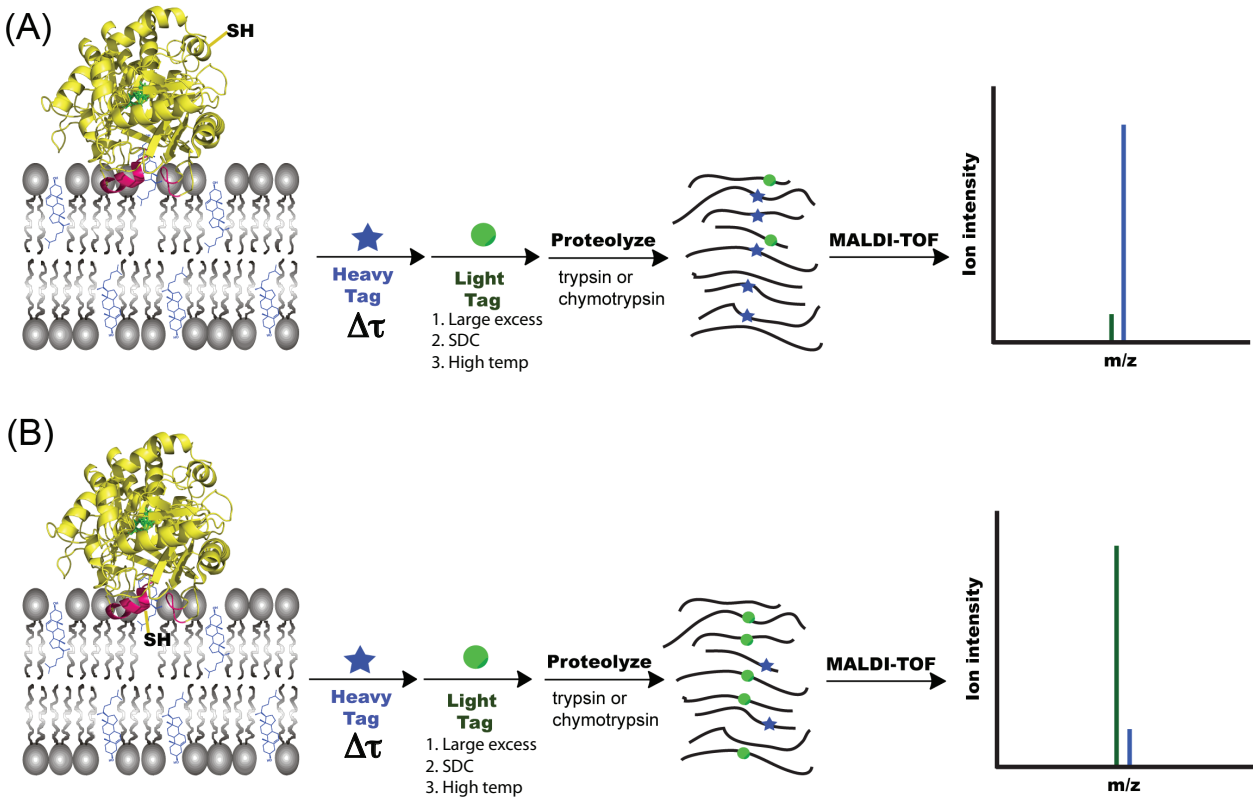

Figure 2.32 The Isotope-Coded Mass Tag (ICMT) strategy for mapping out the binding site of an interfacial enzyme, cholesterol oxidase, at the interface of lipid membrane.
(A) Cysteine residue on the protein surface that is not in membrane contact will be mostly labeled with heavy probe. Denatured protein is labeled with light probe, enzyme is then proteolyzed, and is subsequently analyzed by MALDI-TOF. (B) Cysteine residue on the protein surface that is in membrane contact is protected and is minimally labeled with heavy probe. Denatured protein is labeled with light probe, enzyme is then proteolyzed, and is subsequently analyzed by MALDI-TOF.

The strategy outlined in Figure 2.32 compares the differential reactivity of cysteine thiols; the sulfhydryl that is not in membrane contact (Figure 2.32A) should be mostly labeled with heavy tag whereas the sulfhydryl that is in membrane contact (Figure 2.32B) should be labeled mostly with light probe in the second step.

We labeled single-cysteine and multi-cysteine mutants using the ICMT strategy shown in Figure 2.32. Four conditions, DMPC, DMPC/cholesterol (3/1), DMPC/cholest-4-en-3-one (3/1) vesicles, or in the absence of vesicles, were used in the labeling experiments, and trypsin and chymotrypsin were employed to proteolyze the proteins. The experiments were performed in a time course ranging from 30 sec, 1, 2, 3, 6, 10, 15, to 30 min. There are total 19 cysteine mutation sites, including single-cysteine and multi-cysteine mutants, in all cholesterol oxidase mutants, A32C, L80C, S129C, S153C, T168C, A184C, A205C, T239C, L274C, A276C, A301C, S312C, W333C, T371C, T394C, A407C, A423C, T435C, A465C, and among these mutations, 14 cysteine mutations could be identified from our experimental results. The coverage of the identified cysteine mutations on the protein surface was 74%, and peptides containing five cysteine mutations, S153C (**mut2**), A276C (**mut3**), W333C, T394C (**mut6**), and A407C (**mut4**) could not be identified. The identified and un-identified cysteine mutations from all cholesterol oxidase mutants are summarized in Table 2.7.

We generated two other multi-cysteine mutants overlapping 5 cysteine mutation sites, A32C (**mut1** & **mut5**), T168C (**mut3** & **mut5**), A184C (**mut4** & **mut6**), S312C (**mut2** & **mut5**), and A465C (**mut4** & **mut5**), as internal control. Among these cysteine mutations, 4 out of 5 can be identified from both mutants. A465C is in **mut4** and **mut5** mutants, but it can only be identified in the **mut5** mutant. Trypsin is generally used for protein digestion in proteomics due to its specificity of proteolysis sites, and we also use chymotrypsin to increase coverage of the identified cysteine mutations. Most of the cysteine mutations can be identified in trypsin digest. However, three mutations, A32C (**mut1** & **mut5**), T371C (**mut1**), and A465C (**mut5**) can only be identified in chymotrypsin digest.

Table 2.7 Summary of identified cysteine mutations in cholesterol oxidase mutants.

	L80C	L274C	W333C	**Mut1**	**Mut2**	**Mut3**	**Mut4**	**Mut5**	**Mut6**
A32C	—	—	—	√	—	—	—	√	—
L80C	√	—	—	—	—	—	—	—	—
S129C	—	—	—	√	—	—	—	—	—
S153C	—	—	—	—	nd	—	—	—	—
T168C	—	—	—	—	—	√	—	√	—
A184C	—	—	—	—	—	—	√	—	√
A205C	—	—	—	—	√	—	—	—	—
T239C	—	—	—	—	—	—	√	—	—
L274C	—	√	—	—	—	—	—	—	—
A276C	—	—	—	—	—	nd	—	—	—
A301C	—	—	—	—	—	—	—	—	√
S312C	—	—	—	—	√	—	—	√	—
W333C	—	—	nd	—	—	—	—	—	—
T371C	—	—	—	√	—	—	—	—	—
T394C	—	—	—	—	—	—	—	—	nd
A407C	—	—	—	—	—	—	nd	—	—
A423C	—	—	—	√	—	—	—	—	—
T435C	—	—	—	—	√	—	—	—	—
A465C	—	—	—	—	—	—	nd	√	—

— ≡ not present, √ ≡ detected, nd ≡ not detected.

Single-cysteine mutant L80C (10 μM) was first labeled in the presence of 500 μM DMPC or DMPC/cholest-4-en-3-one (3/1) vesicles with 500 μM **5b-d$_9$** for 1, 2, 5, 10, 30, and 60 min. The mass spectra (Figure 2.33) show a pair of peaks at *m/z* 2016/2025 from peptide$_{72\text{-}87}$. The results showed that the cysteine was all labeled with heavy probe in the first step (Figure 2.33), suggesting that the probe concentration was too high to monitor the changes of labeling with time.

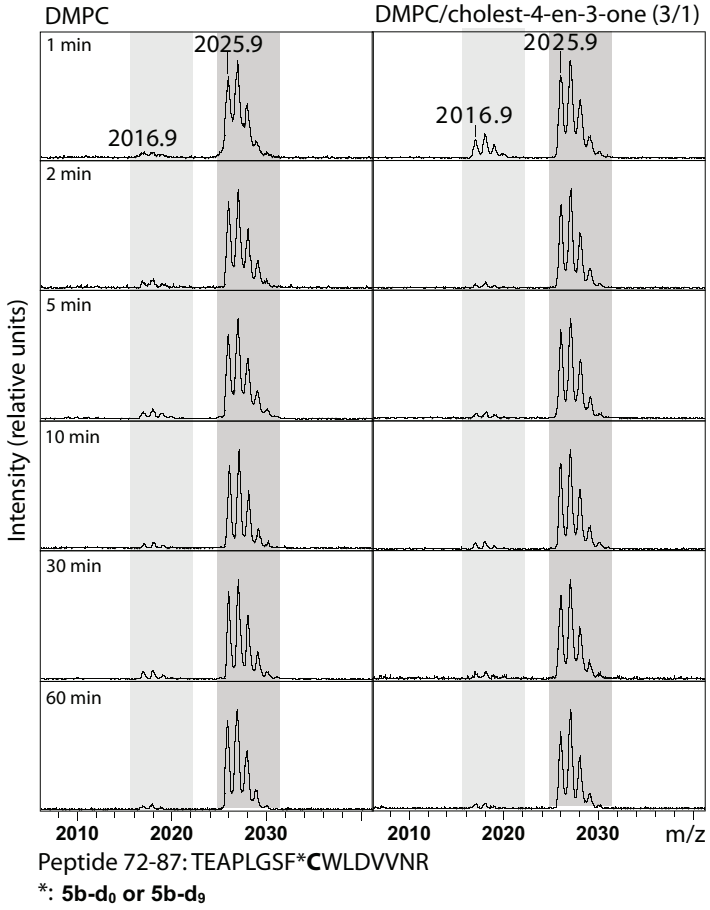

Figure 2.33 Mass spectra of cholesterol oxidase L80C mutant labeling in DMPC and DMPC/cholest-4-en-3-one (3/1) vesicles.
Mass spectra of L80C ICMT labeled peptide$_{72\text{-}87}$ in different lipid conditions. L80C (10 μM) was labeled in the presence of 500 μM lipid vesicles and 500 μM **5b-d$_9$**, aliquots were taken at 1, 2, 5, 10, 30, and 60 min, and 4.95 mM **5b-d$_0$** was added to the reaction. The peaks corresponding to light-labeled peptide are highlighted in light gray, and the peaks corresponding to heavy-labeled peptide are highlighted in dark gray. These experiments were done once.

A lower probe concentration, 100 μM **5b-d$_9$**, was used to label L80C mutant (10 μM) in the presence of 500 μM DMPC, DMPC/cholesterol (3/1), DMPC/cholest-4-en-3-one (3/1)

vesicles, or in the absence of vesicles with the same time course. We could only observe small differences of labeling in the first 5 min (Figure 2.34). However, they reached almost 100% heavy labeling after 5 min. The labeling rates of cysteine were still high at probe concentration of 100 μM. Then we further reduced the probe, **5b-d$_9$**, concentration 4-fold to 25 μM for labeling experiments.

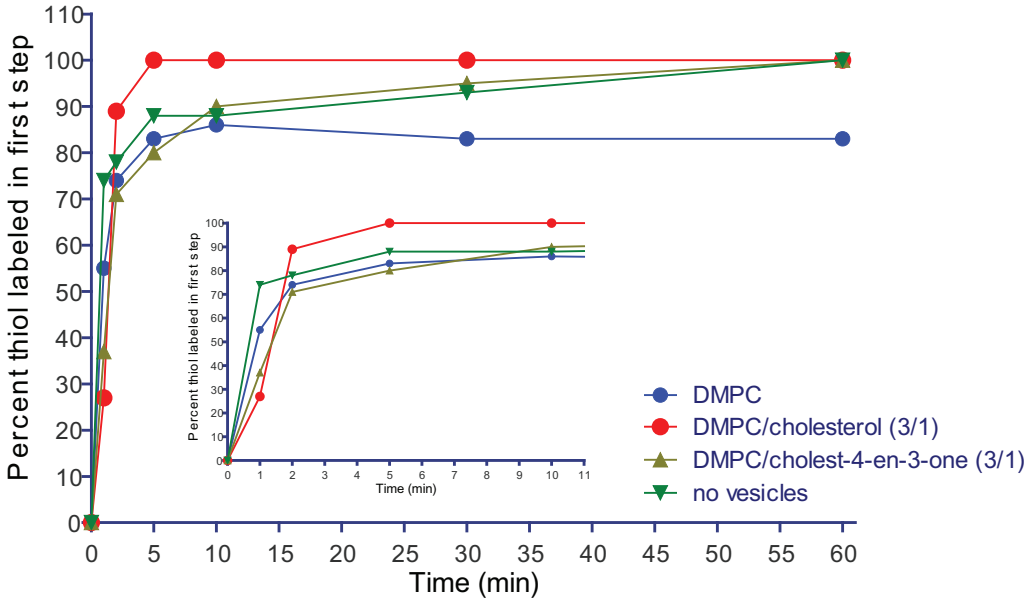

Figure 2.34 Time course labeling of L80C cholesterol oxidase mutant.
Cholesterol oxidase L80C mutants (10 μM) were labeled in the presence of 500 μM DMPC/cholesterol (3/1) vesicles or in the absence of vesicles, with 100 μM **5b-d$_9$**, aliquots were taken at 30 sec, 1, 2, 3, 6, 10, 15, and 30 min, and 4.95 mM **5b-d$_0$** was added to the reaction. Inserted figure is a magnification of the first 10 min. These experiments were done once.

The results of labeling 10 μM L80C mutant with 25 μM **5b-d$_9$** in the presence of 500 μM DMPC, DMPC/cholesterol (3/1), and DMPC/cholest-4-en-3-one (3/1) vesicles, or in the absence of vesicles at different time points are shown in Figure 2.35. The mass spectra (Figure 2.35A) show a pair of peaks at *m/z* 2016/2025 from peptide$_{72\text{-}87}$. The labeling time course under these 4 conditions indicated that in the presence of cholesterol oxidase substrate, cholesterol, the labeling rate of L80C increases. Whereas, the rates of labeling of other 3 conditions remain similar (Figure 2.35B). This result represents that L80C has dynamic labeling profile under the current protocol.

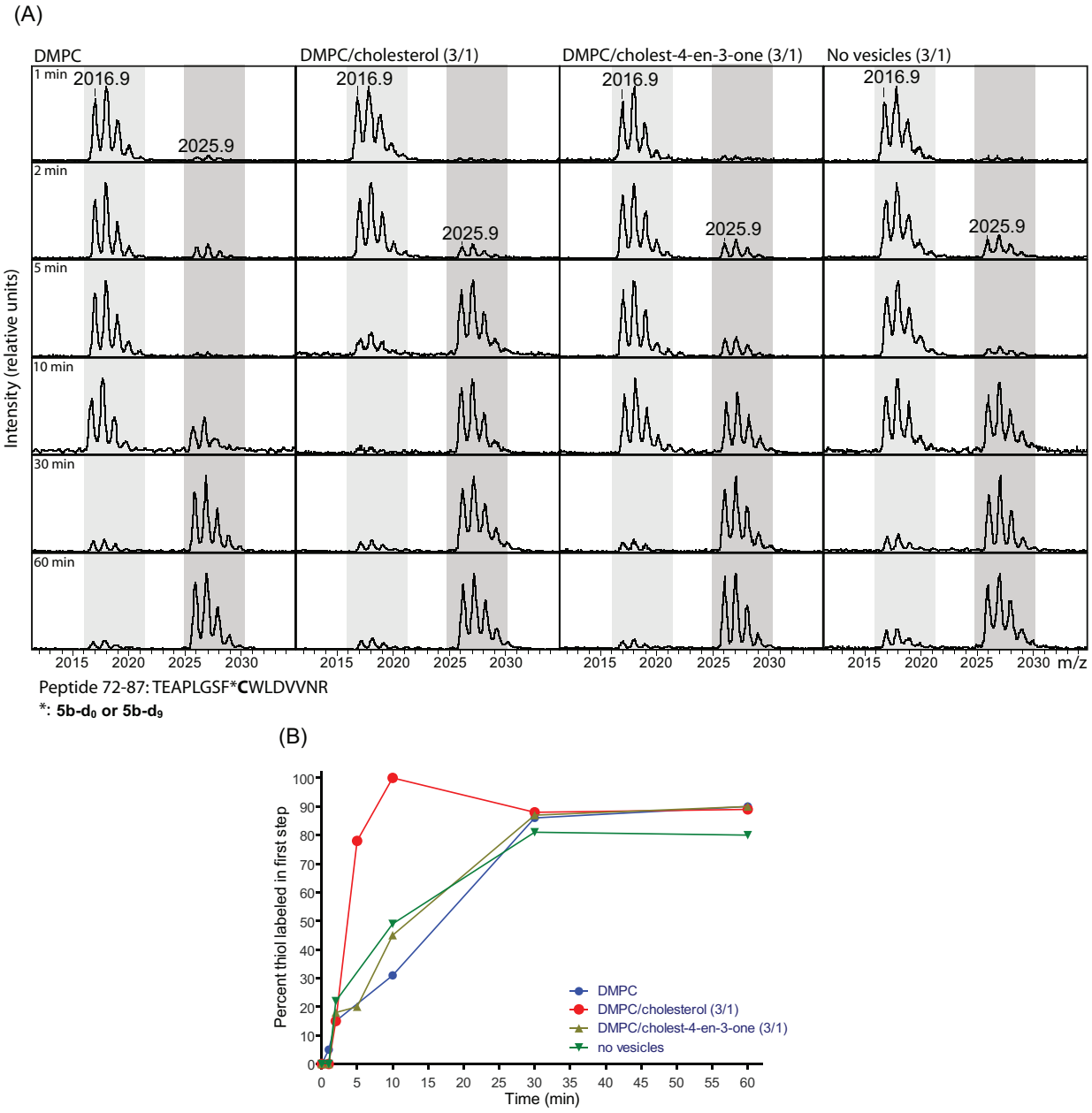

Figure 2.35 Cholesterol oxidase L80C mutant labeling under different lipid conditions.
L80C (10 μM) was labeled in the presence of 500 μM lipid vesicles and 25 μM **5b-d$_9$**, aliquots were taken at 1, 2, 5, 10, 30, and 60 min, and 4.95 mM **5b-d$_0$** was added to the reaction. (A) Mass spectra of L80C ICMT labeled peptide$_{72\text{-}87}$ in different lipid conditions. The peaks corresponding to light-labeled peptide are highlighted in light gray, and the peaks corresponding to heavy-labeled peptide are highlighted in dark gray. (B) Time course of L80C labeling in different lipid conditions. These experiments were done once.

Different protein concentrations were used in labeling experiments with 50 μM **5b-d$_9$** in the presence of 500 μM DMPC/cholesterol (3/1) vesicles or in the absence of vesicles. We used various concentrations (6.6, 8.2, or 10 μM) of **mut2**: S153C/A205C/S312C/T435C, and the

experiments were performed under the same conditions described above from 30 sec to 30 min. The time courses of heavy probe labeling for each mutation site are in Figure 2.36. Three cysteine mutations, A205C, S312C, and T435C showed exposed labeling when 10 μM protein was used. Labeling rate for S312C and T435C were faster than that of A205C in the first 5 min (Figure 2.36 and Table 2.8). The effects on the labeling rate were further tested by using concentration below 10 μM. We performed the same labeling protocol and reaction conditions using 6.6 and 8.2 μM proteins in 500 μM DMPC/cholesterol vesicles and in the absence of vesicles (Figure 2.36). The labeling plateau for A205C thiol reached 60-70% for both enzyme concentrations used, and were lower than that of 10 μM protein used. The rates of labeling for S312C had similar labeling profiles when 10 μM protein was used, and the labeling plateau were lowered by approximately 5-10% in both protein concentrations used. The general trend of lower protein concentrations used in labeling experiments is that both the labeling plateau and labeling rate decrease in certain extent.

When we compared the effects of varying probe concentrations on labeling L80C mutant to the effects of labeling **mut2**, they all showed differences in labeling rates of the cysteine thiols. In the case of L80C mutant labeling with various probe concentrations, we started to monitor slight changes in labeling when probe concentration decreased to 100 μM. However, the changes are not obvious until probe concentration was lowered to 25 or 50 μM. In the case of multi-cysteine mutant labeling experiment, same probe concentration was used to label different concentrations of proteins. We observed changes of the labeling rate in different cysteine labeling. The concentrations of protein 8.2 μM and 6.6 μM used for labeling showed only slightly changes for S312C and A205C thiols labeling plateau. For T435C, the labeling plateau decreased ~ 20% for both lower protein concentrations used. In the labeling of native cysteines, C445 and C452 were labeled at ~ 20% plateau, and C56 was not labeled in first step when 10 μM protein was used. We observed that using lower protein concentration gave slightly higher labeling plateau for C445 and C452.

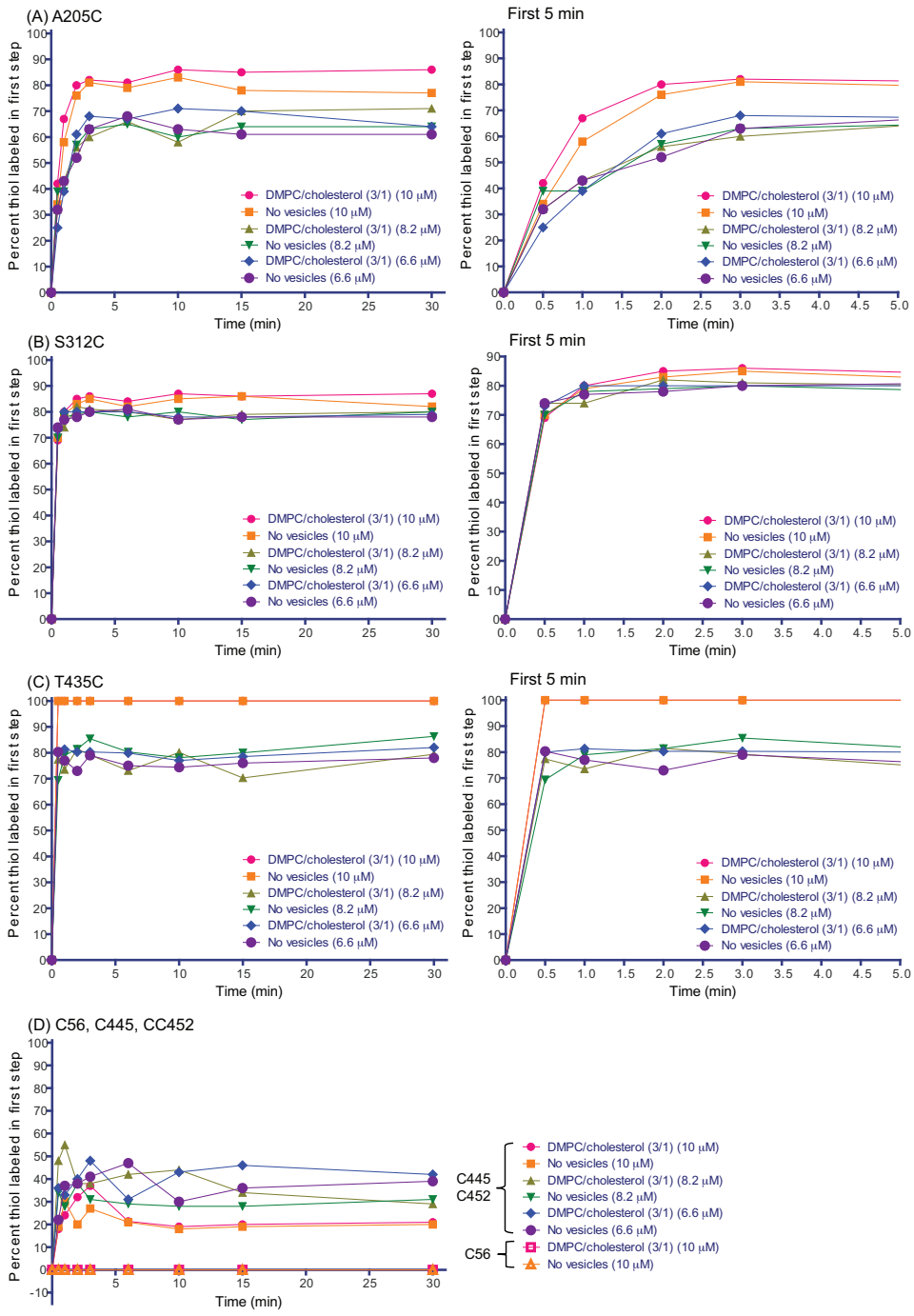

Figure 2.36 Time course labeling of various concentrations of cholesterol oxidase mut2: S153C/A205C/S312C/T435C mutant.

Cholesterol oxidase **mut2** (6.6, 8.2, and 10 μM) were labeled in the presence of 500 μM DMPC/cholesterol (3/1) vesicles or in the absence of vesicles, with 50 μM **5b-d$_9$**, aliquots were taken at 30 sec, 1, 2, 3, 6, 10, 15, and 30 min, and 4.95 mM **5b-d$_0$** was added to the reaction. (A) Time course labeling of A205C. (B) Time course labeling of S312C. (C) Time course labeling of T435C. (D) Time course labeling of C56, C445, and C452. Left: Time course for 30 min. Right: Time course for first 5 min. These experiments were done once.

Table 2.8 Relative cysteine labeling rate in mut2.[a]

	DMPC/cholesterol (3/1)	No vesicles	Time to label 50% (s)	[**mut2**] (μM)	[**5b-d$_9$**] (μM)	[cys][b]/t_{50}×[probe] (s^{-1}) (×10^{-5})
A205C	√	—	39	10	50	513
A205C	—	√	51	10	50	392
A205C	√	—	93	8.2	50	176
A205C	—	√	102	8.2	50	161
A205C	√	—	135	6.6	50	98
A205C	—	√	111	6.6	50	119
S312C	√	—	21	10	50	952
S312C	—	√	21	10	50	952
S312C	√	—	20	8.2	50	820
S312C	—	√	21	8.2	50	781
S312C	√	—	20	6.6	50	660
S312C	—	√	20	6.6	50	660
T435C	√	—	15	10	50	1333
T435C	—	√	15	10	50	1333
T435C	√	—	19	8.2	50	863
T435C	—	√	21	8.2	50	781
T435C	√	—	18	6.6	50	733
T435C	—	√	18	6.6	50	733

[a]Time to label 50% thiol on each cysteine in different protein concentration in the presence or absence of vesicles is reported. The value of cysteine concentration divided by time to label 50% thiol multiplied by probe concentration used in the first step is calculated. This value should be proportion to the average rate constant over the 50% over the 50% of the reaction. [b][cys]: effective cysteine concentration. √ ≡ condition used. — ≡ condition not used. These experiments were done once.

We then performed same labeling experiment for other single-cysteine and multi-cysteine cholesterol oxidase mutants. Cholesterol oxidase mutants (10 μM) were labeled with 50 μM **5b-d_9** in the presence or absence of lipid vesicles for 30 sec, 1, 2, 3, 6, 10, 15, and 30 min. After proteolysis by trypsin or chymotrypsin, samples were analyzed by MALDI-TOF mass spectrometry. We classify the results from the labeling experiments into three categories: dynamic labeling, exposed labeling (labeling in first step), and protected labeling (labeling in second step). Four cysteine mutations, L80C, T168C (**mut3**), A205C (**mut2**) and T239C (**mut4**), show dynamic labeling. Based on the mass spectra, labeling of T239C (**mut4**) mutation can only be found in the absence of vesicles, being digested by trypsin, or it can be found in labeling in DMPC vesicles, being digested by chymotrypsin. The trend of dynamic labeling could be observed, but this mutation is not included for comparison due to low intensity in the mass spectra of T239C (**mut4**) mutation.

Since most of the labeling rates of the protein do not have significant differences between DMPC, DMPC/cholesterol (3/1) and DMPC/cholest-4-en-3-one (3/1) vesicles, we analyzed these data by comparing the rates of labeling in the presence of vesicles with protein substrate (DMPC/cholesterol (3/1) vesicles) and in the absence of vesicles. Time course of dynamic labeling rates for L80C, T168C (**mut3**), and A205C (**mut2**) cysteine mutations are shown in Figure 2.37. The labeling rates of these three cysteine mutations show slightly differences in the presence of DMPC/cholesterol (3/1) vesicles and in the absence of vesicles, especially for L80C mutation labeling. The labeling of T168C (**mut3**) and A205C (**mut2**) might not be distinguishable within the experimental error. The labeling rates increase upon binding to the vesicles for L80C and A205C (**mut2**) mutation sites, whereas the rate of labeling decreases for T168C (**mut3**) mutation. These mutation sites are shown in the crystal structure (PDB entry 1MXT) of wild-type cholesterol oxidase from *Streptomyces* in Figure 2.38. From the structure, L80C and T435C (**mut2**) are in the active site loops (residue 72-87 and 432-438) (*60*), and T168C (**mut3**) and A205C (**mut2**) are on the other two helices. The differential labeling rates of cysteine thiols in the absence or in the presence of lipid vesicles with enzyme substrate reveal that protein might undergo conformational changes upon binding to the lipid membranes. Or the changes of labeling rates were due to the burial of cysteine thiols in the lipid bilayer when protein bound to the membrane.

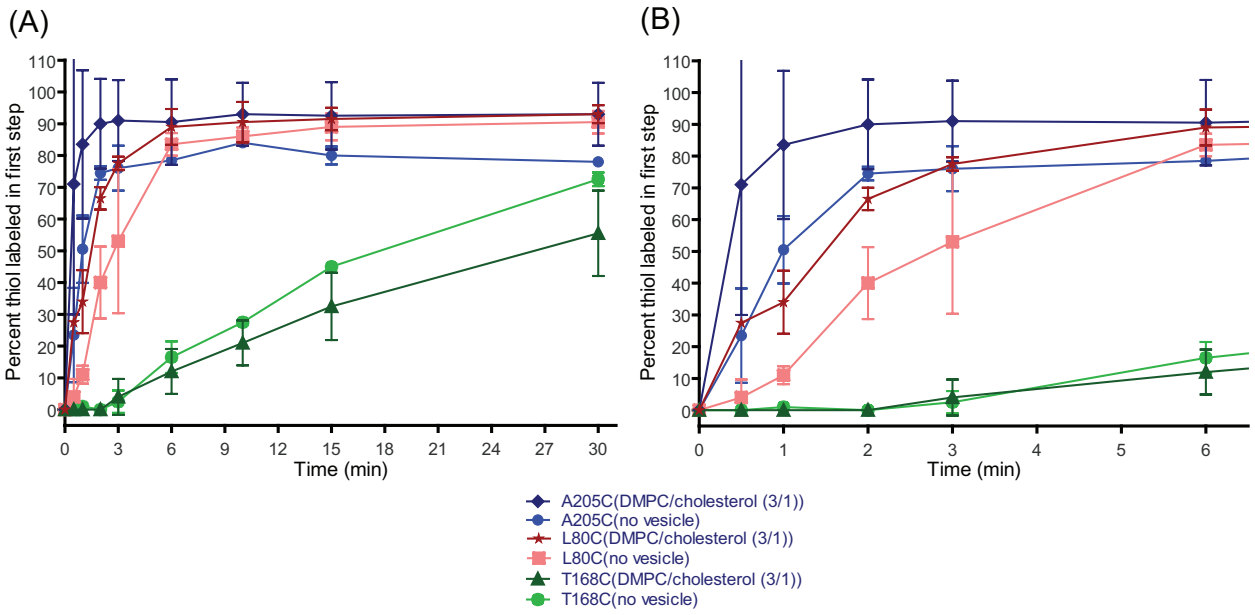

Figure 2.37 Time course labeling of cholesterol oxidase cysteine mutants for L80C, T168C (mut3), and A205C (mut2) mutation sites.
Cholesterol oxidase cysteine mutants (10 μM) were labeled in the presence of 500 μM DMPC/cholesterol (3/1) vesicles or in the absence of vesicles, with 50 μM **5b-d_9**, aliquots were taken at 30 sec, 1, 2, 3, 6, 10, 15, and 30 min, and 4.95 mM **5b-d_0** was added to the reaction. (A) Time course labeling from 0 to 30 min. (B) Magnification of time course labeling in the first 6 min. Errors are standard deviation based on duplicate measurements with two independent labeling experiments.

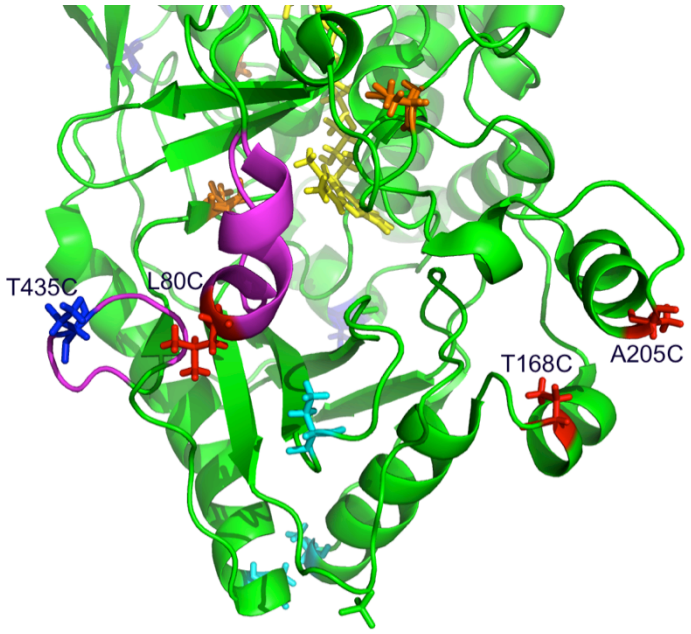

Figure 2.38 Cysteine mutation sites for L80C, T168C (mut3), A205C (mut2), and T435C (mut2) of *Streptomyces* cholesterol oxidase.
Cholesterol oxidase (PDB entry 1MXT) is colored in green, FAD in yellow, two loops (residue 72-87 and 432-438) in purple, L80C, T168C (**mut3**), and A205C (**mut2**) in red, and T435C (**mut2**) in blue. FAD, L80, T168 (**mut3**), A205 (**mut2**), and T435 (**mut2**) are shown in ball-and-stick.

Another labeling type of the cysteine mutations is a exposed labeling. These residues, S129C (**mut1**), L274C, S312C (**mut2** & **mut5**), T435C (**mut2**) and A465C (**mut5**), are labeled in the first step (heavy probe labeled) with plateaus ranging from 70% to 100% in the DMPC/cholesterol (3/1) vesicles or in the absence of vesicles. They are steadily labeled in the first time point, 30 sec, and maintain the same labeling ratio for at least 30 min. The positions of these exposed labeled cysteine mutations in crystal structure are shown in Figure 2.39. Among these cysteine mutations, T435C (**mut2**) mutation is on one of the active site loops (residue 432-438). The mass spectra of S312C (**mut2**) labeled peptides in 4 conditions of vesicles are shown in Figure 2.40. The positions of this type of exposed labeling either in the presence or in the absence of vesicles might not be in contact with lipids upon binding to the membrane, so no differences in labeling is observed.

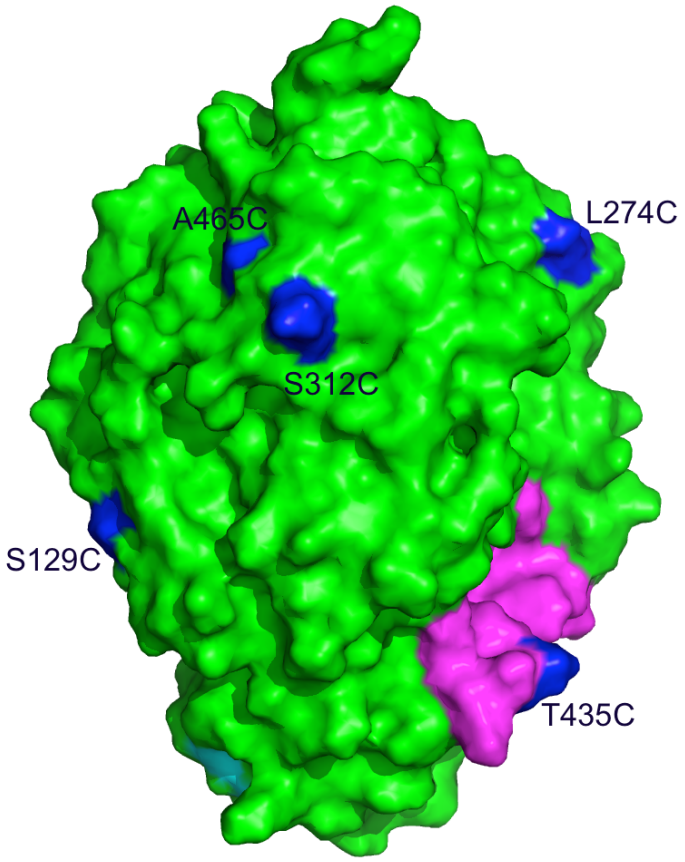

Figure 2.39 Molecular surface representation of positions of exposed labeling cysteine mutations. Cysteine mutation sites for exposed labeling S129C (**mut1**), L274C, S312C (**mut2** & **mut5**), T435C (**mut2**) and A465C (**mut5**) of *Streptomyces* cholesterol oxidase (PDB entry 1MXT). Cholesterol oxidase is colored in green, two loops (residue 72-87 and 432-438) in purple, S129C (**mut1**), L274C, S312C (**mut2** & **mut5**), T435C (**mut2**), and A465C (**mut5**) in blue.

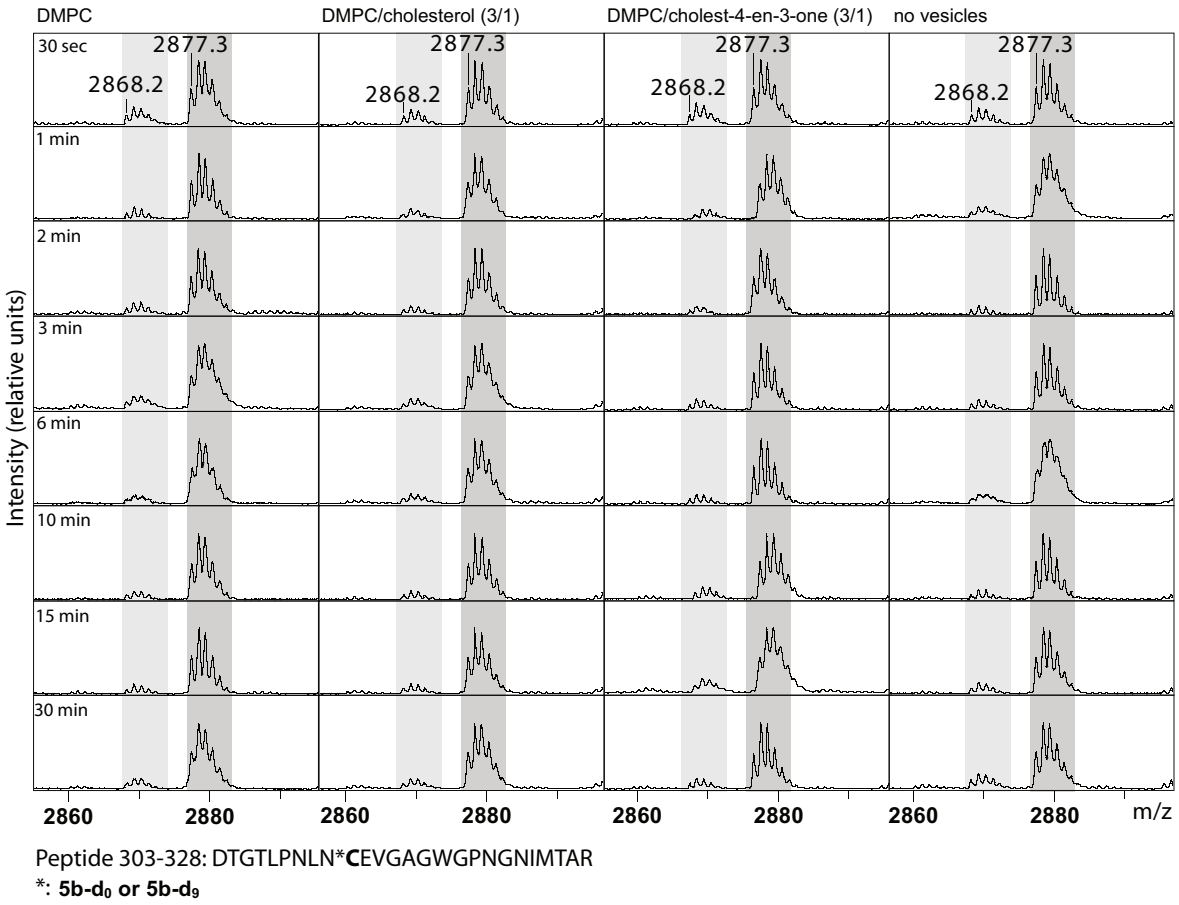

Figure 2.40 Mass spectra of peptide containing S312C (mut2) mutation site from mut2 mutant labeling under different lipid conditions.
Protein (10 μM) was labeled in the presence of 500 μM lipid vesicles and 50 μM **5b-d$_9$**, aliquots were taken at 30 sec, 1, 2, 3, 6, 10, 15, and 30 min, and 4.95 mM **5b-d$_0$** was added to the reaction. Mass spectra of S312C (**mut2**) ICMT labeled peptide$_{303\text{-}328}$ in different lipid conditions. The peaks corresponding to light-labeled peptide are highlighted in light gray, and the peaks corresponding to heavy-labeled peptide are highlighted in dark gray.

The rest of the cysteine mutations, A32C (**mut1** & **mut5**), T168C (**mut5**), A184C (**mut4** & **mut6**), A301C (**mut6**), T371C (**mut1**), and A423C (**mut1**) are only labeled in the second step (protected labeling) regardless of the presence or absence of vesicles. The positions of these light probe labeled cysteine mutations in crystal structure are shown in Figure 2.41. The mass spectra of A301C (**mut6**) labeled peptide in 4 conditions are shown in Figure 2.42. The protected labeling (labeling in second step) cysteine mutations indicate they are possibly in membrane binding sties of the protein sitting on the lipid bilayer or they are buried in the protein local structure. Generally, for these two types of exposed labeling or protected labeling, there were no obvious differences when proteins were labeled with or without vesicles.

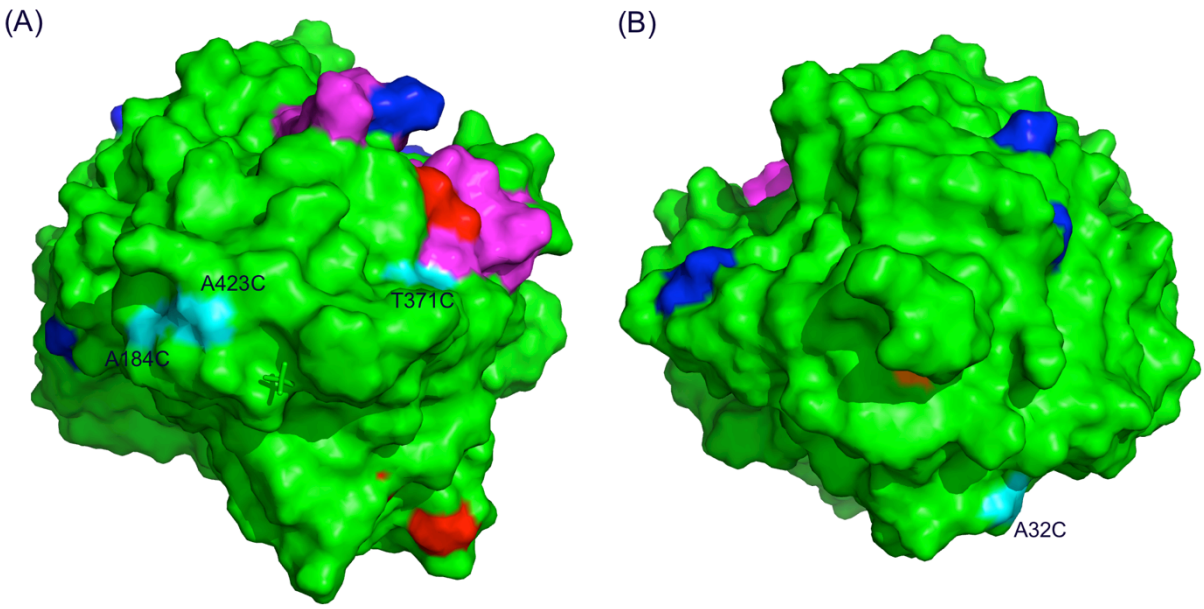

Figure 2.41 Molecular surface representation of positions of protected labeling cysteine mutations. (A) Front view. (B) Back view. Cysteine mutation sites for A32C (**mut1** & **mut5**), A184C (**mut4** & **mut6**), A301C (**mut6**), T371C (**mut1**), and A423C (**mut1**) of *Streptomyces* cholesterol oxidase (PDB entry 1MXT). Cholesterol oxidase is colored in green, two loops (residue 72-87 and 432-438) in purple, A32C (**mut1** & **mut5**), A184C (**mut4** & **mut6**), A301C (**mut6**), T371C (**mut1**), and A423C (**mut1**) in cyan.

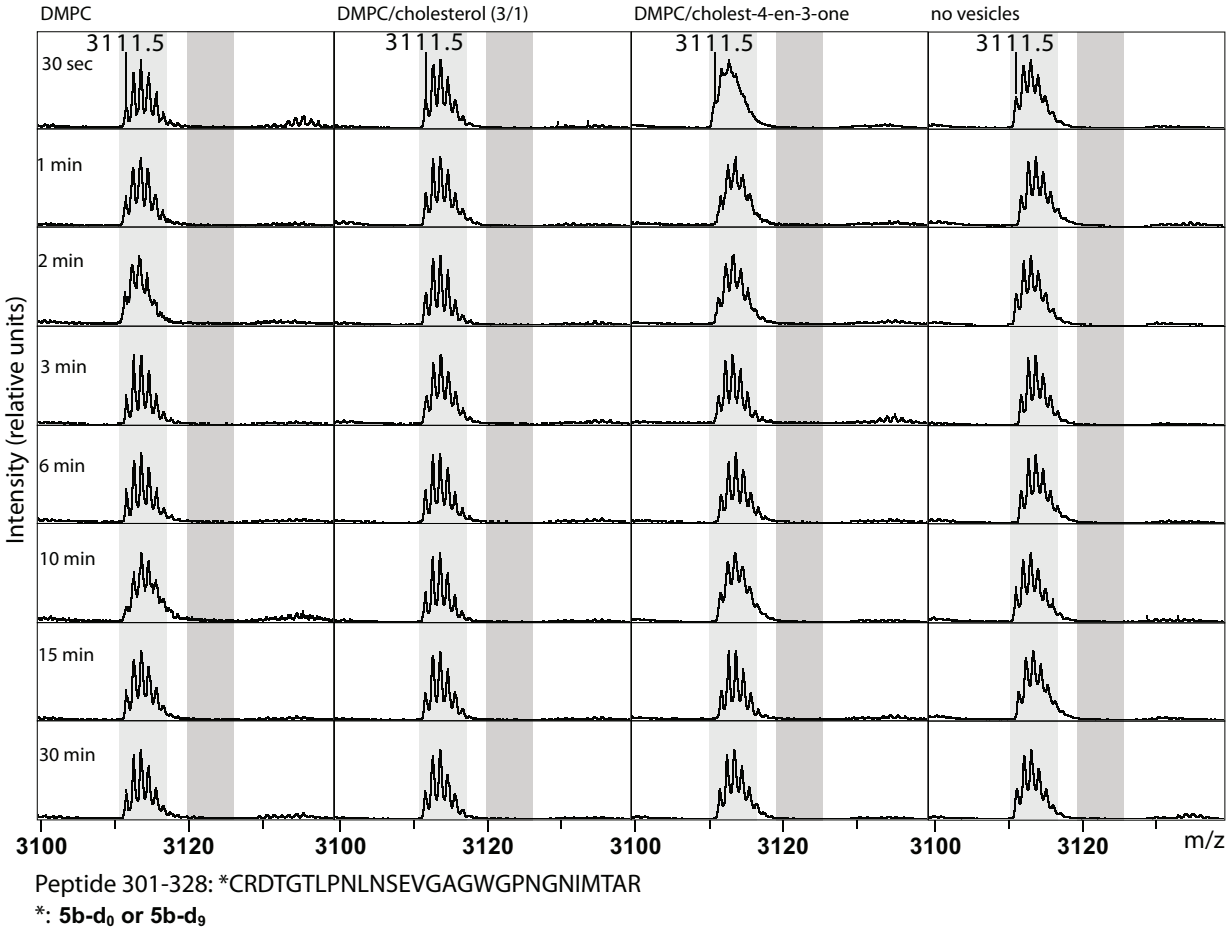

Figure 2.42 Mass spectra of peptide containing A301C (mut6) mutation from mut6 mutant labeling in different lipid conditions.
Protein (10 μM) was labeled in the presence of 500 μM lipid vesicles and 50 μM **5b-d$_9$**, aliquots were taken at 30 sec, 1, 2, 3, 6, 10, 15, and 30 min, and 4.95 mM **5b-d$_0$** was added to the reaction. Mass spectra of A301C (**mut6**) ICMT labeled peptide$_{301\text{-}328}$ in different lipid conditions. The peaks corresponding to light-labeled peptide are highlighted in light gray, and the peaks corresponding to heavy-labeled peptide are highlighted in dark gray.

Among the 5 overlapping cysteine mutations, A32C (**mut1** & **mut5**), T168C (**mut3** & **mut5**), A184C (**mut4** & **mut6**), S312C (**mut2** & **mut5**), and A465C (**mut4** & **mut5**), cysteine mutations of A32C (**mut1** & **mut5**), A184C (**mut4** & **mut6**) and S312C (**mut2** & **mut5**) have comparable results to these mutations in different protein mutants. A465C can only be identified in **mut5** mutant, but not in **mut4** mutant. Interestingly, T168C (**mut3** & **mut5**) mutation shows different results in **mut3** and **mut5** mutants. T168C (**mut3**) mutation shows slow dynamic labeling profile in **mut3** mutant whereas T168C (**mut5**) shows protected labeling for **mut5** mutant. There are totally 6 and 8 cysteines in **mut3** and **mut5** mutants, respectively. Under the

labeling conditions, 10 μM enzyme and 50 μM probe, the effective cysteine concentrations in both mutants are 60 μM and 80 μM, with limited concentration of probe, the differences of labeling results in the same cysteine mutation is observed. The concentration effect is probably responsible for the consequence that T168C in **mut3** shows slow dynamic labeling but T168C in **mut5** shows only protected labeling.

Discussion

We prepared heavy/light ICMT probes as previously described and several single-cysteine and multi-cysteine mutants covering 19 cysteine mutations on the protein surface of cholesterol oxidase. Conventional methods were developed to investigate protein-lipid interactions. Nevertheless, there are still some limitations of these methods. We developed an ICMT strategy as outlined in Figure 2.32 to study cholesterol oxidase-lipid interactions. This method relies on differential reactivity of cysteine thiol to the maleimide of ICMTs, and is analyzed by MALDI-TOF. In this approach, there was no need to remove any of the native cysteine(s), and thus made protein expression easier and efficient. Up to four cysteine residues could be introduced in one protein, and this allowed fast scanning of multiple-sites from one protein at a time.

The labeling reaction protocols were also simplified to make high throughput possible. We took the advantage of the fast dilution of light probe in second step from transmembrane peptide dynamic experiments as outlined in Figure 2.12 (*146*), and this procedure greatly reduces the purification steps. The use of SDC is another benefit in this protocol. SDC can serve as not only denaturing reagent (*182*) but also solubilizing detergent to the hydrophobic proteins (*184*). Cholesterol oxidase is a soluble protein with hydrophobic interior to bind substrate, and the use of SDC to solubilize denatured protein can help protease digestion. SDC is compatible with trypsin in the presence of 1% concentration without interfering protease activity (*185*), and we found that chymotrypsin works well in the same condition as well. SDC can be precipitated and removed by acidifying the reaction solution.

Our procedure simplified purification steps of peptides, and avoided using conventional Ziptip purification protocol. In the Ziptip purification protocol, peptides are first bound to the C18 resin of Ziptip, and then peptides are eluted by mixture of organic solvent/acidic aqueous solution.

We use two proteases, trypsin and chymotrypsin, to digest proteins. The two proteases have different specificity toward the peptide cleavage site, and they will generate different lengths of peptides. Though most of the cysteine containing peptide can be identified in trypsin digest, there are still three of the cysteine mutations, A32C (**mut1** & **mut5**), T371C (**mut1**), and

A465C (**mut5**), which can only be found in chymotrypsin digest. The other advantage of using two proteases is that peaks of cysteine labeled peptides might be overlapping with other peptide peaks in one protease digest result, and they probably can be found from another protease digest result instead. The use of two proteases can also increase cysteine identification coverage, and the results can be used to compare with each other.

When different protein or probe concentrations were used for the labeling experiments, we observed the rates of labeling were concentration dependent. L80C was first labeled with high concentration of probe, 500 μM, and cysteine thiol was almost fully heavy probe labeled (exposed labeling) in 1 min for at least 60 minutes (Figure 2.33). The probe concentration was lowered 5-fold to 100 μM, but it showed all heavy probe labeled (exposed labeling) after 5 minutes (Figure 2.34). We also tried to use probe concentrations at 50 and 25 μM. When 25 μM of probe concentration was used, we observed obvious increase labeling rate in the presence of DMPC/cholesterol (3/1) vesicles (Figure 2.35). We also noticed that the rate of labeling was always faster in the presence of enzyme substrate whether the rate increasing changes are small or large. These results suggest that the L80C mutation on the loop (residue 73-86) is interacting with the lipid vesicles. The changes of labeling rates could be due to the protein conformational changes, such as open of the loop to transport substrate from the membrane to the protein active site. The loop movement makes the L80C thiol either interact with the positively charged headgroup that will result in lower cysteine pK_a or be more accessible to the solvent.

Different protein concentrations were used for **mut2**, and we also observed that the rates of labeling were still concentration dependent. When 10 μM protein was used, A205C (**mut2**) showed fast dynamic labeling. Cysteine mutations of S312C (**mut2**) and T435C (**mut2**) showed steady exposed labeling. We also used the protein concentrations 6.6 μM and 8.2 μM, and the results showed the labeling plateaus were only slightly reduced by 5-10 % compared to 10 μM protein used. The location of T168C (**mut3**) and A205C (**mut2**) are close to each other on the two different α-helices and coil junction position. T168C showed dynamic labeling in one mutant (**mut3**) and steady protected labeling in other mutant (**mut5**). The differences might be the effective cysteine concentrations in both mutant, 60 μM versus 80 μM, for **mut3** and **mut5**, respectively. These changes of labeling profile might be indicative that this region is very likely the binding region of the cholesterol oxidase to the membrane.

We also performed reaction kinetic simulations of **mut2** with probes from current labeling results using Copasi (*189*). We modeled competitive cysteine thiols reactions from 10 μM **mut2** and 50 μM probe, **5b-d$_9$**. There are 8 cysteines in the mutant including 4 native cysteines, C56, C282, C445, and C452, and 4 cysteine mutations, S153C, A205C, S312C, and T435C. Six cysteines were identified from current labeling experiments, but S153C and C282 were not identified. We then used the labeling data and estimated rate constants for S153C and C282 for kinetic simulation. Protein and probe concentration were set to 10 μM and 50 μM. Each cysteine had a concentration of 10 μM, and the effective total cysteine concentration would be 80 μM. The relative second-order rate constants were obtained from the labeling rate from each cysteine identified, and the values were estimated to fit the actual experimental results. The second-order rate constants of the two missing cysteine thiols (S153C and C282) were set to be equal. We made two extreme rate constants (5500 and 1 $M^{-1}s^{-1}$) for the missing cysteines, S153C and C282, and to obtain an idea how the rates of labeling were affected by the two missing cysteine. The simulation shown in fraction cysteine thiol labeled of the 6 cysteine thiols from experiments results (Figure 2.36 and Table 2.8) and 2 cysteine thiols from estimated data was shown in Figure 2.43. The rate constant values of 5500 and 1 $M^{-1}s^{-1}$ for the two missing cysteines (Figure 2.43F) were used to simulate reaction labeling rates for the 8 cysteine thiols, and the results were shown in Figure 2.43 A & B. The three native cysteine, C56, C445, and C452, showed lower labeling rate than that the cysteine mutations on the protein surface. The C56 was all protected labeling, and it showed very low labeling rate. In comparison of Figure 2.43 A & B, the simulation result in Figure 2.43A was close to the actual experimental results. The plateau of labeling for T435C, S312C, A205C, C445, C452, and C56 was 100%, 90%, 80%, 20%, 20%, and 0%, respectively. It is quite possible that the labeling rates for the two missing cysteine thiols are very fast. Since the effective cysteine concentration and probe concentration are 80 μM and 50 μM, respectively, the fraction cysteine thiol labeling will not reach 100% plateau for all cysteines. Therefore, we used this values to simulate the reaction labeling rate for different protein concentrations.

We then used 5, 6.6, and 8.2 μM protein concentrations with 50 μM probe for labeling rate simulations (Figure 2.43 C - E). The effective cysteine concentrations are 40, 52.8, and 65.6 μM for 5, 6.6, and 8.2 μM protein concentration used. In such conditions, the cysteine concentration are closer the probe concentration, and the rates are faster for A205C, S312C,

T435C, S153C, and C282, and might not be able to tell the differential rates. However, the simulation results are not consistent with our experimental data (Figure 2.36). The effective probe concentration should be taken into considerations because insufficient probe concentration will make the labeling rate plateau occur at certain percentage. This reaction rate profile will complicate data interpretation. In general, these simulation results provide valuable information of how the reaction kinetics could be, and could be used to predict the reaction profiles in multi-cysteine mutant system.

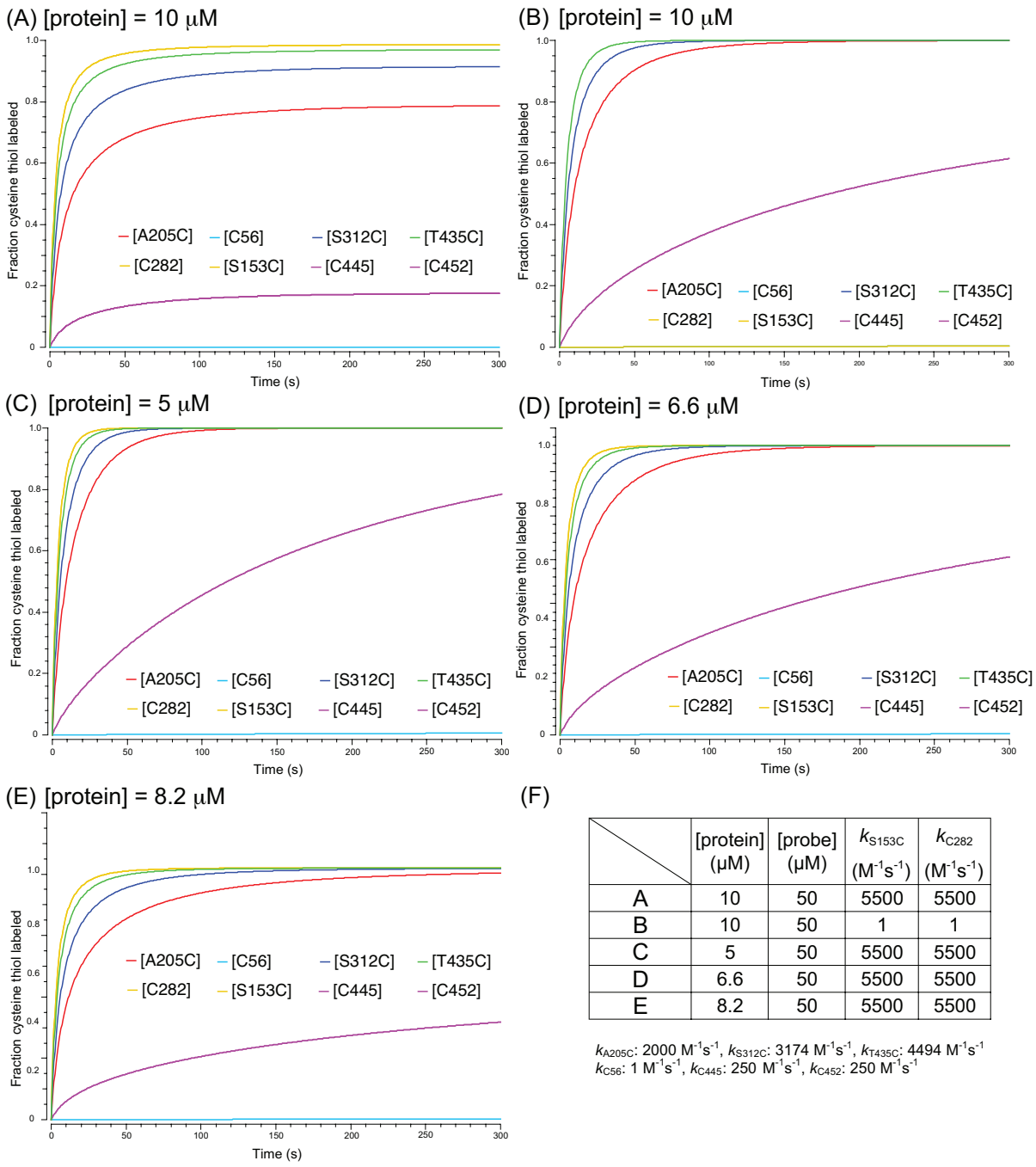

(F)

	[protein] (μM)	[probe] (μM)	k_{S153C} ($M^{-1}s^{-1}$)	k_{C282} ($M^{-1}s^{-1}$)
A	10	50	5500	5500
B	10	50	1	1
C	5	50	5500	5500
D	6.6	50	5500	5500
E	8.2	50	5500	5500

k_{A205C}: 2000 $M^{-1}s^{-1}$, k_{S312C}: 3174 $M^{-1}s^{-1}$, k_{T435C}: 4494 $M^{-1}s^{-1}$
k_{C56}: 1 $M^{-1}s^{-1}$, k_{C445}: 250 $M^{-1}s^{-1}$, k_{C452}: 250 $M^{-1}s^{-1}$

Figure 2.43 Simulation of the rates of cysteine thiols in mut2: S153C/A205C/S312C/T435C mutant. Relative rate constants were obtained from experimental labeling reactions of A205C, S312C, T435C, C56, C445, and C452. Second-order rate constants were estimated based on current labeling experimental results form 10 μM **mut2**: S153C/A205C/S312C/T435C mutant and 50 μM probe, **5b-d$_9$**. Rate constants used of cysteine reaction with probe were 2000, 3174, 4494, 1, 250, and 250 $M^{-1}s^{-1}$ for A205C, S312C, T435C, C56, C445, and C452, respectively. The simulation was performed with Copasi (www.copasi.org)(*189*). Simulation results of various protein and probe concentrations: (A) [protein] = 10 μM, [probe] = 50 μM. (B) [protein] = 10 μM, [probe] = 50 μM. (C) [protein] = 5 μM, [probe] = 50 μM. (D) [protein] = 6.6 μM, [probe] = 50 μM. (E) [protein] = 8.2 μM, [probe] = 50 μM.

We labeled protein mutants with heavy probe **5b-d$_9$** in DMPC, DMPC/cholesterol (3/1), DMPC/cholest-4-en-3-one (3/1) vesicles, or in the absence of vesicles. The majority of the cysteine thiols labeling rates of these selected mutation sites are similar in the four conditions except for some cysteine mutations, L80C, T168C (**mut3**), and A205C (**mut2**) (Figure 2.37). We expect the labeling rate of solvent inaccessible thiol, protected by contacting with membrane, will be slower than that of solvent accessible thiol and the differences should be detectable in our protocol under these conditions. This method relies on the utilization the differential reactivity of cysteine sulfhydryl to the ICMT probes in protein's native conformation in the presence or absence of lipid vesicles. Therefore, the reactivity of sulfhydryl should be examined.

We dispersed the cysteine mutations on the cholesterol oxidase surface, which will result in different sulfhydryl reactivities toward maleimide of the ICMT probe. When we compared the results of labeling from these cysteine mutations, we should first assess the locations of these cysteine mutations. The rates of cysteine thiols labeling are not only altered by interacting with lipid membrane but also are influenced by the conformational changes of the protein itself. We will discuss three types of labeling, dynamic labeling, exposed labeling, and protected labeling from current experimental results.

L80C mutation is known to be in one of the active site loops (residues 73-86), and is shown to interact with lipid headgroups (*60, 104*). The labeling rate of L80C increases upon binding to the membrane, and this could be the evidence that protein makes conformational change upon binding to the membrane (Figure 2.37). This effect is more obvious when lower heavy probe concentration was used to label L80C mutant.

In contrast, T168C (**mut3**) has a slower labeling rate when binding to the membrane. Interestingly, T168C (**mut5**) shows steady protected labeling in the presence and absence of vesicles. This mutation site could probably bind to the membrane during the course of catalysis process or could be involved in the region of protein conformational changes. However, it is also quite possible that the differences might come from the effective cysteine concentrations in both mutant, 60 μM versus 80 μM, for **mut3** and **mut5**, respectively.

From the results shown above, the increase of labeling rate for L80C and A205C (**mut2**) could be explained in two ways. First, protein makes conformational changes, such as open of

the loops, and cysteine thiol of L80C mutant is more accessible to the solvent upon binding to the membrane or upon binding substrate. Second, the loop containing L80C interacts with the lipid headgroup, which is choline in DMPC vesicles, the pK_a of thiol is lowered, and thus increases the labeling rate. Nevertheless, the changes are not as much as we might expect. This phenomenon also suggests that the loop of the protein might only be minimally interacting with the membrane.

In the case of A205C (**mut2**) and T168C (**mut3**), they participate in the interaction with lipid membrane, and they are in a region that protein makes slight conformational changes. It is also possible that the results are due to fast protein on-and-off rate to the surface of the membrane.

When we examine the surface charge distribution of the protein, L80C, T168C, and A205C have negative, positive, and negative charged environment around these cysteine thiols. The inherent cysteine reactivity is also an important factor when we try to interpret the results from the different labeling rates of these cysteine mutations. In order to compare the reactivity of the cysteine mutations introduced to the protein, we compared the solvent accessibility of all these cysteine mutations (*190-193*) (Figure 2.44). Five residues show very low solvent accessibilities, C56, C282, A301C, C445, and C452. In addition to the four native cysteines, A301C is the least accessible to solvent, and it can explain why this mutation behaves as protected labeling. Some of the lower solvent accessible residues, T168C, A184C, and T371C, show protected labeling. As a result, the lower labeling rates of these cysteine mutations might possibly be due to low accessibilities to the probe. The rest of the residues shows medium (~50 $Å^2$) to high (>150 $Å^2$) solvent accessibilities.

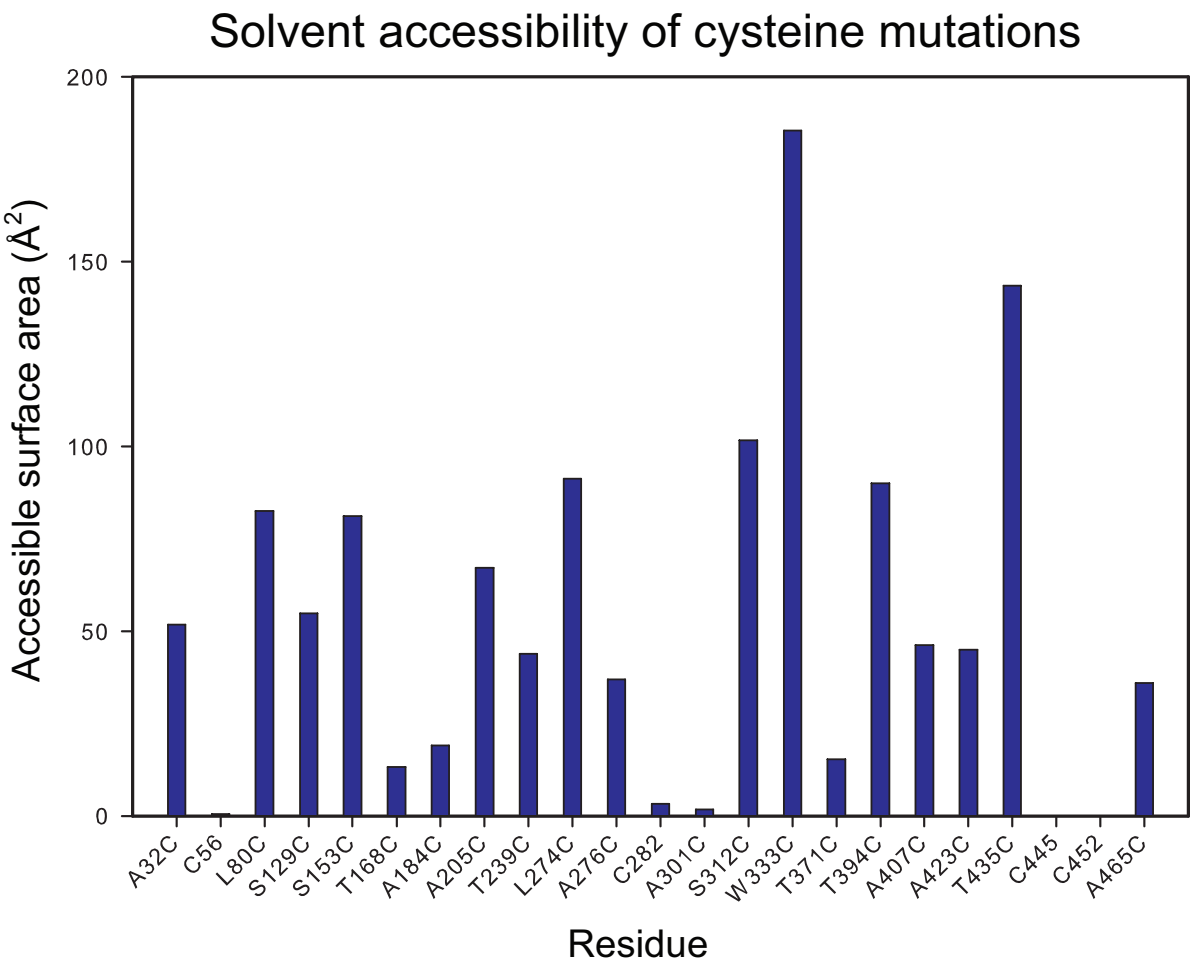

Figure 2.44 Solvent accessibility of cysteine mutations.
Solvent accessibility of native and mutated cysteines in cholesterol oxidase. The solvent accessibility is represented in ASA (accessible surface area, Å^2), and is calculated from cholesterol oxidase crystal structure (PDB entry 1MXT). The solvent accessibility calculation is performed with PDBePISA (Proteins, Interfaces, Structures and Assemblies) (www.ebi.ac.uk/pdbe/pisa/). The ASA of mutation sites are derived from wild-type protein, not substituted cysteines.

Six cysteine mutation sites, A32C (**mut1** & **mut5**), T168C (**mut5**), A184C (**mut4** & **mut6**), A301C (**mut6**), T371C (**mut1**), and A423C (**mut1**), show only protected labeling. All of these cysteine mutations show same results in the four conditions used in labeling experiments. The possible explanations of the all protected labeled cysteine mutations could be either the burial of cysteine in the protein or the cysteine in contact with the membrane that result in the elevated sulfhydryl pK_a.

Figure 2.45 shows that the positions of T168C (**mut5**), A184C (**mut4** & **mut6**), T371C (**mut1**), and A423C (**mut1**) from the cholesterol oxidase crystal structure (PDB entry 1MXT).

They are located near the two loops on a small surface. Based on the experimental results, it is possible the protein binds to the membrane on the small surface region. Two other mutations, A32C (**mut1** & **mut5**) and A301C (**mut6**), are located on the opposite sites of the small surface that could possibly bind to the membrane (Figure 2.46). The surface charge of these two cysteine mutations shows negative charge for A32C (**mut1** & **mut5**) and neutral charge for A301C (**mut6**) (Figure 2.47). However, the position of A301C (**mut6**) in the structure shows that the cysteine mutation is buried in the secondary structure, and is shown to have low solvent accessibility (Figure 2.44). The burial of the cysteine and elevated cysteine pK_a for A301C (**mut6**), and A32C (**mut1** & **mut5**), respectively, might be responsible for slower labeling rates in first step. The surface charge distribution of the cysteine mutation sites, T168C (**mut5**), A184C (**mut4** & **mut6**), T371C (**mut1**) and A423C (**mut1**), on the small surface are all positively charged environments except for T371C (**mut1**) mutation, which is negatively charged. The slower labeling rates of these cysteine mutations should not be due to the elevated pK_as of the cysteine thiols. These mutation sites are highly possible to be in membrane contact, but somehow the labeling rates are also slower even in the absence of vesicles.

Besides inherent pK_as of cysteine thiols affected by surface charges, the other possible reason might be that some lipids bound to the protein during the purification step. The lipid bound cholesterol oxidase will affect UV absorption at 249 nm. We compared the ratio of A_{280nm}/A_{249nm} to determine the relative amounts of lipids bound to the protein. The ratio of A_{280nm}/A_{249nm} for wild-type enzyme was typically 2.56 (*81*). The higher value means less lipids bound to the protein. The ratios of A_{280nm}/A_{249nm} for current expressed wild type, L80C, L274C, W333C, **mut1**, **mut2**, **mut3**, **mut4**, **mut5**, and **mut6** cholesterol oxidases are 2.67, 2.68, 2.73, 2.77, 2.5, 2.75, 2.38, 2.67, 2.65, and 2.72, respectively (Figure 2.29). Most of the proteins have comparable values with the wild-type enzyme. However, we did not know the exact amount of lipid bound to the protein nor the sites of the protein these lipids were bound. Nevertheless, it was possible that the binding region of the protein to the lipid bilayer was occupied with lipid molecules, and it caused these cysteine thiols were still not accessible to the probe even in the absence of vesicles.

The T168C (**mut3** & **mut5**) mutation behaves differently in **mut3** and **mut5**. In **mut3**, the labeling rate showed slow dynamic labeling, but it did not reach plateau (Figure 2.37).

Moreover, the rate of labeling decreased in the presence of vesicles, suggesting that this position was possible to interact with lipid membrane. In **mut5**, T168C showed only protected labeling. It is proposed that the effected cysteine concentrations are responsible for the results, but T168C (**mut3** & **mut5**) should participate in interaction with the lipid bilayer from current data. We can only predict the possible protein binding region to the membrane (Figure 2.45) from current experimental data.

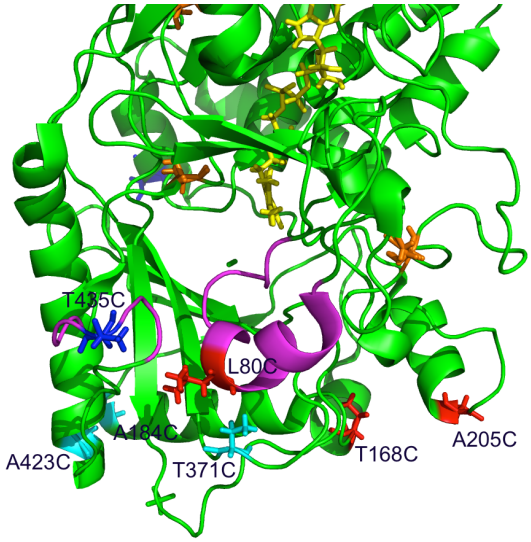

Figure 2.45 Possible binding region of *Streptomyces* cholesterol oxidase to the model membrane. Cholesterol oxidase (PDB entry 1MXT) is colored in green, FAD in yellow, two loops (residue 72-87 and 432-438) in purple, L80C, T168C (**mut3**), and A205C (**mut2**) in red, A184C (**mut4** & **mut6**), A423C (**mut1**), and T371C (**mut1**) in cyan, and T435C (**mut2**) in blue. FAD and cysteine mutation sites are shown in ball-and-stick.

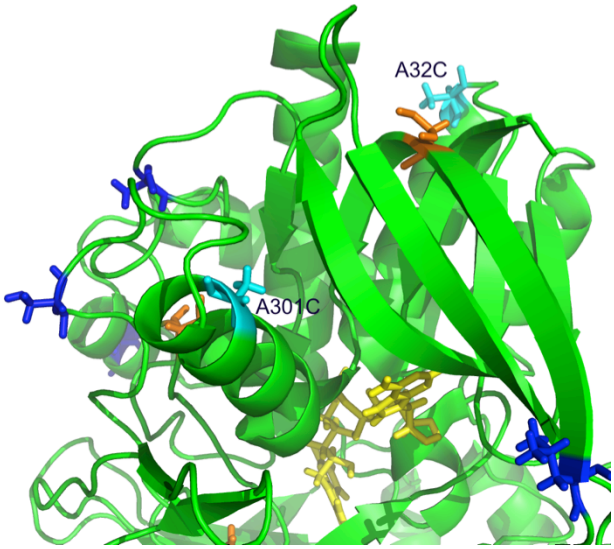

Figure 2.46 Positions of A32C and A301C of *Streptomyces* cholesterol oxidase.
Cholesterol oxidase (PDB entry 1MXT) is colored in green, FAD in yellow, two loops (72-87 and 432-438) in purple, A32C (**mut1** & **mut5**) and A301C (**mut6**) in cyan, and protected labeling residues in blue. FAD and cysteine mutation sites are shown in ball-and-stick.

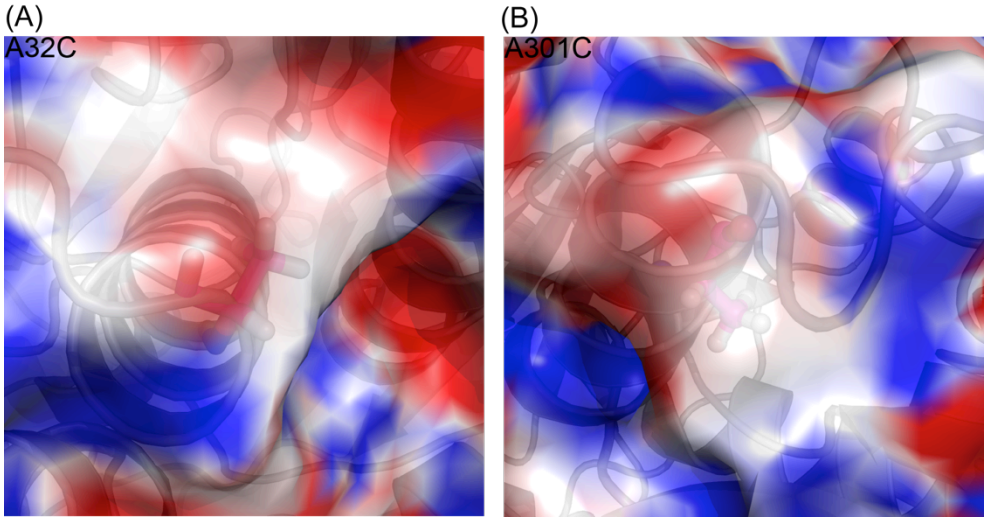

Figure 2.47 Surface charge distribution of A32C and A301C of cholesterol oxidase.
(A) A32C (**mut1** & **mut5**) and (B) A301C (**mut6**) of *Streptomyces* cholesterol oxidase (PDB entry 1MXT). Cholesterol oxidase is colored in gray, and A32C (**mut1** &**mut5**) and A301C (**mut6**) are shown in ball-and-stick. Negative charge, positive charge, and neutral charge are shown in red, blue, and white, respectively.

In the case of exposed cysteine labeling mutations, S129C (**mut1**), L274C, S312C (**mut2** & **mut5**), T435C (**mut2**), and A465C (**mut5**), the heavy probe labeling in the first step (exposed labeling) means that cysteine is accessible to the probe regardless in the presence of vesicles or not. Since the labeling rate is so fast even in the presence of the vesicles, these sites might not be

in the membrane contact region of the protein (Figure 2.32A). The positions of these cysteine mutations in crystal structures shows that besides T435C (**mut2**) which is located on the loop (residue 432-438), all others located on the sites are away from the small proposed protein binding surface (Figure 2.39). In addition, these results also suggest that these mutations probably are not in the protein dynamic moving domains.

The positions of identified cysteine mutation sites of cholesterol oxidase are shown in Figure 2.48. The proposed binding region of cholesterol contains the protected labeling mutations, T168C (**mut5**), A184C (**mut4** & **mut6**), T371C (**mut1**), and, A423C (**mut1**), L80C and T435C (**mut2**) on the two loops, and A205C (**mut2**) that shows dynamic labeling (Figure 2.45).

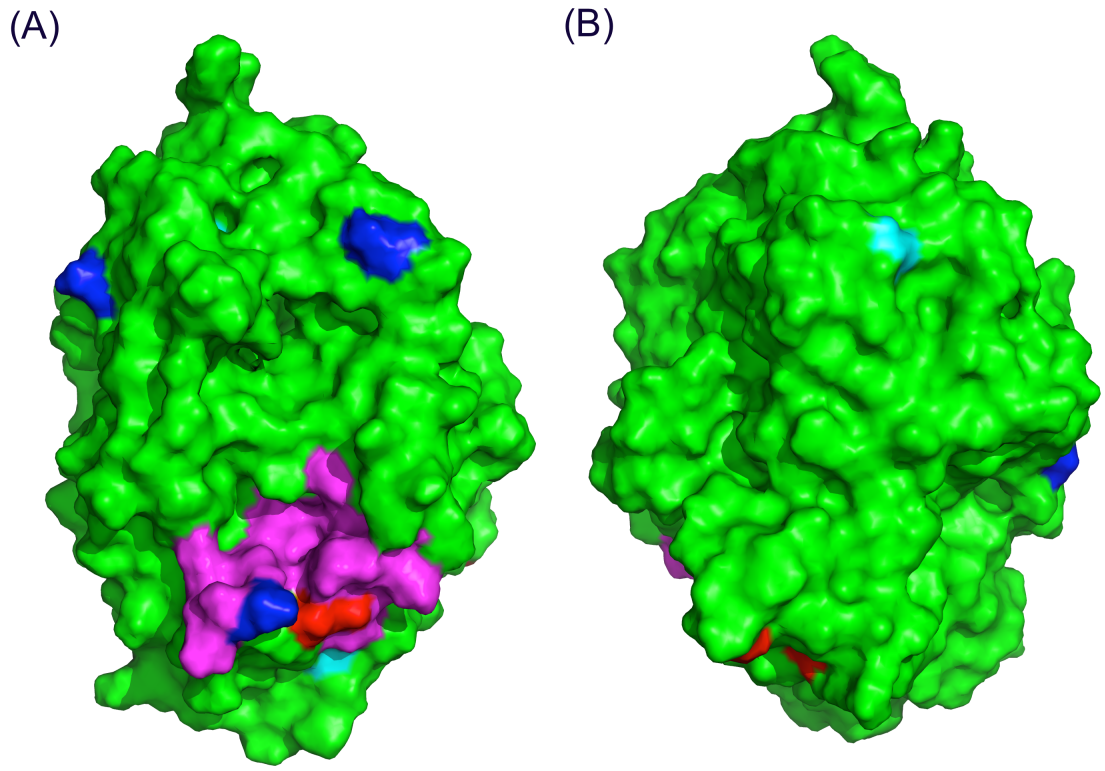

Figure 2.48 Molecular surface representation of positions of cysteine mutations of *Streptomyces* cholesterol oxidase.
(A) Front view. (B) Back view. Cholesterol oxidase (PDB entry 1MXT) is colored in green, two loops (residue 72-87 and 432-438) in purple, dynamic labeling cysteine mutations in red, exposed labeling cysteine mutations in blue, and protected labeling cysteine mutations in cyan.

The reaction kinetics for cysteine thiols in the multi-cysteine mutant are complicated. There are up to 8 cysteine residues, including 4 native cysteines, and they are competing with each other for the same probe at the same time. Even in a single cysteine mutant, there are still 5 cysteines in one protein. The location of 4 native cysteines are shown in Figure 2.49. From the crystal structure, all of the native cysteines are buried inside the protein hydrophobic core. The C56 can be identified in chymotrypsin digest and C445 and C452 can be identified in trypsin digest. The labeling rate of C56 is slow in 10 μM **mut2** mutant, there is nearly no heavy probe labeling in first step (only protected labeling). For C445 and C452, they are identified in the same peptides, and the heavy probe labeling usually ranges from 20 to 30%. The native cysteine thiols generally have lower labeling rates compared to the mutated cysteines of the protein surface. However, in analyzing the kinetics of the cysteine mutations, we still can not neglect the reactions of these native cysteines to the probe.

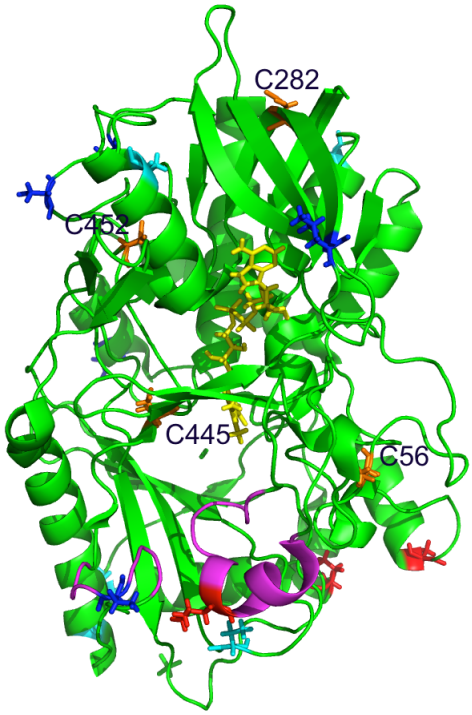

Figure 2.49 Positions of native cysteines of *Streptomyces* cholesterol oxidase.
Cholesterol oxidase (PDB entry 1MXT) is colored in green, FAD in yellow, two loops (72-87 and 432-438) in purple, dynamic labeling cysteine mutations in red, exposed labeling cysteine mutations in blue, protected labeling mutations in cyan, and native cysteines, C56, C282, C445, and C452, in orange. FAD, cysteine mutation sites, and native cysteines are shown in ball-and-stick.

Regarding the sulfhydryl chemistry, the reaction of cysteine thiols to the maleimides are fast, and the stability of maleimide in buffers should be considered (*194*). Maleimides are stable below pH 6 (*195*), and the half-time for hydrolysis of maleimide at pH 7 and pH 9 are approximately 45 h and 1 h, respectively (*196*). We performed our experiment at pH 7, and concentration consumption due to hydrolysis in the time course we used is negligible (approximately 0.3 μM). It was also reported that lysine residues would react with maleimide at pH > 7.5 with long time incubation (*197*). In our working buffer pH and reaction time course (30 sec to 30 min), reaction specificity of cysteine thiols to maleimides should be maintained. It should be noted that reaction rate of thiolate to the hydrogen peroxide which is the by product after reduction of $FADH_2$ to FAD during catalysis is faster than that of protonated thiol (*198*). Nevertheless, we did not detect the oxidized cysteine containing peptide in mass spectra.

Previous data showed that cholesterol oxidase only loosely associates with the membrane (*101*). It is also possible that the region of the protein interacting with membrane is small, so the interacting residues are limited to only several of these cysteine mutations. It is also likely that the interacting residues with the membrane are beyond our designated mutations, and more cysteine mutations are needed to get more information from labeling experiments.

Chapter 3 Experimental Methods

3.1Materials

α-Cyano-4-hydroxycinnamic acid, sinapinic acid, Triton X-100, 5(6)-carboxyfluorescein, and sodium deoxycholate were purchased from Sigma-Aldrich. DL-Dithiothreitol, sodium dodecyl sulfate, tryptone, HEPES, ampicillin, sodium dihydrogen phosphate, sodium hydrogen phosphate, and tris(2-carboxyethyl)phosphine were purchased from Fisher Scientific. Cholic acid sodium salt was obtained from MP Biochemicals, Inc. Cholest-4-en-3-one was purchased from Acros Organics. 2,5-Dihydroxybenzoic acid was purchased from TCI. Phospholipids were purchased from Avanti Polar Lipids, Inc. Oligonucleotides were purchased from Eurofins mwg Operon. Restriction enzymes and trypsin were purchased from New England Biolabs. Chymotrypsin, Rapid DNA Ligation Kit, and Roche High Pure Plasmid Isolation Kit were purchased from Roche Applied Science (Mannheim, Germany). QuickChange Site-Directed Mutagenesis Kit and QuickChange Lightning Multi Site-Directed Mutagenesis Kit were purchased from Stratagene. Isopropyl β-D-1-thiogalactopyranose was purchased from Denville Scientific. Peptide **6** (Ac-$K_2GL_7WLCL_9K_2A$-NH_2), peptide **7** (Ac-$CK_2GL_7WLAL_9K_2A$-NH_2), and peptide **8** (Ac-$K_2CL_7WLAL_9K_2A$-NH_2) were provided by the Keck Laboratory at Yale University. NB-ECD-OMe (5-norbornene-*exo*-carboxyl-glutamate-cysteine-aspartate-α-methyl ester) was provided by Younjoo Lee, PhD, Stony Brook University and synthesized by solution phase methods (*199*). Iodomethane-d_3, chloroform-d_1, and deuterium oxide were purchased from Cambridge Isotope Laboratories, Inc. Solvents were purified with a Pure Process Technology solvent dispensing system.

3.2 General methods

Analytical thin layer chromatography (TLC) was performed on precoated silica gel plates (60F254), flash chromatography was performed with silica gel-60 (230-400 mesh) and Combi-Flash chromatography was performed with RediSep normal phase silica columns (silica gel-60, 230-400 mesh). ^{1}H NMR spectra are reported as chemical shifts in parts per million (ppm) in the following order: (i) multiplicity, (ii) coupling constant in Hz, and (iii) integration. ^{13}C NMR spectra are reported as chemical shifts in ppm. The solvent peak was used as an internal reference. DNA sequencing with an Applied Biosystems 3730 DNA analyzer was performed at the Stony Brook University Sequencing Facility to verify the coding sequencing of the

expression plasmids for all cholesterol oxidase mutants. 2xYT was composed of 16 g tryptone, 10 g yeast extract, and 5 g NaCl per liter.

An MTP 384 target plate was used for MALDI analysis (Bruker Daltonics). Sample preparation for MALDI mass analysis: The matrices were prepared by dissolving α-cyano-4-hydroxycinnamic acid (CHCA, 20 mg/mL) in a 7/3 (v/v) mixture of 5% (v/v) formic acid in H_2O/ACN, 2,5-dihydroxybenzoic acid (DHB, 20 mg/mL) in a 7/3 (v/v) mixture of 0.1% TFA (v/v) in H_2O/ACN or sinapinic acid (SA, 20 mg/mL) in a 7/3 (v/v) mixture of 0.1% TFA (v/v) in H_2O/ACN. Prior to application to the target sample plate, the labeled peptide sample solutions were mixed with matrix in a 1:1 ~ 1:3 ratio (v/v). The sample-matrix mixture (1 μL) was applied onto the MTP384 target plate and was allowed to air dry before acquiring mass spectra.

3.3 Instrumentation

MS Spectra were acquired on a Bruker Autoflex II MALDI-TOF/TOF mass spectrometer operated in the reflectron mode (Bruker Biosciences Corporation). A nitrogen laser UV laser (337 nm, 1-5 ns pulse of max energy 140 μJ, 10 Hz) was used for desorption/ionization. Positive ions were subjected to an accelerating potential of 19.0 kV and 16.9 kV from ion source 1 and ion source 2, respectively and 8.35 kV from the optical lens reflected by reflectron electrodes (20 kV and 9.52 kV), and detected by a microchannel plate (MCP) detector using 4X – 12X voltage gain. The pulsed ion extraction time was 135 ns. Matrix ions were suppressed using a low mass (*m/z* 500) cutoff. Raw mass spectra data were analyzed by Bruker flexAnalysis version 3.0 software.

The purification of organic products was performed on a Teledyne Isco CombiFlash chromatography instrument. Protein purification (butyl sepharose) was performed on a Pharmacia ÄKta explorer. NMR spectra were acquired on Inova 400, Inova 500, Inova 600, or Bruker 400 MHz NMR spectrometers. Fluorescence experiments were performed on a PTI Spectrofluorimeter QM-4/2005-SE with double monochromators. UV/vis spectra and kinetics assays were performed on a Shimadzu UV-2550 UV-visible spectrophotomer (Kyoto. Japan). Masses of organic samples were acquired on a Waters ACQUITY Ultra Performance LC system

equipped with a PDA detector and a SQ detector. Sizes of synthetic vesicles were determined by dynamic light scattering (Brookhaven Instruments, DLS-90)

3.4 Synthesis of ICMTs

4-(3-(*tert*-butoxycarbonylamino)propylamino)-4-oxobut-2-enoic acid (2a) (*130*): *tert*-butyl 3-aminopropylcarbamate (**1a**) (*200*) (11.65 g, 66.90 mmol) in CH_2Cl_2 (100 mL) was added dropwise to a cooled solution of maleic anhydride (6.56 g, 66.90 mmol) in CH_2Cl_2 (150 mL). The solution was stirred for 3 h and was washed with brine (2 x 25mL) and DI water (2 x 25mL). The organic layer was dried over Na_2SO_4 and the solvent was removed under reduced pressure. The product was further purified by column chromatography in Combiflash (linear gradient elution: hexane/EtOAc, 85/15 to 20/80). Yield: 94%. **^{1}H-NMR** (500 MHz, $CDCl_3$) δ 8.23 (s, 1H), 6.36 (d, *J* = 10.0 Hz, 1H), 6.32 (d, *J* = 10.0 Hz, 1H), 4.84 (s, 1H), 3.40 (td, *J* = 10.0 and 5.0 Hz, 2H), 3.22 (td, *J* = 10.0 and 5.0 Hz, 2H), 1.70 (q, *J* = 5.0 Hz, 2H), 1.45 (s, 9H); **^{13}C-NMR** (100MHz, CD_3OD) δ 168.12, 168.03, 158.72, 134.40, 133.50, 80.21, 38.83, 38.46, 30.29, 28.89. **MS** (ESI) Calcd. for $C_{12}H_{20}N_2O_5$ $(M+Na)^+$: 295.13; Found: 295.23.

4-(4-(*tert*-butoxycarbonylamino)butylamino)-4-oxobut-2-enoic acid (2b): Compound **2b** was prepared by the same method as **2a** starting from *tert*-butyl (4-aminobutyl)carbamate (**1b**) and maleic anhydride. Yield: 89%. **^{1}H-NMR** (400 MHz, $CDCl_3$) δ 8.68 (s, 1H), 6.49 (d, *J* = 12.0 Hz, 1H), 6.30 (d, *J* = 12.0 Hz, 1H), 4.82 (s, 1H), 3.39 (td, *J* = 8.0 and 4.0 Hz, 2H), 3.15 (td, *J* = 8.0 and 5.0 Hz, 2H), 1.70 – 1.50 (m, 4H), 1.43 (s, 9H); **^{13}C-NMR** (100MHz, $CDCl_3$) δ 166.25, 165.95, 156.79, 135.62, 131.97, 79.77, 40.29, 39.58, 28.37, 24.59. **MS** (ESI) Calcd. for $C_{13}H_{22}N_2O_5$ $(M+Na)^+$: 309.14; Found: 309.24.

4-(6-(*tert*-butoxycarbonylamino)hexylamino)-4-oxobut-2-enoic acid (2c): Compound **2c** was prepared by the same method as **2a** starting from *tert*-butyl (6-aminohexyl)carbamate (**1c**) and maleic anhydride. Yield: 69%. **^{1}H-NMR** (400 MHz, $CDCl_3$) δ 8.39 (s, 1H), 6.51 (d, *J* = 12.0 Hz, 1H), 6.28 (d, *J* = 12.0 Hz, 1H), 4.73 (t, *J* = 8.0 Hz, 1H), 3.39 (td, *J* = 8.0 and 4.0 Hz, 2H), 3.10 (d, *J* = 8.0 Hz, 2H), 1.59 (td, *J* = 8.0 and 4.0 Hz, 2H), 1.50 – 1.25 (m, 6H), 1.42 (s, 9H); **^{13}C-NMR** (100MHz, $CDCl_3$) δ 166.21, 166.03, 056.53, 135.49, 132.12, 79.34, 39.66, 29.87, 28.38, 28.09, 25.44, 25.20. **MS** (ESI) Calcd. for $C_{15}H_{26}N_2O_5$ $(M+Na)^+$: 337.17; Found: 337.31.

2,2-dimethyl-4,15-dioxo-3,8,11-trioxa-5,14-diazaoctadec-16-en-18-oic acid (2d): Compound **2d** was prepared by the same method as **2a** starting from *tert*-butyl (2-(2-(2-aminoethoxy)ethoxy)ethyl)carbamate (**1d**) and maleic anhydride. Yield: 95%. **^{1}H-NMR** (400 MHz, $CDCl_3$) δ 6.49 (d, *J* = 12.8 Hz, 1H), 6.26 (d, *J* = 12.4 Hz, 1H), 3.65- 3.60 (m, 6H), 3.50 (q, *J* = 6.0 Hz, 4H), 3.22 (t, *J* = 5.6 Hz, 2H), 1.43 (s, 9H); **^{13}C-NMR** (100MHz, CD_3OD) δ 168.02, 167.96, 158.53, 134.07, 133.89, 80.22, 71.44, 71.19, 70.03, 54.95, 41.31, 41.06, 28.89. **MS** (ESI) Calcd. for $C_{15}H_{26}N_2O_7$ $(M+Na)^+$: 369.16; Found: 369.23.

***tert*-butyl 3-(2,5-dioxo-2*H*-pyrrol-1(5*H*)-yl)propylcarbamate (3a) (*130*):** A mixture of **2a** (4.52 g, 16.60 mmol), anhydrous sodium acetate (1.23 g, 14.94 mmol), and acetic anhydride (22.03 g, 215.80 mmol) was heated at 110 °C for 3 h. After the reaction reached completion (monitored by TLC or MS or NMR) , it was cooled to 22 °C, and an ice cold saturated $NaHCO_3$ solution was poured into the reaction mixture to neutralize excess acetic anhydride and acetic acid. The mixture was extracted with CH_2Cl_2, washed with brine and DI water, and dried over Na_2SO_4. After evaporation of the solvent, the product was purified by column chromatography using a Combiflash system (linear gradient elution: hexane/EtOAc, 95/5 to 60/40). Yield: 60%. **^{1}H-NMR** (400 MHz, $CDCl_3$) δ 6.69 (s, 2H), 4.90 (s, 1H), 3.57 (t, *J* = 6.8 Hz, 2H), 3.07 (q, *J* = 6.4 Hz, 2H), 1.74 (q, *J* = 6.4 Hz, 2H), 1.43 (s, 9H); **^{13}C-NMR** (100 MHz, $CDCl_3$) δ 170.87, 155.83, 134.11, 79.21, 37.31, 34.95, 28.79, 28.35**.** **MS** (ESI) Calcd. for $C_{12}H_{18}N_2O_4$ $(M+Na)^+$: 277.12; Found: 277.21.

***tert*-butyl 4-(2,5-dioxo-2*H*-pyrrol-1(5*H*)-yl)butylcarbamate (3b):** Compound **3b** was prepared by the same method as **3a** starting from **2b**. Yield: 55%. **^{1}H-NMR** (400 MHz, $CDCl_3$) δ 6.68 (s, 2H), 4.54 (s, 1H), 3.52 (t, *J* = 8.0 Hz, 2H), 3.12 (d, *J* = 4.0 Hz, 2H), 1.61 (q, *J* = 8.0 Hz, 2H), 1.46 (m, 2H), 1.42 (s, 9H); **^{13}C-NMR** (100 MHz, $CDCl_3$) δ 170.67, 155.81, 133.98, 78.99, 39.88, 37.34, 28.30, 27.26, 25.78. **MS** (ESI) Calcd. for $C_{13}H_{20}N_2O_4$ $(M+Na)^+$: 291.13; Found: 291.24.

***tert*-butyl 6-(2,5-dioxo-2*H*-pyrrol-1(5*H*)-yl)hexylcarbamate (3c):** Compound **3c** was prepared by the same method as **3a** starting from **2c**. Yield: 65%. **^{1}H-NMR** (600 MHz, $CDCl_3$) δ 6.65 (s, 2H), 4.53 (s, 1H), 3.47 (t, *J* = 7.2 Hz, 2H), 3.06 (d, *J* = 6.0 Hz, 2H), 1.54 (q, *J* = 7.2 Hz, 2H), 1.43 (m, 2H), 1.40 (s, 9H), 1.23 – 1.33 (m, 4H); **^{13}C-NMR** (100MHz, $CDCl_3$) δ 170.77,

155.91, 133.97, 78.94, 40.36, 37.65, 29.83, 28.35, 26.28, 26.15. MS (ESI) Calcd. for $C_{15}H_{24}N_2O_4$ $(M+Na)^+$: 319.16; Found: 319.28.

***tert*-butyl 2-(2-(2-(2,5-dioxo-2*H*-pyrrol-1(5*H*)-yl)ethoxy)ethoxy)ethylcarbamate (3d):** Compound **3d** was prepared by the same method as **3a** starting from 2,2-dimethyl-4,15-dioxo-3,8,11-trioxa-5,14-diazaoctadec-16-en-18-oic acid (**2d**). Yield: 65%. **^{1}H-NMR** (500 MHz, $CDCl_3$) δ 6.70 (s, 2H), 5.00 (s, 1H), 3.73 (t, *J* = 5.5 Hz, 2H), 3.64 (t, *J* = 6.0 Hz, 2H), 3.59 (q, *J* = 3.0 Hz, 2H), 3.54 (q, *J* = 3.0 Hz, 2H), 3.49 (t, *J* = 5.0 Hz, 2H), 3.28 (d, *J* = 4.5 Hz, 2H), 1.43 (s, 9H); **^{13}C-NMR** (100MHz, $CDCl_3$) δ 170.53, 155.84, 134.05, 79.04, 70.12, 69.79, 67.69, 40.32, 36.93, 28.31. **MS** (ESI) Calcd. for $C_{15}H_{24}N_2O_6$ $(M+Na)^+$: 351.15; Found: 351.21.

3-(2,5-dioxo-2*H*-pyrrol-1(5*H*)-yl)propan-1-aminium chloride (4a) (*201*): Compound **3a** (3.54 g, 13.92 mmol) was dissolved in CH_2Cl_2 (40 mL) at 22 °C. 4 M HCl in 1, 4- dioxane (15 mL) was added and the solution was stirred at 22 °C for 2 h. The solvent was removed under reduced pressure, and the residue was dried under high vacuum. Yield: 100%. **^{1}H-NMR** (500 MHz, D_2O) δ 6.92 (s, 2H), 3.67 (t, *J* = 7.0 Hz, 2H), 3.06 (t, *J* = 7.0 Hz, 2H), 2.00 (q, *J* = 7.0 Hz, 2H). **MS** (ESI) Calcd. for $C_7H_{11}N_2O_2^+$ $(M+H)^+$: 155.08; Found: 155.10.

4-(2,5-dioxo-2*H*-pyrrol-1(5*H*)-yl)butan-1-aminium chloride (4b): Compound **4b** was prepared by the same method as **4a** starting from **3b**. Yield: 100%. **^{1}H-NMR** (500 MHz, D_2O) δ 6.90 (s, 2H), 3.60 (t, *J* = 7.0 Hz, 2H), 3.05-3.10 (m, 2H), 1.70 (m, 4H). **MS** (ESI) Calcd. for $C_8H_{13}N_2O_2^+$ $(MH)^+$: 169.10; Found: 169.09.

6-(2,5-dioxo-2*H*-pyrrol-1(5*H*)-yl)hexan-1-aminium chloride (1c): Compound **4c** was prepared by the same method as **4a** starting from **3c**. Yield: 100%. ^{1}H-NMR (400 MHz, D_2O) δ 6.60 (s, 2H), 3.25 (t, *J* = 5.6 Hz, 2H), 2.75 (t, *J* = 7.6 Hz, 2H), 1.41 (p, *J* = 7.6 Hz, 2H), 1.32 (p, *J* = 7.6 Hz, 2H), 1.15 (p, *J* = 7.6 Hz, 2H), 1.05 (p, *J* = 6.8 Hz, 2H). **MS** (ESI) Calcd. for $C_{10}H_{17}N_2O_2^+$ $(M+H)^+$: 197.13; Found: 197.10.

2-(2-(2-(2,5-dioxo-2*H*-pyrrol-1(5*H*)-yl)ethoxy)ethoxy)ethanaminium chloride (4d): Compound **4d** was prepared by the same method as **4a** starting from **3d**. Yield: 100%. **^{1}H-NMR** (500 MHz, D_2O) δ 6.91 (s, 2H), 3.70-3.80 (m, 10H), 3.23 (t, *J* = 5.0 Hz, 2H). **MS** (ESI) Calcd. for $C_{10}H_{17}N_2O_4^+$ $(M+H)^+$: 229.12; Found: 229.11.

3-(2,5-dioxo-2*H*-pyrrol-1(5*H*)-yl)-*N,N,N*-trimethylpropan-1-aminium iodide (5a-d_0) (*151*): A mixture of **4a** (2.65 g, 13.9 mmol), iodomethane (9.9 g, 70 mmol), and $KHCO_3$ (7.0 g, 70 mmol) in ACN was stirred at 22 °C under N_2 for 72 h. Solids were removed by filtration, and the solvent was removed from the filtrate under reduced pressure. Maleimide **5a-d_0** was recrystallized from ethanol. Yield: 71%. **^{1}H-NMR** (500 MHz, D_2O) δ 6.92 (s, 2H), 3.68 (t, *J* = 6.5 Hz, 2H), 3.41 (td, *J* = 4.5 and 4.0 Hz, 2H), 3.15 (s, 9H), 2.16 (tt, *J* = 8.0 and 6.5 Hz, 2H); **^{13}C-NMR** (100 MHz, D_2O) δ 172.91, 134.61, 64.01, 53.12, 34.48, 22.13. **mp** = 183 – 183.5 °C. **MS** (ESI) Calcd. for $C_{10}H_{17}N_2O_2^+$ (M^+): 197.13; Found: 197.16.

3-(2,5-dioxo-2*H*-pyrrol-1(5*H*)-yl)-*N,N,N*-trimethyl-d_9-propan-1-aminium iodide (5a-d_9) (*151*): A mixture of **4a** (2.74 g, 14.40 mmol), iodomethane-d_3 (12.48 g, 86.10 mmol), and $KHCO_3$ (8.62 g, 86.10 mmol) in ACN was stirred at 22 °C under N_2 for 72 h. Solids were removed by filtration, and the solvent was removed from the filtrate under reduced pressure. Maleimide **5a-d_9** was recrystallized from ethanol. Yield: 78%. **^{1}H-NMR** (400 MHz, D_2O) δ 6.95 (s, 2H), 3.71 (t, *J* = 6.6 Hz, 2H), 3.45 (td, *J* = 4.7 and 3.6 Hz, 2H), 2.19 (tt, *J* = 8.8 and 6.6 Hz, 2H); **^{13}C-NMR** (100 MHz, D_2O) δ 172.93, 134.65, 63.74, 52.27, 34.53, 22.12. **mp** = 182 – 183 °C. **MS** (ESI) Calcd. for $C_{10}H_8D_9N_2O_2^+$ (M^+): 206.18; Found: 205.99.

4-(2,5-dioxo-2*H*-pyrrol-1(5*H*)-yl)-*N,N,N*-trimethylbutan-1-aminium iodide (5b-d_0): Compound **5b-d_0** was prepared by the same method as **5a-d_0** starting from **4b** and iodomethane. Yield: 74%. **^{1}H-NMR** (400 MHz, D_2O) δ 6.92 (s, 2H), 3.63 (t, *J* = 6.7 Hz, 2H), 3.42 (td, *J* = 5.0 and 4.5 Hz, 2H), 3.17 (s, 9H), 1.84 (tt, *J* = 8.5 and 7.1 Hz, 2H), 1.71 (q, *J* = 7.0 Hz, 2H); **^{13}C-NMR** (100 MHz, D_2O) δ 173.27, 134.48, 65.91, 53.03, 36.71, 24.65, 19.81. mp = 182 – 182.5 °C. **MS** (ESI) Calcd. for $C_{11}H_{19}N_2O_2^+$ (M^+): 211.14; Found: 211.17.

4-(2,5-dioxo-2*H*-pyrrol-1(5*H*)-yl)-*N,N,N*-trimethyl-d_9-butan-1-aminium iodide (5b-d_9): Compound **5b-d_9** was prepared by the same method as **5a-d_9** starting from **4b** and iodomethane-d_3. Yield: 82%. **^{1}H-NMR** (400 MHz, D_2O) δ 6.90 (s, 2H), 3.62 (t, *J* = 6.7 Hz, 2H), 3.40 (td, *J* = 4.5 and 4.0 Hz, 2H), 1.82 (tt, *J* = 8.5 and 7.1 Hz, 2H), 1.70 (q, *J* = 7.0 Hz, 2H); **^{13}C-NMR** (100 MHz, D_2O) δ 173.26, 134.45, 65.60, 51.96, 36.66, 24.62, 19.71. mp = 175-176 °C. **MS** (ESI) Calcd. for $C_{11}H_{10}D_9N_2O_2^+$ (M^+): 220.20; Found: 220.03.

6-(2,5-dioxo-2*H*-pyrrol-1(5*H*)-yl)-*N,N,N*-trimethylhexan-1-aminium iodide (5c-d_0): Compound **5c-d_0** was prepared by the same method as **5a-d_0** starting from **4c** and iodomethane. Yield: 70%. **^{1}H-NMR** (600 MHz, D_2O) δ 6.90 (s, 2H), 3.56 (t, *J* = 6.6 Hz, 2H), 3.36 (td, *J* = 5.4 and 4.2 Hz, 2H), 3.16 (s, 9H), 1.83 (q, *J* = 7.2 Hz, 2H), 1.65 (q, *J* = 7.2 Hz, 2H), 1.38-1.46 (m, 4H); **^{13}C-NMR** (125MHz, D_2O) δ 176.11, 136.98, 69.24, 55.47, 40.06, 29.99, 28.03, 27.57, 24.80. mp = 118.5 - 119 ^{o}C. **MS** (ESI) Calcd. for $C_{13}H_{23}N_2O_2^+$ (M^+): 239.18; Found: 239.18.

6-(2,5-dioxo-2*H*-pyrrol-1(5*H*)-yl)-*N,N,N*-trimethyl-d_9-hexan-1-aminium iodide (5c-d_9): Compound **5c-d_9** was prepared by the same method as **5a-d_9** starting from **4c** and iodomethane-d_3. Yield: 90%. **^{1}H-NMR** (400 MHz, D_2O) δ 6.88 (s, 2H), 3.55 (t, *J* = 7.0 Hz, 2H), 3.34 (td, *J* = 5.0 and 4.3 Hz, 2H), 1.81 (q, *J* = 7.2 Hz, 2H), 1.63 (q, *J* = 7.1 Hz, 2H), 1.35 - 1.47 (m, 4H); **^{13}C-NMR** (100 MHz, D_2O) δ 173.43, 134.35, 66.29, 51.98, 37.44, 27.38, 25.41, 24.94, 22.12. mp 109 - 110 ^{o}C. **MS** (ESI) Calcd. for $C_{13}H_{14}D_9N_2O_2^+$ (M^+): 248.27; Found: 248.31.

2-(2-(2-(2,5-dioxo-2*H*-pyrrol-1(5*H*)-yl)ethoxy)ethoxy)-*N,N,N*-trimethylethanaminium iodide (5d-d_0): Compound **5d-d_0** was prepared by the same method as **5a-d_0** starting from **4d** and iodomethane. Yield: 65%. **^{1}H-NMR** (500 MHz, D_2O) δ 6.93 (s, 2H), 3.99 (tdd, *J* = 3.0, 2.5, and 2.0 Hz, 2H), 3.70 – 3.80 (m, 8H), 3.62 (t, *J* = 5.0 Hz, 2H), 3.23 (s, 9H); **^{13}C-NMR** (100 MHz, D_2O) δ 172.97, 134.53, 69.69, 69.26, 67.76, 65.34, 64.40, 54.04, 37.10. **MS** (ESI) Calcd. for $C_{13}H_{23}N_2O_4^+$ (M^+): 271.18; Found: 271.20.

2-(2-(2-(2,5-dioxo-2*H*-pyrrol-1(5*H*)-yl)ethoxy)ethoxy)-*N,N,N*-trimethyl-d_9-ethanaminium iodide (5d-d_9): Compound **5d-d_9** was prepared by the same method as **5a-d_9** starting from **4d** and iodomethane-d_3. Yield: 51%. **^{1}H-NMR** (400 MHz, D_2O) δ 6.93 (s, 2H), 3.99 (tdd, *J* = 2.8, 2.6, and 2.0 Hz, 2H), 3.70 – 3.80 (m, 8H), 3.62 (t, *J* = 4.8 Hz, 2H); **^{13}C-NMR** (100 MHz, D_2O) δ 172.97, 134.52, 69.67, 69.25, 67.76, 65.04, 64.36, 52.70, 37.08. **MS** (ESI) Calcd. for $C_{13}H_{14}D_9N_2O_4^+$ (M^+): 280.30; Found: 280.33.

3.5 Preparation of lipid vesicles

General preparation method: 100-nm diameter unilamellar vesicles (large unilamellar vesicles, LUV) were made from mixtures of lipids by extrusion (*202*). (LIPEX Extruder,

Northern Lipids Inc., Vancouver, BC Canada) The lipids were mixed in a 25-mL RBF, dried as a thin film under reduced pressure in a rotary evaporator, and evacuated under high vacuum for 2 h. The lipid mixtures were resuspended in 50 mM sodium phosphate, pH 7.0, with vortexing and sonication. Each sample underwent five freeze-thaw cycles at -80 °C and 37 °C. TCEP (final concentration 100 μM) was added to reduce the thiols at 25 °C, and the mixture was extruded 10 times through two stacked 100-nm filters using a N_2 gas pressure of 350-400 psi to provide a homogeneous batch of unilamellar vesicles. The size of the vesicles was confirmed by dynamic light scattering (Brookhaven Instruments, DLS-90). Specific mixtures of lipids used are described below.

DMPC vesicles: 1,2-Dimyristoyl-*sn*-glycero-3-phosphocholine, DMPC (20 μmol) in $CHCl_3$ (3 mL) was dried, and resuspended as described above in 10 mL of 50 mM HEPES, pH 7.0 to yield DMPC vesicles. DMPC/cholesterol (3/1) and DMPC/cholest-4-en-3-one (3/1) vesicles were prepared with same method describe above.

Thiolipid vesicles: 1,2-Dipalmitoyl-*sn*-glycero-3-phosphothioethanol, PTE (sodium salt, 1.6 μmol) and 1-palmitoyl-2-oleoyl-*sn*-glycero-3-phosphocholine, POPC (78.4 μmol) or 1,2-Dipalmitoyl-*sn*-glycero-3-phosphocholine, DPPC (78.4 μmol) were mixed in $CHCl_3$ (3 mL), dried, and resuspended as described above in 20 mL of 50 mM sodium phosphate, pH 7.0 to yield PTE/POPC (2/98) or PTE/DPPC (2/98) vesicles.

Peptide-containing vesicles: Peptide **6** (0.5 μmol), peptide **7**, (0.5 μmol), peptide **8**, (0.5 μmol), or peptide **6**/peptide **7** (1/1, 0.32 μmol each) dissolved in ethanol (3 mL) and POPC (40 μmol) in $CHCl_3$ (3 mL) were mixed, dried, and resuspended as described above in 10 mL of 50 mM sodium phosphate, pH 7.0 to yield peptide **6**/POPC (1/80), peptide **7**/POPC (1/80), peptide **8**/POPC (1/80), or peptide **6**/peptide **7**/POPC (1/1/127) vesicles. The incorporation of peptide into the vesicles was confirmed by monitoring the fluorescence blue shift of the tryptophan emission upon excitation at 280 nm. Other peptide containing vesicles, peptide **7**/DOPC (1/80), peptide **7**/DPPC (1/80), peptide **7**/DOPS (1/80), peptide **7**/DOPG (1/80), peptide **7**/DOPE/DOPC (1/40/40), peptide **7**/POPC/cholesterol (1/76/4), peptide **7**/POPC/cholesterol (1/68/12), peptide **7**/POPC/cholesterol (1/60/20), peptide **7**/POPC/cholesterol (1/44/36), peptide **7**/POPC/cholest-4-en-3-one (1/76/4), peptide **7**/POPC/cholest-4-en-3-one (1/68/12), peptide **7**/POPC/cholest-4-en-3-one (1/60/20), peptide **7**/POPC/cholest-4-en-3-one (1/44/36), peptide **7**/DOPC/cholesterol

(1/60/20), peptide **7**/DPPC/cholesterol (1/64/16), peptide **7**/DPPC/cholesterol (1/48/32), peptide **7**/DPPC/cholest-4-en-3-one (1/64/16), peptide **7**/DPPC/cholest-4-en-3-one (1/48/32), peptide **8**/POPC/cholesterol (1/60/20) or peptide **8**/POPC/cholest-4-en-3-one (1/60/20) vesicles were prepared as described above.

Peptide and thiolipid-containing vesicles: Peptide **7** (0.5 μmol dissolved in ethanol (3 mL), PTE (0.8 μmol), and POPC or DPPC (39.2 μmol) in $CHCl_3$ (3 mL) were mixed, dried, and resuspended in 50 mM sodium phosphate (10 mL, pH 7.0) to yield peptide **7**/POPC/PTE (1/78.4/1.6), or peptide **7**/DPPC/PTE (1/78.4/1.6) vesicles. The incorporation of peptide into the vesicles was confirmed by monitoring the fluorescence blue shift of the tryptophan emission upon excitation at 280 nm.

Vesicles with encapsulated carboxyfluorescein: Peptide **7** (0.5 μmol) dissolved in ethanol (3 mL) and POPC (40 μmol) in $CHCl_3$ (3 mL) were mixed and resuspended in 5 mL 50 mM sodium phosphate, pH 7 containing 5(6)-carboxyfluorescein (0.5 mmol). LUVs were prepared as described above. Excess carboxyfluorescein was removed by size exclusion chromatography (PD-10 column, Sephadex G-25 M, GE Healthcare, Little Chalfont, Buckinghamshire, UK). POPC vesicles encapsulated carboxyfluorescein were prepared as previously described.

Vesicles with encapsulated NB-ECD-OMe: Peptide **7** (0.5 μmol) dissolved in ethanol (3 mL) and POPC (40 μmol) in $CHCl_3$ (3 mL) were mixed, dried, and resuspended in 5 mL of 50 mM sodium phosphate, pH 7 containing NB-ECD-OMe peptide (15 μmol). LUVs were prepared as described above for vesicles with encapsulated carboxyfluorescein.

3.6 Labeling of peptide 6, peptide 7, and peptide 8 with equal molar heavy/light ICMT probes

Peptide **6**, peptide **7**, or peptide **8** (50 μM, 200 μL) was suspended as described above, without the addition of the lipid, in 2 mL of 50 mM sodium phosphate (pH 7.0, with 0.5% SDS w/v) and was reduced with TCEP (1.6 μL, 300 mM stock solution in H_2O, 2.5 mM final concentration**)** at 25 ^oC for 10 min. An equimolar mixture (9 mM each) of **5a-d_0** + **5a-d_9**, **5b-d_0**

+ **5b-d$_9$**, **5c-d$_0$** + **5c-d$_9$**, or **5d-d$_0$** + **5d-d$_9$** was added and the solutions were incubated at 25 ^{o}C for 1 h before analysis by MALDI-TOF mass spectrometry.

3.7 Dye leakage assay

Encapsulated-carboxyfluorescein peptide **7**/POPC (1/80) (285 μM total lipid) or POPC (285 μM total lipid) vesicles (1 mL in fluorescence cuvette) were incubated at 25 ^{o}C. Fluorescence emission intensity (λ_{em} = 517 nm, λ_{ex} = 492 nm) was monitored as a function of time for 75 min. After 65 min, Triton X-100 (30.9 μL, 1% w/v, stock solution in H_2O, 0.03 % w/v, final concentration) was added, and emission intensity monitored for a further 10 min.

3.8 Two-step labeling of encapsulated NB-ECD-OMe in peptide 7/POPC vesicles

Peptide **7**/POPC (1/80) vesicles containing encapsulated NB-ECD-OMe (4 mM total lipid, 200 μL) were incubated at 30 °C. Heavy probe **5a-d$_9$**, **5b-d$_9$**, **5c-d$_9$**, or **5a-d$_9$** (27.3 μL, 50 mM stock solution in H_2O, 6 mM final concentration) was added to the vesicles. 50 μL aliquots were removed after 2, 30, 60, and 90 min, and added to a tube containing DTT (3.8 μL, 100 mM stock solution, 7 mM final concentration). Triton X-100 (1.7 μL, 1% w/v stock solution in H_2O, 0.03% w/v final concentration) was added to the solution. The solution was vortexed and incubated at 25 ^{o}C for 1 h. Light probe **5a-d$_0$**, **5b-d$_0$**, **5c-d$_0$**, or **5a-d$_0$** (9.8 μL, 100 mM stock solution in H_2O, 15 mM final concentration) was added to the solution and the solution was incubated at 25 °C for 1 h before analysis by LC/MS on an Agilent, Kinetex C18 column (2.6 μm, 100Å, 100×2 mm); solvent A: H_2O (0.1% TFA), solvent B: ACN (0.1% TFA); T = 35 °C; 0.6 mL/min; t = 0-1', B = 3%, t = 1-16', B = 3-49%. The integrated areas for both heavy and light peptides are derived from extraction of these masses from total ion counts. The percentage heavy label was calculated as an integrated area of heavy labeled peptide/(integrated area of light labeled peptide + integrated area of heavy labeled peptide). Percent heavy label (%HL) = ($Area_{heavy\ labeled}$)/($Area_{heavy\ labeled}$ + $Area_{light\ labeled}$) at 2, 30, 60, and 90 min. The percentage of heavy label present at 2 min was subtracted from each time point to correct for extra vesicular NB-ECD-OMe peptide remaining from the vesicle preparation. Hence, normalized percent

heavy label at 2, 30, 60, and 90 min = $\%HL_{2min}$ - $\%HL_{2min}$, $\%HL_{30min}$ - $\%HL_{2min}$, $\%HL_{60min}$ - $\%HL_{2min}$, $\%HL_{90min}$ - $\%HL_{2min}$, respectively.

3.9 Two-step labeling of peptide 6 in POPC vesicles

Heavy probe **5a-d_9**, **5b-d_9**, **5c-d_9**, or **5d-d_9** (10 μL, 100 mM stock solution in H_2O, 9 mM final concentration) was added to peptide **6**/POPC (1/80) vesicles (4 mM total lipid, 100 μL), and the mixture was incubated at 30 °C for 1 h. DTT (11 μL, 100 mM stock solution, 10 mM final concentration) and sodium cholate (6.3 μL, 20% w/v, stock solution in H_2O, 0.5 % w/v, final concentration) were added to the solution. The solution was vortexed and incubated at 25 °C for 1 h. Light probe **5a-d_0**, **5b-d_0**, **5c-d_0**, or **5d-d_0** (84 μL, 100 mM stock solution in H_2O, 25 mM final concentration) was added to the solution and the solution was incubated at 75 °C for 1 h before analysis by MALDI-TOF mass spectrometry.

3.10 Two-step labeling of peptide 7 in POPC vesicles

Heavy probe **5a-d_9**, **5b-d_9**, **5c-d_9**, or **5d-d_9** (2.5 μL, 20 mM stock solution in H_2O, 500 μM final concentration) was added to peptide **7**/POPC (1/80) vesicles (4 mM total lipid, 100 μL), and the mixture was incubated at 30 °C for 1 h. DTT (8.3 μL, 20 mM stock solution in H_2O, 1.5 mM final concentration) and Triton X-100 (3.43 μL, 1% w/v, stock solution in H_2O, 0.03 % w/v, final concentration) were added to the solution. The solution was mixed by vortex and incubated at 25 °C for 1 h. Light probe **5a-d_0**, **5b-d_0**, **5c-d_0**, or **5d-d_0** (18 μL, 100 mM stock solution in H_2O, 13.6 mM final concentration) was added to the solution and the solution was incubated at 25 °C for 1 h before analysis by MALDI-TOF mass spectrometry.

3.11 Kinetic labeling of peptides in vesicles

Peptide **7**/POPC (1/80) vesicles (4 mM total lipid, 100 μL) were incubated at 30 °C for 5 min and then heavy probe **5a-d_9** or **5c-d_9** (5 μL, 2.5 mM stock solution in H_2O, 125 μM final concentration) was added to the solution. After 2, 5, 10, 30, 60, 120, 300, 600, or 900 s, light probe **5a-d_0** or **5c-d_0** (26.25 μL, 5 mM stock solution in H_2O, 1.25 mM final concentration) was

added to the solution. Triton X-100 (4.3 μL, 1% w/v, stock solution in H_2O, 0.03% w/v, final concentration) was added, and then the solution was incubated at 25 ^oC for 5 min. Next, DTT (6.5 μL, 100 mM stock solution in H_2O, 4.5 mM final concentration) was added, the solution was vortexed and incubated at 25 ^oC for 5 min before analysis by MALDI-TOF mass spectrometry. Kinetic labeling of peptide **7**/PTE/POPC (1/1.6/78.4), peptide **7**/PTE/DPPC (1/1.6/78.4), peptide **7**/DOPC (1/80), peptide **7**/DPPC (1/80), peptide **7**/DOPS (1/80), peptide **7**/DOPG (1/80), peptide **7**/DOPE/DOPC (1/40/40), peptide **7**/POPC/cholesterol (1/76/4), peptide **7**/POPC/cholesterol (1/68/12), peptide **7**/POPC/cholesterol (1/60/20), peptide **7**/POPC/cholesterol (1/44/36), peptide **7**/POPC/cholest-4-en-3-one (1/76/4), peptide **7**/POPC/cholest-4-en-3-one (1/68/12), peptide **7**/POPC/cholest-4-en-3-one (1/60/20), peptide **7**/POPC/cholest-4-en-3-one (1/44/36), peptide **7**/DOPC/cholesterol (1/60/20), peptide **7**/DPPC/cholesterol (1/64/16), peptide **7**/DPPC/cholesterol (1/48/32), peptide **7**/DPPC/cholest-4-en-3-one (1/64/16), peptide **7**/DPPC/cholest-4-en-3-one (1/48/32), peptide **8**/POPC (1/80), peptide **8**/POPC/cholesterol (1/60/20) or peptide **8**/POPC/cholest-4-en-3-one (1/60/20) vesicles was performed following the same procedure. When heavy probe in first step was used with different concentration, the concentrations of other components would be adjusted accordingly.

In the case of peptide **6**/peptide **7**/POPC (1/1/127) vesicles, 5 mM total lipid (100 μL) was used and after the second labeling step, one sample (**5a-d_9**/**5a-d_0**) was incubated for another 5 min at 30 °C, then vesicles were lysed with sodium cholate (1.75 μL, 20% w/v, stock solution in H_2O, 0.5% w/v final concentration), and an additional aliquot of **5a-d_0** (20 μL, 100 mM stock solution in H_2O, 27 mM final concentration) was added to the mixture that was incubated at 25 ^oC for 1 h before analysis by MALDI-TOF mass spectrometry. Cholate is required for labeling peptide **6** in detergent micelles after vesicle lysis.

In the case of peptide **7**/PTE/POPC (1/1.6/78.4) or peptide **7**/PTE/DPPC (1/1.6/78.4), vesicles were incubated at 30 °C for 5 min and heavy probe **5a-d_9** (10 μL, 5 mM stock solution in H_2O, 455 μM final concentration) was added to the solution. After 2, 5, 10, 30, 60, 120, 300, 600, or 900 s, light probe **5a-d_0** (32.4 μL, 20 mM stock solution in H_2O, 4.55 mM final concentration) was added to the solution that was incubated at 25 ^oC for 5 min. Then Triton X-100 (4.4 μL, 1% w/v, stock solution in H_2O, 0.03% w/v, final concentration) was added, vortexed, and the mixture was incubated at 25 °C for 5 min. DTT (11 μL, 100 mM stock solution

in H_2O, 7 mM final concentration) was added, and the mixture was incubated at 25 ^oC for 5 min before analysis by MALDI-TOF mass spectrometry.

3.12 Two-step labeling of thiolipid vesicles with ICMT probe

PTE/POPC (2/98) or PTE/DPPC (2/98) vesicles (4 mM total lipid, 850 μL) were incubated at 30 ^oC for 5 min, heavy probe **5a-d_9** (10.8 μL, 20 mM stock solution in H_2O, 250 μM final concentration) was added to the vesicles, 100 μL aliquots were removed at 1, 2, 5, 10, 15, 20, 30, and 60 min, and added to a tube containing DTT (11 μL, 20 mM stock solution in H_2O, 2 mM final concentration). Triton X-100 (3.4 μL, 1% w/v stock solution in H_2O, 0.03% w/v final concentration) was added to the solution. The solution was vortexed and incubated at 25 ^oC for 5 min. Light probe **5a-d_0** was added (28.6 μL, 50 mM stock solution in H_2O, 10 mM final concentration) and the solution was incubated at 25 ^oC for 1 h before analysis by MALDI-TOF mass spectrometry. The kinetics of PTE flipping between bilayers were sufficiently slow that this original two-step labeling procedure with a quench step in between addition of the first and second probe could be used.

3.13 Construction of single-cysteine and multi-cysteine cholesterol oxidase mutants

3.13.1 Construction of pCO305, pCO307, and pCO308 for L80C, L274C, and W333C cholesterol oxidase mutants

Previously prepared mutants were subcloned into pCO117, a PKK223-3 expression vector for *Streptomyces* cholesterol oxidase (*203*). The *Xho*I to *Mlu*I fragments of pCO247 (L80C, this work was performed by Dr. David Wolfgang), pCO250 (L274C) (*107*), or HT336-6 (W333C) (*107*) were inserted into the similarly digested pCO117. The plasmids were digested stepwise, first with *Xho*I, followed by *Mlu*I for 1.5 h each at 37 ^oC. The DNA fragments were separated on a 0.8% agarose gel. The 5.5 kb fragment from pCO117 and the 931 bp fragment from pCO247, pCO250 and HT336-6 on agarose gel were isolated and purified using a High Pure PCR Product Purification Kit (Roche Applied Science, Mannheim, Germany). Vector

(from pCO117) and insert (from pCO247, pCO250, and HT336-6) were mixed in 1:4 ratio (v/v), and were ligated with T4 DNA ligase provided by Rapid DNA Ligation Kit for 20 min at rt. All ligated mixtures were transformed into XL1 Blue competent cells, and grown on two LB-ampicillin (200 μg/mL) agar plates at 37 ^{o}C overnight. Two colonies from each plate were picked, and grown in 10 mL LB media respectively. Plasmids were purified by Roche High Pure Plasmid Isolation Kit followed by DNA single digestion by *Hind*III for 1.5 h at 37 ^{o}C.

3.13.2 Construction of pCO309, pCO310, pCO311, pCO312, pCO313, and pCO314 for A32C/S129C/T371C/A423C, S153C/A205C/S312C/T435C, T168C/A276C, A184C/T239C/A407C/A465C, A32C/T168C/S312C/A465C, and A184C/A301C/T394C cholesterol oxidase mutants

With 4 primers containing designated mutation sites (pCO309, A32C: 5'-gctctgcgtctgggtgaa**tgt**ggtgtacagactct-3', S129C: 5'-tggagcccaagcgc**tgc**tacttcgaggagatc-3', T371C: 5'-cggccggcctggag**tgc**tgggtcagcctcta-3', A423C: 5'-tcgaccggatcaacaag**tgc**aacggcacgatctaccg-3') and pCO117 as a template, 30 cycles of PCR were performed with a QuickChange Lightning Multi Site-Directed Mutagenesis Kit (at an annealing temperature of 65 ^{o}C). The procedures were carried out following the instruction manual. The PCR products were transformed into XL10 Gold competent cells provided by the kit and were grown on LB-ampicillin (200 μg/mL) agar plates at 37 ^{o}C overnight. Construction of pCO310 ~ pCO314 followed the same procedures as for pCO309. Primers for pCO310, S153C: 5'-ccgcgccaactgca**tgc**tccgcg-3', A2005C: 5'-cagcgcgaggcc**tgc**ggcgaggtgccc-3', S312C: 5'-cctgccgaacctcaac**tgc**gaggtggg-3', T435C: 5'-cgacctcttcggc**tgc**cagctgaaggcc-3'. Primers for pCO311, T168C: 5'-ccaagtggttcgaggac**tgc**gagtggtacaagttcg-3', A276C: 5'-gacggcaagctcctg**tgc**accaaggagatctc-3', A301C: 5'-ctgctggtgcgc**tgc**cgcgacaccgg-3', T394C: 5'-gtacgacgccgcg**tgc**gaccgcgcgaagc-3'. Primers for pCO312, A184C: 5'-gcaggcgggcaag**tgc**ggtctcggcacc-3', T239C: 5'-cgccgcactcggc**tgc**ggcaaggtcacc-3', A407C: 5'-ccgtgaccagaac**tgc**cccgcggtcaac-3', A465C: 5'-gactacggccgcgtc**tgc**ggttacaagaacct-3'. Primers for pCO313, A32C: 5'-gctctgcgtctgggtgaa**tgt**ggtgtacagactct-3', T168C: 5'-ccaagtggttcgaggac**tgc**gagtggtacaagttcg-3', S312C: 5'-cctgccgaacctcaac**tgc**gaggtggg-3', A465C: 5'-gactacggccgcgtc**tgc**ggttacaagaacct-3'. Primers for pCO314, A184C: 5'-gcaggcgggcaag**tgc**ggtctcggcacc-3', T239C: 5'-cgccgcactcggc**tgc**ggcaaggtcacc-3', A301C: 5'-ctgctggtgcgc**tgc**cgcgacaccgg-3', T394C: 5'-gtacgacgccgcg**tgc**gaccgcgcgaagc-3'.

3.13.3 Mutagenesis of pCO310

With 2 primers containing designated mutation sites E438K (mut2E438K-1: GGCTGCCAGCTG**AAG**GCCTTCGCCG and mut2E438K-2: CGGCGAAGGC**CTT**CAGCTGGCAGCC) and using 686-3 (S153C/A205C/S312C/T435C from pCO117) and 686-5 (S153C/A205C/S312C/T435C from pCO117) as a template respectively, 14 cycles of PCR were performed with QuickChange Site-Directed Mutagenesis Kit at an annealing temperature of 68 ^{o}C. The procedures were carried out following the instruction manual. The PCR products were transformed into XL1 Blue competent cells and were grown on LB-ampicillin (200 μg/mL) agar plates at 37 ^{o}C overnight.

3.13.4 Expression trials for multiple cysteine cholesterol oxidase

Six colonies were randomly chosen from the agar plates of each of these 6 multi-cysteine cholesterol oxidase mutants, and the plasmids were purified using a Roche High Pure Plasmid Isolation Kit. DNA single digestion was performed with *Mlu*I at 37 ^{o}C for 1.5 h, and analyzed on 0.8% agarose gel. The purified plasmids were transformed into BL21(DE3)pLysS competent cells, and were grown on LB-ampicillin (200 μg/mL) agar plates at 37 ^{o}C overnight. A 10-mL mini culture for each plasmid DNA was grown at 37 ^{o}C, IPTG (100 μg/mL) was added at OD_{600nm} value of 0.7 ~ 0.8, and allowed to grow at 28 ^{o}C for additional 25 h. Both un-induced and induced cells were lysed with 5 freeze and thaw cycles, and were analyzed by SDS-PAGE. The supernatant from lysed cells induced by IPTG was assayed with standard conditions (0.025 % (w/v) Triton X-100, 0.02 % (w/v) BSA (bovine serum albumin), and 0.45 mM cholesterol in 2-propanol at 37 ^{o}C).

3.14 Expression and purification of wild-type and mutant cholesterol oxidase

3.14.1 Comparison of cholesterol oxidase over-expression by different plasmids

Plasmids pCO117 (wild-type cholesterol oxidase, derivative of PKK223-3) (*203*), pCO202 (wild-type cholesterol oxidase, derivative of pUC19) (*104*), pCO247 (L80C mutant, derivative of pUC19, this work was performed by Dr. David Wolfgang), and pCO273 (L80C/4CA, 4CA: C56A, C282A, C445A, and C452A, derivative of pET20b) (*107*) were transformed into XL1 Blue competent cells, and were grown on a LB-agar plate containing 200

μg/mL ampicillin. A single colony was selected and grown in 10 mL LB medium at 37 ^{o}C overnight. The plasmids were purified using a Roche High Pure Plasmid Isolation Kit, followed by DNA single (*Hind*III) and double (*Hind*III and *Nde*I) digestions, 1.5 h for each digestion at 37 ^{o}C. Plasmids pCO117, pCO202, pCO247, and pCO273 were then transformed into competent *E. coli* strain BL21(DE3)pLysS cells. An LB-agar plate with 200 μg/mL ampicillin was used to select colonies of the transformed cells. These plates were incubated at 37 ^{o}C overnight. A single colony was picked, and was grown in 10 mL of LB media, containing ampicillin (200 μg/mL), in a sterile tube at 37 ^{o}C. After 8 hours, IPTG (100 μg/mL) was added and the cells were harvested after 20 h of IPTG induction at 18 ^{o}C. Supernatants were discarded, and the pellets were resuspended in 50 mM sodium phosphate buffer, pH 7.0 and spun down at at 4,000 g for 20 min. Cells were lysed by sonication, and analyzed on SDS-PAGE.

3.14.2 Expression and purification of wild-type and mutant cholesterol oxidase

The gene encoding wild-type cholesterol oxidase in the pCO117 plasmid was transformed into competent *E. coli* strain BL21(DE3)pLysS cells. An LB-agar plate containing ampicillin (200 μg/mL) was used to select colonies of the transformed cells. The plate was incubated at 37 ^{o}C overnight. A single colony was picked, and then grown in 10 mL LB media, containing 200 μg/mL ampicillin, in a sterile tube at 37 ^{o}C overnight. The 10-mL inoculated culture was added to 1L of 2xYT media in the shaker at 37 ^{o}C. The cells were grown at 18 ^{o}C for another 20 hours after IPTG (100 μg/mL) induction at OD_{600nm} 0.83. The cells were centrifuged at 4,000 g for 20 min. The pellet was collected, and then resuspended in 50 mL of 50 mM sodium phosphate buffer, pH 7.0. The cells were lysed twice on a Cell Disruptor at 27,000 psi. All subsequent steps were performed at 4 ^{o}C. The cell debris was removed by centrifugation at 135,000 g for 60 min. The supernatant was collected and precipitated with 1.0 M $(NH_4)_2SO_4$. The pellet was discarded after centrifugation at 4,000 g for 20 min. $(NH_4)_2SO_4$ was added to the supernatant to a final concentration of 2.0 M. The pellet was collected after spun down at 4,000 g for 20 minutes, and resuspended in 30 mL of 50 mM sodium phosphate buffer, pH 7.0. The cell solution was desalted by dialysis (NMWCO 6,000-8,000) against 50 mM sodium phosphate buffer, pH 7.0 three times. The dialysate was loaded onto an anion-exchange column of DEAE52 cellulose pre-equilibrated with 50 mM sodium phosphate buffer, pH 7.0. Cholesterol oxidase was eluted using 50 mM sodium phosphate buffer, pH 7.0 and fractions containing the enzyme, determined by SDS-PAGE or activity assay, were subsequently

concentrated by 2.5 M $(NH_4)_2SO_4$ precipitation. The pellet was dissolved in 5 mL of 50 mM sodium phosphate buffer, pH 7.0, and further purified by FPLC using a butyl sepharose column (GE healthcare, Piscataway, NJ). Fractions were collected according to UV/vis A_{280nm} absorption, and were concentrated by Amicon protein concentrator on an YM30 membrane. Protein concentration was determined by UV/vis absorbance at 280 nm (ε = 81,924 $M^{-1}cm^{-1}$, calculated from the molar extinction coefficient of tryptophan and tyrosine). Protein activity was assayed by monitoring the change in A_{240} (ε_{240nm} = 12100 $M^{-1}cm^{-1}$) as a function of time to monitor product cholest-4-en-3-one formation. The assay solution was 0.025% (w/v) Triton X-100, 0.02% (w/v) BSA (bovine serum albumin), and 0.45 mM cholesterol in 2-propanol (2%) in 1 mL total volume at 37 ^oC.

Single cysteine mutants, L80C, L274C, W333C, and multi-cysteine mutants, **mut1**: A32C/S129C/T371C/A423C, **mut2**: S153C/A205C/S312C/T435C, **mut3**: T168C/A276C, **mut4**: A184C/T239C/A407C/A465C, **mut5**: A32C/T168C/S312C/A465C, **mut6**: A184C/A301C/T394C were over-expressed and purified in an analogous fashion to the method described above, except 50 mM sodium phosphate buffer, pH 7.0, containing 1 mM TCEP was used during purification.

3.15 Optimization of expression conditions and expression of ^2H, ^{13}C, and ^{15}N-labeled wild-type cholesterol oxidase

3.15.1 Optimizing expression conditions for ^2H, ^{13}C, and ^{15}N labeled wild-type cholesterol oxidase

The gene carrying wild-type cholesterol oxidase in the pCO117 vector was transformed into *E. coli* strain BL21(DE3)pLysS competent cells. An LB-agar plate containing ampicillin (200 μg/mL) was used to select colonies of the transformed cells at 37 ^oC overnight. Five single colonies were chosen, and grown in five separate test tubes containing 10 mL LB media supplemented with ampicillin (200 μg/mL) at 37 ^oC overnight. The cells were harvested, and the cell pellet was resuspended in five different rich growing media, BIOEXPRESS, ISOGRO, Silantes, Spectra, and M9 minimal media in a volume of 50 mL each. BIOEXPRESS medium was composed of 5 mL un-labeled BIOEXPRESS medium in a total volume of 50 mL D_2O.

ISOGRO medium was composed of 0.5 g ISOGRO (^{15}N-labeled), 90 mg K_2HPO_4, 70 mg KH_2PO_4, 50 mg $MgSO_4$, 7.5 µL $CaCl_2 \cdot H_2O$ (74 mg/mL) in a total volume of 50 mL D_2O. M9 minimal medium was composed of 340 mg Na_2HPO_4, 150 mg KH_2PO_4, 25 mg NaCl, 50 mg $^{15}NH_4Cl$, 200 mg ^{13}C-labeled D-glucose, 5 µL 1 M $CaCl_2$, 50 µL 2 M $MgSO_4$, 500 µL MEM vitamin solution (100X) in a total volume of 50 mL D_2O. Un-labeled Silantes and Spectra media were both ready to use, and 50 mL of each medium was used. The cells were grown in 50 mL cultures containing ampicillin (200 µg/mL) at 37 ^{o}C, and 1 mL of culture was taken for OD_{600nm} measurement every 1 h for 8 h. IPTG (100 µg/mL) was added after the culture reached the desired OD value, and 1 mL of culture was harvested every 2 h after 12 h of IPTG induction for 24 h. The pellet was resuspended in 2 mL of 50 mM sodium phosphate buffer, pH 7.0 and the cells were lysed by 5 freeze and thaw cycles. The supernatant of the lysed cells was used for SDS-PAGE analysis and cholesterol oxidase activity assay.

3.15.2 Expression and purification of ^{2}H, ^{13}C, and ^{15}N labeled wild-type cholesterol oxidase

The gene carrying wild-type cholesterol oxidase in the pCO117 vector was transformed into competent *E. coli* strain BL21(DE3)pLysS cells. An LB-agar plate containing ampiclilin (200 µg/mL) was used to select colonies of the transformed cells. It was incubated at 37 ^{o}C overnight. A single colony was picked and grown in 10 mL of LB media, containing ampicillin (200 µg/mL), in a sterile tube at 37 ^{o}C overnight. The mini-culture was harvested, and the pellet was resuspended in 500 mL BIOEXPRESS medium. The cells were grown at 37 ^{o}C and induced with IPTG (100 µg/mL) once the OD_{600nm} reached 1.35. The cells continued growing at 28 ^{o}C for 34 h and then 18 ^{o}C for 16 h after IPTG induction. The purification procedure was same as for un-labeled wild-type cholesterol oxidase.

3.16 Labeling and digestion of cholesterol oxidase with trypsin and chymotrypsin

A mixture of wild-type cholesterol oxidase (20 µL, 25 µM stock solution, 10 µM final concentration), **5b-d_0**/**5b-d_9** (5 µL, 10 mM stock solution in H_2O, 1 mM final concentration), HEPES pH 7.0 (5 µL, 500 mM stock solution in H_2O, 50 mM final concentration), sodium deoxycholate (5.56 µL, 10 % w/v, stock solution in H_2O, 1 % w/v, final concentration) and 20

μL DDI water was incubated at 70 ^{o}C for 1 h. The solution was cooled to 25 ^{o}C before adding protease. Trypsin (3 μL, 200 ng/μL stock solution in 100 mM NH_4HCO_3) or chymotrypsin (3 μL, 200 ng/μL stock solution in 1 mM HCl solution) was added to the solution and incubated at 37 ^{o}C or 25 ^{o}C for trypsin digest or chymotrypsin digest, respectively. The digestion time for both proteases was 16 ~ 18 h. To the digested sample, 20 μL of 10% TFA in H_2O was added and allowed to incubate at 25 ^{o}C for 10 min. The white deoxycholic acid precipitate was removed by centrifugation at 14000 rpm for 10 min. The clear supernatant was transferred to a new tube, and the precipitate was discarded. An equal volume of sample supernatant (10 μL) and DHB matrix (10 μL, 20 mg/mL in 3/7 (v/v) mixture of 0.1% TFA in H_2O/CAN) was mixed, and was spotted on MTP384 MALDI plate for mass acquisition. Other cysteine mutants, L80C, L274C, W333C, **mut1**: A32C/S129C/T371C/A423C, **mut2**: S153C/A205C/S312C/T435C, **mut3**: T168C/A276C, **mut4**: A184C/T239C/A407C/A465C, **mut5**: A32C/T168C/S312C/A465C and **mut6**: A184C/T239C/T394C were labeled using the same procedure described above.

3.17 Labeling of mutant cholesterol oxidase in the presence or absence of vesicles

Probe **5b-d_9** (45 μL, 500 μM stock solution in H_2O, 50 μM final concentration) was added to a mixture of L80C cholesterol oxidase (180 μL, 25 μM stock solution, 10 μM final concentration), HEPES, pH 7.0 (45 μL, 500 mM stock solution in H_2O, 50 mM final concentration), DMPC/cholesterol (3/1) (112.5 μL, 2 mM stock solution in H_2O, 500 μM final concentration), and DDI water (67.5 μL) to a total volume of 450 μL, and the solution was incubated at 30 ^{o}C for 10 min before adding probe. 50 μL aliquots were removed at 30 sec, 1, 2, 3, 6, 10, 15, and 30 min, and added to a tube containing probe **5b-d_0** (5.5 μL, 50 mM stock solution in H_2O, 4.95 mM final concentration). To the solution was added 6.17 μL 10% sodium deoxycholate, and the mixture was incubated at 25 ^{o}C for 10 min before mixing by vortex. The solution was incubated at 70 ^{o}C for 1h, and was cooled to 25 ^{o}C. Trypsin (3 μL, 200 ng/μL stock solution in 100 mM NH_4HCO_3) or chymotrypsin (3 μL, 200 ng/μL stock solution in 1 mM HCl solution) was added to the solution, and the mixture was incubated at 37 ^{o}C or 25 ^{o}C for trypsin digest or chymotrypsin digest, respectively. The digestion time for both proteases was 16 ~ 18 h. To the digested sample, 20 μL of 10% TFA in H_2O was added and allowed to incubate at 25 ^{o}C

for 10 min. The white deoxycholic acid precipitate was removed by centrifugation at 14000 rpm for 10 min. The clear supernatant was transferred to a new tube and the precipitate was discarded. Equal volumes of the sample supernatant (10 μL) and a DHB matrix (10 μL, 20 mg/mL in 3/7 (v/v) mixture of 0.1% TFA in H_2O/CAN) were mixed, and the mixture was spotted on an MTP384 MALDI plate for mass acquisition. Wild-type enzyme, and cysteine mutants, L274C, W333C, **mut1**: A32C/S129C/T371C/A423C, **mut2**: S153C/A205C/S312C/T435C, **mut3**: T168C/A276C, **mut4**: A184C/T239C/A407C/A465C, **mut5**: A32C/T168C/S312C/A465C and **mut6**: A184C/T239C/T394C were labeled using same procedure described above. Experiments with different lipid compositions, DMPC, DMPC/cholest-4-en-3-one (3/1) utilized the same procedure.

Chapter 4 Conclusion and Future Direction

4.1 Developing membrane impermeable isotope-coded mass tags (ICMTs)

We have designed and synthesized the ICMT probes with both light and heavy (deuterated) versions, **5a-d_0−5d-d_0** and **5a-d_9−5d-d_9**. The probes are comprised of thiol specific maleimide, alkyl(alkoxy) linkers, and a quaternary ammonium group, that also serve as an isotopic coding tag. The syntheses started from relatively cheaper alkyl(alkoxy) diamine, and contained five steps. We incorporated specific/heavy isotope in the last synthetic step, permethylation of amino group using iodomethane, to make the synthesis more cost efficient. This strategy allows selection of ^{13}C or ^{2}H on iodomethane. To prevent isotopic envelope overlap of the light and heavy probe labeled peaks on mass spectrum, we chose deuterated iodomethane in the final step of the synthesis. The final synthetic step to form quaternary ammonium was carefully controlled under mild basic conditions. It required a balance between keeping basicity of the amine and maintaining the maleimide from being hydrolyzed in basic conditions. The protocol used for synthesis provides gram scale for the final products of both light and heavy versions of ICMT probes. This probe is also highly water soluble, and up to 100 mM stock solution can be prepared in water, even for the most hydrophobic probe with 6-carbon alkyl linker. All reagents synthesized are also demonstrated to be membrane impermeable, so they are suitable to be utilized in the labeling experiments for membrane proteins topology studies.

4.2 ICMT approach for transmembrane peptide dynamics

Membrane proteins, including peripheral and integral proteins, play important roles in living systems. These proteins serve as receptors, channels, and signaling complex, and become an initial decision-making center for the cell. It was estimated that the proportion of putative membrane proteins in human genome is approximately 30%. Moreover, over 60% pharmaceutical drug targets are membrane-associated proteins. Hence, the studies of protein-lipid interactions are very important and challenging in structural biology due to the difficulties in membrane protein expression and reconstitution to their native environment. We used a simple model, single span α-helix transmembrane peptide, as model system to study integral protein-lipid interactions.

We present a method for quantitative analysis of the relative ratios of solvent accessible thiols to membrane buried thiols that requires only micrograms quantities of sample and a straightforward experimental protocol in model membrane system. Purification of peptides or lipids is not required. Reaction mixtures are directly mixed with matrix and then analyzed by MALDI-TOF mass spectrometry. There is a minimum of steps involved in the analysis and, consequently, low experimental error. The simplicity of the method makes it amenable to higher throughput sample analysis and faster stopped flow kinetics. The ability of our method to detect the effect of changes in both lipid membrane composition and peptide incorporation on peptide and lipid mobility in the membrane highlights the caution with which the results of biophysical experimental in model systems should be applied to living biological systems with much more complex membranes than typically used in model studies like our own. We expected that our method will be of widespread utility in the future study of membrane-associated proteins in complex cellular contexts due to the simplicity of its application, and the ease with which cysteines can be introduced into native proteins through mutagenesis.

4.3 ICMT strategy for interfacial protein-lipid interactions

Cholesterol oxidase is a water-soluble interfacial enzyme that transiently associates with membrane, and is a model system to study peripheral membrane protein-lipid interactions. The enzyme substrate, cholesterol, is hydrophobic and is embedded in the lipid bilayer. Based on the available crystal structure of this enzyme, kinetics, and mutagenesis studies, cholesterol oxidase will bind to the membrane to allow access of the substrate. High-resolution structure has shown that the protein has two binding domains to accommodate co-factor FAD and cholesterol. These two domains in crystal structure are sequestrated from the bulk solvent, suggesting that protein might have to make conformation changes for substrate binding to the enzyme active site. Previous experimental results have revealed that the two loops (residue 73-86 and 432-438) are involved in the interaction of protein with the membrane. It was shown that one of the loops (residue 73-86) penetrated into the lipid headgroups, but depth of insertion and the extent of protein interaction with lipid bilayer are still unclear.

We outlined a mass spectrometry-based ICMT labeling strategy to study cholesterol oxidase-lipid interactions. This method relies on the differential reactivities of the cysteine thiols introduced on the protein surface based on crystal structure (PDB entry 1MXT). Labeling experiments of the proteins are performed in the presence of lipid vesicles and in the absence of vesicles.

We successfully designed, constructed, and expressed multi-cysteine cholesterol oxidase mutants with high yields. Nineteen cysteine mutation sites are created on the protein surface in 3 single-cysteine and 6 multi-cysteine cholesterol oxidase mutants. We are able to identified 14 cysteine mutations out of the 19 cysteine mutations sites introduced, covering 74% of total cysteine mutations. We also simplified the procedure to utilized fast dilution of heavy probe in the first step with light probe. The sample preparation for MALDI-TOF mass spectrometer analysis was also greatly optimized to make high throughput possible. Trypsin and chymotrypsin were used to proteolyze the proteins after labeling reactions. Most of the cysteine containing peptides can be identified in trypsin digest, and the used of chymotrypsin can increase the number of identified cysteines. The results from chymotrypsin digests can also provide the comparison of the results obtained from trypsin digest.

Single-cysteine mutant, L80C, was first used to optimize reaction conditions because it was shown to participate in protein-lipid interactions from previous results. The reaction rates of the cysteine thiols were probe concentrations dependent when protein concentration was fixed. We then performed labeling experiments on all the mutants in the presence of vesicles and in the absence of vesicles.

Three types of labeling of the cysteine mutations were summarized: dynamic labeling, exposed labeling (labeling in first step), and protected labeling (labeling in second step). The dynamic labeling of L80C, T168C, and A205C shows that these sites are probably involved in the region of protein conformational changes. The rates of labeling differed in the presence of DMPC/cholesterol (3/1) vesicles, or in the absence of vesicles to different extents. When labeling was performed in the presence of DMPC/cholesterol, the rates of labeling increased for L80C and A205C, the rate of labeling decreased for T168C. These results strongly suggest that these residues are participating in protein-lipid interactions. In the case of exposed labeling cysteine thiols, they are all labeled in the first step less than 30 seconds in the presence of DMPC/cholesterol (3/1) vesicles or in the absence of vesicles. The intuitive interpretations of these results are straightforward. These cysteine mutation sites are very likely not to be in membrane contact region for that they are always accessible to the probes. Nevertheless, the other possible scenario is that the protein binding on and off rates on the membrane surface is so fast that makes these sites are highly accessible to the probes. The third type of labeling is a protected labeling (labeling in second step). The slower rates of labeling for these mutation cysteine thiols are possible to be explained as steric hindrance due to secondary structure, an elevated pK_a of thiols due to local electrostatic microenvironments, or the burial of the cysteine thiols in the membrane. The crystal structure is one of the protein conformational states, and proteins are dynamic. The difficulties in interpreting this type of labeling results come from the same labeling trend in the presence and absence of lipid vesicles. The first two accounts, burial in protein or in membrane, could be elucidated when protein was labeled in the absence of vesicles. Any reasons that cause slow labeling rates due to the local structure of the protein should be revealed when protein was labeled in buffers only. However, we are not able to differentiate the differences. Another possible explanation is that the enzyme bound some lipids during purification so that the membrane binding sites of the protein were already occupied with lipids. When we performed the labeling experiments to monitor these cysteine mutation sites in

the presence or absence of vesicles, we cannot see any differences. Even so, we can still propose that A184C, T371C, and A423C are highly possible in membrane contact region of the protein. They are located on the proposed small binding surface of the protein.

From the current experimental results, we can only propose that cholesterol oxidase might bind to the membrane from a small binding surface consisting an area from the two loops to the two α-helices containing T168C (**mut3**) and A205C (**mut2**) mutation sites. However, we still cannot conclude that the extent of the binding area nor the depth of protein penetrating into the membrane. More experimental data are need to support current results as well as gathering new evidences to map out the protein binding sites to the membrane.

Some experiments could be done to further understand the labeling reaction conditions for currently available cysteine mutants. Probe consumption rate for the wild type, single-cysteine, or multi-cysteine mutants could be monitored by UV/vis spectrometer at 300 nm for various concentration of proteins and probes.

Cholesterol oxidase should also be further purified to remove possibly bound lipid to the protein. Same labeling experiments are performed for these further purified mutants might represent more accurate results. It should help to uncover whether the protected labeling (labeling in second step) cysteine mutations are buried in the protein or protected from labeling in the membrane.

As discussed in earlier section, there are several cysteines present competing the same probes, and the concentration of cysteines and probes are constantly changing. One should pick a single-cysteine and a multi-cysteine mutant for extensively review of the reaction kinetics to optimize the working concentrations for both proteins and probes in single composition of vesicles such as DMPC/cholesterol (3/1) vesicles as well as in the absence of vesicles.

Moreover, additional cysteine mutation sites are needed near the proposed binding surface of cholesterol oxidase, especially the region near residues L80, T168, and A205. Since some the cysteine mutations have never been identified, the design of new cysteine mutations should not only follow the considerations discussed in the earlier mutant design section but also search for high intensities peaks by examining the acquired mass spectra.

Although the retention of all native cysteines (C56, C282, C445, and C452) in the original proposal was to simplify and to increase protein expression level, it turned out to be a factor that could compete with other cysteine mutations to the probes. The labeling rates of the identified native cysteines, C56, C445 and C452, are slow ranging from 0% to 40%. In order to reduce complexity of reaction kinetics in multiple cysteine in one mutant, we might have to remove the native cysteines and introduce less than 4 cysteine mutations on the protein surface.

It might also be worthy to generate a cysteine-less cholesterol oxidase with only one cysteine mutation on the protein to derive the authentic second-order rate constant for several cysteine mutations based on current experimental results of the existed designed cysteine mutation sites. From current results, the concentration of protein and probe to use was not very systematic. Higher probe concentration will increase reaction rate, but lower probe concentration might cause early consumption of probes. To achieve pseudo first-order reaction is challenging in multi-cysteine reaction system with various rate constants of various cysteines. Once the rate constants are derived, kinetics simulations of the cysteine labeling with the probes will be more reliable. The optimization of the reaction conditions will be easier when more accurate kinetic constants are available.

The labeling experiments can be performed in lower temperature, e.g. 20 ^{o}C, compared to the currently used temperature 30 ^{o}C. At such temperature, it will slow down probe labeling rates. As long as protein can still bind to the membrane, we can probe if the protein just sits on the membrane surface or is at fast equilibrium between protein on and off the surface of the membrane.

The catalytically inactive protein mutant (H447E/E361Q) should also be used to the labeling experiment. The enzyme is shown to be properly folded as native protein and still associate with model membranes. In such experiments, we can identify if the conformational changes are due to protein binding to the membrane or substrate binding to the protein.

Solution NMR approach can give complementary perspectives of cholesterol oxidase docking to the membrane. We had previous expressed triply labeled (^{2}H, ^{13}C, and ^{15}N) wild-type cholesterol oxidase for 2D and 3D NMR experiments for assignment of native protein. However, only half of the residues could be identified due to hydrophobic interior of the protein

that made the rate of amide deuterium/hydrogen exchange slow. Solution NMR approach is still a good way to provide structure information of how protein can interact with membrane in atomic resolution. Once the assignment of the native protein is complete, a catalytically inactive protein can be expressed using the optimized protocol to study the interplay of protein and model membrane. We also observed shifts of peaks in 2D (^{1}H-^{15}N) TROSY-HSQC experiments when protein was in solution only or with model membrane. Results from the shifts of the peaks strongly suggest that the protein underwent conformation changes in the presence of membrane. This shifting of peaks comes from the residues that are either involved in the protein conformational changes or in the protein binding site to the membrane. These are all valuable information that could help design of mutation site for ICMT labeling approach in the future.

We also expected that the ICMT strategy could be of generally useful method to study protein-lipid interactions, and could be also applied to other systems that are monitoring conformational changes of macromolecule in different states.

References

(1) David L. Nelson, M. M. C. (2004) *Lehninger Principles of Biochemistry*, Worth Publishers Freeman, New York, NY, USA.

(2) Daleke, D. L. (2007) Phospholipid flippases. *J. Biol. Chem. 282*, 821-825.

(3) Devaux, P. F., and Morris, R. (2004) Transmembrane asymmetry and lateral domains in biological membranes. *Traffic 5*, 241-246.

(4) van Klompenburg, W., Paetzel, M., de Jong, J. M., Dalbey, R. E., Demel, R. A., von Heijne, G., and de Kruijff, B. (1998) Phosphatidylethanolamine mediates insertion of the catalytic domain of leader peptidase in membranes. *FEBS Lett. 431*, 75-79.

(5) Oursel, D., Loutelier-Bourhis, C., Orange, N., Chevalier, S., Norris, V., and Lange, C. M. (2007) Lipid composition of membranes of Escherichia coli by liquid chromatography/tandem mass spectrometry using negative electrospray ionization. *Rapid. Commun. Mass Spectrom. 21*, 1721-1728.

(6) Kusumi, A., Tsuda, M., Akino, T., Ohnishi, S., and Terayama, Y. (1983) Protein-phospholipid-cholesterol interaction in the photolysis of invertebrate rhodopsin. *Biochemistry 22*, 1165-1170.

(7) Papahadjopoulos, D., Cowden, M., and Kimelberg, H. (1973) Role of cholesterol in membranes. Effects on phospholipid-protein interactions, membrane permeability and enzymatic activity. *Biochim. Biophys. Acta 330*, 8-26.

(8) Hurley, J. H., and Misra, S. (2000) Signaling and subcellular targeting by membrane-binding domains. *Annu. Rev. Biophys. Biomol. Struct. 29*, 49-79.

(9) Stevens, T. J., and Arkin, I. T. (2000) Do more complex organisms have a greater proportion of membrane proteins in their genomes? *Proteins 39*, 417-420.

(10) Dowhan, W., and Bogdanov, M. (2009) Lipid-dependent membrane protein topogenesis. *Annu. Rev. Biochem. 78*, 515-540.

(11) Cybulski, L. E., and de Mendoza, D. (2011) Bilayer hydrophobic thickness and integral membrane protein function. *Curr. Protein Pept. Sci. 12*, 760-766.

(12) Scott, K. A., Bond, P. J., Ivetac, A., Chetwynd, A. P., Khalid, S., and Sansom, M. S. (2008) Coarse-grained MD simulations of membrane protein-bilayer self-assembly. *Structure 16*, 621-630.

(13) Sanderson, J. M. (2005) Peptide-lipid interactions: insights and perspectives. *Org. Biomol. Chem. 3*, 201-212.

(14) Nyholm, T. K., Ozdirekcan, S., and Killian, J. A. (2007) How protein transmembrane segments sense the lipid environment. *Biochemistry 46*, 1457-1465.

(15) Liu, F., Lewis, R. N., Hodges, R. S., and McElhaney, R. N. (2004) Effect of variations in the structure of a polyleucine-based alpha-helical transmembrane peptide on its interaction with phosphatidylglycerol bilayers. *Biochemistry 43*, 3679-3687.

(16) Killian, J. A., and von Heijne, G. (2000) How proteins adapt to a membrane-water interface. *Trends Biochem. Sci. 25*, 429-434.

(17) White, S. H., and Wimley, W. C. (1999) Membrane protein folding and stability: physical principles. *Annu. Rev. Biophys. Biomol. Struct. 28*, 319-365.

(18) Killian, J. A. (2003) Synthetic peptides as models for intrinsic membrane proteins. *FEBS Lett. 555*, 134-138.

(19) de Planque, M. R., and Killian, J. A. (2003) Protein-lipid interactions studied with designed transmembrane peptides: role of hydrophobic matching and interfacial anchoring. *Mol. Membr. Biol. 20*, 271-284.

(20) Killian, J. A., and Nyholm, T. K. (2006) Peptides in lipid bilayers: the power of simple models. *Curr. Opin. Struct. Biol. 16*, 473-479.

(21) Holt, A., and Killian, J. A. (2010) Orientation and dynamics of transmembrane peptides: the power of simple models. *Eur. Biophys. J. 39*, 609-621.

(22) Killian, J. A., Salemink, I., de Planque, M. R., Lindblom, G., Koeppe, R. E., 2nd, and Greathouse, D. V. (1996) Induction of nonbilayer structures in diacylphosphatidylcholine model membranes by transmembrane alpha-helical peptides: importance of hydrophobic mismatch and proposed role of tryptophans. *Biochemistry 35*, 1037-1045.

(23) Davis, J. H., Clare, D. M., Hodges, R. S., and Bloom, M. (1983) Interaction of a synthetic amphiphilic polypeptide and lipids in a bilayer structure. *Biochemistry 22*, 5298-5305.

(24) London, E., and Shahidullah, K. (2009) Transmembrane vs. non-transmembrane hydrophobic helix topography in model and natural membranes. *Curr. Opin. Struct. Biol. 19*, 464-472.

(25) Ren, J. H., Lew, S., Wang, Z. W., and London, E. (1997) Transmembrane orientation of hydrophobic alpha-helices is regulated both by the relationship of helix length to bilayer thickness and by the cholesterol concentration. *Biochemistry 36*, 10213-10220.

(26) Ren, J. H., Lew, S., Wang, J. Y., and London, E. (1999) Control of the transmembrane orientation and interhelical interactions within membranes by hydrophobic helix length. *Biochemistry 38*, 5905-5912.

(27) Krishnakumar, S. S., and London, E. (2007) Effect of sequence hydrophobicity and bilayer width upon the minimum length required for the formation of transmembrane helices in membranes. *J. Mol. Biol. 374*, 671-687.

(28) Lew, S., Ren, J. H., and London, E. (2000) The effects of polar and/or ionizable residues in the core and flanking regions of hydrophobic helices on transmembrane conformation and oligomerization. *Biochemistry 39*, 9632-9640.

(29) Caputo, G. A., and London, E. (2004) Position and ionization state of Asp in the core of membrane-inserted alpha helices control both the equilibrium between transmembrane and nontransmembrane helix topography and transmembrane helix positioning. *Biochemistry 43*, 8794-8806.

(30) Caputo, G. A., and London, E. (2003) Cumulative effects of amino acid substitutions and hydrophobic mismatch upon the transmembrane stability and conformation of hydrophobic alpha-helices. *Biochemistry 42*, 3275-3285.

(31) Krishnakumar, S. S., and London, E. (2007) The control of transmembrane helix transverse position in membranes by hydrophilic residues. *J. Mol. Biol. 374*, 1251-1269.

(32) Goni, F. M. (2002) Non-permanent proteins in membranes: when proteins come as visitors (review). *Mol. Membr. Biol. 19*, 237-245.

(33) Cho, W. H., and Stahelin, R. V. (2005) Membrane-protein interactions in cell signaling and membrane trafficking. *Annu. Rev. Biophys. Biomol. Struct. 34*, 119-151.

(34) Gelb, M. H., Min, J. H., and Jain, M. K. (2000) Do membrane-bound enzymes access their substrates from the membrane or aqueous phase: interfacial versus non-interfacial enzymes. *Biochim. Biophys. Acta 1488*, 20-27.

(35) Winget, J. M., Pan, Y. H., and Bahnson, B. J. (2006) The interfacial binding surface of phospholipase A2s. *Biochim. Biophys. Acta 1761*, 1260-1269.

(36) Hanakam, F., Gerisch, G., Lotz, S., Alt, T., and Seelig, A. (1996) Binding of hisactophilin I and II to lipid membranes is controlled by a pH-Dependent myristoyl-histidine switch. *Biochemistry 35*, 11036-11044.

(37) Mulgrew-Nesbitt, A., Diraviyam, K., Wang, J., Singh, S., Murray, P., Li, Z., Rogers, L., Mirkovic, N., and Murray, D. (2006) The role of electrostatics in protein-membrane interactions. *Biochim. Biophys. Acta 1761*, 812-826.

(38) Silvius, J. R. (2002) Lipidated peptides as tools for understanding the membrane interactions of lipid-modified proteins. *Curr. Top. Membr. 52*, 371-395.

(39) Medkova, M., and Cho, W. (1999) Interplay of C1 and C2 domains of protein kinase C-alpha in its membrane binding and activation. *J. Biol. Chem. 274*, 19852-19861.

(40) Bittova, L., Sumandea, M., and Cho, W. (1999) A structure-function study of the C2 domain of cytosolic phospholipase A2. Identification of essential calcium ligands and hydrophobic membrane binding residues. *J. Biol. Chem. 274*, 9665-9672.

(41) Ball, A., Nielsen, R., Gelb, M. H., and Robinson, B. H. (1999) Interfacial membrane docking of cytosolic phospholipase A2 C2 domain using electrostatic potential-modulated spin relaxation magnetic resonance. *Proc. Natl. Acad. Sci. U.S.A. 96*, 6637-6642.

(42) Xu, G. Y., McDonagh, T., Yu, H. A., Nalefski, E. A., Clark, J. D., and Cumming, D. A. (1998) Solution structure and membrane interactions of the C2 domain of cytosolic phospholipase A2. *J. Mol. Biol. 280*, 485-500.

(43) Pan, Y. H., Epstein, T. M., Jain, M. K., and Bahnson, B. J. (2001) Five coplanar anion binding sites on one face of phospholipase A2: relationship to interface binding. *Biochemistry 40*, 609-617.

(44) Gelb, M. H., Cho, W. H., and Wilton, D. C. (1999) Interfacial binding of secreted phospholipases A(2): more than electrostatics and a major pole for tryptophan. *Curr. Opin. Struct. Biol. 9*, 428-432.

(45) Lin, Y., Nielsen, R., Murray, D., Hubbell, W. L., Mailer, C., Robinson, B. H., and Gelb, M. H. (1998) Docking phospholipase A2 on membranes using electrostatic potential-modulated spin relaxation magnetic resonance. *Science 279*, 1925-1929.

(46) Rizo, J., and Sudhof, T. C. (1998) C2-domains, structure and function of a universal Ca2+-binding domain. *J. Biol. Chem. 273*, 15879-15882.

(47) Wurmser, A. E., Gary, J. D., and Emr, S. D. (1999) Phosphoinositide 3-kinases and their FYVE domain-containing effectors as regulators of vacuolar/lysosomal membrane trafficking pathways. *J. Biol. Chem. 274*, 9129-9132.

(48) Stenmark, H., Aasland, R., Toh, B. H., and D'Arrigo, A. (1996) Endosomal localization of the autoantigen EEA1 is mediated by a zinc-binding FYVE finger. *J. Biol. Chem. 271*, 24048-24054.

(49) Simonsen, A., Lippe, R., Christoforidis, S., Gaullier, J. M., Brech, A., Callaghan, J., Toh, B. H., Murphy, C., Zerial, M., and Stenmark, H. (1998) EEA1 links PI(3)K function to Rab5 regulation of endosome fusion. *Nature 394*, 494-498.

(50) Nalefski, E. A., and Falke, J. J. (1996) The C2 domain calcium-binding motif: structural and functional diversity. *Protein Sci. 5*, 2375-2390.

(51) Malmberg, N. J., and Falke, J. J. (2005) Use of EPR power saturation to analyze the membrane-docking geometries of peripheral proteins: A applications to C2 domains. *Annu. Rev. Biophys. Biomol. Struct. 34*, 71-90.

(52) Hubbell, W. L., Gross, A., Langen, R., and Lietzow, M. A. (1998) Recent advances in site-directed spin labeling of proteins. *Curr. Opin. Struct. Biol. 8*, 649-656.

(53) Fanucci, G. E., and Cafiso, D. S. (2006) Recent advances and applications of site-directed spin labeling. *Curr. Opin. Struct. Biol. 16*, 644-653.

(54) Drechsler, A., and Separovic, F. (2003) Solid-state NMR structure determination. *IUBMB Life 55*, 515-523.

(55) Opella, S. J., and Marassi, F. M. (2004) Structure determination of membrane proteins by NMR spectroscopy. *Chem. Rev. 104*, 3587-3606.

(56) Watts, A., Burnett, I. J., Glaubitz, C., Grobner, G., Middleton, D. A., Spooner, P. J., Watts, J. A., and Williamson, P. T. (1999) Membrane protein structure determination by solid state NMR. *Nat. Prod. Rep. 16*, 419-423.

(57) Opella, S. J. (2013) Structure determination of membrane proteins by nuclear magnetic resonance spectroscopy. *Annu. Rev. Anal. Chem. 6*, 305-328.

(58) Chattopadhyay, A., and London, E. (1987) Parallax method for direct measurement of membrane penetration depth utilizing fluorescence quenching by spin-labeled phospholipids. *Biochemistry 26*, 39-45.

(59) Abrams, F. S., and London, E. (1993) Extension of the parallax analysis of membrane penetration depth to the polar region of model membranes: use of fluorescence quenching by a spin-label attached to the phospholipid polar headgroup. *Biochemistry 32*, 10826-10831.

(60) Chen, X., Wolfgang, D. E., and Sampson, N. S. (2000) Use of the parallax-quench method to determine the position of the active-site loop of cholesterol oxidase in lipid bilayers. *Biochemistry 39*, 13383-13389.

(61) Burke, J. E., Karbarz, M. J., Deems, R. A., Li, S., Woods, V. L., and Dennis, E. A. (2008) Interaction of group IA phospholipase A2 with metal ions and phospholipid vesicles probed with deuterium exchange mass spectrometry. *Biochemistry 47*, 6451-6459.

(62) Hsu, Y. H., Burke, J. E., Li, S., Woods, V. L., and Dennis, E. A. (2009) Localizing the membrane binding region of group VIA Ca2+-independent phospholipase A2 Using peptide amide hydrogen/deuterium exchange mass spectrometry. *J. Biol. Chem. 284*, 23652-23661.

(63) Morozova, D., Guigas, G., and Weiss, M. (2011) Dynamic Structure Formation of Peripheral Membrane Proteins. *Plos Comput. Biol. 7*, e1002067.

(64) Tieleman, D. P., Marrink, S. J., and Berendsen, H. J. (1997) A computer perspective of membranes: molecular dynamics studies of lipid bilayer systems. *Biochim. Biophys. Acta 1331*, 235-270.

(65) Jaud, S., Tobias, D. J., Falke, J. J., and White, S. H. (2007) Self-induced docking site of a deeply embedded peripheral membrane protein. *Biophys. J. 92*, 517-524.

(66) Rogaski, B., and Klauda, J. B. (2012) Membrane-binding mechanism of a peripheral membrane protein through microsecond molecular dynamics simulations. *J. Mol. Biol. 423*, 847-861.

(67) Hellmich, U. A., and Glaubitz, C. (2009) NMR and EPR studies of membrane transporters. *Biol. Chem. 390*, 815-834.

(68) Altenbach, C., Flitsch, S. L., Khorana, H. G., and Hubbell, W. L. (1989) Structural studies on transmembrane proteins. 2. spin labeling of bacteriorhodopsin mutants at unique cysteines. *Biochemistry 28*, 7806-7812.

(69) Frazier, A. A., Wisner, M. A., Malmberg, N. J., Victor, K. G., Fanucci, G. E., Nalefski, E. A., Falke, J. J., and Cafiso, D. S. (2002) Membrane orientation and position of the C2 domain from cPLA2 by site-directed spin labeling. *Biochemistry 41*, 6282-6292.

(70) Frazier, A. A., Roller, C. R., Havelka, J. J., Hinderliter, A., and Cafiso, D. S. (2003) Membrane-bound orientation and position of the synaptotagmin I C2A domain by site-directed spin labeling. *Biochemistry 42*, 96-105.

(71) Kohout, S. C., Corbalan-Garcia, S., Gomez-Fernandez, J. C., and Falke, J. J. (2003) C2 domain of protein kinase C alpha: elucidation of the membrane docking surface by site-directed fluorescence and spin labeling. *Biochemistry 42*, 1254-1265.

(72) Nalefski, E. A., and Falke, J. J. (1998) Location of the membrane-docking face on the Ca2+-activated C2 domain of cytosolic phospholipase A2. *Biochemistry 37*, 17642-17650.

(73) Toke, O., Maloy, W. L., Kim, S. J., Blazyk, J., and Schaefer, J. (2004) Secondary structure and lipid contact of a peptide antibiotic in phospholipid bilayers by REDOR. *Biophys. J. 87*, 662-674.

(74) Tuzi, S., Uekama, N., Okada, M., Yamaguchi, S., Saito, H., and Yagisawa, H. (2003) Structure and dynamics of the phospholipase C-delta1 pleckstrin homology domain located at the lipid bilayer surface. *J. Biol. Chem. 278*, 28019-28025.

(75) Wales, T. E., and Engen, J. R. (2006) Hydrogen exchange mass spectrometry for the analysis of protein dynamics. *Mass Spectrom. Rev. 25*, 158-170.

(76) Lai, C. L., Landgraf, K. E., Voth, G. A., and Falke, J. J. (2010) Membrane docking geometry and target lipid stoichiometry of membrane-bound PKCα C2 domain: a combined molecular dynamics and experimental study. *J. Mol. Biol. 402*, 301-310.

(77) Balali-Mood, K., Bond, P. J., and Sansom, M. S. P. (2009) Interaction of monotopic membrane enzymes with a lipid bilayer: A Coarse-Grained MD simulation study. *Biochemistry 48*, 2135-2145.

(78) Diraviyam, K., and Murray, D. (2006) Computational analysis of the membrane association of group IIA secreted phospholipases A2: a differential role for electrostatics. *Biochemistry 45*, 2584-2598.

(79) Diraviyam, K., Stahelin, R. V., Cho, W., and Murray, D. (2003) Computer modeling of the membrane interaction of FYVE domains. *J. Mol. Biol. 328*, 721-736.

(80) Kass, I. J., and Sampson, N. S. (1995) The isomerization catalyzed by Brevibacterium sterolicum cholesterol oxidase proceeds stereospecifically with one base. *Biochem. Biophys. Res. Commun. 206*, 688-693.

(81) Sampson, N. S., and Kass, I. J. (1997) Isomerization, but not oxidation, is suppressed by a single point mutation, E361Q, in the reaction catalyzed by cholesterol oxidase. *J. Am. Chem. Soc. 119*, 855-862.

(82) Ghoshroy, K. B., Zhu, W., and Sampson, N. S. (1997) Investigation of membrane disruption in the reaction catalyzed by cholesterol oxidase. *Biochemistry 36*, 6133-6140.

(83) Turfitt, G. E. (1948) The microbiological degradation of steroids. 4. fission of the steroid molecule. *Biochem. J. 42*, 376-383.

(84) Turfitt, G. E. (1944) The microbiological degradation of steroids. 2. Oxidation of cholesterol by Proactinomyces SPP. *Biochem. J. 38*, 492-496.

(85) Turfitt, G. E. (1946) The microbiological degradation of steroids. 3. oxidation of hydroxy-steroids to keto-derivatives by proactinomyces-spp. *Biochem. J. 40*, 79-81.

(86) Richmond, W. (1973) Preparation and properties of a cholesterol oxidase from Nocardia sp and its application to enzymatic assay of total cholesterol in serum. *Clin. Chem. 19*, 1350-1356.

(87) Fukuda, H., Kawakami, Y., and Nakamura, S. (1973) Method to screen anticholesterol substances produced by microbes and a new cholesterol oxidase produced by Streptomyces-violascens. *Chem. Pharm. Bull. 21*, 2057-2060.

(88) Smith, A. G., and Brooks, C. J. W. (1974) Application of cholesterol oxidase in analysis of steroids. *J. Chromatogr. 101*, 373-378.

(89) Lange, Y., Ye, J., and Steck, T. L. (2005) Activation of membrane cholesterol by displacement from phospholipids. *J. Biol. Chem. 280*, 36126-36131.

(90) Elyandouzi, E., and Legrimellec, C. (1992) Cholesterol heterogeneity in the plasma-membrane of epithelial-cells. *Biochemistry 31*, 547-551.

(91) Ahn, K.-w., and Sampson, N. S. (2004) Cholesterol oxidase senses subtle changes in lipid bilayer structure. *Biochemistry 43*, 827-836.

(92) Lario, P. I., Sampson, N., and Vrielink, A. (2003) Sub-atomic resolution crystal structure of cholesterol oxidase: What atomic resolution crystallography reveals about enzyme mechanism and the role of the FAD cofactor in redox activity. *J. Mol. Biol. 326*, 1635-1650.

(93) Vrielink, A., Lloyd, L. F., and Blow, D. M. (1991) Crystal-structure of cholesterol oxidase from Brevibacterium-sterolicum refined at 1.8 Å resolution. *J. Mol. Biol. 219*, 533-554.

(94) Li, J. Y., Vrielink, A., Brick, P., and Blow, D. M. (1993) Crystal-structure of cholesterol oxidase complexed with a steroid substrate - implications for flavin adenine-dinucleotide dependent alcohol oxidases. *Biochemistry 32*, 11507-11515.

(95) Yue, Q. K., Kass, I. J., Sampson, N. S., and Vrielink, A. (1999) Crystal structure determination of cholesterol oxidase from Streptomyces and structural characterization of key active site mutants. *Biochemistry 38*, 4277-4286.

(96) Coulombe, R., Yue, K. Q., Ghisla, S., and Vrielink, A. (2001) Oxygen access to the active site of cholesterol oxidase through a narrow channel is gated by an Arg-Glu pair. *J. Biol. Chem. 276*, 30435-30441.

(97) Kass, I. J., and Sampson, N. S. (1998) The importance of GLU361 position in the reaction catalyzed by cholesterol oxidase. *Bioorg. Med. Chem. Lett. 8*, 2663-2668.

(98) Kass, I. J., and Sampson, N. S. (1998) Evaluation of the role of His447 in the reaction catalyzed by cholesterol oxidase. *Biochemistry 37*, 17990-18000.

(99) Yin, Y., Liu, P., Anderson, R. G. W., and Sampson, N. S. (2002) Construction of a catalytically inactive cholesterol oxidase mutant: investigation of the interplay between active site-residues glutamate 361 and histidine 447. *Arch. Biochem. Biophys. 402*, 235-242.

(100) Yin, Y., Sampson, N. S., Vrielink, A., and Lario, P. I. (2001) The presence of a hydrogen bond between asparagine 485 and the pi system of FAD modulates the redox potential in the reaction catalyzed by cholesterol oxidase. *Biochemistry 40*, 13779-13787.

(101) Sampson, N. S., and Vrielink, A. (2003) Cholesterol oxidases: a study of nature's approach to protein design. *Acc. Chem. Res. 36*, 713-722.

(102) Motteran, L., Pilone, M. S., Molla, G., Ghisla, S., and Pollegioni, L. (2001) Cholesterol oxidase from Brevibacterium sterolicum - The relationship between covalent flavinylation and redox properties. *J. Biol. Chem. 276*, 18024-18030.

(103) Rodrigueza, W. V., Wheeler, J. J., Klimuk, S. K., Kitson, C. N., and Hope, M. J. (1995) Transbilayer movement and net flux of cholesterol and cholesterol sulfate between liposomal membranes. *Biochemistry 34*, 6208-6217.

(104) Sampson, N. S., Kass, I. J., and Ghoshroy, K. B. (1998) Assessment of the role of an ω loop of cholesterol oxidase: a truncated loop mutant has altered substrate specificity. *Biochemistry 37*, 5770-5778.

(105) Ghang, Y.-J. (2008) in *Department of Chemistry*, Stony Brook University, Stony Brook

(106) Heller, H., Schaefer, M., and Schulten, K. (1993) Molecular-dynamics simulation of a bilayer of 200 lipids in the gel and in the liquid-crystal phases. *J. Phys. Chem. 97*, 8343-8360.

(107) Tang, H. (2007) in *Department of Chemistry*, Stony Brook University, Stony Brook.

(108) Mendoza, V. L., and Vachet, R. W. (2009) Probing protein structure by amino acid-specific covalent labeling and mass spectrometry. *Mass Spectrom. Rev. 28*, 785-815.

(109) Hermanson, G. T. (2008) *Bioconjugate Techniques*, Academic Press, San Diego, CA.

(110) Ban, H., Nagano, M., Gavrilyuk, J., Hakamata, W., Inokuma, T., and Barbas, C. F. (2013) Facile and stabile linkages through tyrosine: bioconjugation strategies with the tyrosine-click reaction. *Bioconjug. Chem. 24*, 520-532.

(111) Leitner, A., and Lindner, W. (2004) Current chemical tagging strategies for proteome analysis by mass spectrometry. *J. Chromatogr. B 813*, 1-26.

(112) Leitner, A., and Lindner, W. (2006) Chemistry meets proteomics: The use of chemical tagging reactions for MS-based proteomics. *Proteomics 6*, 5418-5434.

(113) Aebersold, R., and Mann, M. (2003) Mass spectrometry-based proteomics. *Nature 422*, 198-207.

(114) Yates, J. R., Ruse, C. I., and Nakorchevsky, A. (2009) Proteomics by mass spectrometry: approaches, advances, and applications. *Annu. Rev. Biomed. Eng. 11*, 49-79.

(115) Gilis, D., Massar, S., Cerf, N. J., and Rooman, M. (2001) Optimality of the genetic code with respect to protein stability and amino-acid frequencies. *Genome. Biol. 2*, RESEARCH0049.

(116) Chalker, J. M., Bernardes, G. J. L., Lin, Y. A., and Davis, B. G. (2009) Chemical modification of proteins at cysteine: Opportunities in chemistry and biology. *Chem. Asian J. 4*, 630-640.

(117) Jacob, M. H., Amir, D., Ratner, V., Gussakowsky, E., and Haas, E. (2005) Predicting reactivities of protein surface cysteines as part of a strategy for selective multiple labeling. *Biochemistry 44*, 13664-13672.

(118) Bulaj, G., Kortemme, T., and Goldenberg, D. P. (1998) Ionization-reactivity relationships for cysteine thiols in polypeptides. *Biochemistry 37*, 8965-8972.

(119) Kortemme, T., and Creighton, T. E. (1995) Ionisation of cysteine residues at the termini of model α-helical peptides. Relevance to unusual thiol pKa values in proteins of the thioredoxin family. *J. Mol. Biol. 253*, 799-812.

(120) Bogdanov, M., Zhang, W., Xie, J., and Dowhan, W. (2005) Transmembrane protein topology mapping by the substituted cysteine accessibility method (SCAM (TM)): Application to lipid-specific membrane protein topogenesis. *Methods 36*, 148-171.

(121) Krishnasastry, M., Walker, B., Braha, O., and Bayley, H. (1994) Surface labeling of key residues during assembly of the transmembrane pore formed by Staphylococcal alpha-hemolysin. *FEBS Lett. 356*, 66-71.

(122) Snyder, G. H., Cennerazzo, M. J., Karalis, A. J., and Field, D. (1981) Electrostatic influence of local cysteine environments on disulfide exchange kinetics. *Biochemistry 20*, 6509-6519.

(123) Jewell, J. E., Orwick, J., Liu, J., and Miller, K. W. (1999) Functional importance and local environments of the cysteines in the tetracycline resistance protein encoded by plasmid pBR322. *J. Bacteriol. 181*, 1689-1693.

(124) Loo, T. W., and Clarke, D. M. (1995) Membrane topology of a cysteine-less mutant of human P-glycoprotein. *J. Biol. Chem. 270*, 843-848.

(125) Fu, D. X., and Maloney, P. C. (1998) Structure-function relationships in OxlT, the oxalate/formate transporter of Oxalobacter formigenes - Topological features of transmembrane helix 11 as visualized by site-directed fluorescent labeling. *J. Biol. Chem. 273*, 17962-17967.

(126) Harris, T. K., and Turner, G. J. (2002) Structural basis of perturbed pKa values of catalytic groups in enzyme active sites. *IUBMB Life 53*, 85-98.

(127) Zhu, Q. S., and Casey, J. R. (2007) Topology of transmembrane proteins by scanning cysteine accessibility mutagenesis methodology. *Methods 41*, 439-450.

(128) Roberts, D. D., Lewis, S. D., Ballou, D. P., Olson, S. T., and Shafer, J. A. (1986) Reactivity of small thiolate anions and cysteine-25 in papain toward methyl methanethiosulfonate. *Biochemistry 25*, 5595-5601.

(129) Rogers, L. K., Leinweber, B. L., and Smith, C. V. (2006) Detection of reversible protein thiol modifications in tissues. *Anal. Biochem. 358*, 171-184.

(130) Niwayama, S., Kurono, S., and Matsumoto, H. (2001) Synthesis of d-labeled N-alkylmaleimides and application to quantitative peptide analysis by isotope differential mass spectrometry. *Bioorg. Med. Chem. Lett. 11*, 2257-2261.

(131) Akabas, M. H., Stauffer, D. A., Xu, M., and Karlin, A. (1992) Acetylcholine receptor channel structure probed in cysteine-substitution mutants. *Science 258*, 307-310.

(132) Karlin, A., and Akabas, M. H. (1998) Substituted-cysteine accessibility method. *Methods Enzymol. 293*, 123-145.

(133) Sokolowska, I., Wetie, A. G. N., Woods, A. G., and Darie, C. C. (2013) Applications of mass spectrometry in proteomics. *Aust. J. Chem. 66*, 721-733.

(134) Fenn, J. B., Mann, M., Meng, C. K., Wong, S. F., and Whitehouse, C. M. (1989) Electrospray ionization for mass-spectrometry of large biomolecules. *Science 246*, 64-71.

(135) Karas, M., and Hillenkamp, F. (1988) Laser desorption ionization of proteins with molecular masses exceeding 10,000 daltons. *Anal. Chem. 60*, 2299-2301.

(136) Flory, M. R., Griffin, T. J., Martin, D., and Aebersold, R. (2002) Advances in quantitative proteomics using stable isotope tags. *Trends Biotechnol. 20*, S23-S29.

(137) Tao, W. A., and Aebersold, R. (2003) Advances in quantitative proteomics via stable isotope tagging and mass spectrometry. *Curr. Opin. Biotech. 14*, 110-118.

(138) Iliuk, A., Galan, J., and Tao, W. A. (2009) Playing tag with quantitative proteomics. *Anal. Bioanal. Chem. 393*, 503-513.

(139) Boas, U., and Heegaard, P. M. (2004) Dendrimers in drug research. *Chem. Soc. Rev. 33*, 43-63.

(140) Gygi, S. P., Rist, B., Gerber, S. A., Turecek, F., Gelb, M. H., and Aebersold, R. (1999) Quantitative analysis of complex protein mixtures using isotope-coded affinity tags. *Nat. Biotechnol. 17*, 994-999.

(141) Zhang, R., Sioma, C. S., Wang, S., and Regnier, F. E. (2001) Fractionation of isotopically labeled peptides in quantitative proteomics. *Anal. Chem. 73*, 5142-5149.

(142) Zhang, R., Sioma, C. S., Thompson, R. A., Xiong, L., and Regnier, F. E. (2002) Controlling deuterium isotope effects in comparative proteomics. *Anal. Chem. 74*, 3662-3669.

(143) Zhang, R. J., and Regnier, F. E. (2002) Minimizing resolution of isotopically coded peptides in comparative proteomics. *J. Proteome Res. 1*, 139-147.

(144) Qiu, Y., Sousa, E. A., Hewick, R. M., and Wang, J. H. (2002) Acid-labile isotope-coded extractants: a class of reagents for quantitative mass spectrometric analysis of complex protein mixtures. *Anal. Chem. 74*, 4969-4979.

(145) Zhou, H., Ranish, J. A., Watts, J. D., and Aebersold, R. (2002) Quantitative proteome analysis by solid-phase isotope tagging and mass spectrometry. *Nat. Biotechnol. 20*, 512-515.

(146) Su, C. Y., London, E., and Sampson, N. S. (2013) Mapping peptide thiol accessibility in membranes using a quaternary ammonium isotope-coded mass tag (ICMT). *Bioconjug. Chem. 24*, 1235-1247.

(147) Tang, W., and Fang, S. Y. (2008) Mono-acylation of symmetric diamines in the presence of water. *Tetrahedron Lett. 49*, 6003-6006.

(148) Poole, L. B., Klomsiri, C., Knaggs, S. A., Furdui, C. M., Nelson, K. J., Thomas, M. J., Fetrow, J. S., Daniel, L. W., and King, S. B. (2007) Fluorescent and affinity-based tools to detect cysteine sulfenic acid formation in proteins. *Bioconjug. Chem. 18*, 2004-2017.

(149) Dardonville, C., Fernandez-Fernandez, C., Gibbons, S. L., Ryan, G. J., Jagerovic, N., Gabilondo, A. M., Meana, J. J., and Callado, L. F. (2006) Synthesis and pharmacological studies of new hybrid derivatives of fentanyl active at the mu-opioid receptor and I2-imidazoline binding sites. *Bioorg. Med. Chem. 14*, 6570-6580.

(150) Zhao, C., Song, Y. J., Qu, K. G., Ren, J. S., and Qu, X. G. (2010) Luminescent rare-earth complex covalently modified single-walled carbon nanotubes: Design, synthesis, and DNA sequence-dependent red luminescence enhancement. *Chem. Mater. 22*, 5718-5724.

(151) Che, F. Y., and Fricker, L. D. (2005) Quantitative peptidomics of mouse pituitary: comparison of different stable isotopic tags. *J. Mass Spectrom. 40*, 238-249.

(152) Weerapana, E., Wang, C., Simon, G. M., Richter, F., Khare, S., Dillon, M. B. D., Bachovchin, D. A., Mowen, K., Baker, D., and Cravatt, B. F. (2010) Quantitative reactivity profiling predicts functional cysteines in proteomes. *Nature 468*, 790-797.

(153) Viswanadhan, V. N., Ghose, A. K., Revankar, G. R., and Robins, R. K. (1989) Atomic physicochemical parameters for 3 dimensional structure directed quantitative structure - Activity relationships. 4. Additional parameters for hydrophobic and dispersive interactions and their application for an automated superposition of certain naturally-occurring nucleoside antibiotics. *J. Chem. Inf. Comp. Sci. 29*, 163-172.

(154) Klopman, G., Li, J. Y., Wang, S. M., and Dimayuga, M. (1994) Computer automated log P calculations based on an extended group-contribution approach. *J. Chem. Inf. Comp. Sci. 34*, 752-781.

(155) Ren, D., Julka, S., Inerowicz, H. D., and Regnier, F. E. (2004) Enrichment of cysteine-containing peptides from tryptic digests using a quaternary amine tag. *Anal. Chem. 76*, 4522-4530.

(156) Li, J., Ma, H. M., Wang, X. C., Xiong, S. X., Dong, S. Y., and Wang, S. J. (2007) Enhanced detection of thiol peptides by matrix-assisted laser desorption/ionization mass spectrometry after selective derivatization with a tailor-made quaternary ammonium tag containing maleimidyl group. *Rapid. Commun. Mass Spectrom. 21*, 2608-2612.

(157) Shimada, T., Kuyama, H., Sato, T. A., and Tanaka, K. (2012) Development of iodoacetic acid-based cysteine mass tags: detection enhancement for cysteine-containing peptide by matrix-assisted laser desorption/ionization time-of-flight mass spectrometry. *Anal. Biochem. 421*, 785-787.

(158) Paula, S., Sus, W., Tuchtenhagen, J., and Blume, A. (1995) Thermodynamics of micelle formation as a function of temperature – a high-sensitivity titration calorimetry study. *J. Phys. Chem. 99*, 11742-11751.

(159) Shahidullah, K., and London, E. (2008) Effect of lipid composition on the topography of membrane-associated hydrophobic helices: Stabilization of transmembrane topography by anionic lipids. *J. Mol. Biol. 379*, 704-718.

(160) Kucerka, N., Tristram-Nagle, S., and Nagle, J. F. (2005) Structure of fully hydrated fluid phase lipid bilayers with monounsaturated chains. *J. Membr. Biol. 208*, 193-202.

(161) Nezil, F. A., and Bloom, M. (1992) Combined influence of cholesterol and synthetic amphiphillic peptides upon bilayer thickness in model membranes. *Biophys. J. 61*, 1176-1183.

(162) Ellena, J. F., Lackowicz, P., Mongomery, H., and Cafiso, D. S. (2011) Membrane thickness varies around the circumference of the transmembrane protein BtuB. *Biophys. J. 100*, 1280-1287.

(163) Kucerka, N., Nieh, M. P., and Katsaras, J. (2011) Fluid phase lipid areas and bilayer thicknesses of commonly used phosphatidylcholines as a function of temperature. *Biochim. Biophys. Acta 1808*, 2761-2771.

(164) Bretscher, M. S., and Munro, S. (1993) Cholesterol and the Golgi apparatus. *Science 261*, 1280-1281.

(165) Ben-Yashar, V., and Barenholz, Y. (1989) The interaction of cholesterol and cholest-4-en-3-one with dipalmitoylphosphatidylcholine. Comparison based on the use of three fluorophores. *Biochim. Biophys. Acta 985*, 271-278.

(166) Rubenstein, J. R., Smith, B. A., and Mcconnell, H. M. (1979) Lateral diffusion in binary-mixtures of cholesterol and phosphatidylcholines. *Proc. Natl. Acad. Sci. U.S.A. 76*, 15-18.

(167) Reyes Mateo, C., Ulises Acuna, A., and Brochon, J. C. (1995) Liquid-crystalline phases of cholesterol/lipid bilayers as revealed by the fluorescence of trans-parinaric acid. *Biophys. J. 68*, 978-987.

(168) Sankaram, M. B., and Thompson, T. E. (1991) Cholesterol-induced fluid-phase immiscibility in membranes. *Proc. Natl. Acad. Sci. U.S.A. 88*, 8686-8690.

(169) Lad, M. D., Birembaut, F., Clifton, L. A., Frazier, R. A., Webster, J. R., and Green, R. J. (2007) Antimicrobial peptide-lipid binding interactions and binding selectivity. *Biophys. J. 92*, 3575-3586.

(170) Liu, L. P., and Deber, C. M. (1997) Anionic phospholipids modulate peptide insertion into membranes. *Biochemistry 36*, 5476-5482.

(171) McConnell, H. M., and Kornberg, R. D. (1971) Inside-outside transitions of phospholipids in vesicle membranes. *Biochemistry 10*, 1111-1120.

(172) Kol, M. A., de Kroon, A. I. P. M., Rijkers, D. T. S., Killian, J. A., and de Kruijff, B. (2001) Membrane-spanning peptides induce phospholipid flop: A model for

phospholipid translocation across the Inner membrane of E. coli. *Biochemistry 40*, 10500-10506.

(173) Kol, M. A., van Laak, A. N. C., Rijkers, D. T. S., Killian, J. A., de Kroon, A. I. P. M., and de Kruijff, B. (2003) Phospholipid flop induced by transmembrane peptides in model membranes is modulated by lipid composition. *Biochemistry 42*, 231-237.

(174) Kol, M. A., van Dalen, A., de Kroon, A. I., and de Kruijff, B. (2003) Translocation of phospholipids is facilitated by a subset of membrane-spanning proteins of the bacterial cytoplasmic membrane. *J. Biol. Chem. 278*, 24586-24593.

(175) Kunkel, T. A. (1985) Rapid and Efficient Site-Specific Mutagenesis without Phenotypic Selection. *Proc. Natl. Acad. Sci. U.S.A. 82*, 488-492.

(176) Sugimoto, M., Esaki, N., Tanaka, H., and Soda, K. (1989) A Simple and Efficient Method for the Oligonucleotide-Directed Mutagenesis Using Plasmid DNA-Template and Phosphorothioate-Modified Nucleotide. *Anal. Biochem. 179*, 309-311.

(177) Taylor, J. W., Ott, J., and Eckstein, F. (1985) The Rapid Generation of Oligonucleotide-Directed Mutations at High-Frequency Using Phosphorothioate-Modified DNA. *Nucleic Acids Res. 13*, 8765-8785.

(178) Vandeyar, M. A., Weiner, M. P., Hutton, C. J., and Batt, C. A. (1988) A Simple and Rapid Method for the Selection of Oligodeoxynucleotide-Directed Mutants. *Gene 65*, 129-133.

(179) Nelson, M., and Mcclelland, M. (1992) Use of DNA Methyltransferase Endonuclease Enzyme Combinations for Megabase Mapping of Chromosomes. *Methods Enzymol. 216*, 279-303.

(180) Wnendt, S. (1994) Analysis of the Enda Mutation of Escherichia-Coli K12 Strains - Jm103 Behaves Like Enda(+) Wild-type Strains. *Biotechniques 17*, 270-272.

(181) Hogrefe, H. H., Cline, J., Youngblood, G. L., and Allen, R. M. (2002) Creating randomized amino acid libraries with the QuikChange (R) Multi Site-Directed Mutagenesis Kit. *Biotechniques 33*, 1158-+.

(182) Proc, J. L., Kuzyk, M. A., Hardie, D. B., Yang, J., Smith, D. S., Jackson, A. M., Parker, C. E., and Borchers, C. H. (2010) A quantitative study of the effects of chaotropic agents, surfactants, and solvents on the digestion efficiency of human plasma proteins by trypsin. *J. Proteome Res. 9*, 5422-5437.

(183) Zhou, J., Zhou, T. Y., Cao, R., Liu, Z., Shen, J. Y., Chen, P., Wang, X. C., and Liang, S. P. (2006) Evaluation of the application of sodium deoxycholate to proteomic analysis of rat hippocampal plasma membrane. *J. Proteome Res. 5*, 2547-2553.

(184) Masuda, T., Tomita, M., and Ishihama, Y. (2008) Phase transfer surfactant-aided trypsin digestion for membrane proteome analysis. *J. Proteome Res. 7*, 731-740.

(185) Lin, Y., Zhou, J., Bi, D., Chen, P., Wang, X. C., and Liang, S. P. (2008) Sodium-deoxycholate-assisted tryptic digestion and identification of proteolytically resistant proteins. *Anal. Biochem. 377*, 259-266.

(186) Lin, Y., Liu, Y., Li, J. J., Zhao, Y., He, Q. Z., Han, W. J., Chen, P., Wang, X. C., and Liang, S. P. (2010) Evaluation and optimization of removal of an acid-insoluble surfactant for shotgun analysis of membrane proteome. *Electrophoresis 31*, 2705-2713.

(187) Xiang, J., and Sampson, N. S. (2004) Library screening studies to investigate substrate specificity in the reaction catalyzed by cholesterol oxicase. *Protein Eng. Des. Sel. 17*, 341-348.

(188) Sampson, N. S. a. K., S. (2008) in *Proceedings of 3rd International symposium on experimental standard conditions of enzyme characterizations (ESCES)*, Rudesheim/Rhein, Germany, Beilstein-Institut.

(189) Hoops, S., Sahle, S., Gauges, R., Lee, C., Pahle, J., Simus, N., Singhal, M., Xu, L., Mendes, P., and Kummer, U. (2006) Copasi- a complex pathway simulator. *Bioinformatics 22*, 3067-3074.

(190) Shrake, A., and Rupley, J. A. (1973) Environment and Exposure to Solvent of Protein Atoms - Lysozyme and Insulin. *J. Mol. Biol. 79*, 351-371.

(191) Krissinel, E., and Henrick, K. (2007) Inference of macromolecular assemblies from crystalline state. *J. Mol. Biol. 372*, 774-797.

(192) Krissinel, E., and Henrick, K. (2005) Detection of protein assemblies in crystals. *Lect Notes Comput Sc 3695*, 163-174.

(193) Krissinel, E. (2010) Crystal contacts as nature's docking solutions. *J Comput Chem 31*, 133-143.

(194) Hansen, R. E., and Winther, J. R. (2009) An introduction to methods for analyzing thiols and disulfides: Reactions, reagents, and practical considerations. *Anal. Biochem. 394*, 147-158.

(195) Titani, Y., and Tsuruta, Y. (1974) Some chemical and biological characteristics of showdomycin. *J. Antibiot. 27*, 956-962.

(196) Gregory, J. D. (1955) The stability of N-ethylmaleimide and its reaction with sulfhydryl groups. *J. Am. Chem. Soc. 77*, 3922-3923.

(197) Culham, D. E., Hillar, A., Henderson, J., Ly, A., Vernikovska, Y. I., Racher, K. I., Boggs, J. M., and Wood, J. M. (2003) Creation of a fully functional cysteine-less variant of osmosensor and proton-osmoprotectant symporter ProP from Escherichia coli and its application to assess the transporter's membrane orientation. *Biochemistry 42*, 11815-11823.

(198) Winterbourn, C. C., and Metodiewa, D. (1999) Reactivity of biologically important thiol compounds with superoxide and hydrogen peroxide. *Free Radic. Bio. Med. 27*, 322-328.

(199) Baessler, K. A., Lee, Y., Roberts, K. S., Facompre, N., and Sampson, N. S. (2006) Multivalent fertilinβ oligopeptides: The dependence of fertilization inhibition on length and density. *Chem. Biol. 13*, 251-259.

(200) Guy, J., Caron, K., Dufresne, S., Michnick, S. W., Skene, W. G., and Keillor, J. W. (2007) Convergent preparation and photophysical characterization of dimaleimide dansyl fluorogens: elucidation of the maleimide fluorescence quenching mechanism. *J. Am. Chem. Soc. 129*, 11969-11977.

(201) van der Veken, P., Dirksen, E. H. C., Ruijter, E., Elgersma, R. C., Heck, A. J. R., Rijkers, D. T. S., Slijper, M., and Liskamp, R. M. J. (2005) Development of a novel chemical probe for the selective enrichment of phosphorylated serine- and threonine-containing peptides. *ChemBioChem 6*, 2271-2280.

(202) Riaz, M. (1996) Liposomes preparation methods. *Pak. J. Pharm. Sci. 9*, 65-77.

(203) Molnar, I., Hayashi, N., Choi, K. P., Yamamoto, H., Yamashita, M., and Murooka, Y. (1993) Bacterial cholesterol oxidases are able to act as flavoprotein-linked ketosteroid monooxygenases that catalyse the hydroxylation of cholesterol to 4-cholesten-6-ol-3-one. *Mol. Microbiol. 7*, 419-428.

Appendix

Appendix A: List of mass spectra of transmembrane peptide and cholesterol oxidase-lipids labeling experiments.

Appendix 1 List of mass spectra of transmembrane peptide labeling experiments

Note: peptide # in labbook and thesis is different. See below.
Peptide **1** (labbook) = peptide **8** (thesis)
Peptide **2** (labbook) = peptide **6** (thesis)
Peptide **3** (labbook) = peptide **7** (thesis)

#	Page #	Spectrum name	Peptide	[Peptide] mM	Lipids	[Lipids] mM	Probe	[Probe] mM	Time (s)	Buffer
1	p2184	2184-221	peptide 3	50	POPC	4	5a-d9	125	2	50 mM NaPi pH7
2	p2184	2184-231	peptide 3	50	POPC	4	5a-d9	125	5	50 mM NaPi pH7
3	p2184	2184-241	peptide 3	50	POPC	4	5a-d9	125	10	50 mM NaPi pH7
4	p2184	2184-251	peptide 3	50	POPC	4	5a-d9	125	30	50 mM NaPi pH7
5	p2184	2184-261	peptide 3	50	POPC	4	5a-d9	125	60	50 mM NaPi pH7
6	p2184	2184-271	peptide 3	50	POPC	4	5a-d9	125	120	50 mM NaPi pH7
7	p2184	2814-281	peptide 3	50	POPC	4	5a-d9	125	300	50 mM NaPi pH7
8	p2184	2184-291	peptide 3	50	POPC	4	5a-d9	125	2	50 mM NaPi pH7
9	p2184	2184-301	peptide 3	50	POPC	4	5a-d9	125	5	50 mM NaPi pH7
10	p2184	2184-311	peptide 3	50	POPC	4	5a-d9	125	10	50 mM NaPi pH7
11	p2184	2184-321	peptide 3	50	POPC	4	5a-d9	125	30	50 mM NaPi pH7
12	p2184	2184-331	peptide 3	50	POPC	4	5a-d9	125	60	50 mM NaPi pH7
13	p2184	2184-341	peptide 3	50	POPC	4	5a-d9	125	120	50 mM NaPi pH7
14	p2184	2184-351	peptide 3	50	POPC	4	5a-d9	125	300	50 mM NaPi pH7
15	p2184	2184-361	peptide 3	50	POPC	4	5a-d9	125	2	50 mM NaPi pH7
16	p2184	2184-371	peptide 3	50	POPC	4	5a-d9	125	5	50 mM NaPi pH7
17	p2184	2184-381	peptide 3	50	POPC	4	5a-d9	125	10	50 mM NaPi pH7
18	p2184	2184-391	peptide 3	50	POPC	4	5a-d9	125	30	50 mM NaPi pH7
19	p2184	2184-401	peptide 3	50	POPC	4	5a-d9	125	60	50 mM NaPi pH7
20	p2184	2184-411	peptide 3	50	POPC	4	5a-d9	125	120	50 mM NaPi pH7
21	p2184	2184-421	peptide 3	50	POPC	4	5a-d9	125	300	50 mM NaPi pH7
22	p2180	2180-11	peptide 3	50	POPC/cholesterol(75/25)	4	5a-d9	125	2	50 mM NaPi pH7
23	p2180	2180-21	peptide 3	50	POPC/cholesterol(75/25)	4	5a-d9	125	5	50 mM NaPi pH7
24	p2180	2180-31	peptide 3	50	POPC/cholesterol(75/25)	4	5a-d9	125	10	50 mM NaPi pH7
25	p2180	2180-41	peptide 3	50	POPC/cholesterol(75/25)	4	5a-d9	125	30	50 mM NaPi pH7
26	p2180	2180-51	peptide 3	50	POPC/cholesterol(75/25)	4	5a-d9	125	60	50 mM NaPi pH7
27	p2180	2180-61	peptide 3	50	POPC/cholesterol(75/25)	4	5a-d9	125	120	50 mM NaPi pH7
28	p2180	2180-71	peptide 3	50	POPC/cholesterol(75/25)	4	5a-d9	125	300	50 mM NaPi pH7
29	p2180	2180-81	peptide 3	50	POPC/cholesterol(75/25)	4	5a-d9	125	2	50 mM NaPi pH7
30	p2180	2180-91	peptide 3	50	POPC/cholesterol(75/25)	4	5a-d9	125	5	50 mM NaPi pH7
31	p2180	2180-101	peptide 3	50	POPC/cholesterol(75/25)	4	5a-d9	125	10	50 mM NaPi pH7
32	p2180	2180-111	peptide 3	50	POPC/cholesterol(75/25)	4	5a-d9	125	30	50 mM NaPi pH7
33	p2180	2180-121	peptide 3	50	POPC/cholesterol(75/25)	4	5a-d9	125	60	50 mM NaPi pH7
34	p2180	2180-131	peptide 3	50	POPC/cholesterol(75/25)	4	5a-d9	125	120	50 mM NaPi pH7
35	p2180	2180-141	peptide 3	50	POPC/cholesterol(75/25)	4	5a-d9	125	300	50 mM NaPi pH7
36	p2180	2180-151	peptide 3	50	POPC/cholesterol(75/25)	4	5a-d9	125	2	50 mM NaPi pH7
37	p2180	2180-161	peptide 3	50	POPC/cholesterol(75/25)	4	5a-d9	125	5	50 mM NaPi pH7
38	p2180	2180-171	peptide 3	50	POPC/cholesterol(75/25)	4	5a-d9	125	10	50 mM NaPi pH7
39	p2180	2180-181	peptide 3	50	POPC/cholesterol(75/25)	4	5a-d9	125	30	50 mM NaPi pH7
40	p2180	2180-191	peptide 3	50	POPC/cholesterol(75/25)	4	5a-d9	125	60	50 mM NaPi pH7
41	p2180	2180-201	peptide 3	50	POPC/cholesterol(75/25)	4	5a-d9	125	120	50 mM NaPi pH7
42	p2180	2180-211	peptide 3	50	POPC/cholesterol(75/25)	4	5a-d9	125	300	50 mM NaPi pH7
43	p2188	2188-11	peptide 3	50	POPC/cholest-4-en-3-one(75/25)	4	5a-d9	125	2	50 mM NaPi pH7
44	p2188	2188-21	peptide 3	50	POPC/cholest-4-en-3-one(75/25)	4	5a-d9	125	5	50 mM NaPi pH7
45	p2188	2188-31	peptide 3	50	POPC/cholest-4-en-3-one(75/25)	4	5a-d9	125	10	50 mM NaPi pH7
46	p2188	2188-41	peptide 3	50	POPC/cholest-4-en-3-one(75/25)	4	5a-d9	125	30	50 mM NaPi pH7
47	p2188	2188-51	peptide 3	50	POPC/cholest-4-en-3-one(75/25)	4	5a-d9	125	60	50 mM NaPi pH7
48	p2188	2188-61	peptide 3	50	POPC/cholest-4-en-3-one(75/25)	4	5a-d9	125	120	50 mM NaPi pH7
49	p2188	2188-71	peptide 3	50	POPC/cholest-4-en-3-one(75/25)	4	5a-d9	125	300	50 mM NaPi pH7

50	p2188	2188-81	peptide 3	50	POPC/cholest-4-en-3-one(75/25)	4	5a-d9	125	2	50 mM NaPi pH7
51	p2188	2188-91	peptide 3	50	POPC/cholest-4-en-3-one(75/25)	4	5a-d9	125	5	50 mM NaPi pH7
52	p2188	2188-101	peptide 3	50	POPC/cholest-4-en-3-one(75/25)	4	5a-d9	125	10	50 mM NaPi pH7
53	p2188	2188-111	peptide 3	50	POPC/cholest-4-en-3-one(75/25)	4	5a-d9	125	30	50 mM NaPi pH7
54	p2188	2188-121	peptide 3	50	POPC/cholest-4-en-3-one(75/25)	4	5a-d9	125	60	50 mM NaPi pH7
55	p2188	2188-131	peptide 3	50	POPC/cholest-4-en-3-one(75/25)	4	5a-d9	125	120	50 mM NaPi pH7
56	p2188	2188-141	peptide 3	50	POPC/cholest-4-en-3-one(75/25)	4	5a-d9	125	300	50 mM NaPi pH7
57	p2188	2188-151	peptide 3	50	POPC/cholest-4-en-3-one(75/25)	4	5a-d9	125	2	50 mM NaPi pH7
58	p2188	2188-161	peptide 3	50	POPC/cholest-4-en-3-one(75/25)	4	5a-d9	125	5	50 mM NaPi pH7
59	p2188	2188-171	peptide 3	50	POPC/cholest-4-en-3-one(75/25)	4	5a-d9	125	10	50 mM NaPi pH7
60	p2188	2188-181	peptide 3	50	POPC/cholest-4-en-3-one(75/25)	4	5a-d9	125	30	50 mM NaPi pH7
61	p2188	2188-191	peptide 3	50	POPC/cholest-4-en-3-one(75/25)	4	5a-d9	125	60	50 mM NaPi pH7
62	p2188	2188-201	peptide 3	50	POPC/cholest-4-en-3-one(75/25)	4	5a-d9	125	120	50 mM NaPi pH7
63	p2188	2188-211	peptide 3	50	POPC/cholest-4-en-3-one(75/25)	4	5a-d9	125	300	50 mM NaPi pH7
64	p2205	2205-11	peptide 1	50	POPC	4	5a-d9	250	2	50 mM NaPi pH7
65	p2205	2205-21	peptide 1	50	POPC	4	5a-d9	250	5	50 mM NaPi pH7
66	p2205	2205-31	peptide 1	50	POPC	4	5a-d9	250	10	50 mM NaPi pH7
67	p2205	2205-41	peptide 1	50	POPC	4	5a-d9	250	30	50 mM NaPi pH7
68	p2205	2205-51	peptide 1	50	POPC	4	5a-d9	250	60	50 mM NaPi pH7
69	p2205	2205-61	peptide 1	50	POPC	4	5a-d9	250	120	50 mM NaPi pH7
70	p2205	2205-71	peptide 1	50	POPC	4	5a-d9	250	300	50 mM NaPi pH7
71	p2205	2205-81	peptide 1	50	POPC	4	5a-d9	250	600	50 mM NaPi pH7
72	p2205	2205-91	peptide 1	50	POPC	4	5a-d9	250	900	50 mM NaPi pH7
73	p2205	2205-101	peptide 1	50	POPC	4	5a-d9	250	2	50 mM NaPi pH7
74	p2205	2205-111	peptide 1	50	POPC	4	5a-d9	250	5	50 mM NaPi pH7
75	p2205	2205-121	peptide 1	50	POPC	4	5a-d9	250	10	50 mM NaPi pH7
76	p2205	2205-131	peptide 1	50	POPC	4	5a-d9	250	30	50 mM NaPi pH7
77	p2205	2205-141	peptide 1	50	POPC	4	5a-d9	250	60	50 mM NaPi pH7
78	p2205	2205-151	peptide 1	50	POPC	4	5a-d9	250	120	50 mM NaPi pH7
79	p2205	2205-161	peptide 1	50	POPC	4	5a-d9	250	300	50 mM NaPi pH7
80	p2205	2205-171	peptide 1	50	POPC	4	5a-d9	250	600	50 mM NaPi pH7
81	p2205	2205-181	peptide 1	50	POPC	4	5a-d9	250	900	50 mM NaPi pH7
82	p2205	2205-191	peptide 1	50	POPC	4	5a-d9	250	2	50 mM NaPi pH7
83	p2205	2205-201	peptide 1	50	POPC	4	5a-d9	250	5	50 mM NaPi pH7
84	p2205	2205-211	peptide 1	50	POPC	4	5a-d9	250	10	50 mM NaPi pH7
85	p2205	2205-221	peptide 1	50	POPC	4	5a-d9	250	30	50 mM NaPi pH7
86	p2205	2205-231	peptide 1	50	POPC	4	5a-d9	250	60	50 mM NaPi pH7
87	p2205	2205-241	peptide 1	50	POPC	4	5a-d9	250	120	50 mM NaPi pH7
88	p2205	2205-251	peptide 1	50	POPC	4	5a-d9	250	300	50 mM NaPi pH7
89	p2205	2205-261	peptide 1	50	POPC	4	5a-d9	250	600	50 mM NaPi pH7
90	p2205	2205-271	peptide 1	50	POPC	4	5a-d9	250	900	50 mM NaPi pH7
91	p2197	2197-11	peptide 1	50	POPC/cholesterol(75/25)	4	5a-d9	250	2	50 mM NaPi pH7
92	p2197	2197-21	peptide 1	50	POPC/cholesterol(75/25)	4	5a-d9	250	5	50 mM NaPi pH7
93	p2197	2197-31	peptide 1	50	POPC/cholesterol(75/25)	4	5a-d9	250	10	50 mM NaPi pH7
94	p2197	2197-41	peptide 1	50	POPC/cholesterol(75/25)	4	5a-d9	250	30	50 mM NaPi pH7
95	p2197	2197-51	peptide 1	50	POPC/cholesterol(75/25)	4	5a-d9	250	60	50 mM NaPi pH7
96	p2197	2197-61	peptide 1	50	POPC/cholesterol(75/25)	4	5a-d9	250	120	50 mM NaPi pH7
97	p2197	2197-71	peptide 1	50	POPC/cholesterol(75/25)	4	5a-d9	250	300	50 mM NaPi pH7
98	p2197	2197-81	peptide 1	50	POPC/cholesterol(75/25)	4	5a-d9	250	600	50 mM NaPi pH7
99	p2197	2197-91	peptide 1	50	POPC/cholesterol(75/25)	4	5a-d9	250	900	50 mM NaPi pH7
100	p2197	2197-101	peptide 1	50	POPC/cholesterol(75/25)	4	5a-d9	250	2	50 mM NaPi pH7
101	p2197	2197-111	peptide 1	50	POPC/cholesterol(75/25)	4	5a-d9	250	5	50 mM NaPi pH7
102	p2197	2197-121	peptide 1	50	POPC/cholesterol(75/25)	4	5a-d9	250	10	50 mM NaPi pH7
103	p2197	2197-131	peptide 1	50	POPC/cholesterol(75/25)	4	5a-d9	250	30	50 mM NaPi pH7
104	p2197	2197-141	peptide 1	50	POPC/cholesterol(75/25)	4	5a-d9	250	60	50 mM NaPi pH7
105	p2197	2197-151	peptide 1	50	POPC/cholesterol(75/25)	4	5a-d9	250	120	50 mM NaPi pH7
106	p2197	2197-161	peptide 1	50	POPC/cholesterol(75/25)	4	5a-d9	250	300	50 mM NaPi pH7
107	p2197	2197-171	peptide 1	50	POPC/cholesterol(75/25)	4	5a-d9	250	600	50 mM NaPi pH7

108	p2197	2197-181	peptide 1	50	POPC/cholesterol(75/25)	4	5a-d9	250	900	50 mM NaPi pH7
109	p2197	2197-191	peptide 1	50	POPC/cholesterol(75/25)	4	5a-d9	250	2	50 mM NaPi pH7
110	p2197	2197-201	peptide 1	50	POPC/cholesterol(75/25)	4	5a-d9	250	5	50 mM NaPi pH7
111	p2197	2197-211	peptide 1	50	POPC/cholesterol(75/25)	4	5a-d9	250	10	50 mM NaPi pH7
112	p2197	2197-221	peptide 1	50	POPC/cholesterol(75/25)	4	5a-d9	250	30	50 mM NaPi pH7
113	p2197	2197-231	peptide 1	50	POPC/cholesterol(75/25)	4	5a-d9	250	60	50 mM NaPi pH7
114	p2197	2197-241	peptide 1	50	POPC/cholesterol(75/25)	4	5a-d9	250	120	50 mM NaPi pH7
115	p2197	2197-251	peptide 1	50	POPC/cholesterol(75/25)	4	5a-d9	250	300	50 mM NaPi pH7
116	p2197	2197-261	peptide 1	50	POPC/cholesterol(75/25)	4	5a-d9	250	600	50 mM NaPi pH7
117	p2197	2197-271	peptide 1	50	POPC/cholesterol(75/25)	4	5a-d9	250	900	50 mM NaPi pH7
118	p2202	2202-11	peptide 1	50	POPC/cholest-4-en-3-one(75/25)	4	5a-d9	250	2	50 mM NaPi pH7
119	p2202	2202-21	peptide 1	50	POPC/cholest-4-en-3-one(75/25)	4	5a-d9	250	5	50 mM NaPi pH7
120	p2202	2202-31	peptide 1	50	POPC/cholest-4-en-3-one(75/25)	4	5a-d9	250	10	50 mM NaPi pH7
121	p2202	2202-41	peptide 1	50	POPC/cholest-4-en-3-one(75/25)	4	5a-d9	250	30	50 mM NaPi pH7
122	p2202	2202-51	peptide 1	50	POPC/cholest-4-en-3-one(75/25)	4	5a-d9	250	60	50 mM NaPi pH7
123	p2202	2202-61	peptide 1	50	POPC/cholest-4-en-3-one(75/25)	4	5a-d9	250	120	50 mM NaPi pH7
124	p2202	2202-71	peptide 1	50	POPC/cholest-4-en-3-one(75/25)	4	5a-d9	250	300	50 mM NaPi pH7
125	p2202	2202-81	peptide 1	50	POPC/cholest-4-en-3-one(75/25)	4	5a-d9	250	600	50 mM NaPi pH7
126	p2202	2202-91	peptide 1	50	POPC/cholest-4-en-3-one(75/25)	4	5a-d9	250	900	50 mM NaPi pH7
127	p2202	2202-101	peptide 1	50	POPC/cholest-4-en-3-one(75/25)	4	5a-d9	250	2	50 mM NaPi pH7
128	p2202	2202-111	peptide 1	50	POPC/cholest-4-en-3-one(75/25)	4	5a-d9	250	5	50 mM NaPi pH7
129	p2202	2202-121	peptide 1	50	POPC/cholest-4-en-3-one(75/25)	4	5a-d9	250	10	50 mM NaPi pH7
130	p2202	2202-131	peptide 1	50	POPC/cholest-4-en-3-one(75/25)	4	5a-d9	250	30	50 mM NaPi pH7
131	p2202	2202-141	peptide 1	50	POPC/cholest-4-en-3-one(75/25)	4	5a-d9	250	60	50 mM NaPi pH7
132	p2202	2202-151	peptide 1	50	POPC/cholest-4-en-3-one(75/25)	4	5a-d9	250	120	50 mM NaPi pH7
133	p2202	2202-161	peptide 1	50	POPC/cholest-4-en-3-one(75/25)	4	5a-d9	250	300	50 mM NaPi pH7
134	p2202	2202-171	peptide 1	50	POPC/cholest-4-en-3-one(75/25)	4	5a-d9	250	600	50 mM NaPi pH7
135	p2202	2202-181	peptide 1	50	POPC/cholest-4-en-3-one(75/25)	4	5a-d9	250	900	50 mM NaPi pH7
136	p2202	2202-191	peptide 1	50	POPC/cholest-4-en-3-one(75/25)	4	5a-d9	250	2	50 mM NaPi pH7
137	p2202	2202-201	peptide 1	50	POPC/cholest-4-en-3-one(75/25)	4	5a-d9	250	5	50 mM NaPi pH7
138	p2202	2202-211	peptide 1	50	POPC/cholest-4-en-3-one(75/25)	4	5a-d9	250	10	50 mM NaPi pH7
139	p2202	2202-221	peptide 1	50	POPC/cholest-4-en-3-one(75/25)	4	5a-d9	250	30	50 mM NaPi pH7
140	p2202	2202-231	peptide 1	50	POPC/cholest-4-en-3-one(75/25)	4	5a-d9	250	60	50 mM NaPi pH7
141	p2202	2202-241	peptide 1	50	POPC/cholest-4-en-3-one(75/25)	4	5a-d9	250	120	50 mM NaPi pH7
142	p2202	2202-251	peptide 1	50	POPC/cholest-4-en-3-one(75/25)	4	5a-d9	250	300	50 mM NaPi pH7
143	p2202	2202-261	peptide 1	50	POPC/cholest-4-en-3-one(75/25)	4	5a-d9	250	600	50 mM NaPi pH7
144	p2202	2202-271	peptide 1	50	POPC/cholest-4-en-3-one(75/25)	4	5a-d9	250	900	50 mM NaPi pH7
145	p2586	2586-11	peptide 3	50	POPC/cholesterol(95/5)	4	5a-d9	250	2	50 mM NaPi pH7
146	p2586	2586-21	peptide 3	50	POPC/cholesterol(95/5)	4	5a-d9	250	5	50 mM NaPi pH7
147	p2586	2586-31	peptide 3	50	POPC/cholesterol(95/5)	4	5a-d9	250	10	50 mM NaPi pH7
148	p2586	2586-41	peptide 3	50	POPC/cholesterol(95/5)	4	5a-d9	250	30	50 mM NaPi pH7
149	p2586	2586-51	peptide 3	50	POPC/cholesterol(95/5)	4	5a-d9	250	60	50 mM NaPi pH7
150	p2586	2586-61	peptide 3	50	POPC/cholesterol(95/5)	4	5a-d9	250	120	50 mM NaPi pH7
151	p2586	2586-71	peptide 3	50	POPC/cholesterol(95/5)	4	5a-d9	250	300	50 mM NaPi pH7
152	p2586	2586-81	peptide 3	50	POPC/cholesterol(95/5)	4	5a-d9	250	600	50 mM NaPi pH7
153	p2586	2586-91	peptide 3	50	POPC/cholesterol(95/5)	4	5a-d9	250	900	50 mM NaPi pH7
154	p2586	2586-101	peptide 3	50	POPC/cholesterol(95/5)	4	5a-d9	250	2	50 mM NaPi pH7
155	p2586	2586-111	peptide 3	50	POPC/cholesterol(95/5)	4	5a-d9	250	5	50 mM NaPi pH7
156	p2586	2586-121	peptide 3	50	POPC/cholesterol(95/5)	4	5a-d9	250	10	50 mM NaPi pH7
157	p2586	2586-131	peptide 3	50	POPC/cholesterol(95/5)	4	5a-d9	250	30	50 mM NaPi pH7
158	p2586	2586-141	peptide 3	50	POPC/cholesterol(95/5)	4	5a-d9	250	60	50 mM NaPi pH7
159	p2586	2586-151	peptide 3	50	POPC/cholesterol(95/5)	4	5a-d9	250	120	50 mM NaPi pH7
160	p2586	2586-161	peptide 3	50	POPC/cholesterol(95/5)	4	5a-d9	250	300	50 mM NaPi pH7
161	p2586	2586-171	peptide 3	50	POPC/cholesterol(95/5)	4	5a-d9	250	600	50 mM NaPi pH7
162	p2586	2586-181	peptide 3	50	POPC/cholesterol(95/5)	4	5a-d9	250	900	50 mM NaPi pH7
163	p2586	2586-191	peptide 3	50	POPC/cholesterol(95/5)	4	5a-d9	250	2	50 mM NaPi pH7
164	p2586	2586-201	peptide 3	50	POPC/cholesterol(95/5)	4	5a-d9	250	5	50 mM NaPi pH7
165	p2586	2586-211	peptide 3	50	POPC/cholesterol(95/5)	4	5a-d9	250	10	50 mM NaPi pH7

166	p2586	2586-221	peptide 3	50	POPC/cholesterol(95/5)	4	5a-d9	250	30	50 mM NaPi pH7
167	p2586	2586-231	peptide 3	50	POPC/cholesterol(95/5)	4	5a-d9	250	60	50 mM NaPi pH7
168	p2586	2586-241	peptide 3	50	POPC/cholesterol(95/5)	4	5a-d9	250	120	50 mM NaPi pH7
169	p2586	2586-251	peptide 3	50	POPC/cholesterol(95/5)	4	5a-d9	250	300	50 mM NaPi pH7
170	p2586	2586-261	peptide 3	50	POPC/cholesterol(95/5)	4	5a-d9	250	600	50 mM NaPi pH7
171	p2586	2586-271	peptide 3	50	POPC/cholesterol(95/5)	4	5a-d9	250	900	50 mM NaPi pH7
172	p2598	2598-11	peptide 3	50	POPC/cholesterol(85/15)	4	5a-d9	250	2	50 mM NaPi pH7
173	p2598	2598-21	peptide 3	50	POPC/cholesterol(85/15)	4	5a-d9	250	5	50 mM NaPi pH7
174	p2598	2598-31	peptide 3	50	POPC/cholesterol(85/15)	4	5a-d9	250	10	50 mM NaPi pH7
175	p2598	2598-41	peptide 3	50	POPC/cholesterol(85/15)	4	5a-d9	250	30	50 mM NaPi pH7
176	p2598	2598-51	peptide 3	50	POPC/cholesterol(85/15)	4	5a-d9	250	60	50 mM NaPi pH7
177	p2598	2598-61	peptide 3	50	POPC/cholesterol(85/15)	4	5a-d9	250	120	50 mM NaPi pH7
178	p2598	2598-71	peptide 3	50	POPC/cholesterol(85/15)	4	5a-d9	250	300	50 mM NaPi pH7
179	p2598	2598-81	peptide 3	50	POPC/cholesterol(85/15)	4	5a-d9	250	600	50 mM NaPi pH7
180	p2598	2598-91	peptide 3	50	POPC/cholesterol(85/15)	4	5a-d9	250	900	50 mM NaPi pH7
181	p2598	2598-101	peptide 3	50	POPC/cholesterol(85/15)	4	5a-d9	250	2	50 mM NaPi pH7
182	p2598	2598-111	peptide 3	50	POPC/cholesterol(85/15)	4	5a-d9	250	5	50 mM NaPi pH7
183	p2598	2598-121	peptide 3	50	POPC/cholesterol(85/15)	4	5a-d9	250	10	50 mM NaPi pH7
184	p2598	2598-131	peptide 3	50	POPC/cholesterol(85/15)	4	5a-d9	250	30	50 mM NaPi pH7
185	p2598	2598-141	peptide 3	50	POPC/cholesterol(85/15)	4	5a-d9	250	60	50 mM NaPi pH7
186	p2598	2598-151	peptide 3	50	POPC/cholesterol(85/15)	4	5a-d9	250	120	50 mM NaPi pH7
187	p2598	2598-161	peptide 3	50	POPC/cholesterol(85/15)	4	5a-d9	250	300	50 mM NaPi pH7
188	p2598	2598-171	peptide 3	50	POPC/cholesterol(85/15)	4	5a-d9	250	600	50 mM NaPi pH7
189	p2598	2598-181	peptide 3	50	POPC/cholesterol(85/15)	4	5a-d9	250	900	50 mM NaPi pH7
190	p2598	2598-191	peptide 3	50	POPC/cholesterol(85/15)	4	5a-d9	250	2	50 mM NaPi pH7
191	p2598	2598-201	peptide 3	50	POPC/cholesterol(85/15)	4	5a-d9	250	5	50 mM NaPi pH7
192	p2598	2598-211	peptide 3	50	POPC/cholesterol(85/15)	4	5a-d9	250	10	50 mM NaPi pH7
193	p2598	2598-221	peptide 3	50	POPC/cholesterol(85/15)	4	5a-d9	250	30	50 mM NaPi pH7
194	p2598	2598-231	peptide 3	50	POPC/cholesterol(85/15)	4	5a-d9	250	60	50 mM NaPi pH7
195	p2598	2598-241	peptide 3	50	POPC/cholesterol(85/15)	4	5a-d9	250	120	50 mM NaPi pH7
196	p2598	2598-251	peptide 3	50	POPC/cholesterol(85/15)	4	5a-d9	250	300	50 mM NaPi pH7
197	p2598	2598-261	peptide 3	50	POPC/cholesterol(85/15)	4	5a-d9	250	600	50 mM NaPi pH7
198	p2598	2598-271	peptide 3	50	POPC/cholesterol(85/15)	4	5a-d9	250	900	50 mM NaPi pH7
199	p2800	2800-11	peptide 3	50	POPC/cholesterol(55/45)	4	5a-d9	250	2	50 mM NaPi pH7
200	p2800	2800-21	peptide 3	50	POPC/cholesterol(55/45)	4	5a-d9	250	5	50 mM NaPi pH7
201	p2800	2800-31	peptide 3	50	POPC/cholesterol(55/45)	4	5a-d9	250	10	50 mM NaPi pH7
202	p2800	2800-41	peptide 3	50	POPC/cholesterol(55/45)	4	5a-d9	250	30	50 mM NaPi pH7
203	p2800	2800-51	peptide 3	50	POPC/cholesterol(55/45)	4	5a-d9	250	60	50 mM NaPi pH7
204	p2800	2800-61	peptide 3	50	POPC/cholesterol(55/45)	4	5a-d9	250	120	50 mM NaPi pH7
205	p2800	2800-71	peptide 3	50	POPC/cholesterol(55/45)	4	5a-d9	250	300	50 mM NaPi pH7
206	p2800	2800-81	peptide 3	50	POPC/cholesterol(55/45)	4	5a-d9	250	600	50 mM NaPi pH7
207	p2800	2800-91	peptide 3	50	POPC/cholesterol(55/45)	4	5a-d9	250	900	50 mM NaPi pH7
208	p2800	2800-101	peptide 3	50	POPC/cholesterol(55/45)	4	5a-d9	250	2	50 mM NaPi pH7
209	p2800	2800-111	peptide 3	50	POPC/cholesterol(55/45)	4	5a-d9	250	5	50 mM NaPi pH7
210	p2800	2800-121	peptide 3	50	POPC/cholesterol(55/45)	4	5a-d9	250	10	50 mM NaPi pH7
211	p2800	2800-131	peptide 3	50	POPC/cholesterol(55/45)	4	5a-d9	250	30	50 mM NaPi pH7
212	p2800	2800-141	peptide 3	50	POPC/cholesterol(55/45)	4	5a-d9	250	60	50 mM NaPi pH7
213	p2800	2800-151	peptide 3	50	POPC/cholesterol(55/45)	4	5a-d9	250	120	50 mM NaPi pH7
214	p2800	2800-161	peptide 3	50	POPC/cholesterol(55/45)	4	5a-d9	250	300	50 mM NaPi pH7
215	p2800	2800-171	peptide 3	50	POPC/cholesterol(55/45)	4	5a-d9	250	600	50 mM NaPi pH7
216	p2800	2800-181	peptide 3	50	POPC/cholesterol(55/45)	4	5a-d9	250	900	50 mM NaPi pH7
217	p2800	2800-191	peptide 3	50	POPC/cholesterol(55/45)	4	5a-d9	250	2	50 mM NaPi pH7
218	p2800	2800-201	peptide 3	50	POPC/cholesterol(55/45)	4	5a-d9	250	5	50 mM NaPi pH7
219	p2800	2800-211	peptide 3	50	POPC/cholesterol(55/45)	4	5a-d9	250	10	50 mM NaPi pH7
220	p2800	2800-221	peptide 3	50	POPC/cholesterol(55/45)	4	5a-d9	250	30	50 mM NaPi pH7
221	p2800	2800-231	peptide 3	50	POPC/cholesterol(55/45)	4	5a-d9	250	60	50 mM NaPi pH7
222	p2800	2800-241	peptide 3	50	POPC/cholesterol(55/45)	4	5a-d9	250	120	50 mM NaPi pH7
223	p2800	2800-251	peptide 3	50	POPC/cholesterol(55/45)	4	5a-d9	250	300	50 mM NaPi pH7

224	p2800	2800-261	peptide 3	50	POPC/cholesterol(55/45)	4	5a-d9	250	600	50 mM NaPi pH7
225	p2800	2800-271	peptide 3	50	POPC/cholesterol(55/45)	4	5a-d9	250	900	50 mM NaPi pH7
226	p2608	2608-11	peptide 3	50	POPC/cholest-4-en-3-one(95/5)	4	5a-d9	250	2	50 mM NaPi pH7
227	p2608	2608-21	peptide 3	50	POPC/cholest-4-en-3-one(95/5)	4	5a-d9	250	5	50 mM NaPi pH7
228	p2608	2608-31	peptide 3	50	POPC/cholest-4-en-3-one(95/5)	4	5a-d9	250	10	50 mM NaPi pH7
229	p2608	2608-41	peptide 3	50	POPC/cholest-4-en-3-one(95/5)	4	5a-d9	250	30	50 mM NaPi pH7
230	p2608	2608-51	peptide 3	50	POPC/cholest-4-en-3-one(95/5)	4	5a-d9	250	60	50 mM NaPi pH7
231	p2608	2608-61	peptide 3	50	POPC/cholest-4-en-3-one(95/5)	4	5a-d9	250	120	50 mM NaPi pH7
232	p2608	2608-71	peptide 3	50	POPC/cholest-4-en-3-one(95/5)	4	5a-d9	250	300	50 mM NaPi pH7
233	p2608	2608-81	peptide 3	50	POPC/cholest-4-en-3-one(95/5)	4	5a-d9	250	600	50 mM NaPi pH7
234	p2608	2608-91	peptide 3	50	POPC/cholest-4-en-3-one(95/5)	4	5a-d9	250	900	50 mM NaPi pH7
235	p2608	2608-101	peptide 3	50	POPC/cholest-4-en-3-one(95/5)	4	5a-d9	250	2	50 mM NaPi pH7
236	p2608	2608-111	peptide 3	50	POPC/cholest-4-en-3-one(95/5)	4	5a-d9	250	5	50 mM NaPi pH7
237	p2608	2608-121	peptide 3	50	POPC/cholest-4-en-3-one(95/5)	4	5a-d9	250	10	50 mM NaPi pH7
238	p2608	2608-131	peptide 3	50	POPC/cholest-4-en-3-one(95/5)	4	5a-d9	250	30	50 mM NaPi pH7
239	p2608	2608-141	peptide 3	50	POPC/cholest-4-en-3-one(95/5)	4	5a-d9	250	60	50 mM NaPi pH7
240	p2608	2608-151	peptide 3	50	POPC/cholest-4-en-3-one(95/5)	4	5a-d9	250	120	50 mM NaPi pH7
241	p2608	2608-161	peptide 3	50	POPC/cholest-4-en-3-one(95/5)	4	5a-d9	250	300	50 mM NaPi pH7
242	p2608	2608-171	peptide 3	50	POPC/cholest-4-en-3-one(95/5)	4	5a-d9	250	600	50 mM NaPi pH7
243	p2608	2608-181	peptide 3	50	POPC/cholest-4-en-3-one(95/5)	4	5a-d9	250	900	50 mM NaPi pH7
244	p2608	2608-191	peptide 3	50	POPC/cholest-4-en-3-one(95/5)	4	5a-d9	250	2	50 mM NaPi pH7
245	p2608	2608-201	peptide 3	50	POPC/cholest-4-en-3-one(95/5)	4	5a-d9	250	5	50 mM NaPi pH7
246	p2608	2608-211	peptide 3	50	POPC/cholest-4-en-3-one(95/5)	4	5a-d9	250	10	50 mM NaPi pH7
247	p2608	2608-221	peptide 3	50	POPC/cholest-4-en-3-one(95/5)	4	5a-d9	250	30	50 mM NaPi pH7
248	p2608	2608-231	peptide 3	50	POPC/cholest-4-en-3-one(95/5)	4	5a-d9	250	60	50 mM NaPi pH7
249	p2608	2608-241	peptide 3	50	POPC/cholest-4-en-3-one(95/5)	4	5a-d9	250	120	50 mM NaPi pH7
250	p2608	2608-251	peptide 3	50	POPC/cholest-4-en-3-one(95/5)	4	5a-d9	250	300	50 mM NaPi pH7
251	p2608	2608-261	peptide 3	50	POPC/cholest-4-en-3-one(95/5)	4	5a-d9	250	600	50 mM NaPi pH7
252	p2608	2608-271	peptide 3	50	POPC/cholest-4-en-3-one(95/5)	4	5a-d9	250	900	50 mM NaPi pH7
253	p2612	2612-11	peptide 3	50	POPC/cholest-4-en-3-one(85/15)	4	5a-d9	250	2	50 mM NaPi pH7
254	p2612	2612-21	peptide 3	50	POPC/cholest-4-en-3-one(85/15)	4	5a-d9	250	5	50 mM NaPi pH7
255	p2612	2612-31	peptide 3	50	POPC/cholest-4-en-3-one(85/15)	4	5a-d9	250	10	50 mM NaPi pH7
256	p2612	2612-41	peptide 3	50	POPC/cholest-4-en-3-one(85/15)	4	5a-d9	250	30	50 mM NaPi pH7
257	p2612	2612-51	peptide 3	50	POPC/cholest-4-en-3-one(85/15)	4	5a-d9	250	60	50 mM NaPi pH7
258	p2612	2612-61	peptide 3	50	POPC/cholest-4-en-3-one(85/15)	4	5a-d9	250	120	50 mM NaPi pH7
259	p2612	2612-71	peptide 3	50	POPC/cholest-4-en-3-one(85/15)	4	5a-d9	250	300	50 mM NaPi pH7
260	p2612	2612-81	peptide 3	50	POPC/cholest-4-en-3-one(85/15)	4	5a-d9	250	600	50 mM NaPi pH7
261	p2612	2612-91	peptide 3	50	POPC/cholest-4-en-3-one(85/15)	4	5a-d9	250	900	50 mM NaPi pH7
262	p2612	2612-101	peptide 3	50	POPC/cholest-4-en-3-one(85/15)	4	5a-d9	250	2	50 mM NaPi pH7
263	p2612	2612-111	peptide 3	50	POPC/cholest-4-en-3-one(85/15)	4	5a-d9	250	5	50 mM NaPi pH7
264	p2612	2612-121	peptide 3	50	POPC/cholest-4-en-3-one(85/15)	4	5a-d9	250	10	50 mM NaPi pH7
265	p2612	2612-131	peptide 3	50	POPC/cholest-4-en-3-one(85/15)	4	5a-d9	250	30	50 mM NaPi pH7
266	p2612	2612-141	peptide 3	50	POPC/cholest-4-en-3-one(85/15)	4	5a-d9	250	60	50 mM NaPi pH7
267	p2612	2612-151	peptide 3	50	POPC/cholest-4-en-3-one(85/15)	4	5a-d9	250	120	50 mM NaPi pH7
268	p2612	2612-161	peptide 3	50	POPC/cholest-4-en-3-one(85/15)	4	5a-d9	250	300	50 mM NaPi pH7
269	p2612	2612-171	peptide 3	50	POPC/cholest-4-en-3-one(85/15)	4	5a-d9	250	600	50 mM NaPi pH7
270	p2612	2612-181	peptide 3	50	POPC/cholest-4-en-3-one(85/15)	4	5a-d9	250	900	50 mM NaPi pH7
271	p2612	2612-191	peptide 3	50	POPC/cholest-4-en-3-one(85/15)	4	5a-d9	250	2	50 mM NaPi pH7
272	p2612	2612-201	peptide 3	50	POPC/cholest-4-en-3-one(85/15)	4	5a-d9	250	5	50 mM NaPi pH7
273	p2612	2612-211	peptide 3	50	POPC/cholest-4-en-3-one(85/15)	4	5a-d9	250	10	50 mM NaPi pH7
274	p2612	2612-221	peptide 3	50	POPC/cholest-4-en-3-one(85/15)	4	5a-d9	250	30	50 mM NaPi pH7
275	p2612	2612-231	peptide 3	50	POPC/cholest-4-en-3-one(85/15)	4	5a-d9	250	60	50 mM NaPi pH7
276	p2612	2612-241	peptide 3	50	POPC/cholest-4-en-3-one(85/15)	4	5a-d9	250	120	50 mM NaPi pH7
277	p2612	2612-251	peptide 3	50	POPC/cholest-4-en-3-one(85/15)	4	5a-d9	250	300	50 mM NaPi pH7
278	p2612	2612-261	peptide 3	50	POPC/cholest-4-en-3-one(85/15)	4	5a-d9	250	600	50 mM NaPi pH7
279	p2612	2612-271	peptide 3	50	POPC/cholest-4-en-3-one(85/15)	4	5a-d9	250	900	50 mM NaPi pH7
280	p2675	2675-11	peptide 3	50	POPC/cholest-4-en-3-one(55/45)	4	5a-d9	250	2	50 mM NaPi pH7
281	p2675	2675-21	peptide 3	50	POPC/cholest-4-en-3-one(55/45)	4	5a-d9	250	5	50 mM NaPi pH7

282	p2675	2675-31	peptide 3	50	POPC/cholest-4-en-3-one(55/45)	4	5a-d9	250	10	50 mM NaPi pH7
283	p2675	2675-41	peptide 3	50	POPC/cholest-4-en-3-one(55/45)	4	5a-d9	250	30	50 mM NaPi pH7
284	p2675	2675-51	peptide 3	50	POPC/cholest-4-en-3-one(55/45)	4	5a-d9	250	60	50 mM NaPi pH7
285	p2675	2675-61	peptide 3	50	POPC/cholest-4-en-3-one(55/45)	4	5a-d9	250	120	50 mM NaPi pH7
286	p2675	2675-71	peptide 3	50	POPC/cholest-4-en-3-one(55/45)	4	5a-d9	250	300	50 mM NaPi pH7
287	p2675	2675-81	peptide 3	50	POPC/cholest-4-en-3-one(55/45)	4	5a-d9	250	600	50 mM NaPi pH7
288	p2675	2675-91	peptide 3	50	POPC/cholest-4-en-3-one(55/45)	4	5a-d9	250	900	50 mM NaPi pH7
289	p2675	2675-101	peptide 3	50	POPC/cholest-4-en-3-one(55/45)	4	5a-d9	250	2	50 mM NaPi pH7
290	p2675	2675-111	peptide 3	50	POPC/cholest-4-en-3-one(55/45)	4	5a-d9	250	5	50 mM NaPi pH7
291	p2675	2675-121	peptide 3	50	POPC/cholest-4-en-3-one(55/45)	4	5a-d9	250	10	50 mM NaPi pH7
292	p2675	2675-131	peptide 3	50	POPC/cholest-4-en-3-one(55/45)	4	5a-d9	250	30	50 mM NaPi pH7
293	p2675	2675-141	peptide 3	50	POPC/cholest-4-en-3-one(55/45)	4	5a-d9	250	60	50 mM NaPi pH7
294	p2675	2675-151	peptide 3	50	POPC/cholest-4-en-3-one(55/45)	4	5a-d9	250	120	50 mM NaPi pH7
295	p2675	2675-161	peptide 3	50	POPC/cholest-4-en-3-one(55/45)	4	5a-d9	250	300	50 mM NaPi pH7
296	p2675	2675-171	peptide 3	50	POPC/cholest-4-en-3-one(55/45)	4	5a-d9	250	600	50 mM NaPi pH7
297	p2675	2675-181	peptide 3	50	POPC/cholest-4-en-3-one(55/45)	4	5a-d9	250	900	50 mM NaPi pH7
298	p2675	2675-191	peptide 3	50	POPC/cholest-4-en-3-one(55/45)	4	5a-d9	250	2	50 mM NaPi pH7
299	p2675	2675-201	peptide 3	50	POPC/cholest-4-en-3-one(55/45)	4	5a-d9	250	5	50 mM NaPi pH7
300	p2675	2675-211	peptide 3	50	POPC/cholest-4-en-3-one(55/45)	4	5a-d9	250	10	50 mM NaPi pH7
301	p2675	2675-221	peptide 3	50	POPC/cholest-4-en-3-one(55/45)	4	5a-d9	250	30	50 mM NaPi pH7
302	p2675	2675-231	peptide 3	50	POPC/cholest-4-en-3-one(55/45)	4	5a-d9	250	60	50 mM NaPi pH7
303	p2675	2675-241	peptide 3	50	POPC/cholest-4-en-3-one(55/45)	4	5a-d9	250	120	50 mM NaPi pH7
304	p2675	2675-251	peptide 3	50	POPC/cholest-4-en-3-one(55/45)	4	5a-d9	250	300	50 mM NaPi pH7
305	p2675	2675-261	peptide 3	50	POPC/cholest-4-en-3-one(55/45)	4	5a-d9	250	600	50 mM NaPi pH7
306	p2675	2675-271	peptide 3	50	POPC/cholest-4-en-3-one(55/45)	4	5a-d9	250	900	50 mM NaPi pH7
307	p2900	2900-11	peptide 3	50	DOPC	4	5a-d9	250	2	50 mM NaPi pH7
308	p2900	2900-21	peptide 3	50	DOPC	4	5a-d9	250	5	50 mM NaPi pH7
309	p2900	2900-31	peptide 3	50	DOPC	4	5a-d9	250	10	50 mM NaPi pH7
310	p2900	2900-41	peptide 3	50	DOPC	4	5a-d9	250	30	50 mM NaPi pH7
311	p2900	2900-51	peptide 3	50	DOPC	4	5a-d9	250	60	50 mM NaPi pH7
312	p2900	2900-61	peptide 3	50	DOPC	4	5a-d9	250	120	50 mM NaPi pH7
313	p2900	2900-71	peptide 3	50	DOPC	4	5a-d9	250	300	50 mM NaPi pH7
314	p2900	2900-81	peptide 3	50	DOPC	4	5a-d9	250	600	50 mM NaPi pH7
315	p2900	2900-91	peptide 3	50	DOPC	4	5a-d9	250	900	50 mM NaPi pH7
316	p2900	2900-101	peptide 3	50	DOPC	4	5a-d9	250	2	50 mM NaPi pH7
317	p2900	2900-111	peptide 3	50	DOPC	4	5a-d9	250	5	50 mM NaPi pH7
318	p2900	2900-121	peptide 3	50	DOPC	4	5a-d9	250	10	50 mM NaPi pH7
319	p2900	2900-131	peptide 3	50	DOPC	4	5a-d9	250	30	50 mM NaPi pH7
320	p2900	2900-141	peptide 3	50	DOPC	4	5a-d9	250	60	50 mM NaPi pH7
321	p2900	2900-151	peptide 3	50	DOPC	4	5a-d9	250	120	50 mM NaPi pH7
322	p2900	2900-161	peptide 3	50	DOPC	4	5a-d9	250	300	50 mM NaPi pH7
323	p2900	2900-171	peptide 3	50	DOPC	4	5a-d9	250	600	50 mM NaPi pH7
324	p2900	2900-181	peptide 3	50	DOPC	4	5a-d9	250	900	50 mM NaPi pH7
325	p2900	2900-191	peptide 3	50	DOPC	4	5a-d9	250	2	50 mM NaPi pH7
326	p2900	2900-201	peptide 3	50	DOPC	4	5a-d9	250	5	50 mM NaPi pH7
327	p2900	2900-211	peptide 3	50	DOPC	4	5a-d9	250	10	50 mM NaPi pH7
328	p2900	2900-221	peptide 3	50	DOPC	4	5a-d9	250	30	50 mM NaPi pH7
329	p2900	2900-231	peptide 3	50	DOPC	4	5a-d9	250	60	50 mM NaPi pH7
330	p2900	2900-241	peptide 3	50	DOPC	4	5a-d9	250	120	50 mM NaPi pH7
331	p2900	2900-251	peptide 3	50	DOPC	4	5a-d9	250	300	50 mM NaPi pH7
332	p2900	2900-261	peptide 3	50	DOPC	4	5a-d9	250	600	50 mM NaPi pH7
333	p2900	2900-271	peptide 3	50	DOPC	4	5a-d9	250	900	50 mM NaPi pH7
334	p2902	2902-11	peptide 3	50	DOPC/cholesterol(75/25)	4	5a-d9	250	2	50 mM NaPi pH7
335	p2902	2902-21	peptide 3	50	DOPC/cholesterol(75/25)	4	5a-d9	250	5	50 mM NaPi pH7
336	p2902	2902-31	peptide 3	50	DOPC/cholesterol(75/25)	4	5a-d9	250	10	50 mM NaPi pH7
337	p2902	2902-41	peptide 3	50	DOPC/cholesterol(75/25)	4	5a-d9	250	30	50 mM NaPi pH7
338	p2902	2902-51	peptide 3	50	DOPC/cholesterol(75/25)	4	5a-d9	250	60	50 mM NaPi pH7
339	p2902	2902-61	peptide 3	50	DOPC/cholesterol(75/25)	4	5a-d9	250	120	50 mM NaPi pH7

340	p2902	2902-71	peptide 3	50	DOPC/cholesterol(75/25)	4	5a-d9	250	300	50 mM NaPi pH7
341	p2902	2902-81	peptide 3	50	DOPC/cholesterol(75/25)	4	5a-d9	250	600	50 mM NaPi pH7
342	p2902	2902-91	peptide 3	50	DOPC/cholesterol(75/25)	4	5a-d9	250	900	50 mM NaPi pH7
343	p2902	2902-101	peptide 3	50	DOPC/cholesterol(75/25)	4	5a-d9	250	2	50 mM NaPi pH7
344	p2902	2902-111	peptide 3	50	DOPC/cholesterol(75/25)	4	5a-d9	250	5	50 mM NaPi pH7
345	p2902	2902-121	peptide 3	50	DOPC/cholesterol(75/25)	4	5a-d9	250	10	50 mM NaPi pH7
346	p2902	2902-131	peptide 3	50	DOPC/cholesterol(75/25)	4	5a-d9	250	30	50 mM NaPi pH7
347	p2902	2902-141	peptide 3	50	DOPC/cholesterol(75/25)	4	5a-d9	250	60	50 mM NaPi pH7
348	p2902	2902-151	peptide 3	50	DOPC/cholesterol(75/25)	4	5a-d9	250	120	50 mM NaPi pH7
349	p2902	2902-161	peptide 3	50	DOPC/cholesterol(75/25)	4	5a-d9	250	300	50 mM NaPi pH7
350	p2902	2902-171	peptide 3	50	DOPC/cholesterol(75/25)	4	5a-d9	250	600	50 mM NaPi pH7
351	p2902	2902-181	peptide 3	50	DOPC/cholesterol(75/25)	4	5a-d9	250	900	50 mM NaPi pH7
352	p2902	2902-191	peptide 3	50	DOPC/cholesterol(75/25)	4	5a-d9	250	2	50 mM NaPi pH7
353	p2902	2902-201	peptide 3	50	DOPC/cholesterol(75/25)	4	5a-d9	250	5	50 mM NaPi pH7
354	p2902	2902-211	peptide 3	50	DOPC/cholesterol(75/25)	4	5a-d9	250	10	50 mM NaPi pH7
355	p2902	2902-221	peptide 3	50	DOPC/cholesterol(75/25)	4	5a-d9	250	30	50 mM NaPi pH7
356	p2902	2902-231	peptide 3	50	DOPC/cholesterol(75/25)	4	5a-d9	250	60	50 mM NaPi pH7
357	p2902	2902-241	peptide 3	50	DOPC/cholesterol(75/25)	4	5a-d9	250	120	50 mM NaPi pH7
358	p2902	2902-251	peptide 3	50	DOPC/cholesterol(75/25)	4	5a-d9	250	300	50 mM NaPi pH7
359	p2902	2902-261	peptide 3	50	DOPC/cholesterol(75/25)	4	5a-d9	250	600	50 mM NaPi pH7
360	p2902	2902-271	peptide 3	50	DOPC/cholesterol(75/25)	4	5a-d9	250	900	50 mM NaPi pH7
361	p2421	2421-11	peptide 3	50	DPPC	4	5a-d9	455	2	50 mM NaPi pH7
362	p2421	2421-21	peptide 3	50	DPPC	4	5a-d9	455	5	50 mM NaPi pH7
363	p2421	2421-31	peptide 3	50	DPPC	4	5a-d9	455	10	50 mM NaPi pH7
364	p2421	2421-41	peptide 3	50	DPPC	4	5a-d9	455	30	50 mM NaPi pH7
365	p2421	2421-51	peptide 3	50	DPPC	4	5a-d9	455	60	50 mM NaPi pH7
366	p2421	2421-61	peptide 3	50	DPPC	4	5a-d9	455	120	50 mM NaPi pH7
367	p2421	2421-71	peptide 3	50	DPPC	4	5a-d9	455	300	50 mM NaPi pH7
368	p2421	2421-81	peptide 3	50	DPPC	4	5a-d9	455	600	50 mM NaPi pH7
369	p2421	2421-91	peptide 3	50	DPPC	4	5a-d9	455	900	50 mM NaPi pH7
370	p2421	2421-101	peptide 3	50	DPPC	4	5a-d9	455	2	50 mM NaPi pH7
371	p2421	2421-111	peptide 3	50	DPPC	4	5a-d9	455	5	50 mM NaPi pH7
372	p2421	2421-121	peptide 3	50	DPPC	4	5a-d9	455	10	50 mM NaPi pH7
373	p2421	2421-131	peptide 3	50	DPPC	4	5a-d9	455	30	50 mM NaPi pH7
374	p2421	2421-141	peptide 3	50	DPPC	4	5a-d9	455	60	50 mM NaPi pH7
375	p2421	2421-151	peptide 3	50	DPPC	4	5a-d9	455	120	50 mM NaPi pH7
376	p2421	2421-161	peptide 3	50	DPPC	4	5a-d9	455	300	50 mM NaPi pH7
377	p2421	2421-171	peptide 3	50	DPPC	4	5a-d9	455	600	50 mM NaPi pH7
378	p2421	2421-181	peptide 3	50	DPPC	4	5a-d9	455	900	50 mM NaPi pH7
379	p2421	2421-191	peptide 3	50	DPPC	4	5a-d9	455	2	50 mM NaPi pH7
380	p2421	2421-201	peptide 3	50	DPPC	4	5a-d9	455	5	50 mM NaPi pH7
381	p2421	2421-211	peptide 3	50	DPPC	4	5a-d9	455	10	50 mM NaPi pH7
382	p2421	2421-221	peptide 3	50	DPPC	4	5a-d9	455	30	50 mM NaPi pH7
383	p2421	2421-231	peptide 3	50	DPPC	4	5a-d9	455	60	50 mM NaPi pH7
384	p2421	2421-241	peptide 3	50	DPPC	4	5a-d9	455	120	50 mM NaPi pH7
385	p2421	2421-251	peptide 3	50	DPPC	4	5a-d9	455	300	50 mM NaPi pH7
386	p2421	2421-261	peptide 3	50	DPPC	4	5a-d9	455	600	50 mM NaPi pH7
387	p2421	2421-271	peptide 3	50	DPPC	4	5a-d9	455	900	50 mM NaPi pH7
388	p2660	2660-11	peptide 3	50	DPPC/cholesterol(80/20)	4	5a-d9	250	2	50 mM NaPi pH7
389	p2660	2660-21	peptide 3	50	DPPC/cholesterol(80/20)	4	5a-d9	250	5	50 mM NaPi pH7
390	p2660	2660-31	peptide 3	50	DPPC/cholesterol(80/20)	4	5a-d9	250	10	50 mM NaPi pH7
391	p2660	2660-41	peptide 3	50	DPPC/cholesterol(80/20)	4	5a-d9	250	30	50 mM NaPi pH7
392	p2660	2660-51	peptide 3	50	DPPC/cholesterol(80/20)	4	5a-d9	250	60	50 mM NaPi pH7
393	p2660	2660-61	peptide 3	50	DPPC/cholesterol(80/20)	4	5a-d9	250	120	50 mM NaPi pH7
394	p2660	2660-71	peptide 3	50	DPPC/cholesterol(80/20)	4	5a-d9	250	300	50 mM NaPi pH7
395	p2660	2660-81	peptide 3	50	DPPC/cholesterol(80/20)	4	5a-d9	250	600	50 mM NaPi pH7
396	p2660	2660-91	peptide 3	50	DPPC/cholesterol(80/20)	4	5a-d9	250	900	50 mM NaPi pH7
397	p2660	2660-101	peptide 3	50	DPPC/cholesterol(80/20)	4	5a-d9	250	2	50 mM NaPi pH7

398	p2660	2660-111	peptide 3	50	DPPC/cholesterol(80/20)	4	5a-d9	250	5	50 mM NaPi pH7
399	p2660	2660-121	peptide 3	50	DPPC/cholesterol(80/20)	4	5a-d9	250	10	50 mM NaPi pH7
400	p2660	2660-131	peptide 3	50	DPPC/cholesterol(80/20)	4	5a-d9	250	30	50 mM NaPi pH7
401	p2660	2660-141	peptide 3	50	DPPC/cholesterol(80/20)	4	5a-d9	250	60	50 mM NaPi pH7
402	p2660	2660-151	peptide 3	50	DPPC/cholesterol(80/20)	4	5a-d9	250	120	50 mM NaPi pH7
403	p2660	2660-161	peptide 3	50	DPPC/cholesterol(80/20)	4	5a-d9	250	300	50 mM NaPi pH7
404	p2660	2660-171	peptide 3	50	DPPC/cholesterol(80/20)	4	5a-d9	250	600	50 mM NaPi pH7
405	p2660	2660-181	peptide 3	50	DPPC/cholesterol(80/20)	4	5a-d9	250	900	50 mM NaPi pH7
406	p2660	2660-191	peptide 3	50	DPPC/cholesterol(80/20)	4	5a-d9	250	2	50 mM NaPi pH7
407	p2660	2660-201	peptide 3	50	DPPC/cholesterol(80/20)	4	5a-d9	250	5	50 mM NaPi pH7
408	p2660	2660-211	peptide 3	50	DPPC/cholesterol(80/20)	4	5a-d9	250	10	50 mM NaPi pH7
409	p2660	2660-221	peptide 3	50	DPPC/cholesterol(80/20)	4	5a-d9	250	30	50 mM NaPi pH7
410	p2660	2660-231	peptide 3	50	DPPC/cholesterol(80/20)	4	5a-d9	250	60	50 mM NaPi pH7
411	p2660	2660-241	peptide 3	50	DPPC/cholesterol(80/20)	4	5a-d9	250	120	50 mM NaPi pH7
412	p2660	2660-251	peptide 3	50	DPPC/cholesterol(80/20)	4	5a-d9	250	300	50 mM NaPi pH7
413	p2660	2660-261	peptide 3	50	DPPC/cholesterol(80/20)	4	5a-d9	250	600	50 mM NaPi pH7
414	p2660	2660-271	peptide 3	50	DPPC/cholesterol(80/20)	4	5a-d9	250	900	50 mM NaPi pH7
415	p2669	2669-11	peptide 3	50	DPPC/cholesterol(60/40)	4	5a-d9	250	2	50 mM NaPi pH7
416	p2669	2669-21	peptide 3	50	DPPC/cholesterol(60/40)	4	5a-d9	250	5	50 mM NaPi pH7
417	p2669	2669-31	peptide 3	50	DPPC/cholesterol(60/40)	4	5a-d9	250	10	50 mM NaPi pH7
418	p2669	2669-41	peptide 3	50	DPPC/cholesterol(60/40)	4	5a-d9	250	30	50 mM NaPi pH7
419	p2669	2669-51	peptide 3	50	DPPC/cholesterol(60/40)	4	5a-d9	250	60	50 mM NaPi pH7
420	p2669	2669-61	peptide 3	50	DPPC/cholesterol(60/40)	4	5a-d9	250	120	50 mM NaPi pH7
421	p2669	2669-71	peptide 3	50	DPPC/cholesterol(60/40)	4	5a-d9	250	300	50 mM NaPi pH7
422	p2669	2669-81	peptide 3	50	DPPC/cholesterol(60/40)	4	5a-d9	250	600	50 mM NaPi pH7
423	p2669	2669-91	peptide 3	50	DPPC/cholesterol(60/40)	4	5a-d9	250	900	50 mM NaPi pH7
424	p2669	2669-101	peptide 3	50	DPPC/cholesterol(60/40)	4	5a-d9	250	2	50 mM NaPi pH7
425	p2669	2669-111	peptide 3	50	DPPC/cholesterol(60/40)	4	5a-d9	250	5	50 mM NaPi pH7
426	p2669	2669-121	peptide 3	50	DPPC/cholesterol(60/40)	4	5a-d9	250	10	50 mM NaPi pH7
427	p2669	2669-131	peptide 3	50	DPPC/cholesterol(60/40)	4	5a-d9	250	30	50 mM NaPi pH7
428	p2669	2669-141	peptide 3	50	DPPC/cholesterol(60/40)	4	5a-d9	250	60	50 mM NaPi pH7
429	p2669	2669-151	peptide 3	50	DPPC/cholesterol(60/40)	4	5a-d9	250	120	50 mM NaPi pH7
430	p2669	2669-161	peptide 3	50	DPPC/cholesterol(60/40)	4	5a-d9	250	300	50 mM NaPi pH7
431	p2669	2669-171	peptide 3	50	DPPC/cholesterol(60/40)	4	5a-d9	250	600	50 mM NaPi pH7
432	p2669	2669-181	peptide 3	50	DPPC/cholesterol(60/40)	4	5a-d9	250	900	50 mM NaPi pH7
433	p2669	2669-191	peptide 3	50	DPPC/cholesterol(60/40)	4	5a-d9	250	2	50 mM NaPi pH7
434	p2669	2669-201	peptide 3	50	DPPC/cholesterol(60/40)	4	5a-d9	250	5	50 mM NaPi pH7
435	p2669	2669-211	peptide 3	50	DPPC/cholesterol(60/40)	4	5a-d9	250	10	50 mM NaPi pH7
436	p2669	2669-221	peptide 3	50	DPPC/cholesterol(60/40)	4	5a-d9	250	30	50 mM NaPi pH7
437	p2669	2669-231	peptide 3	50	DPPC/cholesterol(60/40)	4	5a-d9	250	60	50 mM NaPi pH7
438	p2669	2669-241	peptide 3	50	DPPC/cholesterol(60/40)	4	5a-d9	250	120	50 mM NaPi pH7
439	p2669	2669-251	peptide 3	50	DPPC/cholesterol(60/40)	4	5a-d9	250	300	50 mM NaPi pH7
440	p2669	2669-261	peptide 3	50	DPPC/cholesterol(60/40)	4	5a-d9	250	600	50 mM NaPi pH7
441	p2669	2669-271	peptide 3	50	DPPC/cholesterol(60/40)	4	5a-d9	250	900	50 mM NaPi pH7
442	p2807	2807-11	peptide 3	50	DPPC/cholest-4-en-3-one(80/20)	4	5a-d9	250	2	50 mM NaPi pH7
443	p2807	2807-21	peptide 3	50	DPPC/cholest-4-en-3-one(80/20)	4	5a-d9	250	5	50 mM NaPi pH7
444	p2807	2807-31	peptide 3	50	DPPC/cholest-4-en-3-one(80/20)	4	5a-d9	250	10	50 mM NaPi pH7
445	p2807	2807-41	peptide 3	50	DPPC/cholest-4-en-3-one(80/20)	4	5a-d9	250	30	50 mM NaPi pH7
446	p2807	2807-51	peptide 3	50	DPPC/cholest-4-en-3-one(80/20)	4	5a-d9	250	60	50 mM NaPi pH7
447	p2807	2807-61	peptide 3	50	DPPC/cholest-4-en-3-one(80/20)	4	5a-d9	250	120	50 mM NaPi pH7
448	p2807	2807-71	peptide 3	50	DPPC/cholest-4-en-3-one(80/20)	4	5a-d9	250	300	50 mM NaPi pH7
449	p2807	2807-81	peptide 3	50	DPPC/cholest-4-en-3-one(80/20)	4	5a-d9	250	600	50 mM NaPi pH7
450	p2807	2807-91	peptide 3	50	DPPC/cholest-4-en-3-one(80/20)	4	5a-d9	250	900	50 mM NaPi pH7
451	p2807	2807-101	peptide 3	50	DPPC/cholest-4-en-3-one(80/20)	4	5a-d9	250	2	50 mM NaPi pH7
452	p2807	2807-111	peptide 3	50	DPPC/cholest-4-en-3-one(80/20)	4	5a-d9	250	5	50 mM NaPi pH7
453	p2807	2807-121	peptide 3	50	DPPC/cholest-4-en-3-one(80/20)	4	5a-d9	250	10	50 mM NaPi pH7
454	p2807	2807-131	peptide 3	50	DPPC/cholest-4-en-3-one(80/20)	4	5a-d9	250	30	50 mM NaPi pH7
455	p2807	2807-141	peptide 3	50	DPPC/cholest-4-en-3-one(80/20)	4	5a-d9	250	60	50 mM NaPi pH7

456	p2807	2807-151	peptide 3	50	DPPC/cholest-4-en-3-one(80/20)	4	5a-d9	250	120	50 mM NaPi pH7
457	p2807	2807-161	peptide 3	50	DPPC/cholest-4-en-3-one(80/20)	4	5a-d9	250	300	50 mM NaPi pH7
458	p2807	2807-171	peptide 3	50	DPPC/cholest-4-en-3-one(80/20)	4	5a-d9	250	600	50 mM NaPi pH7
459	p2807	2807-181	peptide 3	50	DPPC/cholest-4-en-3-one(80/20)	4	5a-d9	250	900	50 mM NaPi pH7
460	p2807	2807-191	peptide 3	50	DPPC/cholest-4-en-3-one(80/20)	4	5a-d9	250	2	50 mM NaPi pH7
461	p2807	2807-201	peptide 3	50	DPPC/cholest-4-en-3-one(80/20)	4	5a-d9	250	5	50 mM NaPi pH7
462	p2807	2807-211	peptide 3	50	DPPC/cholest-4-en-3-one(80/20)	4	5a-d9	250	10	50 mM NaPi pH7
463	p2807	2807-221	peptide 3	50	DPPC/cholest-4-en-3-one(80/20)	4	5a-d9	250	30	50 mM NaPi pH7
464	p2807	2807-231	peptide 3	50	DPPC/cholest-4-en-3-one(80/20)	4	5a-d9	250	60	50 mM NaPi pH7
465	p2807	2807-241	peptide 3	50	DPPC/cholest-4-en-3-one(80/20)	4	5a-d9	250	120	50 mM NaPi pH7
466	p2807	2807-251	peptide 3	50	DPPC/cholest-4-en-3-one(80/20)	4	5a-d9	250	300	50 mM NaPi pH7
467	p2807	2807-261	peptide 3	50	DPPC/cholest-4-en-3-one(80/20)	4	5a-d9	250	600	50 mM NaPi pH7
468	p2807	2807-271	peptide 3	50	DPPC/cholest-4-en-3-one(80/20)	4	5a-d9	250	900	50 mM NaPi pH7
469	p2814	2814-11	peptide 3	50	DPPC/cholest-4-en-3-one(60/40)	4	5a-d9	250	2	50 mM NaPi pH7
470	p2814	2814-21	peptide 3	50	DPPC/cholest-4-en-3-one(60/40)	4	5a-d9	250	5	50 mM NaPi pH7
471	p2814	2814-31	peptide 3	50	DPPC/cholest-4-en-3-one(60/40)	4	5a-d9	250	10	50 mM NaPi pH7
472	p2814	2814-41	peptide 3	50	DPPC/cholest-4-en-3-one(60/40)	4	5a-d9	250	30	50 mM NaPi pH7
473	p2814	2814-51	peptide 3	50	DPPC/cholest-4-en-3-one(60/40)	4	5a-d9	250	60	50 mM NaPi pH7
474	p2814	2814-61	peptide 3	50	DPPC/cholest-4-en-3-one(60/40)	4	5a-d9	250	120	50 mM NaPi pH7
475	p2814	2814-71	peptide 3	50	DPPC/cholest-4-en-3-one(60/40)	4	5a-d9	250	300	50 mM NaPi pH7
476	p2814	2814-81	peptide 3	50	DPPC/cholest-4-en-3-one(60/40)	4	5a-d9	250	600	50 mM NaPi pH7
477	p2814	2814-91	peptide 3	50	DPPC/cholest-4-en-3-one(60/40)	4	5a-d9	250	900	50 mM NaPi pH7
478	p2814	2814-101	peptide 3	50	DPPC/cholest-4-en-3-one(60/40)	4	5a-d9	250	2	50 mM NaPi pH7
479	p2814	2814-111	peptide 3	50	DPPC/cholest-4-en-3-one(60/40)	4	5a-d9	250	5	50 mM NaPi pH7
480	p2814	2814-121	peptide 3	50	DPPC/cholest-4-en-3-one(60/40)	4	5a-d9	250	10	50 mM NaPi pH7
481	p2814	2814-131	peptide 3	50	DPPC/cholest-4-en-3-one(60/40)	4	5a-d9	250	30	50 mM NaPi pH7
482	p2814	2814-141	peptide 3	50	DPPC/cholest-4-en-3-one(60/40)	4	5a-d9	250	60	50 mM NaPi pH7
483	p2814	2814-151	peptide 3	50	DPPC/cholest-4-en-3-one(60/40)	4	5a-d9	250	120	50 mM NaPi pH7
484	p2814	2814-161	peptide 3	50	DPPC/cholest-4-en-3-one(60/40)	4	5a-d9	250	300	50 mM NaPi pH7
485	p2814	2814-171	peptide 3	50	DPPC/cholest-4-en-3-one(60/40)	4	5a-d9	250	600	50 mM NaPi pH7
486	p2814	2814-181	peptide 3	50	DPPC/cholest-4-en-3-one(60/40)	4	5a-d9	250	900	50 mM NaPi pH7
487	p2814	2814-191	peptide 3	50	DPPC/cholest-4-en-3-one(60/40)	4	5a-d9	250	2	50 mM NaPi pH7
488	p2814	2814-201	peptide 3	50	DPPC/cholest-4-en-3-one(60/40)	4	5a-d9	250	5	50 mM NaPi pH7
489	p2814	2814-211	peptide 3	50	DPPC/cholest-4-en-3-one(60/40)	4	5a-d9	250	10	50 mM NaPi pH7
490	p2814	2814-221	peptide 3	50	DPPC/cholest-4-en-3-one(60/40)	4	5a-d9	250	30	50 mM NaPi pH7
491	p2814	2814-231	peptide 3	50	DPPC/cholest-4-en-3-one(60/40)	4	5a-d9	250	60	50 mM NaPi pH7
492	p2814	2814-241	peptide 3	50	DPPC/cholest-4-en-3-one(60/40)	4	5a-d9	250	120	50 mM NaPi pH7
493	p2814	2814-251	peptide 3	50	DPPC/cholest-4-en-3-one(60/40)	4	5a-d9	250	300	50 mM NaPi pH7
494	p2814	2814-261	peptide 3	50	DPPC/cholest-4-en-3-one(60/40)	4	5a-d9	250	600	50 mM NaPi pH7
495	p2814	2814-271	peptide 3	50	DPPC/cholest-4-en-3-one(60/40)	4	5a-d9	250	900	50 mM NaPi pH7
496	p2306	2306-11	peptide 3	50	POPC/PTE(98/2)	4	5a-d9	455	2	50 mM NaPi pH7
497	p2306	2306-21	peptide 3	50	POPC/PTE(98/2)	4	5a-d9	455	5	50 mM NaPi pH7
498	p2306	2306-31	peptide 3	50	POPC/PTE(98/2)	4	5a-d9	455	10	50 mM NaPi pH7
499	p2306	2306-41	peptide 3	50	POPC/PTE(98/2)	4	5a-d9	455	30	50 mM NaPi pH7
500	p2306	2306-51	peptide 3	50	POPC/PTE(98/2)	4	5a-d9	455	60	50 mM NaPi pH7
501	p2306	2306-61	peptide 3	50	POPC/PTE(98/2)	4	5a-d9	455	120	50 mM NaPi pH7
502	p2306	2306-71	peptide 3	50	POPC/PTE(98/2)	4	5a-d9	455	300	50 mM NaPi pH7
503	p2306	2306-81	peptide 3	50	POPC/PTE(98/2)	4	5a-d9	455	600	50 mM NaPi pH7
504	p2306	2306-91	peptide 3	50	POPC/PTE(98/2)	4	5a-d9	455	900	50 mM NaPi pH7
505	p2306	2306-101	peptide 3	50	POPC/PTE(98/2)	4	5a-d9	455	2	50 mM NaPi pH7
506	p2306	2306-111	peptide 3	50	POPC/PTE(98/2)	4	5a-d9	455	5	50 mM NaPi pH7
507	p2306	2306-121	peptide 3	50	POPC/PTE(98/2)	4	5a-d9	455	10	50 mM NaPi pH7
508	p2306	2306-131	peptide 3	50	POPC/PTE(98/2)	4	5a-d9	455	30	50 mM NaPi pH7
509	p2306	2306-141	peptide 3	50	POPC/PTE(98/2)	4	5a-d9	455	60	50 mM NaPi pH7
510	p2306	2306-151	peptide 3	50	POPC/PTE(98/2)	4	5a-d9	455	120	50 mM NaPi pH7
511	p2306	2306-161	peptide 3	50	POPC/PTE(98/2)	4	5a-d9	455	300	50 mM NaPi pH7
512	p2306	2306-171	peptide 3	50	POPC/PTE(98/2)	4	5a-d9	455	600	50 mM NaPi pH7
513	p2306	2306-181	peptide 3	50	POPC/PTE(98/2)	4	5a-d9	455	900	50 mM NaPi pH7

514	p2306	2306-191	peptide 3	50	POPC/PTE(98/2)	4	5a-d9	455	2	50 mM NaPi pH7
515	p2306	2306-201	peptide 3	50	POPC/PTE(98/2)	4	5a-d9	455	5	50 mM NaPi pH7
516	p2306	2306-211	peptide 3	50	POPC/PTE(98/2)	4	5a-d9	455	10	50 mM NaPi pH7
517	p2306	2306-221	peptide 3	50	POPC/PTE(98/2)	4	5a-d9	455	30	50 mM NaPi pH7
518	p2306	2306-231	peptide 3	50	POPC/PTE(98/2)	4	5a-d9	455	60	50 mM NaPi pH7
519	p2306	2306-241	peptide 3	50	POPC/PTE(98/2)	4	5a-d9	455	120	50 mM NaPi pH7
520	p2306	2306-251	peptide 3	50	POPC/PTE(98/2)	4	5a-d9	455	300	50 mM NaPi pH7
521	p2306	2306-261	peptide 3	50	POPC/PTE(98/2)	4	5a-d9	455	600	50 mM NaPi pH7
522	p2306	2306-271	peptide 3	50	POPC/PTE(98/2)	4	5a-d9	455	900	50 mM NaPi pH7
523	p2337	2337-11	peptide 3	50	DPPC/PTE(98/2)	4	5a-d9	455	2	50 mM NaPi pH7
524	p2337	2337-21	peptide 3	50	DPPC/PTE(98/2)	4	5a-d9	455	5	50 mM NaPi pH7
525	p2337	2337-31	peptide 3	50	DPPC/PTE(98/2)	4	5a-d9	455	10	50 mM NaPi pH7
526	p2337	2337-41	peptide 3	50	DPPC/PTE(98/2)	4	5a-d9	455	30	50 mM NaPi pH7
527	p2337	2337-51	peptide 3	50	DPPC/PTE(98/2)	4	5a-d9	455	60	50 mM NaPi pH7
528	p2337	2337-61	peptide 3	50	DPPC/PTE(98/2)	4	5a-d9	455	120	50 mM NaPi pH7
529	p2337	2337-71	peptide 3	50	DPPC/PTE(98/2)	4	5a-d9	455	300	50 mM NaPi pH7
530	p2337	2337-81	peptide 3	50	DPPC/PTE(98/2)	4	5a-d9	455	600	50 mM NaPi pH7
531	p2337	2337-91	peptide 3	50	DPPC/PTE(98/2)	4	5a-d9	455	900	50 mM NaPi pH7
532	p2337	2337-101	peptide 3	50	DPPC/PTE(98/2)	4	5a-d9	455	2	50 mM NaPi pH7
533	p2337	2337-111	peptide 3	50	DPPC/PTE(98/2)	4	5a-d9	455	5	50 mM NaPi pH7
534	p2337	2337-121	peptide 3	50	DPPC/PTE(98/2)	4	5a-d9	455	10	50 mM NaPi pH7
535	p2337	2337-131	peptide 3	50	DPPC/PTE(98/2)	4	5a-d9	455	30	50 mM NaPi pH7
536	p2337	2337-141	peptide 3	50	DPPC/PTE(98/2)	4	5a-d9	455	60	50 mM NaPi pH7
537	p2337	2337-151	peptide 3	50	DPPC/PTE(98/2)	4	5a-d9	455	120	50 mM NaPi pH7
538	p2337	2337-161	peptide 3	50	DPPC/PTE(98/2)	4	5a-d9	455	300	50 mM NaPi pH7
539	p2337	2337-171	peptide 3	50	DPPC/PTE(98/2)	4	5a-d9	455	600	50 mM NaPi pH7
540	p2337	2337-181	peptide 3	50	DPPC/PTE(98/2)	4	5a-d9	455	900	50 mM NaPi pH7
541	p2337	2337-191	peptide 3	50	DPPC/PTE(98/2)	4	5a-d9	455	2	50 mM NaPi pH7
542	p2337	2337-201	peptide 3	50	DPPC/PTE(98/2)	4	5a-d9	455	5	50 mM NaPi pH7
543	p2337	2337-211	peptide 3	50	DPPC/PTE(98/2)	4	5a-d9	455	10	50 mM NaPi pH7
544	p2337	2337-221	peptide 3	50	DPPC/PTE(98/2)	4	5a-d9	455	30	50 mM NaPi pH7
545	p2337	2337-231	peptide 3	50	DPPC/PTE(98/2)	4	5a-d9	455	60	50 mM NaPi pH7
546	p2337	2337-241	peptide 3	50	DPPC/PTE(98/2)	4	5a-d9	455	120	50 mM NaPi pH7
547	p2337	2337-251	peptide 3	50	DPPC/PTE(98/2)	4	5a-d9	455	300	50 mM NaPi pH7
548	p2337	2337-261	peptide 3	50	DPPC/PTE(98/2)	4	5a-d9	455	600	50 mM NaPi pH7
549	p2337	2337-271	peptide 3	50	DPPC/PTE(98/2)	4	5a-d9	455	900	50 mM NaPi pH7
550	p2028	2028-191	peptide 3	50	POPC	4	5c-d9	125	2	50 mM NaPi pH7
551	p2028	2028-201	peptide 3	50	POPC	4	5c-d9	125	5	50 mM NaPi pH7
552	p2028	2028-211	peptide 3	50	POPC	4	5c-d9	125	10	50 mM NaPi pH7
553	p2028	2028-221	peptide 3	50	POPC	4	5c-d9	125	30	50 mM NaPi pH7
554	p2028	2028-231	peptide 3	50	POPC	4	5c-d9	125	60	50 mM NaPi pH7
555	p2028	2028-241	peptide 3	50	POPC	4	5c-d9	125	120	50 mM NaPi pH7
556	p2028	2028-251	peptide 3	50	POPC	4	5c-d9	125	2	50 mM NaPi pH7
557	p2028	2028-261	peptide 3	50	POPC	4	5c-d9	125	5	50 mM NaPi pH7
558	p2028	2028-271	peptide 3	50	POPC	4	5c-d9	125	10	50 mM NaPi pH7
559	p2028	2028-281	peptide 3	50	POPC	4	5c-d9	125	30	50 mM NaPi pH7
560	p2028	2028-291	peptide 3	50	POPC	4	5c-d9	125	60	50 mM NaPi pH7
561	p2028	2028-301	peptide 3	50	POPC	4	5c-d9	125	120	50 mM NaPi pH7
562	p2028	2028-311	peptide 3	50	POPC	4	5c-d9	125	2	50 mM NaPi pH7
563	p2028	2028-321	peptide 3	50	POPC	4	5c-d9	125	5	50 mM NaPi pH7
564	p2028	2028-331	peptide 3	50	POPC	4	5c-d9	125	10	50 mM NaPi pH7
565	p2028	2028-341	peptide 3	50	POPC	4	5c-d9	125	30	50 mM NaPi pH7
566	p2028	2028-351	peptide 3	50	POPC	4	5c-d9	125	60	50 mM NaPi pH7
567	p2028	2028-361	peptide 3	50	POPC	4	5c-d9	125	120	50 mM NaPi pH7
568	p2033	2033-11	peptide 2/3	31.25	POPC	5	5a-d9	125	2	50 mM NaPi pH7
569	p2033	2033-21	peptide 2/3	31.25	POPC	5	5a-d9	125	5	50 mM NaPi pH7
570	p2033	2033-31	peptide 2/3	31.25	POPC	5	5a-d9	125	10	50 mM NaPi pH7
571	p2033	2033-41	peptide 2/3	31.25	POPC	5	5a-d9	125	30	50 mM NaPi pH7

572	p2033	2033-51	peptide 2/3	31.25	POPC	5	5a-d9	125	60	50 mM NaPi pH7
573	p2033	2033-61	peptide 2/3	31.25	POPC	5	5a-d9	125	120	50 mM NaPi pH7
574	p2069	2069-11	peptide 2/3	31.25	POPC	5	5a-d9	125	2	50 mM NaPi pH7
575	p2069	2069-21	peptide 2/3	31.25	POPC	5	5a-d9	125	5	50 mM NaPi pH7
576	p2069	2069-31	peptide 2/3	31.25	POPC	5	5a-d9	125	10	50 mM NaPi pH7
577	p2069	2069-41	peptide 2/3	31.25	POPC	5	5a-d9	125	30	50 mM NaPi pH7
578	p2069	2069-51	peptide 2/3	31.25	POPC	5	5a-d9	125	60	50 mM NaPi pH7
579	p2069	2069-61	peptide 2/3	31.25	POPC	5	5a-d9	125	120	50 mM NaPi pH7
580	p2069	2069-71	peptide 2/3	31.25	POPC	5	5a-d9	125	2	50 mM NaPi pH7
581	p2069	2069-81	peptide 2/3	31.25	POPC	5	5a-d9	125	5	50 mM NaPi pH7
582	p2069	2069-91	peptide 2/3	31.25	POPC	5	5a-d9	125	10	50 mM NaPi pH7
583	p2069	2069-101	peptide 2/3	31.25	POPC	5	5a-d9	125	30	50 mM NaPi pH7
584	p2069	2069-111	peptide 2/3	31.25	POPC	5	5a-d9	125	60	50 mM NaPi pH7
585	p2069	2069-121	peptide 2/3	31.25	POPC	5	5a-d9	125	120	50 mM NaPi pH7
586	p2033	2033-71	peptide 2/3	31.25	POPC	5	5c-d9	125	2	50 mM NaPi pH7
587	p2033	2033-81	peptide 2/3	31.25	POPC	5	5c-d9	125	5	50 mM NaPi pH7
588	p2033	2033-91	peptide 2/3	31.25	POPC	5	5c-d9	125	10	50 mM NaPi pH7
589	p2033	2033-101	peptide 2/3	31.25	POPC	5	5c-d9	125	30	50 mM NaPi pH7
590	p2033	2033-111	peptide 2/3	31.25	POPC	5	5c-d9	125	60	50 mM NaPi pH7
591	p2033	2033-121	peptide 2/3	31.25	POPC	5	5c-d9	125	120	50 mM NaPi pH7
592	p2069	2069-131	peptide 2/3	31.25	POPC	5	5c-d9	125	2	50 mM NaPi pH7
593	p2069	2069-141	peptide 2/3	31.25	POPC	5	5c-d9	125	5	50 mM NaPi pH7
594	p2069	2069-151	peptide 2/3	31.25	POPC	5	5c-d9	125	10	50 mM NaPi pH7
595	p2069	2069-161	peptide 2/3	31.25	POPC	5	5c-d9	125	30	50 mM NaPi pH7
596	p2069	2069-171	peptide 2/3	31.25	POPC	5	5c-d9	125	60	50 mM NaPi pH7
597	p2069	2069-181	peptide 2/3	31.25	POPC	5	5c-d9	125	120	50 mM NaPi pH7
598	p2069	2069-191	peptide 2/3	31.25	POPC	5	5c-d9	125	2	50 mM NaPi pH7
599	p2069	2069-201	peptide 2/3	31.25	POPC	5	5c-d9	125	5	50 mM NaPi pH7
600	p2069	2069-211	peptide 2/3	31.25	POPC	5	5c-d9	125	10	50 mM NaPi pH7
601	p2069	2069-221	peptide 2/3	31.25	POPC	5	5c-d9	125	30	50 mM NaPi pH7
602	p2069	2069-231	peptide 2/3	31.25	POPC	5	5c-d9	125	60	50 mM NaPi pH7
603	p2069	2069-241	peptide 2/3	31.25	POPC	5	5c-d9	125	120	50 mM NaPi pH7
604	p2073	2073-11	peptide 2/3	31.25	POPC	5	5a-d0	125	2	50 mM NaPi pH7
605	p2073	2073-21	peptide 2/3	31.25	POPC	5	5a-d0	125	5	50 mM NaPi pH7
606	p2073	2073-31	peptide 2/3	31.25	POPC	5	5a-d0	125	10	50 mM NaPi pH7
607	p2073	2073-41	peptide 2/3	31.25	POPC	5	5a-d0	125	30	50 mM NaPi pH7
608	p2073	2073-51	peptide 2/3	31.25	POPC	5	5a-d0	125	60	50 mM NaPi pH7
609	p2073	2073-61	peptide 2/3	31.25	POPC	5	5a-d0	125	120	50 mM NaPi pH7
610	p2073	2073-71	peptide 2/3	31.25	POPC	5	5a-d0	125	2	50 mM NaPi pH7
611	p2073	2073-81	peptide 2/3	31.25	POPC	5	5a-d0	125	5	50 mM NaPi pH7
612	p2073	2073-91	peptide 2/3	31.25	POPC	5	5a-d0	125	10	50 mM NaPi pH7
613	p2073	2073-101	peptide 2/3	31.25	POPC	5	5a-d0	125	30	50 mM NaPi pH7
614	p2073	2073-111	peptide 2/3	31.25	POPC	5	5a-d0	125	60	50 mM NaPi pH7
615	p2073	2073-121	peptide 2/3	31.25	POPC	5	5a-d0	125	120	50 mM NaPi pH7
616	p2073	2073-131	peptide 2/3	31.25	POPC	5	5a-d0	125	2	50 mM NaPi pH7
617	p2073	2073-141	peptide 2/3	31.25	POPC	5	5a-d0	125	5	50 mM NaPi pH7
618	p2073	2073-151	peptide 2/3	31.25	POPC	5	5a-d0	125	10	50 mM NaPi pH7
619	p2073	2073-161	peptide 2/3	31.25	POPC	5	5a-d0	125	30	50 mM NaPi pH7
620	p2073	2073-171	peptide 2/3	31.25	POPC	5	5a-d0	125	60	50 mM NaPi pH7
621	p2073	2073-181	peptide 2/3	31.25	POPC	5	5a-d0	125	120	50 mM NaPi pH7
622	p2073	2073-191	peptide 2/3	31.25	POPC	5	5c-d0	125	2	50 mM NaPi pH7
623	p2073	2073-201	peptide 2/3	31.25	POPC	5	5c-d0	125	5	50 mM NaPi pH7
624	p2073	2073-211	peptide 2/3	31.25	POPC	5	5c-d0	125	10	50 mM NaPi pH7
625	p2073	2073-221	peptide 2/3	31.25	POPC	5	5c-d0	125	30	50 mM NaPi pH7
626	p2073	2073-231	peptide 2/3	31.25	POPC	5	5c-d0	125	60	50 mM NaPi pH7
627	p2073	2073-241	peptide 2/3	31.25	POPC	5	5c-d0	125	120	50 mM NaPi pH7
628	p2073	2073-251	peptide 2/3	31.25	POPC	5	5c-d0	125	2	50 mM NaPi pH7
629	p2073	2073-261	peptide 2/3	31.25	POPC	5	5c-d0	125	5	50 mM NaPi pH7

630	p2073	2073-271	peptide 2/3	31.25	POPC	5	5c-d0	125	10	50 mM NaPi pH7
631	p2073	2073-281	peptide 2/3	31.25	POPC	5	5c-d0	125	30	50 mM NaPi pH7
632	p2073	2073-291	peptide 2/3	31.25	POPC	5	5c-d0	125	60	50 mM NaPi pH7
633	p2073	2073-301	peptide 2/3	31.25	POPC	5	5c-d0	125	120	50 mM NaPi pH7
634	p2073	2073-311	peptide 2/3	31.25	POPC	5	5c-d0	125	2	50 mM NaPi pH7
635	p2073	2073-321	peptide 2/3	31.25	POPC	5	5c-d0	125	5	50 mM NaPi pH7
636	p2073	2073-331	peptide 2/3	31.25	POPC	5	5c-d0	125	10	50 mM NaPi pH7
637	p2073	2073-341	peptide 2/3	31.25	POPC	5	5c-d0	125	30	50 mM NaPi pH7
638	p2073	2073-351	peptide 2/3	31.25	POPC	5	5c-d0	125	60	50 mM NaPi pH7
639	p2073	2073-361	peptide 2/3	31.25	POPC	5	5c-d0	125	120	50 mM NaPi pH7
640	p2840	2840-11	peptide 3	50	DOPC/DOPE(1:1)	4	5a-d9	250	2	50 mM NaPi pH7
641	p2840	2840-21	peptide 3	50	DOPC/DOPE(1:1)	4	5a-d9	250	5	50 mM NaPi pH7
642	p2840	2840-31	peptide 3	50	DOPC/DOPE(1:1)	4	5a-d9	250	10	50 mM NaPi pH7
643	p2840	2840-41	peptide 3	50	DOPC/DOPE(1:1)	4	5a-d9	250	30	50 mM NaPi pH7
644	p2840	2840-51	peptide 3	50	DOPC/DOPE(1:1)	4	5a-d9	250	60	50 mM NaPi pH7
645	p2840	2840-61	peptide 3	50	DOPC/DOPE(1:1)	4	5a-d9	250	120	50 mM NaPi pH7
646	p2840	2840-71	peptide 3	50	DOPC/DOPE(1:1)	4	5a-d9	250	300	50 mM NaPi pH7
647	p2840	2840-81	peptide 3	50	DOPC/DOPE(1:1)	4	5a-d9	250	600	50 mM NaPi pH7
648	p2840	2840-91	peptide 3	50	DOPC/DOPE(1:1)	4	5a-d9	250	900	50 mM NaPi pH7
649	p2840	2840-101	peptide 3	50	DOPC/DOPE(1:1)	4	5a-d9	250	2	50 mM NaPi pH7
650	p2840	2840-111	peptide 3	50	DOPC/DOPE(1:1)	4	5a-d9	250	5	50 mM NaPi pH7
651	p2840	2840-121	peptide 3	50	DOPC/DOPE(1:1)	4	5a-d9	250	10	50 mM NaPi pH7
652	p2840	2840-131	peptide 3	50	DOPC/DOPE(1:1)	4	5a-d9	250	30	50 mM NaPi pH7
653	p2840	2840-141	peptide 3	50	DOPC/DOPE(1:1)	4	5a-d9	250	60	50 mM NaPi pH7
654	p2840	2840-151	peptide 3	50	DOPC/DOPE(1:1)	4	5a-d9	250	120	50 mM NaPi pH7
655	p2840	2840-161	peptide 3	50	DOPC/DOPE(1:1)	4	5a-d9	250	300	50 mM NaPi pH7
656	p2840	2840-171	peptide 3	50	DOPC/DOPE(1:1)	4	5a-d9	250	600	50 mM NaPi pH7
657	p2840	2840-181	peptide 3	50	DOPC/DOPE(1:1)	4	5a-d9	250	900	50 mM NaPi pH7
658	p2840	2840-191	peptide 3	50	DOPC/DOPE(1:1)	4	5a-d9	250	2	50 mM NaPi pH7
659	p2840	2840-201	peptide 3	50	DOPC/DOPE(1:1)	4	5a-d9	250	5	50 mM NaPi pH7
660	p2840	2840-211	peptide 3	50	DOPC/DOPE(1:1)	4	5a-d9	250	10	50 mM NaPi pH7
661	p2840	2840-221	peptide 3	50	DOPC/DOPE(1:1)	4	5a-d9	250	30	50 mM NaPi pH7
662	p2840	2840-231	peptide 3	50	DOPC/DOPE(1:1)	4	5a-d9	250	60	50 mM NaPi pH7
663	p2840	2840-241	peptide 3	50	DOPC/DOPE(1:1)	4	5a-d9	250	120	50 mM NaPi pH7
664	p2840	2840-251	peptide 3	50	DOPC/DOPE(1:1)	4	5a-d9	250	300	50 mM NaPi pH7
665	p2840	2840-261	peptide 3	50	DOPC/DOPE(1:1)	4	5a-d9	250	600	50 mM NaPi pH7
666	p2840	2840-271	peptide 3	50	DOPC/DOPE(1:1)	4	5a-d9	250	900	50 mM NaPi pH7
667	p2875	2875-11	peptide 3	50	DOPS	4	5a-d9	250	2	50 mM NaPi pH7
668	p2875	2875-21	peptide 3	50	DOPS	4	5a-d9	250	5	50 mM NaPi pH7
669	p2875	2875-31	peptide 3	50	DOPS	4	5a-d9	250	10	50 mM NaPi pH7
670	p2875	2875-41	peptide 3	50	DOPS	4	5a-d9	250	30	50 mM NaPi pH7
671	p2875	2875-51	peptide 3	50	DOPS	4	5a-d9	250	60	50 mM NaPi pH7
672	p2875	2875-61	peptide 3	50	DOPS	4	5a-d9	250	120	50 mM NaPi pH7
673	p2875	2875-71	peptide 3	50	DOPS	4	5a-d9	250	300	50 mM NaPi pH7
674	p2875	2875-81	peptide 3	50	DOPS	4	5a-d9	250	600	50 mM NaPi pH7
675	p2875	2875-91	peptide 3	50	DOPS	4	5a-d9	250	900	50 mM NaPi pH7
676	p2875	2875-101	peptide 3	50	DOPS	4	5a-d9	250	2	50 mM NaPi pH7
677	p2875	2875-111	peptide 3	50	DOPS	4	5a-d9	250	5	50 mM NaPi pH7
678	p2875	2875-121	peptide 3	50	DOPS	4	5a-d9	250	10	50 mM NaPi pH7
679	p2875	2875-131	peptide 3	50	DOPS	4	5a-d9	250	30	50 mM NaPi pH7
680	p2875	2875-141	peptide 3	50	DOPS	4	5a-d9	250	60	50 mM NaPi pH7
681	p2875	2875-151	peptide 3	50	DOPS	4	5a-d9	250	120	50 mM NaPi pH7
682	p2875	2875-161	peptide 3	50	DOPS	4	5a-d9	250	300	50 mM NaPi pH7
683	p2875	2875-171	peptide 3	50	DOPS	4	5a-d9	250	600	50 mM NaPi pH7
684	p2875	2875-181	peptide 3	50	DOPS	4	5a-d9	250	900	50 mM NaPi pH7
685	p2875	2875-191	peptide 3	50	DOPS	4	5a-d9	250	2	50 mM NaPi pH7
686	p2875	2875-201	peptide 3	50	DOPS	4	5a-d9	250	5	50 mM NaPi pH7
687	p2875	2875-211	peptide 3	50	DOPS	4	5a-d9	250	10	50 mM NaPi pH7

688	p2875	2875-221	peptide 3	50	DOPS	4	5a-d9	250	30	50 mM NaPi pH7
689	p2875	2875-231	peptide 3	50	DOPS	4	5a-d9	250	60	50 mM NaPi pH7
690	p2875	2875-241	peptide 3	50	DOPS	4	5a-d9	250	120	50 mM NaPi pH7
691	p2875	2875-251	peptide 3	50	DOPS	4	5a-d9	250	300	50 mM NaPi pH7
692	p2875	2875-261	peptide 3	50	DOPS	4	5a-d9	250	600	50 mM NaPi pH7
693	p2875	2875-271	peptide 3	50	DOPS	4	5a-d9	250	900	50 mM NaPi pH7
694	p2877	2877-11	peptide 3	50	DOPG	4	5a-d9	250	2	50 mM NaPi pH7
695	p2877	2877-21	peptide 3	50	DOPG	4	5a-d9	250	5	50 mM NaPi pH7
696	p2877	2877-31	peptide 3	50	DOPG	4	5a-d9	250	10	50 mM NaPi pH7
697	p2877	2877-41	peptide 3	50	DOPG	4	5a-d9	250	30	50 mM NaPi pH7
698	p2877	2877-51	peptide 3	50	DOPG	4	5a-d9	250	60	50 mM NaPi pH7
699	p2877	2877-61	peptide 3	50	DOPG	4	5a-d9	250	120	50 mM NaPi pH7
700	p2877	2877-71	peptide 3	50	DOPG	4	5a-d9	250	300	50 mM NaPi pH7
701	p2877	2877-81	peptide 3	50	DOPG	4	5a-d9	250	600	50 mM NaPi pH7
702	p2877	2877-91	peptide 3	50	DOPG	4	5a-d9	250	900	50 mM NaPi pH7
703	p2877	2877-101	peptide 3	50	DOPG	4	5a-d9	250	2	50 mM NaPi pH7
704	p2877	2877-111	peptide 3	50	DOPG	4	5a-d9	250	5	50 mM NaPi pH7
705	p2877	2877-121	peptide 3	50	DOPG	4	5a-d9	250	10	50 mM NaPi pH7
706	p2877	2877-131	peptide 3	50	DOPG	4	5a-d9	250	30	50 mM NaPi pH7
707	p2877	2877-141	peptide 3	50	DOPG	4	5a-d9	250	60	50 mM NaPi pH7
708	p2877	2877-151	peptide 3	50	DOPG	4	5a-d9	250	120	50 mM NaPi pH7
709	p2877	2877-161	peptide 3	50	DOPG	4	5a-d9	250	300	50 mM NaPi pH7
710	p2877	2877-171	peptide 3	50	DOPG	4	5a-d9	250	600	50 mM NaPi pH7
711	p2877	2877-181	peptide 3	50	DOPG	4	5a-d9	250	900	50 mM NaPi pH7
712	p2877	2877-191	peptide 3	50	DOPG	4	5a-d9	250	2	50 mM NaPi pH7
713	p2877	2877-201	peptide 3	50	DOPG	4	5a-d9	250	5	50 mM NaPi pH7
714	p2877	2877-211	peptide 3	50	DOPG	4	5a-d9	250	10	50 mM NaPi pH7
715	p2877	2877-221	peptide 3	50	DOPG	4	5a-d9	250	30	50 mM NaPi pH7
716	p2877	2877-231	peptide 3	50	DOPG	4	5a-d9	250	60	50 mM NaPi pH7
717	p2877	2877-241	peptide 3	50	DOPG	4	5a-d9	250	120	50 mM NaPi pH7
718	p2877	2877-251	peptide 3	50	DOPG	4	5a-d9	250	300	50 mM NaPi pH7
719	p2877	2877-261	peptide 3	50	DOPG	4	5a-d9	250	600	50 mM NaPi pH7
720	p2877	2877-271	peptide 3	50	DOPG	4	5a-d9	250	900	50 mM NaPi pH7

Appendix 2 List of mass spectra of cholesterol oxidase-lipids labeling experiments

Note: For naming simpilicity of multi-cysteine mutants. See below for details.
Mutant 1: A32C/S129C/T371C/A423C
Mutant 2: S153C/A205C/S312C/T435C
Mutant 3: T168C/A276C
Mutant 4: A184C/T239C/A407C/A465C
Mutant 5: A32C/T168C/S312C/A465C
Mutant 6: A184C/A301C/T394C

#	Page #	Spectrum name	Cholesterol oxidase mutant	[ChoA] mM	Lipids	[Lipids] mM	Probe	[Probe] mM	Time (min)	Protease	Buffer
1	p2645	2645-11	L80C	10	DMPC	500	5b-d9	500	1	trypsin	50 mM HEPES pH7
2	p2645	2645-21	L80C	10	DMPC	500	5b-d9	500	2	trypsin	50 mM HEPES pH7
3	p2645	2645-31	L80C	10	DMPC	500	5b-d9	500	5	trypsin	50 mM HEPES pH7
4	p2645	2645-41	L80C	10	DMPC	500	5b-d9	500	10	trypsin	50 mM HEPES pH7
5	p2645	2645-51	L80C	10	DMPC	500	5b-d9	500	30	trypsin	50 mM HEPES pH7
6	p2645	2645-61	L80C	10	DMPC	500	5b-d9	500	60	trypsin	50 mM HEPES pH7
7	p2650	2650-11	L80C	10	DMPC/cholest-4-en-3-one(3/1)	500	5b-d9	500	1	trypsin	50 mM HEPES pH7
8	p2650	2650-21	L80C	10	DMPC/cholest-4-en-3-one(3/1)	500	5b-d9	500	2	trypsin	50 mM HEPES pH7
9	p2650	2650-31	L80C	10	DMPC/cholest-4-en-3-one(3/1)	500	5b-d9	500	5	trypsin	50 mM HEPES pH7
10	p2650	2650-41	L80C	10	DMPC/cholest-4-en-3-one(3/1)	500	5b-d9	500	10	trypsin	50 mM HEPES pH7
11	p2650	2650-51	L80C	10	DMPC/cholest-4-en-3-one(3/1)	500	5b-d9	500	30	trypsin	50 mM HEPES pH7
12	p2650	2650-61	L80C	10	DMPC/cholest-4-en-3-one(3/1)	500	5b-d9	500	60	trypsin	50 mM HEPES pH7
13	p2650	2650-71	L80C	10	DMPC/cholest-4-en-3-one(3/1)	500	5b-d9	100	1	trypsin	50 mM HEPES pH7
14	p2650	2650-81	L80C	10	DMPC/cholest-4-en-3-one(3/1)	500	5b-d9	100	2	trypsin	50 mM HEPES pH7
15	p2650	2650-91	L80C	10	DMPC/cholest-4-en-3-one(3/1)	500	5b-d9	100	5	trypsin	50 mM HEPES pH7
16	p2650	2650-101	L80C	10	DMPC/cholest-4-en-3-one(3/1)	500	5b-d9	100	10	trypsin	50 mM HEPES pH7
17	p2650	2650-111	L80C	10	DMPC/cholest-4-en-3-one(3/1)	500	5b-d9	100	30	trypsin	50 mM HEPES pH7
18	p2650	2650-121	L80C	10	DMPC/cholest-4-en-3-one(3/1)	500	5b-d9	100	60	trypsin	50 mM HEPES pH7
19	p2655	2655-11	L80C	10	DMPC	500	5b-d9	100	1	trypsin	50 mM HEPES pH7
20	p2655	2655-21	L80C	10	DMPC	500	5b-d9	100	2	trypsin	50 mM HEPES pH7
21	p2655	2655-31	L80C	10	DMPC	500	5b-d9	100	5	trypsin	50 mM HEPES pH7
22	p2655	2655-41	L80C	10	DMPC	500	5b-d9	100	10	trypsin	50 mM HEPES pH7
23	p2655	2655-51	L80C	10	DMPC	500	5b-d9	100	30	trypsin	50 mM HEPES pH7
24	p2655	2655-61	L80C	10	DMPC	500	5b-d9	100	60	trypsin	50 mM HEPES pH7
25	p2655	2655-71	L80C	10	DMPC/cholesterol(3/1)	500	5b-d9	100	1	trypsin	50 mM HEPES pH7
26	p2655	2655-81	L80C	10	DMPC/cholesterol(3/1)	500	5b-d9	100	2	trypsin	50 mM HEPES pH7
27	p2655	2655-91	L80C	10	DMPC/cholesterol(3/1)	500	5b-d9	100	5	trypsin	50 mM HEPES pH7
28	p2655	2655-101	L80C	10	DMPC/cholesterol(3/1)	500	5b-d9	100	10	trypsin	50 mM HEPES pH7
29	p2655	2655-111	L80C	10	DMPC/cholesterol(3/1)	500	5b-d9	100	30	trypsin	50 mM HEPES pH7
30	p2655	2655-121	L80C	10	DMPC/cholesterol(3/1)	500	5b-d9	100	60	trypsin	50 mM HEPES pH7
31	p2655	2655-131	L80C	10	no vesicles	0	5b-d9	100	1	trypsin	50 mM HEPES pH7
32	p2655	2655-141	L80C	10	no vesicles	0	5b-d9	100	2	trypsin	50 mM HEPES pH7
33	p2655	2655-151	L80C	10	no vesicles	0	5b-d9	100	5	trypsin	50 mM HEPES pH7
34	p2655	2655-161	L80C	10	no vesicles	0	5b-d9	100	10	trypsin	50 mM HEPES pH7
35	p2655	2655-171	L80C	10	no vesicles	0	5b-d9	100	30	trypsin	50 mM HEPES pH7
36	p2655	2655-181	L80C	10	no vesicles	0	5b-d9	100	60	trypsin	50 mM HEPES pH7
37	p2655	2655-191	L80C	10	DMPC	500	5b-d9	25	1	trypsin	50 mM HEPES pH7
38	p2655	2655-201	L80C	10	DMPC	500	5b-d9	25	2	trypsin	50 mM HEPES pH7
39	p2655	2655-211	L80C	10	DMPC	500	5b-d9	25	5	trypsin	50 mM HEPES pH7
40	p2655	2655-221	L80C	10	DMPC	500	5b-d9	25	10	trypsin	50 mM HEPES pH7
41	p2655	2655-231	L80C	10	DMPC	500	5b-d9	25	30	trypsin	50 mM HEPES pH7
42	p2655	2655-241	L80C	10	DMPC	500	5b-d9	25	60	trypsin	50 mM HEPES pH7
43	p2655	2655-251	L80C	10	DMPC/cholesterol(3/1)	500	5b-d9	25	1	trypsin	50 mM HEPES pH7
44	p2655	2655-261	L80C	10	DMPC/cholesterol(3/1)	500	5b-d9	25	2	trypsin	50 mM HEPES pH7
45	p2655	2655-271	L80C	10	DMPC/cholesterol(3/1)	500	5b-d9	25	5	trypsin	50 mM HEPES pH7

46	p2655	2655-281	L80C	10	DMPC/cholesterol(3/1)	500	5b-d9	25	10	trypsin	50 mM HEPES pH7
47	p2655	2655-291	L80C	10	DMPC/cholesterol(3/1)	500	5b-d9	25	30	trypsin	50 mM HEPES pH7
48	p2655	2655-301	L80C	10	DMPC/cholesterol(3/1)	500	5b-d9	25	60	trypsin	50 mM HEPES pH7
49	p2655	2655-311	L80C	10	DMPC/cholest-4-en-3-one(3/1)	500	5b-d9	25	1	trypsin	50 mM HEPES pH7
50	p2655	2655-321	L80C	10	DMPC/cholest-4-en-3-one(3/1)	500	5b-d9	25	2	trypsin	50 mM HEPES pH7
51	p2655	2655-331	L80C	10	DMPC/cholest-4-en-3-one(3/1)	500	5b-d9	25	5	trypsin	50 mM HEPES pH7
52	p2655	2655-341	L80C	10	DMPC/cholest-4-en-3-one(3/1)	500	5b-d9	25	10	trypsin	50 mM HEPES pH7
53	p2655	2655-351	L80C	10	DMPC/cholest-4-en-3-one(3/1)	500	5b-d9	25	30	trypsin	50 mM HEPES pH7
54	p2655	2655-361	L80C	10	DMPC/cholest-4-en-3-one(3/1)	500	5b-d9	25	60	trypsin	50 mM HEPES pH7
55	p2655	2655-371	L80C	10	no vesicles	0	5b-d9	25	1	trypsin	50 mM HEPES pH7
56	p2655	2655-381	L80C	10	no vesicles	0	5b-d9	25	2	trypsin	50 mM HEPES pH7
57	p2655	2655-391	L80C	10	no vesicles	0	5b-d9	25	5	trypsin	50 mM HEPES pH7
58	p2655	2655-401	L80C	10	no vesicles	0	5b-d9	25	10	trypsin	50 mM HEPES pH7
59	p2655	2655-411	L80C	10	no vesicles	0	5b-d9	25	30	trypsin	50 mM HEPES pH7
60	p2655	2655-421	L80C	10	no vesicles	0	5b-d9	25	60	trypsin	50 mM HEPES pH7
61	p2851	2851-11	WT	10	DMPC	500	5b-d9	50	0.5	trypsin	50 mM HEPES pH7
62	p2851	2851-21	WT	10	DMPC	500	5b-d9	50	1	trypsin	50 mM HEPES pH7
63	p2851	2851-31	WT	10	DMPC	500	5b-d9	50	2	trypsin	50 mM HEPES pH7
64	p2851	2851-41	WT	10	DMPC	500	5b-d9	50	3	trypsin	50 mM HEPES pH7
65	p2851	2851-51	WT	10	DMPC	500	5b-d9	50	6	trypsin	50 mM HEPES pH7
66	p2851	2851-61	WT	10	DMPC	500	5b-d9	50	10	trypsin	50 mM HEPES pH7
67	p2851	2851-71	WT	10	DMPC	500	5b-d9	50	15	trypsin	50 mM HEPES pH7
68	p2851	2851-81	WT	10	DMPC	500	5b-d9	50	30	trypsin	50 mM HEPES pH7
69	p2851	2851-91	L80C	10	DMPC	500	5b-d9	50	0.5	trypsin	50 mM HEPES pH7
70	p2851	2851-101	L80C	10	DMPC	500	5b-d9	50	1	trypsin	50 mM HEPES pH7
71	p2851	2851-111	L80C	10	DMPC	500	5b-d9	50	2	trypsin	50 mM HEPES pH7
72	p2851	2851-121	L80C	10	DMPC	500	5b-d9	50	3	trypsin	50 mM HEPES pH7
73	p2851	2851-131	L80C	10	DMPC	500	5b-d9	50	6	trypsin	50 mM HEPES pH7
74	p2851	2851-141	L80C	10	DMPC	500	5b-d9	50	10	trypsin	50 mM HEPES pH7
75	p2851	2851-151	L80C	10	DMPC	500	5b-d9	50	15	trypsin	50 mM HEPES pH7
76	p2851	2851-161	L80C	10	DMPC	500	5b-d9	50	30	trypsin	50 mM HEPES pH7
77	p2851	2851-171	L274C	10	DMPC	500	5b-d9	50	0.5	trypsin	50 mM HEPES pH7
78	p2851	2851-181	L274C	10	DMPC	500	5b-d9	50	1	trypsin	50 mM HEPES pH7
79	p2851	2851-191	L274C	10	DMPC	500	5b-d9	50	2	trypsin	50 mM HEPES pH7
80	p2851	2851-201	L274C	10	DMPC	500	5b-d9	50	3	trypsin	50 mM HEPES pH7
81	p2851	2851-211	L274C	10	DMPC	500	5b-d9	50	6	trypsin	50 mM HEPES pH7
82	p2851	2851-221	L274C	10	DMPC	500	5b-d9	50	10	trypsin	50 mM HEPES pH7
83	p2851	2851-231	L274C	10	DMPC	500	5b-d9	50	15	trypsin	50 mM HEPES pH7
84	p2851	2851-241	L274C	10	DMPC	500	5b-d9	50	30	trypsin	50 mM HEPES pH7
85	p2851	2851-251	W333C	10	DMPC	500	5b-d9	50	0.5	trypsin	50 mM HEPES pH7
86	p2851	2851-261	W333C	10	DMPC	500	5b-d9	50	1	trypsin	50 mM HEPES pH7
87	p2851	2851-271	W333C	10	DMPC	500	5b-d9	50	2	trypsin	50 mM HEPES pH7
88	p2851	2851-281	W333C	10	DMPC	500	5b-d9	50	3	trypsin	50 mM HEPES pH7
89	p2851	2851-291	W333C	10	DMPC	500	5b-d9	50	6	trypsin	50 mM HEPES pH7
90	p2851	2851-301	W333C	10	DMPC	500	5b-d9	50	10	trypsin	50 mM HEPES pH7
91	p2851	2851-311	W333C	10	DMPC	500	5b-d9	50	15	trypsin	50 mM HEPES pH7
92	p2851	2851-321	W333C	10	DMPC	500	5b-d9	50	30	trypsin	50 mM HEPES pH7
93	p2851	2851-331	mutant 1	10	DMPC	500	5b-d9	50	0.5	trypsin	50 mM HEPES pH7
94	p2851	2851-341	mutant 1	10	DMPC	500	5b-d9	50	1	trypsin	50 mM HEPES pH7
95	p2851	2851-351	mutant 1	10	DMPC	500	5b-d9	50	2	trypsin	50 mM HEPES pH7
96	p2851	2851-361	mutant 1	10	DMPC	500	5b-d9	50	3	trypsin	50 mM HEPES pH7
97	p2851	2851-371	mutant 1	10	DMPC	500	5b-d9	50	6	trypsin	50 mM HEPES pH7
98	p2851	2851-381	mutant 1	10	DMPC	500	5b-d9	50	10	trypsin	50 mM HEPES pH7
99	p2851	2851-391	mutant 1	10	DMPC	500	5b-d9	50	15	trypsin	50 mM HEPES pH7
100	p2851	2851-401	mutant 1	10	DMPC	500	5b-d9	50	30	trypsin	50 mM HEPES pH7
101	p2851	2851-411	mutant 2	10	DMPC	500	5b-d9	50	0.5	trypsin	50 mM HEPES pH7
102	p2851	2851-421	mutant 2	10	DMPC	500	5b-d9	50	1	trypsin	50 mM HEPES pH7
103	p2851	2851-431	mutant 2	10	DMPC	500	5b-d9	50	2	trypsin	50 mM HEPES pH7

104	p2851	2851-441	mutant 2	10	DMPC	500	5b-d9	50	3	trypsin	50 mM HEPES pH7
105	p2851	2851-451	mutant 2	10	DMPC	500	5b-d9	50	6	trypsin	50 mM HEPES pH7
106	p2851	2851-461	mutant 2	10	DMPC	500	5b-d9	50	10	trypsin	50 mM HEPES pH7
107	p2851	2851-471	mutant 2	10	DMPC	500	5b-d9	50	15	trypsin	50 mM HEPES pH7
108	p2851	2851-481	mutant 2	10	DMPC	500	5b-d9	50	30	trypsin	50 mM HEPES pH7
109	p2851	2851-491	mutant 3	10	DMPC	500	5b-d9	50	0.5	trypsin	50 mM HEPES pH7
110	p2851	2851-501	mutant 3	10	DMPC	500	5b-d9	50	1	trypsin	50 mM HEPES pH7
111	p2851	2851-511	mutant 3	10	DMPC	500	5b-d9	50	2	trypsin	50 mM HEPES pH7
112	p2851	2851-521	mutant 3	10	DMPC	500	5b-d9	50	3	trypsin	50 mM HEPES pH7
113	p2851	2851-531	mutant 3	10	DMPC	500	5b-d9	50	6	trypsin	50 mM HEPES pH7
114	p2851	2851-541	mutant 3	10	DMPC	500	5b-d9	50	10	trypsin	50 mM HEPES pH7
115	p2851	2851-551	mutant 3	10	DMPC	500	5b-d9	50	15	trypsin	50 mM HEPES pH7
116	p2851	2851-561	mutant 3	10	DMPC	500	5b-d9	50	30	trypsin	50 mM HEPES pH7
117	p2851	2851-571	mutant 4	10	DMPC	500	5b-d9	50	0.5	trypsin	50 mM HEPES pH7
118	p2851	2851-581	mutant 4	10	DMPC	500	5b-d9	50	1	trypsin	50 mM HEPES pH7
119	p2851	2851-591	mutant 4	10	DMPC	500	5b-d9	50	2	trypsin	50 mM HEPES pH7
120	p2851	2851-601	mutant 4	10	DMPC	500	5b-d9	50	3	trypsin	50 mM HEPES pH7
121	p2851	2851-611	mutant 4	10	DMPC	500	5b-d9	50	6	trypsin	50 mM HEPES pH7
122	p2851	2851-621	mutant 4	10	DMPC	500	5b-d9	50	10	trypsin	50 mM HEPES pH7
123	p2851	2851-631	mutant 4	10	DMPC	500	5b-d9	50	15	trypsin	50 mM HEPES pH7
124	p2851	2851-641	mutant 4	10	DMPC	500	5b-d9	50	30	trypsin	50 mM HEPES pH7
125	p2851	2851-651	mutant 5	10	DMPC	500	5b-d9	50	0.5	trypsin	50 mM HEPES pH7
126	p2851	2851-661	mutant 5	10	DMPC	500	5b-d9	50	1	trypsin	50 mM HEPES pH7
127	p2851	2851-671	mutant 5	10	DMPC	500	5b-d9	50	2	trypsin	50 mM HEPES pH7
128	p2851	2851-681	mutant 5	10	DMPC	500	5b-d9	50	3	trypsin	50 mM HEPES pH7
129	p2851	2851-691	mutant 5	10	DMPC	500	5b-d9	50	6	trypsin	50 mM HEPES pH7
130	p2851	2851-701	mutant 5	10	DMPC	500	5b-d9	50	10	trypsin	50 mM HEPES pH7
131	p2851	2851-711	mutant 5	10	DMPC	500	5b-d9	50	15	trypsin	50 mM HEPES pH7
132	p2851	2851-721	mutant 5	10	DMPC	500	5b-d9	50	30	trypsin	50 mM HEPES pH7
133	p2851	2851-731	mutant 6	10	DMPC	500	5b-d9	50	0.5	trypsin	50 mM HEPES pH7
134	p2851	2851-741	mutant 6	10	DMPC	500	5b-d9	50	1	trypsin	50 mM HEPES pH7
135	p2851	2851-751	mutant 6	10	DMPC	500	5b-d9	50	2	trypsin	50 mM HEPES pH7
136	p2851	2851-761	mutant 6	10	DMPC	500	5b-d9	50	3	trypsin	50 mM HEPES pH7
137	p2851	2851-771	mutant 6	10	DMPC	500	5b-d9	50	6	trypsin	50 mM HEPES pH7
138	p2851	2851-781	mutant 6	10	DMPC	500	5b-d9	50	10	trypsin	50 mM HEPES pH7
139	p2851	2851-791	mutant 6	10	DMPC	500	5b-d9	50	15	trypsin	50 mM HEPES pH7
140	p2851	2851-801	mutant 6	10	DMPC	500	5b-d9	50	30	trypsin	50 mM HEPES pH7
141	p2865	2865-11	WT	10	DMPC	500	5b-d9	50	0.5	chymotrypsin	50 mM HEPES pH7
142	p2865	2865-21	WT	10	DMPC	500	5b-d9	50	1	chymotrypsin	50 mM HEPES pH7
143	p2865	2865-31	WT	10	DMPC	500	5b-d9	50	2	chymotrypsin	50 mM HEPES pH7
144	p2865	2865-41	WT	10	DMPC	500	5b-d9	50	3	chymotrypsin	50 mM HEPES pH7
145	p2865	2865-51	WT	10	DMPC	500	5b-d9	50	6	chymotrypsin	50 mM HEPES pH7
146	p2865	2865-61	WT	10	DMPC	500	5b-d9	50	10	chymotrypsin	50 mM HEPES pH7
147	p2865	2865-71	WT	10	DMPC	500	5b-d9	50	15	chymotrypsin	50 mM HEPES pH7
148	p2865	2865-81	WT	10	DMPC	500	5b-d9	50	30	chymotrypsin	50 mM HEPES pH7
149	p2865	2865-91	L80C	10	DMPC	500	5b-d9	50	0.5	chymotrypsin	50 mM HEPES pH7
150	p2865	2865-101	L80C	10	DMPC	500	5b-d9	50	1	chymotrypsin	50 mM HEPES pH7
151	p2865	2865-111	L80C	10	DMPC	500	5b-d9	50	2	chymotrypsin	50 mM HEPES pH7
152	p2865	2865-121	L80C	10	DMPC	500	5b-d9	50	3	chymotrypsin	50 mM HEPES pH7
153	p2865	2865-131	L80C	10	DMPC	500	5b-d9	50	6	chymotrypsin	50 mM HEPES pH7
154	p2865	2865-141	L80C	10	DMPC	500	5b-d9	50	10	chymotrypsin	50 mM HEPES pH7
155	p2865	2865-151	L80C	10	DMPC	500	5b-d9	50	15	chymotrypsin	50 mM HEPES pH7
156	p2865	2865-161	L80C	10	DMPC	500	5b-d9	50	30	chymotrypsin	50 mM HEPES pH7
157	p2865	2865-171	L274C	10	DMPC	500	5b-d9	50	0.5	chymotrypsin	50 mM HEPES pH7
158	p2865	2865-181	L274C	10	DMPC	500	5b-d9	50	1	chymotrypsin	50 mM HEPES pH7
159	p2865	2865-191	L274C	10	DMPC	500	5b-d9	50	2	chymotrypsin	50 mM HEPES pH7
160	p2865	2865-201	L274C	10	DMPC	500	5b-d9	50	3	chymotrypsin	50 mM HEPES pH7
161	p2865	2865-211	L274C	10	DMPC	500	5b-d9	50	6	chymotrypsin	50 mM HEPES pH7

162	p2865	2865-221	L274C	10	DMPC	500	5b-d9	50	10	chymotrypsin	50 mM HEPES pH7
163	p2865	2865-231	L274C	10	DMPC	500	5b-d9	50	15	chymotrypsin	50 mM HEPES pH7
164	p2865	2865-241	L274C	10	DMPC	500	5b-d9	50	30	chymotrypsin	50 mM HEPES pH7
165	p2865	2865-251	W333C	10	DMPC	500	5b-d9	50	0.5	chymotrypsin	50 mM HEPES pH7
166	p2865	2865-261	W333C	10	DMPC	500	5b-d9	50	1	chymotrypsin	50 mM HEPES pH7
167	p2865	2865-271	W333C	10	DMPC	500	5b-d9	50	2	chymotrypsin	50 mM HEPES pH7
168	p2865	2865-281	W333C	10	DMPC	500	5b-d9	50	3	chymotrypsin	50 mM HEPES pH7
169	p2865	2865-291	W333C	10	DMPC	500	5b-d9	50	6	chymotrypsin	50 mM HEPES pH7
170	p2865	2865-301	W333C	10	DMPC	500	5b-d9	50	10	chymotrypsin	50 mM HEPES pH7
171	p2865	2865-311	W333C	10	DMPC	500	5b-d9	50	15	chymotrypsin	50 mM HEPES pH7
172	p2865	2865-321	W333C	10	DMPC	500	5b-d9	50	30	chymotrypsin	50 mM HEPES pH7
173	p2865	2865-331	mutant 1	10	DMPC	500	5b-d9	50	0.5	chymotrypsin	50 mM HEPES pH7
174	p2865	2865-341	mutant 1	10	DMPC	500	5b-d9	50	1	chymotrypsin	50 mM HEPES pH7
175	p2865	2865-351	mutant 1	10	DMPC	500	5b-d9	50	2	chymotrypsin	50 mM HEPES pH7
176	p2865	2865-361	mutant 1	10	DMPC	500	5b-d9	50	3	chymotrypsin	50 mM HEPES pH7
177	p2865	2865-371	mutant 1	10	DMPC	500	5b-d9	50	6	chymotrypsin	50 mM HEPES pH7
178	p2865	2865-381	mutant 1	10	DMPC	500	5b-d9	50	10	chymotrypsin	50 mM HEPES pH7
179	p2865	2865-391	mutant 1	10	DMPC	500	5b-d9	50	15	chymotrypsin	50 mM HEPES pH7
180	p2865	2865-401	mutant 1	10	DMPC	500	5b-d9	50	30	chymotrypsin	50 mM HEPES pH7
181	p2865	2865-411	mutant 2	10	DMPC	500	5b-d9	50	0.5	chymotrypsin	50 mM HEPES pH7
182	p2865	2865-421	mutant 2	10	DMPC	500	5b-d9	50	1	chymotrypsin	50 mM HEPES pH7
183	p2865	2865-431	mutant 2	10	DMPC	500	5b-d9	50	2	chymotrypsin	50 mM HEPES pH7
184	p2865	2865-441	mutant 2	10	DMPC	500	5b-d9	50	3	chymotrypsin	50 mM HEPES pH7
185	p2865	2865-451	mutant 2	10	DMPC	500	5b-d9	50	6	chymotrypsin	50 mM HEPES pH7
186	p2865	2865-461	mutant 2	10	DMPC	500	5b-d9	50	10	chymotrypsin	50 mM HEPES pH7
187	p2865	2865-471	mutant 2	10	DMPC	500	5b-d9	50	15	chymotrypsin	50 mM HEPES pH7
188	p2865	2865-481	mutant 2	10	DMPC	500	5b-d9	50	30	chymotrypsin	50 mM HEPES pH7
189	p2865	2865-491	mutant 3	10	DMPC	500	5b-d9	50	0.5	chymotrypsin	50 mM HEPES pH7
190	p2865	2865-501	mutant 3	10	DMPC	500	5b-d9	50	1	chymotrypsin	50 mM HEPES pH7
191	p2865	2865-511	mutant 3	10	DMPC	500	5b-d9	50	2	chymotrypsin	50 mM HEPES pH7
192	p2865	2865-521	mutant 3	10	DMPC	500	5b-d9	50	3	chymotrypsin	50 mM HEPES pH7
193	p2865	2865-531	mutant 3	10	DMPC	500	5b-d9	50	6	chymotrypsin	50 mM HEPES pH7
194	p2865	2865-541	mutant 3	10	DMPC	500	5b-d9	50	10	chymotrypsin	50 mM HEPES pH7
195	p2865	2865-551	mutant 3	10	DMPC	500	5b-d9	50	15	chymotrypsin	50 mM HEPES pH7
196	p2865	2865-561	mutant 3	10	DMPC	500	5b-d9	50	30	chymotrypsin	50 mM HEPES pH7
197	p2865	2865-571	mutant 4	10	DMPC	500	5b-d9	50	0.5	chymotrypsin	50 mM HEPES pH7
198	p2865	2865-581	mutant 4	10	DMPC	500	5b-d9	50	1	chymotrypsin	50 mM HEPES pH7
199	p2865	2865-591	mutant 4	10	DMPC	500	5b-d9	50	2	chymotrypsin	50 mM HEPES pH7
200	p2865	2865-601	mutant 4	10	DMPC	500	5b-d9	50	3	chymotrypsin	50 mM HEPES pH7
201	p2865	2865-611	mutant 4	10	DMPC	500	5b-d9	50	6	chymotrypsin	50 mM HEPES pH7
202	p2865	2865-621	mutant 4	10	DMPC	500	5b-d9	50	10	chymotrypsin	50 mM HEPES pH7
203	p2865	2865-631	mutant 4	10	DMPC	500	5b-d9	50	15	chymotrypsin	50 mM HEPES pH7
204	p2865	2865-641	mutant 4	10	DMPC	500	5b-d9	50	30	chymotrypsin	50 mM HEPES pH7
205	p2865	2865-651	mutant 5	10	DMPC	500	5b-d9	50	0.5	chymotrypsin	50 mM HEPES pH7
206	p2865	2865-661	mutant 5	10	DMPC	500	5b-d9	50	1	chymotrypsin	50 mM HEPES pH7
207	p2865	2865-671	mutant 5	10	DMPC	500	5b-d9	50	2	chymotrypsin	50 mM HEPES pH7
208	p2865	2865-681	mutant 5	10	DMPC	500	5b-d9	50	3	chymotrypsin	50 mM HEPES pH7
209	p2865	2865-691	mutant 5	10	DMPC	500	5b-d9	50	6	chymotrypsin	50 mM HEPES pH7
210	p2865	2865-701	mutant 5	10	DMPC	500	5b-d9	50	10	chymotrypsin	50 mM HEPES pH7
211	p2865	2865-711	mutant 5	10	DMPC	500	5b-d9	50	15	chymotrypsin	50 mM HEPES pH7
212	p2865	2865-721	mutant 5	10	DMPC	500	5b-d9	50	30	chymotrypsin	50 mM HEPES pH7
213	p2865	2865-731	mutant 6	10	DMPC	500	5b-d9	50	0.5	chymotrypsin	50 mM HEPES pH7
214	p2865	2865-741	mutant 6	10	DMPC	500	5b-d9	50	1	chymotrypsin	50 mM HEPES pH7
215	p2865	2865-751	mutant 6	10	DMPC	500	5b-d9	50	2	chymotrypsin	50 mM HEPES pH7
216	p2865	2865-761	mutant 6	10	DMPC	500	5b-d9	50	3	chymotrypsin	50 mM HEPES pH7
217	p2865	2865-771	mutant 6	10	DMPC	500	5b-d9	50	6	chymotrypsin	50 mM HEPES pH7
218	p2865	2865-781	mutant 6	10	DMPC	500	5b-d9	50	10	chymotrypsin	50 mM HEPES pH7
219	p2865	2865-791	mutant 6	10	DMPC	500	5b-d9	50	15	chymotrypsin	50 mM HEPES pH7

220	p2865	2865-801	mutant 6	10	DMPC	500	5b-d9	50	30	chymotrypsin	50 mM HEPES pH7
221	p2855	2855-11	WT	10	DMPC/cholesterol(3/1)	500	5b-d9	50	0.5	trypsin	50 mM HEPES pH7
222	p2855	2855-21	WT	10	DMPC/cholesterol(3/1)	500	5b-d9	50	1	trypsin	50 mM HEPES pH7
223	p2855	2855-31	WT	10	DMPC/cholesterol(3/1)	500	5b-d9	50	2	trypsin	50 mM HEPES pH7
224	p2855	2855-41	WT	10	DMPC/cholesterol(3/1)	500	5b-d9	50	3	trypsin	50 mM HEPES pH7
225	p2855	2855-51	WT	10	DMPC/cholesterol(3/1)	500	5b-d9	50	6	trypsin	50 mM HEPES pH7
226	p2855	2855-61	WT	10	DMPC/cholesterol(3/1)	500	5b-d9	50	10	trypsin	50 mM HEPES pH7
227	p2855	2855-71	WT	10	DMPC/cholesterol(3/1)	500	5b-d9	50	15	trypsin	50 mM HEPES pH7
228	p2855	2855-81	WT	10	DMPC/cholesterol(3/1)	500	5b-d9	50	30	trypsin	50 mM HEPES pH7
229	p2855	2855-91	L80C	10	DMPC/cholesterol(3/1)	500	5b-d9	50	0.5	trypsin	50 mM HEPES pH7
230	p2855	2855-101	L80C	10	DMPC/cholesterol(3/1)	500	5b-d9	50	1	trypsin	50 mM HEPES pH7
231	p2855	2855-111	L80C	10	DMPC/cholesterol(3/1)	500	5b-d9	50	2	trypsin	50 mM HEPES pH7
232	p2855	2855-121	L80C	10	DMPC/cholesterol(3/1)	500	5b-d9	50	3	trypsin	50 mM HEPES pH7
233	p2855	2855-131	L80C	10	DMPC/cholesterol(3/1)	500	5b-d9	50	6	trypsin	50 mM HEPES pH7
234	p2855	2855-141	L80C	10	DMPC/cholesterol(3/1)	500	5b-d9	50	10	trypsin	50 mM HEPES pH7
235	p2855	2855-151	L80C	10	DMPC/cholesterol(3/1)	500	5b-d9	50	15	trypsin	50 mM HEPES pH7
236	p2855	2855-161	L80C	10	DMPC/cholesterol(3/1)	500	5b-d9	50	30	trypsin	50 mM HEPES pH7
237	p2855	2855-171	L274C	10	DMPC/cholesterol(3/1)	500	5b-d9	50	0.5	trypsin	50 mM HEPES pH7
238	p2855	2855-181	L274C	10	DMPC/cholesterol(3/1)	500	5b-d9	50	1	trypsin	50 mM HEPES pH7
239	p2855	2855-191	L274C	10	DMPC/cholesterol(3/1)	500	5b-d9	50	2	trypsin	50 mM HEPES pH7
240	p2855	2855-201	L274C	10	DMPC/cholesterol(3/1)	500	5b-d9	50	3	trypsin	50 mM HEPES pH7
241	p2855	2855-211	L274C	10	DMPC/cholesterol(3/1)	500	5b-d9	50	6	trypsin	50 mM HEPES pH7
242	p2855	2855-221	L274C	10	DMPC/cholesterol(3/1)	500	5b-d9	50	10	trypsin	50 mM HEPES pH7
243	p2855	2855-231	L274C	10	DMPC/cholesterol(3/1)	500	5b-d9	50	15	trypsin	50 mM HEPES pH7
244	p2855	2855-241	L274C	10	DMPC/cholesterol(3/1)	500	5b-d9	50	30	trypsin	50 mM HEPES pH7
245	p2855	2855-251	W333C	10	DMPC/cholesterol(3/1)	500	5b-d9	50	0.5	trypsin	50 mM HEPES pH7
246	p2855	2855-261	W333C	10	DMPC/cholesterol(3/1)	500	5b-d9	50	1	trypsin	50 mM HEPES pH7
247	p2855	2855-271	W333C	10	DMPC/cholesterol(3/1)	500	5b-d9	50	2	trypsin	50 mM HEPES pH7
248	p2855	2855-281	W333C	10	DMPC/cholesterol(3/1)	500	5b-d9	50	3	trypsin	50 mM HEPES pH7
249	p2855	2855-291	W333C	10	DMPC/cholesterol(3/1)	500	5b-d9	50	6	trypsin	50 mM HEPES pH7
250	p2855	2855-301	W333C	10	DMPC/cholesterol(3/1)	500	5b-d9	50	10	trypsin	50 mM HEPES pH7
251	p2855	2855-311	W333C	10	DMPC/cholesterol(3/1)	500	5b-d9	50	15	trypsin	50 mM HEPES pH7
252	p2855	2855-321	W333C	10	DMPC/cholesterol(3/1)	500	5b-d9	50	30	trypsin	50 mM HEPES pH7
253	p2855	2855-331	mutant 1	10	DMPC/cholesterol(3/1)	500	5b-d9	50	0.5	trypsin	50 mM HEPES pH7
254	p2855	2855-341	mutant 1	10	DMPC/cholesterol(3/1)	500	5b-d9	50	1	trypsin	50 mM HEPES pH7
255	p2855	2855-351	mutant 1	10	DMPC/cholesterol(3/1)	500	5b-d9	50	2	trypsin	50 mM HEPES pH7
256	p2855	2855-361	mutant 1	10	DMPC/cholesterol(3/1)	500	5b-d9	50	3	trypsin	50 mM HEPES pH7
257	p2855	2855-371	mutant 1	10	DMPC/cholesterol(3/1)	500	5b-d9	50	6	trypsin	50 mM HEPES pH7
258	p2855	2855-381	mutant 1	10	DMPC/cholesterol(3/1)	500	5b-d9	50	10	trypsin	50 mM HEPES pH7
259	p2855	2855-391	mutant 1	10	DMPC/cholesterol(3/1)	500	5b-d9	50	15	trypsin	50 mM HEPES pH7
260	p2855	2855-401	mutant 1	10	DMPC/cholesterol(3/1)	500	5b-d9	50	30	trypsin	50 mM HEPES pH7
261	p2855	2855-411	mutant 2	10	DMPC/cholesterol(3/1)	500	5b-d9	50	0.5	trypsin	50 mM HEPES pH7
262	p2855	2855-421	mutant 2	10	DMPC/cholesterol(3/1)	500	5b-d9	50	1	trypsin	50 mM HEPES pH7
263	p2855	2855-431	mutant 2	10	DMPC/cholesterol(3/1)	500	5b-d9	50	2	trypsin	50 mM HEPES pH7
264	p2855	2855-441	mutant 2	10	DMPC/cholesterol(3/1)	500	5b-d9	50	3	trypsin	50 mM HEPES pH7
265	p2855	2855-451	mutant 2	10	DMPC/cholesterol(3/1)	500	5b-d9	50	6	trypsin	50 mM HEPES pH7
266	p2855	2855-461	mutant 2	10	DMPC/cholesterol(3/1)	500	5b-d9	50	10	trypsin	50 mM HEPES pH7
267	p2855	2855-471	mutant 2	10	DMPC/cholesterol(3/1)	500	5b-d9	50	15	trypsin	50 mM HEPES pH7
268	p2855	2855-481	mutant 2	10	DMPC/cholesterol(3/1)	500	5b-d9	50	30	trypsin	50 mM HEPES pH7
269	p2855	2855-491	mutant 3	10	DMPC/cholesterol(3/1)	500	5b-d9	50	0.5	trypsin	50 mM HEPES pH7
270	p2855	2855-501	mutant 3	10	DMPC/cholesterol(3/1)	500	5b-d9	50	1	trypsin	50 mM HEPES pH7
271	p2855	2855-511	mutant 3	10	DMPC/cholesterol(3/1)	500	5b-d9	50	2	trypsin	50 mM HEPES pH7
272	p2855	2855-521	mutant 3	10	DMPC/cholesterol(3/1)	500	5b-d9	50	3	trypsin	50 mM HEPES pH7
273	p2855	2855-531	mutant 3	10	DMPC/cholesterol(3/1)	500	5b-d9	50	6	trypsin	50 mM HEPES pH7
274	p2855	2855-541	mutant 3	10	DMPC/cholesterol(3/1)	500	5b-d9	50	10	trypsin	50 mM HEPES pH7
275	p2855	2855-551	mutant 3	10	DMPC/cholesterol(3/1)	500	5b-d9	50	15	trypsin	50 mM HEPES pH7
276	p2855	2855-561	mutant 3	10	DMPC/cholesterol(3/1)	500	5b-d9	50	30	trypsin	50 mM HEPES pH7
277	p2855	2855-571	mutant 4	10	DMPC/cholesterol(3/1)	500	5b-d9	50	0.5	trypsin	50 mM HEPES pH7

278	p2855	2855-581	mutant 4	10	DMPC/cholesterol(3/1)	500	5b-d9	50	1	trypsin	50 mM HEPES pH7
279	p2855	2855-591	mutant 4	10	DMPC/cholesterol(3/1)	500	5b-d9	50	2	trypsin	50 mM HEPES pH7
280	p2855	2855-601	mutant 4	10	DMPC/cholesterol(3/1)	500	5b-d9	50	3	trypsin	50 mM HEPES pH7
281	p2855	2855-611	mutant 4	10	DMPC/cholesterol(3/1)	500	5b-d9	50	6	trypsin	50 mM HEPES pH7
282	p2855	2855-621	mutant 4	10	DMPC/cholesterol(3/1)	500	5b-d9	50	10	trypsin	50 mM HEPES pH7
283	p2855	2855-631	mutant 4	10	DMPC/cholesterol(3/1)	500	5b-d9	50	15	trypsin	50 mM HEPES pH7
284	p2855	2855-641	mutant 4	10	DMPC/cholesterol(3/1)	500	5b-d9	50	30	trypsin	50 mM HEPES pH7
285	p2855	2855-651	mutant 5	10	DMPC/cholesterol(3/1)	500	5b-d9	50	0.5	trypsin	50 mM HEPES pH7
286	p2855	2855-661	mutant 5	10	DMPC/cholesterol(3/1)	500	5b-d9	50	1	trypsin	50 mM HEPES pH7
287	p2855	2855-671	mutant 5	10	DMPC/cholesterol(3/1)	500	5b-d9	50	2	trypsin	50 mM HEPES pH7
288	p2855	2855-681	mutant 5	10	DMPC/cholesterol(3/1)	500	5b-d9	50	3	trypsin	50 mM HEPES pH7
289	p2855	2855-691	mutant 5	10	DMPC/cholesterol(3/1)	500	5b-d9	50	6	trypsin	50 mM HEPES pH7
290	p2855	2855-701	mutant 5	10	DMPC/cholesterol(3/1)	500	5b-d9	50	10	trypsin	50 mM HEPES pH7
291	p2855	2855-711	mutant 5	10	DMPC/cholesterol(3/1)	500	5b-d9	50	15	trypsin	50 mM HEPES pH7
292	p2855	2855-721	mutant 5	10	DMPC/cholesterol(3/1)	500	5b-d9	50	30	trypsin	50 mM HEPES pH7
293	p2855	2855-731	mutant 6	10	DMPC/cholesterol(3/1)	500	5b-d9	50	0.5	trypsin	50 mM HEPES pH7
294	p2855	2855-741	mutant 6	10	DMPC/cholesterol(3/1)	500	5b-d9	50	1	trypsin	50 mM HEPES pH7
295	p2855	2855-751	mutant 6	10	DMPC/cholesterol(3/1)	500	5b-d9	50	2	trypsin	50 mM HEPES pH7
296	p2855	2855-761	mutant 6	10	DMPC/cholesterol(3/1)	500	5b-d9	50	3	trypsin	50 mM HEPES pH7
297	p2855	2855-771	mutant 6	10	DMPC/cholesterol(3/1)	500	5b-d9	50	6	trypsin	50 mM HEPES pH7
298	p2855	2855-781	mutant 6	10	DMPC/cholesterol(3/1)	500	5b-d9	50	10	trypsin	50 mM HEPES pH7
299	p2855	2855-791	mutant 6	10	DMPC/cholesterol(3/1)	500	5b-d9	50	15	trypsin	50 mM HEPES pH7
300	p2855	2855-801	mutant 6	10	DMPC/cholesterol(3/1)	500	5b-d9	50	30	trypsin	50 mM HEPES pH7
301	p2860	2860-11	WT	10	DMPC/cholesterol(3/1)	500	5b-d9	50	0.5	chymotrypsin	50 mM HEPES pH7
302	p2860	2860-21	WT	10	DMPC/cholesterol(3/1)	500	5b-d9	50	1	chymotrypsin	50 mM HEPES pH7
303	p2860	2860-31	WT	10	DMPC/cholesterol(3/1)	500	5b-d9	50	2	chymotrypsin	50 mM HEPES pH7
304	p2860	2860-41	WT	10	DMPC/cholesterol(3/1)	500	5b-d9	50	3	chymotrypsin	50 mM HEPES pH7
305	p2860	2860-51	WT	10	DMPC/cholesterol(3/1)	500	5b-d9	50	6	chymotrypsin	50 mM HEPES pH7
306	p2860	2860-61	WT	10	DMPC/cholesterol(3/1)	500	5b-d9	50	10	chymotrypsin	50 mM HEPES pH7
307	p2860	2860-71	WT	10	DMPC/cholesterol(3/1)	500	5b-d9	50	15	chymotrypsin	50 mM HEPES pH7
308	p2860	2860-81	WT	10	DMPC/cholesterol(3/1)	500	5b-d9	50	30	chymotrypsin	50 mM HEPES pH7
309	p2860	2860-91	L80C	10	DMPC/cholesterol(3/1)	500	5b-d9	50	0.5	chymotrypsin	50 mM HEPES pH7
310	p2860	2860-101	L80C	10	DMPC/cholesterol(3/1)	500	5b-d9	50	1	chymotrypsin	50 mM HEPES pH7
311	p2860	2860-111	L80C	10	DMPC/cholesterol(3/1)	500	5b-d9	50	2	chymotrypsin	50 mM HEPES pH7
312	p2860	2860-121	L80C	10	DMPC/cholesterol(3/1)	500	5b-d9	50	3	chymotrypsin	50 mM HEPES pH7
313	p2860	2860-131	L80C	10	DMPC/cholesterol(3/1)	500	5b-d9	50	6	chymotrypsin	50 mM HEPES pH7
314	p2860	2860-141	L80C	10	DMPC/cholesterol(3/1)	500	5b-d9	50	10	chymotrypsin	50 mM HEPES pH7
315	p2860	2860-151	L80C	10	DMPC/cholesterol(3/1)	500	5b-d9	50	15	chymotrypsin	50 mM HEPES pH7
316	p2860	2860-161	L80C	10	DMPC/cholesterol(3/1)	500	5b-d9	50	30	chymotrypsin	50 mM HEPES pH7
317	p2860	2860-171	L274C	10	DMPC/cholesterol(3/1)	500	5b-d9	50	0.5	chymotrypsin	50 mM HEPES pH7
318	p2860	2860-181	L274C	10	DMPC/cholesterol(3/1)	500	5b-d9	50	1	chymotrypsin	50 mM HEPES pH7
319	p2860	2860-191	L274C	10	DMPC/cholesterol(3/1)	500	5b-d9	50	2	chymotrypsin	50 mM HEPES pH7
320	p2860	2860-201	L274C	10	DMPC/cholesterol(3/1)	500	5b-d9	50	3	chymotrypsin	50 mM HEPES pH7
321	p2860	2860-211	L274C	10	DMPC/cholesterol(3/1)	500	5b-d9	50	6	chymotrypsin	50 mM HEPES pH7
322	p2860	2860-221	L274C	10	DMPC/cholesterol(3/1)	500	5b-d9	50	10	chymotrypsin	50 mM HEPES pH7
323	p2860	2860-231	L274C	10	DMPC/cholesterol(3/1)	500	5b-d9	50	15	chymotrypsin	50 mM HEPES pH7
324	p2860	2860-241	L274C	10	DMPC/cholesterol(3/1)	500	5b-d9	50	30	chymotrypsin	50 mM HEPES pH7
325	p2860	2860-251	W333C	10	DMPC/cholesterol(3/1)	500	5b-d9	50	0.5	chymotrypsin	50 mM HEPES pH7
326	p2860	2860-261	W333C	10	DMPC/cholesterol(3/1)	500	5b-d9	50	1	chymotrypsin	50 mM HEPES pH7
327	p2860	2860-271	W333C	10	DMPC/cholesterol(3/1)	500	5b-d9	50	2	chymotrypsin	50 mM HEPES pH7
328	p2860	2860-281	W333C	10	DMPC/cholesterol(3/1)	500	5b-d9	50	3	chymotrypsin	50 mM HEPES pH7
329	p2860	2860-291	W333C	10	DMPC/cholesterol(3/1)	500	5b-d9	50	6	chymotrypsin	50 mM HEPES pH7
330	p2860	2860-301	W333C	10	DMPC/cholesterol(3/1)	500	5b-d9	50	10	chymotrypsin	50 mM HEPES pH7
331	p2860	2860-311	W333C	10	DMPC/cholesterol(3/1)	500	5b-d9	50	15	chymotrypsin	50 mM HEPES pH7
332	p2860	2860-321	W333C	10	DMPC/cholesterol(3/1)	500	5b-d9	50	30	chymotrypsin	50 mM HEPES pH7
333	p2860	2860-331	mutant 1	10	DMPC/cholesterol(3/1)	500	5b-d9	50	0.5	chymotrypsin	50 mM HEPES pH7
334	p2860	2860-341	mutant 1	10	DMPC/cholesterol(3/1)	500	5b-d9	50	1	chymotrypsin	50 mM HEPES pH7
335	p2860	2860-351	mutant 1	10	DMPC/cholesterol(3/1)	500	5b-d9	50	2	chymotrypsin	50 mM HEPES pH7

336	p2860	2860-361	mutant 1	10	DMPC/cholesterol(3/1)	500	5b-d9	50	3	chymotrypsin	50 mM HEPES pH7
337	p2860	2860-371	mutant 1	10	DMPC/cholesterol(3/1)	500	5b-d9	50	6	chymotrypsin	50 mM HEPES pH7
338	p2860	2860-381	mutant 1	10	DMPC/cholesterol(3/1)	500	5b-d9	50	10	chymotrypsin	50 mM HEPES pH7
339	p2860	2860-391	mutant 1	10	DMPC/cholesterol(3/1)	500	5b-d9	50	15	chymotrypsin	50 mM HEPES pH7
340	p2860	2860-401	mutant 1	10	DMPC/cholesterol(3/1)	500	5b-d9	50	30	chymotrypsin	50 mM HEPES pH7
341	p2860	2860-411	mutant 2	10	DMPC/cholesterol(3/1)	500	5b-d9	50	0.5	chymotrypsin	50 mM HEPES pH7
342	p2860	2860-421	mutant 2	10	DMPC/cholesterol(3/1)	500	5b-d9	50	1	chymotrypsin	50 mM HEPES pH7
343	p2860	2860-431	mutant 2	10	DMPC/cholesterol(3/1)	500	5b-d9	50	2	chymotrypsin	50 mM HEPES pH7
344	p2860	2860-441	mutant 2	10	DMPC/cholesterol(3/1)	500	5b-d9	50	3	chymotrypsin	50 mM HEPES pH7
345	p2860	2860-451	mutant 2	10	DMPC/cholesterol(3/1)	500	5b-d9	50	6	chymotrypsin	50 mM HEPES pH7
346	p2860	2860-461	mutant 2	10	DMPC/cholesterol(3/1)	500	5b-d9	50	10	chymotrypsin	50 mM HEPES pH7
347	p2860	2860-471	mutant 2	10	DMPC/cholesterol(3/1)	500	5b-d9	50	15	chymotrypsin	50 mM HEPES pH7
348	p2860	2860-481	mutant 2	10	DMPC/cholesterol(3/1)	500	5b-d9	50	30	chymotrypsin	50 mM HEPES pH7
349	p2860	2860-491	mutant 3	10	DMPC/cholesterol(3/1)	500	5b-d9	50	0.5	chymotrypsin	50 mM HEPES pH7
350	p2860	2860-501	mutant 3	10	DMPC/cholesterol(3/1)	500	5b-d9	50	1	chymotrypsin	50 mM HEPES pH7
351	p2860	2860-511	mutant 3	10	DMPC/cholesterol(3/1)	500	5b-d9	50	2	chymotrypsin	50 mM HEPES pH7
352	p2860	2860-521	mutant 3	10	DMPC/cholesterol(3/1)	500	5b-d9	50	3	chymotrypsin	50 mM HEPES pH7
353	p2860	2860-531	mutant 3	10	DMPC/cholesterol(3/1)	500	5b-d9	50	6	chymotrypsin	50 mM HEPES pH7
354	p2860	2860-541	mutant 3	10	DMPC/cholesterol(3/1)	500	5b-d9	50	10	chymotrypsin	50 mM HEPES pH7
355	p2860	2860-551	mutant 3	10	DMPC/cholesterol(3/1)	500	5b-d9	50	15	chymotrypsin	50 mM HEPES pH7
356	p2860	2860-561	mutant 3	10	DMPC/cholesterol(3/1)	500	5b-d9	50	30	chymotrypsin	50 mM HEPES pH7
357	p2860	2860-571	mutant 4	10	DMPC/cholesterol(3/1)	500	5b-d9	50	0.5	chymotrypsin	50 mM HEPES pH7
358	p2860	2860-581	mutant 4	10	DMPC/cholesterol(3/1)	500	5b-d9	50	1	chymotrypsin	50 mM HEPES pH7
359	p2860	2860-591	mutant 4	10	DMPC/cholesterol(3/1)	500	5b-d9	50	2	chymotrypsin	50 mM HEPES pH7
360	p2860	2860-601	mutant 4	10	DMPC/cholesterol(3/1)	500	5b-d9	50	3	chymotrypsin	50 mM HEPES pH7
361	p2860	2860-611	mutant 4	10	DMPC/cholesterol(3/1)	500	5b-d9	50	6	chymotrypsin	50 mM HEPES pH7
362	p2860	2860-621	mutant 4	10	DMPC/cholesterol(3/1)	500	5b-d9	50	10	chymotrypsin	50 mM HEPES pH7
363	p2860	2860-631	mutant 4	10	DMPC/cholesterol(3/1)	500	5b-d9	50	15	chymotrypsin	50 mM HEPES pH7
364	p2860	2860-641	mutant 4	10	DMPC/cholesterol(3/1)	500	5b-d9	50	30	chymotrypsin	50 mM HEPES pH7
365	p2860	2860-651	mutant 5	10	DMPC/cholesterol(3/1)	500	5b-d9	50	0.5	chymotrypsin	50 mM HEPES pH7
366	p2860	2860-661	mutant 5	10	DMPC/cholesterol(3/1)	500	5b-d9	50	1	chymotrypsin	50 mM HEPES pH7
367	p2860	2860-671	mutant 5	10	DMPC/cholesterol(3/1)	500	5b-d9	50	2	chymotrypsin	50 mM HEPES pH7
368	p2860	2860-681	mutant 5	10	DMPC/cholesterol(3/1)	500	5b-d9	50	3	chymotrypsin	50 mM HEPES pH7
369	p2860	2860-691	mutant 5	10	DMPC/cholesterol(3/1)	500	5b-d9	50	6	chymotrypsin	50 mM HEPES pH7
370	p2860	2860-701	mutant 5	10	DMPC/cholesterol(3/1)	500	5b-d9	50	10	chymotrypsin	50 mM HEPES pH7
371	p2860	2860-711	mutant 5	10	DMPC/cholesterol(3/1)	500	5b-d9	50	15	chymotrypsin	50 mM HEPES pH7
372	p2860	2860-721	mutant 5	10	DMPC/cholesterol(3/1)	500	5b-d9	50	30	chymotrypsin	50 mM HEPES pH7
373	p2860	2860-731	mutant 6	10	DMPC/cholesterol(3/1)	500	5b-d9	50	0.5	chymotrypsin	50 mM HEPES pH7
374	p2860	2860-741	mutant 6	10	DMPC/cholesterol(3/1)	500	5b-d9	50	1	chymotrypsin	50 mM HEPES pH7
375	p2860	2860-751	mutant 6	10	DMPC/cholesterol(3/1)	500	5b-d9	50	2	chymotrypsin	50 mM HEPES pH7
376	p2860	2860-761	mutant 6	10	DMPC/cholesterol(3/1)	500	5b-d9	50	3	chymotrypsin	50 mM HEPES pH7
377	p2860	2860-771	mutant 6	10	DMPC/cholesterol(3/1)	500	5b-d9	50	6	chymotrypsin	50 mM HEPES pH7
378	p2860	2860-781	mutant 6	10	DMPC/cholesterol(3/1)	500	5b-d9	50	10	chymotrypsin	50 mM HEPES pH7
379	p2860	2860-791	mutant 6	10	DMPC/cholesterol(3/1)	500	5b-d9	50	15	chymotrypsin	50 mM HEPES pH7
380	p2860	2860-801	mutant 6	10	DMPC/cholesterol(3/1)	500	5b-d9	50	30	chymotrypsin	50 mM HEPES pH7
381	p2853	2853-11	WT	10	DMPC/cholest-4-en-3-one(3/1)	500	5b-d9	50	0.5	trypsin	50 mM HEPES pH7
382	p2853	2853-21	WT	10	DMPC/cholest-4-en-3-one(3/1)	500	5b-d9	50	1	trypsin	50 mM HEPES pH7
383	p2853	2853-31	WT	10	DMPC/cholest-4-en-3-one(3/1)	500	5b-d9	50	2	trypsin	50 mM HEPES pH7
384	p2853	2853-41	WT	10	DMPC/cholest-4-en-3-one(3/1)	500	5b-d9	50	3	trypsin	50 mM HEPES pH7
385	p2853	2853-51	WT	10	DMPC/cholest-4-en-3-one(3/1)	500	5b-d9	50	6	trypsin	50 mM HEPES pH7
386	p2853	2853-61	WT	10	DMPC/cholest-4-en-3-one(3/1)	500	5b-d9	50	10	trypsin	50 mM HEPES pH7
387	p2853	2853-71	WT	10	DMPC/cholest-4-en-3-one(3/1)	500	5b-d9	50	15	trypsin	50 mM HEPES pH7
388	p2853	2853-81	WT	10	DMPC/cholest-4-en-3-one(3/1)	500	5b-d9	50	30	trypsin	50 mM HEPES pH7
389	p2853	2853-91	L80C	10	DMPC/cholest-4-en-3-one(3/1)	500	5b-d9	50	0.5	trypsin	50 mM HEPES pH7
390	p2853	2853-101	L80C	10	DMPC/cholest-4-en-3-one(3/1)	500	5b-d9	50	1	trypsin	50 mM HEPES pH7
391	p2853	2853-111	L80C	10	DMPC/cholest-4-en-3-one(3/1)	500	5b-d9	50	2	trypsin	50 mM HEPES pH7
392	p2853	2853-121	L80C	10	DMPC/cholest-4-en-3-one(3/1)	500	5b-d9	50	3	trypsin	50 mM HEPES pH7
393	p2853	2853-131	L80C	10	DMPC/cholest-4-en-3-one(3/1)	500	5b-d9	50	6	trypsin	50 mM HEPES pH7

394	p2853	2853-141	L80C	10	DMPC/cholest-4-en-3-one(3/1)	500	5b-d9	50	10	trypsin	50 mM HEPES pH7
395	p2853	2853-151	L80C	10	DMPC/cholest-4-en-3-one(3/1)	500	5b-d9	50	15	trypsin	50 mM HEPES pH7
396	p2853	2853-161	L80C	10	DMPC/cholest-4-en-3-one(3/1)	500	5b-d9	50	30	trypsin	50 mM HEPES pH7
397	p2853	2853-171	L274C	10	DMPC/cholest-4-en-3-one(3/1)	500	5b-d9	50	0.5	trypsin	50 mM HEPES pH7
398	p2853	2853-181	L274C	10	DMPC/cholest-4-en-3-one(3/1)	500	5b-d9	50	1	trypsin	50 mM HEPES pH7
399	p2853	2853-191	L274C	10	DMPC/cholest-4-en-3-one(3/1)	500	5b-d9	50	2	trypsin	50 mM HEPES pH7
400	p2853	2853-201	L274C	10	DMPC/cholest-4-en-3-one(3/1)	500	5b-d9	50	3	trypsin	50 mM HEPES pH7
401	p2853	2853-211	L274C	10	DMPC/cholest-4-en-3-one(3/1)	500	5b-d9	50	6	trypsin	50 mM HEPES pH7
402	p2853	2853-221	L274C	10	DMPC/cholest-4-en-3-one(3/1)	500	5b-d9	50	10	trypsin	50 mM HEPES pH7
403	p2853	2853-231	L274C	10	DMPC/cholest-4-en-3-one(3/1)	500	5b-d9	50	15	trypsin	50 mM HEPES pH7
404	p2853	2853-241	L274C	10	DMPC/cholest-4-en-3-one(3/1)	500	5b-d9	50	30	trypsin	50 mM HEPES pH7
405	p2853	2853-251	W333C	10	DMPC/cholest-4-en-3-one(3/1)	500	5b-d9	50	0.5	trypsin	50 mM HEPES pH7
406	p2853	2853-261	W333C	10	DMPC/cholest-4-en-3-one(3/1)	500	5b-d9	50	1	trypsin	50 mM HEPES pH7
407	p2853	2853-271	W333C	10	DMPC/cholest-4-en-3-one(3/1)	500	5b-d9	50	2	trypsin	50 mM HEPES pH7
408	p2853	2853-281	W333C	10	DMPC/cholest-4-en-3-one(3/1)	500	5b-d9	50	3	trypsin	50 mM HEPES pH7
409	p2853	2853-291	W333C	10	DMPC/cholest-4-en-3-one(3/1)	500	5b-d9	50	6	trypsin	50 mM HEPES pH7
410	p2853	2853-301	W333C	10	DMPC/cholest-4-en-3-one(3/1)	500	5b-d9	50	10	trypsin	50 mM HEPES pH7
411	p2853	2853-311	W333C	10	DMPC/cholest-4-en-3-one(3/1)	500	5b-d9	50	15	trypsin	50 mM HEPES pH7
412	p2853	2853-321	W333C	10	DMPC/cholest-4-en-3-one(3/1)	500	5b-d9	50	30	trypsin	50 mM HEPES pH7
413	p2853	2853-331	mutant 1	10	DMPC/cholest-4-en-3-one(3/1)	500	5b-d9	50	0.5	trypsin	50 mM HEPES pH7
414	p2853	2853-341	mutant 1	10	DMPC/cholest-4-en-3-one(3/1)	500	5b-d9	50	1	trypsin	50 mM HEPES pH7
415	p2853	2853-351	mutant 1	10	DMPC/cholest-4-en-3-one(3/1)	500	5b-d9	50	2	trypsin	50 mM HEPES pH7
416	p2853	2853-361	mutant 1	10	DMPC/cholest-4-en-3-one(3/1)	500	5b-d9	50	3	trypsin	50 mM HEPES pH7
417	p2853	2853-371	mutant 1	10	DMPC/cholest-4-en-3-one(3/1)	500	5b-d9	50	6	trypsin	50 mM HEPES pH7
418	p2853	2853-381	mutant 1	10	DMPC/cholest-4-en-3-one(3/1)	500	5b-d9	50	10	trypsin	50 mM HEPES pH7
419	p2853	2853-391	mutant 1	10	DMPC/cholest-4-en-3-one(3/1)	500	5b-d9	50	15	trypsin	50 mM HEPES pH7
420	p2853	2853-401	mutant 1	10	DMPC/cholest-4-en-3-one(3/1)	500	5b-d9	50	30	trypsin	50 mM HEPES pH7
421	p2853	2853-411	mutant 2	10	DMPC/cholest-4-en-3-one(3/1)	500	5b-d9	50	0.5	trypsin	50 mM HEPES pH7
422	p2853	2853-421	mutant 2	10	DMPC/cholest-4-en-3-one(3/1)	500	5b-d9	50	1	trypsin	50 mM HEPES pH7
423	p2853	2853-431	mutant 2	10	DMPC/cholest-4-en-3-one(3/1)	500	5b-d9	50	2	trypsin	50 mM HEPES pH7
424	p2853	2853-441	mutant 2	10	DMPC/cholest-4-en-3-one(3/1)	500	5b-d9	50	3	trypsin	50 mM HEPES pH7
425	p2853	2853-451	mutant 2	10	DMPC/cholest-4-en-3-one(3/1)	500	5b-d9	50	6	trypsin	50 mM HEPES pH7
426	p2853	2853-461	mutant 2	10	DMPC/cholest-4-en-3-one(3/1)	500	5b-d9	50	10	trypsin	50 mM HEPES pH7
427	p2853	2853-471	mutant 2	10	DMPC/cholest-4-en-3-one(3/1)	500	5b-d9	50	15	trypsin	50 mM HEPES pH7
428	p2853	2853-481	mutant 2	10	DMPC/cholest-4-en-3-one(3/1)	500	5b-d9	50	30	trypsin	50 mM HEPES pH7
429	p2853	2853-491	mutant 3	10	DMPC/cholest-4-en-3-one(3/1)	500	5b-d9	50	0.5	trypsin	50 mM HEPES pH7
430	p2853	2853-501	mutant 3	10	DMPC/cholest-4-en-3-one(3/1)	500	5b-d9	50	1	trypsin	50 mM HEPES pH7
431	p2853	2853-511	mutant 3	10	DMPC/cholest-4-en-3-one(3/1)	500	5b-d9	50	2	trypsin	50 mM HEPES pH7
432	p2853	2853-521	mutant 3	10	DMPC/cholest-4-en-3-one(3/1)	500	5b-d9	50	3	trypsin	50 mM HEPES pH7
433	p2853	2853-531	mutant 3	10	DMPC/cholest-4-en-3-one(3/1)	500	5b-d9	50	6	trypsin	50 mM HEPES pH7
434	p2853	2853-541	mutant 3	10	DMPC/cholest-4-en-3-one(3/1)	500	5b-d9	50	10	trypsin	50 mM HEPES pH7
435	p2853	2853-551	mutant 3	10	DMPC/cholest-4-en-3-one(3/1)	500	5b-d9	50	15	trypsin	50 mM HEPES pH7
436	p2853	2853-561	mutant 3	10	DMPC/cholest-4-en-3-one(3/1)	500	5b-d9	50	30	trypsin	50 mM HEPES pH7
437	p2853	2853-571	mutant 4	10	DMPC/cholest-4-en-3-one(3/1)	500	5b-d9	50	0.5	trypsin	50 mM HEPES pH7
438	p2853	2853-581	mutant 4	10	DMPC/cholest-4-en-3-one(3/1)	500	5b-d9	50	1	trypsin	50 mM HEPES pH7
439	p2853	2853-591	mutant 4	10	DMPC/cholest-4-en-3-one(3/1)	500	5b-d9	50	2	trypsin	50 mM HEPES pH7
440	p2853	2853-601	mutant 4	10	DMPC/cholest-4-en-3-one(3/1)	500	5b-d9	50	3	trypsin	50 mM HEPES pH7
441	p2853	2853-611	mutant 4	10	DMPC/cholest-4-en-3-one(3/1)	500	5b-d9	50	6	trypsin	50 mM HEPES pH7
442	p2853	2853-621	mutant 4	10	DMPC/cholest-4-en-3-one(3/1)	500	5b-d9	50	10	trypsin	50 mM HEPES pH7
443	p2853	2853-631	mutant 4	10	DMPC/cholest-4-en-3-one(3/1)	500	5b-d9	50	15	trypsin	50 mM HEPES pH7
444	p2853	2853-641	mutant 4	10	DMPC/cholest-4-en-3-one(3/1)	500	5b-d9	50	30	trypsin	50 mM HEPES pH7
445	p2853	2853-651	mutant 5	10	DMPC/cholest-4-en-3-one(3/1)	500	5b-d9	50	0.5	trypsin	50 mM HEPES pH7
446	p2853	2853-661	mutant 5	10	DMPC/cholest-4-en-3-one(3/1)	500	5b-d9	50	1	trypsin	50 mM HEPES pH7
447	p2853	2853-671	mutant 5	10	DMPC/cholest-4-en-3-one(3/1)	500	5b-d9	50	2	trypsin	50 mM HEPES pH7
448	p2853	2853-681	mutant 5	10	DMPC/cholest-4-en-3-one(3/1)	500	5b-d9	50	3	trypsin	50 mM HEPES pH7
449	p2853	2853-691	mutant 5	10	DMPC/cholest-4-en-3-one(3/1)	500	5b-d9	50	6	trypsin	50 mM HEPES pH7
450	p2853	2853-701	mutant 5	10	DMPC/cholest-4-en-3-one(3/1)	500	5b-d9	50	10	trypsin	50 mM HEPES pH7
451	p2853	2853-711	mutant 5	10	DMPC/cholest-4-en-3-one(3/1)	500	5b-d9	50	15	trypsin	50 mM HEPES pH7

452	p2853	2853-721	mutant 5	10	DMPC/cholest-4-en-3-one(3/1)	500	5b-d9	50	30	trypsin	50 mM HEPES pH7
453	p2853	2853-731	mutant 6	10	DMPC/cholest-4-en-3-one(3/1)	500	5b-d9	50	0.5	trypsin	50 mM HEPES pH7
454	p2853	2853-741	mutant 6	10	DMPC/cholest-4-en-3-one(3/1)	500	5b-d9	50	1	trypsin	50 mM HEPES pH7
455	p2853	2853-751	mutant 6	10	DMPC/cholest-4-en-3-one(3/1)	500	5b-d9	50	2	trypsin	50 mM HEPES pH7
456	p2853	2853-761	mutant 6	10	DMPC/cholest-4-en-3-one(3/1)	500	5b-d9	50	3	trypsin	50 mM HEPES pH7
457	p2853	2853-771	mutant 6	10	DMPC/cholest-4-en-3-one(3/1)	500	5b-d9	50	6	trypsin	50 mM HEPES pH7
458	p2853	2853-781	mutant 6	10	DMPC/cholest-4-en-3-one(3/1)	500	5b-d9	50	10	trypsin	50 mM HEPES pH7
459	p2853	2853-791	mutant 6	10	DMPC/cholest-4-en-3-one(3/1)	500	5b-d9	50	15	trypsin	50 mM HEPES pH7
460	p2853	2853-801	mutant 6	10	DMPC/cholest-4-en-3-one(3/1)	500	5b-d9	50	30	trypsin	50 mM HEPES pH7
461	p2863	2863-11	WT	10	DMPC/cholest-4-en-3-one(3/1)	500	5b-d9	50	0.5	chymotrypsin	50 mM HEPES pH7
462	p2863	2863-21	WT	10	DMPC/cholest-4-en-3-one(3/1)	500	5b-d9	50	1	chymotrypsin	50 mM HEPES pH7
463	p2863	2863-31	WT	10	DMPC/cholest-4-en-3-one(3/1)	500	5b-d9	50	2	chymotrypsin	50 mM HEPES pH7
464	p2863	2863-41	WT	10	DMPC/cholest-4-en-3-one(3/1)	500	5b-d9	50	3	chymotrypsin	50 mM HEPES pH7
465	p2863	2863-51	WT	10	DMPC/cholest-4-en-3-one(3/1)	500	5b-d9	50	6	chymotrypsin	50 mM HEPES pH7
466	p2863	2863-61	WT	10	DMPC/cholest-4-en-3-one(3/1)	500	5b-d9	50	10	chymotrypsin	50 mM HEPES pH7
467	p2863	2863-71	WT	10	DMPC/cholest-4-en-3-one(3/1)	500	5b-d9	50	15	chymotrypsin	50 mM HEPES pH7
468	p2863	2863-81	WT	10	DMPC/cholest-4-en-3-one(3/1)	500	5b-d9	50	30	chymotrypsin	50 mM HEPES pH7
469	p2863	2863-91	L80C	10	DMPC/cholest-4-en-3-one(3/1)	500	5b-d9	50	0.5	chymotrypsin	50 mM HEPES pH7
470	p2863	2863-101	L80C	10	DMPC/cholest-4-en-3-one(3/1)	500	5b-d9	50	1	chymotrypsin	50 mM HEPES pH7
471	p2863	2863-111	L80C	10	DMPC/cholest-4-en-3-one(3/1)	500	5b-d9	50	2	chymotrypsin	50 mM HEPES pH7
472	p2863	2863-121	L80C	10	DMPC/cholest-4-en-3-one(3/1)	500	5b-d9	50	3	chymotrypsin	50 mM HEPES pH7
473	p2863	2863-131	L80C	10	DMPC/cholest-4-en-3-one(3/1)	500	5b-d9	50	6	chymotrypsin	50 mM HEPES pH7
474	p2863	2863-141	L80C	10	DMPC/cholest-4-en-3-one(3/1)	500	5b-d9	50	10	chymotrypsin	50 mM HEPES pH7
475	p2863	2863-151	L80C	10	DMPC/cholest-4-en-3-one(3/1)	500	5b-d9	50	15	chymotrypsin	50 mM HEPES pH7
476	p2863	2863-161	L80C	10	DMPC/cholest-4-en-3-one(3/1)	500	5b-d9	50	30	chymotrypsin	50 mM HEPES pH7
477	p2863	2863-171	L274C	10	DMPC/cholest-4-en-3-one(3/1)	500	5b-d9	50	0.5	chymotrypsin	50 mM HEPES pH7
478	p2863	2863-181	L274C	10	DMPC/cholest-4-en-3-one(3/1)	500	5b-d9	50	1	chymotrypsin	50 mM HEPES pH7
479	p2863	2863-191	L274C	10	DMPC/cholest-4-en-3-one(3/1)	500	5b-d9	50	2	chymotrypsin	50 mM HEPES pH7
480	p2863	2863-201	L274C	10	DMPC/cholest-4-en-3-one(3/1)	500	5b-d9	50	3	chymotrypsin	50 mM HEPES pH7
481	p2863	2863-211	L274C	10	DMPC/cholest-4-en-3-one(3/1)	500	5b-d9	50	6	chymotrypsin	50 mM HEPES pH7
482	p2863	2863-221	L274C	10	DMPC/cholest-4-en-3-one(3/1)	500	5b-d9	50	10	chymotrypsin	50 mM HEPES pH7
483	p2863	2863-231	L274C	10	DMPC/cholest-4-en-3-one(3/1)	500	5b-d9	50	15	chymotrypsin	50 mM HEPES pH7
484	p2863	2863-241	L274C	10	DMPC/cholest-4-en-3-one(3/1)	500	5b-d9	50	30	chymotrypsin	50 mM HEPES pH7
485	p2863	2863-251	W333C	10	DMPC/cholest-4-en-3-one(3/1)	500	5b-d9	50	0.5	chymotrypsin	50 mM HEPES pH7
486	p2863	2863-261	W333C	10	DMPC/cholest-4-en-3-one(3/1)	500	5b-d9	50	1	chymotrypsin	50 mM HEPES pH7
487	p2863	2863-271	W333C	10	DMPC/cholest-4-en-3-one(3/1)	500	5b-d9	50	2	chymotrypsin	50 mM HEPES pH7
488	p2863	2863-281	W333C	10	DMPC/cholest-4-en-3-one(3/1)	500	5b-d9	50	3	chymotrypsin	50 mM HEPES pH7
489	p2863	2863-291	W333C	10	DMPC/cholest-4-en-3-one(3/1)	500	5b-d9	50	6	chymotrypsin	50 mM HEPES pH7
490	p2863	2863-301	W333C	10	DMPC/cholest-4-en-3-one(3/1)	500	5b-d9	50	10	chymotrypsin	50 mM HEPES pH7
491	p2863	2863-311	W333C	10	DMPC/cholest-4-en-3-one(3/1)	500	5b-d9	50	15	chymotrypsin	50 mM HEPES pH7
492	p2863	2863-321	W333C	10	DMPC/cholest-4-en-3-one(3/1)	500	5b-d9	50	30	chymotrypsin	50 mM HEPES pH7
493	p2863	2863-331	mutant 1	10	DMPC/cholest-4-en-3-one(3/1)	500	5b-d9	50	0.5	chymotrypsin	50 mM HEPES pH7
494	p2863	2863-341	mutant 1	10	DMPC/cholest-4-en-3-one(3/1)	500	5b-d9	50	1	chymotrypsin	50 mM HEPES pH7
495	p2863	2863-351	mutant 1	10	DMPC/cholest-4-en-3-one(3/1)	500	5b-d9	50	2	chymotrypsin	50 mM HEPES pH7
496	p2863	2863-361	mutant 1	10	DMPC/cholest-4-en-3-one(3/1)	500	5b-d9	50	3	chymotrypsin	50 mM HEPES pH7
497	p2863	2863-371	mutant 1	10	DMPC/cholest-4-en-3-one(3/1)	500	5b-d9	50	6	chymotrypsin	50 mM HEPES pH7
498	p2863	2863-381	mutant 1	10	DMPC/cholest-4-en-3-one(3/1)	500	5b-d9	50	10	chymotrypsin	50 mM HEPES pH7
499	p2863	2863-391	mutant 1	10	DMPC/cholest-4-en-3-one(3/1)	500	5b-d9	50	15	chymotrypsin	50 mM HEPES pH7
500	p2863	2863-401	mutant 1	10	DMPC/cholest-4-en-3-one(3/1)	500	5b-d9	50	30	chymotrypsin	50 mM HEPES pH7
501	p2863	2863-411	mutant 2	10	DMPC/cholest-4-en-3-one(3/1)	500	5b-d9	50	0.5	chymotrypsin	50 mM HEPES pH7
502	p2863	2863-421	mutant 2	10	DMPC/cholest-4-en-3-one(3/1)	500	5b-d9	50	1	chymotrypsin	50 mM HEPES pH7
503	p2863	2863-431	mutant 2	10	DMPC/cholest-4-en-3-one(3/1)	500	5b-d9	50	2	chymotrypsin	50 mM HEPES pH7
504	p2863	2863-441	mutant 2	10	DMPC/cholest-4-en-3-one(3/1)	500	5b-d9	50	3	chymotrypsin	50 mM HEPES pH7
505	p2863	2863-451	mutant 2	10	DMPC/cholest-4-en-3-one(3/1)	500	5b-d9	50	6	chymotrypsin	50 mM HEPES pH7
506	p2863	2863-461	mutant 2	10	DMPC/cholest-4-en-3-one(3/1)	500	5b-d9	50	10	chymotrypsin	50 mM HEPES pH7
507	p2863	2863-471	mutant 2	10	DMPC/cholest-4-en-3-one(3/1)	500	5b-d9	50	15	chymotrypsin	50 mM HEPES pH7
508	p2863	2863-481	mutant 2	10	DMPC/cholest-4-en-3-one(3/1)	500	5b-d9	50	30	chymotrypsin	50 mM HEPES pH7
509	p2863	2863-491	mutant 3	10	DMPC/cholest-4-en-3-one(3/1)	500	5b-d9	50	0.5	chymotrypsin	50 mM HEPES pH7

510	p2863	2863-501	mutant 3	10	DMPC/cholest-4-en-3-one(3/1)	500	5b-d9	50	1	chymotrypsin	50 mM HEPES pH7
511	p2863	2863-511	mutant 3	10	DMPC/cholest-4-en-3-one(3/1)	500	5b-d9	50	2	chymotrypsin	50 mM HEPES pH7
512	p2863	2863-521	mutant 3	10	DMPC/cholest-4-en-3-one(3/1)	500	5b-d9	50	3	chymotrypsin	50 mM HEPES pH7
513	p2863	2863-531	mutant 3	10	DMPC/cholest-4-en-3-one(3/1)	500	5b-d9	50	6	chymotrypsin	50 mM HEPES pH7
514	p2863	2863-541	mutant 3	10	DMPC/cholest-4-en-3-one(3/1)	500	5b-d9	50	10	chymotrypsin	50 mM HEPES pH7
515	p2863	2863-551	mutant 3	10	DMPC/cholest-4-en-3-one(3/1)	500	5b-d9	50	15	chymotrypsin	50 mM HEPES pH7
516	p2863	2863-561	mutant 3	10	DMPC/cholest-4-en-3-one(3/1)	500	5b-d9	50	30	chymotrypsin	50 mM HEPES pH7
517	p2863	2863-571	mutant 4	10	DMPC/cholest-4-en-3-one(3/1)	500	5b-d9	50	0.5	chymotrypsin	50 mM HEPES pH7
518	p2863	2863-581	mutant 4	10	DMPC/cholest-4-en-3-one(3/1)	500	5b-d9	50	1	chymotrypsin	50 mM HEPES pH7
519	p2863	2863-591	mutant 4	10	DMPC/cholest-4-en-3-one(3/1)	500	5b-d9	50	2	chymotrypsin	50 mM HEPES pH7
520	p2863	2863-601	mutant 4	10	DMPC/cholest-4-en-3-one(3/1)	500	5b-d9	50	3	chymotrypsin	50 mM HEPES pH7
521	p2863	2863-611	mutant 4	10	DMPC/cholest-4-en-3-one(3/1)	500	5b-d9	50	6	chymotrypsin	50 mM HEPES pH7
522	p2863	2863-621	mutant 4	10	DMPC/cholest-4-en-3-one(3/1)	500	5b-d9	50	10	chymotrypsin	50 mM HEPES pH7
523	p2863	2863-631	mutant 4	10	DMPC/cholest-4-en-3-one(3/1)	500	5b-d9	50	15	chymotrypsin	50 mM HEPES pH7
524	p2863	2863-641	mutant 4	10	DMPC/cholest-4-en-3-one(3/1)	500	5b-d9	50	30	chymotrypsin	50 mM HEPES pH7
525	p2863	2863-651	mutant 5	10	DMPC/cholest-4-en-3-one(3/1)	500	5b-d9	50	0.5	chymotrypsin	50 mM HEPES pH7
526	p2863	2863-661	mutant 5	10	DMPC/cholest-4-en-3-one(3/1)	500	5b-d9	50	1	chymotrypsin	50 mM HEPES pH7
527	p2863	2863-671	mutant 5	10	DMPC/cholest-4-en-3-one(3/1)	500	5b-d9	50	2	chymotrypsin	50 mM HEPES pH7
528	p2863	2863-681	mutant 5	10	DMPC/cholest-4-en-3-one(3/1)	500	5b-d9	50	3	chymotrypsin	50 mM HEPES pH7
529	p2863	2863-691	mutant 5	10	DMPC/cholest-4-en-3-one(3/1)	500	5b-d9	50	6	chymotrypsin	50 mM HEPES pH7
530	p2863	2863-701	mutant 5	10	DMPC/cholest-4-en-3-one(3/1)	500	5b-d9	50	10	chymotrypsin	50 mM HEPES pH7
531	p2863	2863-711	mutant 5	10	DMPC/cholest-4-en-3-one(3/1)	500	5b-d9	50	15	chymotrypsin	50 mM HEPES pH7
532	p2863	2863-721	mutant 5	10	DMPC/cholest-4-en-3-one(3/1)	500	5b-d9	50	30	chymotrypsin	50 mM HEPES pH7
533	p2863	2863-731	mutant 6	10	DMPC/cholest-4-en-3-one(3/1)	500	5b-d9	50	0.5	chymotrypsin	50 mM HEPES pH7
534	p2863	2863-741	mutant 6	10	DMPC/cholest-4-en-3-one(3/1)	500	5b-d9	50	1	chymotrypsin	50 mM HEPES pH7
535	p2863	2863-751	mutant 6	10	DMPC/cholest-4-en-3-one(3/1)	500	5b-d9	50	2	chymotrypsin	50 mM HEPES pH7
536	p2863	2863-761	mutant 6	10	DMPC/cholest-4-en-3-one(3/1)	500	5b-d9	50	3	chymotrypsin	50 mM HEPES pH7
537	p2863	2863-771	mutant 6	10	DMPC/cholest-4-en-3-one(3/1)	500	5b-d9	50	6	chymotrypsin	50 mM HEPES pH7
538	p2863	2863-781	mutant 6	10	DMPC/cholest-4-en-3-one(3/1)	500	5b-d9	50	10	chymotrypsin	50 mM HEPES pH7
539	p2863	2863-791	mutant 6	10	DMPC/cholest-4-en-3-one(3/1)	500	5b-d9	50	15	chymotrypsin	50 mM HEPES pH7
540	p2863	2863-801	mutant 6	10	DMPC/cholest-4-en-3-one(3/1)	500	5b-d9	50	30	chymotrypsin	50 mM HEPES pH7
541	p2809	2809-11	WT	10	no vesicles	0	5b-d9	50	0.5	trypsin	50 mM HEPES pH7
542	p2809	2809-21	WT	10	no vesicles	0	5b-d9	50	1	trypsin	50 mM HEPES pH7
543	p2809	2809-31	WT	10	no vesicles	0	5b-d9	50	2	trypsin	50 mM HEPES pH7
544	p2809	2809-41	WT	10	no vesicles	0	5b-d9	50	3	trypsin	50 mM HEPES pH7
545	p2809	2809-51	WT	10	no vesicles	0	5b-d9	50	6	trypsin	50 mM HEPES pH7
546	p2809	2809-61	WT	10	no vesicles	0	5b-d9	50	10	trypsin	50 mM HEPES pH7
547	p2809	2809-71	WT	10	no vesicles	0	5b-d9	50	15	trypsin	50 mM HEPES pH7
548	p2809	2809-81	WT	10	no vesicles	0	5b-d9	50	30	trypsin	50 mM HEPES pH7
549	p2809	2809-91	L80C	10	no vesicles	0	5b-d9	50	0.5	trypsin	50 mM HEPES pH7
550	p2809	2809-101	L80C	10	no vesicles	0	5b-d9	50	1	trypsin	50 mM HEPES pH7
551	p2809	2809-111	L80C	10	no vesicles	0	5b-d9	50	2	trypsin	50 mM HEPES pH7
552	p2809	2809-121	L80C	10	no vesicles	0	5b-d9	50	3	trypsin	50 mM HEPES pH7
553	p2809	2809-131	L80C	10	no vesicles	0	5b-d9	50	6	trypsin	50 mM HEPES pH7
554	p2809	2809-141	L80C	10	no vesicles	0	5b-d9	50	10	trypsin	50 mM HEPES pH7
555	p2809	2809-151	L80C	10	no vesicles	0	5b-d9	50	15	trypsin	50 mM HEPES pH7
556	p2809	2809-161	L80C	10	no vesicles	0	5b-d9	50	30	trypsin	50 mM HEPES pH7
557	p2809	2809-171	L274C	10	no vesicles	0	5b-d9	50	0.5	trypsin	50 mM HEPES pH7
558	p2809	2809-181	L274C	10	no vesicles	0	5b-d9	50	1	trypsin	50 mM HEPES pH7
559	p2809	2809-191	L274C	10	no vesicles	0	5b-d9	50	2	trypsin	50 mM HEPES pH7
560	p2809	2809-201	L274C	10	no vesicles	0	5b-d9	50	3	trypsin	50 mM HEPES pH7
561	p2809	2809-211	L274C	10	no vesicles	0	5b-d9	50	6	trypsin	50 mM HEPES pH7
562	p2809	2809-221	L274C	10	no vesicles	0	5b-d9	50	10	trypsin	50 mM HEPES pH7
563	p2809	2809-231	L274C	10	no vesicles	0	5b-d9	50	15	trypsin	50 mM HEPES pH7
564	p2809	2809-241	L274C	10	no vesicles	0	5b-d9	50	30	trypsin	50 mM HEPES pH7
565	p2809	2809-251	W333C	10	no vesicles	0	5b-d9	50	0.5	trypsin	50 mM HEPES pH7
566	p2809	2809-261	W333C	10	no vesicles	0	5b-d9	50	1	trypsin	50 mM HEPES pH7
567	p2809	2809-271	W333C	10	no vesicles	0	5b-d9	50	2	trypsin	50 mM HEPES pH7

568	p2809	2809-281	W333C	10	no vesicles	0	5b-d9	50	3	trypsin	50 mM HEPES pH7
569	p2809	2809-291	W333C	10	no vesicles	0	5b-d9	50	6	trypsin	50 mM HEPES pH7
570	p2809	2809-301	W333C	10	no vesicles	0	5b-d9	50	10	trypsin	50 mM HEPES pH7
571	p2809	2809-311	W333C	10	no vesicles	0	5b-d9	50	15	trypsin	50 mM HEPES pH7
572	p2809	2809-321	W333C	10	no vesicles	0	5b-d9	50	30	trypsin	50 mM HEPES pH7
573	p2809	2809-331	mutant 1	10	no vesicles	0	5b-d9	50	0.5	trypsin	50 mM HEPES pH7
574	p2809	2809-341	mutant 1	10	no vesicles	0	5b-d9	50	1	trypsin	50 mM HEPES pH7
575	p2809	2809-351	mutant 1	10	no vesicles	0	5b-d9	50	2	trypsin	50 mM HEPES pH7
576	p2809	2809-361	mutant 1	10	no vesicles	0	5b-d9	50	3	trypsin	50 mM HEPES pH7
577	p2809	2809-371	mutant 1	10	no vesicles	0	5b-d9	50	6	trypsin	50 mM HEPES pH7
578	p2809	2809-381	mutant 1	10	no vesicles	0	5b-d9	50	10	trypsin	50 mM HEPES pH7
579	p2809	2809-391	mutant 1	10	no vesicles	0	5b-d9	50	15	trypsin	50 mM HEPES pH7
580	p2809	2809-401	mutant 1	10	no vesicles	0	5b-d9	50	30	trypsin	50 mM HEPES pH7
581	p2809	2809-411	mutant 2	10	no vesicles	0	5b-d9	50	0.5	trypsin	50 mM HEPES pH7
582	p2809	2809-421	mutant 2	10	no vesicles	0	5b-d9	50	1	trypsin	50 mM HEPES pH7
583	p2809	2809-431	mutant 2	10	no vesicles	0	5b-d9	50	2	trypsin	50 mM HEPES pH7
584	p2809	2809-441	mutant 2	10	no vesicles	0	5b-d9	50	3	trypsin	50 mM HEPES pH7
585	p2809	2809-451	mutant 2	10	no vesicles	0	5b-d9	50	6	trypsin	50 mM HEPES pH7
586	p2809	2809-461	mutant 2	10	no vesicles	0	5b-d9	50	10	trypsin	50 mM HEPES pH7
587	p2809	2809-471	mutant 2	10	no vesicles	0	5b-d9	50	15	trypsin	50 mM HEPES pH7
588	p2809	2809-481	mutant 2	10	no vesicles	0	5b-d9	50	30	trypsin	50 mM HEPES pH7
589	p2809	2809-491	mutant 3	10	no vesicles	0	5b-d9	50	0.5	trypsin	50 mM HEPES pH7
590	p2809	2809-501	mutant 3	10	no vesicles	0	5b-d9	50	1	trypsin	50 mM HEPES pH7
591	p2809	2809-511	mutant 3	10	no vesicles	0	5b-d9	50	2	trypsin	50 mM HEPES pH7
592	p2809	2809-521	mutant 3	10	no vesicles	0	5b-d9	50	3	trypsin	50 mM HEPES pH7
593	p2809	2809-531	mutant 3	10	no vesicles	0	5b-d9	50	6	trypsin	50 mM HEPES pH7
594	p2809	2809-541	mutant 3	10	no vesicles	0	5b-d9	50	10	trypsin	50 mM HEPES pH7
595	p2809	2809-551	mutant 3	10	no vesicles	0	5b-d9	50	15	trypsin	50 mM HEPES pH7
596	p2809	2809-561	mutant 3	10	no vesicles	0	5b-d9	50	30	trypsin	50 mM HEPES pH7
597	p2809	2809-571	mutant 4	10	no vesicles	0	5b-d9	50	0.5	trypsin	50 mM HEPES pH7
598	p2809	2809-581	mutant 4	10	no vesicles	0	5b-d9	50	1	trypsin	50 mM HEPES pH7
599	p2809	2809-591	mutant 4	10	no vesicles	0	5b-d9	50	2	trypsin	50 mM HEPES pH7
600	p2809	2809-601	mutant 4	10	no vesicles	0	5b-d9	50	3	trypsin	50 mM HEPES pH7
601	p2809	2809-611	mutant 4	10	no vesicles	0	5b-d9	50	6	trypsin	50 mM HEPES pH7
602	p2809	2809-621	mutant 4	10	no vesicles	0	5b-d9	50	10	trypsin	50 mM HEPES pH7
603	p2809	2809-631	mutant 4	10	no vesicles	0	5b-d9	50	15	trypsin	50 mM HEPES pH7
604	p2809	2809-641	mutant 4	10	no vesicles	0	5b-d9	50	30	trypsin	50 mM HEPES pH7
605	p2809	2809-651	mutant 5	10	no vesicles	0	5b-d9	50	0.5	trypsin	50 mM HEPES pH7
606	p2809	2809-661	mutant 5	10	no vesicles	0	5b-d9	50	1	trypsin	50 mM HEPES pH7
607	p2809	2809-671	mutant 5	10	no vesicles	0	5b-d9	50	2	trypsin	50 mM HEPES pH7
608	p2809	2809-681	mutant 5	10	no vesicles	0	5b-d9	50	3	trypsin	50 mM HEPES pH7
609	p2809	2809-691	mutant 5	10	no vesicles	0	5b-d9	50	6	trypsin	50 mM HEPES pH7
610	p2809	2809-701	mutant 5	10	no vesicles	0	5b-d9	50	10	trypsin	50 mM HEPES pH7
611	p2809	2809-711	mutant 5	10	no vesicles	0	5b-d9	50	15	trypsin	50 mM HEPES pH7
612	p2809	2809-721	mutant 5	10	no vesicles	0	5b-d9	50	30	trypsin	50 mM HEPES pH7
613	p2809	2809-731	mutant 6	10	no vesicles	0	5b-d9	50	0.5	trypsin	50 mM HEPES pH7
614	p2809	2809-741	mutant 6	10	no vesicles	0	5b-d9	50	1	trypsin	50 mM HEPES pH7
615	p2809	2809-751	mutant 6	10	no vesicles	0	5b-d9	50	2	trypsin	50 mM HEPES pH7
616	p2809	2809-761	mutant 6	10	no vesicles	0	5b-d9	50	3	trypsin	50 mM HEPES pH7
617	p2809	2809-771	mutant 6	10	no vesicles	0	5b-d9	50	6	trypsin	50 mM HEPES pH7
618	p2809	2809-781	mutant 6	10	no vesicles	0	5b-d9	50	10	trypsin	50 mM HEPES pH7
619	p2809	2809-791	mutant 6	10	no vesicles	0	5b-d9	50	15	trypsin	50 mM HEPES pH7
620	p2809	2809-801	mutant 6	10	no vesicles	0	5b-d9	50	30	trypsin	50 mM HEPES pH7
621	p2809	2809-811	WT	10	no vesicles	0	5b-d9	50	0.5	chymotrypsin	50 mM HEPES pH7
622	p2809	2809-821	WT	10	no vesicles	0	5b-d9	50	1	chymotrypsin	50 mM HEPES pH7
623	p2809	2809-831	WT	10	no vesicles	0	5b-d9	50	2	chymotrypsin	50 mM HEPES pH7
624	p2809	2809-841	WT	10	no vesicles	0	5b-d9	50	3	chymotrypsin	50 mM HEPES pH7
625	p2809	2809-851	WT	10	no vesicles	0	5b-d9	50	6	chymotrypsin	50 mM HEPES pH7

626	p2809	2809-861	WT	10	no vesicles	0	5b-d9	50	10	chymotrypsin	50 mM HEPES pH7
627	p2809	2809-871	WT	10	no vesicles	0	5b-d9	50	15	chymotrypsin	50 mM HEPES pH7
628	p2809	2809-881	WT	10	no vesicles	0	5b-d9	50	30	chymotrypsin	50 mM HEPES pH7
629	p2809	2809-891	L80C	10	no vesicles	0	5b-d9	50	0.5	chymotrypsin	50 mM HEPES pH7
630	p2809	2809-901	L80C	10	no vesicles	0	5b-d9	50	1	chymotrypsin	50 mM HEPES pH7
631	p2809	2809-911	L80C	10	no vesicles	0	5b-d9	50	2	chymotrypsin	50 mM HEPES pH7
632	p2809	2809-921	L80C	10	no vesicles	0	5b-d9	50	3	chymotrypsin	50 mM HEPES pH7
633	p2809	2809-931	L80C	10	no vesicles	0	5b-d9	50	6	chymotrypsin	50 mM HEPES pH7
634	p2809	2809-941	L80C	10	no vesicles	0	5b-d9	50	10	chymotrypsin	50 mM HEPES pH7
635	p2809	2809-951	L80C	10	no vesicles	0	5b-d9	50	15	chymotrypsin	50 mM HEPES pH7
636	p2809	2809-961	L80C	10	no vesicles	0	5b-d9	50	30	chymotrypsin	50 mM HEPES pH7
637	p2809	2809-971	L274C	10	no vesicles	0	5b-d9	50	0.5	chymotrypsin	50 mM HEPES pH7
638	p2809	2809-981	L274C	10	no vesicles	0	5b-d9	50	1	chymotrypsin	50 mM HEPES pH7
639	p2809	2809-991	L274C	10	no vesicles	0	5b-d9	50	2	chymotrypsin	50 mM HEPES pH7
640	p2809	2809-1001	L274C	10	no vesicles	0	5b-d9	50	3	chymotrypsin	50 mM HEPES pH7
641	p2809	2809-1011	L274C	10	no vesicles	0	5b-d9	50	6	chymotrypsin	50 mM HEPES pH7
642	p2809	2809-1021	L274C	10	no vesicles	0	5b-d9	50	10	chymotrypsin	50 mM HEPES pH7
643	p2809	2809-1031	L274C	10	no vesicles	0	5b-d9	50	15	chymotrypsin	50 mM HEPES pH7
644	p2809	2809-1041	L274C	10	no vesicles	0	5b-d9	50	30	chymotrypsin	50 mM HEPES pH7
645	p2809	2809-1051	W333C	10	no vesicles	0	5b-d9	50	0.5	chymotrypsin	50 mM HEPES pH7
646	p2809	2809-1061	W333C	10	no vesicles	0	5b-d9	50	1	chymotrypsin	50 mM HEPES pH7
647	p2809	2809-1071	W333C	10	no vesicles	0	5b-d9	50	2	chymotrypsin	50 mM HEPES pH7
648	p2809	2809-1081	W333C	10	no vesicles	0	5b-d9	50	3	chymotrypsin	50 mM HEPES pH7
649	p2809	2809-1091	W333C	10	no vesicles	0	5b-d9	50	6	chymotrypsin	50 mM HEPES pH7
650	p2809	2809-1101	W333C	10	no vesicles	0	5b-d9	50	10	chymotrypsin	50 mM HEPES pH7
651	p2809	2809-1111	W333C	10	no vesicles	0	5b-d9	50	15	chymotrypsin	50 mM HEPES pH7
652	p2809	2809-1121	W333C	10	no vesicles	0	5b-d9	50	30	chymotrypsin	50 mM HEPES pH7
653	p2809	2809-1131	mutant 1	10	no vesicles	0	5b-d9	50	0.5	chymotrypsin	50 mM HEPES pH7
654	p2809	2809-1141	mutant 1	10	no vesicles	0	5b-d9	50	1	chymotrypsin	50 mM HEPES pH7
655	p2809	2809-1151	mutant 1	10	no vesicles	0	5b-d9	50	2	chymotrypsin	50 mM HEPES pH7
656	p2809	2809-1161	mutant 1	10	no vesicles	0	5b-d9	50	3	chymotrypsin	50 mM HEPES pH7
657	p2809	2809-1171	mutant 1	10	no vesicles	0	5b-d9	50	6	chymotrypsin	50 mM HEPES pH7
658	p2809	2809-1181	mutant 1	10	no vesicles	0	5b-d9	50	10	chymotrypsin	50 mM HEPES pH7
659	p2809	2809-1191	mutant 1	10	no vesicles	0	5b-d9	50	15	chymotrypsin	50 mM HEPES pH7
660	p2809	2809-1201	mutant 1	10	no vesicles	0	5b-d9	50	30	chymotrypsin	50 mM HEPES pH7
661	p2809	2809-1211	mutant 2	10	no vesicles	0	5b-d9	50	0.5	chymotrypsin	50 mM HEPES pH7
662	p2809	2809-1221	mutant 2	10	no vesicles	0	5b-d9	50	1	chymotrypsin	50 mM HEPES pH7
663	p2809	2809-1231	mutant 2	10	no vesicles	0	5b-d9	50	2	chymotrypsin	50 mM HEPES pH7
664	p2809	2809-1241	mutant 2	10	no vesicles	0	5b-d9	50	3	chymotrypsin	50 mM HEPES pH7
665	p2809	2809-1251	mutant 2	10	no vesicles	0	5b-d9	50	6	chymotrypsin	50 mM HEPES pH7
666	p2809	2809-1261	mutant 2	10	no vesicles	0	5b-d9	50	10	chymotrypsin	50 mM HEPES pH7
667	p2809	2809-1271	mutant 2	10	no vesicles	0	5b-d9	50	15	chymotrypsin	50 mM HEPES pH7
668	p2809	2809-1281	mutant 2	10	no vesicles	0	5b-d9	50	30	chymotrypsin	50 mM HEPES pH7
669	p2809	2809-1291	mutant 3	10	no vesicles	0	5b-d9	50	0.5	chymotrypsin	50 mM HEPES pH7
670	p2809	2809-1301	mutant 3	10	no vesicles	0	5b-d9	50	1	chymotrypsin	50 mM HEPES pH7
671	p2809	2809-1311	mutant 3	10	no vesicles	0	5b-d9	50	2	chymotrypsin	50 mM HEPES pH7
672	p2809	2809-1321	mutant 3	10	no vesicles	0	5b-d9	50	3	chymotrypsin	50 mM HEPES pH7
673	p2809	2809-1331	mutant 3	10	no vesicles	0	5b-d9	50	6	chymotrypsin	50 mM HEPES pH7
674	p2809	2809-1341	mutant 3	10	no vesicles	0	5b-d9	50	10	chymotrypsin	50 mM HEPES pH7
675	p2809	2809-1351	mutant 3	10	no vesicles	0	5b-d9	50	15	chymotrypsin	50 mM HEPES pH7
676	p2809	2809-1361	mutant 3	10	no vesicles	0	5b-d9	50	30	chymotrypsin	50 mM HEPES pH7
677	p2809	2809-1371	mutant 4	10	no vesicles	0	5b-d9	50	0.5	chymotrypsin	50 mM HEPES pH7
678	p2809	2809-1381	mutant 4	10	no vesicles	0	5b-d9	50	1	chymotrypsin	50 mM HEPES pH7
679	p2809	2809-1391	mutant 4	10	no vesicles	0	5b-d9	50	2	chymotrypsin	50 mM HEPES pH7
680	p2809	2809-1401	mutant 4	10	no vesicles	0	5b-d9	50	3	chymotrypsin	50 mM HEPES pH7
681	p2809	2809-1411	mutant 4	10	no vesicles	0	5b-d9	50	6	chymotrypsin	50 mM HEPES pH7
682	p2809	2809-1421	mutant 4	10	no vesicles	0	5b-d9	50	10	chymotrypsin	50 mM HEPES pH7
683	p2809	2809-1431	mutant 4	10	no vesicles	0	5b-d9	50	15	chymotrypsin	50 mM HEPES pH7

684	p2809	2809-1441	mutant 4	10	no vesicles	0	5b-d9	50	30	chymotrypsin	50 mM HEPES pH7
685	p2809	2809-1451	mutant 5	10	no vesicles	0	5b-d9	50	0.5	chymotrypsin	50 mM HEPES pH7
686	p2809	2809-1461	mutant 5	10	no vesicles	0	5b-d9	50	1	chymotrypsin	50 mM HEPES pH7
687	p2809	2809-1471	mutant 5	10	no vesicles	0	5b-d9	50	2	chymotrypsin	50 mM HEPES pH7
688	p2809	2809-1481	mutant 5	10	no vesicles	0	5b-d9	50	3	chymotrypsin	50 mM HEPES pH7
689	p2809	2809-1491	mutant 5	10	no vesicles	0	5b-d9	50	6	chymotrypsin	50 mM HEPES pH7
690	p2809	2809-1501	mutant 5	10	no vesicles	0	5b-d9	50	10	chymotrypsin	50 mM HEPES pH7
691	p2809	2809-1511	mutant 5	10	no vesicles	0	5b-d9	50	15	chymotrypsin	50 mM HEPES pH7
692	p2809	2809-1521	mutant 5	10	no vesicles	0	5b-d9	50	30	chymotrypsin	50 mM HEPES pH7
693	p2809	2809-1531	mutant 6	10	no vesicles	0	5b-d9	50	0.5	chymotrypsin	50 mM HEPES pH7
694	p2809	2809-1541	mutant 6	10	no vesicles	0	5b-d9	50	1	chymotrypsin	50 mM HEPES pH7
695	p2809	2809-1551	mutant 6	10	no vesicles	0	5b-d9	50	2	chymotrypsin	50 mM HEPES pH7
696	p2809	2809-1561	mutant 6	10	no vesicles	0	5b-d9	50	3	chymotrypsin	50 mM HEPES pH7
697	p2809	2809-1571	mutant 6	10	no vesicles	0	5b-d9	50	6	chymotrypsin	50 mM HEPES pH7
698	p2809	2809-1581	mutant 6	10	no vesicles	0	5b-d9	50	10	chymotrypsin	50 mM HEPES pH7
699	p2809	2809-1591	mutant 6	10	no vesicles	0	5b-d9	50	15	chymotrypsin	50 mM HEPES pH7
700	p2809	2809-1601	mutant 6	10	no vesicles	0	5b-d9	50	30	chymotrypsin	50 mM HEPES pH7
701	p2870	2870-11	WT	10	no vesicles	0	5b-d9	50	0.5	trypsin	50 mM HEPES pH7
702	p2870	2870-21	WT	10	no vesicles	0	5b-d9	50	1	trypsin	50 mM HEPES pH7
703	p2870	2870-31	WT	10	no vesicles	0	5b-d9	50	2	trypsin	50 mM HEPES pH7
704	p2870	2870-41	WT	10	no vesicles	0	5b-d9	50	3	trypsin	50 mM HEPES pH7
705	p2870	2870-51	WT	10	no vesicles	0	5b-d9	50	6	trypsin	50 mM HEPES pH7
706	p2870	2870-61	WT	10	no vesicles	0	5b-d9	50	10	trypsin	50 mM HEPES pH7
707	p2870	2870-71	WT	10	no vesicles	0	5b-d9	50	15	trypsin	50 mM HEPES pH7
708	p2870	2870-81	WT	10	no vesicles	0	5b-d9	50	30	trypsin	50 mM HEPES pH7
709	p2870	2870-91	L80C	10	no vesicles	0	5b-d9	50	0.5	trypsin	50 mM HEPES pH7
710	p2870	2870-101	L80C	10	no vesicles	0	5b-d9	50	1	trypsin	50 mM HEPES pH7
711	p2870	2870-111	L80C	10	no vesicles	0	5b-d9	50	2	trypsin	50 mM HEPES pH7
712	p2870	2870-121	L80C	10	no vesicles	0	5b-d9	50	3	trypsin	50 mM HEPES pH7
713	p2870	2870-131	L80C	10	no vesicles	0	5b-d9	50	6	trypsin	50 mM HEPES pH7
714	p2870	2870-141	L80C	10	no vesicles	0	5b-d9	50	10	trypsin	50 mM HEPES pH7
715	p2870	2870-151	L80C	10	no vesicles	0	5b-d9	50	15	trypsin	50 mM HEPES pH7
716	p2870	2870-161	L80C	10	no vesicles	0	5b-d9	50	30	trypsin	50 mM HEPES pH7
717	p2870	2870-171	L274C	10	no vesicles	0	5b-d9	50	0.5	trypsin	50 mM HEPES pH7
718	p2870	2870-181	L274C	10	no vesicles	0	5b-d9	50	1	trypsin	50 mM HEPES pH7
719	p2870	2870-191	L274C	10	no vesicles	0	5b-d9	50	2	trypsin	50 mM HEPES pH7
720	p2870	2870-201	L274C	10	no vesicles	0	5b-d9	50	3	trypsin	50 mM HEPES pH7
721	p2870	2870-211	L274C	10	no vesicles	0	5b-d9	50	6	trypsin	50 mM HEPES pH7
722	p2870	2870-221	L274C	10	no vesicles	0	5b-d9	50	10	trypsin	50 mM HEPES pH7
723	p2870	2870-231	L274C	10	no vesicles	0	5b-d9	50	15	trypsin	50 mM HEPES pH7
724	p2870	2870-241	L274C	10	no vesicles	0	5b-d9	50	30	trypsin	50 mM HEPES pH7
725	p2870	2870-251	W333C	10	no vesicles	0	5b-d9	50	0.5	trypsin	50 mM HEPES pH7
726	p2870	2870-261	W333C	10	no vesicles	0	5b-d9	50	1	trypsin	50 mM HEPES pH7
727	p2870	2870-271	W333C	10	no vesicles	0	5b-d9	50	2	trypsin	50 mM HEPES pH7
728	p2870	2870-281	W333C	10	no vesicles	0	5b-d9	50	3	trypsin	50 mM HEPES pH7
729	p2870	2870-291	W333C	10	no vesicles	0	5b-d9	50	6	trypsin	50 mM HEPES pH7
730	p2870	2870-301	W333C	10	no vesicles	0	5b-d9	50	10	trypsin	50 mM HEPES pH7
731	p2870	2870-311	W333C	10	no vesicles	0	5b-d9	50	15	trypsin	50 mM HEPES pH7
732	p2870	2870-321	W333C	10	no vesicles	0	5b-d9	50	30	trypsin	50 mM HEPES pH7
733	p2870	2870-331	mutant 1	10	no vesicles	0	5b-d9	50	0.5	trypsin	50 mM HEPES pH7
734	p2870	2870-341	mutant 1	10	no vesicles	0	5b-d9	50	1	trypsin	50 mM HEPES pH7
735	p2870	2870-351	mutant 1	10	no vesicles	0	5b-d9	50	2	trypsin	50 mM HEPES pH7
736	p2870	2870-361	mutant 1	10	no vesicles	0	5b-d9	50	3	trypsin	50 mM HEPES pH7
737	p2870	2870-371	mutant 1	10	no vesicles	0	5b-d9	50	6	trypsin	50 mM HEPES pH7
738	p2870	2870-381	mutant 1	10	no vesicles	0	5b-d9	50	10	trypsin	50 mM HEPES pH7
739	p2870	2870-391	mutant 1	10	no vesicles	0	5b-d9	50	15	trypsin	50 mM HEPES pH7
740	p2870	2870-401	mutant 1	10	no vesicles	0	5b-d9	50	30	trypsin	50 mM HEPES pH7
741	p2870	2870-411	mutant 2	10	no vesicles	0	5b-d9	50	0.5	trypsin	50 mM HEPES pH7

742	p2870	2870-421	mutant 2	10	no vesicles	0	5b-d9	50	1	trypsin	50 mM HEPES pH7
743	p2870	2870-431	mutant 2	10	no vesicles	0	5b-d9	50	2	trypsin	50 mM HEPES pH7
744	p2870	2870-441	mutant 2	10	no vesicles	0	5b-d9	50	3	trypsin	50 mM HEPES pH7
745	p2870	2870-451	mutant 2	10	no vesicles	0	5b-d9	50	6	trypsin	50 mM HEPES pH7
746	p2870	2870-461	mutant 2	10	no vesicles	0	5b-d9	50	10	trypsin	50 mM HEPES pH7
747	p2870	2870-471	mutant 2	10	no vesicles	0	5b-d9	50	15	trypsin	50 mM HEPES pH7
748	p2870	2870-481	mutant 2	10	no vesicles	0	5b-d9	50	30	trypsin	50 mM HEPES pH7
749	p2870	2870-491	mutant 3	10	no vesicles	0	5b-d9	50	0.5	trypsin	50 mM HEPES pH7
750	p2870	2870-501	mutant 3	10	no vesicles	0	5b-d9	50	1	trypsin	50 mM HEPES pH7
751	p2870	2870-511	mutant 3	10	no vesicles	0	5b-d9	50	2	trypsin	50 mM HEPES pH7
752	p2870	2870-521	mutant 3	10	no vesicles	0	5b-d9	50	3	trypsin	50 mM HEPES pH7
753	p2870	2870-531	mutant 3	10	no vesicles	0	5b-d9	50	6	trypsin	50 mM HEPES pH7
754	p2870	2870-541	mutant 3	10	no vesicles	0	5b-d9	50	10	trypsin	50 mM HEPES pH7
755	p2870	2870-551	mutant 3	10	no vesicles	0	5b-d9	50	15	trypsin	50 mM HEPES pH7
756	p2870	2870-561	mutant 3	10	no vesicles	0	5b-d9	50	30	trypsin	50 mM HEPES pH7
757	p2870	2870-571	mutant 4	10	no vesicles	0	5b-d9	50	0.5	trypsin	50 mM HEPES pH7
758	p2870	2870-581	mutant 4	10	no vesicles	0	5b-d9	50	1	trypsin	50 mM HEPES pH7
759	p2870	2870-591	mutant 4	10	no vesicles	0	5b-d9	50	2	trypsin	50 mM HEPES pH7
760	p2870	2870-601	mutant 4	10	no vesicles	0	5b-d9	50	3	trypsin	50 mM HEPES pH7
761	p2870	2870-611	mutant 4	10	no vesicles	0	5b-d9	50	6	trypsin	50 mM HEPES pH7
762	p2870	2870-621	mutant 4	10	no vesicles	0	5b-d9	50	10	trypsin	50 mM HEPES pH7
763	p2870	2870-631	mutant 4	10	no vesicles	0	5b-d9	50	15	trypsin	50 mM HEPES pH7
764	p2870	2870-641	mutant 4	10	no vesicles	0	5b-d9	50	30	trypsin	50 mM HEPES pH7
765	p2870	2870-651	mutant 5	10	no vesicles	0	5b-d9	50	0.5	trypsin	50 mM HEPES pH7
766	p2870	2870-661	mutant 5	10	no vesicles	0	5b-d9	50	1	trypsin	50 mM HEPES pH7
767	p2870	2870-671	mutant 5	10	no vesicles	0	5b-d9	50	2	trypsin	50 mM HEPES pH7
768	p2870	2870-681	mutant 5	10	no vesicles	0	5b-d9	50	3	trypsin	50 mM HEPES pH7
769	p2870	2870-691	mutant 5	10	no vesicles	0	5b-d9	50	6	trypsin	50 mM HEPES pH7
770	p2870	2870-701	mutant 5	10	no vesicles	0	5b-d9	50	10	trypsin	50 mM HEPES pH7
771	p2870	2870-711	mutant 5	10	no vesicles	0	5b-d9	50	15	trypsin	50 mM HEPES pH7
772	p2870	2870-721	mutant 5	10	no vesicles	0	5b-d9	50	30	trypsin	50 mM HEPES pH7
773	p2870	2870-731	mutant 6	10	no vesicles	0	5b-d9	50	0.5	trypsin	50 mM HEPES pH7
774	p2870	2870-741	mutant 6	10	no vesicles	0	5b-d9	50	1	trypsin	50 mM HEPES pH7
775	p2870	2870-751	mutant 6	10	no vesicles	0	5b-d9	50	2	trypsin	50 mM HEPES pH7
776	p2870	2870-761	mutant 6	10	no vesicles	0	5b-d9	50	3	trypsin	50 mM HEPES pH7
777	p2870	2870-771	mutant 6	10	no vesicles	0	5b-d9	50	6	trypsin	50 mM HEPES pH7
778	p2870	2870-781	mutant 6	10	no vesicles	0	5b-d9	50	10	trypsin	50 mM HEPES pH7
779	p2870	2870-791	mutant 6	10	no vesicles	0	5b-d9	50	15	trypsin	50 mM HEPES pH7
780	p2870	2870-801	mutant 6	10	no vesicles	0	5b-d9	50	30	trypsin	50 mM HEPES pH7
781	p2872	2872-11	WT	10	no vesicles	0	5b-d9	50	0.5	chymotrypsin	50 mM HEPES pH7
782	p2872	2872-21	WT	10	no vesicles	0	5b-d9	50	1	chymotrypsin	50 mM HEPES pH7
783	p2872	2872-31	WT	10	no vesicles	0	5b-d9	50	2	chymotrypsin	50 mM HEPES pH7
784	p2872	2872-41	WT	10	no vesicles	0	5b-d9	50	3	chymotrypsin	50 mM HEPES pH7
785	p2872	2872-51	WT	10	no vesicles	0	5b-d9	50	6	chymotrypsin	50 mM HEPES pH7
786	p2872	2872-61	WT	10	no vesicles	0	5b-d9	50	10	chymotrypsin	50 mM HEPES pH7
787	p2872	2872-71	WT	10	no vesicles	0	5b-d9	50	15	chymotrypsin	50 mM HEPES pH7
788	p2872	2872-81	WT	10	no vesicles	0	5b-d9	50	30	chymotrypsin	50 mM HEPES pH7
789	p2872	2872-91	L80C	10	no vesicles	0	5b-d9	50	0.5	chymotrypsin	50 mM HEPES pH7
790	p2872	2872-101	L80C	10	no vesicles	0	5b-d9	50	1	chymotrypsin	50 mM HEPES pH7
791	p2872	2872-111	L80C	10	no vesicles	0	5b-d9	50	2	chymotrypsin	50 mM HEPES pH7
792	p2872	2872-121	L80C	10	no vesicles	0	5b-d9	50	3	chymotrypsin	50 mM HEPES pH7
793	p2872	2872-131	L80C	10	no vesicles	0	5b-d9	50	6	chymotrypsin	50 mM HEPES pH7
794	p2872	2872-141	L80C	10	no vesicles	0	5b-d9	50	10	chymotrypsin	50 mM HEPES pH7
795	p2872	2872-151	L80C	10	no vesicles	0	5b-d9	50	15	chymotrypsin	50 mM HEPES pH7
796	p2872	2872-161	L80C	10	no vesicles	0	5b-d9	50	30	chymotrypsin	50 mM HEPES pH7
797	p2872	2872-171	L274C	10	no vesicles	0	5b-d9	50	0.5	chymotrypsin	50 mM HEPES pH7
798	p2872	2872-181	L274C	10	no vesicles	0	5b-d9	50	1	chymotrypsin	50 mM HEPES pH7
799	p2872	2872-191	L274C	10	no vesicles	0	5b-d9	50	2	chymotrypsin	50 mM HEPES pH7

800	p2872	2872-201	L274C	10	no vesicles	0	5b-d9	50	3	chymotrypsin	50 mM HEPES pH7
801	p2872	2872-211	L274C	10	no vesicles	0	5b-d9	50	6	chymotrypsin	50 mM HEPES pH7
802	p2872	2872-221	L274C	10	no vesicles	0	5b-d9	50	10	chymotrypsin	50 mM HEPES pH7
803	p2872	2872-231	L274C	10	no vesicles	0	5b-d9	50	15	chymotrypsin	50 mM HEPES pH7
804	p2872	2872-241	L274C	10	no vesicles	0	5b-d9	50	30	chymotrypsin	50 mM HEPES pH7
805	p2872	2872-251	W333C	10	no vesicles	0	5b-d9	50	0.5	chymotrypsin	50 mM HEPES pH7
806	p2872	2872-261	W333C	10	no vesicles	0	5b-d9	50	1	chymotrypsin	50 mM HEPES pH7
807	p2872	2872-271	W333C	10	no vesicles	0	5b-d9	50	2	chymotrypsin	50 mM HEPES pH7
808	p2872	2872-281	W333C	10	no vesicles	0	5b-d9	50	3	chymotrypsin	50 mM HEPES pH7
809	p2872	2872-291	W333C	10	no vesicles	0	5b-d9	50	6	chymotrypsin	50 mM HEPES pH7
810	p2872	2872-301	W333C	10	no vesicles	0	5b-d9	50	10	chymotrypsin	50 mM HEPES pH7
811	p2872	2872-311	W333C	10	no vesicles	0	5b-d9	50	15	chymotrypsin	50 mM HEPES pH7
812	p2872	2872-321	W333C	10	no vesicles	0	5b-d9	50	30	chymotrypsin	50 mM HEPES pH7
813	p2872	2872-331	mutant 1	10	no vesicles	0	5b-d9	50	0.5	chymotrypsin	50 mM HEPES pH7
814	p2872	2872-341	mutant 1	10	no vesicles	0	5b-d9	50	1	chymotrypsin	50 mM HEPES pH7
815	p2872	2872-351	mutant 1	10	no vesicles	0	5b-d9	50	2	chymotrypsin	50 mM HEPES pH7
816	p2872	2872-361	mutant 1	10	no vesicles	0	5b-d9	50	3	chymotrypsin	50 mM HEPES pH7
817	p2872	2872-371	mutant 1	10	no vesicles	0	5b-d9	50	6	chymotrypsin	50 mM HEPES pH7
818	p2872	2872-381	mutant 1	10	no vesicles	0	5b-d9	50	10	chymotrypsin	50 mM HEPES pH7
819	p2872	2872-391	mutant 1	10	no vesicles	0	5b-d9	50	15	chymotrypsin	50 mM HEPES pH7
820	p2872	2872-401	mutant 1	10	no vesicles	0	5b-d9	50	30	chymotrypsin	50 mM HEPES pH7
821	p2872	2872-411	mutant 2	10	no vesicles	0	5b-d9	50	0.5	chymotrypsin	50 mM HEPES pH7
822	p2872	2872-421	mutant 2	10	no vesicles	0	5b-d9	50	1	chymotrypsin	50 mM HEPES pH7
823	p2872	2872-431	mutant 2	10	no vesicles	0	5b-d9	50	2	chymotrypsin	50 mM HEPES pH7
824	p2872	2872-441	mutant 2	10	no vesicles	0	5b-d9	50	3	chymotrypsin	50 mM HEPES pH7
825	p2872	2872-451	mutant 2	10	no vesicles	0	5b-d9	50	6	chymotrypsin	50 mM HEPES pH7
826	p2872	2872-461	mutant 2	10	no vesicles	0	5b-d9	50	10	chymotrypsin	50 mM HEPES pH7
827	p2872	2872-471	mutant 2	10	no vesicles	0	5b-d9	50	15	chymotrypsin	50 mM HEPES pH7
828	p2872	2872-481	mutant 2	10	no vesicles	0	5b-d9	50	30	chymotrypsin	50 mM HEPES pH7
829	p2872	2872-491	mutant 3	10	no vesicles	0	5b-d9	50	0.5	chymotrypsin	50 mM HEPES pH7
830	p2872	2872-501	mutant 3	10	no vesicles	0	5b-d9	50	1	chymotrypsin	50 mM HEPES pH7
831	p2872	2872-511	mutant 3	10	no vesicles	0	5b-d9	50	2	chymotrypsin	50 mM HEPES pH7
832	p2872	2872-521	mutant 3	10	no vesicles	0	5b-d9	50	3	chymotrypsin	50 mM HEPES pH7
833	p2872	2872-531	mutant 3	10	no vesicles	0	5b-d9	50	6	chymotrypsin	50 mM HEPES pH7
834	p2872	2872-541	mutant 3	10	no vesicles	0	5b-d9	50	10	chymotrypsin	50 mM HEPES pH7
835	p2872	2872-551	mutant 3	10	no vesicles	0	5b-d9	50	15	chymotrypsin	50 mM HEPES pH7
836	p2872	2872-561	mutant 3	10	no vesicles	0	5b-d9	50	30	chymotrypsin	50 mM HEPES pH7
837	p2872	2872-571	mutant 4	10	no vesicles	0	5b-d9	50	0.5	chymotrypsin	50 mM HEPES pH7
838	p2872	2872-581	mutant 4	10	no vesicles	0	5b-d9	50	1	chymotrypsin	50 mM HEPES pH7
839	p2872	2872-591	mutant 4	10	no vesicles	0	5b-d9	50	2	chymotrypsin	50 mM HEPES pH7
840	p2872	2872-601	mutant 4	10	no vesicles	0	5b-d9	50	3	chymotrypsin	50 mM HEPES pH7
841	p2872	2872-611	mutant 4	10	no vesicles	0	5b-d9	50	6	chymotrypsin	50 mM HEPES pH7
842	p2872	2872-621	mutant 4	10	no vesicles	0	5b-d9	50	10	chymotrypsin	50 mM HEPES pH7
843	p2872	2872-631	mutant 4	10	no vesicles	0	5b-d9	50	15	chymotrypsin	50 mM HEPES pH7
844	p2872	2872-641	mutant 4	10	no vesicles	0	5b-d9	50	30	chymotrypsin	50 mM HEPES pH7
845	p2872	2872-651	mutant 5	10	no vesicles	0	5b-d9	50	0.5	chymotrypsin	50 mM HEPES pH7
846	p2872	2872-661	mutant 5	10	no vesicles	0	5b-d9	50	1	chymotrypsin	50 mM HEPES pH7
847	p2872	2872-671	mutant 5	10	no vesicles	0	5b-d9	50	2	chymotrypsin	50 mM HEPES pH7
848	p2872	2872-681	mutant 5	10	no vesicles	0	5b-d9	50	3	chymotrypsin	50 mM HEPES pH7
849	p2872	2872-691	mutant 5	10	no vesicles	0	5b-d9	50	6	chymotrypsin	50 mM HEPES pH7
850	p2872	2872-701	mutant 5	10	no vesicles	0	5b-d9	50	10	chymotrypsin	50 mM HEPES pH7
851	p2872	2872-711	mutant 5	10	no vesicles	0	5b-d9	50	15	chymotrypsin	50 mM HEPES pH7
852	p2872	2872-721	mutant 5	10	no vesicles	0	5b-d9	50	30	chymotrypsin	50 mM HEPES pH7
853	p2872	2872-731	mutant 6	10	no vesicles	0	5b-d9	50	0.5	chymotrypsin	50 mM HEPES pH7
854	p2872	2872-741	mutant 6	10	no vesicles	0	5b-d9	50	1	chymotrypsin	50 mM HEPES pH7
855	p2872	2872-751	mutant 6	10	no vesicles	0	5b-d9	50	2	chymotrypsin	50 mM HEPES pH7
856	p2872	2872-761	mutant 6	10	no vesicles	0	5b-d9	50	3	chymotrypsin	50 mM HEPES pH7
857	p2872	2872-771	mutant 6	10	no vesicles	0	5b-d9	50	6	chymotrypsin	50 mM HEPES pH7

858	p2872	2872-781	mutant 6	10	no vesicles	0	5b-d9	50	10	chymotrypsin	50 mM HEPES pH7
859	p2872	2872-791	mutant 6	10	no vesicles	0	5b-d9	50	15	chymotrypsin	50 mM HEPES pH7
860	p2872	2872-801	mutant 6	10	no vesicles	0	5b-d9	50	30	chymotrypsin	50 mM HEPES pH7
861	p2916	2916-11	L80C	5	DMPC/cholesterol(3/1)	500	5b-d9	50	0.5	trypsin	50 mM HEPES pH7
862	p2916	2916-21	L80C	5	DMPC/cholesterol(3/1)	500	5b-d9	50	1	trypsin	50 mM HEPES pH7
863	p2916	2916-31	L80C	5	DMPC/cholesterol(3/1)	500	5b-d9	50	2	trypsin	50 mM HEPES pH7
864	p2916	2916-41	L80C	5	DMPC/cholesterol(3/1)	500	5b-d9	50	3	trypsin	50 mM HEPES pH7
865	p2916	2916-51	L80C	5	DMPC/cholesterol(3/1)	500	5b-d9	50	6	trypsin	50 mM HEPES pH7
866	p2916	2916-61	L80C	5	DMPC/cholesterol(3/1)	500	5b-d9	50	10	trypsin	50 mM HEPES pH7
867	p2916	2916-71	L80C	5	DMPC/cholesterol(3/1)	500	5b-d9	50	15	trypsin	50 mM HEPES pH7
868	p2916	2916-81	L80C	5	DMPC/cholesterol(3/1)	500	5b-d9	50	30	trypsin	50 mM HEPES pH7
869	p2916	2916-91	L80C	5	no vesicles	0	5b-d9	50	0.5	trypsin	50 mM HEPES pH7
870	p2916	2916-101	L80C	5	no vesicles	0	5b-d9	50	1	trypsin	50 mM HEPES pH7
871	p2916	2916-111	L80C	5	no vesicles	0	5b-d9	50	2	trypsin	50 mM HEPES pH7
872	p2916	2916-121	L80C	5	no vesicles	0	5b-d9	50	3	trypsin	50 mM HEPES pH7
873	p2916	2916-131	L80C	5	no vesicles	0	5b-d9	50	6	trypsin	50 mM HEPES pH7
874	p2916	2916-141	L80C	5	no vesicles	0	5b-d9	50	10	trypsin	50 mM HEPES pH7
875	p2916	2916-151	L80C	5	no vesicles	0	5b-d9	50	15	trypsin	50 mM HEPES pH7
876	p2916	2916-161	L80C	5	no vesicles	0	5b-d9	50	30	trypsin	50 mM HEPES pH7
877	p2916	2916-171	L80C	5	DMPC/cholesterol(3/1)	500	5d-d9	50	0.5	trypsin	50 mM HEPES pH7
878	p2916	2916-181	L80C	5	DMPC/cholesterol(3/1)	500	5d-d9	50	1	trypsin	50 mM HEPES pH7
879	p2916	2916-191	L80C	5	DMPC/cholesterol(3/1)	500	5d-d9	50	2	trypsin	50 mM HEPES pH7
880	p2916	2916-201	L80C	5	DMPC/cholesterol(3/1)	500	5d-d9	50	3	trypsin	50 mM HEPES pH7
881	p2916	2916-211	L80C	5	DMPC/cholesterol(3/1)	500	5d-d9	50	6	trypsin	50 mM HEPES pH7
882	p2916	2916-221	L80C	5	DMPC/cholesterol(3/1)	500	5d-d9	50	10	trypsin	50 mM HEPES pH7
883	p2916	2916-231	L80C	5	DMPC/cholesterol(3/1)	500	5d-d9	50	15	trypsin	50 mM HEPES pH7
884	p2916	2916-241	L80C	5	DMPC/cholesterol(3/1)	500	5d-d9	50	30	trypsin	50 mM HEPES pH7
885	p2916	2916-251	L80C	5	no vesicles	0	5d-d9	50	0.5	trypsin	50 mM HEPES pH7
886	p2916	2916-261	L80C	5	no vesicles	0	5d-d9	50	1	trypsin	50 mM HEPES pH7
887	p2916	2916-271	L80C	5	no vesicles	0	5d-d9	50	2	trypsin	50 mM HEPES pH7
888	p2916	2916-281	L80C	5	no vesicles	0	5d-d9	50	3	trypsin	50 mM HEPES pH7
889	p2916	2916-291	L80C	5	no vesicles	0	5d-d9	50	6	trypsin	50 mM HEPES pH7
890	p2916	2916-301	L80C	5	no vesicles	0	5d-d9	50	10	trypsin	50 mM HEPES pH7
891	p2916	2916-311	L80C	5	no vesicles	0	5d-d9	50	15	trypsin	50 mM HEPES pH7
892	p2916	2916-321	L80C	5	no vesicles	0	5d-d9	50	30	trypsin	50 mM HEPES pH7
893	p2916	2916-331	mutant 2	5	DMPC/cholesterol(3/1)	500	5b-d9	50	0.5	trypsin	50 mM HEPES pH7
894	p2916	2916-341	mutant 2	5	DMPC/cholesterol(3/1)	500	5b-d9	50	1	trypsin	50 mM HEPES pH7
895	p2916	2916-351	mutant 2	5	DMPC/cholesterol(3/1)	500	5b-d9	50	2	trypsin	50 mM HEPES pH7
896	p2916	2916-361	mutant 2	5	DMPC/cholesterol(3/1)	500	5b-d9	50	3	trypsin	50 mM HEPES pH7
897	p2916	2916-371	mutant 2	5	DMPC/cholesterol(3/1)	500	5b-d9	50	6	trypsin	50 mM HEPES pH7
898	p2916	2916-381	mutant 2	5	DMPC/cholesterol(3/1)	500	5b-d9	50	10	trypsin	50 mM HEPES pH7
899	p2916	2916-391	mutant 2	5	DMPC/cholesterol(3/1)	500	5b-d9	50	15	trypsin	50 mM HEPES pH7
900	p2916	2916-401	mutant 2	5	DMPC/cholesterol(3/1)	500	5b-d9	50	30	trypsin	50 mM HEPES pH7
901	p2916	2916-411	mutant 2	5	no vesicles	0	5b-d9	50	0.5	trypsin	50 mM HEPES pH7
902	p2916	2916-421	mutant 2	5	no vesicles	0	5b-d9	50	1	trypsin	50 mM HEPES pH7
903	p2916	2916-431	mutant 2	5	no vesicles	0	5b-d9	50	2	trypsin	50 mM HEPES pH7
904	p2916	2916-441	mutant 2	5	no vesicles	0	5b-d9	50	3	trypsin	50 mM HEPES pH7
905	p2916	2916-451	mutant 2	5	no vesicles	0	5b-d9	50	6	trypsin	50 mM HEPES pH7
906	p2916	2916-461	mutant 2	5	no vesicles	0	5b-d9	50	10	trypsin	50 mM HEPES pH7
907	p2916	2916-471	mutant 2	5	no vesicles	0	5b-d9	50	15	trypsin	50 mM HEPES pH7
908	p2916	2916-481	mutant 2	5	no vesicles	0	5b-d9	50	30	trypsin	50 mM HEPES pH7
909	p2916	2916-491	mutant 2	5	DMPC/cholesterol(3/1)	500	5d-d9	50	0.5	trypsin	50 mM HEPES pH7
910	p2916	2916-501	mutant 2	5	DMPC/cholesterol(3/1)	500	5d-d9	50	1	trypsin	50 mM HEPES pH7
911	p2916	2916-511	mutant 2	5	DMPC/cholesterol(3/1)	500	5d-d9	50	2	trypsin	50 mM HEPES pH7
912	p2916	2916-521	mutant 2	5	DMPC/cholesterol(3/1)	500	5d-d9	50	3	trypsin	50 mM HEPES pH7
913	p2916	2916-531	mutant 2	5	DMPC/cholesterol(3/1)	500	5d-d9	50	6	trypsin	50 mM HEPES pH7
914	p2916	2916-541	mutant 2	5	DMPC/cholesterol(3/1)	500	5d-d9	50	10	trypsin	50 mM HEPES pH7
915	p2916	2916-551	mutant 2	5	DMPC/cholesterol(3/1)	500	5d-d9	50	15	trypsin	50 mM HEPES pH7

916	p2916	2916-561	mutant 2	5	DMPC/cholesterol(3/1)	500	5d-d9	50	30	trypsin	50 mM HEPES pH7
917	p2916	2916-571	mutant 2	5	no vesicles	0	5d-d9	50	0.5	trypsin	50 mM HEPES pH7
918	p2916	2916-581	mutant 2	5	no vesicles	0	5d-d9	50	1	trypsin	50 mM HEPES pH7
919	p2916	2916-591	mutant 2	5	no vesicles	0	5d-d9	50	2	trypsin	50 mM HEPES pH7
920	p2916	2916-601	mutant 2	5	no vesicles	0	5d-d9	50	3	trypsin	50 mM HEPES pH7
921	p2916	2916-611	mutant 2	5	no vesicles	0	5d-d9	50	6	trypsin	50 mM HEPES pH7
922	p2916	2916-621	mutant 2	5	no vesicles	0	5d-d9	50	10	trypsin	50 mM HEPES pH7
923	p2916	2916-631	mutant 2	5	no vesicles	0	5d-d9	50	15	trypsin	50 mM HEPES pH7
924	p2916	2916-641	mutant 2	5	no vesicles	0	5d-d9	50	30	trypsin	50 mM HEPES pH7
925	p2918	2918-11	mutant 2	10	DMPC/cholesterol(3/1)	500	5d-d9	50	0.5	trypsin	50 mM HEPES pH7
926	p2918	2918-21	mutant 2	10	DMPC/cholesterol(3/1)	500	5d-d9	50	1	trypsin	50 mM HEPES pH7
927	p2918	2918-31	mutant 2	10	DMPC/cholesterol(3/1)	500	5d-d9	50	2	trypsin	50 mM HEPES pH7
928	p2918	2918-41	mutant 2	10	DMPC/cholesterol(3/1)	500	5d-d9	50	3	trypsin	50 mM HEPES pH7
929	p2918	2918-51	mutant 2	10	DMPC/cholesterol(3/1)	500	5d-d9	50	6	trypsin	50 mM HEPES pH7
930	p2918	2918-61	mutant 2	10	DMPC/cholesterol(3/1)	500	5d-d9	50	10	trypsin	50 mM HEPES pH7
931	p2918	2918-71	mutant 2	10	DMPC/cholesterol(3/1)	500	5d-d9	50	15	trypsin	50 mM HEPES pH7
932	p2918	2918-81	mutant 2	10	DMPC/cholesterol(3/1)	500	5d-d9	50	30	trypsin	50 mM HEPES pH7
933	p2918	2918-91	mutant 2	10	no vesicles	0	5d-d9	50	0.5	trypsin	50 mM HEPES pH7
934	p2918	2918-101	mutant 2	10	no vesicles	0	5d-d9	50	1	trypsin	50 mM HEPES pH7
935	p2918	2918-111	mutant 2	10	no vesicles	0	5d-d9	50	2	trypsin	50 mM HEPES pH7
936	p2918	2918-121	mutant 2	10	no vesicles	0	5d-d9	50	3	trypsin	50 mM HEPES pH7
937	p2918	2918-131	mutant 2	10	no vesicles	0	5d-d9	50	6	trypsin	50 mM HEPES pH7
938	p2918	2918-141	mutant 2	10	no vesicles	0	5d-d9	50	10	trypsin	50 mM HEPES pH7
939	p2918	2918-151	mutant 2	10	no vesicles	0	5d-d9	50	15	trypsin	50 mM HEPES pH7
940	p2918	2918-161	mutant 2	10	no vesicles	0	5d-d9	50	30	trypsin	50 mM HEPES pH7
941	p2918	2918-171	mutant 2	10	DMPC/cholesterol(3/1)	500	5d-d9	50	0.5	chymotrypsin	50 mM HEPES pH7
942	p2918	2918-181	mutant 2	10	DMPC/cholesterol(3/1)	500	5d-d9	50	1	chymotrypsin	50 mM HEPES pH7
943	p2918	2918-191	mutant 2	10	DMPC/cholesterol(3/1)	500	5d-d9	50	2	chymotrypsin	50 mM HEPES pH7
944	p2918	2918-201	mutant 2	10	DMPC/cholesterol(3/1)	500	5d-d9	50	3	chymotrypsin	50 mM HEPES pH7
945	p2918	2918-211	mutant 2	10	DMPC/cholesterol(3/1)	500	5d-d9	50	6	chymotrypsin	50 mM HEPES pH7
946	p2918	2918-221	mutant 2	10	DMPC/cholesterol(3/1)	500	5d-d9	50	10	chymotrypsin	50 mM HEPES pH7
947	p2918	2918-231	mutant 2	10	DMPC/cholesterol(3/1)	500	5d-d9	50	15	chymotrypsin	50 mM HEPES pH7
948	p2918	2918-241	mutant 2	10	DMPC/cholesterol(3/1)	500	5d-d9	50	30	chymotrypsin	50 mM HEPES pH7
949	p2918	2918-251	mutant 2	10	no vesicles	0	5d-d9	50	0.5	chymotrypsin	50 mM HEPES pH7
950	p2918	2918-261	mutant 2	10	no vesicles	0	5d-d9	50	1	chymotrypsin	50 mM HEPES pH7
951	p2918	2918-271	mutant 2	10	no vesicles	0	5d-d9	50	2	chymotrypsin	50 mM HEPES pH7
952	p2918	2918-281	mutant 2	10	no vesicles	0	5d-d9	50	3	chymotrypsin	50 mM HEPES pH7
953	p2918	2918-291	mutant 2	10	no vesicles	0	5d-d9	50	6	chymotrypsin	50 mM HEPES pH7
954	p2918	2918-301	mutant 2	10	no vesicles	0	5d-d9	50	10	chymotrypsin	50 mM HEPES pH7
955	p2918	2918-311	mutant 2	10	no vesicles	0	5d-d9	50	15	chymotrypsin	50 mM HEPES pH7
956	p2918	2918-321	mutant 2	10	no vesicles	0	5d-d9	50	30	chymotrypsin	50 mM HEPES pH7
957	p2921	2921-11	mutant 2	6.6	DMPC/cholesterol(3/1)	500	5d-d9	50	0.5	trypsin	50 mM HEPES pH7
958	p2921	2921-21	mutant 2	6.6	DMPC/cholesterol(3/1)	500	5d-d9	50	1	trypsin	50 mM HEPES pH7
959	p2921	2921-31	mutant 2	6.6	DMPC/cholesterol(3/1)	500	5d-d9	50	2	trypsin	50 mM HEPES pH7
960	p2921	2921-41	mutant 2	6.6	DMPC/cholesterol(3/1)	500	5d-d9	50	3	trypsin	50 mM HEPES pH7
961	p2921	2921-51	mutant 2	6.6	DMPC/cholesterol(3/1)	500	5d-d9	50	6	trypsin	50 mM HEPES pH7
962	p2921	2921-61	mutant 2	6.6	DMPC/cholesterol(3/1)	500	5d-d9	50	10	trypsin	50 mM HEPES pH7
963	p2921	2921-71	mutant 2	6.6	DMPC/cholesterol(3/1)	500	5d-d9	50	15	trypsin	50 mM HEPES pH7
964	p2921	2921-81	mutant 2	6.6	DMPC/cholesterol(3/1)	500	5d-d9	50	30	trypsin	50 mM HEPES pH7
965	p2921	2921-91	mutant 2	6.6	no vesicles	0	5d-d9	50	0.5	trypsin	50 mM HEPES pH7
966	p2921	2921-101	mutant 2	6.6	no vesicles	0	5d-d9	50	1	trypsin	50 mM HEPES pH7
967	p2921	2921-111	mutant 2	6.6	no vesicles	0	5d-d9	50	2	trypsin	50 mM HEPES pH7
968	p2921	2921-121	mutant 2	6.6	no vesicles	0	5d-d9	50	3	trypsin	50 mM HEPES pH7
969	p2921	2921-131	mutant 2	6.6	no vesicles	0	5d-d9	50	6	trypsin	50 mM HEPES pH7
970	p2921	2921-141	mutant 2	6.6	no vesicles	0	5d-d9	50	10	trypsin	50 mM HEPES pH7
971	p2921	2921-151	mutant 2	6.6	no vesicles	0	5d-d9	50	15	trypsin	50 mM HEPES pH7
972	p2921	2921-161	mutant 2	6.6	no vesicles	0	5d-d9	50	30	trypsin	50 mM HEPES pH7
973	p2923	2923-11	mutant 2	8.2	DMPC/cholesterol(3/1)	500	5d-d9	50	0.5	trypsin	50 mM HEPES pH7

974	p2923	2923-21	mutant 2	8.2	DMPC/cholesterol(3/1)	500	5d-d9	50	1	trypsin	50 mM HEPES pH7
975	p2923	2923-31	mutant 2	8.2	DMPC/cholesterol(3/1)	500	5d-d9	50	2	trypsin	50 mM HEPES pH7
976	p2923	2923-41	mutant 2	8.2	DMPC/cholesterol(3/1)	500	5d-d9	50	3	trypsin	50 mM HEPES pH7
977	p2923	2923-51	mutant 2	8.2	DMPC/cholesterol(3/1)	500	5d-d9	50	6	trypsin	50 mM HEPES pH7
978	p2923	2923-61	mutant 2	8.2	DMPC/cholesterol(3/1)	500	5d-d9	50	10	trypsin	50 mM HEPES pH7
979	p2923	2923-71	mutant 2	8.2	DMPC/cholesterol(3/1)	500	5d-d9	50	15	trypsin	50 mM HEPES pH7
980	p2923	2923-81	mutant 2	8.2	DMPC/cholesterol(3/1)	500	5d-d9	50	30	trypsin	50 mM HEPES pH7
981	p2923	2923-91	mutant 2	8.2	no vesicles	0	5d-d9	50	0.5	trypsin	50 mM HEPES pH7
982	p2923	2923-101	mutant 2	8.2	no vesicles	0	5d-d9	50	1	trypsin	50 mM HEPES pH7
983	p2923	2923-111	mutant 2	8.2	no vesicles	0	5d-d9	50	2	trypsin	50 mM HEPES pH7
984	p2923	2923-121	mutant 2	8.2	no vesicles	0	5d-d9	50	3	trypsin	50 mM HEPES pH7
985	p2923	2923-131	mutant 2	8.2	no vesicles	0	5d-d9	50	6	trypsin	50 mM HEPES pH7
986	p2923	2923-141	mutant 2	8.2	no vesicles	0	5d-d9	50	10	trypsin	50 mM HEPES pH7
987	p2923	2923-151	mutant 2	8.2	no vesicles	0	5d-d9	50	15	trypsin	50 mM HEPES pH7
988	p2923	2923-161	mutant 2	8.2	no vesicles	0	5d-d9	50	30	trypsin	50 mM HEPES pH7

Appendix B: NMR and mass spectra for the ICMTs

Appendix 3 ^{1}H-NMR spectrum of compound 2a

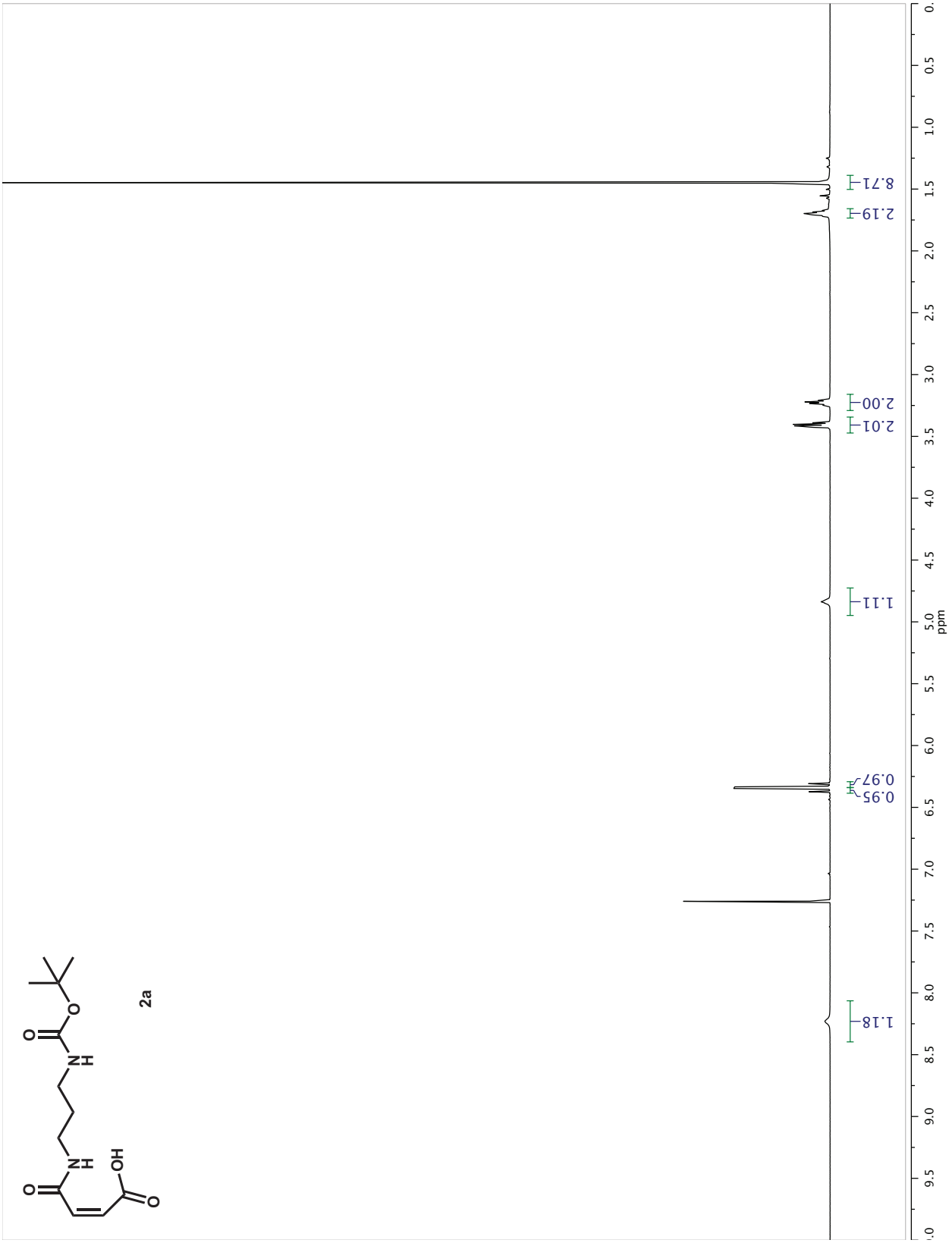

Appendix 4 ^{13}C-NMR spectrum of compound 2a

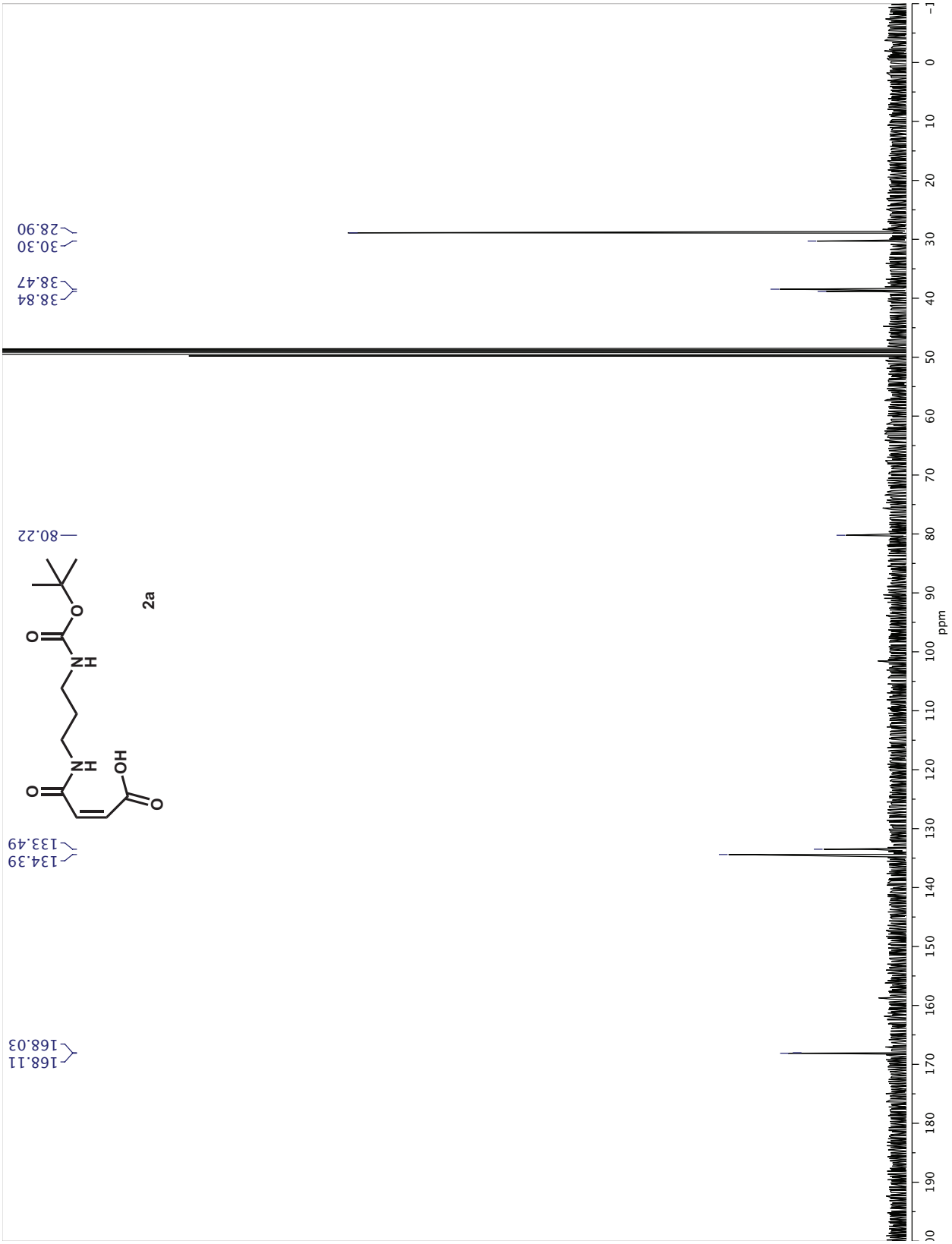

Appendix 5 ^{1}H-NMR of spectrum of compound 2b

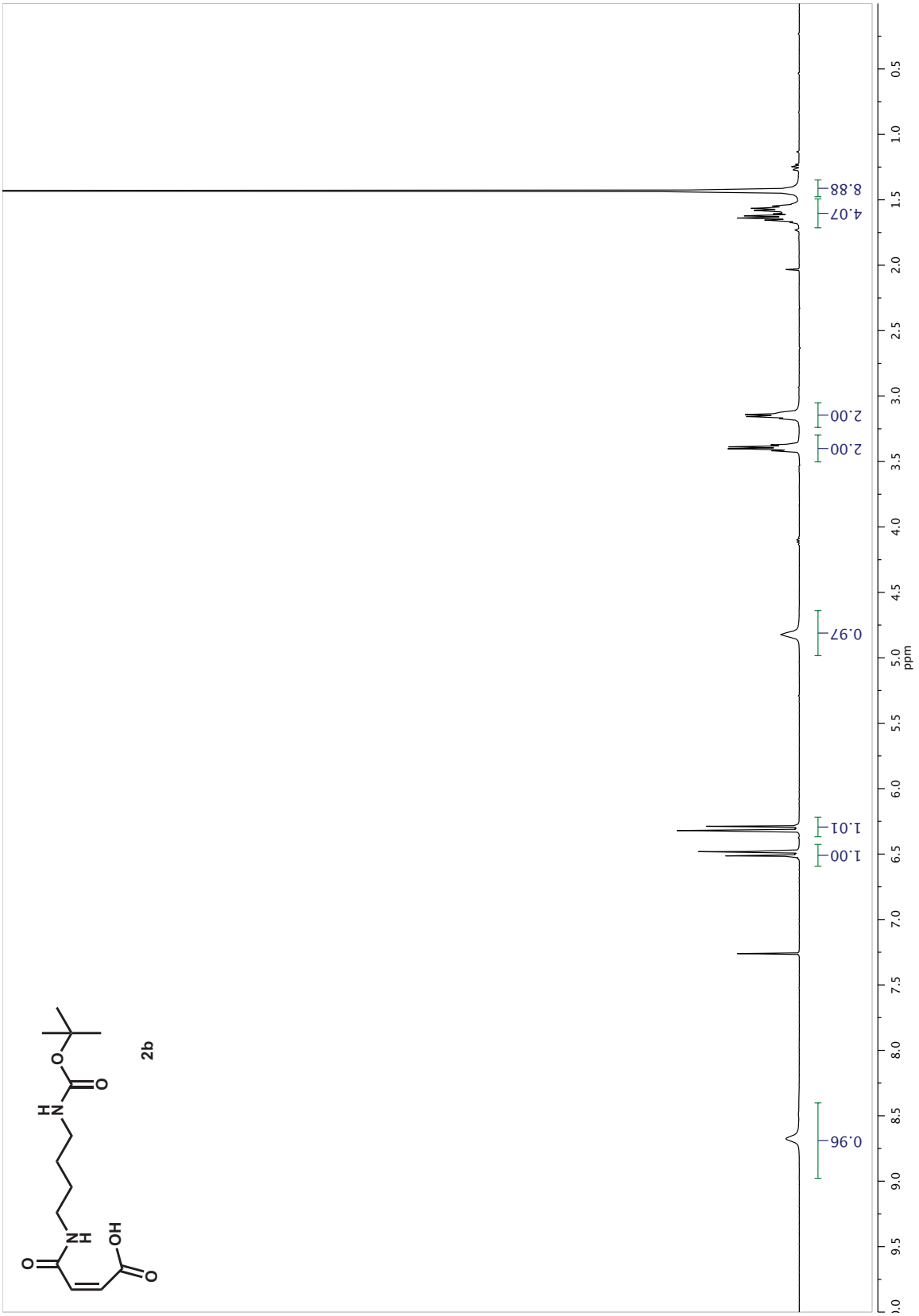

Appendix 6 ^{13}C-NMR of spectrum of compound 2b

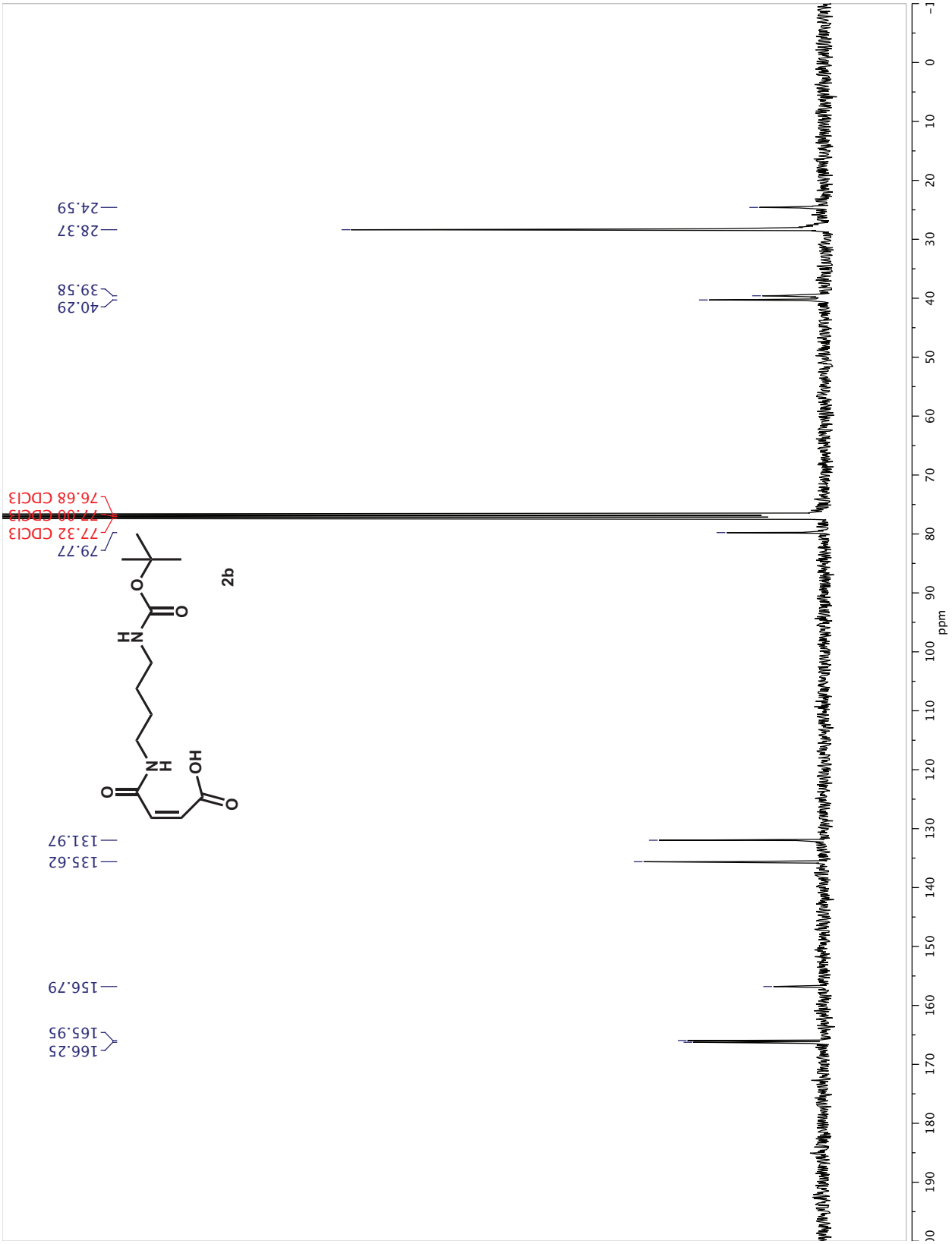

Appendix 7 ^{1}H-NMR of spectrum of compound 2c

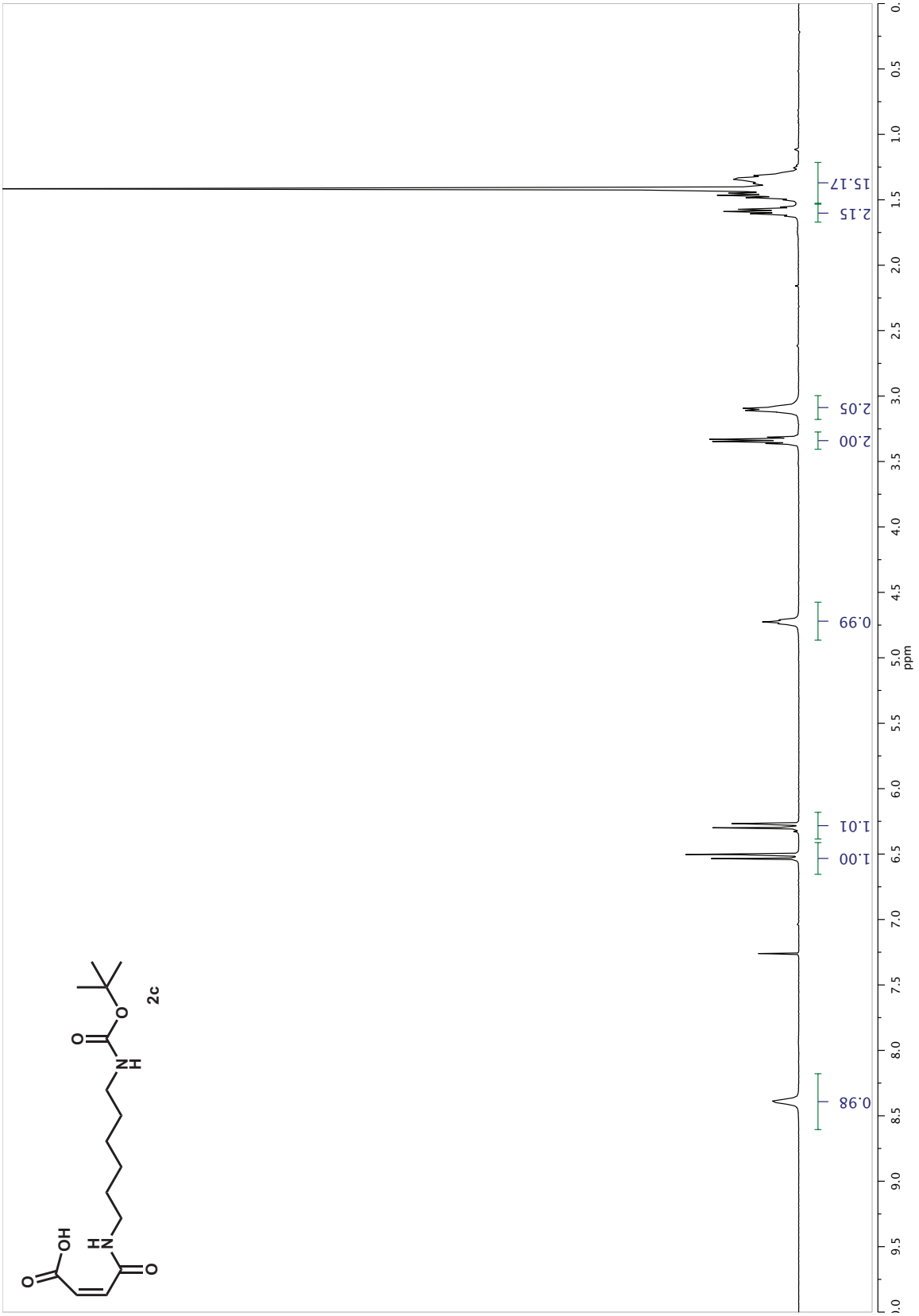

Appendix 8 ^{13}C-NMR of spectrum of compound 2c

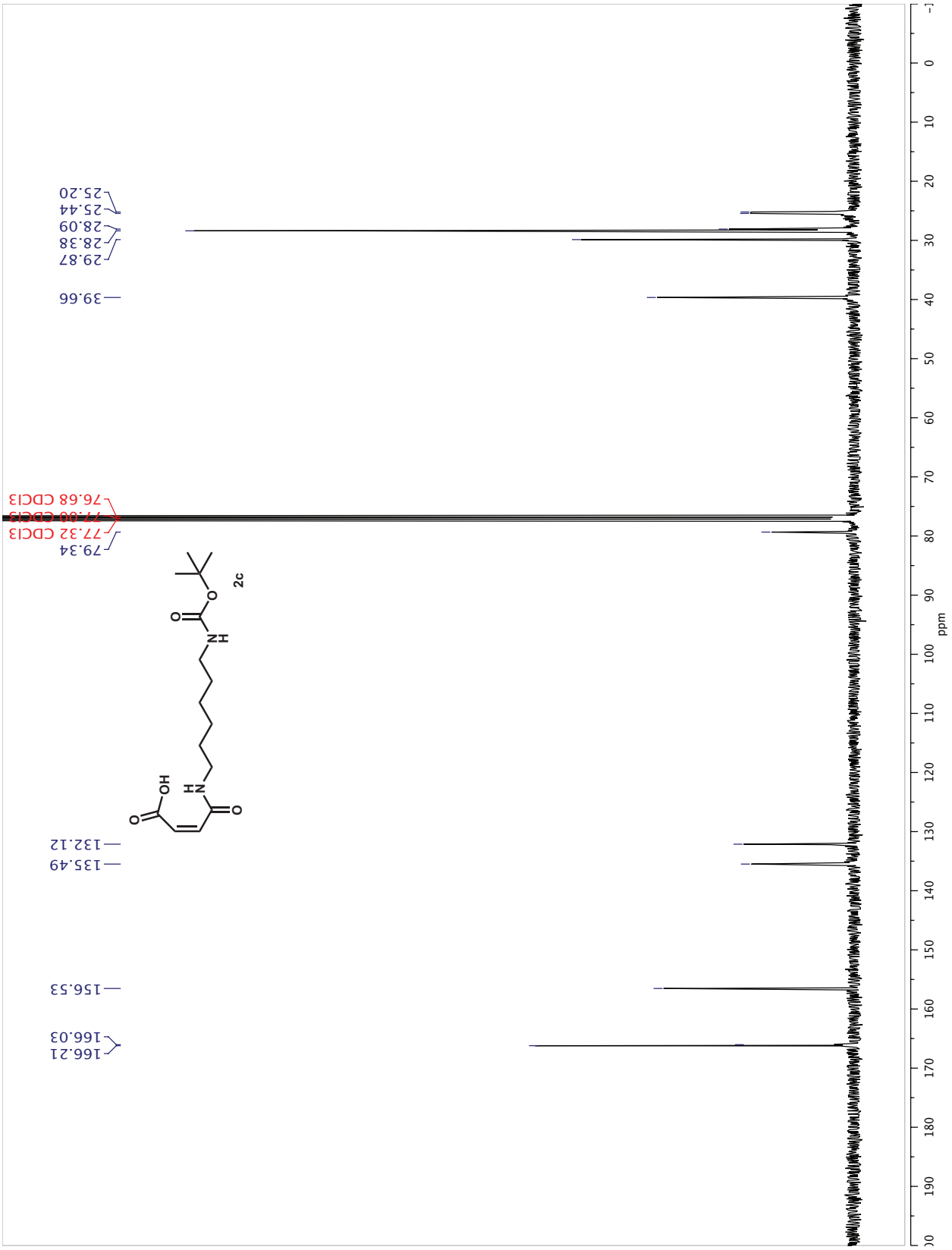

Appendix 9 ^{1}H-NMR of spectrum of compound 2d

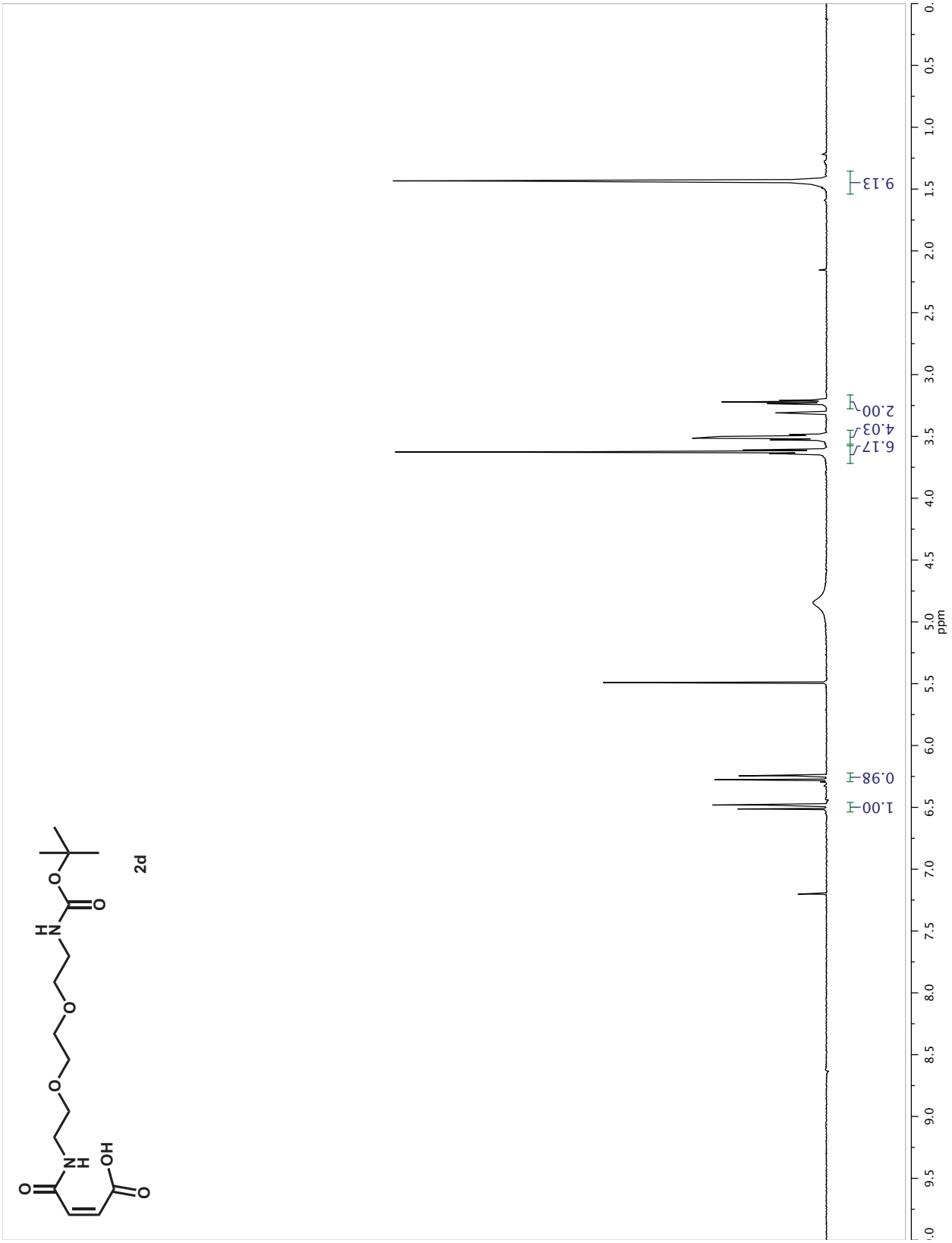

Appendix 10 ^{13}C-NMR of spectrum of compound 2d

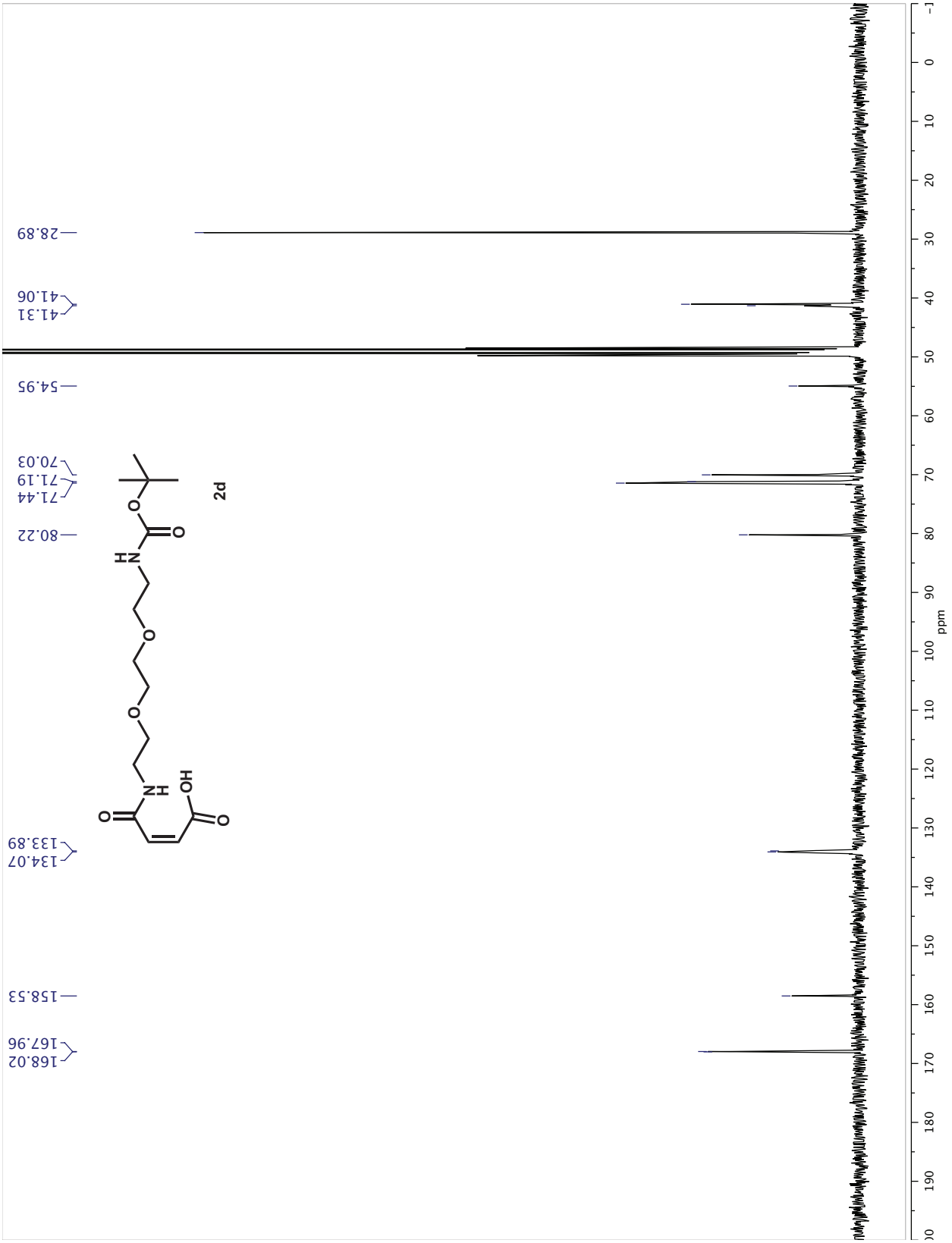

Appendix 11 ^{1}H-NMR of spectrum of compound 3a

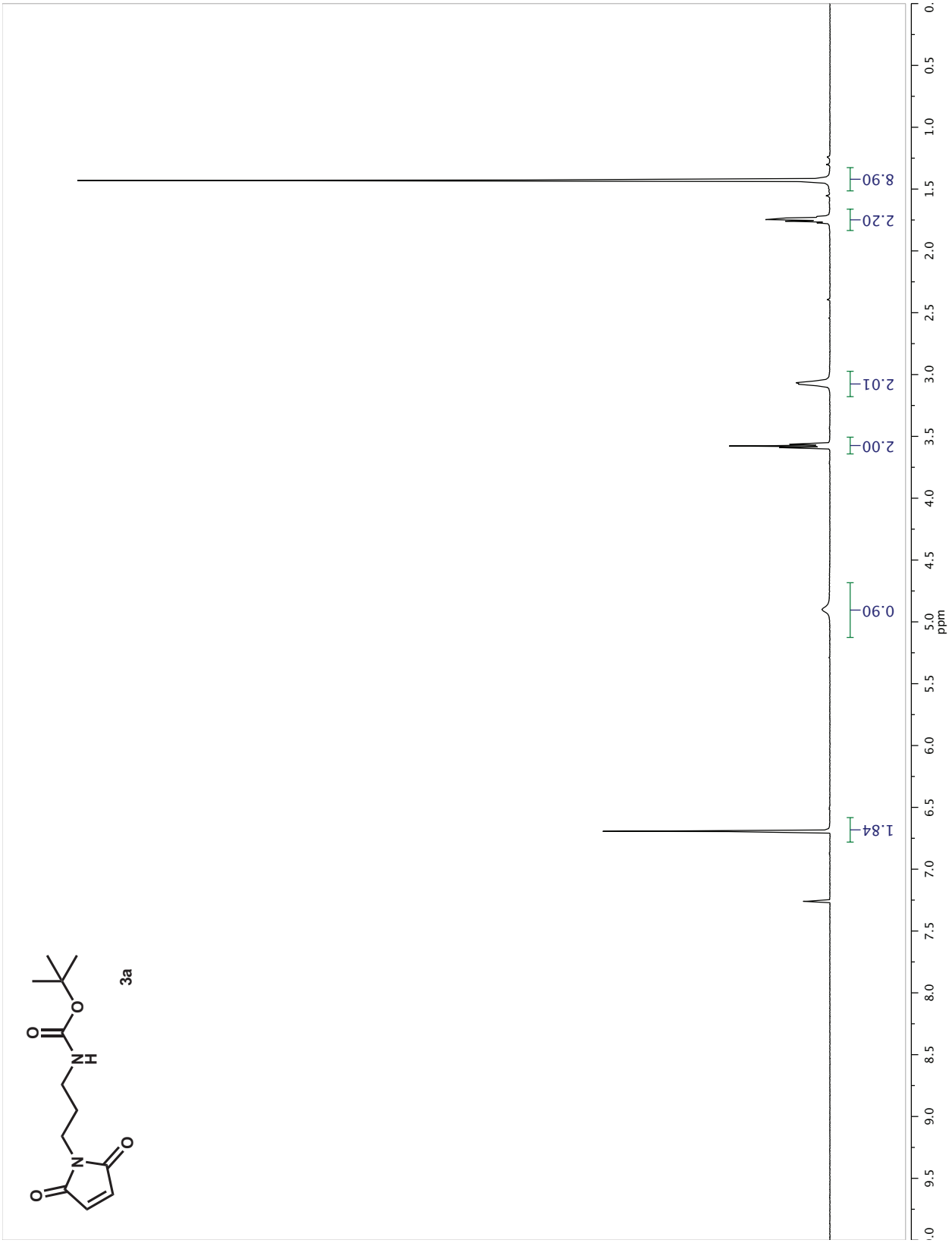

Appendix 12 ^{13}C-NMR of spectrum of compound 3a

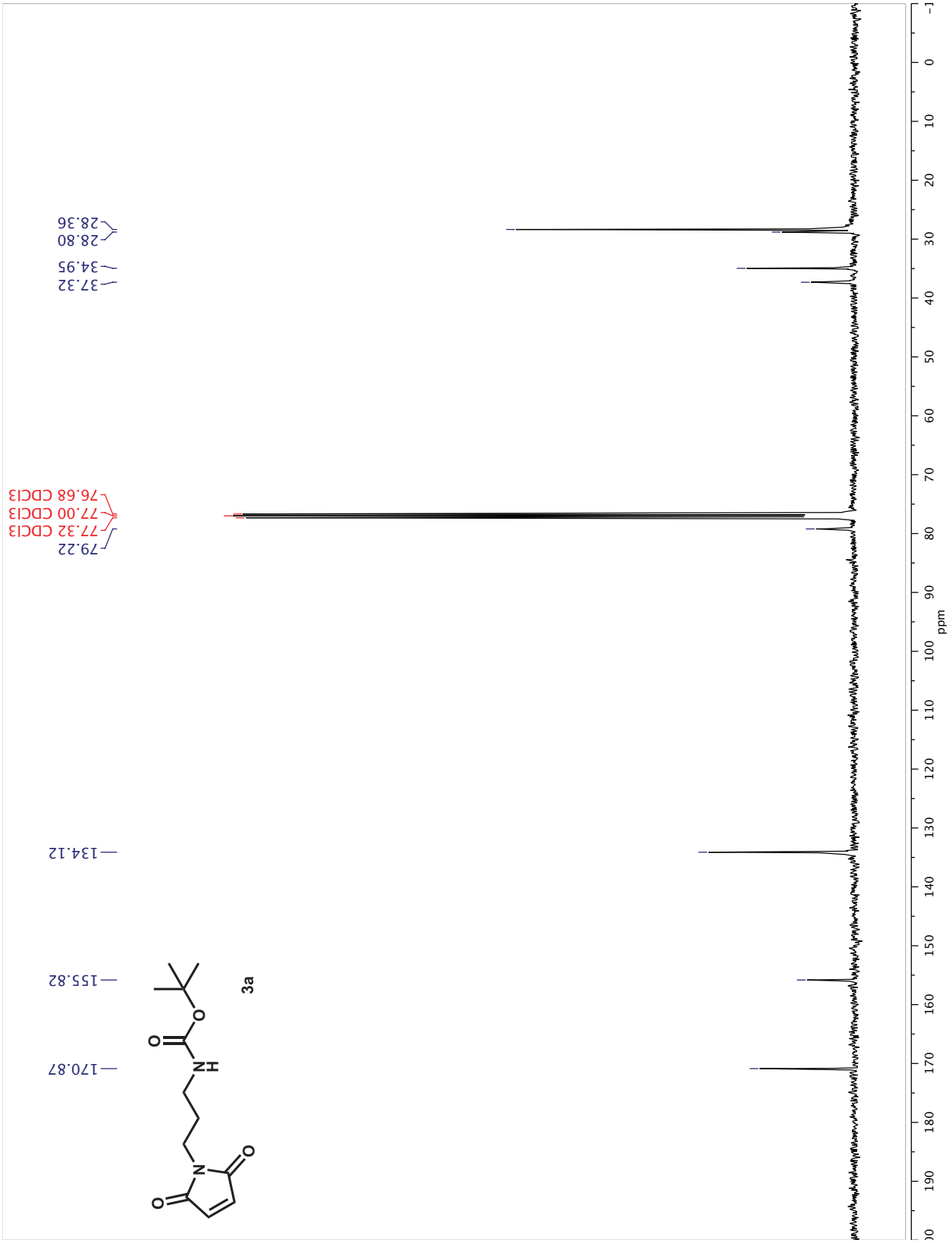

Appendix 13 ^{1}H-NMR of spectrum of compound 3b

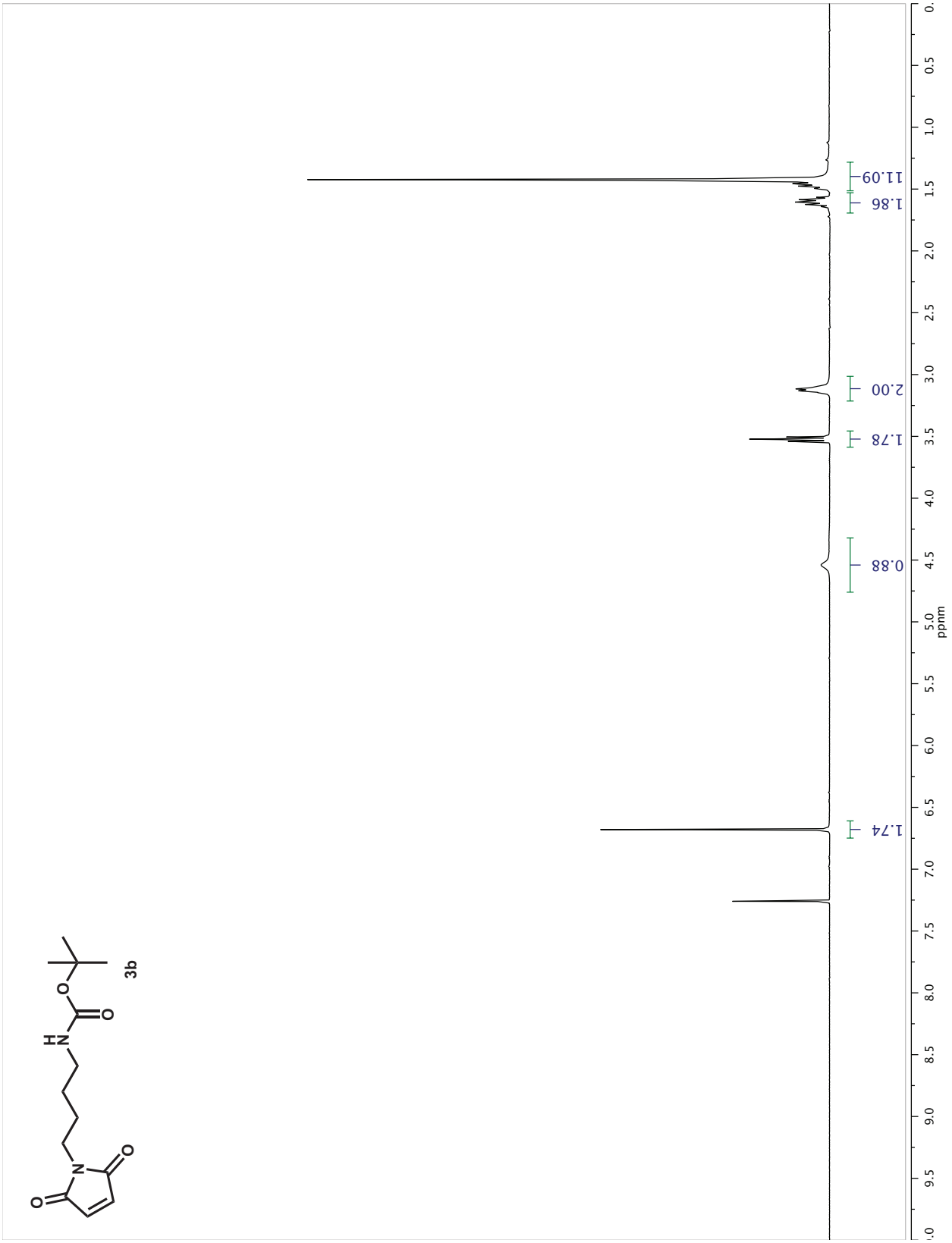

Appendix 14 ^{13}C-NMR of spectrum of compound 3b

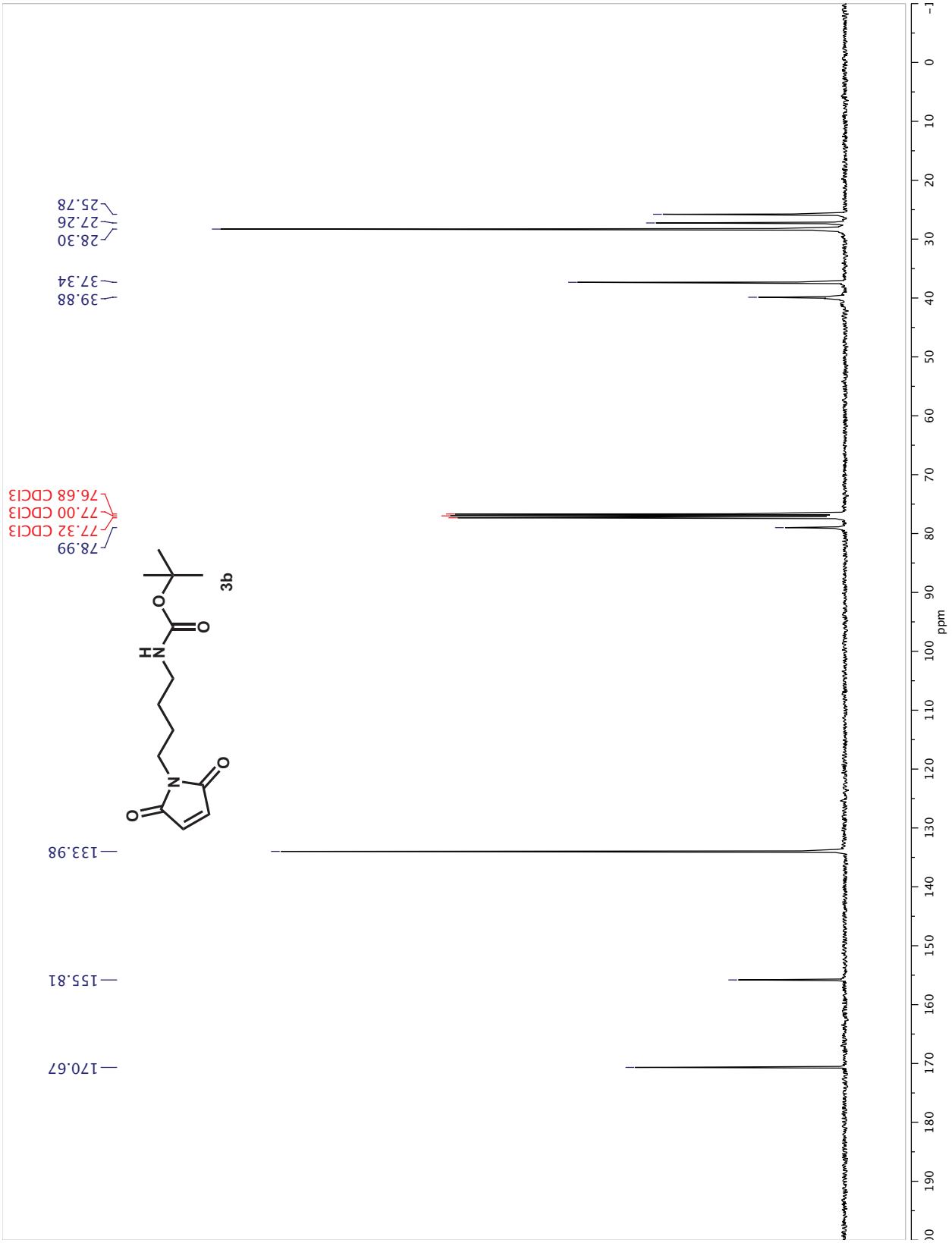

Appendix 15 ^{1}H-NMR of spectrum of compound 3c

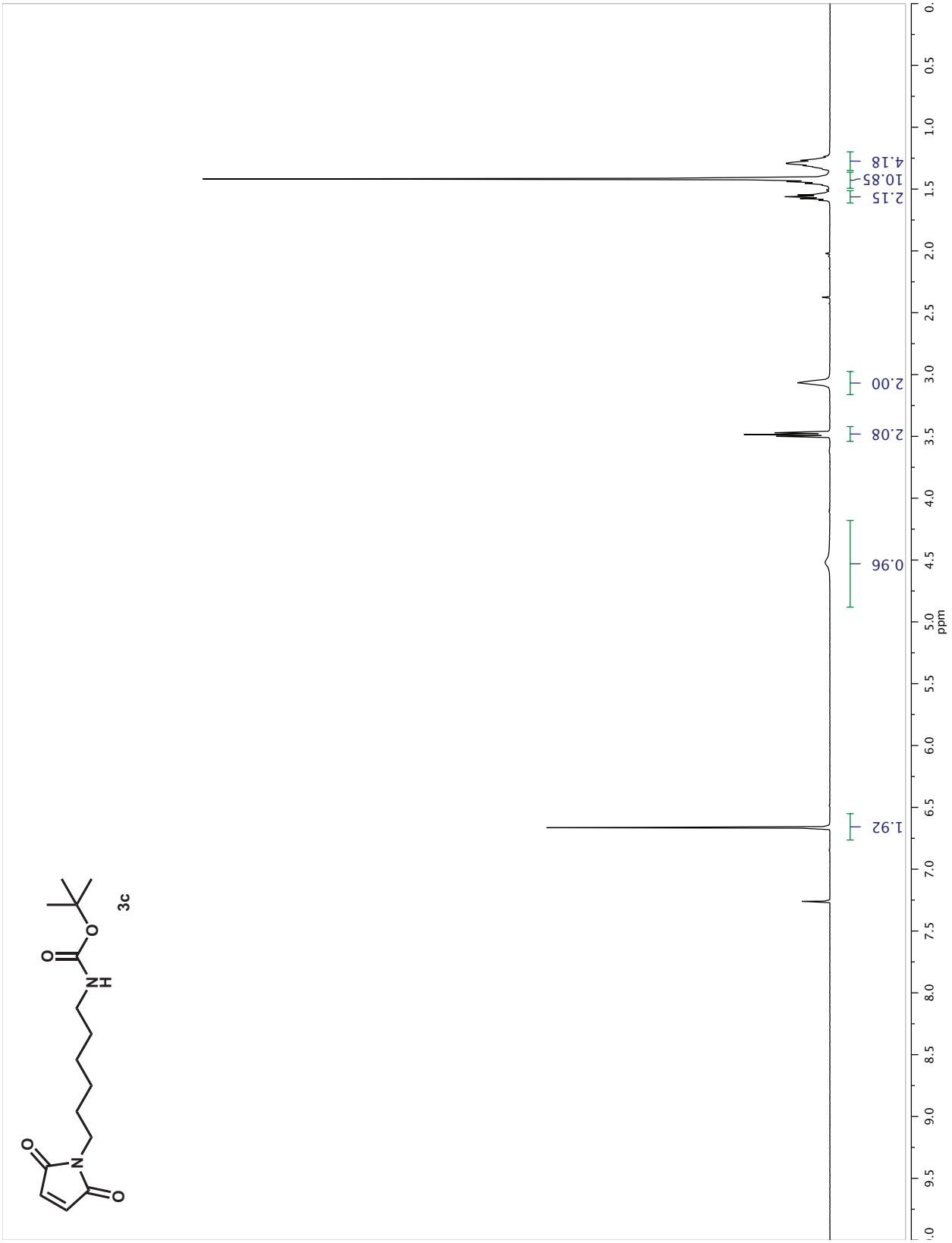

Appendix 16 ^{13}C-NMR of spectrum of compound 3c

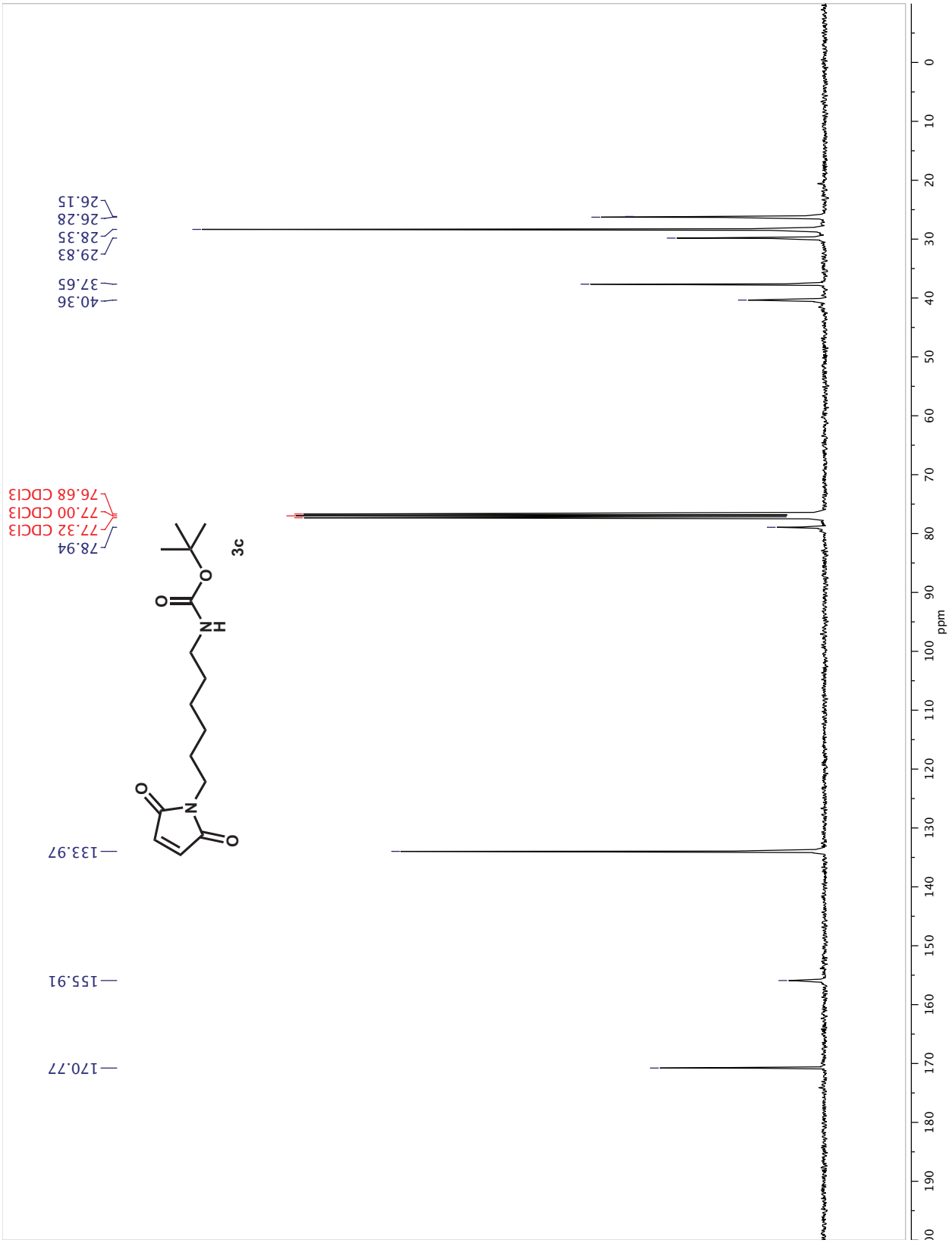

Appendix 17 ^{1}H-NMR of spectrum of compound 3d

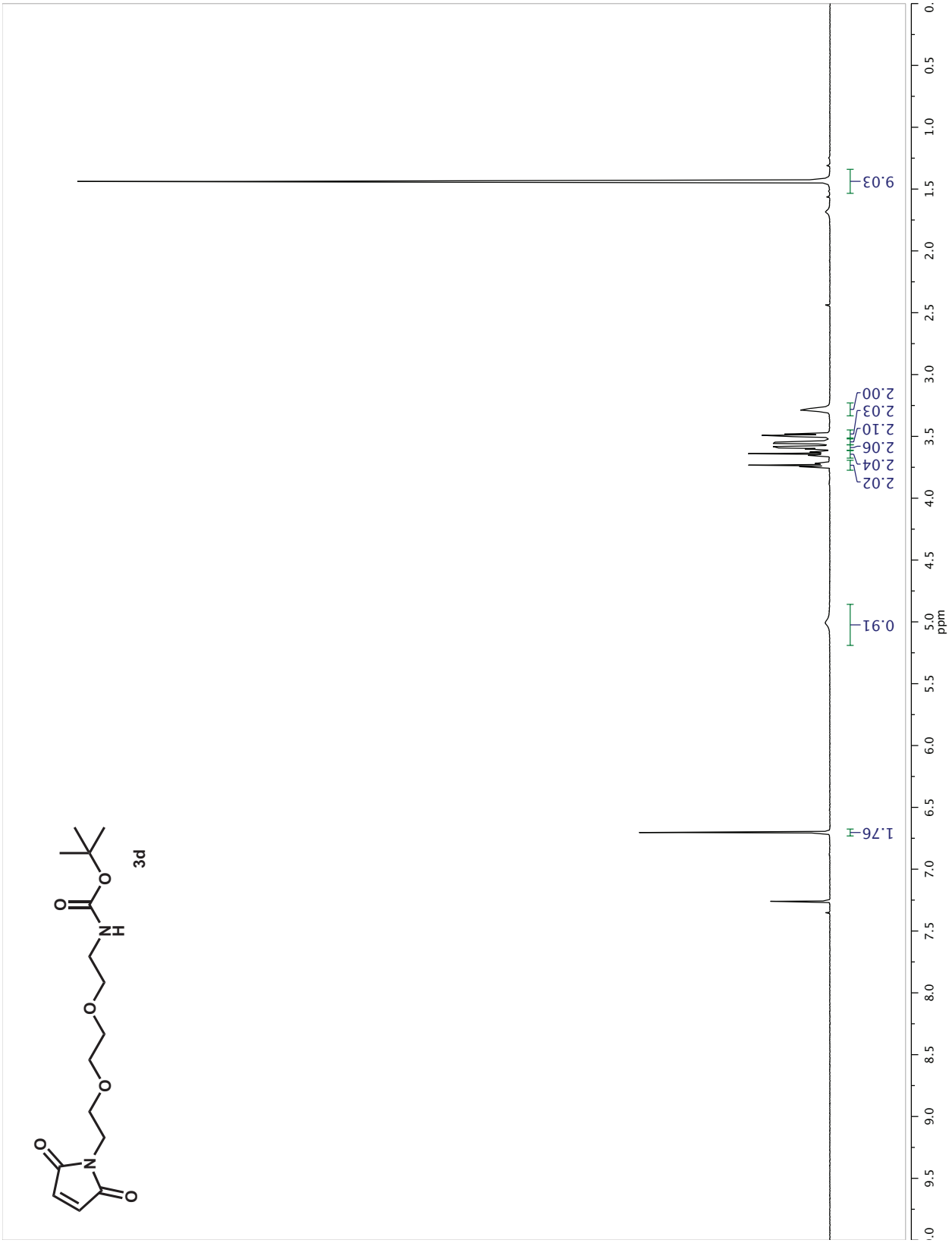

Appendix 18 ^{13}C-NMR of spectrum of compound 3d

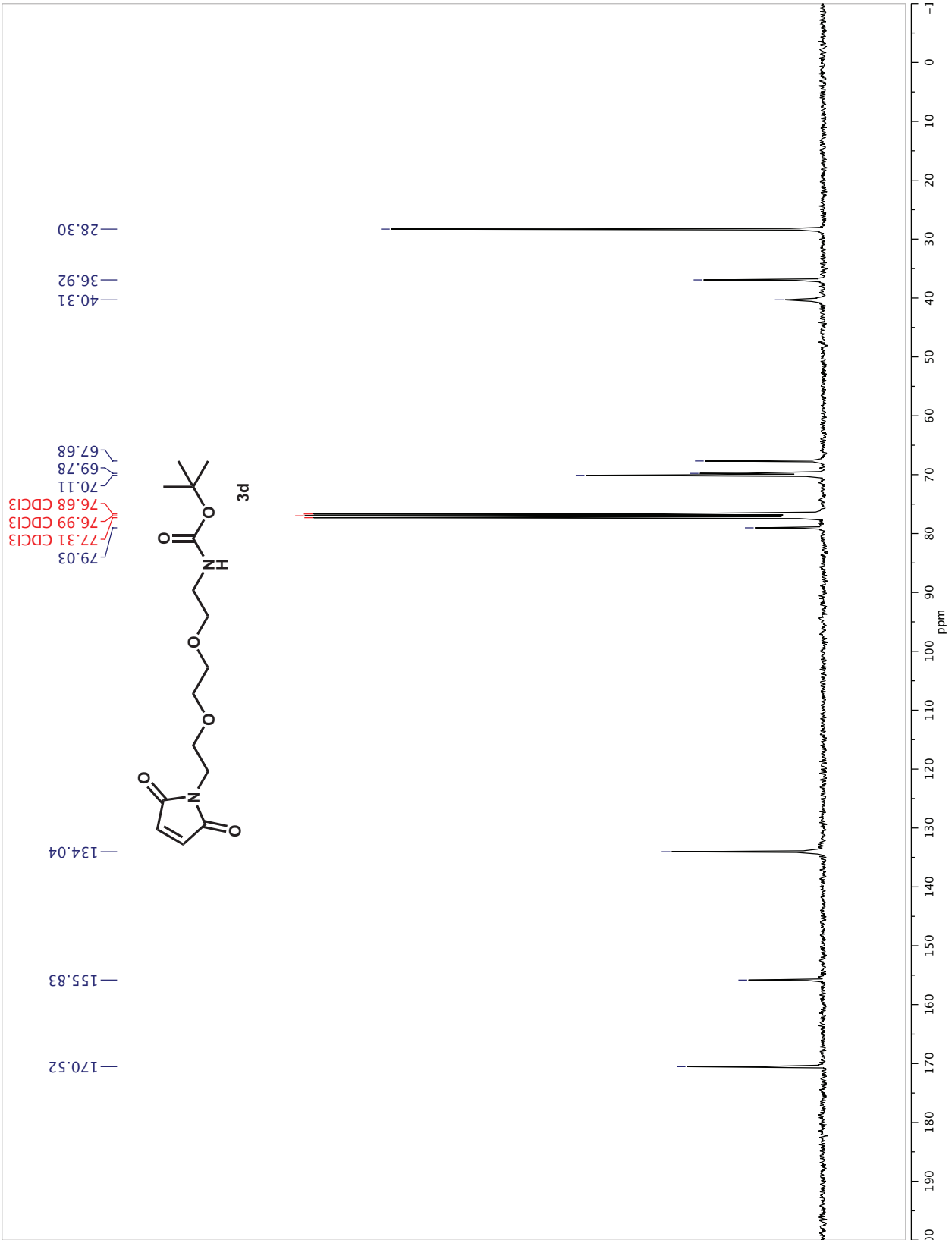

Appendix 19 1H-NMR of spectrum of compound 4a

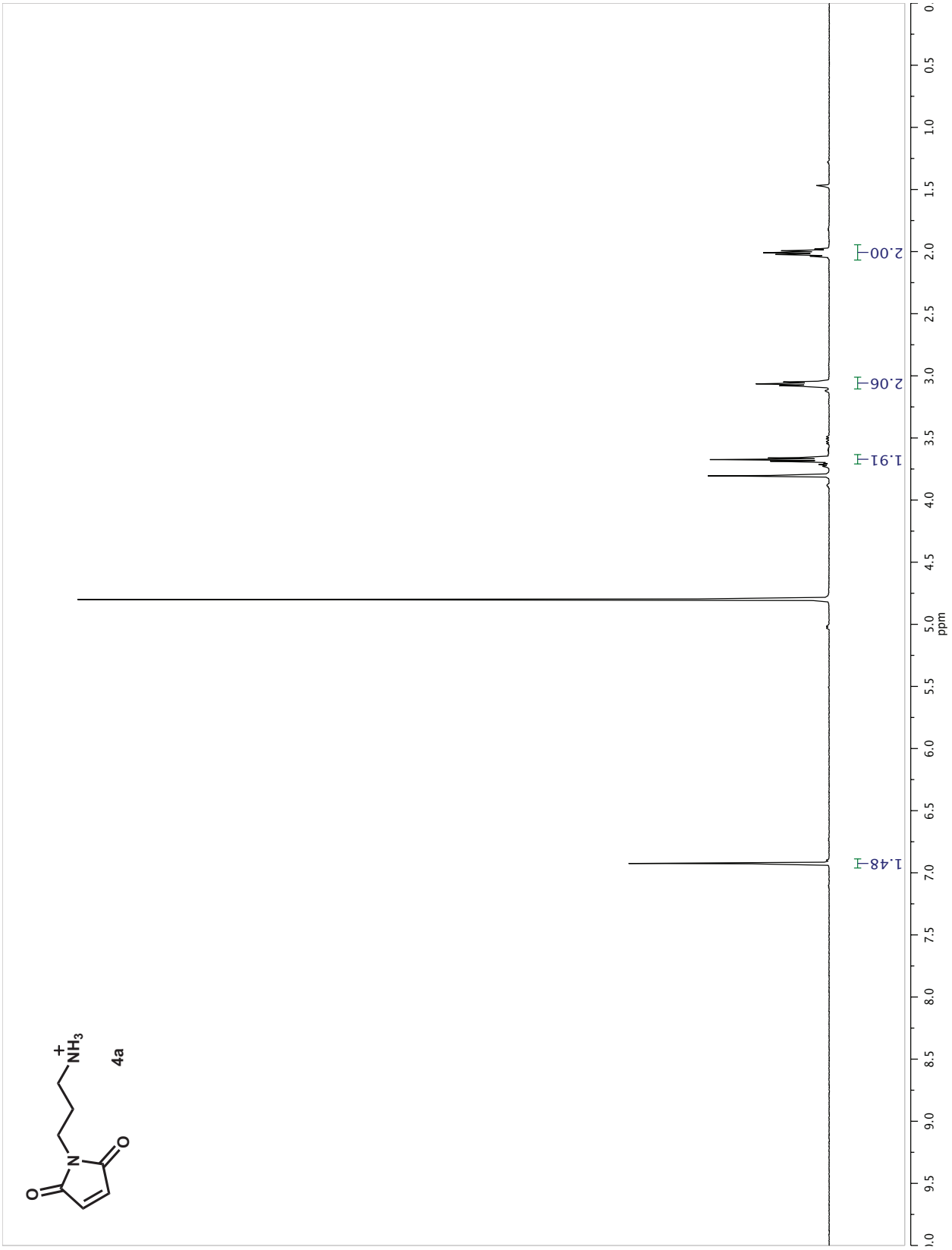

Appendix 20 ^{1}H-NMR of spectrum of compound 4b

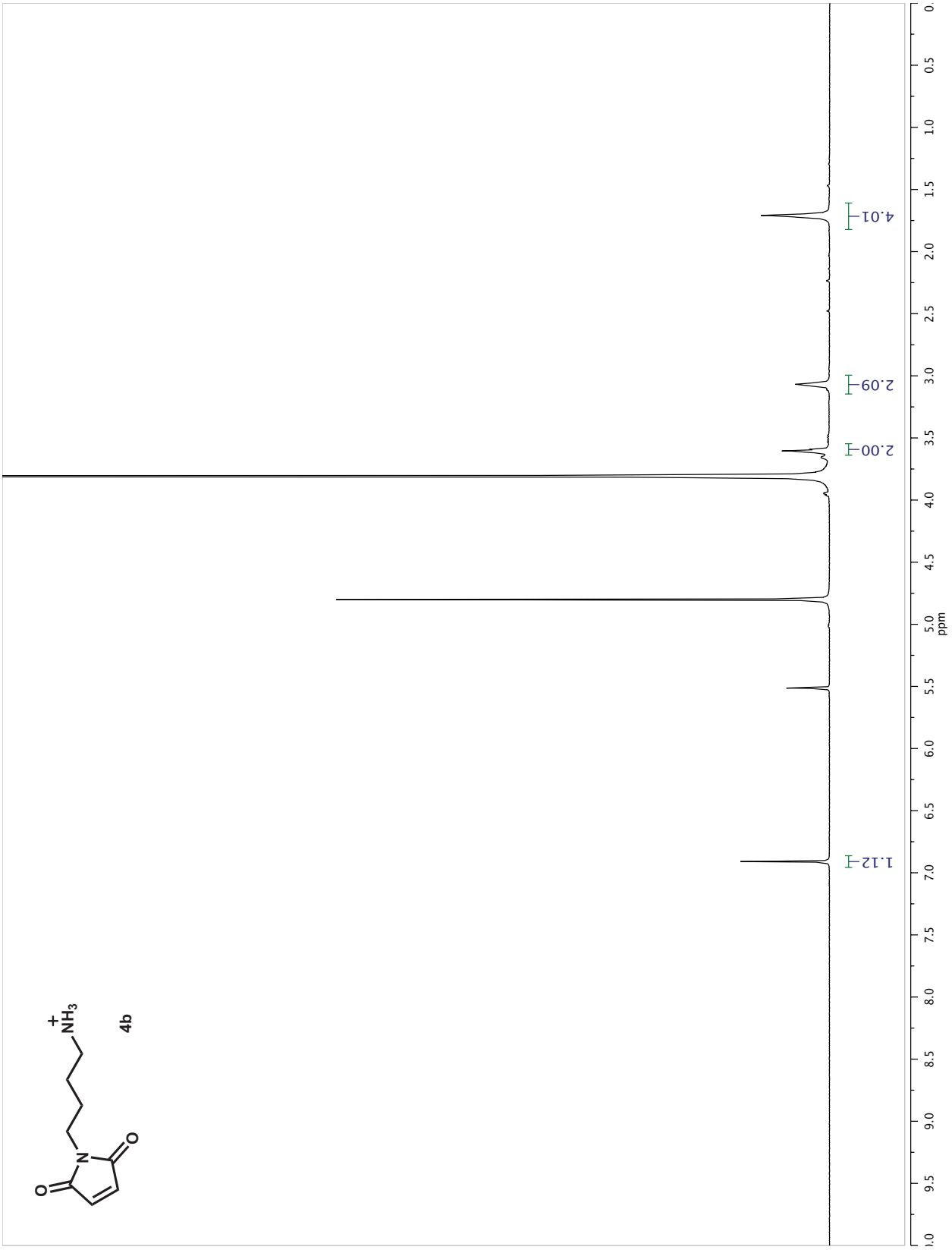

Appendix 21 ^{1}H-NMR of spectrum of compound 4c

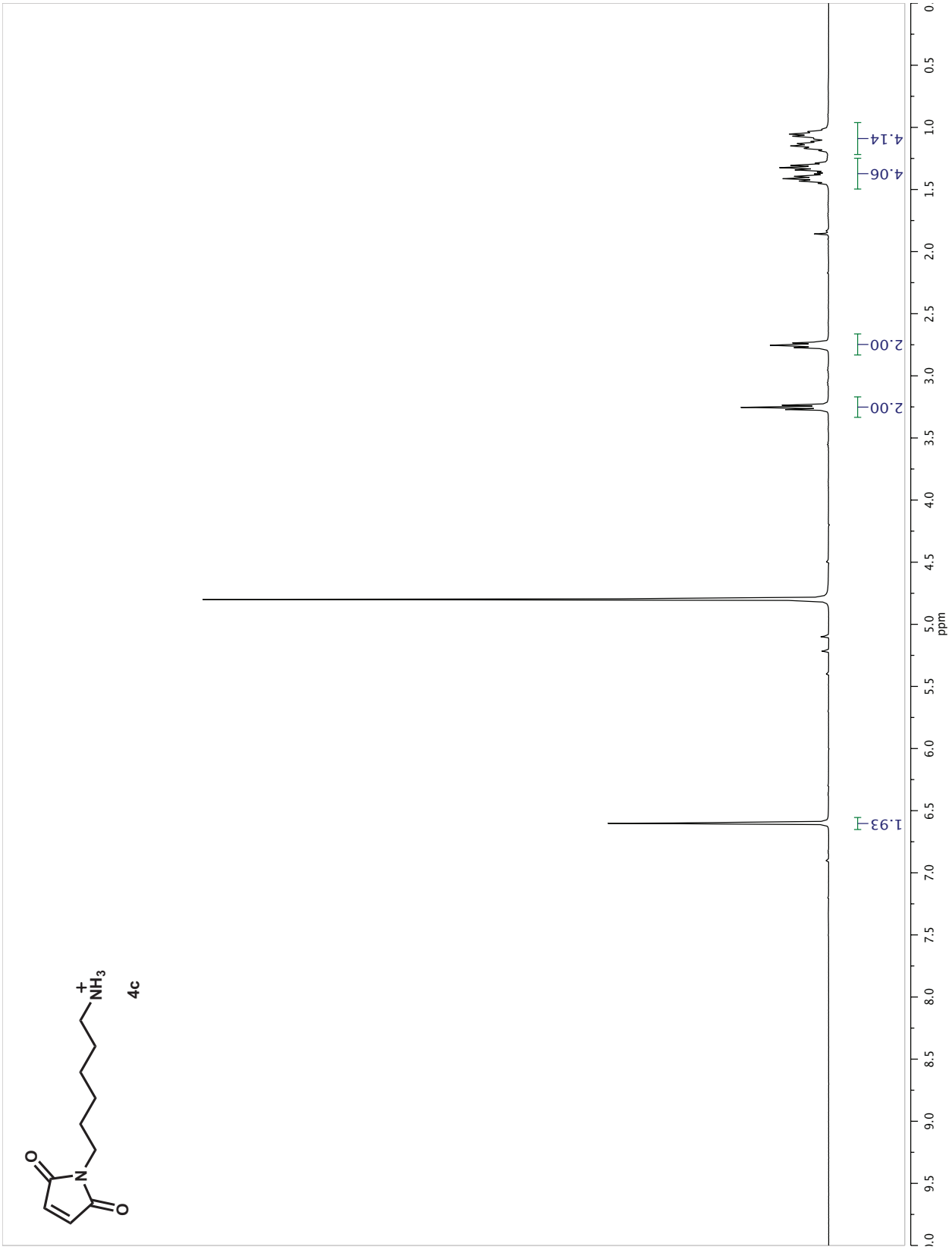

Appendix 22 ^{1}H-NMR of spectrum of compound 4d

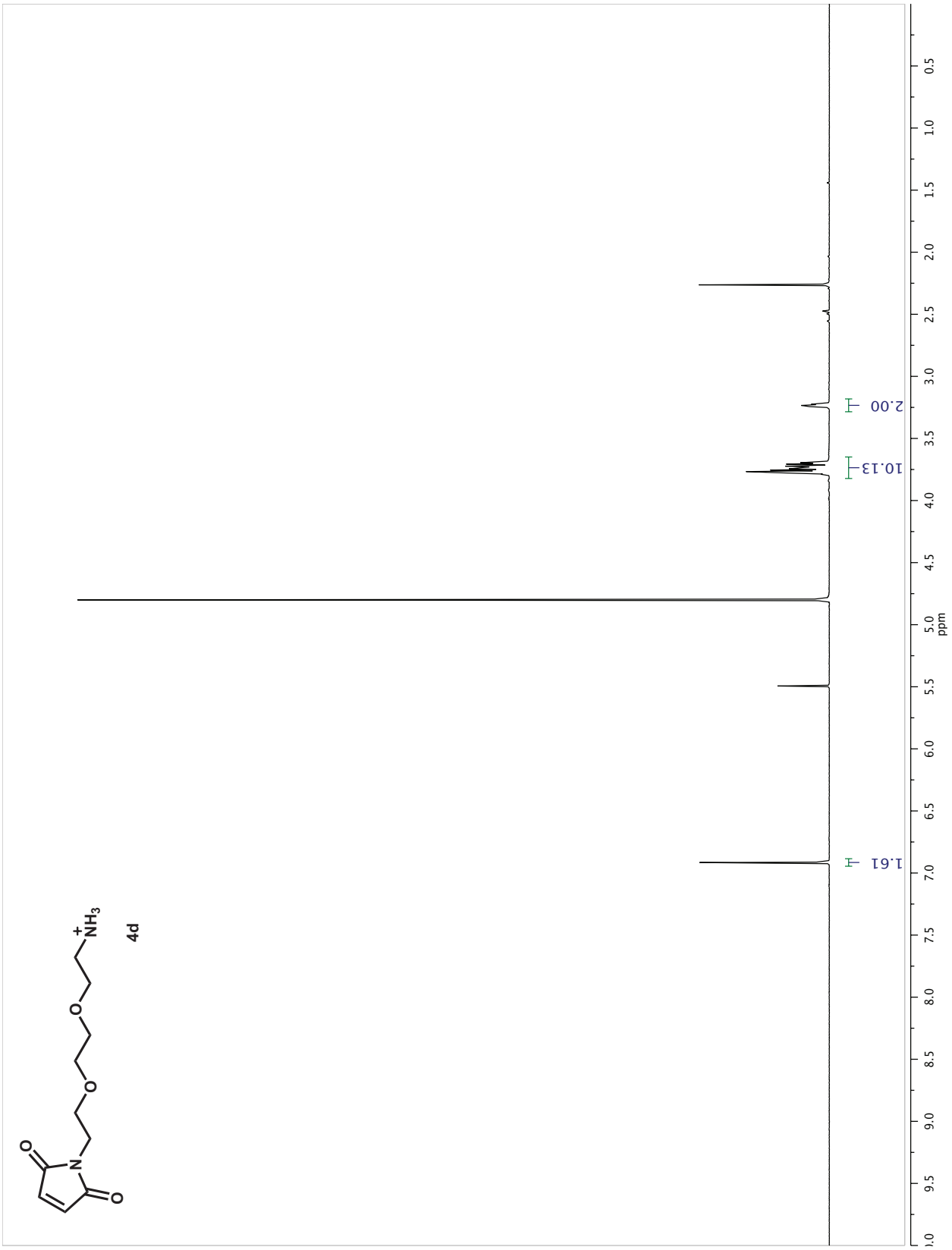

Appendix 23 ^{1}H-NMR of spectrum of compound 5a-d_0

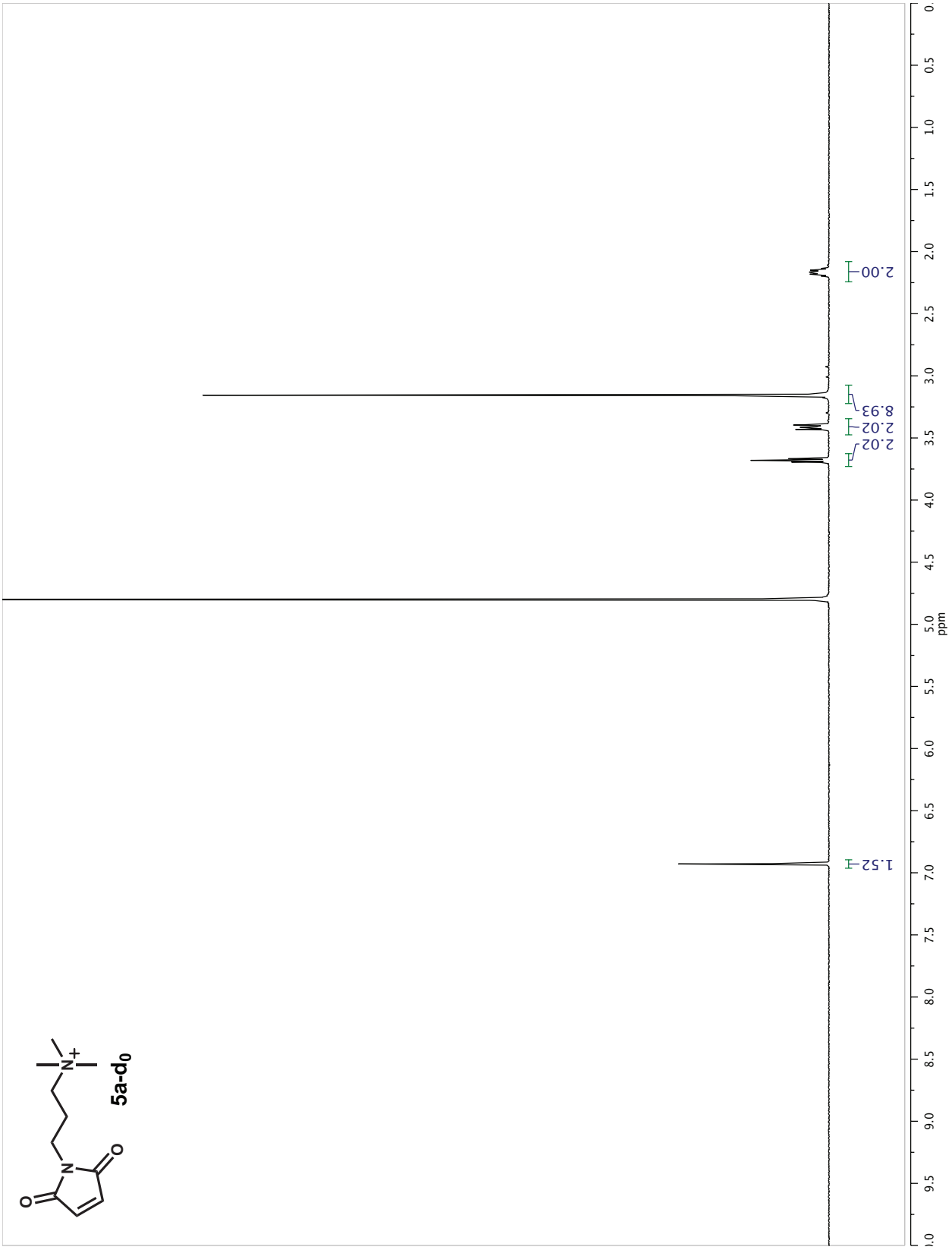

Appendix 24 ^{13}C-NMR of spectrum of compound 5a-d_0

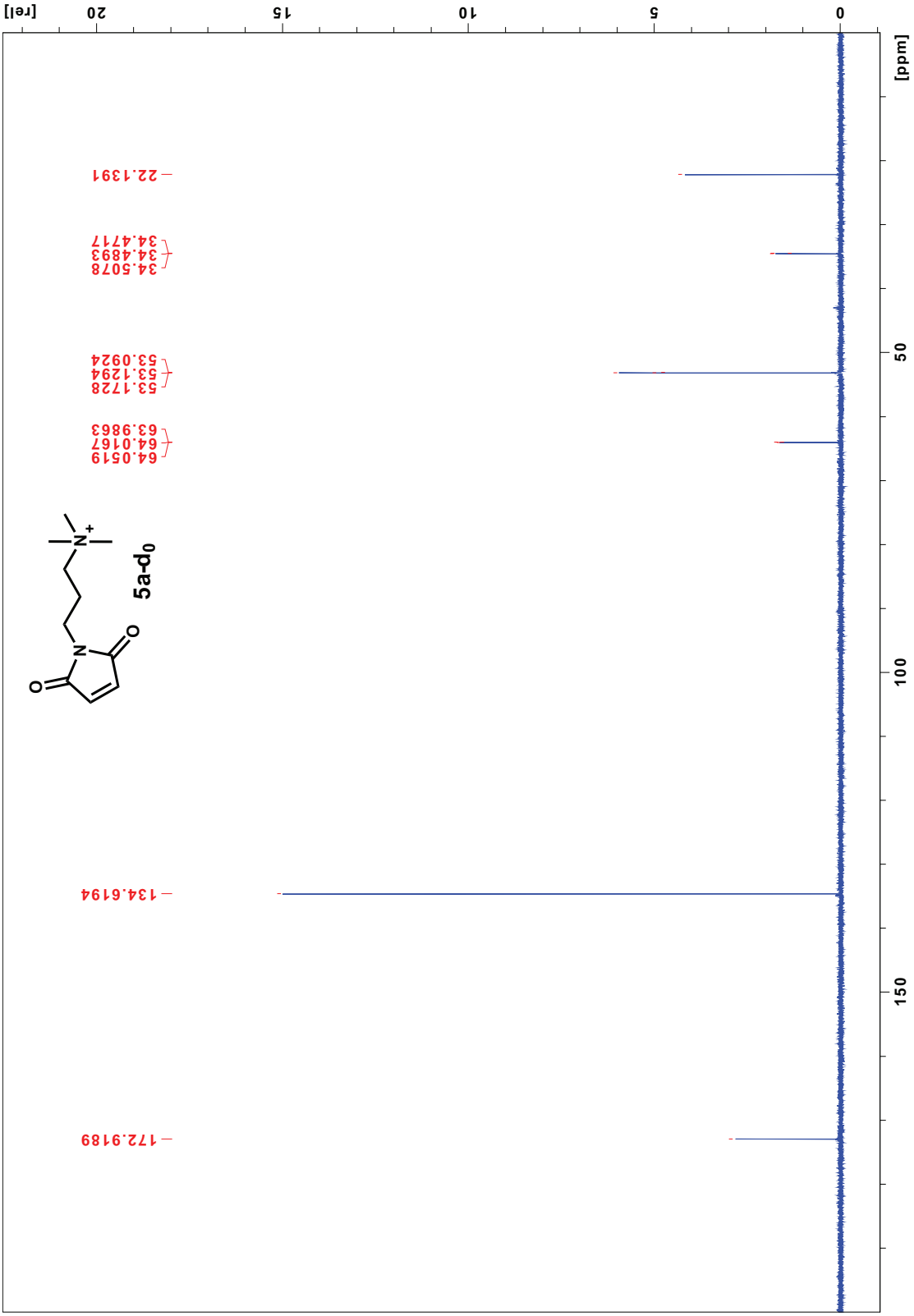

Appendix 25 ^{1}H-NMR of spectrum of compound 5a-d_9

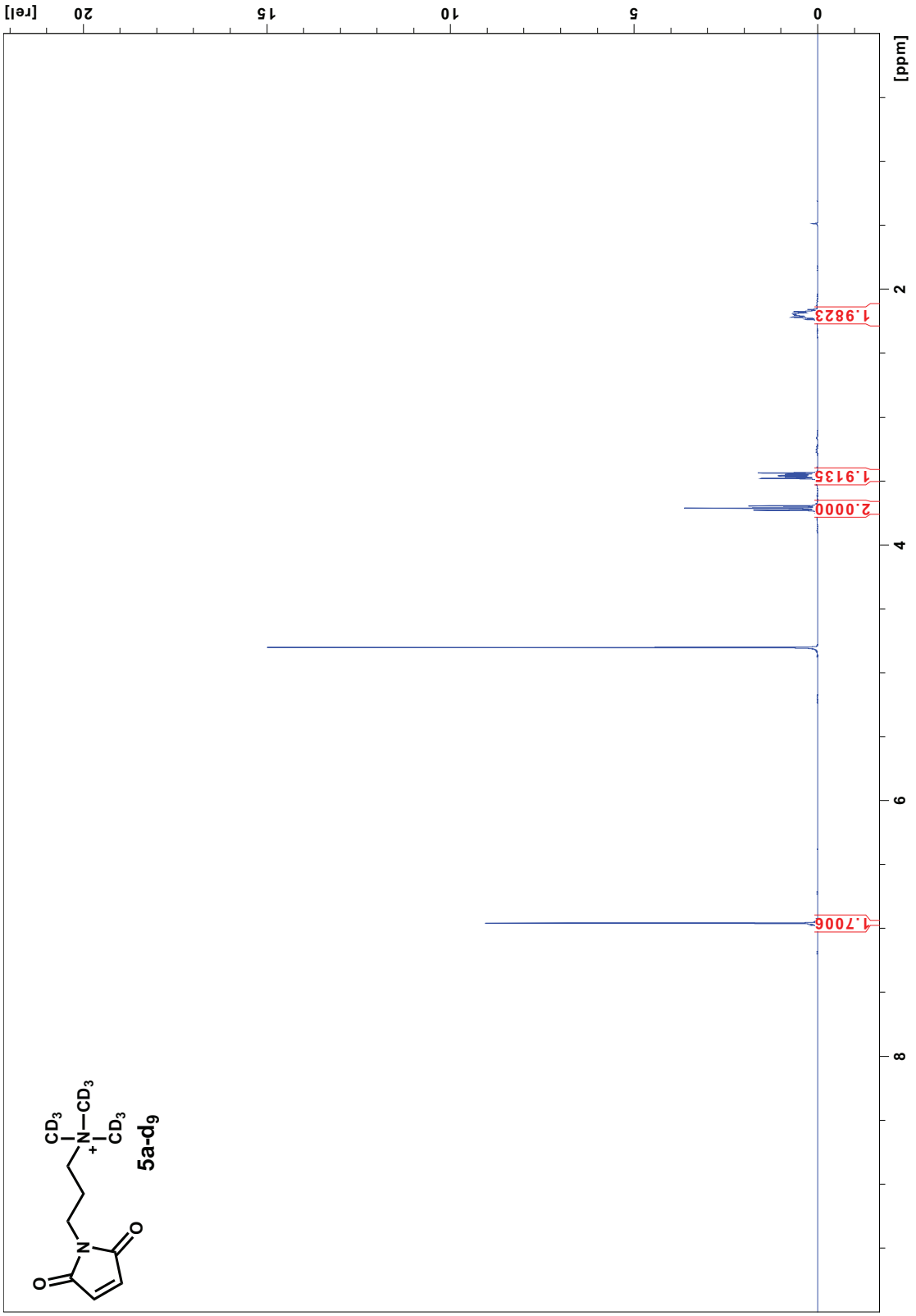

Appendix 26 ^{13}C-NMR of spectrum of compound 5a-d$_9$

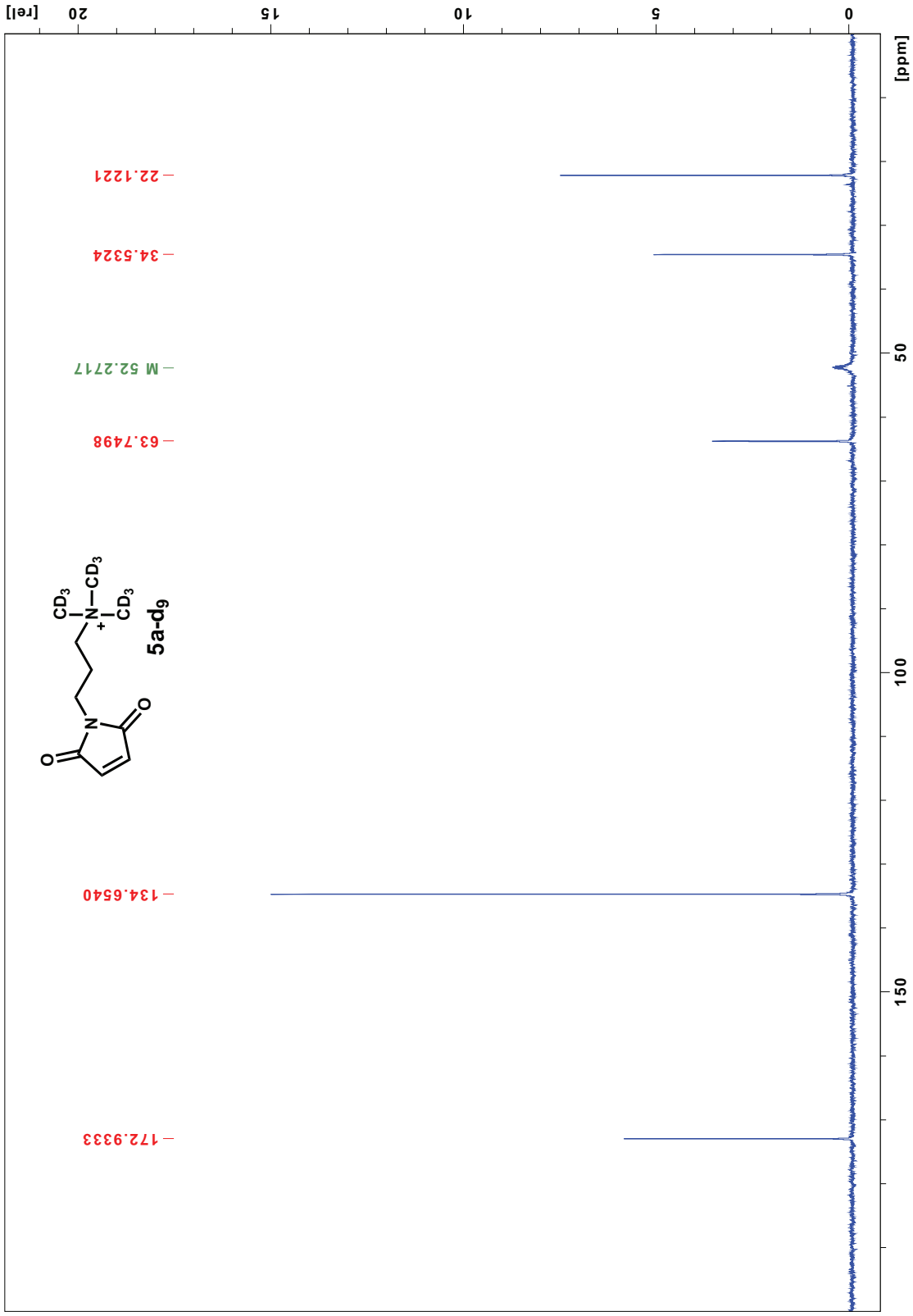

Appendix 27 ^{1}H-NMR of spectrum of compound 5b-d_0

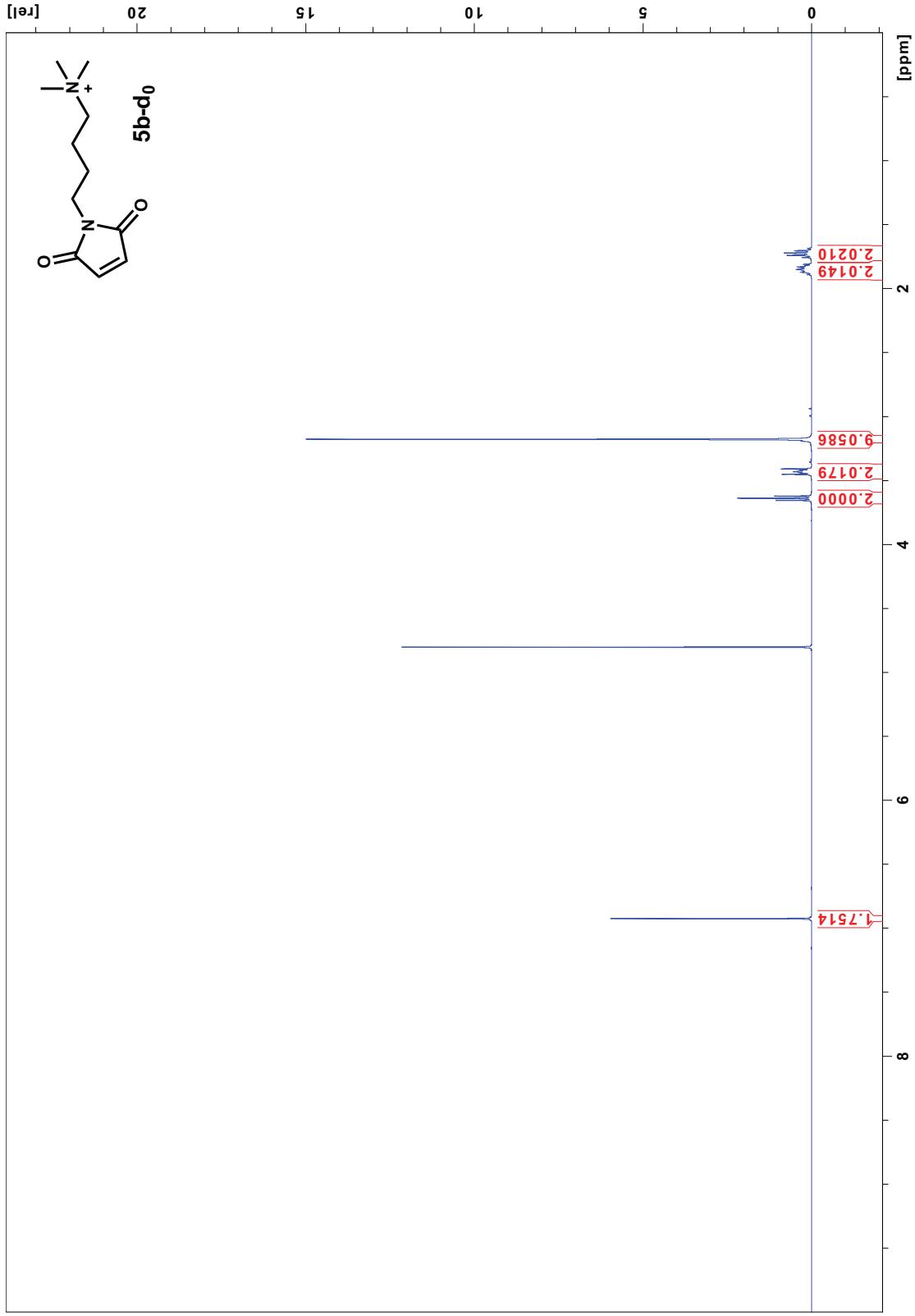

Appendix 28 ^{13}C-NMR of spectrum of compound 5b-d_0

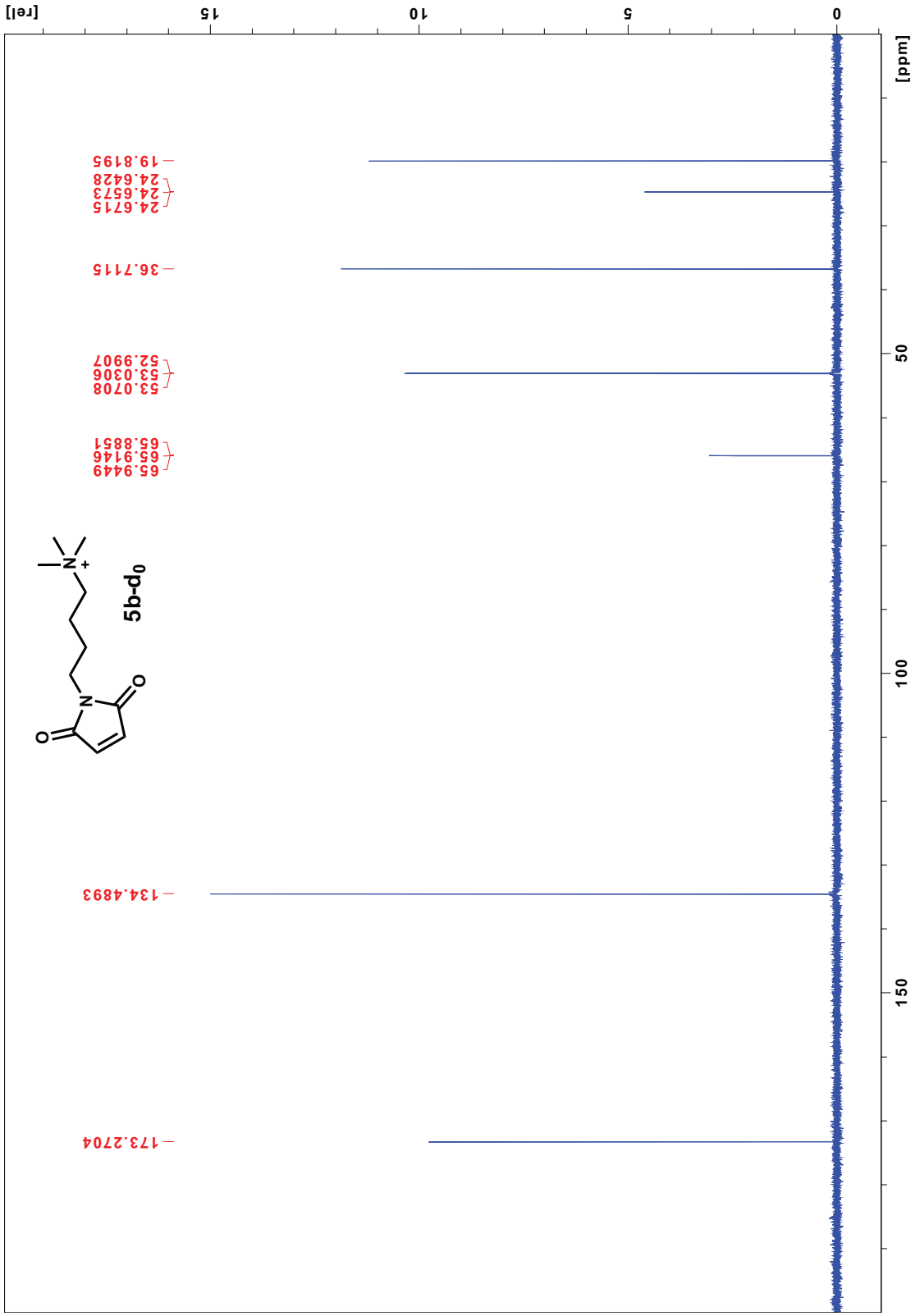

Appendix 29 ^{1}H-NMR of spectrum of compound 5b-d$_9$

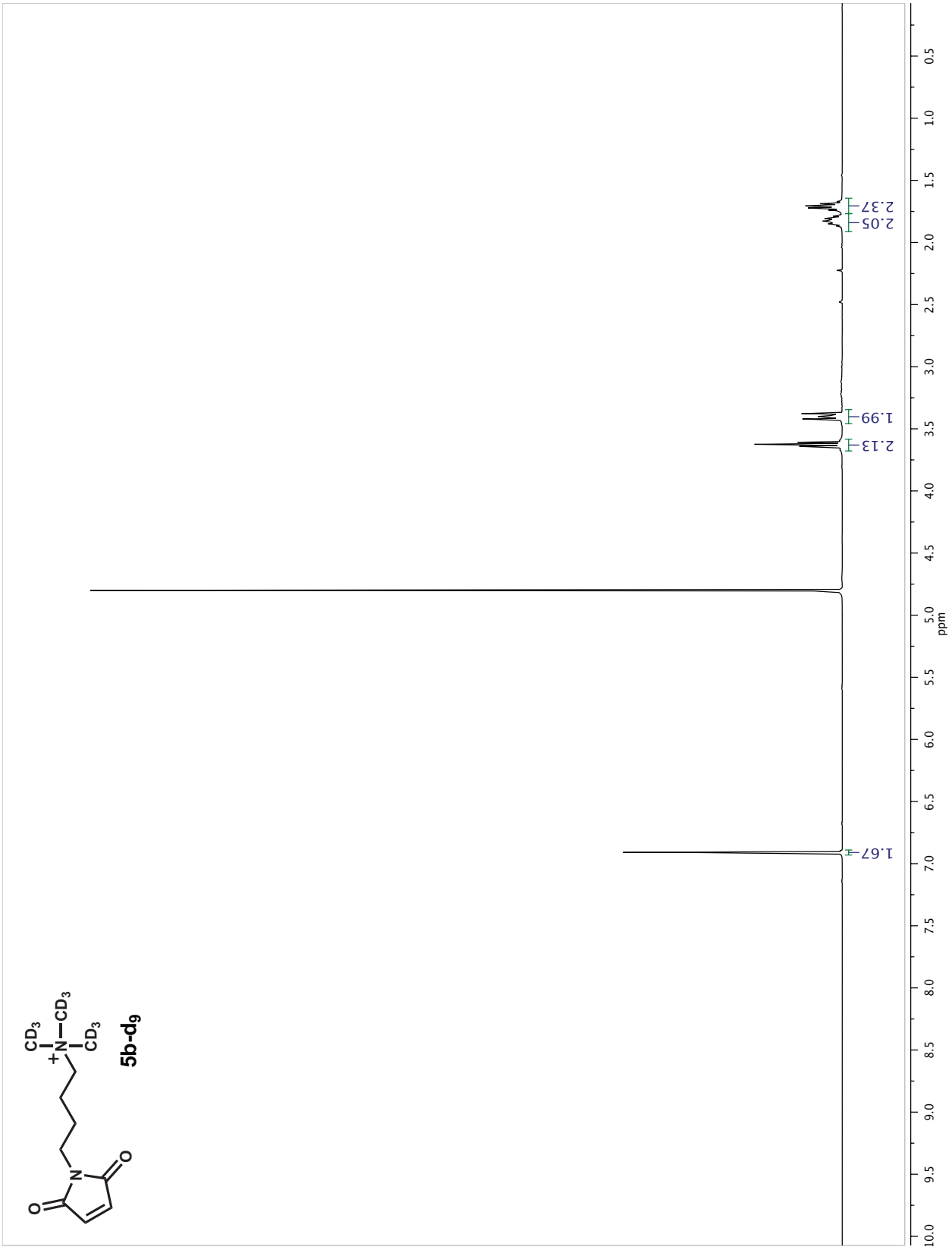

Appendix 30 ^{13}C-NMR of spectrum of compound 5b-d_9

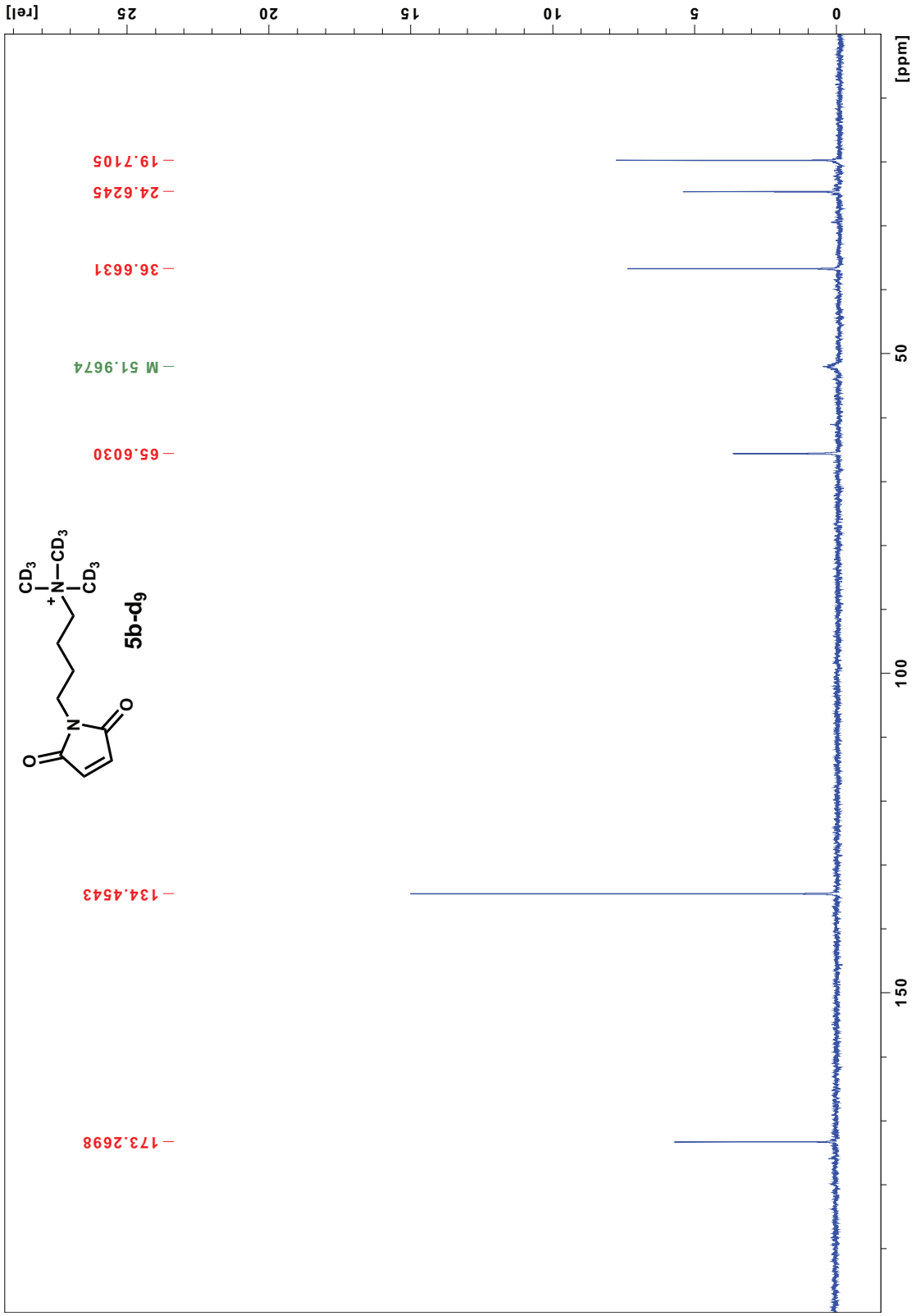

Appendix 31 ^{1}H-NMR of spectrum of compound 5c-d_0

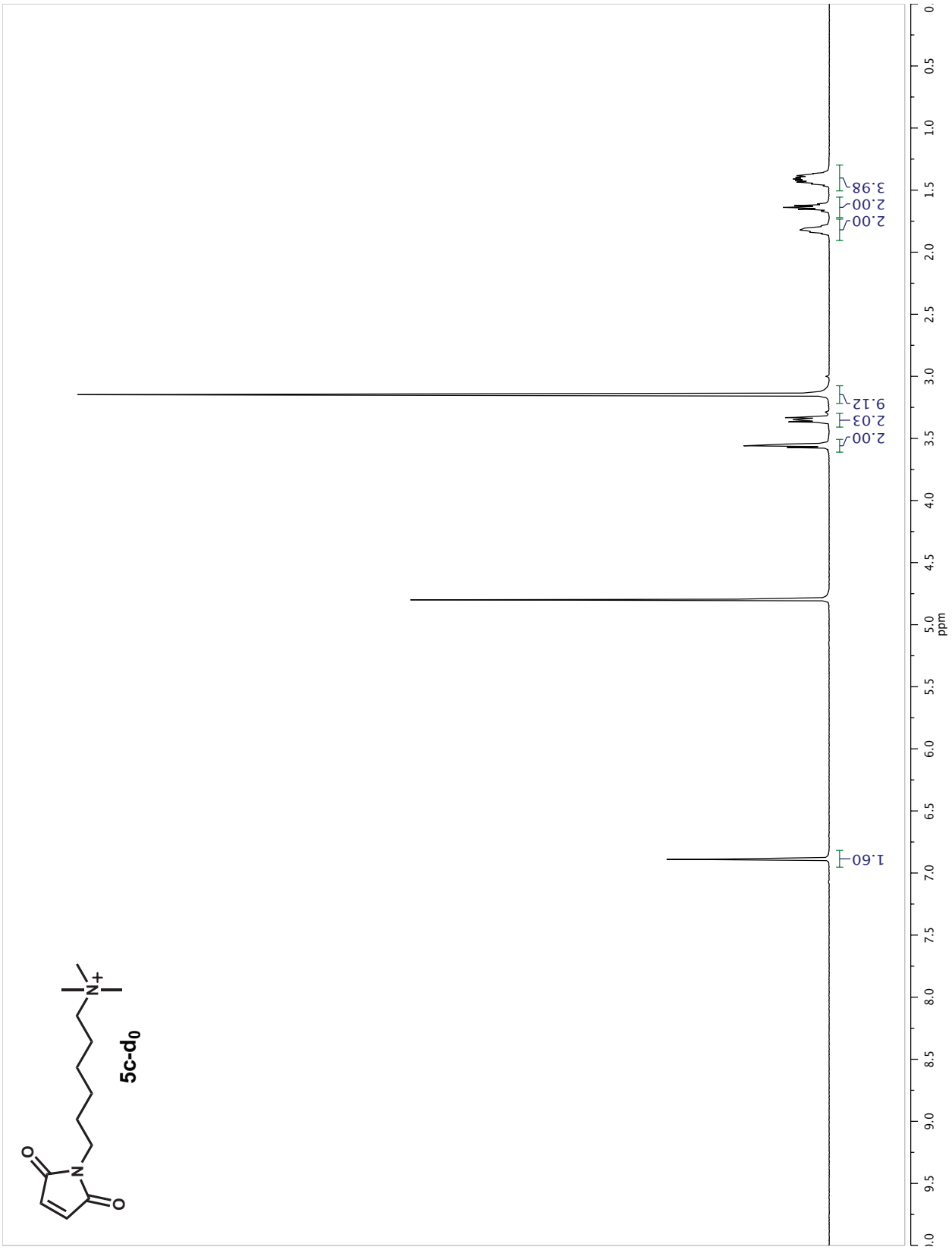

Appendix 32 ^{13}C-NMR of spectrum of compound 5c-d_0

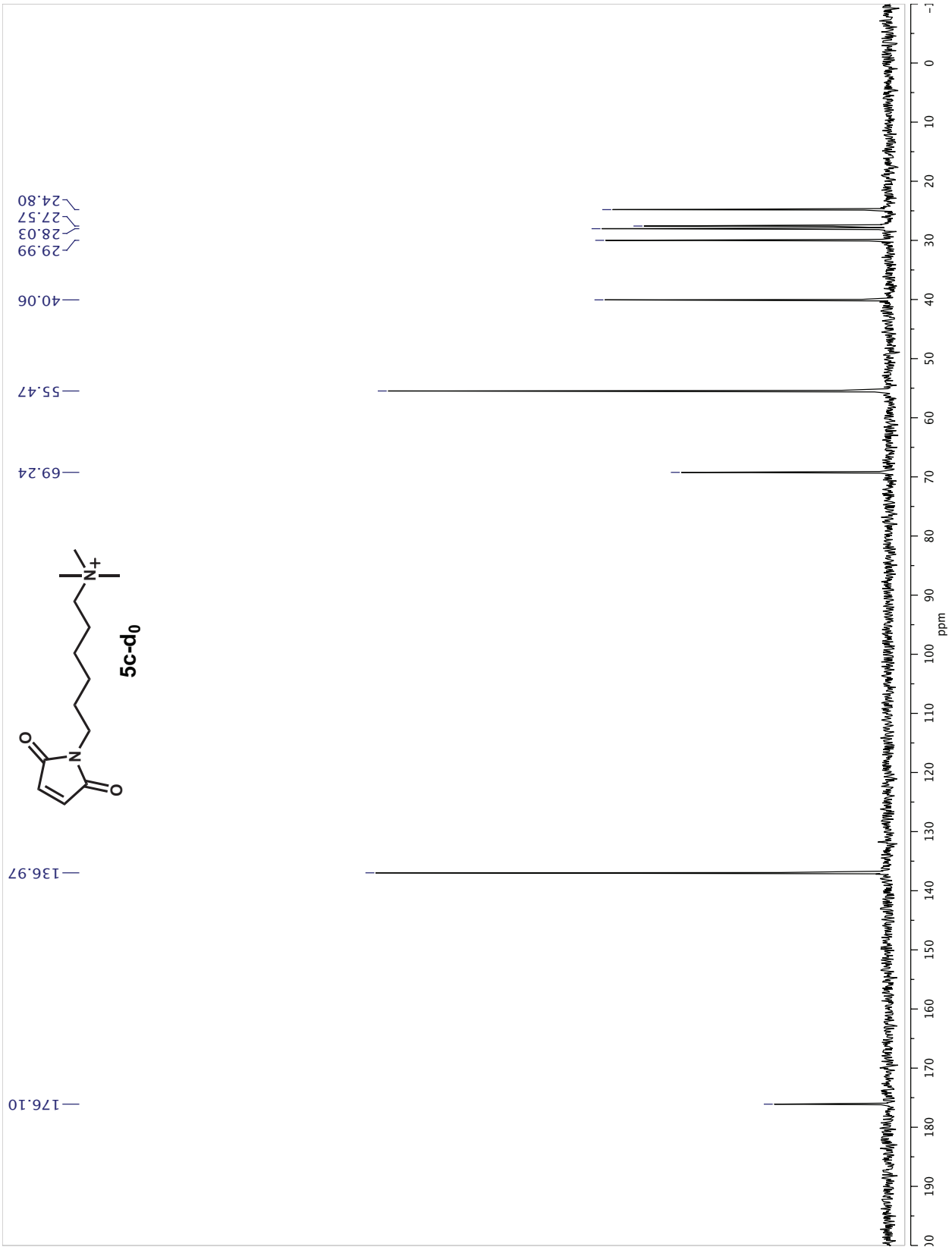

Appendix 33 ^{1}H-NMR of spectrum of compound 5c-d_9

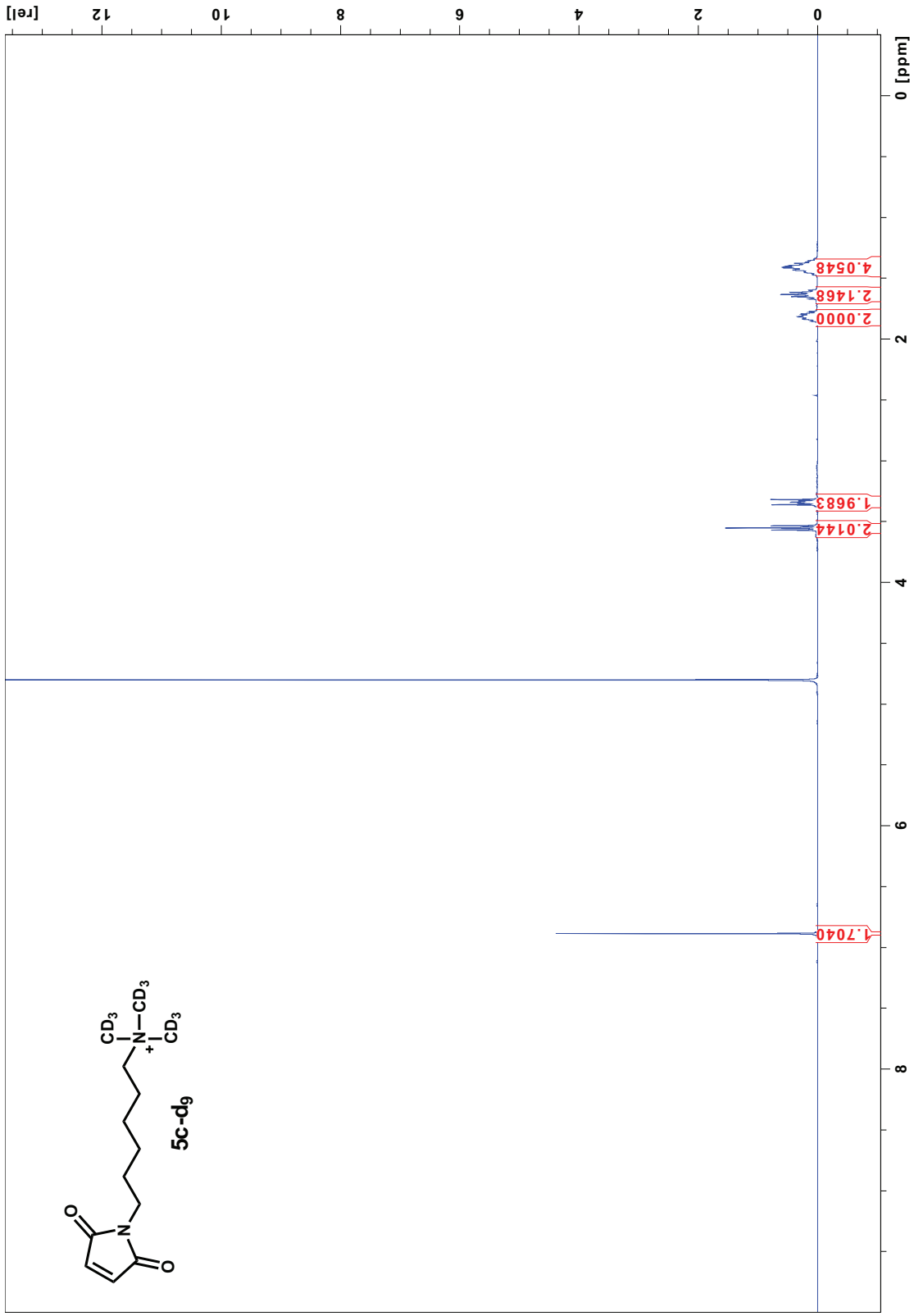

Appendix 34 ^{13}C-NMR of spectrum of compound 5c-d$_9$

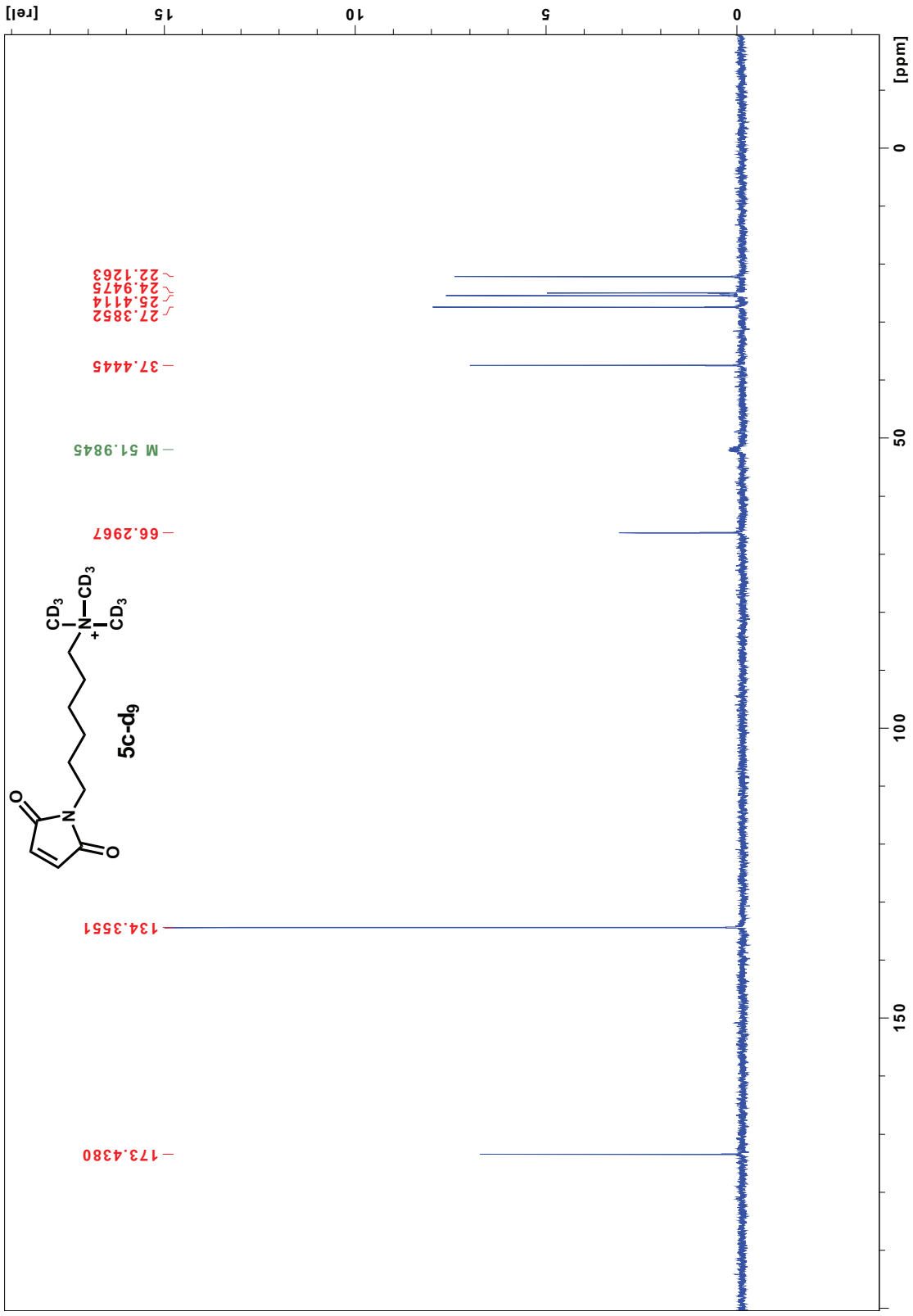

Appendix 35 ^{1}H-NMR of spectrum of compound 5d-d_0

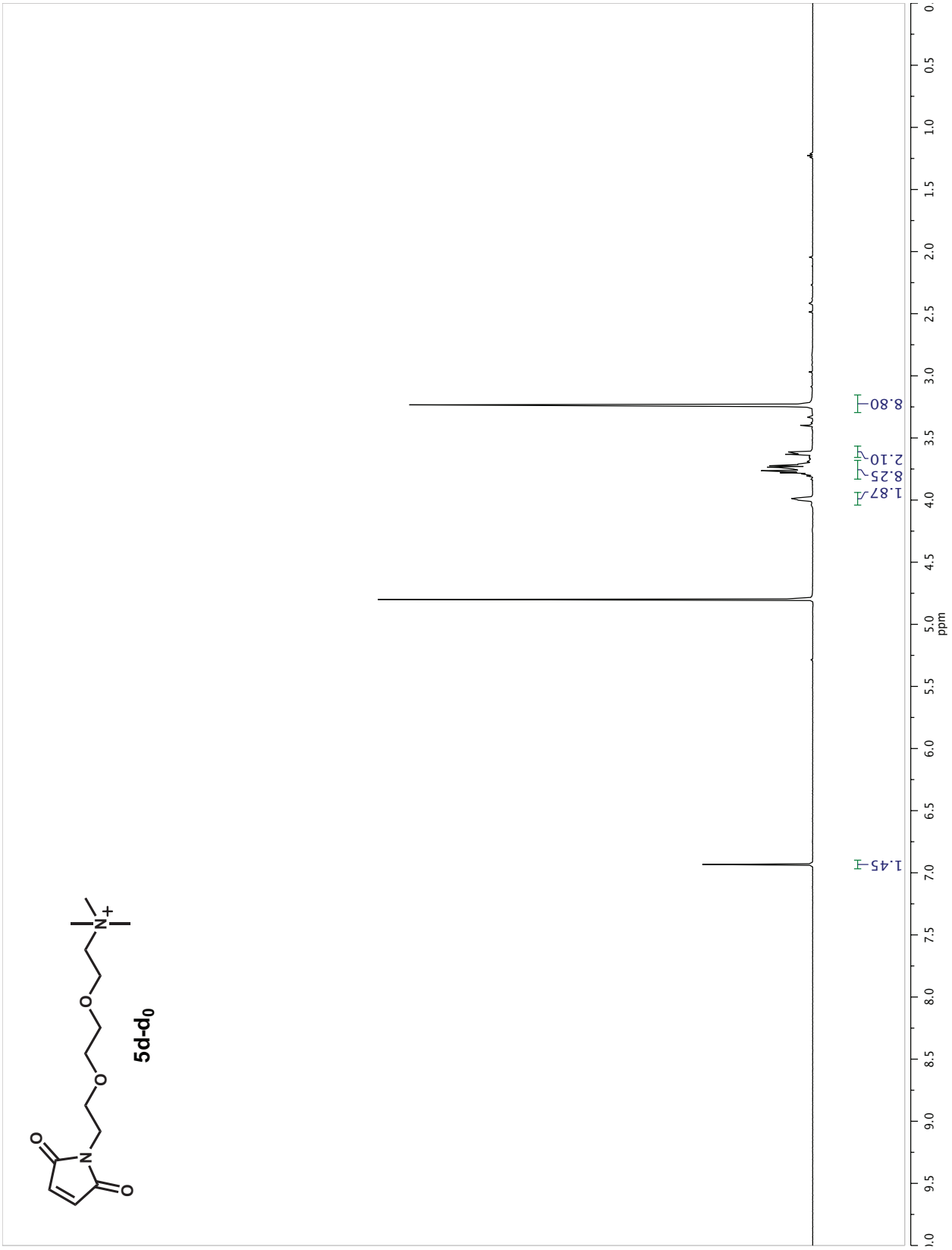

Appendix 36 ^{13}C-NMR of spectrum of compound 5d-d_0

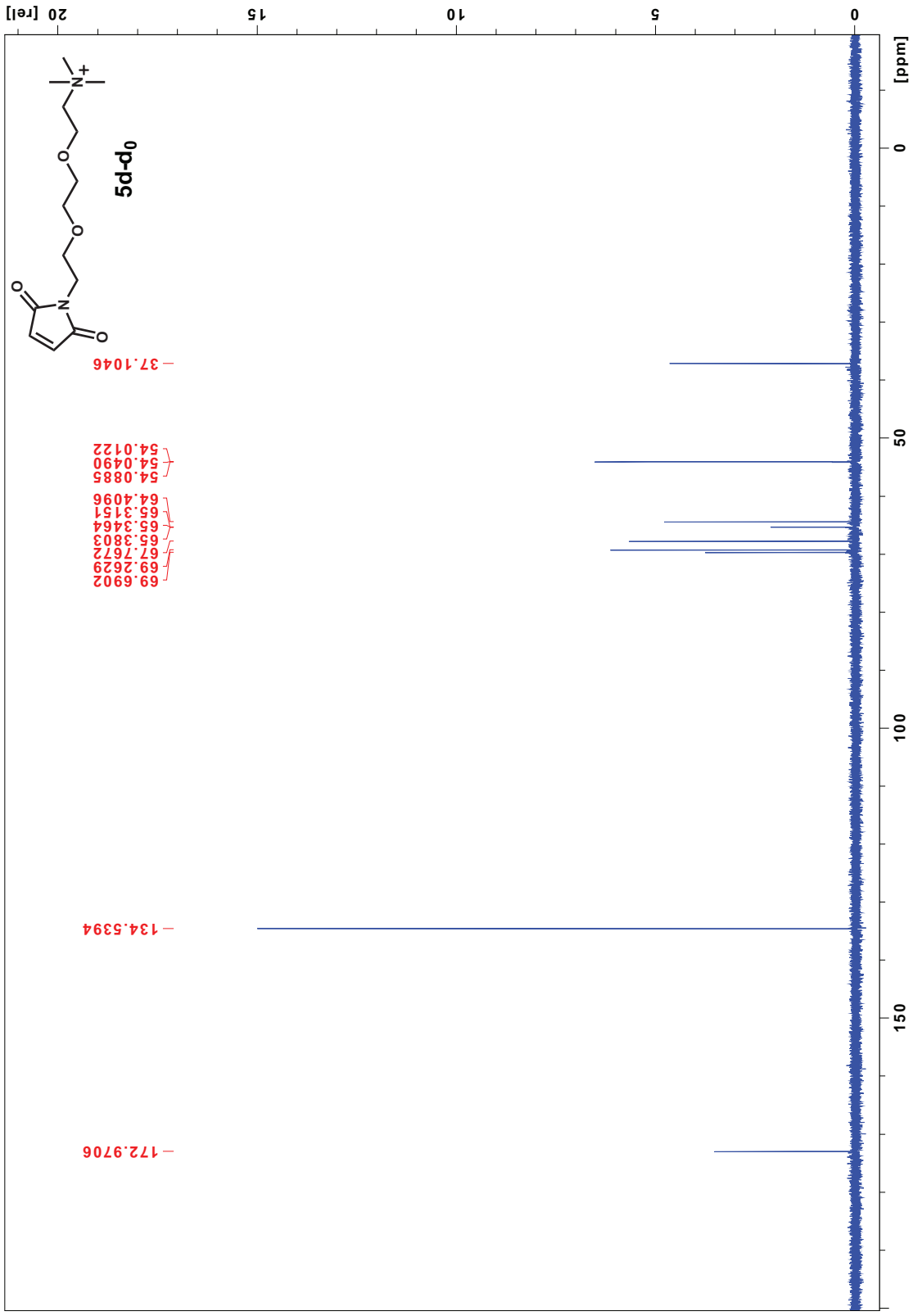

Appendix 37 ^{1}H-NMR of spectrum of compound 5d-d$_9$

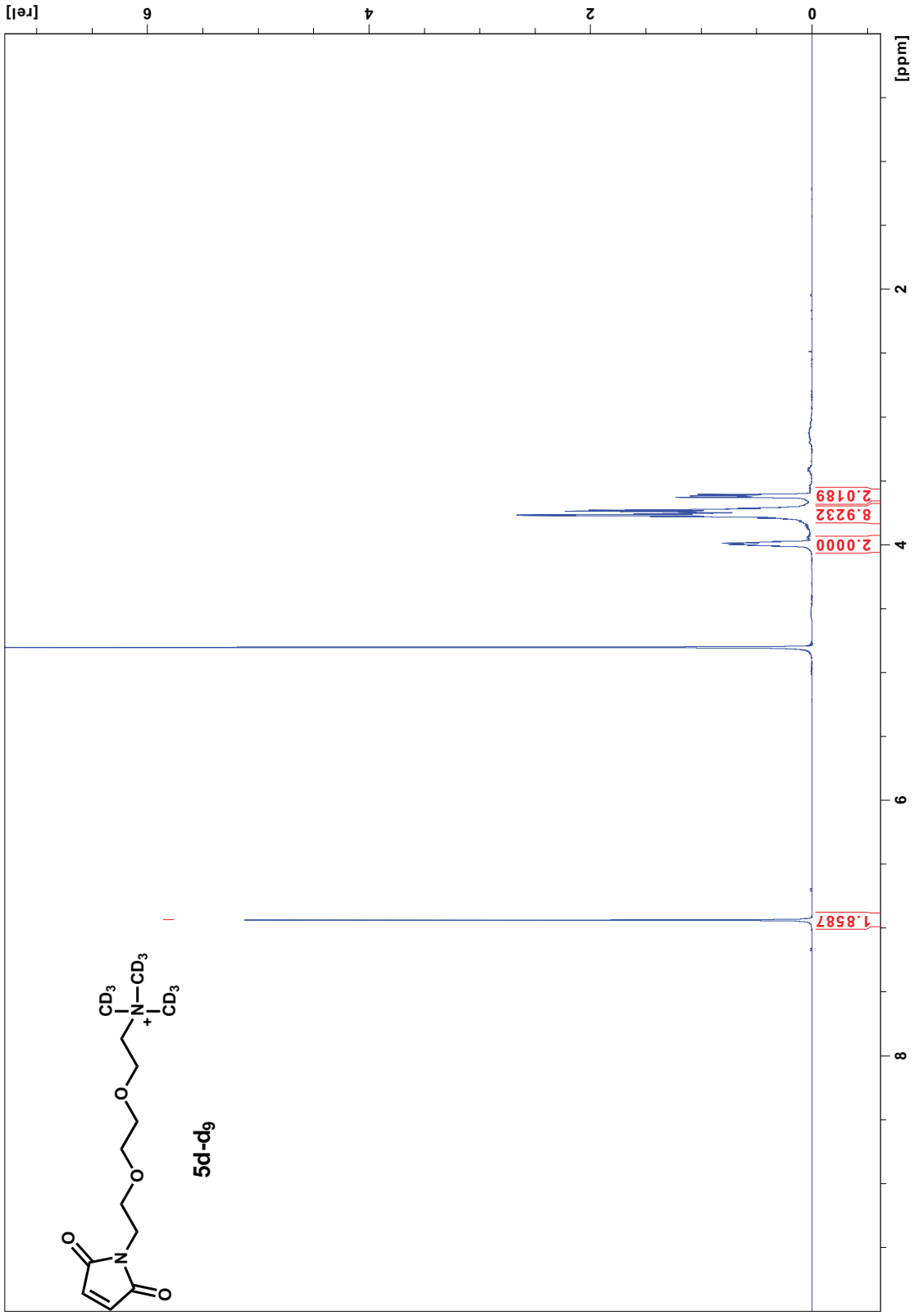

Appendix 38 ^{13}C-NMR of spectrum of compound 5d-d$_9$

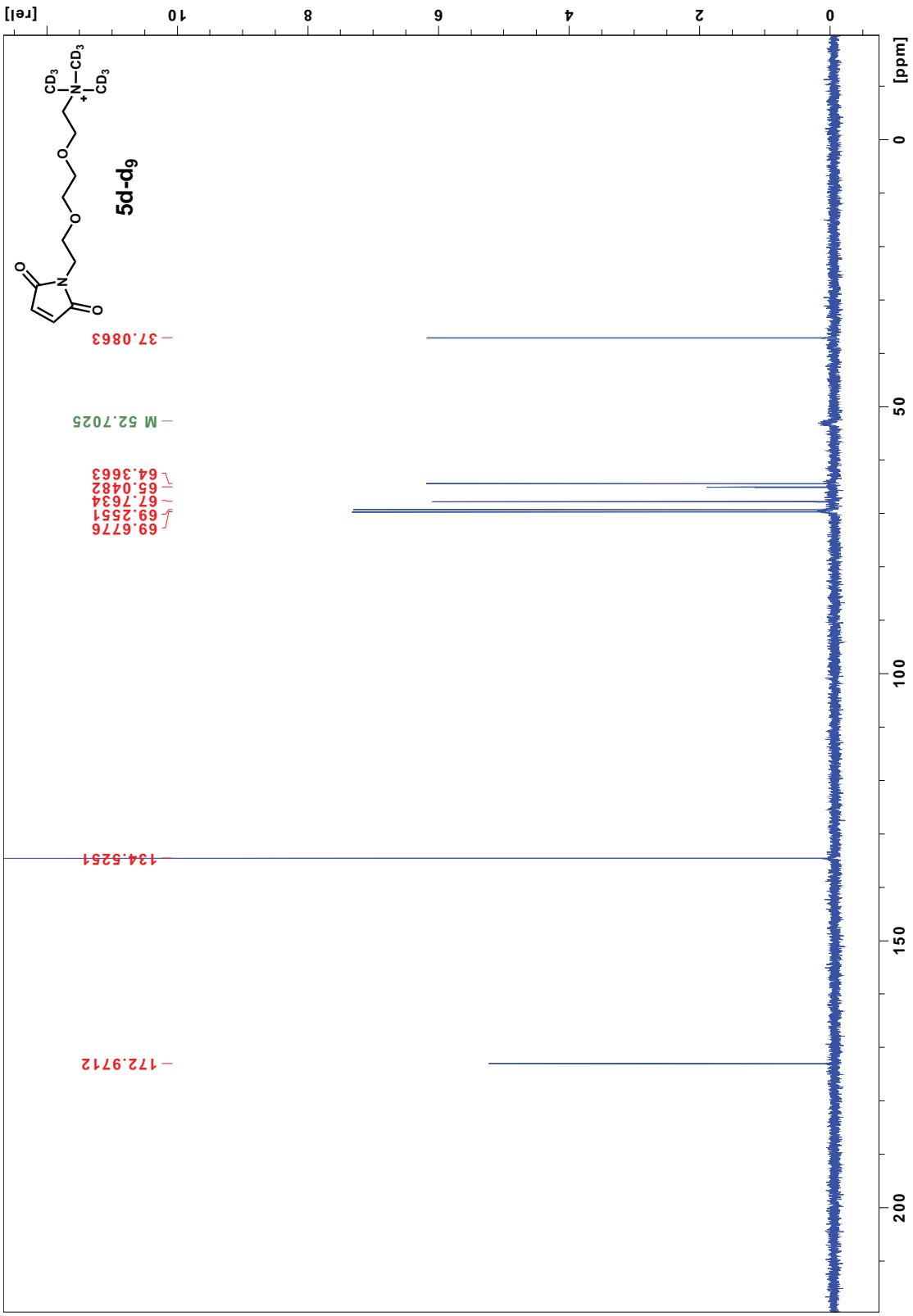

Appendix 39 Mass of spectrum of compound 5a-d_0

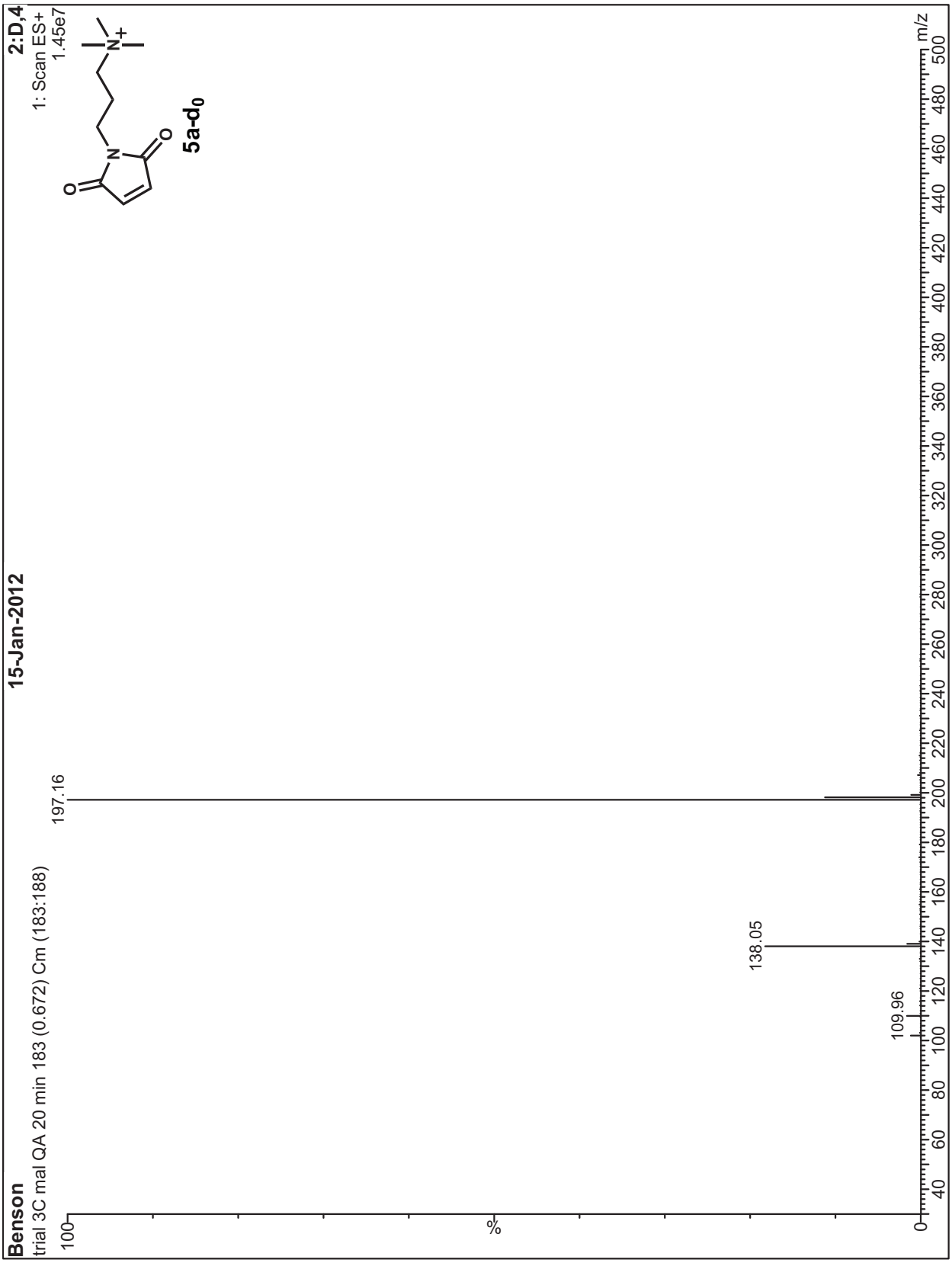

Appendix 40 Mass of spectrum of compound 5a-d_9

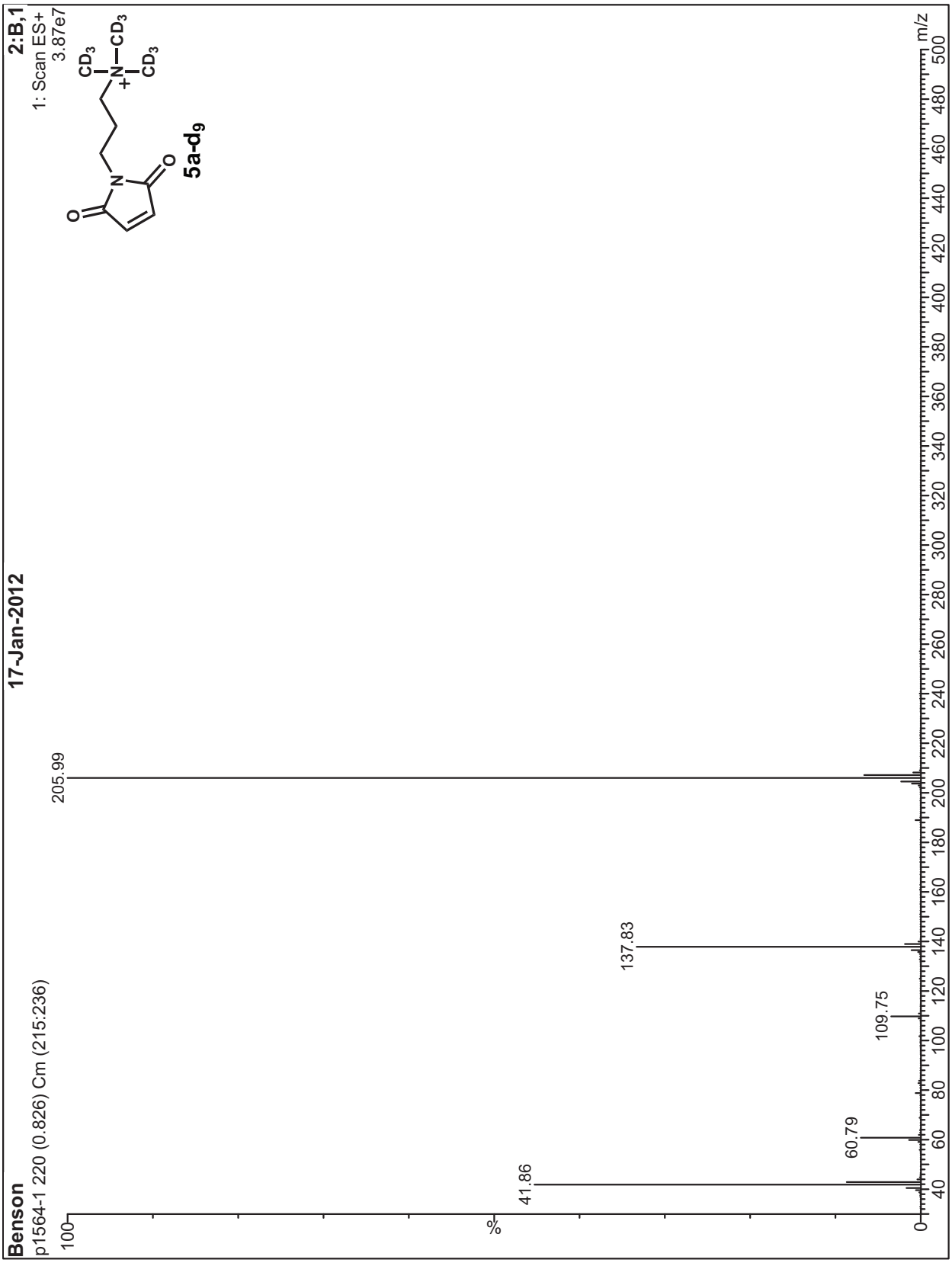

Appendix 41 Mass of spectrum of compound 5b-d_0

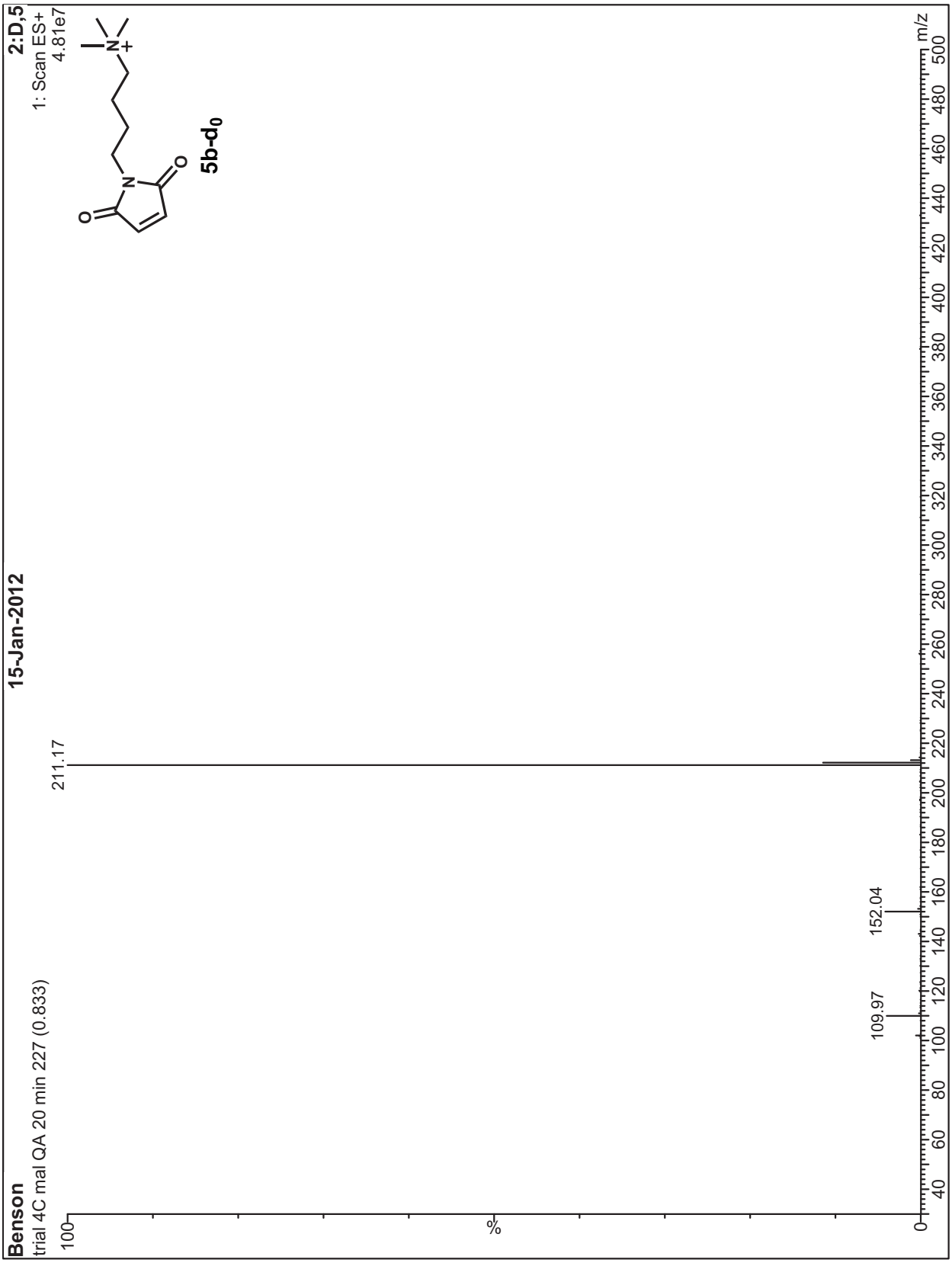

Appendix 42 Mass of spectrum of compound 5b-d_9

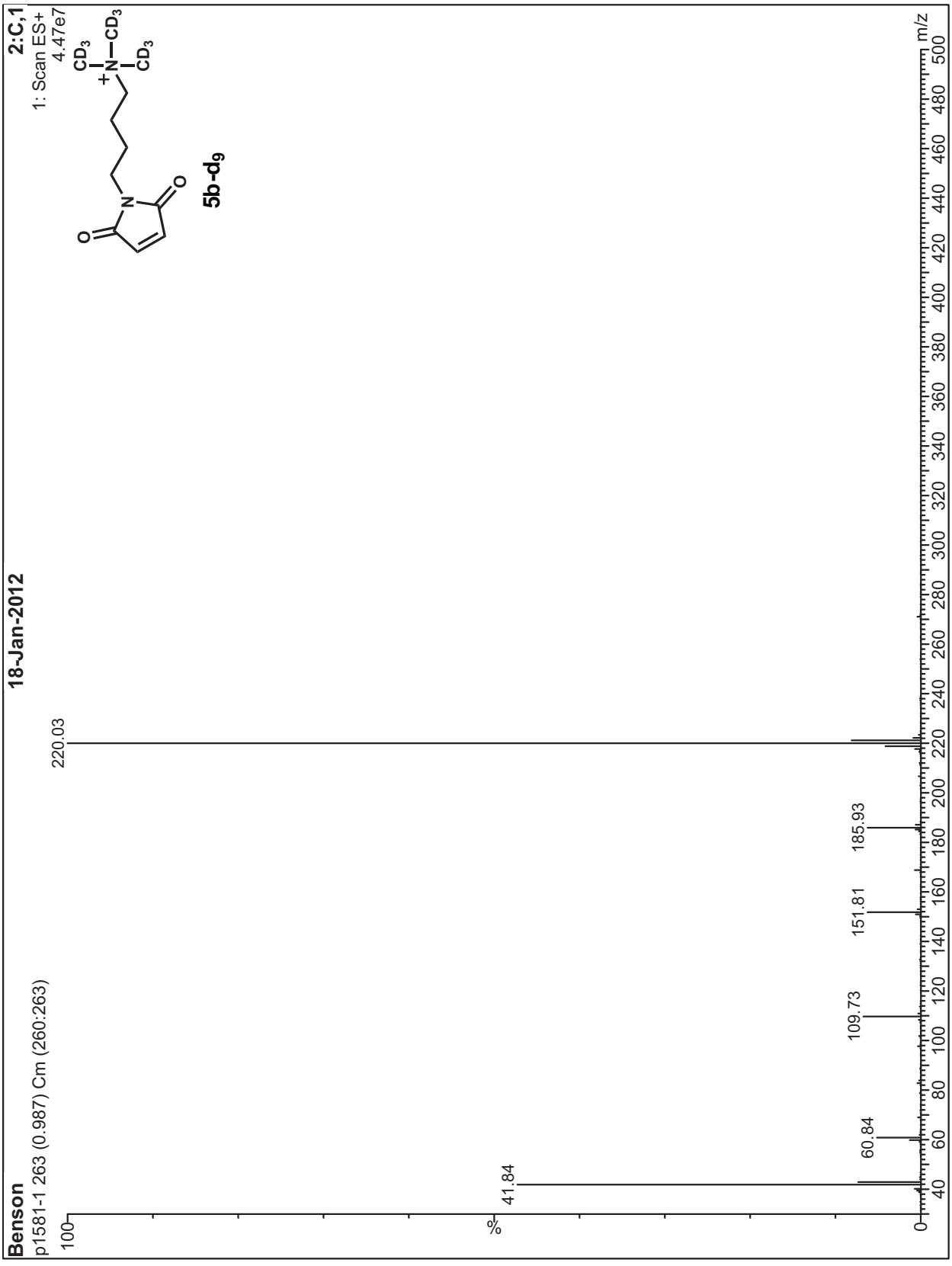

Appendix 43 Mass of spectrum of compound 5c-d_0

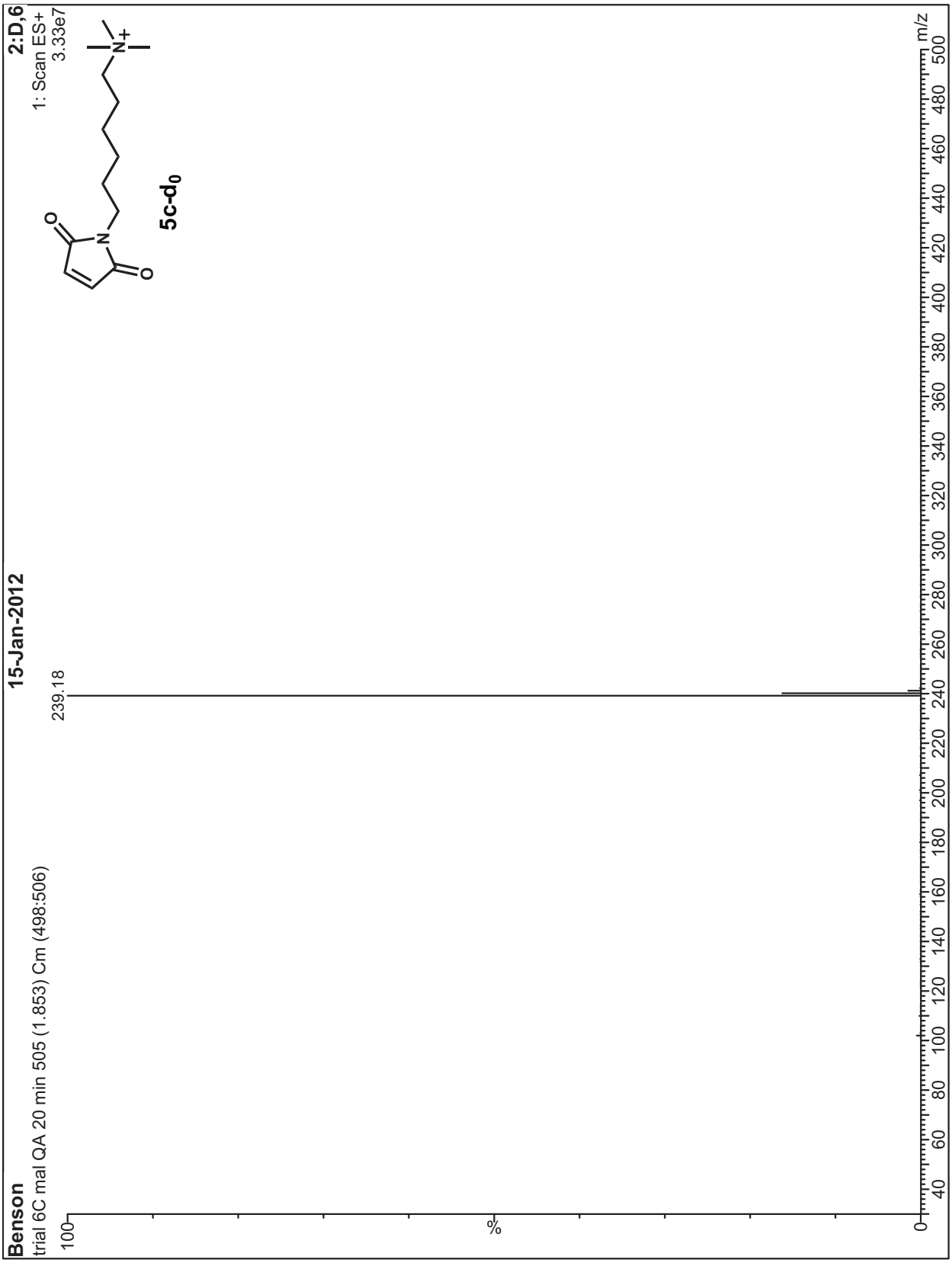

Appendix 44 Mass of spectrum of compound 5c-d_9

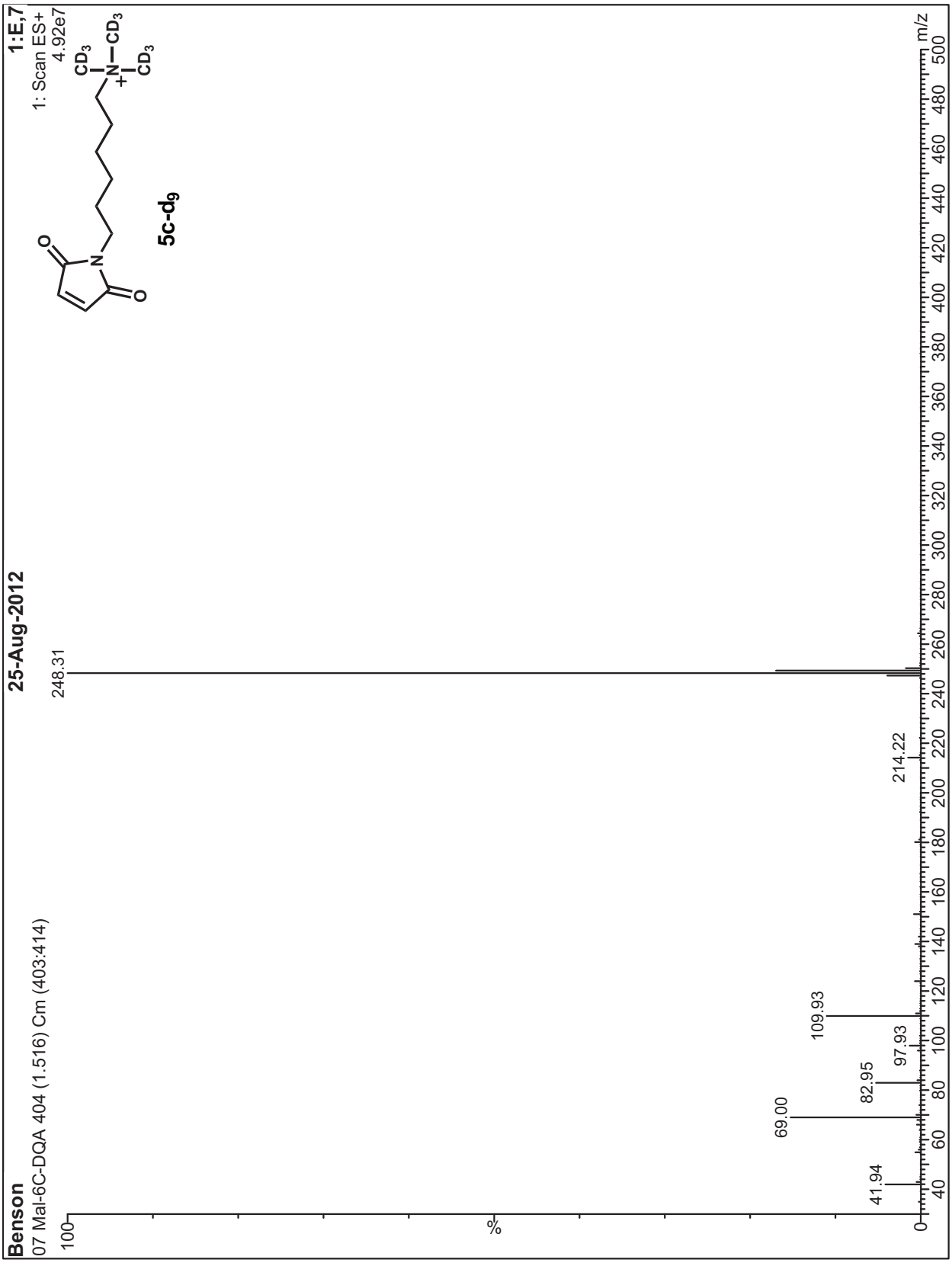

Appendix 45 Mass of spectrum of compound 5d-d_0

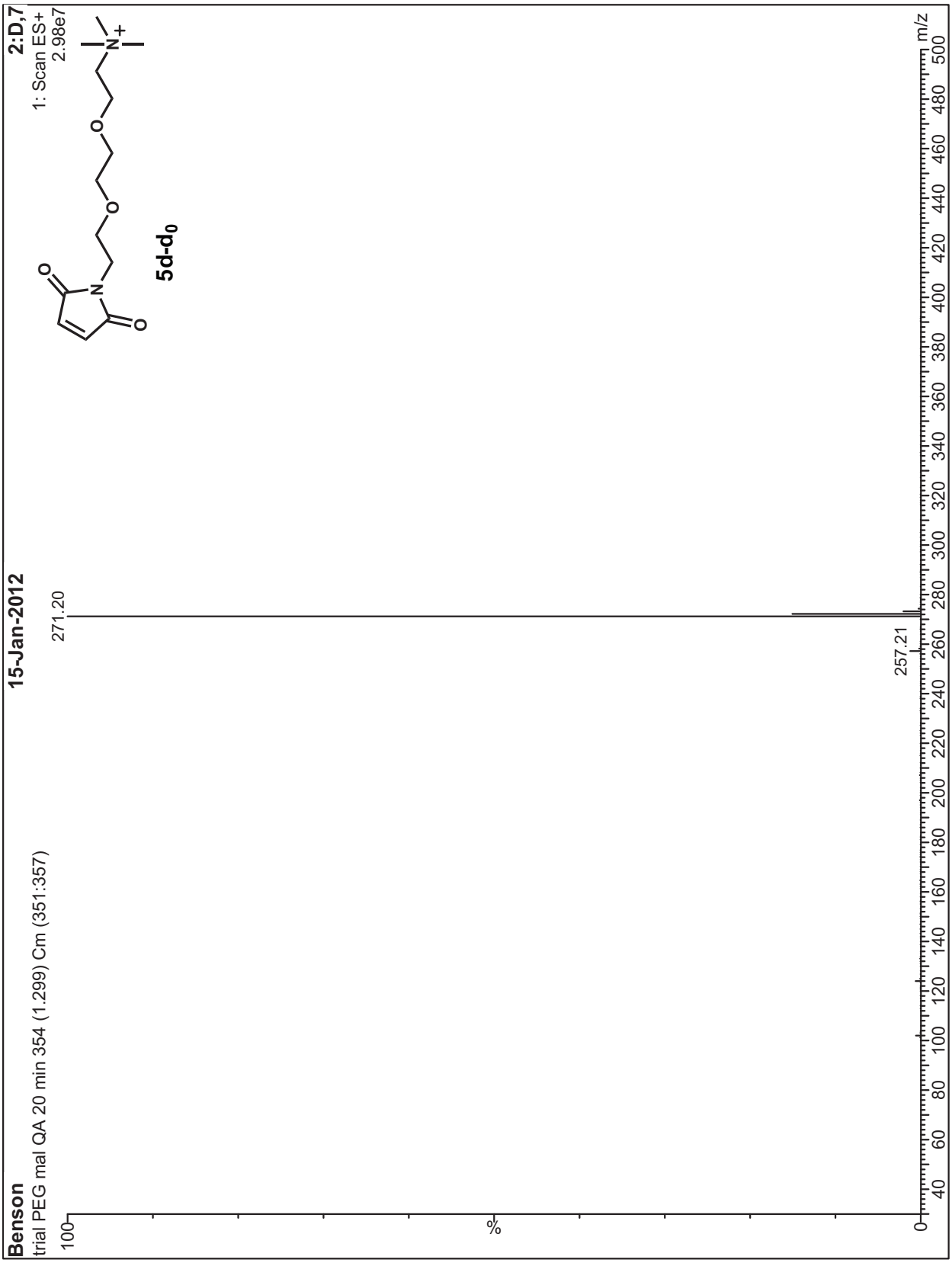

Appendix 46 Mass of spectrum of compound 5d-d_9